ACTA CHIMICA

ACADEMIAE SCIENTIARUM HUNGARICAE

ADIUVANTIBUS

V. BRUCKNER, GY. DEÁK, K. POLINSZKY,
E. PUNGOR, G. SCHAY, Z. G. SZABÓ

REDIGIT

B. LENGYEL

TOMUS 76 FASCICULUS 1

AKADÉMIAI KIADÓ, BUDAPEST

1973

ACTA CHIM. (BUDAPEST) ACASA 76 (1) 1–112 (1973)

ACTA CHIMICA

A MAGYAR TUDOMÁNYOS AKADÉMIA KÉMIAI TUDOMÁNYOK OSZTÁLYÁNAK IDEGEN NYELVŰ KÖZLEMÉNYEI

SZERKESZTI

LENGYEL BÉLA

TECHNIKAI SZERKESZTŐK

DEÁK GYULA és HARASZTHY-PAPP MELINDA

Az Acta Chimica német, angol, francia és orosz nyelven közöl értekezéseket a kémiai tudományok köréből.

Az Acta Chimica változó terjedelmű füzetekben jelenik meg, egy-egy kötet négy füzetből áll. Évente átlag négy kötet jelenik meg.

A közlésre szánt kéziratok a szerkesztőség címére (Budapest 112/91 Műegyetem) küldendők.

Ugyanerre a címre küldendő minden szerkesztőségi levelezés. A szerkesztőség kéziratokat nem ad vissza.

Megrendelhető a belföld számára az „Akadémiai Kiadó"-nál (1363 Budapest Pf 24. Bankszámla 215-11488), a külföld számára pedig a „Kultúra" Könyv- és Hírlap Külkereskedelmi Vállalatnál (1389 Budapest 62, P.O.B. 149 Bankszámla: 218-10-990) vagy annak külföldi képviseleteinél és bizományosainál.

Die Acta Chimica veröffentlichen Abhandlungen aus dem Bereiche der chemischen Wissenschaften in deutscher, englischer, französischer und russischer Sprache.

Die Acta Chimica erscheinen in Heften wechselnden Umfanges. Vier Hefte bilden einen Band. Jährlich erscheinen 4 Bände.

Die zur Veröffentlichung bestimmten Manuskripte sind an folgende Adresse zu senden:

Acta Chimica
Budapest 112/91 Műegyetem

An die gleiche Anschrift ist auch jede für die Redaktion bestimmte Korrespondenz zu richten. Abonnementspreis pro Band: $ 24,00.

Bestellbar bei dem Buch- und Zeitungs-Außenhandels-Unternehmen »*Kultúra*« (1389 Budapest 62, P.O.B. 149 Bankkonto Nr. 212-10-990) oder bei seinen Auslandsvertretungen und Kommissionären.

ACTA CHIMICA

ACADEMIAE SCIENTIARUM HUNGARICAE

ADIUVANTIBUS

V. BRUCKNER, GY. DEÁK, K. POLINSZKY,
E. PUNGOR, G. SCHAY, Z. G. SZABÓ

REDIGIT

B. LENGYEL

TOMUS 76

AKADÉMIAI KIADÓ, BUDAPEST

1973

ACTA CHIM. (BUDAPEST)

ACTA CHIMICA

TOMUS 76

Fasciculus 1: 1973
Fasciculus 2: 1973
Fasciculus 3: 1973
Fasciculus 4: 1973

INDEX

Acta Chimica Academiae Scientiarum Hungaricae, Tomus 76 (1), pp. 1—11 (1973)

UNTERSUCHUNG DER ZUSAMMENSETZUNG VON EINHEIMISCHEN UND AUSLÄNDISCHEN ÄTHERISCHEN ÖLEN, I

KOMBINIERTE METHODE ZUR ANALYSE VON ÄTHERISCHEN ÖLEN MITTELS WIRKSAMER TRENNUNG DER GEMISCHE UND INSTRUMENTELLER IDENTIFIZIERUNG DER KOMPONENTEN

K. BÉLAFI-RÉTHY*, S. IGLEWSKI*, E. KERÉNYI* und R. KOLTA**

*(*Ungarisches Erdöl- und Erdgas-Forschungsinstitut, Veszprém und **Betrieb für Kosmetik und Haushaltschemie, Budapest)*

Eingegangen am 14. Februar 1972

Zwecks Aufklärung der Zusammensetzung von ätherischen Ölen wurde eine kombinierte Analysenmethode entwickelt, die auf wirksamer Trennung und danach folgender instrumenteller Strukturuntersuchung der Komponenten beruht. Die quantitative Analyse der Öle wurde mittels Kapillar-Gaschromatographie durchgeführt. Zur qualitativen Analyse ließen sich die Komponenten voneinander trennen, d. h., durch Kombinierung von Rektifikation, Elutions-Flüssigkeitschromatographie, präparativer Gaschromatographie und chemischer Trennung aus den ätherischen Ölen in reinem Zustand herstellen. Die Identifizierung der Komponenten wurde durch Anwendung von IR- und UV-Spektrometrie, Massenspektrometrie, Kernresonanz-Spektrometrie und chemischen Methoden erreicht. Die kombinierte Analysenmethode wird am Beispiel der Untersuchung eines importierten »dementholisierten« Minzöls aus Mentha arvensis vorgeführt.

Die Aufklärung der Zusammensetzung von ätherischen Ölen ist für die Lebensmittelindustrie und für die kosmetische, pharmazeutische und organisch-chemische Industrie von großer Bedeutung. Die Anwendung bzw. die Anwendbarkeit der ätherischen Öle beruht wesentlich auf der Gegenwart einer oder mehrerer Hauptkomponenten, während die Gegenwart von Nebenkomponenten die Brauchbarkeit bedeutend beeinflussen bzw. modifizieren kann [1].

Bis zur Mitte der fünfziger Jahre stützte sich die Untersuchung der Zusammensetzung hauptsächlich auf *chemische Methoden* und beschränkte sich auf die Identifizierung und Bestimmung der wichtigsten oder am meisten charakteristischen Komponenten [2]. Eine bedeutende Entwicklung erlebte die Bestimmung der Zusammensetzung durch die Anwendung der *Gaschromatographie* und *Dünnschichtchromatographie*; diese vermittelten eine viel eingehendere Kenntnis der Zusammensetzung zahlreicher ätherischer Öle [3]. Bei den chromatographischen Untersuchungen erfolgt die qualitative Analyse der Komponenten meistens durch die Untersuchung der Retentionsverhalten mit Hilfe von Modellsubstanzen; auf diese Weise ist jedoch die Identifizierung — gerade wenn es sich um unbekannte Komponenten handelt — oft undurchführbar oder irreführend. Demzufolge sind die in der Fachliteratur veröffentlichten und nur auf chromatographischer Analyse beruhenden Zusammen-

setzungsdaten ziemlich lückenhaft und nicht immer verläßlich (z. B. [4, 51]). Über die spektrometrische Untersuchung der getrennten Komponenten wurde bisher in nur sehr wenigen Arbeiten berichtet (z. B. [6, 7]), so daß die Zusammensetzung bei der Mehrzahl der ätherischen Öle auch heute noch nur in groben Zügen bekannt ist.

Kombinierte Methode zur Analyse von ätherischen Ölen

Einer der Ausgangspunkte unserer Methode war die Erfahrung, daß eine *eindeutige Identifizierung* der Komponenten nur mittels spektrometrischer Methoden möglich ist, weiterhin daß die Vorbedingung der spektrometrischen Identifizierung die Trennung der einzelnen Komponenten in ausreichender Reinheit ist. Demgemäß beruht die qualitative Analyse nach unserer Methode auf der Herstellung und der instrumentellen Strukturbestimmung der reinen Komponenten.

Der zweite Ausgangspunkt war die Erfahrung, daß die Komponenten der ätherischen Öle unter entsprechenden Bedingungen mittels Kapillar-Gaschromatographie analytisch getrennt und mit befriedigender Genauigkeit *quantitativ bestimmt* werden können. Die quantitative Analyse wird daher bei unseren Untersuchungen mit Kapillar-Gaschromatographie durchgeführt.

Das Schema der entwickelten Methode zur Analyse der ätherischen Öle ist in Abb. 1 dargestellt. Demgemäß wird die Probe des zu untersuchenden ätherischen Öles zwecks qualitativer Analyse zuerst durch Flüssigkeitschromatographie in Kohlenwasserstoffe und Kohlenwasserstoffderivate getrennt.

Aus dem hauptsächlich aus *Terpenen* bestehenden Kohlenwasserstoffgemisch werden dann mittels wirksamer Rektifikation Monoterpene, Sesquiterpene, gegebenenfalls Kohlenwasserstoffe höherer Kohlenstoffatomzahl gewonnen. Aus den engen Kohlenwasserstoff-Fraktionen werden endlich mittels grober und anschließend feiner präparativer Gaschromatographie reine oder fast reine Kohlenwassertoffe erhalten. Bei einfacher Kohlenwasserstoff-Zusammensetzung fällt die Rektifikation aus und das Kohlenwasserstoffgemisch wird unmittelbar der präparativen Gaschromatographie unterworfen. Sämtliche Trennungsoperationen werden durch Kapillar-Gaschromatographie kontrolliert.

Das hauptsächlich sauerstoffhaltige *Terpenderivate enthaltende Gemisch* wird ebenfalls mittels Rektifikation in Monoterpenderivate, Sesquiterpenderivate, Diterpenderivate, gegebenenfalls in sauerstoffhaltige Derivate anderer Kohlenstoffatomzahl getrennt. Bei den Terpenderivaten kann man auch so vorgehen, daß Alkohole, Aldehyde-Ketone, Karbonsäuren und Ester durch verschiedene chemische Methoden aus dem Gemisch gewonnen werden. Die reinen Verbindungen werden aus diesen Fraktionen engen Siedepunktbereiches durch präparative Gaschromatographie hergestellt. Die Rektifika-

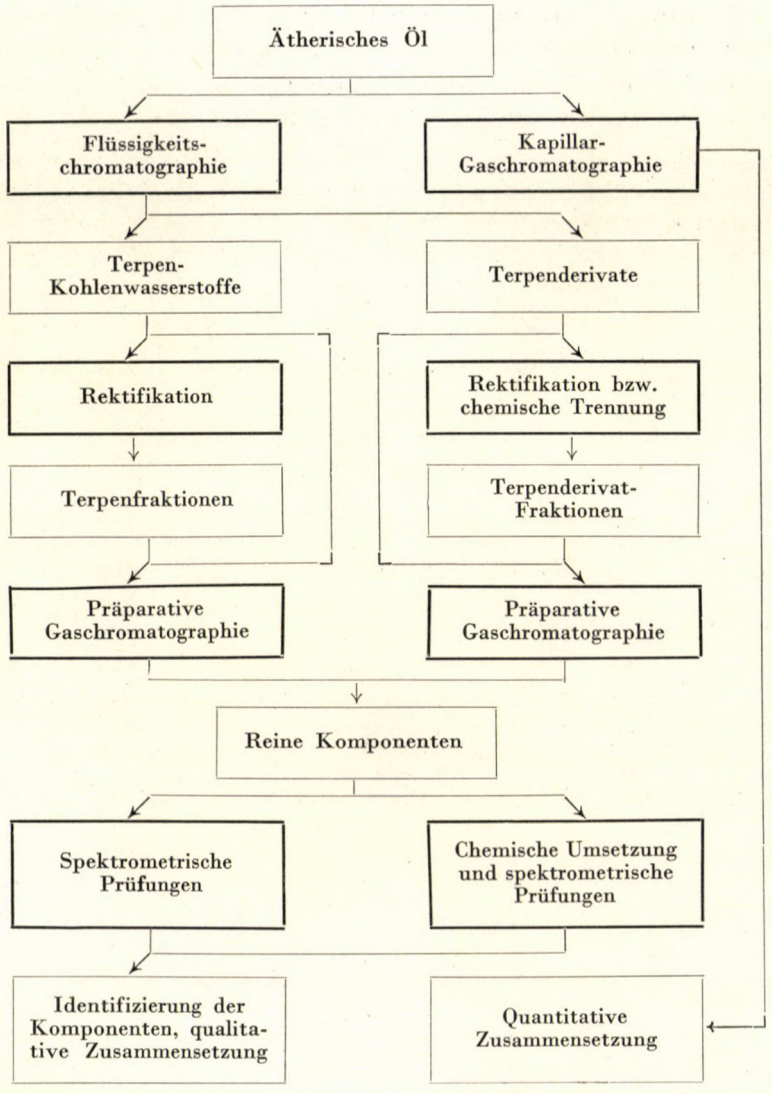

Abb. 1. Schema der zur Analyse von ätherischen Ölen ausgearbeiteten kombinierten Methode

tion oder die chemische Trennung wird nur bei Gemischen verwickelter Zusammensetzung angewendet, häufig kann das Gemisch unmittelbar der präparativen Geschromatographie unterworfen werden. Auch hier wird die Wirksamkeit der Trennung durch Kapillar-Gaschromatographie kontrolliert.

Die *reinen Komponenten* wurden durch Studieren ihrer verschiedenen Spektren bzw. durch Untersuchung der Spektren der verwandten Verbindungen identifiziert, in die sie eindeutig umgesetzt wurden. Dazu ließen sich vor

allem IR- und UV-Spektrometrie, Massenspektrometrie und Kernresonanz-Spektrometrie verwenden. Dabei wurden zur Bestätigung der Struktur in der Literatur veröffentlichte Spektren in Betracht gezogen und in einzelnen Fällen Synthesen von Modellverbindungen, eventuell chemische Methoden herangezogen.

Die *quantitative Analyse* der zu untersuchenden Probe bestand aus der quantitativen Auswertung der Kapillar-Gaschromatogramme des ätherischen Öles und ihrer getrennten Grundfraktionen.

Trennung der Komponenten

Die Kohlenwasserstoffe und Kohlenwasserstoffderivate wurden mit Hilfe von Elutions-Flüssigkeitschromatographie an Silikagel getrennt. Die chromatographische Säule war eine 1400 mm lange Glasröhre mit 35 mm innerem Durchmesser und war mit einem ausgeweiteten Flüssigkeitsbehälter und mit einer verjüngten Ausflußöffnung versehen. Die Säule wurde zur Trennung mit aktiviertem Silikagel der Firma Davison (Korngröße 100—200 mesh) gefüllt. Die Menge der zu trennenden ätherischen Ölprobe pro Zyklus war je nach der Zusammensetzung 150—250 g. Die Kohlenwasserstoffe wurden mit *n*-Hexan, die Kohlenwasserstoffderivate mit Methanol eluiert. In einigen Fällen wurde, um die vollkommene Trennung der beiden Verbindungsgruppen zu fördern, Elution mit Benzol zwischengeschaltet. Das Elutionsmittel ließ sich aus den erhaltenen Fraktionen durch gelindes Erwärmen unter Vakuum entfernen.

In bestimmten Fällen wurden die flüssigkeitschromatographischen Grundfraktionen durch Rektifikation *mittels Halbmikro-Drehbandkolonne*, Monoterpene bzw. Monoterpenderivate, Sesquiterpene bzw. Sesquiterpenderivate, gegebenenfalls in Fraktionen höherer Kohlenstoffatomzahl getrennt. Das zur Rektifikation angewandte Gerät bestand aus einer 500 mm langen Kolonne mit 6 mm innerem Durchmesser, versehen mit einem zugeschmolzenen Vakuummantel und einem totraumfreien Kopfteil. In der Kolonne befindet sich ein säurefestes Stahlband, das durch magnetischen Antrieb mit einer Umdrehungszahl von 1000—3000 U/min rotiert. Unten ist die Kolonne mit einem Siedekolben, oben mit einem Kühler und einer Vorlage verbunden. Die elektrisch geheizte und mit magnetischer Rücklaufregelung versehene Kolonne kann bis etwa 250 °C Kopftemperatur und 1 Torr Druck verwendet werden. Ihre Trennfähigkeit entspricht bei optimaler Belastung einer Trennstufenzahl von 35; ihr Betriebsinhalt und ihr Druckverlust sind gering [8, 9]. Die gewöhnlich getrennte Menge betrug 5—60 g. Der Destillationsdruck wurde jeweils so gewählt, daß die Temperatur im Kolben 150—160 °C nicht überstieg.

Bei Kohlenwasserstoffderivat-Gemischen bzw. -Fraktionen komplizierter Zusammensetzung wurden auch *chemische Methoden* zur Trennung der Komponenten angewendet. Eine gut bewährte Kombination bestand aus der Gewinnung von Borsäureestern der ursprünglichen Alkohole, aus der Verarbeitung der Ester mittels Hydrolyse und ähnlicher Umsetzung der entstandenen Alkohole und aus der Trennung der Aldehyde und Ketone durch deren Hydrierung und danach folgende Borsäureesterbildung. Die aus den Borsäureestergemischen schrittweise zurückgewonnenen Alkoholgemische bestehen aus Alkoholen, deren Struktur den ursprünglichen Sauerstoffderivaten entspricht, wodurch die Untersuchung der aus vielerlei Verbindungen zusammengesetzten Gemische zur Identifizierung der Terpenalkohole vereinfacht wird [10]. Auch andere, selektive und quantitative chemische Trennungen wurden für bestimmte Derivatgruppen, insbesondere für Oxoverbindungen, mit Erfolg verwendet [11, 12].

Die Anreicherung oder Herstellung der einzelnen Komponenten bei Gemischen, die aus wenigen Bestandteilen ähnlicher Struktur bestehen, erfolgte meistens in zwei Schritten mittels *präparativer Gaschromatographie*. Zur *Grobpräparierung* wurde teils das Gerät Fractovap P von der Firma Carlo Erba, teils das Gerät Chrom III von der Firma Kovo verwendet. Die Kolonne war 4 m lang, mit einem inneren Durchmesser von 10 mm. Die Füllung bestand meistens aus dem Träger MH-1 [13] mit 10% Carbowax-20 M benetzt. Die Einwaage betrug hier etwa 1—5 ml. Als Trägergas wurde Wasserstoff verwendet. Die Trennungstemperatur wurde je nach den Siedepunkten und Wärmeempfindlichkeiten der Komponenten gewählt.

Die *Feinpräparierung* der angereicherten Komponenten erfolgte anfänglich mit einem für analytische Zwecke gebauten und in unserem Institut für präparative Zwecke modifizierten Gerät Typ GCHF 18 von der Firma W. Giede, später mit dem Grät Typ 105 von der Firma Pye. Bei dem mit Vorlagesystem versehenen Giede-Gerät wurde eine 4 m lange Säule mit 4 mm innerem Durchmesser verwendet. Die Verteilungsphase war hier meistens ebenfalls Carbowax-20 M. Die Geschwindigkeit des Wasserstoff-Trägergases betrug 2 Liter/h. Im Pye-Gerät bastand die Füllung der Säule (Abmessungen 5 m $\times$ 6 mm) aus mit Carbowax-20 M benetztem Celit. Die Geschwindigkeit des Argon-Trägergases betrug hier 1,5 Liter/h. Bei der Feinpräparierung wurden Einwaagen von 10—200 μl verwendet; die Versuchstemperatur wurde auch in diesen Fällen der Natur der Komponenten entsprechend gewählt.

Die bei den Trennungen erhaltenen reinen Verbindungen ermöglichten — außer der Sicherung der Vorbedingungen für die Identifizierung der Komponenten — die Untersuchung zahlreicher, bisher wenig studierter oder unbekannter Komponenten der ätherischen Öle.

Identifizierung der Komponenten

Die *IR Spektren* der abgetrennten reinen Komponenten wurden mit den Geräten UR-10 bzw. UR-20 von der Firma Carl Zeiss, Jena aufgenommen. Dabei wurden Prismen und Küvetten aus KBr, NaCl und LiF und Schichtdicken von meistens 0,0025 oder 0,01 cm verwendet. Das Wellenzahlgebiet lag zwischen 4000 und 400 cm^{-1}.

Zur Aufnahme der *UV-Spektren* wurde ein registrierendes Spektrophotometer mit doppeltem Strahlengang von der Firma Perkin-Elmer (Mod. 137) benützt. Die Schichtdicke betrug 0,1—4,0 cm; die Proben wurden mit aromatenfreiem Benzin oder mit Alkohol verdünnt.

Die *Massenspektren* der Komponenten wurden mit dem Massenspektrometer MI 1305 (System Nier) von der Firma ZEME aufgenommen. Der Meßbereich des Gerätes beträgt 1—400 Masseneinheiten, das Auflösungsvermögen 300. Das für chemisch-analytische Zwecke geeignete Einwaagesystem des Gerätes wurde in unserem Institut hergestellt, es war aber für Proben hohen Siedepunktes ungeeignet. Die Beschleunigungsspannung betrug bei den Messungen 4 kV und die Ionisierspannung 50 V. Die Aufnahmegeschwindigkeit war einheitlich etwa 2 Masseneinheiten pro Minute.

Zur Aufnahme der *Kernresonanzspektren* wurde früher das Gerät ZKR-60 von der Firma Zeiss verwendet. Die Aufnahmen ließen sich in 10%igen Lösungen mit Tetrachlorkohlenstoff durchführen. Der Meßbereich lag (bezogen auf Tetramethylsilan) zwischen Verschiebungswerten (δ) von 0 und 8 ppm. Später wurden die Spektren mit dem Gerät Varian T-60 aufgenommen. Dieses arbeitet mit einer Frequenz von 60 MHz und einer Induktionsstärke von 14 KG; sein Auflösungsvermögen beträgt 0,4 Hz.

Bei der Identifizierung der reinen Komponenten von ätherischen Ölen ergab sich häufig die Notwendigkeit, die Spektren der *chemisch eindeutig umgesetzten Derivate* der Komponenten zu untersuchen. In dieser Beziehung wurden vor allem ungesättigte Kohlenwasserstoffe durch Hydrieren in gesättigte umgewandelt, gegebenenfalls wurde der Sauerstoffgehalt bestimmter Sauerstoffderivate durch Hydrieren entfernt. Die Spektren der durch Reduktion erhaltenen Kohlenwasserstoffe trugen zur genauen Klärung der Kohlenstoff-Skelettstruktur bei. Die *Mikrohydrierung* wurde mit Substanzmengen von einigen Zehntel Gramm bei 200—250 °C in einem Mikroreaktor durchgeführt, der mit Palladiumkatalysator auf Aluminiumoxyd-Träger gefüllt war [14]. Bei sauerstoffhaltigen Derivaten wurden außer der Hydrierung auch andere chemische Umsetzungen angewandt [10]. Bei der Identifizierung der reinen Komponenten ergab sich auch die Gelegenheit zum Registrieren von Spektren wenig bekannter oder bisher unbekannter Komponenten ätherischer Öle.

Quantitative Analyse

Zur quantitativen Analyse der zu untersuchenden ätherischen Öle und zur Kontrolle der mittels Flüssigkeitschromatographie oder anderer Methoden erhaltenen Grundfraktionen wurde die *Kapillar-Gaschromatographie* verwendet. Dabei wurden die Geräte Carlo Erba P-AID/F, KOVO Chrom III und Pye 105 benützt. In den meisten Fällen wurde mit einem 50 m langen Kapillarrohr mit einem inneren Durchmesser von 0,25 mm gearbeitet; die Verteilungsphase war Carbowax 1000, die Analysentemperatur lag zwischen 100 und 150 °C, die Strömungsgeschwindigkeit des Argon-Trägergases um etwa 1,5 ml/Min. Die Auswertung der Geschromatogramme erfolgte teils durch Planimetrieren, teils unter Anwendung eines Integrators; dabei wurden, wenn nötig, auch die Empfindlichkeitsfaktoren der Komponenten in Betracht gezogen. Die aus den zur quantitativen Analyse und zur Kontrolle der Fraktionen aufgenommenen Gaschromatogrammen erhaltene laufende Numerierung der Komponenten war zugleich der Ausgangspunkt für die qualitative Analyse.

Analysenbeispiel eines »dementholisierten« Minzöles ausländischer Herkunft

Das Öl der Pflanze *Mentha arvensis* ist der wichtigste Rohstoff des in der Lebensmittelindustrie, in der kosmetischen und pharmazeutischen Industrie ausgedehnt verwendeten Menthols. Aus dem Öl wird das Menthol im allgemeinen durch Filtrieren, durch Kühlen und Filtrieren oder eventuell durch Umkristallisieren mit Lösungsmitteln gewonnen. Das dementholisierte Minzöl enthält noch beträchtliche Mengen an Menthol und läßt sich deshalb vor allem in kosmetischen Produkten als Riechstoff verwenden. Um die kombinierte Analysenmethode zu kontrollieren, wurde von uns zuerst die Zusammensetzung eines aus Brasilien importierten »dementholisierten« Minzöls untersucht.

Bei der Untersuchung dieser Probe wurde die entwickelte kombinierte Methode — wegen der verhältnismäßig großen Zahl der zur Verfügung stehenden Literaturangaben [1, 2] und der nicht allzu komplizierten Zusammensetzung — in einer etwas vereinfachten Form angewendet und einige Trennungs- und Identifizierungsschritte wurden weggelassen. Die durchgeführten Operationen und Prüfungen sind in *Tab. I* zusammengefaßt. Die Identifizierung der angereicherten oder reinen Komponenten wird im folgenden an zwei Beispielen vorgeführt.

Im Kapillar-Gaschromatogramm des Minzöls zeigt das mit Nr. 3 bezeichnete Peak die Gegenwart einer geringen Menge (0,2 Gew.%) einer Komponente an, die sich gemäß der flüssigkeitschromatographischen Trennung und gaschromatographischen Aufnahme als Terpenkohlenwasserstoff erwies. Aufgrund

Tabelle I

Operationen und Prüfungen bei der Bestimmung der Zusammensetzung eines »dementholisierten« Minzöls

Operation bzw. Prüfung.	Ergebnis
Messen von physikalischen Konstanten des ätherischen Öles	Grunddaten, orientierende qualitative Informationen
Analitische Gaschromatographie des ätherischen Öles	Zahl der Komponenten, quantitative Zusammensetzung
Flüssigkeitschromatographische Trennung des ätherischen Öles	Terpen-Kohlenwasserstoffe und Terpenderivate
Analytische Gaschromatographie der Terpenfraktion und der Terpenderivat-Fraktion	Ergänzende Angaben über die Anzahl der Komponenten und über die quantitative Zusammensetzung
Präparative und mikropräparative gaschromatographische Trennung der Terpenfraktion und der Terpenderivat-Fraktion	Angereicherte oder reine Komponenten
Hydrierung einzelner angereicherter oder reiner Komponenten	Reine oder angereicherte gesättigte Kohlenwasserstoffe
Aufnahme des Massenspektrums, des IR-Spektrums und des Kernresonanz-Spektrums der angereicherten oder reinen Komponenten bzw. der hydrierten Produkte	Spektren reiner Substanzen, Informationen über die Natur der Komponenten
Verarbeitung der Informationen	Qualitative Zusammensetzung, Identifizierung der Komponenten

des Massenspektrums ergab sich das Molekulargewicht dieser Komponente zu 136, ihre Bruttoformel zu $C_{10}H_{16}$. Die Hydrierung der Komponente ergab — wie gaschromatographisch und spektrometrisch festgestellt werden konnte — 2,6-Dimethyloktan; die gesuchte Komponente war also ein 2,6-Dimethyloktatrien-Isomer. Es sind insgesamt 42 Isomere möglich, die keine kumulierten Doppelbindungen enthalten; von diesen sind nur 9 Isomere bekannt, und im Falle von 6 Isomeren (c-α-Ocymen, tr-α-Ocymen, c-β-Ocymen, tr-β-Ocymen, α-Myrcen und β-Myrcen) kennt man auch die Spektren [15]. Die bekannten Spektren der Isomere weisen neben ähnlichen Spektrumteilen auch mit ihrer chemischen Struktur übereinstimmende charakteristische Abweichungen auf. Bei uns wurden nur IR-spektrometrische und massenspektrometrische Aufnahmen der Komponente Nr. 3 gemacht; diese standen in guter Übereinstimmung mit den bekannten Spektren und mit der Struktur des β-Myrcens (2-Methyl-6-Methylen-2,7-Oktadien). Die Zuordnung der Spektrumteile ermöglichte den Ausschluß der Anwesenheit anderer Isomere. Demzufolge konnte die Komponente Nr. 3 als β-Myrcen identifiziert werden.

Die Möglichkeit der Anwesenheit von β-Myrcen im Minzöl wird auch in der Fachliteratur erwähnt [1].

Im Kapillar-Geschromatogramm des »dementholisierten« Minzöls zeigt das quantitativ auswertbare Peak Nr 11 die Gegenwart einer Komponente in Mengen von 0,1 Gew.% an. Die Ergebnisse der flüssigkeitschromatographischen Trennung wiesen auf Terpenalkohol hin, jedoch gelang es wegen der geringen Menge und des mit Neomenthol identischen Retentionsverhaltens nicht, die Komponente in reinem Zustand zu isolieren. Die Einzelheiten des IR-Spektrums der angereicherten Probe und sonstige Beobachtungen sprachen dafür, daß es sich um einen ungesättigten Terpenalkohol handelt, dessen Skelettstruktur der des Menthols ähnlich ist. Da die Fachliteratur nur drei derartige Alkohole kennt (Pulegol, Isopulegol und Piperitol) [1, 2], beweist die bei der angereicherten und nur gesättigte Verunreinigung (Neomenthol) enthaltenden Probe gefundene IR-Bande bei 890 cm^{-1}, die einer endständigen Doppelbindung zuzuordnen ist, daß es sich um Isopulegol (1-Methyl-4-Isopropenyl-Cyclohexanol-3) handelt. Die Konformation des vorliegenden Isopulegols (*d*- und *l*-Isopulegol, *d*- und *l*-Neoisopulegol oder *d*- und *l*-Neoiso-Isopulegol) wurde nicht bestimmt.

Bis jetzt wurde die Anwesenheit von Isopulegol im Öl der Mentha arvensis noch nicht festgestellt [1].

Die durch Flüssigkeitschromatographie und präparative Gaschromatographie erhaltenen oder angereicherten Komponenten wurden, wie aus den angeführten Beispielen hervorgeht, aufgrund der verschiedenen aufgenommenen Spektren und mit Hilfe der Spektrumaufnahmen von Modellsubstanzen, der zu Verfügung stehenden bekannten Spektren, der Assignation der Spektrumbanden und gegebenenfalls der zusätzlichen Informationen (z. B. mittels chemischer Umsetzungen) identifiziert. In *Tab. II* sind die Methoden und Ergebnisse der Identifizierung, die relativen Retentionszeiten (Limonen = 100) und die Mengen (in Gew.%) der in auswertbaren Konzentrationen (0,1 Gew.% oder mehr) vorliegenden Komponenten angeführt. Die gaschromatographischen Angaben stammen in diesem Falle aus Aufnahmen, die mit einem Gerät P-AID/F von der Firma Carlo Erba und mit einer mit Carbowax-1000 benetzten Kapillarsäule von 50 m Länge bereitet wurden. Die Temperatur betrug 125° und die Geschwindigkeit des Argon-Trägergases 1,6 ml/Min. Außer den in der Tabelle angeführten Komponenten konnte die Gegenwart von geringen (unterhalb 0,1 Gew.% liegenden) Mengen an 3,7-Dimethyl-1,6-Oktadienol-3, Neoisomenthol, ε-Cadinen und weiteren 10 unbekannten Komponenten (hauptsächlich Sesquiterpenen) nachgewiesen werden.

Demgemäß enthält das untersuchte dementholisierte Minzöl insgesamt 34 nachweisbare Komponenten, davon liegen 21 Komponenten in auswertbaren Mengen vor; diese bilden den 99,3prozentigen Anteil des Minzöls. Von diesen letzteren konnten 17 Komponenten, d.h. 98,5 Gew.% des Minzöls identifiziert werden. Die nicht identifizierten wesentlichen Komponenten waren alle Sesquiterpene in der Größenordnung von je 0,1%.

Tabelle II

Identifizierung und Mengenanteil der signifikanten Komponenten eines »dementholisierten« Minzöls

Nr.	Methode der Identifizierung				Komponente	Relative Retention	Gew. %
	Modell-verbindung	Bekannte Spektren	Zuordnung der Spektrumbanden	Zusätzliche Informationen			
1			+	+	α-Pinen	81	0,7
2			+	+	β-Pinen	91	0,6
3		+	+	+	β-Myrcen	93	0,2
4		+	+	+	Limonen	100	5,4
5	+		+		1,8-Cineol	104	0,2
6		+	+	+	*p*-Cymol	104	0,2
7			+	+	2,6-Dimethylok-tanol-2	140	0,4
8				+	Sesquiterpen	191	0,1
9			+	+	Menthon	191	31,6
10				+	Sesquiterpen	208	0,3
11		+	+		Isomenthon	208	8,7
12	+	+	+		Menthylacetat	253	5,5
13		+	+	+	Neomenthol	273	4,8
14			+	+	Isopulegol	290	0,1
15		+			Cariophyllen	307	1,7
16		+	+	+	Menthol	330	32,7
17		+	+	+	Isomenthol	356	1,5
18			+	+	Sesquiterpen	403	0,2
19		+	+		Piperiton	450	4,1
20				+	Sesquiterpen	518	0,2
21		+	+		Chalamenen	741	0,1
							Σ 99,3

Der zur Trennung der Komponenten verwendete präparative Gaschromatograph Carlo Erba Fractovap-P wurde vom Organisch-chemischen Lehrstuhl der Universität für chemische Industrie, Veszprém zu Verfügung gestellt; die Kernresonanzspektren wurden mit dem Gerät ZKR-60 am Organisch-chemischen Lehrstuhl der L. Eötvös-Universität, Budapest aufgenommen. Es sei an dieser Stelle beiden Lehrstühlen unser Dank ausgesprochen.

LITERATUR

1. Gildemeister, E., Hoffmann, F.: Die ätherischen Öle. Band I—VII, Akademie-Verlag, Berlin, 1956—1961
2. Guenther, R.: The essential oils. Volume I—III, Nostrand Co., New York, 1949
3. Guenther, E., Kulka, K., Rogers, J. A.: Anal. Chem., **31,** 679 (1959); Anal. Chem., **33,** No. 5, 37R (1961); Anal. Chem. **35,** No. 5, 39R (1963); Guenther, E., Rogers, J. A., Gilbertson, G., Koenig, R. T.: Anal. Chem., **37,** No. 5, 46R (1965); Guenther, E.,

GILBERTSON, G., KOENIG, R. T., BROTHERS, F.: Anal. Chem., **39,** No. 5, 47R. (1967); GUENTHER, E., GILBERTSON, G. KOENIG, R. T.: Anal. Chem., **41,** No. 5, 40R (1969); Anal. Chem., **43,** No. 5, 45R (1971)
4. SLATER, A. C.: Chem. Ind. (London), **1961,** 833
5. THIHÁK, E., VÁGUJFALVI, A.: Herba Hung., **1,** 95. (1962)
6. TSUBAKI, N., NISHIMURA, K., HIROSE, Y.: Bull. Chem. Soc. Japan, **39,** 312. (1966)
7. VLAHOV, R., HOLUB, M., OGNYANOV, I., HEROUT, V.: Coll. Czech., Chem. Comm. **32,** 808. (1967)
8. Ungarisches Patent No. 154692 (1966)
9. KERÉNYI, E., BÖRZSÖNYI, M., HANÁK, F.: Magy. Kém. Foly. **71,** 386 (1965)
10. BÉLAFI-RÉTHY, K., KÁNTOR, M., RÉPÁSY, O., KERÉNYI, E.: Erdöl u. Kohle, **24,** 19 (1971)
11. MÁZOR, L.: Szerveskémiai Analízis I—III. Műszaki Könyvkiadó, Budapest, 1961—1963
12. ETTRE, L. S., MCFADDEN, W. H.: Ancillary Techniques of Gas Chromatography. Wiley Interscience, New York—Sidney—London—Toronto, 1969
13. Ungarisches Patent No. 152671 (1965)
14. SINGLIAR, M., SESTRIENKOVA, M.: Sborník Prác VUP, Nováky, **1,** 39 (1965)
15. AHLONG, G., SEIBL, J., KOVÁTS, E.: Ann. Chem., **675,** 83 (1967)

Katalin BÉLAFI-RÉTHY
Stanislaw IGLEWSKI
Ervin KERÉNYI
Veszprém, Wartha V. u. 1—3. Hungary.

Rezső KOLTA
1113 Budapest, Bocskai út 90.

Acta Chimica Academiae Scientiarum Hungaricae, Tomus 76 (1), pp. 13—20 (1973)

STUDY OF PROBLEMS ARISING IN THE MOLECULAR WEIGHT DETERMINATION BY THE APPROXIMATE SEDIMENTATION EQUILIBRIUM METHODS

M. BLAZSÓ and A. CZUPPON

(Center for Studies on Chemical Structures, Hungarian Academy of Sciences, Budapest)

Received February 28, 1972

The present work is aimed at eliminating uncertainties in evaluating and handling ultracentrifugal data of approximate sedimentation equilibria for the determination of the molecular weight of polydisperse macromolecular materials in non-ideal solutions. The Lamme differential equation has been solved numerically for the Archibald conditions, taking into account the concentration dependence of diffusion and sedimentation coefficients as well. From the solution the following experimental conditions have been obtained for the applicability of linear extrapolation of the concentration gradient to the meniscus on the Schlieren pattern

$$\frac{2D}{S\omega^2 r^2} > 0.05 \quad \text{and} \quad Dt > 0.75 \times 10^{-2} \text{cm}^2 .$$

In the case of non-ideal solutions and/or polydisperse solutes the apparent molecular weight changes with time. In this case linear extrapolation with respect to $t^{1/2}$ has been shown to give better results than that with respect to t. The use of the Trautman diagram for linear extrapolation of the concentration gradient to the initial concentration and for determining M_z was extended to non-ideal solutions.

Introduction

The ultracentrifugal molecular weight determinations of macromolecules are based on the Svedberg equation expressing the proportionality of the molecular weight and the ratio of the sedimentation (S) and diffusion (D) coefficients. In sedimentation equilibria this ratio is determined by the Lamme differential equation as follows:

$$\frac{\partial c}{\partial t} = \frac{1}{r} \cdot \frac{\partial}{\partial r}\left[rD \frac{\partial c}{\partial r} - S\omega^2 r^2 c \right] = 0 \tag{1}$$

where c is the solution concentration, r is the distance from the center of rotation, t is the time and ω is the angular velocity.

For the meniscus and bottom of the ultracentrifugal cell ARCHIBALD [1] extended the validity of equation (1) for non-equilibrium conditions. In this way it becomes possible to evaluate the molecular weight by the following expression:

$$\frac{S}{D} = \frac{1}{\omega^2} \cdot \frac{\left(\frac{\partial c}{\partial r}\right)_m}{r_m c_m} \tag{2}$$

where subscript m denotes the meniscus.

ARCHIBALD's simple and rapid method is strictly valid only in the case of monodisperse materials and ideal solutions, since otherwise expression (2) varies with time during the experiment. Several efforts have been made to extent the method [2–5]. For polydisperse ideal systems KEGELES [4] has demonstrated that the value at $t = 0$ equals the weight average of S/D. Values for $t = 0$ are obtained by extrapolation. Most of the authors extrapolate to zero time linearly, others by assuming proportionality to the square root of time. Both assumption are arbitrary. In the case of non-ideal systems, for the values at $t = 0$ the following expression is valid (KEGELES [4]):

$$\left(\frac{D}{S}\right)_{w,\mathrm{app}} = \left(\frac{D}{S}\right)_{w} + B^* c + (0)c^2 + \ldots \tag{3}$$

where B^* is proportional to the second virial coefficient [6].

TRAUTMAN, on the other hand, in the case of polydisperse ideal systems, regarded $(\delta c/\delta r)_m$ as a function of the meniscus concentration and proposed extrapolation to the initial concentration [7]. He has shown that the substitution of this extrapolated value and of the initial concentration into Eq. (2) leads to the weight average of S/D. Moreover, he has also shown that the slope of the $(\delta c/\delta r)_m$ *vs.* c_m curve in the point $c_m = c_0$ corresponds to the z average.

Numerical solution of the Lamme equation if S/D depends on the concentration

The ARCHIBALD and TRAUTMAN methods involve values of concentration and concentration gradient at the meniscus. Their evaluation is done by extrapolation which, in turn, requires certain information about the concentration distribution. The variation of the meniscus concentration and its gradient as a function of time becomes important when the ratio of these values also changes with time because of non-ideality and polydispersity. In this case an extrapolation to the initial state (zero time) is needed. Therefore, solution of the Lamme equation is necessary for a study of the conditions for correct extrapolations.

LA BAR [8] and YPHANTIS [5] solved the Lamme equation for the case of ideal solutions and drew some conclusions regarding the above mentioned extrapolations. The purpose of the present paper is to extend their studies for non-ideal solutions, numerically solving the Lamme equation for a monodisperse solute in the case when both S and D depend on the concentration.

For the concentration dependence the following functions were used:

$$S = \frac{S_0}{1 + kc} \tag{4}$$

$$D = D_0(1 + k_D c) \tag{5}$$

where k and k_D are constants.

First, the Lamme equation is re-written in terms of dimensionless parameters:

$$x = \left(\frac{r}{r_m}\right)^2; \quad \tau = 2w^2 S_0 t; \quad \Theta(x, \tau) = \frac{c(r, t)}{c_0};$$

$$\varepsilon = \frac{2D_0}{S_0 w^2 r_m^2}; \quad \alpha = kc_0; \quad \beta = k_D c_0.$$

This leads to the equation

$$\frac{\partial\Theta}{\partial\tau} = \frac{\partial}{\partial x}\left\{x\left[\varepsilon\frac{\partial\Theta}{\partial x}(1+\beta\Theta) - \frac{\Theta}{1+\alpha\Theta}\right]\right\} \tag{6}$$

to the initial condition:

$$\Theta = 1 \quad \left[1 < x < \left(\frac{r_b}{r_m}\right)^2; \quad \tau = 0\right]$$

and to the boundary condition:

$$\varepsilon\frac{\partial\Theta}{\partial x}(1+\beta\Theta) = \frac{\Theta}{1+\alpha\Theta} \quad \left[x = 1 \quad \text{or} \quad x\left(\frac{r_b}{r_m}\right)^2; \quad \tau > 0\right]$$

where r_b is the distance of the cell bottom from the center of rotation.

We computed Θ and $\delta\Theta/\delta x$ values in the range $x = 1$ to $x = 1.4$ (corresponding approximately to the common ultracentrifugal cell length), for fixed values of the other independent variable τ. This again was varied in the range from zero to a time when a finite meniscus concentration still existed, and the constant concentration range between bottom and meniscus did not disappear.

The values for the constants of the Lamme equation were chosen so that they reflected all the cases of practical importance. The following ranges have been considered:

$$\varepsilon\text{: } 0.01 - 0.20; \quad \alpha\text{: } 0 - 1.0; \quad \beta\text{: } -0.5 - +0.5.$$

The equation has been solved numerically by the grid method. The estimation of errors was carried out on the basis of the Runge principle.

Application of the calculated solutions

1. Evaluation of the concentration gradient at the meniscus

The simplest way of evaluating the refraction index gradient at the meniscus on the pattern of the ultracentrifugal cell taken by Schlieren optics would be the linear extrapolation from the non-distorted part of the gradient curve. LA BAR [8] — who examined the possible errors of this extrapolation for ideal solutions, solving the Lamme equation by the Faxén approximation — found that, within less than 5% error, the concentration gradient is a linear function of r, in a range of 0.75 mm in the neighbourhood of the meniscus when $\epsilon > 0.5$ and $Dt = 10^{-2}$ cm^2. Unfortunately, this condition corresponds to a very small concentration change at the meniscus ($\Delta\Theta < 0.05$).

In our calculations we assumed linearity only for about half of LA BAR's range ($1.005 \leqslant x \leqslant 1.015$) and found that the error of the extrapolated value does not exceed 5% if $\epsilon > 0.05$ and $\epsilon\tau > 6\times10^{-4}$ ($Dt > 0.75\times10^{-2}$ cm^2). This is a better approximation of the usual experimental conditions. Our calculations were not limited to the case of ideal solutions. Moreover, if conditions $\epsilon > 0.05$ and $\epsilon\tau > 6\times10^{-4}$ are fulfilled for the component characterized by the smallest value of ϵ, we obtain the same results for polydisperse solutes. For ideal solutions this is a simple conclusion if there is no interaction between the solutes of different size.

2. Time dependence of the apparent molecular weight

In Figs 1. and 2 the calculated relative apparent molecular weights are plotted against time and the square root of time, respectively, for solutions of

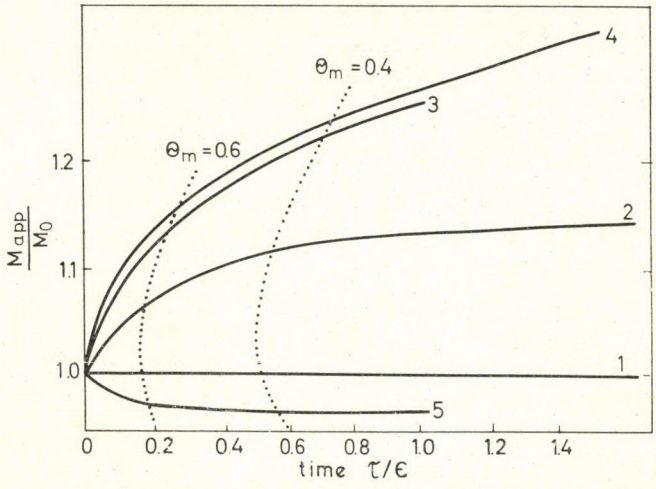

Fig. 1. Variation of apparent molecular weight as a function of time. The different curves refer to non-ideal solutions characterized by the following constants. 1. $\alpha=0$, $\beta = 0$; 2. $\alpha = 0.2$, $\beta = 0$; 3. $\alpha = 0.5$, $\beta = 0$; 4. $\alpha = 0.2$, $\beta = +0.2$; 5. $\alpha = 0.2$, $\beta = -0.2$

different deviations from ideality. The relative apparent molecular weight is the ratio to the value at zero time. In order to show the direct relation of the numerical values on the x axes to the real experimental time, we have shown the curves of two relative concentrations of the meniscus (Θ_m) by dotted lines. The comparison of Figs 1 and 2 is convincing: the linear extrapolation of the apparent molecular weight against the square root of time leads to a much smaller error than that against time.

The same statement is valid in the case of an ideal solution if the change of the apparent molecular weight is caused by polydispersity. Linear extrapolation with respect to $t^{1/2}$ seems to be good enough if Θ_m values below 0.6 are avoided. Fig. 3 shows the functions calculated for model mixtures of two components in equal weights, characterized in Table I. Since the dimensionless τ involves S_0 changing from component to component, the time scale

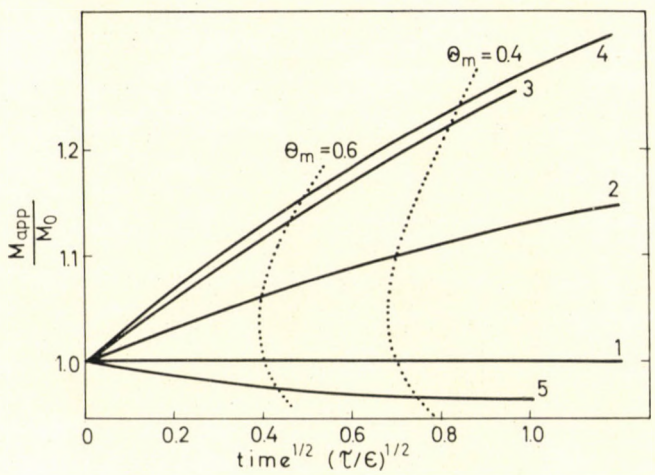

Fig. 2. Variation of apparent molecular weight as a function of the square root of time. Notations as in Fig. 1

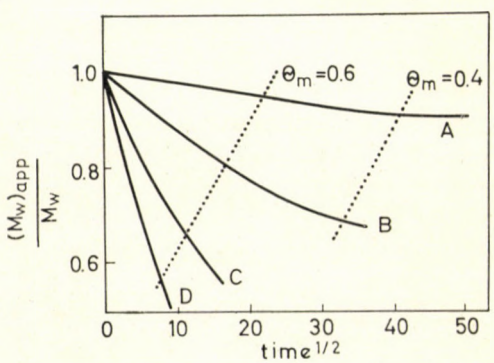

Fig. 3. Variation of apparent molecular weight as a function of the square root of time for ideal solutions of two-component model mixtures characterized in Table I

has to be returned to t. For this reason $\tau/t=2\omega^2 S_0$ values are also given in addition to $1/\epsilon$ for all components in the table.

3. Determination of the z-average molecular weight in non-ideal solutions

As already mentioned, Trautman has shown that the z-average molecular weight can be determined by taking the initial slope of the $(\partial c/\partial r)_m$ *vs.* c_m

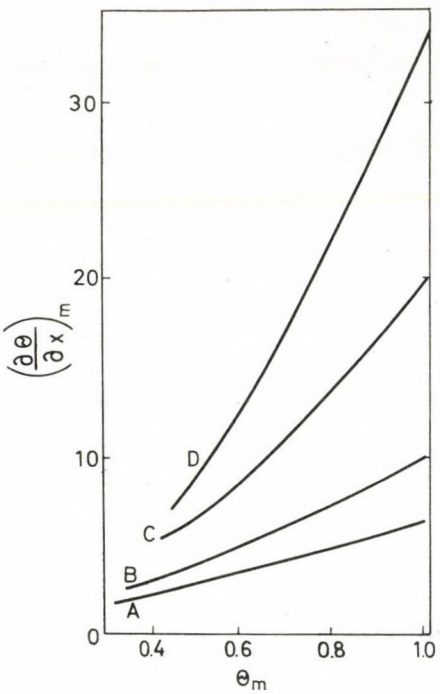

Fig. 4. Trautman diagram of four two-component model mixtures characterized in Table I in ideal solutions

function [7]. Figure 4 shows the Trautman diagram plotted for the model mixtures of Table I. The slope of the curve at $\Theta_m = 1$ is equal to the corresponding z averages. For non-ideal solutions, the meniscus concentration gradient as a function of the concentration is also nearly linear in a relatively wide range of meniscus concentrations according to the calculated data given in Fig. 5. Therefore, we can extrapolate also by the Trautman diagram in order to obtain the apparent weight average molecular weights in non-ideal solutions, and at the same time we can evaluate the initial slopes corresponding to the apparent z-average molecular weight as follows:

$$(M_z)_{\text{app}} = \frac{d[(M_w)_{\text{app}} \cdot c]}{dc} \,. \tag{7}$$

Table I

Characterization of two-component model mixtures used for the numerical calculations

Model	COMPONENTS				$(1/\varepsilon)_w$	$(1/\varepsilon)_z$	$\frac{(1/\varepsilon)_z}{(1/\varepsilon)_w}$
	1		2				
	$1/\varepsilon$	$2\,\omega^2 S_0 \times$ sec	$1/\varepsilon$	$2\,\omega^2 S_0 \times$ sec			
A	4	5×10^{-5}	8	7×10^{-5}	6	6.67	1.11
B	4	5×10^{-5}	16	1×10^{-4}	10	13.6	1.36
C	4	5×10^{-5}	36	1.5×10^{-4}	20	32.8	1.64
D	4	5×10^{-5}	64	2×10^{-4}	34	60.4	1.78

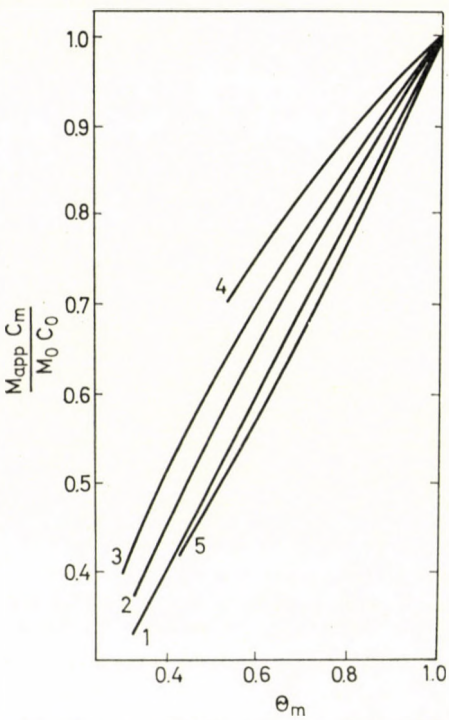

Fig. 5. Trautman diagram of various non-ideal solutions characterized by the following constants. 1. $\alpha = 0, \beta = 0$; 2. $\alpha = 0.2, \beta = 0$; 3. $\alpha = 0.2, \beta = +0.2$; 4. $\alpha = 1.0, \beta = 0$; 5. $\alpha = 0.2, \beta = -0.2$

Nevertheless, the apparent z-average values have to be extrapolated to infinite dilution as well. In order to demonstrate the concentration dependence of the z-average values, we start from Eq. (3) expressing the concentration dependence of the weight average molecular weight. The terms of second and higher powers of concentration are negligible in the expression when the solution is sufficiently dilute.

$$\left(\frac{1}{M_w}\right)_{\text{app}} = \frac{1}{M_w} + Bc \tag{8}$$

where B is the second virial coefficient. Inserting this into Eq. (7) we have:

$$\frac{d}{dc}\left(\frac{M_w \cdot c}{1+M_w Bc}\right) = \frac{M_z}{(1+M_w Bc)^2} \,. \tag{9}$$

Generally, in Eq. (9) the square term is not negligible. Since the ratio of apparent weight average and z-average molecular weight depends on the concentration as follows:

$$\frac{(M_w)_{\text{app}}}{(M_z)_{\text{app}}} = \frac{M_w}{M_z}(1+M_w Bc) \tag{10}$$

we suggest linear extrapolation to infinite dilution by means of Eq. (10).

*

The authors gratefully acknowledge the assistance of Mr. I. SZEPESVÁRI of the Computer Center of the Hungarian Academy of Sciences, who has written the program for the Ural 2 computer and carried out the numerical solutions of the Lamme differential equation.

REFERENCES

1. ARCHIBALD, W. J.: J. Phys. Colloid Chem., **51,** 1204 (1947)
2. KLAINER, M., KEGELES, G.: J. Phys. Chem., **59,** 952 (1955)
3. GINSBURG, A., APPEL, P., SCHACHMAN, H. K.: Arch. Biochem. and Biophys., **65,** 545 (1956)
4. KEGELES, G., KLAINER, S. M., SALEM, W. J.: J. Phys. Chem., **61,** 1286 (1957)
5. YPHANTIS, D. A.: J. Phys. Chem., **63,** 1742 (1959)
6. FUJITA, H., INAGAKI, H., KOTAKA, T., UTIYAMA, H.: J. Phys. Chem., **66,** 4 (1962)
7. TRAUTMAN, R., CRAMPTON, C. F.: J. Amer. Chem. Soc., **81,** 4036 (1959)
8. LA BAR, F. E.: Biochemistry, **5,** 2362 (1966)

Marianne BLAZSÓ; 1088 Budapest, Múzeum krt 6—8.
Alfréd CZUPPON; 1088 Budapest, Puskin u. 11—13.

Acta Chimica Academiae Scientiarum Hungaricae, Tomus 76 (1), pp. 21—27 (1973)

INVESTIGATION OF THE RATE OF CORROSION OF IRON IN ACETONE–WATER–SODIUM ACETATE MIXTURES

J. DÉVAY, R. RATKOVICS-SCHÜTZ and L. MÉSZÁROS

(Department of Physical Chemistry, University of Chemical Engineering, Veszprém and Research Group of Electrochemistry of the Hungarian Academy of Sciences, Veszprém)

Received March 2, 1972

The kinetic parameters of the dissolution of iron were studied in acetone–water–sodium acetate mixtures. The polarization curves were measured by using a potentiostat equipment with automatic compensation of the resistance polarization because of the high resistance of the solutions. The slopes of the Tafel's plots were measured and the corrosion-current density values of iron were evaluated in various mixtures.

The constant (b) of Tafel's equation was found to be independent of the acetone concentration while a decrease of the constant was observed by increasing the acetate concentration. The corrosion-current density decreased by increasing acetone concentration while acetate ion concentration had an opposite effect.

Several workers have investigated the electrochemical properties and corrosion of iron because of the great practical importance of the latter. Here we report on an investigation aimed at studying the effect of acetone on the kinetics of iron dissolution in acetone–water–sodium acetate mixtures.

The method used was the measurement of the polarization resistanc and the evaluation of the corrosion current density (i_{corr}) characteristto the rate of corrosion. Constants b_a and b_k characteristic to the anod- and cathodic processes, respectively, were obtained from the slope of th Tafel's plots. The corrosion current density was calculated according to th following formula (1)

$$i_c = \frac{1}{R_p} \frac{b_a \cdot b_k}{b_a + b_k} \tag{1}$$

where $R_p = (dE/di)_{i=0}$ is the polarization resistance, as determined from the polarization curve in the neighbourhood of some mV of the steady-state potential. The determination of the above-mentioned constants would have been inaccurate by the usual potentiostatic method because of the high resistance of the mixtures ($\varrho = 15$—1000 Ohm cm). Thus, an automatic compensating system was employed for the elimination of resistance polarization in the measurement of the polarization curves (2).

The experimental equipment is shown in Fig. 1. The details have been reported previously [2]. The measurements were performed in a three-electrode cell. The working electrode V was an iron foil with a surface area of 0.25 cm^2 sealed in a glass tube by means of Epokitt resin. A normal calomel electrode K

served as reference electrode, while the platinum electrode E was the counter electrode. The working electrode was polarized in the potential range from 0 to $\pm$2.5 V. Prior to the measurements, the surface of the electrodes was cleaned by means of emery paper and etched in dilute sulphuric acid for 5 minutes, then rinsed with distilled water and dried.

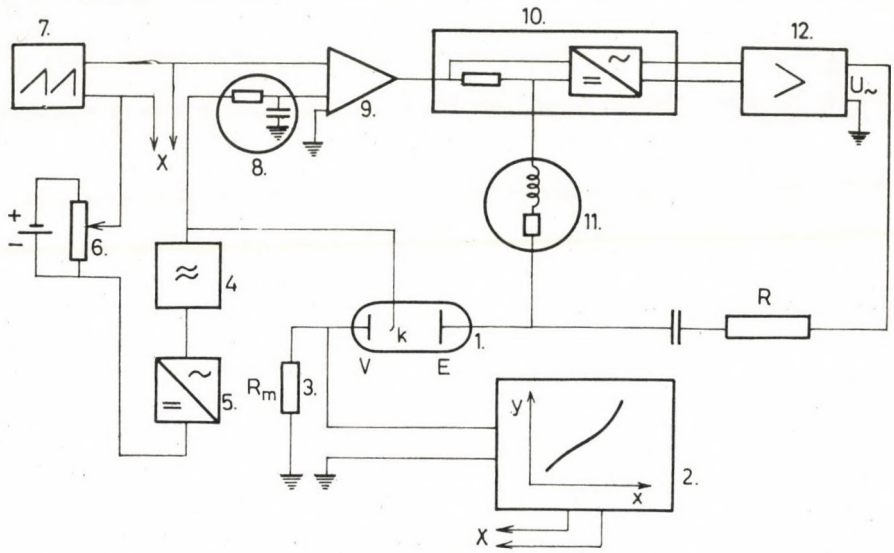

Fig. 1. Block diagram of the equipment. 1. Cell; 2. X—Y recorder; 3. Measuring resistance; 4. Wave analyser; 5. Demodulator; 6. Potentiometer; 7. Kipp generator; 8. Filter circuit; 9. Potentiostat; 10. Modulator; 11. Filter circuit; 12. Amplifier

The sodium acetate concentration of the solutions was 0.01, 0.05, 0.1 and 0.5 *M*, respectively. The acetone content of the solutions was varied from 0 to 30 per cent. Analytical grade reagents were employed for the preparation of the solutions. The electrodes were pretreated before each measurement. The measurements were performed at room temperature.

A few examples of the polarization curves are shown in Figs 2 through 5. The plots obtained by employing the automatic compensation system are indicated by full lines while the dotted lines refer to the measurements performed without compensating the resistance polarization. It is apparent that the two types of curves differ considerably.

The slopes of Tafel's plots were determined by means of the linearization of the polarization curves and examined as a function of the concentration of sodium acetate and acetone, respectively. The constants are listed in Table I. It is apparent from the data that the values referring to the anodic and cathodic processes, respectively, were independent from the acetone concentration in solutions containing an equal amount of sodium acetate. b_a and b_k decreased

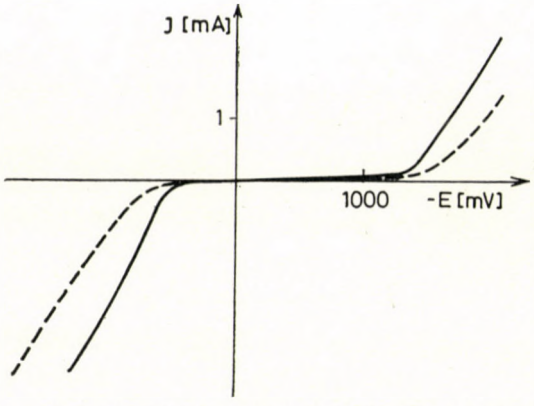

Fig. 2. Polarization curve of the iron electrode in a 0.01 *N* sodium acetate solution containing 10 per cent acetone

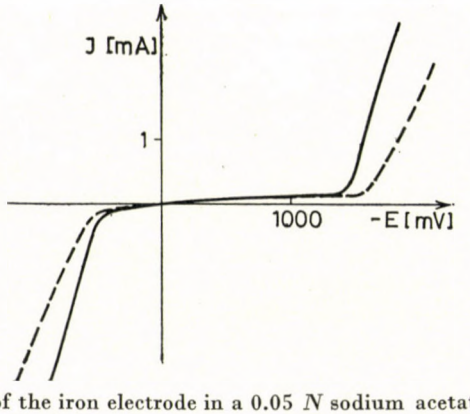

Fig. 3. Polarization curve of the iron electrode in a 0.05 *N* sodium acetate solution containing 20 per cent acetone

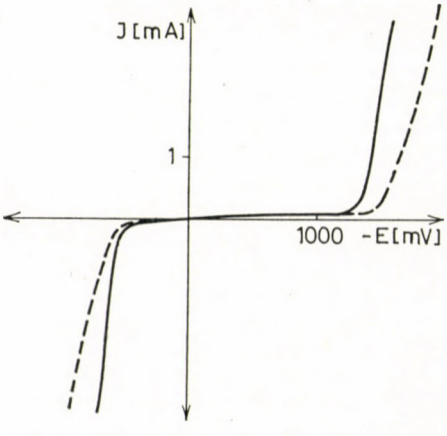

Fig. 4. Polarization curve of the iron electrode in a 0.1 *N* sodium acetate solution containing 10 per cent acetone

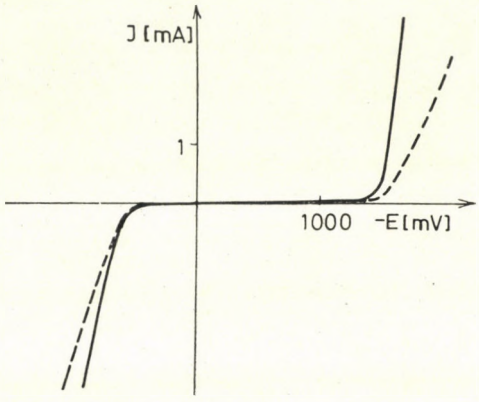

Fig. 5. Polarization curve of the iron electrode in a 0.5 *N* sodium acetate solution containing 10 per cent acetone

Table I

CH_3COONa C[M]	Acetone per cent	Cathodic process b [V]	Anodic process b [V]	i_{corr} [$\mu A/cm^2$]
0.01	0	0.111	0.177	68.5
0.01	10	0.099	0.152	55.5
0.01	20	0.109	0.161	50.4
0.01	30	0.098	0.204	47.5
average:		0.104	0.174	
0.05	0	0.100	0.137	104
0.05	10	0.091	0.170	90.7
0.05	20	0.096	0.140	70.6
0.05	30	0.103	0.121	68
average:		0.097	0.142	
0.1	0	0.087	0.124	127
0.1	10	0.074	0.087	109
0.1	20	0.073	0.098	92.5
0.1	30	0.083	0.110	80.8
average:		0.079	0.105	
0.5	0	0.067	0.087	147.5
0.5	10	0.074	0.085	134
0.5	20	0.074	0.073	123
0.5	30	0.063	0.096	112
average:		0.069	0.085	

by increasing the sodium acetate concentration, as shown in Fig. 6 representing the mean values of the constants as a function of the sodium acetate concentration.

The measurement of the polarization resistance of the systems was performed by means of the above mentioned equipment without employing the

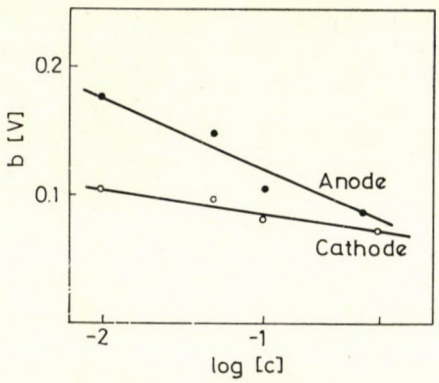

Fig. 6. b constants of Tafel's equation as plotted *vs.* the sodium acetate concentration

automatic compensation system. The compensation of the ohmic potential drop was not necessary in this case, as the current flowing through the electrode was in the order of some μA only, in the neighbourhood of a few mV of the steady-state potential, thus the ohmic potential drop on the resistance of the solution was negligible as compared to the polarization voltage.

The results of the measurement of polarization resistance are shown in Fig. 7. It is apparent in Fig. 7 that in this potential range the polarization curves were linear to a fairly good approximation, and the slopes differ considerably.

The effect of resistance R_m had to be taken into consideration in the evaluation of the polarization resistance on the basis of the measured data. The voltage recorded on the axis of the current–potential curve was the sum of the electrode potential and the voltage, iR_m, appearing on the standard resistance.

$$U = E + iR_m \tag{2}$$

where

U is the measured voltage
E is the electrode potential
i is the current intensity
R_m is the standard resistance

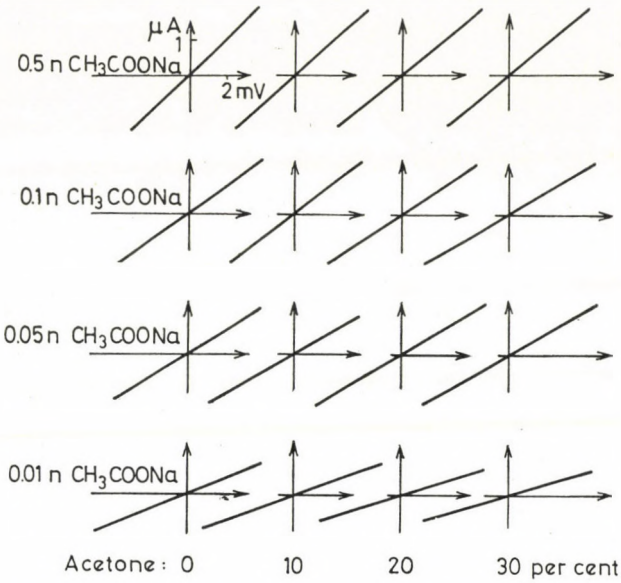

Fig. 7. Corrosion current density data as a function of sodium acetate and acetone concentrations, respectively

The derivation of Eq. 2 at $i = 0$ yields

$$\left(\frac{dU}{di}\right)_{i=0} = \left(\frac{dE}{di_{i=0}}\right) + R_m, \tag{3}$$

and it follows that the polarization resistance (R_p) is

$$R_p = \left(\frac{dE}{di}\right)_{i=0} = \left(\frac{dU}{di}\right)_{i=0} - R_m . \tag{4}$$

The values of $(dU/di)_{i=0}$ were determined by a graphic differentiation of the curves represented in Fig. 7, while the corrosion current densities were evaluated by means of Eq. 1 and the above-mentioned values of b_a and b_k.

The corrosion current densities expressed in $\mu A/cm^2$ units are shown as a function of the acetone concentration in Fig. 8.

It is apparent that the corrosion current densities decreased by increasing acetone concentration, while an increase in the concentration of acetate ions had an opposite effect. The concentration of acetate ions apparently affected the corrosion current density values in the acetone–water–sodium acetate mixtures to a considerable extent, similarly to the case reported by Kiss *et al.* [3] relating to the anodic dissolution of iron in glacial acetic acid. Acetate ions

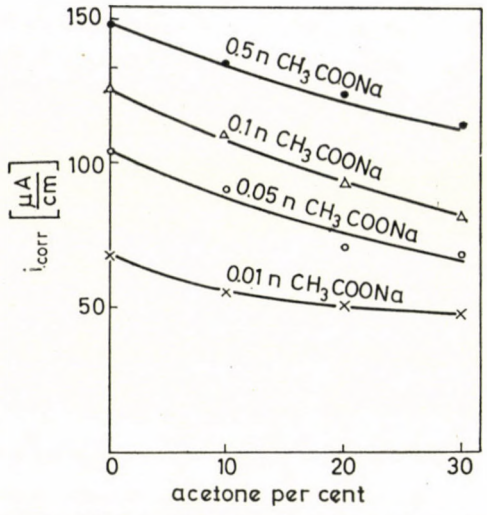

Fig. 8. Corrosion current density data as a function of the acetone concentration

were found to exhibit a catalytic effect similar to the one shown by hydroxil ions in aqueous medium [3]. An increase in acetone concentration slightly influenced the effect of acetate ions. However, the corrosion current density decreased by an increase in acetone concentration in solutions containing constant amounts of sodium acetate in the concentration range of the latter investigated in this work.

REFERENCES

1. KAESCHE, H.: Die Korrosion der Metalle. Springer-Verlag, Berlin, (1966)
2. DÉVAY, J., LENGYEL, B. jr., MÉSZÁROS, L.: Magy. Kém. Foly. **76**, 212 (1970)
3. KISS, L., DO NGOC LIEN, VARSÁNYI, L. M.: Magy. Kém. Foly. **76**, 371 (1970)

József DÉVAY
R. RATKOVICS-SCHÜTZ
Lajos MÉSZÁROS
8201 Veszprém, Schönherz Z. u. 10. Hungary

Acta Chimica Academiae Scientiarum Hungaricae, Tomus 76 (1), pp. 29—50 (1973)

HIGHER HARMONIC A. C. POLAROGRAPHY OF MULTICOMPONENT SYSTEMS

J. Dévay, T. Garai, B. Palágyi-Fényes, L. Mészáros and Sayed Sabat Abd-El Rehim*

(Department of Physical Chemistry, University of Chemical Engineering, Veszprém, and Research Group of Electrochemistry of the Hungarian Academy of Sciences, Veszprém)

Received March 2, 1972

Second and third harmonic A.C. polarography was used for the simultaneous determination of depolarizers having half-wave potentials differing by less than 150 mV. The results showed that in such cases the above techniques were more convenient than D.C. or fundamental harmonic A.C. polarography.

The relative merits of second and third harmonic A.C. polarography were also discussed. The simultaneous determination of two electroactive species could be performed in a concentration ratio depending on the quality of the depolarizers even when the difference in the respective half-wave potentials is 40 mV only.

In our previous communication [1] we have dealt with the application in chemical analysis of the second and third harmonic A.C. current flowing through the cell containing a d.m.e. — when a small amplitude sinusoidal A.C. voltage is superimposed on the D.C. polarizing potential. It has been proved experimentally that the sensitivity of higher harmonic A.C. polarographic analysis is higher by at least one order of magnitude than that of conventional D.C. or fundamental harmonic A.C. polarography as the effect of the double-layer capacity, i.e., the interference caused by the condenser current is eliminated. This is in accordance with theoretical expectations [2]. Further, the effect of the ohmic potential drop across the cell resistance has been investigated both theoretically and experimentally in order to establish optimum working conditions in higher harmonic A.C. polarographic analysis [3].

The present paper deals with the simultaneous determination of ions in the case when their respective half-wave potentials differ by less than 200 mV. It is well-known that under these circumstances D.C. polarographic analysis is not reliable.

Breyer *et al.* [4] have shown that the determination of a given component in fundamental harmonic A.C. polarography is not hindered by the presence of a relatively large amount of an ion having a half-wave potential more positive than that of the depolarizer to be determined when the difference of the half-wave potentials of the components is greater than 150 to 200 mV. Even in the case when the difference of the half-wave potentials of

* On study leave from Ain-Shamps University, Cairo, UAR.

the depolarizers is smaller than 150 mV, quantitative evaluation of the polarogram obtained by this technique is still feasible under favourable circumstances [5]. However, the simultaneous determination of such depolarizers in fundamental harmonic A.C. polarography can be carried out with some accuracy only when the components have approximately equal diffusion currents. Furthermore, the evaluation of the data of multicomponent systems is rather cumbersome even in this case, as the polarograms of each depolarizer are to be traced separately and the concentrations of the components are to be calculated by means of geometrical plotting [4]. When the diffusion currents of the components are different, the error in the concentration determination of the depolarizer having a smaller diffusion current tends to increase and if there is a sufficiently large difference in the diffusion currents of the components, even the presence of the depolarizer is hardly detectable.

BOND and CANTERFORD [5] have recently made a thorough study on the simultaneous determination of two electroactive species by fundamental harmonic A.C. polarography and they have concluded that the maximum values exhibited at the half-wave potential of each depolarizer were only suitable for qualitative analysis in the case of overlapping waves. The authors have recommended the use of a selective complexing agent to increase the difference in the half-wave potentials of the depolarizers to be determined. Thus, a complete separation of the waves can be achieved.

BAUER [6] and NEEB [7] have suggested that the measurement of the second harmonic A.C. current can be used more advantageously than the fundamental harmonic for the analysis of multicomponent systems. In NEEB's paper some quantitative data are also presented regarding the simultaneous determination of some depolarizers having half-wave potentials differing by approx. 200 mV. However, NEEB did not examine in detail such depolarizer systems where the difference in the half-wave potentials is less than 200 mV, though the latter are especially worth of interest. According to NEEB, the simultaneous determination of indium and thallium in perchloric acid is not feasible by the measurement of the second harmonic A.C. current, as the difference in the respective half-wave potentials of these ions is about 50 mV, while even a hundredfold excess of cadmium and a thousandfold excess of indium does not hinder the determination of 4 μg/ml lead. The former ions have half-wave potentials more negative by approximately 150 to 200 mV than that of lead.

Considering the fact that only meager data have been published in the literature, it was deemed necessary to examine systematically the simultaneous determination of various depolarizers by means of higher harmonic A.C. polarography.

It has been established (*cf.* [1], [8]) that the first, second and third harmonic A.C. polarographic currents *vs.* potential functions have similar forms

to the first, second and third derivatives, respectively, of the D.C. current *vs.* potential functions. Thus, the fundamental harmonic A.C. component exhibits a maximum at the half-wave potential of the electroactive species and tends to the condenser current flowing through the double-layer capacity at more positive and more negative potential, respectively, than the half-wave potential. The amplitude of the second harmonic A.C. current *vs.* potential functions exhibit two peak values in the case of fast polarographic reactions at potentials equal to

$$\eta_{max} = \eta_{1/2} \pm \frac{0.034}{z} \text{ [volt]} \tag{1}$$

where z is the number of electrons involved in the electrode reaction and $\eta_{1/2}$ is the half-wave potential, while the curves have a minimum near to or at the half-wave potential. The minimum is zero and it is located at the half-wave potential in the case of reversible polarographic reactions. The second harmonic A.C. current shows a rapid decrease when the potential is made more negative than that corresponding to the negative peak potential. Similarly, the second harmonic A.C. current rapidly decreases at more positive potentials than the positive peak potential as shown in Fig. 1.

Fig. 1 represents a second harmonic A.C. polarogram of 1.10^{-5} M Pb^{2+} in 1 M $HClO_4$ as supporting electrolyte. It is apparent in Fig. 1 that the second harmonic A.C. was found practically negligible at ± 70 mV as referred to the half-wave potential.

The amplitude of the third harmonic A.C. component *vs.* potential function exhibits one maximum at the half-wave potential and two ones at more positive and more negative potentials, respectively, than the half-wave potential. The former potentials are equal to

$$\eta_{1,2} = \eta_{1/2} \pm \frac{0.060}{z} \text{ [volt]} \tag{2}$$

(where the notations are the same as in Eq. 1). The two lateral peak values are one third of the central peak in the case of a reversible polarographic reaction. The potentials corresponding to the minimum amplitudes between the peak values are equal to the peak potentials of the second harmonic (*cf.* Eq. 1). The minima are equal to zero in the case of reversible polarographic reactions. A third harmonic A.C. polarogram is shown in Fig. 2 as a function of the potential for $5 \cdot 10^{-5}$ M Pb^{2+} in 1M $HClO_4$. The rapid decrease in the current at more negative and more positive potentials than the respective lateral peak values is clearly apparent. The decrease in the intensity of the A.C. harmonic components with the potential is shown in Fig. 3, representing

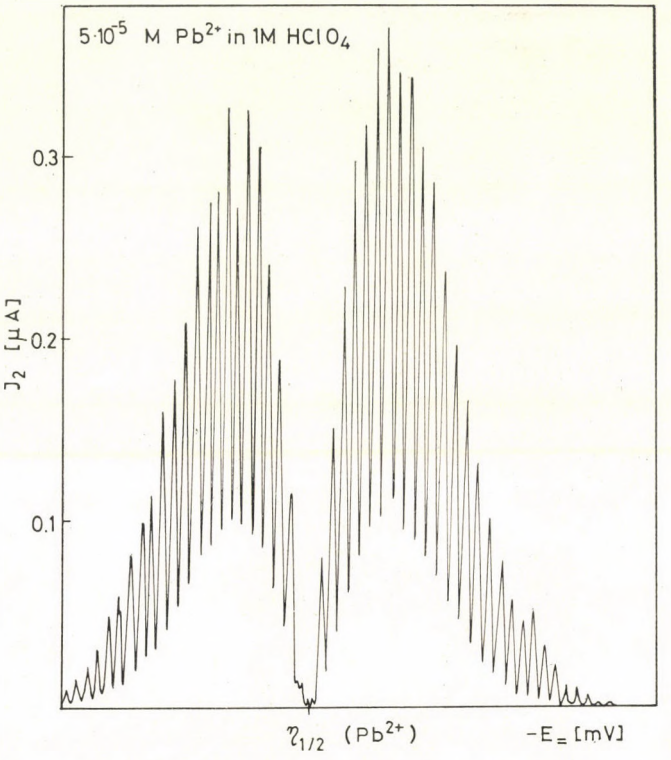

Fig. 1. Second harmonic A.C. polarogram of 5.10^{-5} *M* Pb^{2+} in 1 *M* $HClO_4$ as supporting electrolyte

the logarithm of the ratios of the second harmonic (full line) and the third harmonic (dotted line) A.C. current to their maximum values, respectively, as a function of the absolute value of the D.C. potential, the half-wave potential being taken as the origin of the abscissa, in the case of reductions where one and two electrons, respectively, are exchanged in the electrode reactions.

In the case of reversible A.C. polarographic reactions the amplitudes of the harmonic components of the A.C. current as functions of the D.C. potential are symmetrical to the half-wave potential. Hence the analysis of a depolarizer is equally influenced by any component having either more positive or more negative half-wave potential than that of the ion to be determined. Thus, only the absolute value of the potential as referred to the half-wave potential is represented in Fig. 3.

The plots show that the decrease in the second harmonic A.C. current at more negative (or more positive) potentials than the corresponding peak potential becomes increasingly rapid when the number of electrons involved in the electrode reaction is higher. *E.g.*, the calculations show that in the

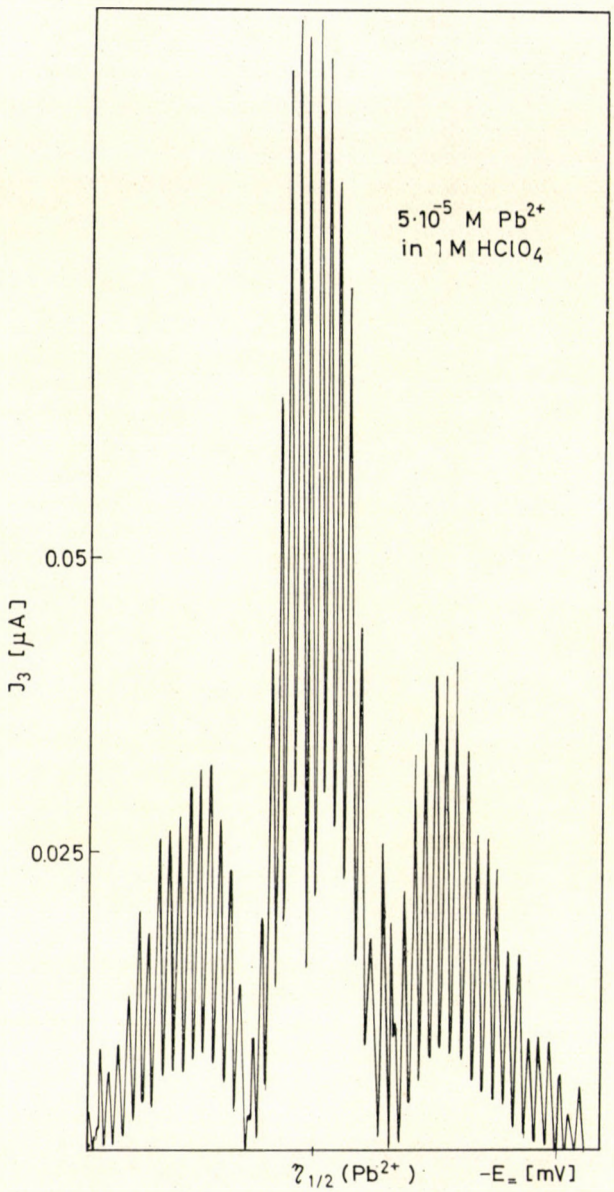

Fig. 2. Third harmonic A.C. polarogram of 5.10^{-5} *M* Pb^{2+} in 1 *M* $HClO_4$ as supporting electrolyte

case of $z = 1$, the second harmonic A.C. current is about 1 per cent of its maximum value at a potential 150 mV more negative (or more positive) than the half-wave potential. In the case of a two-electron electrode reaction the sec-

ond harmonic A.C. current attains 1 per cent of its peak value when the absolute value of the potential is 85 mV as measured from the half-wave potential, while at a potential 150 mV more negative (or more positive) than the latter, the A.C. current decreases to 0.01 per cent, *i.e.*, it is practically negligible. It is apparent in Fig. 3 that the relative decrease in the current inten-

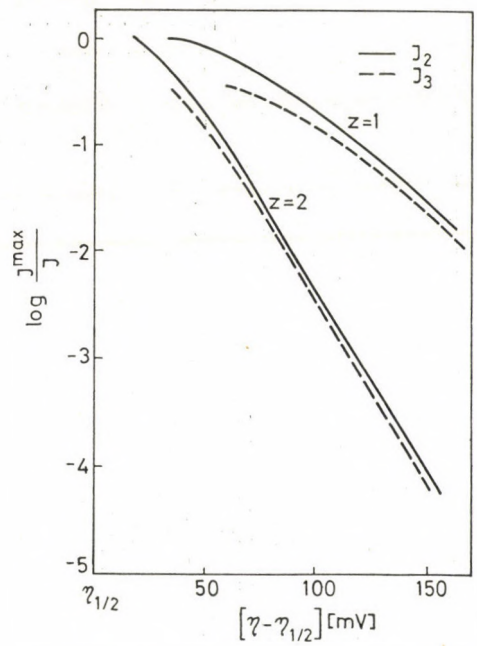

Fig. 3. The relative decrease of the second and third harmonic A.C. current intensity as a function of the potential for $z = 1$ and 2

sity of the third harmonic A.C. component is slightly larger than that of the second harmonic. It is noteworthy that the effect of the cell resistance has been neglected in the calculation of the relative decrease in the intensity of the A.C. harmonics. According to recent studies [3] the amplitude of the A.C. harmonics decreases due to cell resistance, while the difference in the peak potentials of the second harmonic increases.

The maximum value appearing at the half-wave potential of the third harmonic A.C. component is affected by the ohmic potential drop to a relatively larger extent than the other two peaks. Thus, the slope of the curve representing the relative decrease in the intensity of the second harmonic A.C. is decreased to a similar extent than that of the third harmonic A.C. component due to cell resistance. Thus, according to these calculations, the simultaneous analysis of depolarizers having a difference of 150 mV or more in their

half-wave potentials is practically simple in higher harmonic A.C. polarography. However, the cases when this difference is about 100 mV or less, deserve further examinations.

In addition to the relative decrease in the current intensity of the higher harmonic A.C. components, two other factors affect the simultaneous determination of two or more depolarizers in the case of reversible polarographic reactions. Namely, the number of electrons involved in the electrode reaction and the change in the relative phase angles of the A.C. harmonics as a function of the potential. (In the case of slow transition reactions the heterogeneous rate constants and the transfer coefficients also modify the current *vs.* potential relations.) (*cf. e.g.* [2], [8], [9])

The formulas relating to the A.C. polarographic currents [2], [8] indicate that the potential range of the current *vs.* potential functions is smaller when the number of electrons involved in the electrode reaction is higher, as it is apparent in Fig. 3.

The simultaneous determination of two electroactive species is also affected by the fact that the second harmonic A.C. component increases proportionally to the third power of the number of electrons involved in the reduction, while the third harmonic increases proportionally to the fourth power of the number of electrons. Consequently, the depolarizer involving a higher number of electrons in its electrode reaction, interferes to a larger extent in the determination of an electroactive species involving a smaller number of electrons in its reduction than *vice versa*. Obviously, this effect is more pronounced in the case of the third harmonic than in that of the second harmonic A.C. component.

The following considerations refer to the phase angles of the A.C. harmonics. The theory of the A.C. polarography of a reversible electrode reaction indicates that the phase angles of the second harmonic A.C. current referred to that of the fundamental harmonic are 45° and 225° at the respective peak values [8], [10], if adsorption does not take place on the electrode surface [11]. SMITH's [12] phase selective measurements as well as the results of KOOIJMAN and SLUYTERS [13] proved this fact experimentally. It is obvious that the resultant of the second harmonic A.C. components of the diffusion currents of various ions at a given potential is obtained by vectorial summation as represented in Fig. 4. The pointed line shows the phase sensitive second harmonic A.C. polarogram of a one-electron reaction, while the dotted line represents that of a two-electron electrode reaction, the half-wave potential of the latter being more negative by 50 mV than that of the former electrode process. The resultant of the two components is represented by a full line. This calculated example shows that at potentials more negative (or more positive) than the half-wave potentials of both components, the amplitude of the resultant second harmonic current is increased, as the phase angles of each

components are nearly equal. The superposition of the second harmonic A.C. currents of the two depolarizers at potentials between the respective half-wave potentials result in a current of relatively small amplitude, as the phase angles of the components differ by nearly 180°.

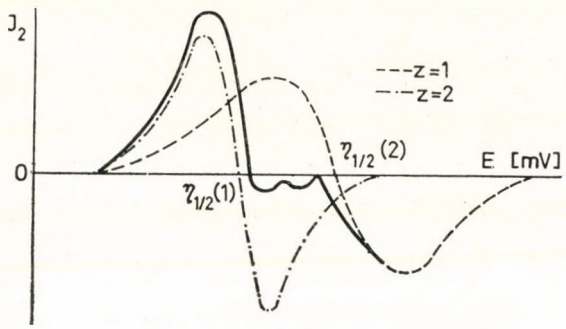

Fig. 4. Vectorial summation of second harmonic A.C. polarograms (–.–.– $z = 1$, ———— $z = 2$), (——— resultant polarogram) in case of 50 mV difference in the half-wave potentials of the respective depolarizers

On the basis of these theoretical considerations the maximum amplitudes appearing at more positive and more negative potentials than the half-wave potentials of both ions can be used for their respective determination when both are simultaneously present in the solution.

The relative concentration of the ions when their half-wave potentials are very close, obviously represent a limitation in the evaluation of the polarograms (*cf.* Fig. 3).

According to the results referring to the third harmonic A.C. component [2], the phase angles of the peak values at the half-wave potential and at more negative (or more positive) potentials than the latter differ by 180°. Consequently, in the case of the reduction of two depolarizers involving z_1 and z_2 electrons, respectively, in the electrode reaction, the peaks of the third harmonics at the respective half-wave potentials decrease proportionally to the current of the other ion appearing at the same potential when the difference in the half-wave potentials is

$$|(\eta_{1/2})_1 - (\eta_{1/2})_2| > 0.034 \left(\frac{1}{z_1} + \frac{1}{z_2}\right) \text{[volt]}$$

as in Fig. 5/a. However, when

$$|(\eta_{1/2})_1 - (\eta_{1/2})_2| < 0.034 \left(\frac{1}{z_1} + \frac{1}{z_2}\right) \text{[volt]} \qquad (4)$$

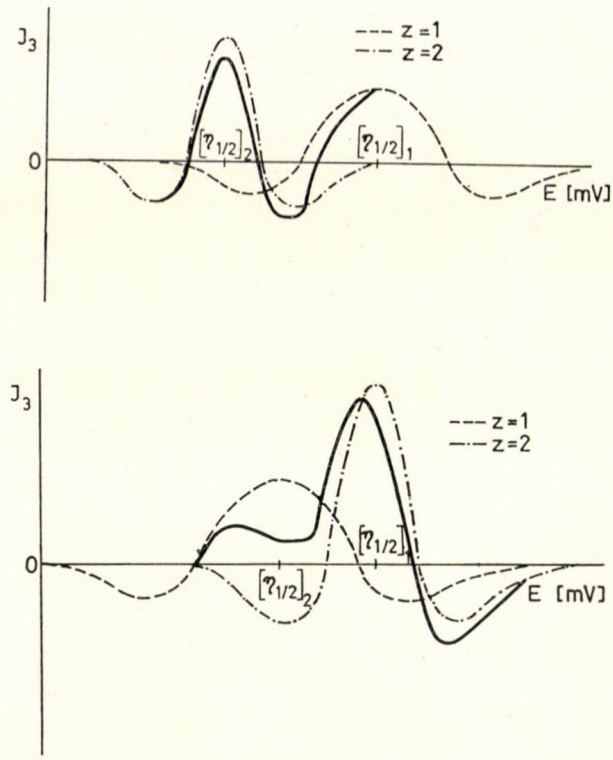

b)

Fig. 5. Vectorial summation of third harmonic A.C. polarograms (explanation in the text)

as in Fig. 5/b, the summation of the diffusion currents of the two electroactive species follows the same considerations as in the case of the fundamental harmonic A.C. current [5]. Namely, the third harmonic A.C. polarographic current at any potential is the vectorial resultant of the current relating to each depolarizer. The peak currents of the depolarizers are generally indistinct in the latter case, except when the current relating to one of the depolarizers is negligible as compared to that relating to the other because of the large difference in the respective concentrations and the number of electrons involved in the electrode reaction. We can conclude as a consequence of these considerations that second harmonic A.C. polarography is generally more advantageous than the third harmonic one for the simultaneous determination of two or more depolarizers when the respective half-wave potentials are close to one another. However, third harmonic A.C. polarography can be useful to eliminate the interference of a one-electron reduction in the determination of a depolarizer involving a larger number of electrons in the electrode reaction.

Experimental part

The measurements were made on a modified A.C. Polarographic Unit attached to a Controlled Potential Polarograph of RADELKIS type OH 102 [14]. The block diagram of the instrument is shown in Fig. 6. The polarographic cell employed in the measurement contained three electrodes. A calomel reference electrode was placed near to the dropping mercury electrode to control the potential of the latter, while a mercury pool served as counter electrode. The D.C. polarizing voltage (E) supplied by the D.C. polarograph was branched to one input of the potentiostat (P) built into the instrument. The variable amplitude A.C. voltage was generated by an oscillator (O) tuned exactly to 60 s^{-1} and superimposed on the D.C.

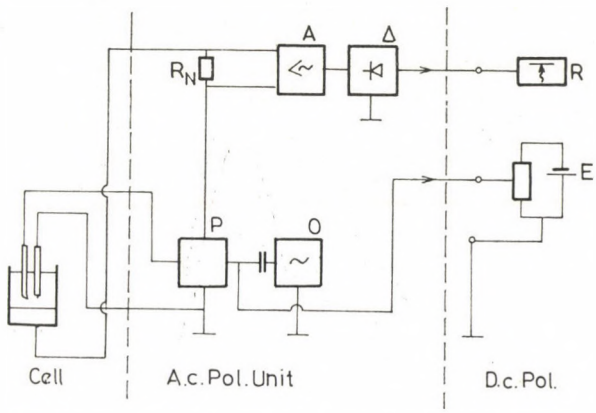

Fig. 6. Block diagram of the A.C. polarographic instruments

voltage and was also stabilized by the potentiostat. The reference electrode was branched to the other input of the potentiostat, while the output of the latter controlled the current of the cell through the counter electrode in order to secure that the potential of the working electrode referred to the reference electrode should be equal to the voltage of the voltage devider (E) branched to the input. The A.C. current flowing through the cell is obtained by measuring the A.C. voltage proportional to the A.C. current on the standard resistance (R) inserted into the counter electrode circuit. A selective vacuum tube voltmeter (A) provided for the measurement of either the fundamental harmonic or the second or the third harmonic components of the A.C. current. The output of the vacuum tube voltmeter was recorded after rectification (Δ) by the pen recorder (R) of the D.C. polarograph. Thus A.C. polarograms were automatically recorded. The instrument was operated at 10 mV (effective) 60 c.p.s. A.C. voltage throughout the experiments. The drop time of the d.m.e. was adjusted to about 5s. The test solutions were prepared using reagent grade chemicals. The test solutions were deaerated with pure nitrogen prior to the measurements.

Measurements were carried out in solutions containing lead(II) and thallium(I) ions at various concentrations in 1 *M* HCl and 1 *M* $HClO_4$, respectively, as supporting electrolytes, as well as in solutions containing cadmium(II) and indium(III) ions at various concentrations in 1*M* HCl as supporting electrolyte. Solutions of lead and cadmium ions were also tested.

Results

The experimental results are in general agreement with the theoretical expectations.

Fig. 7 represents the polarogram of a solution containing 5.10^{-4} *M* Pb^{2+} and $5 \cdot 10^{-4}$ *M* Tl^{+} in 1 *M* HCl as supporting electrolyte. The half-wave

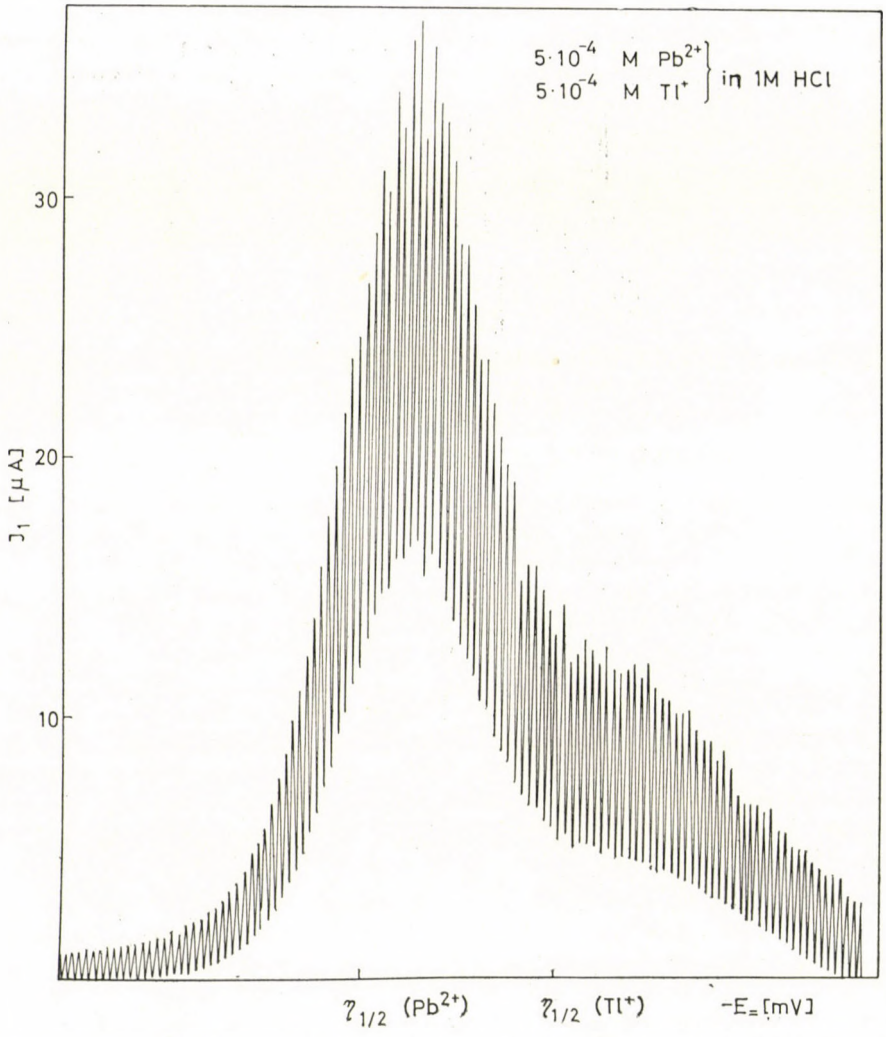

Fig. 7. a) Fundamental harmonic, *b*) second harmonic and *c*) third harmonic A.C. polarogram of 5.10^{-4} M Pb^{2+} and 5.10^{-4} M Tl^{+} in 1 M HCl as supporting electrolyte

potentials of the reduction of lead(II) and thallium(I) in 1 *M* HCl as supporting electrolyte are —0.435 and —0.475 V *vs.* S.C.E., respectively [10]. Fig. 7/a shows the fundamental harmonic A.C. polarogram of the system. It is apparent that the thallium(I) peak is just discernable on the latter curve, while on the second harmonic A.C. polarogram in Fig. 7/b the positive peak of lead(II) and the negative peak of thallium(I) are well-developed and they could be employed for the quantitative evaluation of lead and thallium concentration, respectively, of solutions containing these ions in the presence of each other.

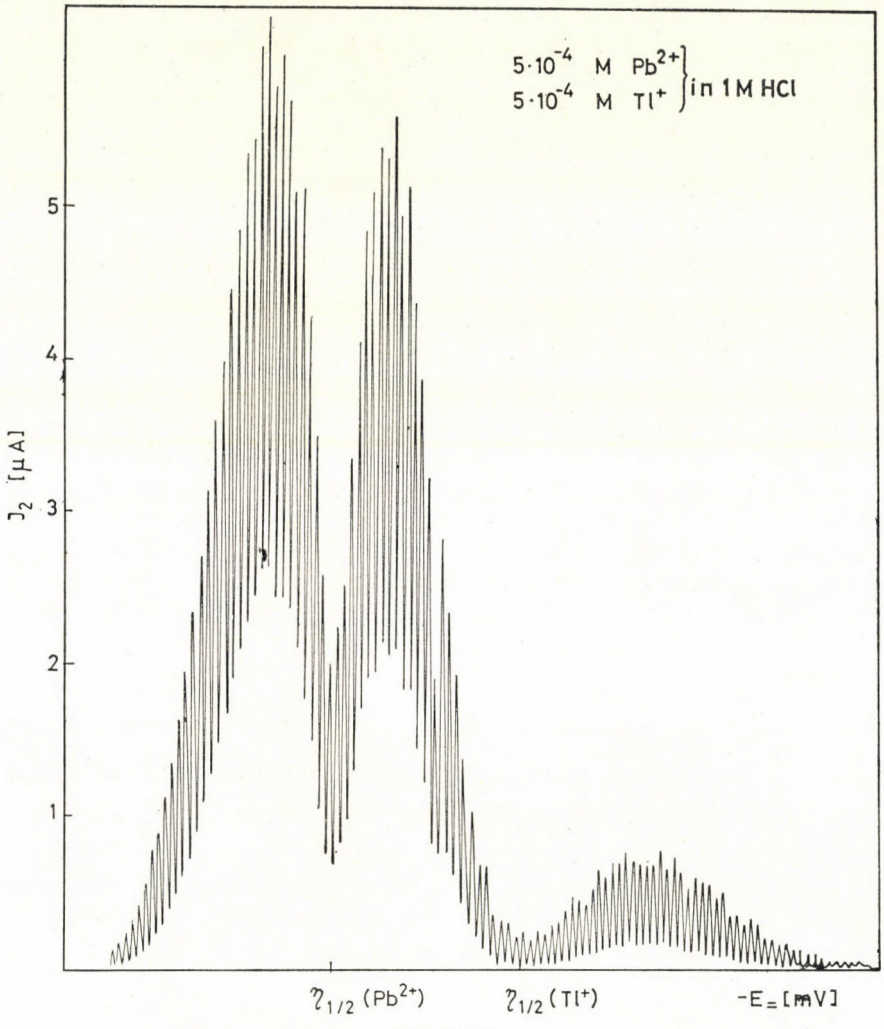

Fig. 7. b)

The negative peak of lead(II) and the positive peak of thallium(I) do not exhibit a linear relation with the concentration of the respective ion. Though the half-wave potentials of lead (II) and thallium(I) differ by only 40 mV in 1 *M* HCl as supporting electrolyte, the concentration of *e.g.* $1 \cdot 10^{-5}$ to 1.10^{-4} *M* Tl^+ can be determined in the presence of lead (II) up to a five- to sevenfold excess of the latter. The determination of *e.g.* $1 \cdot 10^{-5}$ *M* Pb^{2+} was possible even in the presence of a twentyfold excess of thallium(I).

It is apparent from Fig. 3 that the second harmonic A.C. current exhibits a less rapid decrease with potential (the half-wave potential being taken as

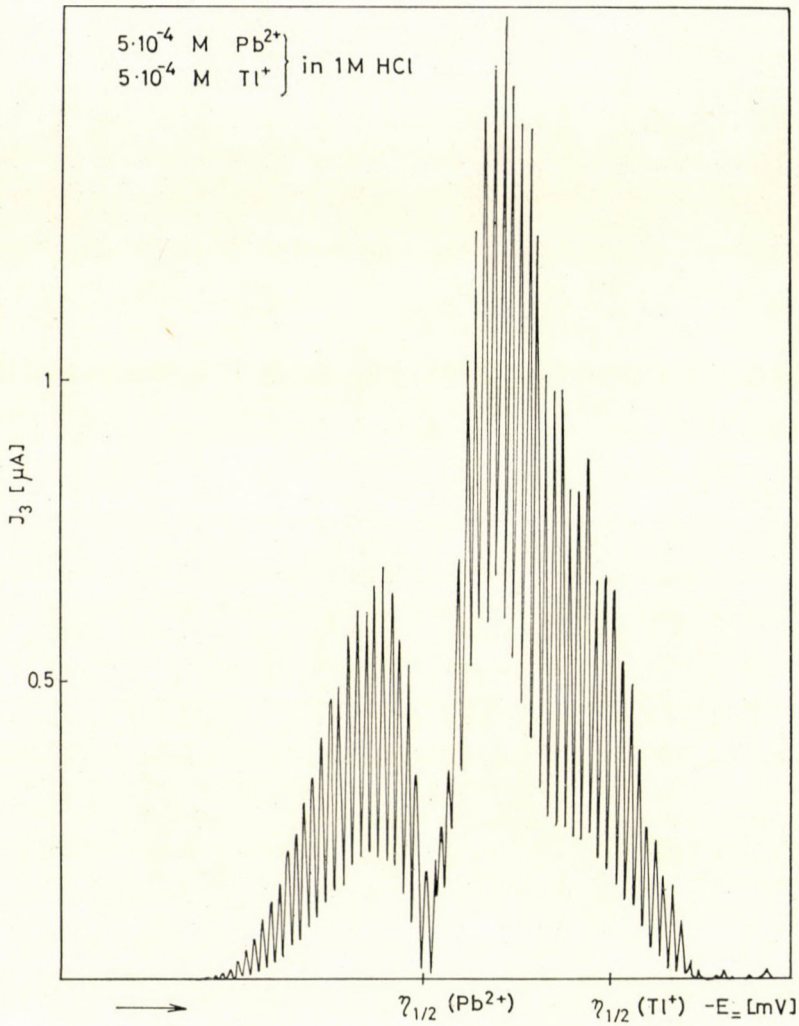

Fig. 7. c)

origin) when the number of electrons involved in the electrode reaction is one than in cases when this number is higher. Thus a depolarizer of a one-electron electrode reaction interferes in the determinations in a wider potential range than an ion of a two- or three-electron electrode reaction. However, it is also to be taken into consideration that the second harmonic A.C. current is proportional to the third power of the number of electrons involved in the electrode reaction (1) and thus the second harmonic A.C. current of a depolarizer is considerably higher — at a given concentration — when higher number of electrons are involved and an A.C. voltage of equal amplitude and

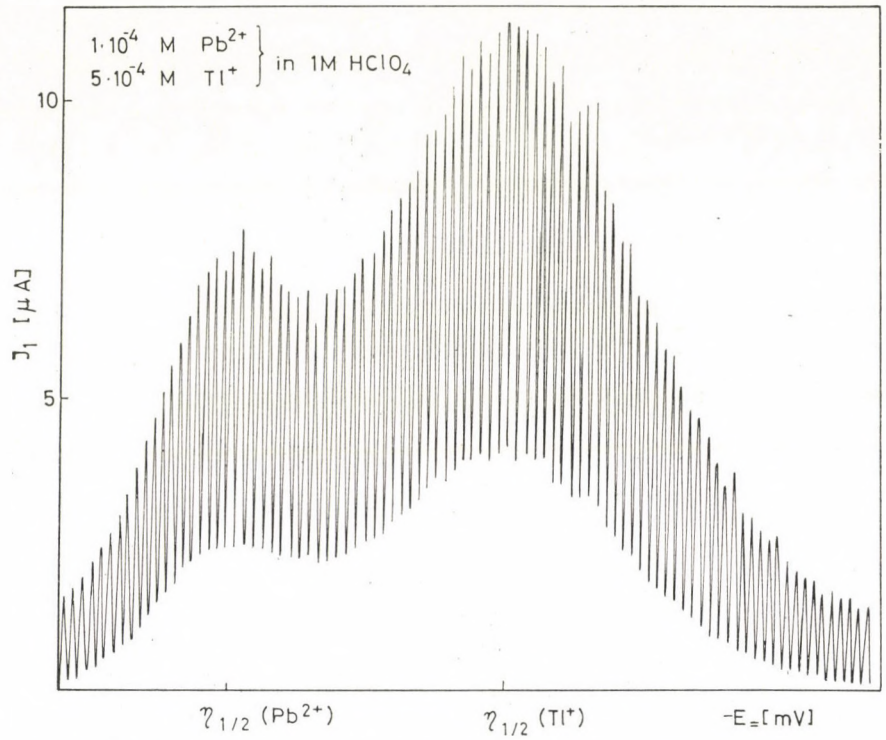

Fig. 8. a) Fundamental harmonic, *b)* second harmonic and *c)* third harmonic A.C. polarogram of 1.10^{-4} *M* Pb^{2+} and 5.10^{-4} *M* Tl^{+} and of 5.10^{-4} *M* Pb^{2+} and 3.10^{-4} *M* Tl^{+}, respectively, in 1 *M* $HClO_4$ as supporting electrolyte

frequency is used (the diffusion coefficients of the various depolarizers do not differ to a great extent). These effects account for the experimental result that the presence of lead (II) ions causes a more severe interference in the determination of thallium(I) than *vice versa*. Fig. 7/c represents the third harmonic A.C. current of the above mixture as a function of the potential. The quantitative evaluation of the curve is not possible, as the respective half-wave potentials of the two ions are very close to one another.

The separation of these ions could be further improved to a certain extent by using A.C. voltage of an amplitude lower than 10 mV. In this case, however, at low concentrations the A.C. current becomes very low.

As far as the simultaneous analytical determination of lead(II) and thallium(I) is concerned, it is more practical to employ 1 *M* $HClO_4$ as supporting electrolyte instead of 1 *M* HCl because in the former the half-wave potentials of lead(II) and thallium(I) (−0.400 V and −0.485 V), respectively, as referred to a saturated calomel electrode [15] differ by 85 mV, thus the separation of the peaks is much improved.

Fig. 8 represents a polarogram of $1 \cdot 10^{-4}$ *M* Pb^{2+} and $5 \cdot 10^{-4}$ *M* Tl^{+} in 1 *M* $HClO_4$ as supporting electrolyte. It is apparent in Fig. 8/a that the fundamental harmonic is also better developed than in the previous case represented in Fig. 7. Fig. 8/b shows the second harmonic A.C. polarogram of the system. The determination of the concentration of lead(II) is based again on the measurement of the peak current at a more positive potential than

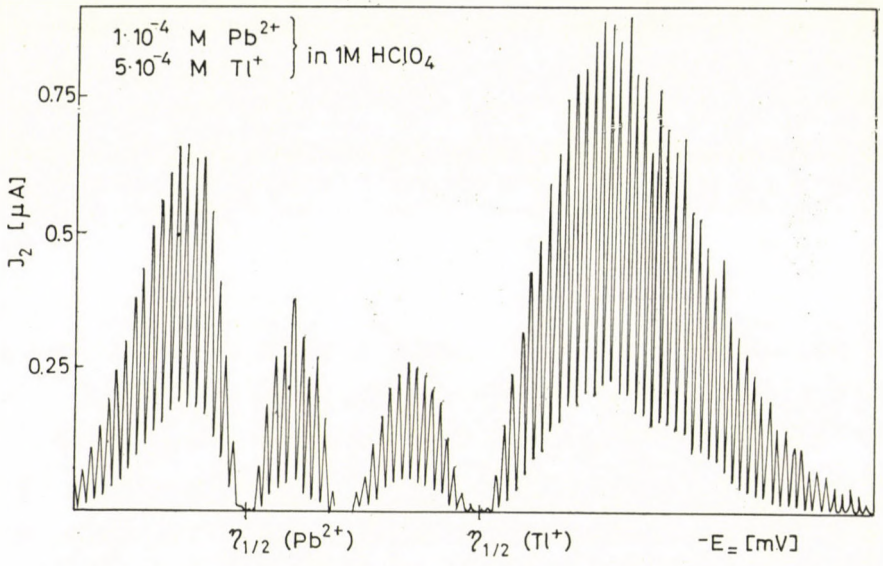

Fig. 8. b)

the half-wave potential of lead(II), while the negative peak of thallium(I) serves the evaluation of its concentration. Plotting the usual calibration curves, the determination of *e.g.* $1 \cdot 10^{-5}$ to $1 \cdot 10^{-4}$ *M* thallium(I) in the presence of a twentyfold excess of lead(II) is still possible, while *e.g.* $1 \cdot 10^{-5}$ *M* Pb^{2+} can be detected even when the concentration of thallium(I) in the system is fifty time higher than that of lead(II).

The third harmonic A.C. polarogram of the system is shown in Fig. 8/c. The peaks appearing at the half-wave potential of the respective ions are suitable for the determination of the respective concentrations on account of the larger difference in the half-wave potentials. (The part of the polarogram in the potential range of the reduction of thallium(I) was traced at a higher sensitivity setting of the instrument than the rest of the polarogram.) It is noteworthy that the peak related to lead(II) is about fifteen times greater than that of thallium(I), as the third harmonic A.C. current is proportional to the fourth power of the number of electrons involved in the electrode reaction.

Observing the calculated curves represented in Fig. 3 one can predict that in the case of electrode reactions where two or more electrons are involved, the simultaneous determination of the depolarizers is even more convenient. A solution containing cadmium(II) and indium(III) in the presence of each other illustrates this case. Though the difference of the half-wave potentials

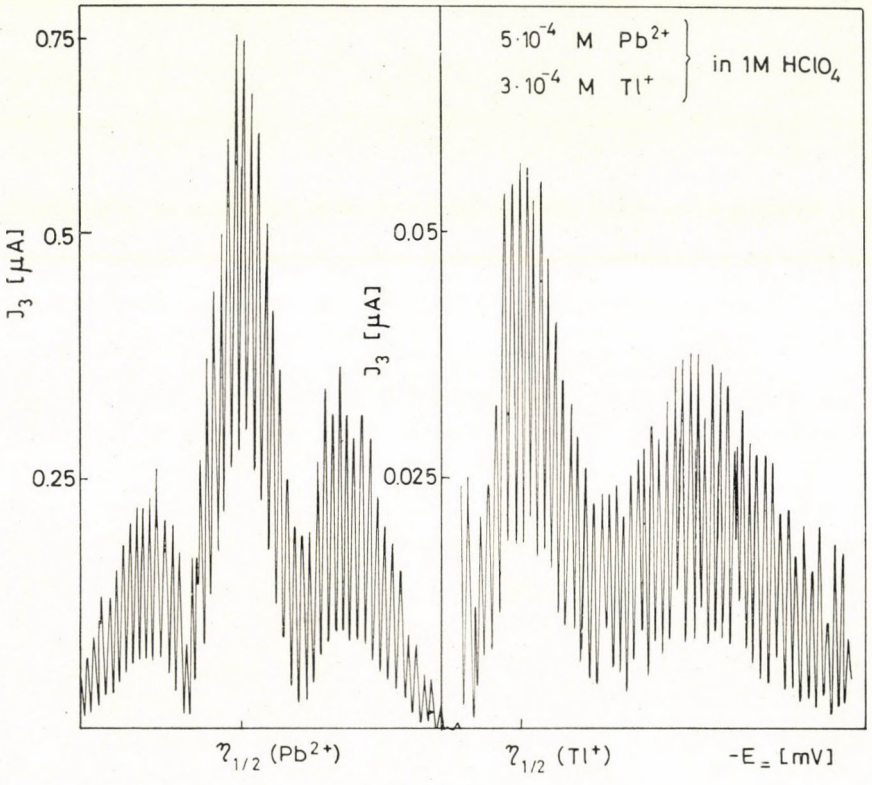

Fig. 8. c)

of cadmium(II) and indium(III), respectively, is only 40 mV in 1 *M* HCl as supporting electrolyte [15], the simultaneous determination of both ions is feasible within wide limits of concentration. Fig. 9 shows a typical polarogram of the above system, containing $5 \cdot 10^{-4}$ *M* Cd^{2+} and $1 \cdot 10^{-4}$ *M* In^{3+} in 1 *M* HCl as the supporting electrolyte. Fig. 9/a representing the fundamental harmonic polarogram exhibits a slight shouldering at the half-wave potential of indium(III) which is not suitable for the quantitative determination of the latter. However, on the second harmonic polarogram of the system shown in Fig. 9/b, the negative peak of indium(III) and the positive peak of cadmium(II) are clearly separated. The third peak in the middle of the polaro-

gram is the resultant of the A.C. currents caused by the reduction of cadmium (II) and indium(III) at potentials between the respective half-wave potentials.

Fig. 9/c represents the third harmonic A.C. polarogram of the above system. (The second part of the polarogram, in the potential range of the half-wave potential of cadmium(II) was recorded at a higher sensitivity of the

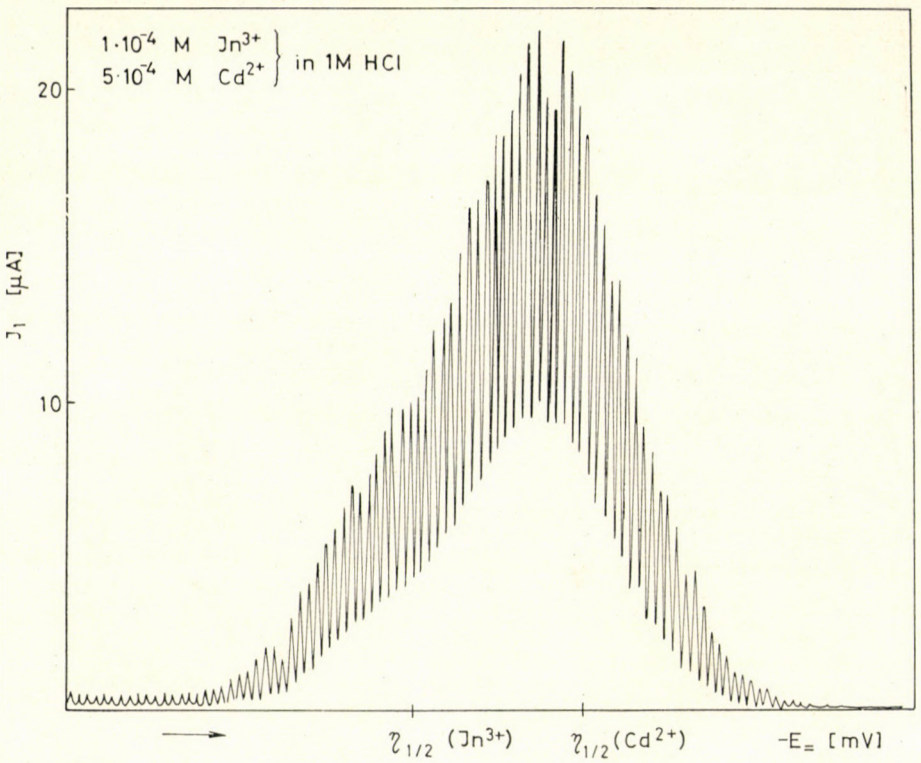

Fig. 9. a) Fundamental harmonic, *b)* second harmonic and *c)* third harmonic A.C. polarogram of 1.10^{-4} *M* In^{3+} and 5.10^{-4} M Cd^{2+} and of 1.10^{-4} *M* In^{3+} and 5.10^{-5} *M* Cd^{2+}, respectively, in 1 *M* HCl as supporting electrolyte

instrument than the first part of the polarogram.) The maxima appearing at the half-wave potentials can be used for the evaluation of the respective concentrations of the depolarizers.

The determination of the concentration of the depolarizers is carried out by means of calibration curves, as usual in polarography. It is advisable to trace sets of polarograms where the concentration of one of the ions is kept constant while the other is varied over the concentration range where its determination is feasible. Such a calibration curve is shown in Fig. 10 representing the values of the positive peak of the second harmonic A.C. current

of indium(III) in the presence of various concentrations of cadmium(II) ions in 1 *M* HCl as supporting electrolyte. It is apparent in Fig. 10 that the straight lines corresponding to various cadmium(II) concentrations are parallelly shifted at increasing cadmium(II) concentration and the intercepts of these lines with the ordinate, *i.e.*, the current intensities extrapolated to zero

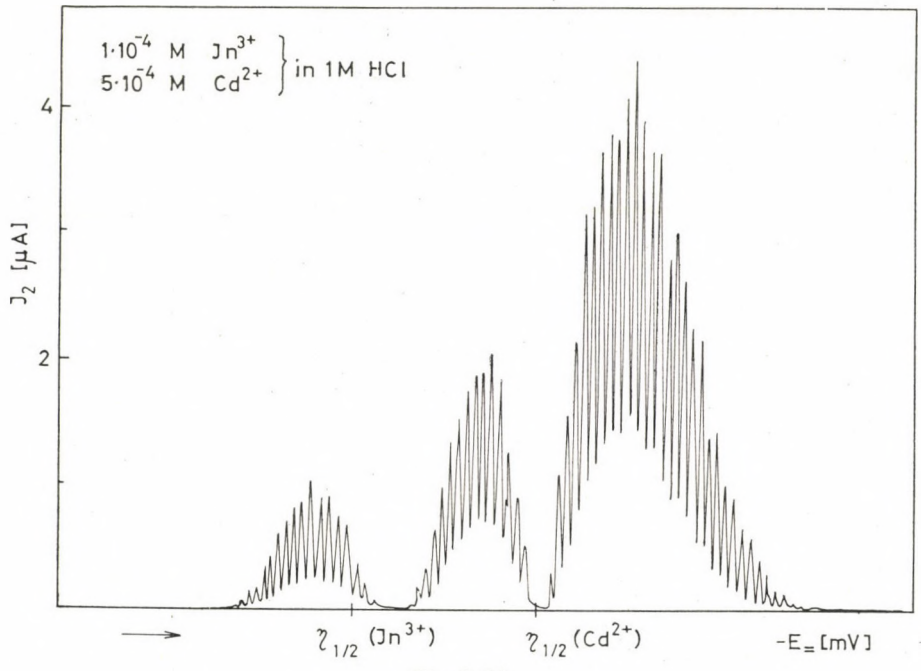

Fig. 9. b)

indium(III) concentration are proportional to the cadmium(II) concentration. This is in accordance with the theoretical interpretation given above regarding the superposition of second harmonic currents of various depolarizers.

Thus, the determination of *e.g.* $1 \cdot 10^{-4}$ *M* In^{3+} is not affected by a tenfold excess of cadmium(II), while the determination of *e.g.* $1 \cdot 10^{-5}$ *M* Cd^{2+} is still possible when an approximately twentyfold excess of indium(III) is present.

Fig. 11 also represents the calibration curve of indium(III). The peak values of the third harmonic A.C. current are plotted as a function of the indium(III) concentration in solutions containing various amounts of cadmium(II). It is apparent in Fig. 11 that $1 \cdot 10^{-4}$ *M* Cd^{2+} did not interfere in the determination of $5 \cdot 10^{-5}$ to $3 \cdot 10^{-4}$ *M* In^{3+}. In the presence of $5 \cdot 10^{-4}$ *M* Cd^{2+} the curves are parallelly shifted to smaller current intensities as the

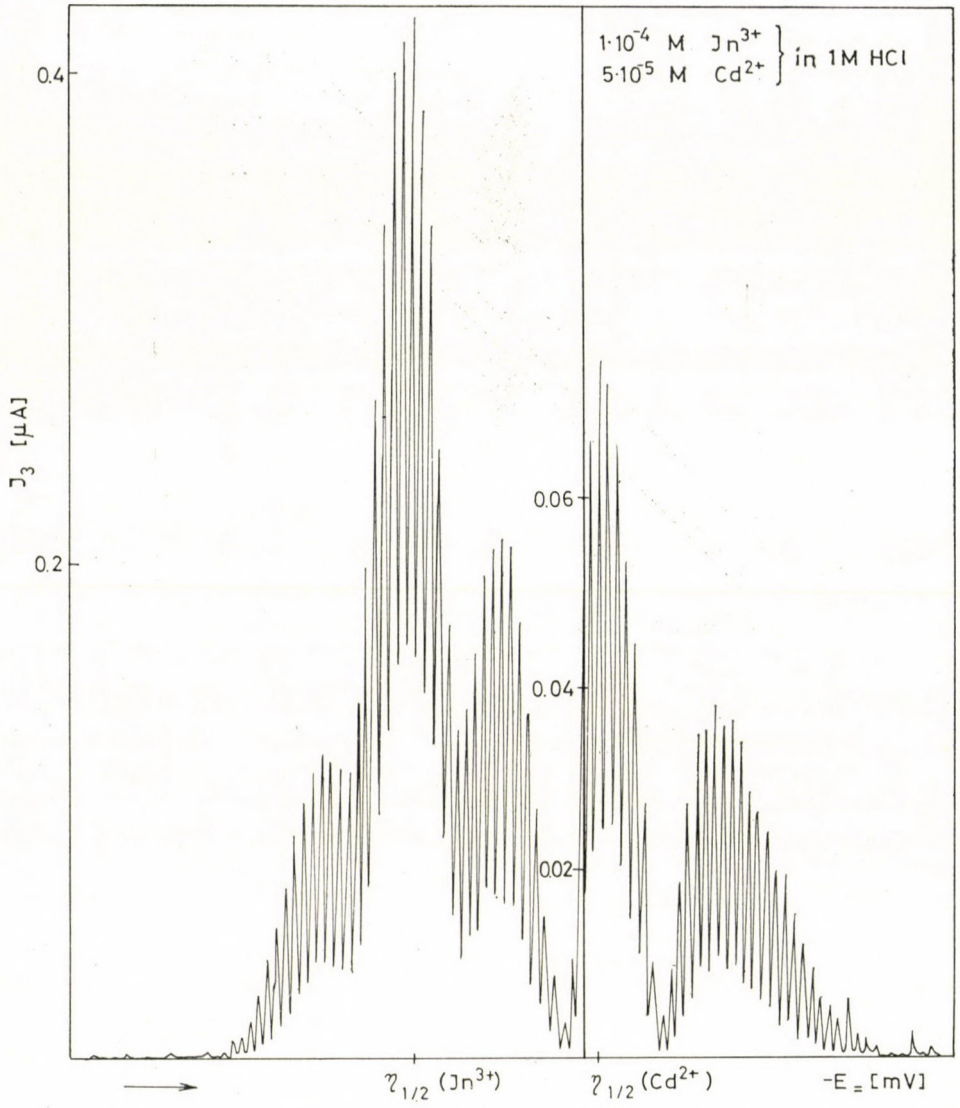

Fig. 9, c)

diffusion current of cadmium(II) at the half-wave potential of indium(III) lowers the peak value of the third harmonic current of the reduction of indium(III), as the difference in the phase angles of these components is 180° at the given potential.

The above examples concerning the simultaneous determination of various ions demonstrate some limiting cases where the difference in the half-

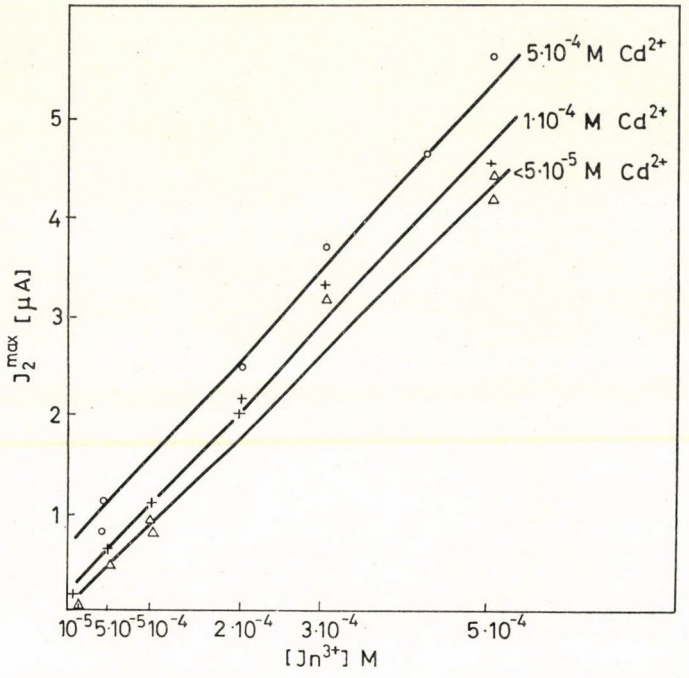

Fig. 10. Maximum values of the second harmonic A.C. current intensities as functions of the indium(III) concentration in the presence of various amounts of cadmium(II) in 1 *M* HCl as supporting electrolyte

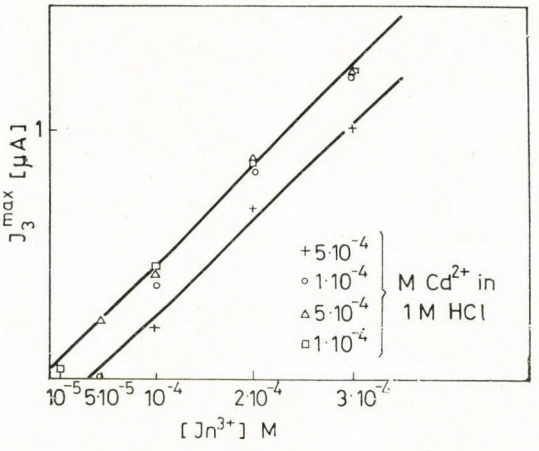

Fig. 11. Maximum values of the third harmonic A.C. current intensities as functions of the indium(III) concentration in the presence of various amounts of cadmium(II) in 1 *M* HCl as supporting electrolyte

wave potentials of the respective ions is small. Practically no mutual interference is encountered in the simultaneous determination of the depolarizers when the difference in their respective half-wave potentials is higher than 150 mV. For instance, the calibration curves of $1 \cdot 10^{-6}$ to $1 \cdot 10^{-3}$ M lead(II) and cadmium(II), respectively, are not altered even when the other ion is present in $1 \cdot 10^{-33}$ M concentration.

The results of these experiments lead to the conclusion that second and third harmonic A.C. polarography is a useful technique for the analysis of multicomponent systems even in such cases when the half-wave potentials of the components differ by less than 200 mV.

The experimental results — in accordance with theoretical expectations — established that the simultaneous determination of two or more ions could be performed by higher harmonic A.C. polarography even in such cases when fundamental harmonic A.C. polarography was found to be inefficient. The range of the concentration ratios of the depolarizers which permitted the quantitative evaluation of the polarograms in a given case depended on the number of electrons involved in the electrode reaction of each component and on the difference in the half-wave potentials of the depolarizers as well as on the kinetic parameters of the polarographic reaction when the latter cannot be considered reversible.

Second harmonic A.C. polarography was found to be more advantageous than third harmonic A.C. polarography in the cases investigated in this study. The determinations were feasible in a larger range of the concentration ratios of the depolarizers and by a smaller difference in the half-wave potentials of the latter when second harmonic A.C. polarography was employed than in the case of third harmonic A.C. polarography. This conclusion, however, cannot be accepted as a general one, as some properties of the third harmonic A.C. component (as *e.g.*, the proportionality of the latter to the forth power of the number of electrons involved in the electrode reaction) may advantageously be employed in certain cases.

REFERENCES

1. Dévay, J., Garai, T., Mészáros, L., Palágyi-Fényes, B.: Magy. Kém. Foly. **75,** 460 (1969): Hung. Sci. Instr. 1969, No. 15, 1.
2. Dévay J., Mészáros, L., Garai, T.: Acta Chim. Hung. **58,** 141 (1968)
3. Dévay, J., Mészáros, L., Garai, T.: Acta Chim. Hung. **60,** 67 (1969): **61,** 279 (1969)
4. Breyer, B., Gutman, F., Hacobian, S.: Austr. J. Sci. Research **A3,** 567 (1950)
5. Bond, A. M., Canterford, J. H.: Anal. Chem. **43,** 393 (1971)
6. Bauer, H. H.: J. Electroanal. Chem. **1,** 2 (1959)
7. Neeb, R.: Z. Anal. Chem. **188,** 401 (1962)
8. Smith, D. E.: Electroanalytical Chemistry Vol. I. (Ed.: Bard, A. J.) Marcel Dekker Inc., New-York, 1966
9. McCord, T. G., Smith, D. E.: Anal. Chem. **40,** 289 (1968)
10. Senda, M., Tachi, I.: Bull. Chem. Soc. Japan **28,** 632 (1955)
11. Senda, M., Delahay, P.: J. Am. Chem. Soc. **83,** 3763 (1961)
12. Smith, D. E.: Anal. Chem. **35,** 1811 (1963)

13. KOOIJMAN, D. J., SLUYTERS, J. H.: Rec. Trav. Chim. Pays-Bas **83,** 587 (1964)
14. DÉVAY, J., GARAI, T., JUHÁSZ, B., MÉSZÁROS, L., PUNGOR, É.: Hung. Sci. Instr. 1968. No. 13, 25
15. MEITES, L.: Polarographic Techniques. Interscience, New York 1965

József DÉVAY
Tibor GARAI
B. PALÁGYI-FÉNYES
Lajos MÉSZÁROS

8201 Veszprém, Schőnherz Z. u. 12. Hungary

SAYED SABAT ABD-EL REHIM; Ain Shamps University, Faculty of Science. Cairo, Egypt.

Acta Chimica Academiae Scientiarum Hungaricae, Tomus 76 (1), pp. 51—68 (1973)

DETERMINATION OF THE HETEROGENEOUS RATE CONSTANT OF THE TRANSITION REACTION BY MEANS OF THE HARMONIC ANALYSIS OF THE CURRENT ON THE ELECTRODE POLARIZED BY A SINUSOIDAL A.C. VOLTAGE SUPERIMPOSED ON THE D.C. POTENTIAL

J. DÉVAY, T. GARAI and L. MÉSZÁROS

(Department of Physical Chemistry, University of Chemical Engineering, Veszprém, and Research Group of Electrochemistry, Hungarian Academy of Sciences, Veszprém)

Received March 2, 1972

The determination of the heterogeneous rate constant of the transition reaction has been examined by means of the second and third harmonic components of the a.c. current flowing through the electrode polarized by a small amplitude sinusoidal a.c. voltage superimposed on the d.c. potential. The rate constant can be evaluated by comparing the experimental data with the curves calculated by a computer program.

In previous communications [1, 2] a mathematical treatment has been given of the current passing through a redox electrode under the effect of an a.c. voltage superimposed on the d.c. potential in the case of transfer and diffusion polarization. Expressions have been derived for the harmonic a.c. components as a function of the potential, the amplitude and frequency of the a.c. voltage, the concentration of the electroactive species in the solution, as well as of the kinetic parameters of the electrode reaction, namely the heterogeneous rate constant and the transfer coefficient.

In the present paper the possibility of the determination of the heterogeneous rate constant will be discussed on the basis of computations performed using the above-mentioned relations.

GRAHAME [3], GERISCHER [4] and KAMBARA [5] pioneered the study of the influence of the rate of the charge-transfer reaction on the Faradaic impedance and on the fundamental harmonic a. c. polarography.

MATSUDA derived a generalized equation of the a.c. fundamental harmonic passing through the d.m.e. for the case of both reversible polarographic reactions [6] and charge-transfer polarization [7]. Matsuda's theoretical calculations have shown that the maximum current intensity of the fundamental harmonic decreases with the decreasing rate of the transfer reaction, other parameters, such as frequency and amplitude of the a.c. voltage, etc., being equal. The potential corresponding to the maximum a.c. intensity is equal to the half-wave potential and is independent of the transfer coefficient in the case of relatively rapid electrode reactions ($k > 1 \times 10^{-2}$ cms^{-1}). However, if the transfer reaction is slow, the peak potential differs from the half-

wave potential. The shift in the peak potential is a complicated function of the rate constant of the electrode reaction, the transfer coefficient and the frequency of the a.c. voltage. The maximum current of the fundamental harmonic depends linearly on the square root of the angular frequency of the a.c. voltage if the rate constant of the transfer reaction is relatively high ($k > 1 \times 10^{-2}$ cms^{-1}) (the current passing through the double layer capacitance is disregarded). A deviation from the above linear relationship is observed in the case of low reaction rates ($k < 1 \times 10^{-2}$ cms^{-1}). The extent of this deviation is considerably affected by the transfer coefficient. At a low rate constant of the transfer reaction the current of the fundamental harmonic as a function of the d.c. potential is symmetrical with respect to the peak potential only if the transfer coefficient is $\alpha = 0.5$. At other values of the transfer coefficient the shape of the current–potential curve depends on the rate constant and the transfer coefficient as well as on the frequency of the a.c. voltage.

SMITH and MCCORD [8] extended their calculations on the a.c. passing through the d.m.e. to very low rate constant charge-transfer reaction ($k \cong 1 \times 10^{-6}$ cms^{-1}) and showed that—contrary to previous expectations — an a.c. fundamental harmonic was detectable even in these cases, however, the a.c. density was very low.

The second harmonic component of the a.c. passing through the electrode polarized by an a.c. voltage superimposed on the d.c. potential was also the subject of numerous studies (*cf.* Ref. [1]).

The current density *vs.* potential function of the second harmonic a.c. component was found to be more sensitive to the kinetic parameters of the electrode reaction than the fundamental harmonic [9].

VAN CAKENBERGHE [10] noted that the potential corresponding to the maximum value of the second harmonic was affected by the transfer coefficient and the latter could be calculated from the shift of the potential corresponding to the minimum value of the second harmonic relative to the half-wave potential. BAUER and ELVING [11] employed this method for the determination of the transfer coefficient of various electrode reactions. However, REINMUTH [12] questioned the reliability of this technique because the minimum value of the second harmonic is zero only when $\alpha = 0.5$.

BAUER [3] studied the dependence of the a.c. second harmonic on the rate constant of the electrode reaction and on the transfer coefficient. Numerical calculations showed that these parameters effect the dependence of the second harmonic a.c. intensity on the d.c. potential and the ratio of the two maximum values. BAUER concluded that the periodic functions describing the concentration changes at the electrode surface and the effect of the sinusoidal a.c. voltage did not contain higher harmonics. Later BAUER and FOO [14] corrected this statement.

McCORD and SMITH [15] derived the formulas for the second harmonic component of the a.c. polarographic current as a function of the d.c. potential and performed numerical calculations in order to evaluate the effect of the kinetic parameters of the electrode reaction on the second harmonic a.c. polarogram and on its frequency dependence. Smith's treatment was based on MATSUDA's theory [7], thus due consideration was given to the effect of the drop time of the d.m.e. on the a.c. second harmonic, as Matsuda employed the "expanding plane" electrode model in his calculations. According to SMITH'S theoretical treatment the current density and the phase angle of the second harmonic as a function of the d.c. potential was affected to a greater extent by the drop time of the d.m.e. in the case of a slow transfer reaction than in the case of a reversible polarographic process [9, 16]. The kinetic parameters of an electrode reaction cannot be evaluated in an explicit form from the formulas relating to the second harmonic a.c. intensity and thus they could only be determined by a comparison of the experimental data and the functions calculated, assuming various kinetic parameters. The diffusion coefficients of the components taking part in the electrode reaction and the half-wave potential have to be calculated from independent measurements [15]. Our mathematical treatment [1] has led to the same general results. The third harmonic component of the a.c. intensity was also examined [2].

Results

Our theory concerning the harmonic components of the a.c. passing through the electrode polarized by a small amplitude sinusoidal voltage superimposed on the d.c. potential is based on the solution of the equation of linear diffusion with appropriate boundary conditions and refers to well-defined hydrodynamic conditions. The current density of the fundamental, the second and of the third harmonic a.c. components were given as functions of the time average value of the overpotential ($\eta_{=}$), the amplitude ($\eta_{\sim}$) and the angular frequency (ω) of the a.c. voltage, the concentration of the components taking part in the electrode reaction (c_{10}, c_{20}), as well as the transfer coefficient (α) and the heterogeneous rate constant of charge-transfer reaction (k). The kinetic parameters of the electrode reaction could not be obtained in an explicit form as the mathematical expressions were too complicated. However, the dependence of the amplitude of the a.c. harmonic components on the kinetic parameters could be investigated by means of numerical calculations assuming various values of the parameters (ω, $\eta_{=}$, $\eta_{\sim}$, c_{10}, c_{20}) susceptible to experimental control.

The programming and the calculations were performed by the Computer Center of the Hungarian Academy of Sciences.

We present here some of the results of these calculations. The calculations were made on some simplifying assumptions, namely $c_{10} = c_{20}$ and $D_1 = D_2$, *i. e.*, the concentrations and the diffusion coefficients of both the oxidized and the reduced form of the component taking part in the redox reaction were assumed to be equal; further, the cell resistance was assumed to be zero. It is easier to make a comprehensive survey of the results with these assumptions. The parameters employed in the calculation were the following: $c_{10} = c_{20} = 1 \times 10^{-4}$ mol/l, $D_1 = D_2 = 1 \times 10^{-5}$ cm^2 s^{-1}, $C = 25\ \mu$F, $\omega = 500$ s^{-1}, $\eta_\sim = 1 \times 10^{-3}$ V, $z = 2$ and $z = 1$ in the calculations relating to the third harmonic a.c. density; the values of the heterogeneous rate constants and of the transfer coefficients are indicated in the Figures.

1. Fundamental harmonic a.c. component of the current

The results of the calculations concerning the fundamental harmonic are shown in Figs 1 to 3. Fig. 1 represents the current density of the a.c. fundamental harmonic as a function of the d.c. potential for various charge-transfer rate constants. The transfer coefficient was assumed to be $\alpha = 0.5$.

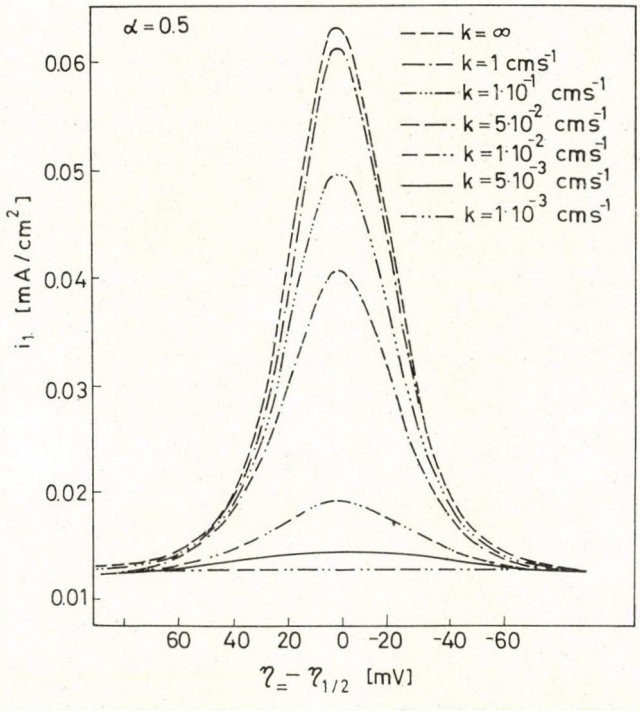

Fig. 1. Fundamental harmonic a.c. density as a function of the potential in the case of $\infty \geqslant k \geqslant 1 \times 10^{-3}$ cms^{-1} and $\alpha = 0.5$ (other parameters in the text)

It is apparent from Fig. 1 that the curves relating to the fundamental harmonic exhibit a maximum at the half-wave potential, while at more positive and more negative potentials than the latter they rapidly decrease and tend to a limiting value corresponding to the current across the electric double layer. Thus the fundamental harmonic a.c. component is the vectorial sum of the Faradaic current and the condenser current. The maximum current density of the fundamental harmonic decreases with decreasing values of the rate constant. The decrease in the maximum current density of the fundamental harmonic, as compared to the case of $k \to \infty$, is not greater than 5 per cent in the range of $\infty > k > 1$ cms^{-1}. However, at values of the rate constant ranging from $1 \times 10^{-1} > k > 1 \times 10^{-3}$, this decrease becomes very important.

Fig. 2 illustrates the influence of the transfer coefficient on the a.c. fundamental harmonic *vs.* potential curves. The parameters of the curves in Figs 2 and 1 are identical except that the transfer coefficients are $\alpha = 0.7$ and $\alpha = 0.5$, respectively. A comparison of Figs 1 and 2 indicates that the shape of the curves is not modified when the transfer coefficient differs from $\alpha = 0.5$ at $k > 1 \times 10^{-1}$cms^{-1} in the case of the parameters employed in the calculations. However, at lower values of the rate constant ($1 \times 10^{-1} > k >$

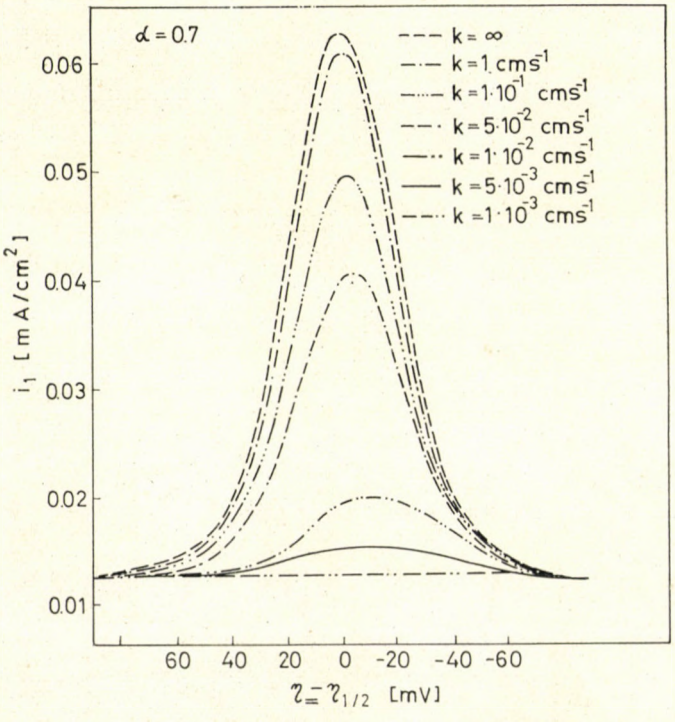

Fig. 2. Fundamental harmonic a.c. density as a function of the potential in the case of $\infty > k > 1 \times 10^{-3}$ cms^{-1} and $\alpha = 0.7$ (other parameters in the text)

1×10^{-3} cms^{-1}) the symmetry of the fundamental harmonic a.c. functions related to the half-wave potential is altered, i.e. the maximum of the fundamental harmonic a.c. density is exhibited at a potential differing from the half-wave potential. The peak potential is more positive than the half-wave potential when the transfer coefficient is $\alpha < 0.5$, while the opposite occurs when $\alpha > 0.5$.

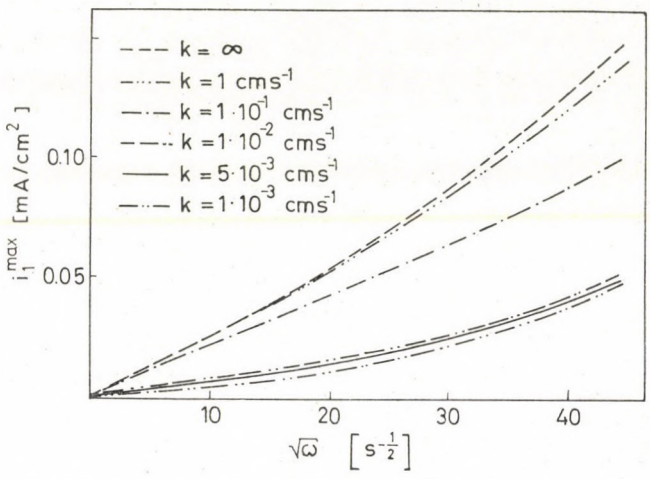

Fig. 3. Maximum current density of fundamental harmonic a.c. as a function of the square root of the frequency of the a.c. voltage

In Fig. 3 the effect of the frequency of the a.c. voltage on the a.c. fundamental harmonic peak currents is shown for various values of the charge-transfer rate constant. The maximum values of the fundamental harmonic a.c. are plotted against the square root of the angular frequency of the a.c. voltage. It is apparent from Fig. 3 that the peak values of the fundamental harmonic linearly increase as a function of the square root of the angular frequency when $k > 1 \times 10^{-1}$ cms^{-1} and $\omega < 200$ s^{-1}, while the curves are convex from below when $\omega > 200$ s^{-1}. These results can be explained by the fact that the condenser current proportional to ωC is negligible compared to the Faradaic current when $\omega < 200$ s^{-1} in the case of the parameters employed in the calculations. The Faradaic component of the fundamental harmonic a.c. decreases with decreasing rate constants of the electrode reaction in the range $1 \times 10^{-1} > k > 1 \times 10^{-3}$ cms^{-1}. Consequently, it becomes gradually smaller as compared to the current passing through the impedance of the double-layer capacity. At about $k = 1 \times 10^{-3}$ cms^{-1}, the current density of the fundamental harmonic a.c. Faradaic current is so small, that it is practically indiscernible from the current passing through

the impedance of the double-layer capacity. Thus, the results concerning the fundamental harmonic a.c. density are in good agreement with the results described in the literature (cf. MATSUDA [6, 7], SMITH [9], etc.).

2. Second harmonic a.c. component of the current

The second harmonic a.c. density deserves a more detailed examination.

First, the effect of the heterogeneous rate constant on the second harmonic is considered, assuming $\alpha = 0.5$.

The second harmonic a.c. density is shown in Fig. 4 as a function of the d.c. potential assuming the above parameter values in the case of $\alpha = 0.5$ and $\infty > k > 1 \times 10^{-3}$ cms^{-1}. It is apparent from Fig. 4 that the amplitude of the second harmonic a.c. density exhibits a minimum at the half-wave potential and two maxima, one at more positive and one at more negative potentials than the latter. The difference of the peak potential and the half-wave potential depends on the number of electrons involved in the electrode reaction and on the heterogeneous rate constant. The current density of the second harmonic decreases with the decreasing rate constant of the electrode reaction when $k > 1 \times 10^{-3}$ cms^{-1}. It is interesting to note that only a slight decrease of about 5 to 10% in the maximum current density of the second harmonic is found when the rate constant is $k > 1$ cms^{-1} as compared to the case when $k \to \infty$. However, the second harmonic current density rapidly decreases at lower values of the rate constant ($k < 1 \times 10^{-1}$ cms^{-1}). The latter considerably affects the magnitude of the current density of the second harmonic in the range of $1 \times 10^{-1} > k > 1 \times 10^{-3}$ cms^{-1}. The decrease in the rate constant also modifies the shape of the current-potential curve. Thus, the difference in the potentials corresponding to the maximum values of the second harmonic increases with a decreasing rate constant.

It is apparent from Fig. 4 that the curves are symmetrical with respect to the half-wave potential when $\alpha = 0.5$. However, this symmetry is not maintained at $\alpha \neq 0.5$. The asymmetry of the curves is enhanced by decreasing rate constants and by an increasing deviation of the transfer coefficient from $\alpha = 0.5$. It is noteworthy that, according to the calculations of SMITH *et al.* [8], based on the 'expanding plane' electrode model of the d.m.e., the symmetry of the second harmonic *vs.* potential curve is not maintained, even when $\alpha = 0.5$, in the range of rate constants: $1 \times 10^{-2} > k > 1 \times 10^{-4}$ cms^{-1}. Thus, according to these authors, the second harmonic a.c. density *vs.* potential functions are symmetrical with respect to the half-wave potential only when $k > 1 \times 10^{-2}$ cms^{-1} and $\alpha = 0.5$.

The effect of the transfer coefficient on the second harmonic a.c. component at various values of the rate constant is shown in Fig. 5 representing the

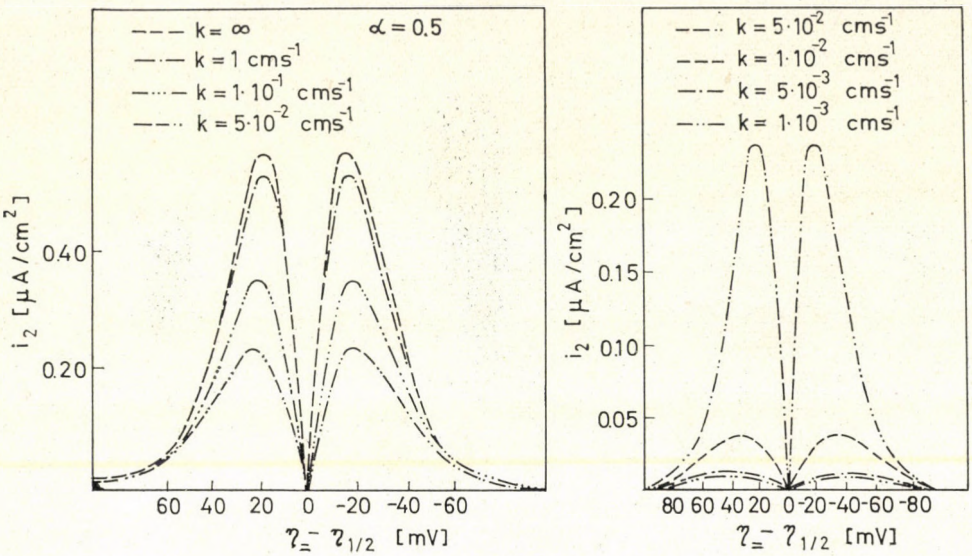

Fig. 4. Second harmonic. a.c. current density as a function of the potential in the case of $\infty \geqslant k \geqslant 1 \times 10^{-3}$ cms^{-1} and $\alpha = 0.5$ (other parameters in the text)

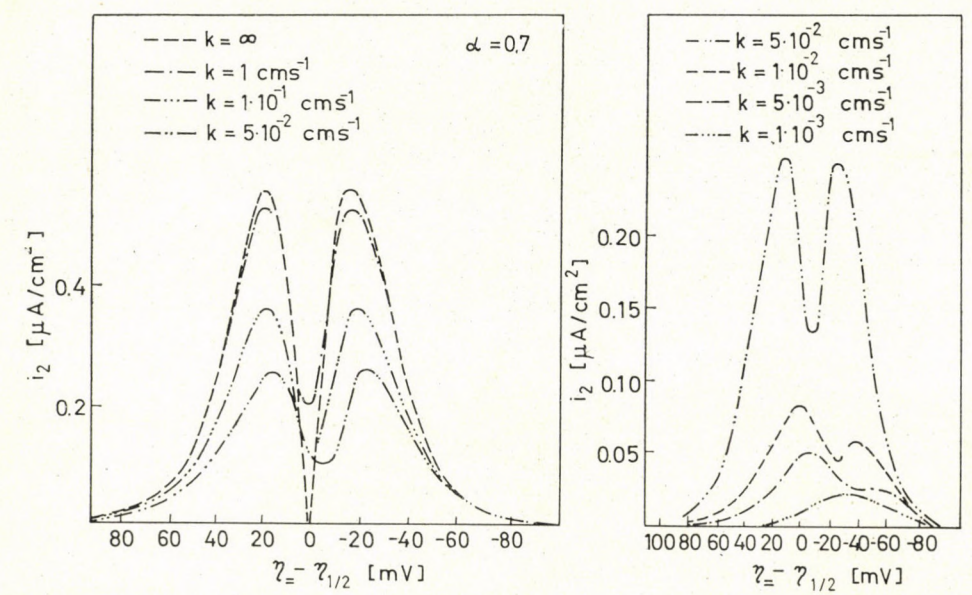

Fig. 5. Second harmonic a.c. current density as a function of the potential in the case of $\infty \geqslant k \geqslant 1 \times 10^{-3}$ cms^{-1} and $\alpha = 0.7$ (other parameters in the text)

function for $\infty > k > 1 \times 10^{-3}$ cms^{-1} and $\alpha = 0.7$. It is apparent from Fig. 5 that the curves are practically independent of the transfer coefficient when $k > 1$ cms^{-1}, as in this case the deviation from the curves calculated for $\alpha = 0.5$ is smaller than the expected experimental error. The deviation of the transfer coefficient from $\alpha = 0.5$ is manifested by the distortion of the symmetry of the curves when $k < 1$ cms^{-1}. It is noticeable in Fig. 5 that the ratio of

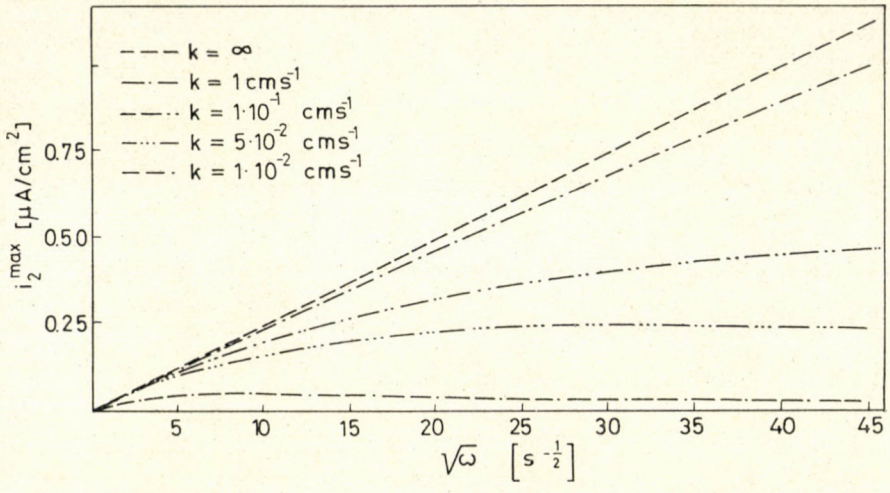

Fig. 6. Maximum second harmonic a.c. current density as a function of the square root of the frequency of a.c. voltage in the case of $\infty \geqslant k \geqslant 1 \times 10^{-2}$ cms^{-1}

the maximum values of the second harmonic a.c. polarograms differs from unity. This difference increases with the increasing deviation of the transfer coefficient from $\alpha = 0.5$. The shape of the second harmonic *vs.* potential curves is considerably altered, when $\alpha = 0.7$ and the rate of the electrode reaction is $k < 1 \times 10^{-1}$ cms^{-1}. The minimum amplitude of the second harmonic is not zero and the potential corresponding to this minimum is shifted towards more negative values from the half-wave potential. This shift in the potential increases with the increasing frequency of the a.c. voltage and with the decreasing rate constant of the charge-transfer reaction. The minimum of the current density differs from zero when $\alpha \neq 0.5$ [12].

It is noteworthy that in the case of $\alpha \neq 0.5$ the functions obtained for transfer coefficients of α and $1-\alpha$ are mirror images.

The dependence of the second harmonic a.c. current density on the frequency is shown in Figs 6 and 7, where the peak values of the current are plotted against the square root of the frequency of the a.c. voltage for various values of the heterogeneous rate constant.

It is apparent from the curves that the maxima of the second harmonic current densities increase linearly with the square root of the angular frequency of the a.c. voltage in the case of reversible polarographic reactions. However, at smaller values of the rate constant, the slope of the curves decreases. The deviation of the curves from linearity exhibited at $k \to \infty$ is not larger than 10

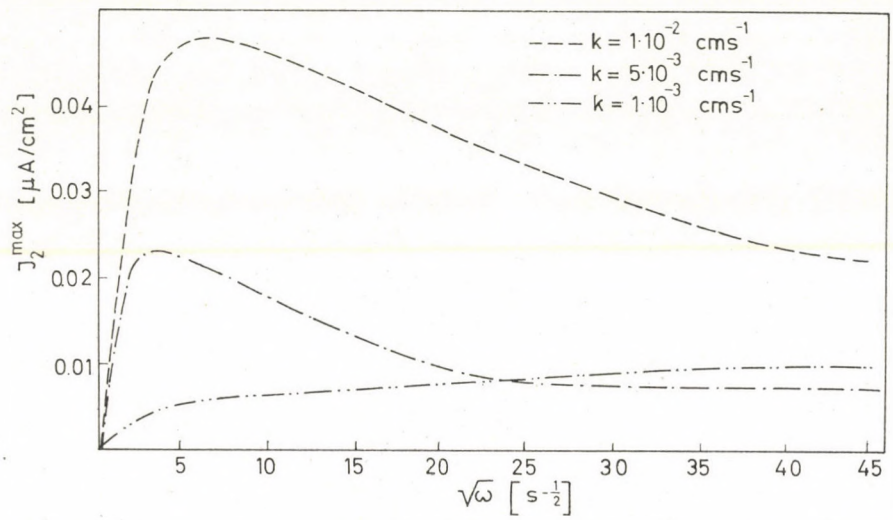

Fig. 7. Maximum second harmonic a.c. density as a function of the square root of the frequency of a.c. voltage in the case of $1\times10^{-3} \leqslant k \leqslant 1\times10^{-2}$ cms^{-1}

per cent in the frequency range most suitable for the measurements ($\omega < 2000$ s^{-1}) when $k > 1$ cms^{-1}, while the peak values of the second harmonic a.c. densities tend to a limiting value with increasing frequencies in the range of heterogeneous rate constants $1\times10^{-1} > k\, 5\times10^{-2}$ cms^{-1}, as shown in Fig. 6. It is noteworthy that the curves representing the peak values of the second harmonic a.c. density as plotted against the square root of the frequency exhibit maxima at lower frequencies ($\omega < 200$ s^{-1}) in the case of $1\times10^{-2} > k > 1\times10^{-3}$ cms^{-1}. The maximum is shifted to lower frequencies with decreasing values of the heterogeneous rate constant.

3. Third harmonic a.c. component of the current

Many analogies can be found between the functions relating to the third harmonic a.c. component of the current and the above data on the second harmonic, as it is apparent from Fig. 8 representing the amplitude of the third harmonic a.c. current density plotted against the potential for $\infty > k$

$\geqslant 1\times10^{-2}$ cms^{-1} and $\alpha = 0.5$. The curves exhibit a maximum at the half-wave potential and two other maxima at more positive and more negative potentials, respectively, than the half-wave potential. Two minima appear between the peak values at potentials corresponding to the maxima of the second harmonic a.c. component.

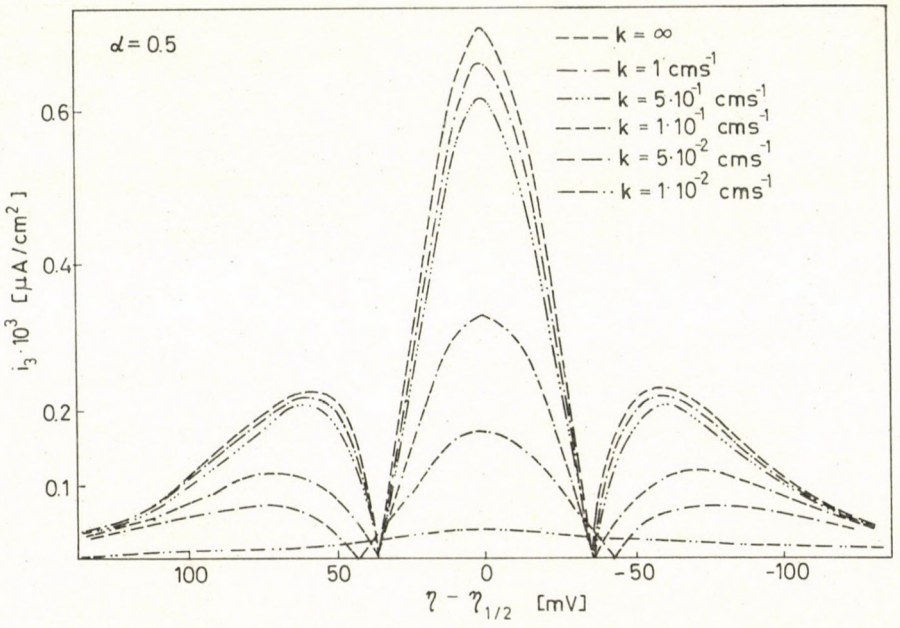

Fig. 8. Third harmonic a.c. density as a function of the potential in the case of $\infty \geqslant k \geqslant 1\times10^{-2}$ cms^{-1} and $\alpha = 0.5$ (other parameters in the text)

The functions relating to the third harmonic a.c. component are symmetrical with respect to the half-wave potential when $\alpha = 0.5$ as in the case of the second harmonic a.c. density *vs.* potential curves. At smaller values of the heterogeneous rate constant, the amplitude of the third harmonic a.c. density decreases, while the differences between the peak potentials and the half-wave potential, as well as between the potentials corresponding to the minimum current density increase. The ratio of the maxima appearing at the half-wave potential and at more negative (or more positive) potentials than the latter decreases with decreasing values of the heterogeneous rate constant. The maximum appearing at the half-wave potential is three times larger than the others in the case of diffusion polarization, while it is 1.8 times larger only when $k = 1\times10^{-2}$ cms^{-1}.

The effect of the transfer coefficient on the third harmonic a.c. density *vs.* potential functions is shown in Fig. 9. The parameters employed in the

calculations were the same as in the case of Fig. 8, except that $\alpha = 0.7$ was assumed instead of $\alpha = 0.5$. The symmetry of the curves with respect to the half-wave potential is distorted at transfer coefficient values differing from $\alpha = 0.5$, similarly to the case of the functions relating to the second harmonic a.c. component. This phenomenon is observed at lower frequencies by decreasing values of the rate constant and by increasing deviation of the trans-

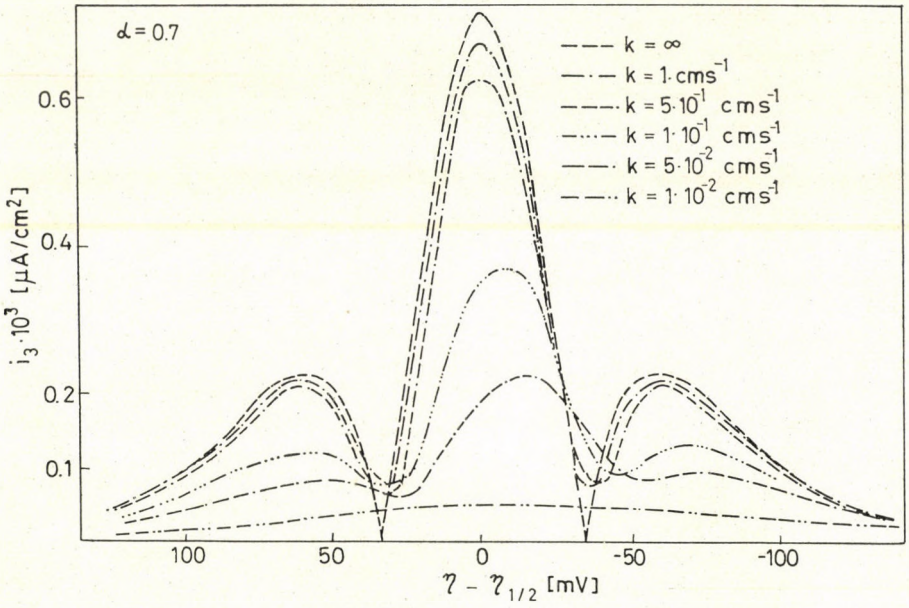

Fig. 9. Third harmonic a.c. density as a function of the potential in the case of $\infty \geqslant k \geqslant 1\times10^{-2}$ cms^{-1} and $\alpha = 0.7$, for $z = 1$ (other parameters in the text)

fer coefficient from $\alpha = 0.5$. For smaller values of the rate constant, the peak value appearing at the half-wave potential is shifted towards more negative potentials when $\alpha > 0.5$. The maxima exhibited at more positive and more negative potentials than the half-wave potential gradually disappear. Two peak values are observed at sufficiently high frequencies in the case of $k < 1\times10^{-2}$ cms^{-1}.

If other parameters are identical, the functions belonging to α and $1-\alpha$ in the case of the third harmonic a.c. component are mirror images of each other. The dependence of the maximum amplitudes of the third harmonic a.c. component on the square root of the frequency is similar to that of the second harmonic peak values (Fig. 10). It is noteworthy, however, that the deviation from linearity is larger and is observed at lower frequency values in the former case.

4. Determination of the heterogeneous rate constant of the charge-transfer reaction

The results of the calculations briefly outlined in the previous paragraphs lead to the conclusion that the heterogeneous rate constant of the charge-transfer reaction can be determined by the measurement of the harmonic components of the current as a function of the potential and the angular frequency of the a.c. voltage superimposed on the d.c. polarizing potential.

The results obtained in this study relating to the fundamental harmonic a.c. component (*i.e.* the Faradaic impedance) are in good agreement with the results reported in the literature [5—10]. As far as the determination of the kinetic parameters of the transfer reaction is concerned, the study of the higher harmonic components of the current appears to be superior to the investigation of the fundamental harmonic by virtue of the elimination, or at least considerable decrease, of the interfering effect caused by the current flowing through the double-layer capacity. The results relating to both the second and the third harmonic a.c. component give evidence that these techniques are fruitful in the range of rate constants $1 > k > 5 \times 10^{-3}$ cms^{-1}. The harmonic components of the a.c. are equal within the experimental error to the relationships valid for diffusion polarization in the case a relatively rapid charge-transfer reaction ($k > 1$ cms^{-1}.) Thus, the results concerning the kinetic parameters of the electrode reaction become unreliable. On the other hand, the potential and frequency dependence of the higher harmonic components of the a.c. are only slightly affected by the rate constant of the charge-transfer reaction when the latter is relatively slow ($k < 5 \times 10^{-3}$ cms^{-1}) and the measurement of small currents also causes experimental difficulties in these cases. The study of the d.c. polarization curves yields reliable data when $k \approx 1 \times 10^{-3}$ cms^{-1} [18].

The experimental method for determining the rate constant of the charge-transfer reaction consists in the selective measurement of the a.c. harmonic components as functions of the potential, by the superposition of a small amplitude sinusoidal a.c. voltage at various frequencies. The a.c. harmonic components *vs.* potential plots are obtained from the experimental results after correction for the ohmic potential drop across the cell resistance [19]. The experimental results are compared with the calculated data by means of a computer program. The rate constant and the transfer coefficient of the electrode reaction are evaluated by fitting the experimental curves to the calculated ones in the frequency range employed in the experiments.

The frequency dependence of the peak values of the a.c. harmonic components yields informative data on the proper selection of the range of parameter values needed in the computer program and gives an approximate value of the rate constant of the charge-transfer reaction.

It is apparent from Figs 6, 7 and 11 relating to the second harmonic, as well as from Figs 10 and 12 relating to the third harmonic, that the peak current density varies linearly with the square root of the a.c. frequency, irrespective of the value of the transfer coefficient, when $k > 1 \times 10^{-1}$ cms^{-1}. A deviation is observed from the linear relation valid for diffusion polariza-

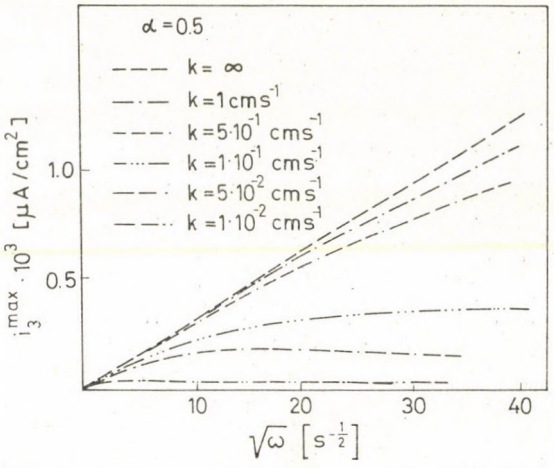

Fig. 10. Maximum third harmonic a.c. current density as a function of the square root of the a.c. frequency

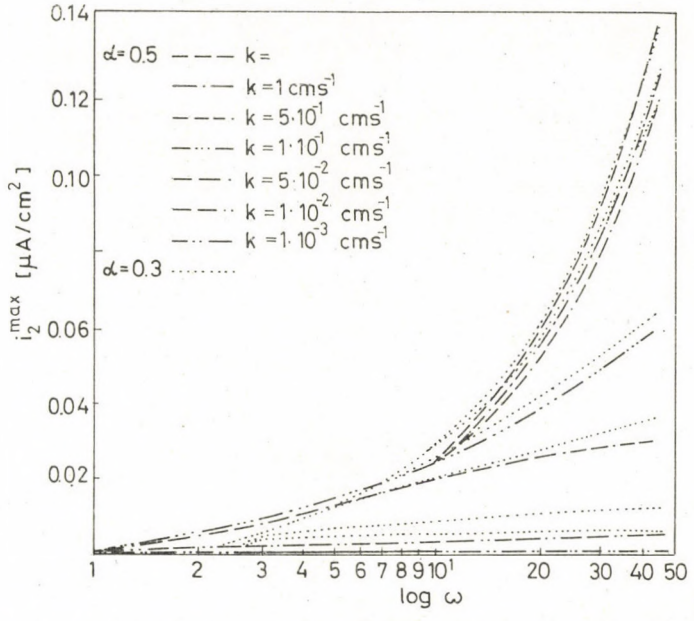

Fig. 11. Maximum second harmonic a.c. current density as a function of the logarithm of the a.c. frequency

tion by decreasing values of the rate constant of the heterogeneous reaction ($k < 1 \times 10^{-1}$ cms^{-1}); the smaller the rate constant, the lower the frequency at which this occurs. The peak values of the current density gradually become proportional to the logarithm of the frequency at the rate constant $k < 1 \times 10^{-1}$ cms^{-1}. It is apparent from Figs 11 and 12 that the maximum amplitudes of the higher harmonics are not independent of the transfer coefficient at small values of the rate constant. However, the determination of approximate data is not prevented by these deviations. The a.c. harmonic components *vs.* potentia

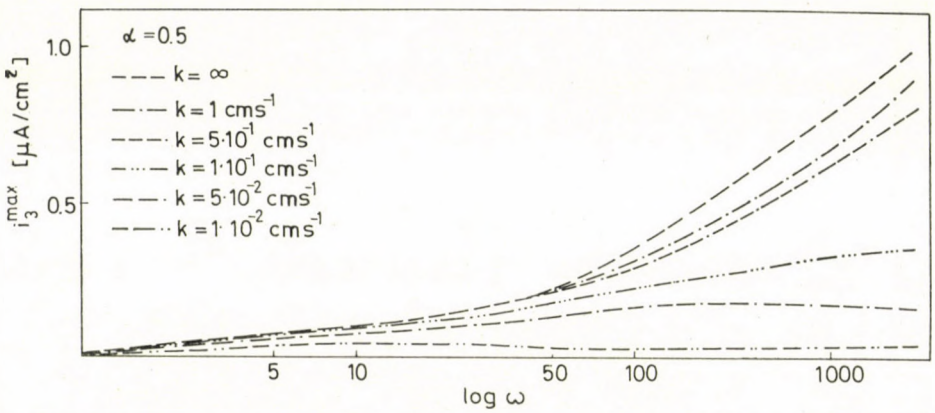

Fig. 12. Maximum third harmonic a.c. current density as a function of the logarithm of the a.c. frequency

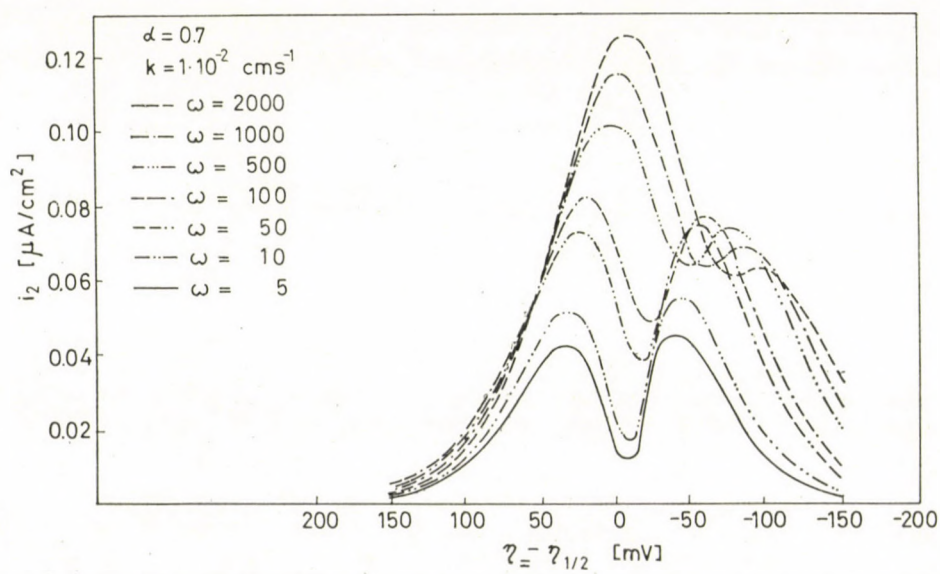

Fig. 13. Second harmonic a.c. current density as a function of the potential in the case of $5 \leqslant \omega \leqslant 2000$ s^{-1} and $\alpha = 0.7$ ($z = 1$; other parameters in the text)

curves at various a.c. frequencies also give a certain amount of information. An example of this is shown in Figs 13 and 14 representing the amplitude of the second and the third harmonic a.c. component, respectively, as a function of the potential at various frequencies, assuming $k = 1 \times 10^{-2}$ cms^{-1} and $\alpha = 0.7$. At low frequencies the curves are slightly different from those calculated for the case of diffusion polarization. It is also apparent from Fig. 13 that the minimum of the second harmonic is not equal to zero and the potential cor-

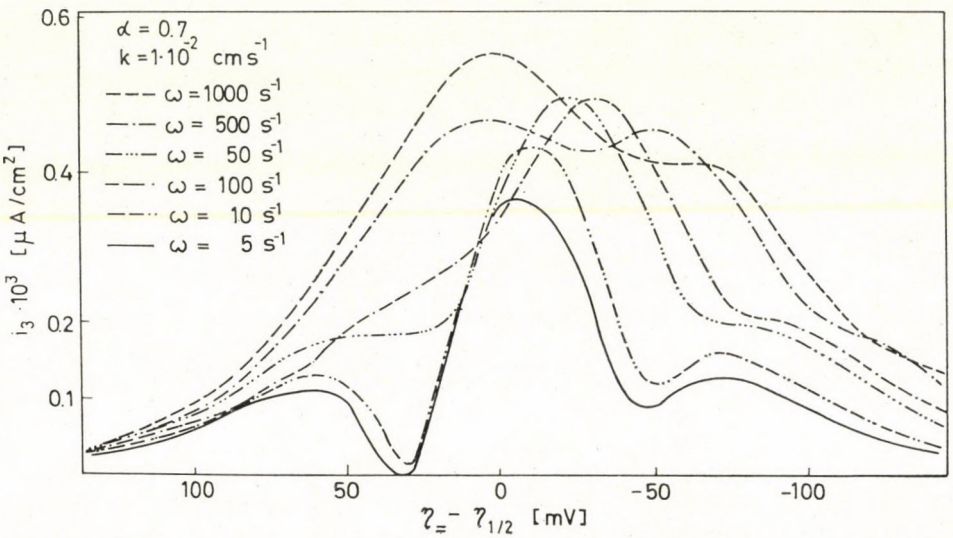

Fig. 14. Third harmonic a.c. current density as a function of the potential in the case of $5 \leqslant \omega \leqslant 2000$ s^{-1} and $\alpha = 0.7$ ($z = 1$; other parameters in the text)

responding to the minimum is shifted towards more negative potentials at $\omega < 100\ s^{-1}$, while the ratio of the maximum amplitudes considerably deviates from unity, at higher frequencies (in contrast to the case of $\alpha = 0.5$). At sufficiently high frequencies only one maximum is observed and an inflexion point appears instead of the minimum. It is apparent from Fig. 14 that in the case of the third harmonic a.c. component the minima become indefinite in the frequency range $\omega < 100$ s^{-1}, while at higher frequencies two approximately equal maxima are exhibited instead of the peak values appearing at the half-wave potential. The ratio of the peak values differs from unity upon further increasing the frequency. These phenomena are observed at lower frequencies when the rate constant becomes smaller. Thus, the evaluation of the results is facilitated by extending the measurements to lower frequencies ($\omega < 50$ s^{-1}).

It is noteworthy that the difference between the potential corresponding to the minimum of the second harmonic a.c. component and the half-wave potential (calculated for the reversible polarographic reaction) depends charac-

teristically on the frequency for $\alpha \neq 0.5$. It is apparent from Fig. 15 that the difference of the minimum potential of the second harmonic a.c. component and of the half-wave potential ($\Delta\eta = \eta_{min} - \eta_{1/2}$) increases linearly with the square root of the frequency in the range $\omega < 1000\ s^{-1}$ when $k \geq 1 \times 10^{-2}$ cms^{-1}. However, the plot is only linear at $\omega < 100\ s^{-1}$ when $k = 5 \times 10^{-3}$ cms^{-1}. In the latter case $\Delta\eta$ is a linear function of the logarithm of the frequency in the range $50 < \omega < 500\ s^{-1}$. At higher values of the rate constant the logarithmic $\Delta\eta$ *vs.* ω relation is observed from higher frequencies. The dependence on the frequency of the difference between the peak potential of the third harmonic a.c. component and the reversible half-wave potential is similar to that encountered in the previous case.

In the present paper we focused our interest mainly on the determination of the rate constant of the charge-transfer reaction by examining the

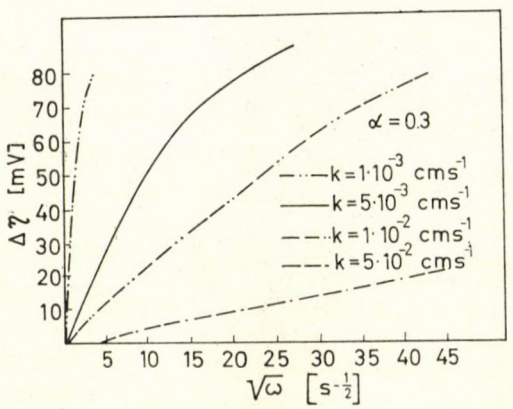

a)

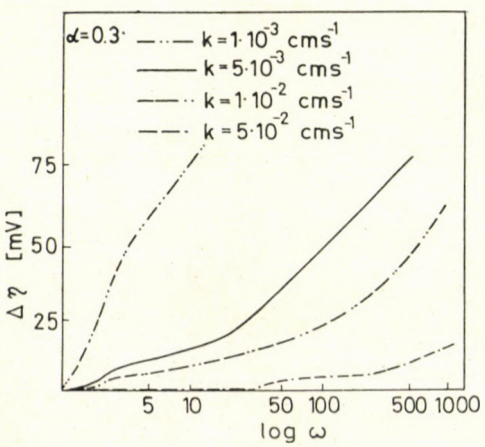

Fig. 15. Difference of the peak potential of the second harmonic a.c. density and the half-wave potential as a function of a) square root, and b) logarithm of the a.c. frequency in the case of $\alpha = 0.3$.

second and third harmonic components of the a.c. current flowing through the electrode polarized by a small amplitude sinusoidal a.c. voltage superimposed on the potential. The determination of the transfer coefficient and the investigation of the effect of hydrodynamic parameters will be described in a subsequent paper.

REFERENCES

1. DÉVAY, J., MÉSZÁROS, L., GARAI, T.: Acta Chim. Acad. Sic. Hung., **58,** 141 (1968)
2. DÉVAY, J., MÉSZÁROS, L., GARAI, T.: Acta Chim. Acad. Sci. Hung. (In press)
3. GRAHAME, D. D.: J. Electrochem. Soc., **99,** 370C (1952)
4. GERISCHER, H.: Z. phys. Chem. N. F. **1,** 278 (1954)
5. KAMBARA, T.: Z. Phys. Chem. N. F. **5,** 52 (1955)
6. MATSUDA, H.: Z. Electrochem., **61,** 489 (1967)
7. MATSUDA, H.: Z. Electrochem., **62,** 997 (1958)
8. SMITH, D. E., MCCORD, T. G.: Anal. Chem., **40,** 474 (1968)
9. SMITH, D. E.: Electroanalytical Chemistry. Vol. 1. Ed. A. J. Bard, Marcel Dekker, New York 1966
10. VAN CAKENBERGHE, J.: Bull. Soc. Chim. Belge, **60,** 3 (1951)
11. BAUER, H. H., ELVING, P. J.: Anal. Chem., **30,** 341 (1958)
12. REINMUTH, W. H.: Anal. Chem., **36,** 211R (1964)
13. BAUER, H. H.: Austr. J. Chem., **17,** 591, 715 (1964)
14. BAUER, H. H., FOO, D. C. S.: Austr. J. Chem., **19,** 1103 (1966)
15. MCCORD, T. G., SMITH, D. E.: Anal. Chem., **40,** 289 (1968)
16. MCCORD, T. G., BROWN, E. R., SMITH, D. E.: Anal. Chem., **38,** 1615 (1966)
17. MCCORD, T. G., SMITH, D. E.: Anal. Chem., **41,** 131 (1969)
18. ERDEY-GRÚZ, T.: Elektródfolyamatok kinetikája (in Hungarian), Akadémiai Könyvkiadó, Budapest 1969
19. DÉVAY, J., MÉSZÁROS, L., GARAI, T.: Acta Chim. Acad. Sci. Hung., **60,** 67 (1969)

József DÉVAY
Tibor GARAI
Lajos MÉSZÁROS
8201 Veszprém, Schönherz Z. u. 12. Hungary

Acta Chimica Academiae Scientiarum Hungaricae, Tomus 76 (1), pp. 69—80 (1973)

EQUILIBRIUM TREATMENT OF THE WATER–ACETONE SYSTEM

M. SIMONYI, J. KARDOS and A. NESZMÉLYI

(Central Research Institute for Chemistry of the Hungarian Academy of Sciences, Budapest)

Received March 13, 1972

Two simple equilibrium models have been outlined to interpret experimental chemical shifts in water–acetone mixtures. The first model covers a wide range: $0.9 > > x_{H_2O} > 0.02$ and implies a solvate exchange in which any one molecule is an active participant. Equilibrium constants determined by three different resonance techniques equal 0.62 (water ^1H); 2.04 (carbonyl ^{17}O) and 1.32 (carbonyl ^{13}C) unequivocally suggesting that water-water solvation slightly dominates over the water–acetone one. The second model seems to be valid for the range $0.14 > x_{H_2O} > 0$ and implies stepwise hydrogen bonding between water and acetone but neglects water–water interaction. Since the second model considers three individual water states, it is non-determinate and can be tested only by introducing arbitrary equilibrium constants.

Introduction

In a previous study on hydrogen isotope exchange between water and hydroquinone, acetone has been used as a medium [1]. NMR spectroscopy provides good possibility for studying the more simple, two-component water–acetone system owing to chemical shift dependences on the concentration*. Recently there is increasing interest in studying the properties of solvent mixtures [2, 3] and in interpreting medium effects [4]. Several papers dealing with investigations of water–acetone mixtures have been published [5, 6, 7] but the question whether the results would be consistent with any simple model of the mixture has not been considered. Attempts to characterize the water–acetone system in terms of simple equilibrium treatments are presented here.

Experimental

REANAL acetone of analytical grade was used after drying on P_2O_5 and bidistilli ng. Water–acetone mixtures were prepared by weighing both components. Mixtures of low water concentrations were prepared by diluting aqueous acetone with dehydrated acetone. The lowest water concentration was determined by the NMR spectrum measuring the line intensity. The NMR spectra were recorded at 60 MHz on an AEI spectrometer Type RS-Z. Proton chemical shifts were calibrated by the normal side-band technique. The line positions were measured relative to acetone methyl protons, with a precision of 0.1 Hz (0.0017 ppm). Spectra were obtained at 25 ± 1 °C. The overall precision of chemical shift measurements — in a situation quite similar to ours — has been thoroughly investigated by F. PODO and V. VITI [3]. On that basis we estimate our error in chemical shift data to be not greater than ± 0.010 ppm.

* The statement in [1] that the proton chemical shift of water is independent of the concentration in the range $0 < [H_2O] < 5.0$ mole/l, is erroneous.

Results

Unfortunately, different authors have usually referred their proton magnetic resonance data to different reference signals. It could be of some help in clarifying the situation to collect all those NMR lines in a graph which might be involved in particular studies.

There are different published values for monomer water solved in several media and in the gas phase [8, 9, 10, 11]. Though some of these values are contra-

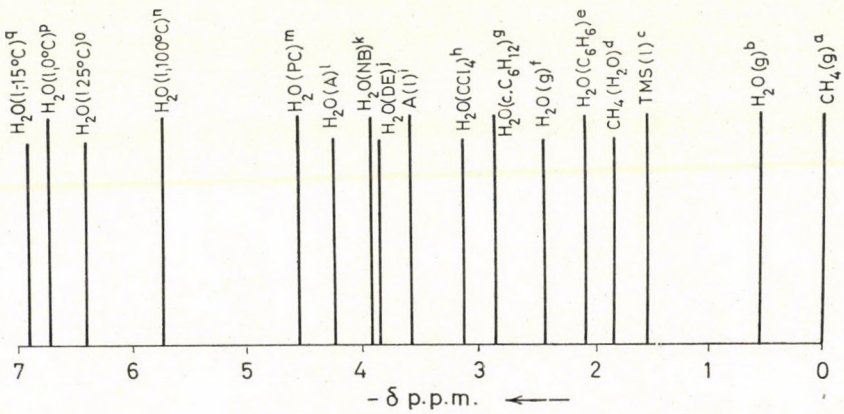

Fig. 1. Positions of some NMR lines referred to gaseous methane (~20 atm, 180 °C). The chemical species and shifts in p.p.m. are as follows: *a*, CH_4(g): 0.00; *b*, H_2O(g): —0.56 [8]; *c*, TMS (*l*): —1.54 (calculated); *d*, CH_4 (solved in H_2O, 25 °C): —1.84 [8]; *e*, H_2O (solved in C_6H_6, 25 °C): —2.10 [9]; *f*, H_2O(g): —2.44 [10]; *g*, H_2O (solved in cyclohexane, 25 °C): —2.86 [8]; *h*, H_2O (solved in CCl_4, 25 °C): —3.12 [8]; *i*, Acetone (*l*): —3.57 (calculated); *j*, H_2O (solved in 1,2-dichloroethane, 25 °C): —3.85 [9]; *k*, H_2O (solved in nitrobenzene, 25 °C): —3.91 [9]; *l*, H_2O (in acetone 25 °C, $x_{H_2O} \to 0$): —4.25 (this work); *m*, H_2O (solved in propylene carbonate): —4.54 [11]; *n*, H_2O (*l*, 100 °C): —5.72 [8]; *o*, H_2O (*l*, 25 °C): —6.43 [8]; *p*, H_2O (*l*, 0 °C): —6.72 [8]; *q*, H_2O (*l*, —15 °C): —6.91 [8]

dictory, it is clear that they cover a relatively wide range of magnetic field (Fig. 1) which is located between the more reliable chemical shift of water vapour [8] and that of pure liquid water*.

The proton magnetic resonance spectra of water–acetone mixtures consist of two main lines, *i.e.* that of the methyl and OH protons. The chemical shift of water moves in an approximately 2.2 ppm wide interval, as the concentration varies. The chemical shift of the methyl protons is also dependent on concentration but to a much less extent. De JEU [7] published a figure on the concentration dependence of the chemical shift of acetone protons in a range of approximately 0.16 ppm when the mole fraction of acetone (x_X) varied

* The large drift caused by an inert solvent on the chemical shift of water as compared to water vapour is in close agreement with MAYO's conclusion on solvation effects [12]. The same can be seen on the CH_4 line drifted when CH_4 is solved by water.

between 0.2 and 0.8. In case of $x_X < 0.2$ the chemical shift of methyl protons was essentially constant.

Table I

Chemical shift of the water protons at 25 °C referred to the acetone protons in water–acetone mixtures

$^{x}H_2O$	$-\sigma$, p. p. m.
0.0007	0.705
0.0015	0.710
0.0026	0.736
0.0032	0.740
0.0052	0.720
0.0080	0.770
0.0131	0.758
0.0152	0.784
0.0159	0.770
0.0259	0.805
0.0314	0.820
0.0356	0.852
0.0510	0.882
0.0759	0.943
0.1208	1.178
0.1315	1.235
0.1428	1.208
0.2200	1.363
0.2772	1.572
0.4650	1.892
0.7010	2.223
1.0000	2.633

We have measured the chemical shift of water protons referred to the acetone signal (Table I). The shift of the methyl protons can be estimated by comparing our results with that of SATAKE *et al.* [5] who referred their results to TMS. The difference between the curves in Fig. 3 is in agreement with the dependence of the methyl chemical shift published by DE JEU [7].

Our measurements as well as those of SATAKE *et al.* [5] are insufficent to observe the unexpected maximum of the water chemical shift at mixtures of about 3 mole per cent [6]. That suggests the stabilisation of water structure by interstitial solute molecules [6, 13], in contrast to views that no profound changes may be expected by small changes in the concentration of a predomin-

antly aqueous medium [14, 15]. The extreme behaviour of the chemical shift dependence mentioned above represents only a slight deviation (~0.03 ppm) from the monotonous curve and will therefore be neglected.

The water–acetone system has also been studied by carbonyl ^{13}C and ^{17}O resonance methods [7]. These data will be used in one of the simple models to be outlined.

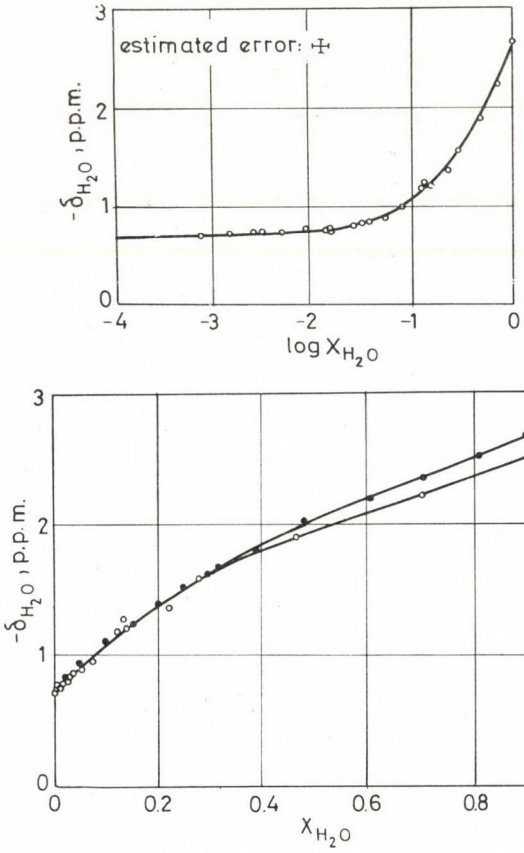

Figs 2 and *3*. Dependence of the chemical shift of water protons as a function of the concentration of water–acetone mixtures. Key: ○ this work, referred to the actual acetone signal; ● original measurements of [5], recalculated so as to be referred to a virtually constant acetone signal

The first model

The shift of the position of an NMR signal with concentration is usually interpreted to be the consequence of a rapid exchange between different (*e.g.* bonded and free) states [8]. This results in the

$$\delta_{exp} = \sum_i \alpha_i \delta_i \qquad (1)$$

weighted average of the individual δ_i chemical shifts. If the δ_i values are known, the system is determinate for *not more than* two different individual states [16]. Since we have only two independent equations (Eq. [1] and $\sum_i \alpha_i = 1$), α_i weighting factors cannot be calculated in case of three or more individual states, hence, the system is then regarded as non-determinate by NMR measurements.

Would the approximation of two independent states be valid for a proton involved in hydrogen bond, the equilibrium constant of a hydrogen-bonded complex of 1 : 1 composition could be determined by the equation

$$K_{1:1} = \frac{1-\alpha_1}{\alpha_1 \{C_a - C_d (1-\alpha_1)\}} \qquad (2)^*$$

where α_1 is the weighting factor of the free proton state, C_a and C_d are total concentrations of the proton acceptor and proton donor, respectively.

In the first simple model, we distinguish *only two* individual states to see how far the experimental data will allow us *to make* the system determinate. These two states are

a., water protons solvated by acetone molecules and

b., water protons solvated by water molecules.

It is assumed that these two states are involved in the equilibrium

$$H_w + aX \rightleftharpoons H_x + bH_2O \qquad (3)$$

where H_w and H_x stand for water protons solvated by water and acetone, respectively, while a and b are average stoichiometric numbers of acetone and water molecules needed to exchange the solvate shell. Since all water protons should be in either of the two states (according to our assumption), the total water concentration can be given by

$$[H_2O]_0 = \frac{[H_x]}{\alpha_1} = \frac{[H_w]}{1-\alpha_1} \qquad (4)$$

where α_1 denotes the weighting factor of water protons solvated by acetone molecules. As for individual chemical shifts, the limiting values in pure acetone and in pure water may be used (Fig. 1) and α_1 can be determined from Eq. [1]. Assuming that molecules either solvated or participating in solvate shells are all active X or H_2O species of the equilibrium, we can write:

$$K = \frac{[H_x]\,[H_2O]_0^b}{[H_w]\,[X]_0^a} = \frac{\alpha_1\,[H_2O]_0^b}{(1-\alpha_1)\,[X]_0^a}. \qquad (5)$$

* This equation is given as Eq. (35) in [16] in a misprinted form.

Substituting the chemical shifts for α_1, Eq. (5) can be given the form:

$$\frac{\delta_{exp}-\delta_{H_2O}}{\delta_x-\delta_{exp}} = K\frac{[X]_0^a}{[H_2O]_0^b} \tag{6}$$

where δ_x and δ_{H_2O} are limiting values of the chemical shift in pure acetone and water, respectively. The logarithm of Eq. (6) has a simple form only if $a = b$. In this case we have

$$\log\frac{\delta_{exp}-\delta_{H_2O}}{\delta_x-\delta_{exp}} = \log K + a\log\frac{[X]_0}{[H_2O]_0} \; . \tag{7}$$

Eq. (7) represents a straight line, according to which the logarithm of the chemical shift ratio depends on the logarithm of total concentration ratio. The slope gives the stoichiometric number while the intercept equals log K. If, on the contrary, Eq. (7) is a curve, then a and b are not equal or the above model is unsatisfactory.

Since carbonyl ^{17}O and ^{13}C chemical shifts are also available [7], we may apply the simple model also to these results by distinguishing two different states (solvated by water or acetone) for the oxygen and carbon atom of the carbonyl group and deriving similar equations as (7). Thus three different sets of data afford the test of Eq. (7) (Fig. 4).

For plotting ^{17}O and ^{13}C curves, the original data of DE JEU [7] have been used. In case of proton resonance, some points of the curve itself in Fig. 2 were used since our measurements extended to low water concentration that was near the δ_x limiting value and the experimental scatter would have been highly magnified by using Eq. (7). Fig. 4 indicates that all the three

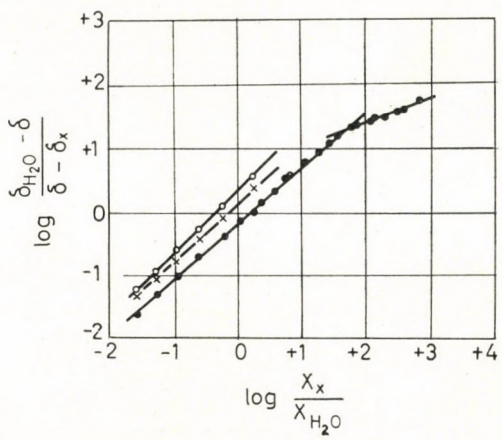

Fig. 4. Test of Eq. (7). Key: ○ carbonyl ^{17}O resonance data [7]; × carbonyl ^{13}C resonance data [7]; ● water proton resonance data taken from the curve in Fig. 2

different sets of experiments satisfy the linearity of Eq. (7) within a wide concentration range, thus suggesting the equality of the stoichiometric numbers a and b. In the range of low water concentrations, the proton resonance data show significant deviation from the straight line. The concentration where linearity ceases is $x_{H_2O} \sim 0.02$ which is equivalent to ~ 0.3 M water. It seems probable that below this concentration water molecules are separated from each other to such an extent that water-solvated protons may no more exist, hence our model cannot be applied.

The parameters of Eq. (7), determined from Fig. 4 are given in Table II.

Table II

Parameters of Eq. (7)

Method	a	log K	K
Water proton resonance	0.88	—0.21	0.62
Carbonyl ^{17}O resonance	0.98	0.31	2.04
Carbonyl ^{13}C resonance	0.92	0.12	1.32

Although the above model has been originally outlined for the convenience of having a determinate system, in light of the results shown in Fig. 4 we may realize that this model is tenable and probably gives some information on the properties of water–acetone mixtures. Before interpreting the data in Table II, it is necessary to explain more thoroughly the equilibrium given by Eq. (3). It is essentially a solvation equilibrium in which any particle may act either as a solute or as a solvent molecule. By studying the process on three independent ways — collecting informations on three different atoms (H, O and C) — we may compare the solvation effects of the corresponding sites. The water protons are probably in both states involved in hydrogen bonds, hence the results characterize the difference between the two hydrogen bonds. The carbonyl oxygen atom is bonded when solvated with water, while it is free when solvated with acetone. The carbonyl carbon atom probably cannot be directly involved in hydrogen bonding though it may be a 'sensor' for the hydrogen bonding on the oxygen atom. An important feature of hydrogen bonding is that it is seriously affected by non-specific solvation phenomena [16—19]. Hence, even if water–acetone hydrogen bonding would be the basic reason determining the properties of the system, it may be differently reflected through the three differently solvated molecular sites [20].

According to the values given in Table II, less then one molecule is sufficient on an average for the solvate exchange process in both directions. The reciprocal of 'a' values may be interpreted as the 'functionality' of molecules participating in the solvate exchange. Since these functionalities slightly

exceed unity, the existence of molecules involved simultaneously in two solvates may be assumed. This conclusion is, however, connected with the fulfilment of the physical conditions of Eq. (1). The K value from proton resonance is 0.62 suggesting that water–water solvation slightly dominates over the water–acetone one in an equimolar mixture in accordance with the statement that the water–water hydrogen bond is stronger than the other one [6]. Similar conclusion may be drawn from the heteroresonance studies since the K values are greater than one suggesting that the acetone–acetone solvation slightly dominates over the acetone–water one*. Moreover, the reciprocal of the K values from ^{17}O and ^{13}C studies is close to that obtained from proton resonance studies, and the differences between them can be accounted for by considering different solvations on the three atoms. The idea that different equilibrium constants may hold for different types of contact between the segments of which the component molecules are composed, has been put forward by HUGGINS [21] as a fundamental concept of his new solution theory [22].

Thus, the above simple model offers surprisingly acceptable results. Two weaknesses are, however, implied:

a) the model does not hold in cases of low water concentrations;

b) it treats water protons as if they were separated from each other and not linked, at least, pairwise to one oxygen atom.

The second simple model tries to improve these weaknesses.

The second model

At low water concentrations water–water interaction may be excluded, hence, the chemical shift dependence is due to the different possible solvations of water protons by acetone molecules. Thus we may write stepwise hydrogen bonding equilibria:

$$\mathrm{HOH} + \mathrm{X} \overset{K_1}{\rightleftharpoons} \mathrm{HOH} \ldots \mathrm{X} \tag{8}$$

$$\mathrm{HOH} \ldots \mathrm{X} + \mathrm{X} \overset{K_2}{\rightleftharpoons} \mathrm{X} \ldots \mathrm{HOH} \ldots \mathrm{X}. \tag{9}$$

The two equilibria imply three different states for water, *i.e.* free, partly bonded and doubly bonded species. As far as water–water interaction can be neglected, all water molecules are involved in one of the three states. Consequently, if the probabilities of the states are α, β and γ, the following equations are valid for the mole fractions of the three individual states:

$$x_{\mathrm{X} \ldots \mathrm{HOH} \ldots \mathrm{X}} = \alpha \, x_{\mathrm{H_2O}} \tag{10}$$

* Eq. (3) is written as water–acetone hydrogen bond formation for ^1H nuclei while it represents the fission of water–acetone hydrogen bonds for ^{13}C and ^{17}O nuclei.

$$x_{\mathrm{HOH}\ldots\mathrm{X}} = \beta\, x_{\mathrm{H_2O}} \tag{11}$$

$$x_{\mathrm{HOH}} = \gamma\, x_{\mathrm{H_2O}} \tag{12}$$

and, obviously,

$$\alpha + \beta + \gamma = 1. \tag{13}$$

The equilibrium constants are as follows:

$$K_1 = \frac{\beta x_{\mathrm{H_2O}}}{\gamma\, x_{\mathrm{H_2O}}\, x_{[\mathrm{X}]}} = \frac{\beta}{\gamma\, x_{[\mathrm{X}]}} \tag{14}$$

and

$$K_2 = \frac{\alpha}{\beta\, x_{[\mathrm{X}]}}\,. \tag{15}$$

While $x_{\mathrm{H_2O}}$ is the total water content expressed in mole fraction, $x_{[\mathrm{X}]}$ refers to the 'equilibrium' acetone concentration which is different from the total concentration, x_{X}^0,

$$x_{[\mathrm{X}]} = x_{\mathrm{X}}^0 - x_{\mathrm{H_2O}}\,(2\alpha+\beta). \tag{16}$$

The experimental chemical shift can be given by

$$\delta_{\mathrm{exp}} = \alpha\delta_1 + \beta\delta_a + \gamma\delta_4 \tag{17}$$

where δ_1 and δ_4 are the individual chemical shifts for doubly bonded and free water molecules, respectively, while δ_a is an average value of δ_2 and δ_3 corresponding to the equimolar protons in the partly bonded water molecule. From Eqs (13), (14) and (15), the probability factors can be expressed, as follows:

$$\alpha = \frac{K_1 K_2\, x_{[\mathrm{X}]}^2}{K_1 K_2 x_{[\mathrm{X}]}^2 + K_1 x_{[\mathrm{X}]} + 1} \tag{18}$$

$$\beta = \frac{K_1\, x_{[\mathrm{X}]}}{K_1 K_2 x_{[\mathrm{X}]}^2 + K_1 x_{[\mathrm{X}]} + 1} \tag{19}$$

$$\gamma = \frac{1}{K_1 K_2 x_{[\mathrm{X}]}^2 + K_1 x_{[\mathrm{X}]} + 1}\,. \tag{20}$$

The above expressions can be substituted into Eq. (17) which will then contain five unknown quantities (two equilibrium constants and three individual chemical shifts). We have no reason for substituting the limiting values of δ_{exp} in water and acetone for δ_1 and δ_4, respectively. The chemical shifts in pure water depend on the concentration of 'structured' and 'unstructured' water [11] which are not similar in structure to a species doubly bonded to acetone molecules. On the other hand, we are now dealing with mixtures of

low water concentration where overwhelmingly water monomers exist and δ_{exp} still varies with concentration. We may *arbitrarily* choose the H_2O(*c.* C_6H_{12}) line for δ_4 (*cf.* Fig. 1).

Since the values of δ_1 and δ_a cannot even be estimated, we have still four unknown quantities which is far more than allowable in a single equation is a straight line depending on $x_{[X]}$. The following values were used: $\delta_4 = 0.71$ relative to acetone; $K_1 = 1.0$; $K_2 = 0.1$. The plot of Eq. (21) is shown in Fig. 5.

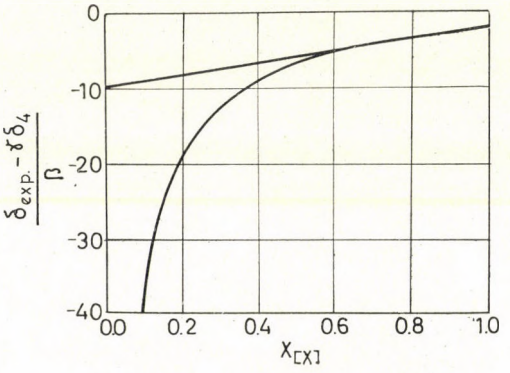

Fig. 5. Test of the second model

for a determinate system. Hence, there is no hope to obtain accurate values for these quantities.

We may, however, test our second model in the following way. By substituting *arbitrary* values for the equilibrium constants, only δ_1 and δ_a remain unknown. As far as the model has some validity, these individual shifts should be constant. Eq. (17) in the rearranged form

$$\frac{\delta_{exp} - \gamma\delta_4}{\beta} = \frac{\alpha}{\beta}\delta_1 + \delta_a = K_2\,\delta_1\,x_{[X]} + \delta_a \qquad (21)$$

Since the equilibrium constants have been chosen arbitrarily, only the fact is important that at low water concentrations we get a straight line. Deviation from linearity begins at $x_{[X]} \simeq 0.77$ that corresponds to $x_{H_2O} = 0.16$ or 2.5 M water concentration. It is one order of magnitude higher than the value obtained from the first model to the limit of water solvated water protons. Thus, it seems that the second model would be partly valid in a concentration range where water–water interaction might take place. It is, however, true that the curve does not provide a very sensitive indication of the deviation from linearity. We may conclude that our second simple model can be fitted to the experimental data in the range of $0.8 < x_{[X]} < 1.0$ or $0.14 > x_{H_2O} > 0$. This particular treatment gives $\delta_a = -9.70$ ppm and $\delta_1 = -76$ ppm that is of no importance in light of the arbitrary values introduced.

Conclusion

In spite of the complex character of water structure, NMR data of water–acetone mixtures may be rationalized by means of very simple models if no attempt is made to cover the entire concentration range. Of the two models outlined, the first allows a somewhat deeper insight into the physical nature of the system, and suggests that the basic reason of the chemical shift dependence is a solvate exchange equilibrium. Since this type of interaction is weak, it is different from a chemical equilibrium. All molecules participate in the solvate exchange, hence there is no bonded molecule in the chemical sense. Essentially, one molecule is sufficient to cause a solvate exchange*. In other words, the consideration of the first neighbour is sufficient to account for the magnetic behaviour of nuclei. The first model cannot be applied in case of mixtures of low water concentration. The second model resembling the chemical equilibrium appears to be valid just at low water concentrations where water–water interactions can be practically disregarded.

*

We are grateful to Miss F. Podo for helpful discussions, and to Miss I. Kovács for her participation in the experiments. The suggestion of Prof. Maurice L. Huggins on the applicability of his structon theory to our data is gratefully acknowledged.

REFERENCES

1. Neszmélyi, A., Simonyi, M., Tüdős, F.: Acta Chim. Acad. Sci. Hung. (Budapest) **53,** 369 (1967)
2. Covington, A. K., Jones, P.: Hydrogen-bonded Solvent Systems. Taylor and Francis Ltd. London, 1968
3. Podo, F., Viti, V.: Rapporto No. 33/1969, Istituto Superiore di Sanità, Roma
4. Coetzee, J. F., Ritchie, C.D.: Solute-Solvent Interactions. Dekker, New York, 1969
5. Satake, I., Arita, M., Kimizuka, H., Matuura, R.: Bull. Chem. Soc. Japan **39,** 597 (1966)
6. Glew, D. N., Mak, H. D., Rath, N. S.: p. 195 in Ref. 2.
7. de Jeu, W. H.: J. Phys. Chem. **74,** 822 (1970)
8. Hindmann, J. C.: J. Chem. Phys. **44,** 4582 (1966)
9. Ödberg, L., Högfeldt, E.: Acta Chem. Scand. **23,** 1330 (1969)
10. Pople, J. A., Schneider, G. W., Bernstein, H. J.: High-Resolution Nuclear Magnetic Resonance. McGraw-Hill Book Co. New York, 1959
11. Cogley, D. R., Butler, J. N., Grunwald, E.: J. Phys. Chem. **75,** 1477 (1971)
12. Mayo, F. R.: J. Am. Chem. Soc. **89,** 2655 (1967)
13. Macdonald, D. D., Smith, M. D., Hyne, J. B.: Can. J. Chem. **49,** 2817 (1971)
14. Bates, R. G.: p. 49 in Ref. 2.
15. Le Narvor, A., Gentric, E., Saumagne, P.: Can. J. Chem. **49,** 1933 (1971)
16. Simonyi, M., Tüdős, F.: Adv. Phys. Org. Chem. **9,** 127 (1971)
17. Scott, R., DePalma, D., Vinogradov, S.: J. Phys. Chem. **72,** 3192 (1968)
18. Eastman, J. W., Rehfeld, S. J.: J. Phys. Chem. **74,** 1438 (1970)

* It has recently been shown [23] that organic solvates of phenol comprise only one molecule of the solvent.

19. PAOLLIO, L., BECKER, E. D.: J. Magn. Res. **2,** 168 (1970)
20. LAMOTTE, M., GERHOLD, G. A., JOUSSOT-DUBIEN, J.: J. Chim. Phys. **67,** 2006 (1970)
21. HUGGINS, M. L.: J. Phys. Chem. **74,** 371 (1970)
22. HUGGINS, M. L.: Disc. Faraday Soc. **49,** 175 (1970)
HUGGINS, M. L.: Polymer **12,** 389 (1971)
HUGGINS, M. L.: J. Phys. Chem. **75,** 1255 (1971)
HUGGINS, M. L.: Macromolecules **4,** 274 (1971)
23. KORENMAN, YA. I.: Zhur. Fiz. Khim. **46,** 77 (1972)

Miklós SIMONYI
Julianna KARDOS
András NESZMÉLYI
1025 Budapest, Pusztaszeri út 59—67.

Acta Chimica Academiae Scientiarum Hungaricae, Tomus 76 (1), pp. 81—94 (1973)

ACYLATION OF DISUBSTITUTED CYANAMIDES WITH PHOSGENE, I

PREPARATION AND SOME REACTIONS OF 1,3,5-TRICHLORO-2,4-DIAZAPENTADIENE DERIVATIVES

Z. Csűrös*, R. Soós*, Á. Antus-Ercsényi**, I. Bitter* and J. Tamás***

*(*Institute of Organic Chemical Technology, Technical University, Budapest, ** Chinoin Pharmaceutical and Chemical Works and *** Chemical and Structure Research Laboratory of the Hungarian Academy of Sciences, Budapest)*

Received October 1, 1971

The structure and mechanism of formation of dialkyl-[1,3,5-trichloro-5-dialkylamino-2,4-diazapentadiene-(2,4)-ylidene]-ammonium chlorides, obtained from the reaction of disubstituted cyanamides with phosgene, were investigated. The structural relationship between these compounds and chloromethylenedialkylammonium chlorides was confirmed by spectroscopic methods. The effects of water and heat on the derivatives prepared were studied and the structures of the compounds resulting from these processesverified.

Bredereck and Richter [1] prepared a compound with N-acylchloroformamidine structure (1) from dimethylcyanamide and *p*-nitrobenzoyl chloride.

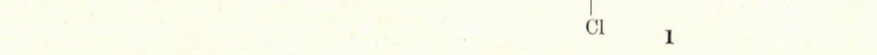

1

Salt-like products of type **2** were obtained from dimethylcyanamide, N-cyanopiperidine and N-cyanomorpholine with the more reactive bifunctional phosgene; the structures are very similar to those of the amide chlorides resulting from the reaction of N,N-dialkyl acid amides and phosgene.

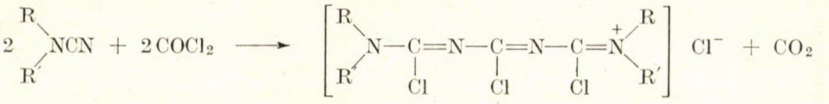

2

2a: R=R′=CH_3—
2b: R+R′= —$(CH_2)_2$—O—$(CH_2)_2$—
2c: R+R′= —$(CH_2)_5$—
2d: R=R′=CH_3CH_2—
2e: R=R′=$CH_3CH_2CH_2$—
2f: R=R′=$(CH_3)_2CH$—
2g: R=R′=$CH_3(CH_2)_3$—
2h: R=CH_3—; R′=C_6H_5—

According to the authors mentioned above, the reaction is strongly dependent on the space requirement of groups R and R′ and their conjugation conditions. No reaction takes place with diethylcyanamide and N-methyl-N-

phenylcyanamide, since the collision due to the free rotation of the methyl groups in the former compound and the conjugative interaction between the phenyl group and the free electron pair of the amine nitrogen in N-methyl-N-phenylcyanamide, prevent the formation of a salt-like product of type **2.** The cyclic structure of N-cyanomorpholine and N-cyanopiperidine hinders the rotation of the methyl groups in the β position, therefore compounds **2b** and **2c** can be obtained in the phosgenation reaction.

This explanation is in contradiction with the usual ideas about steric hindrance. Collisions due to free rotation always decrease the reaction rate but, in general, they do not prevent the occurrence of a reaction. Therefore, in our work the interaction of various substituted cyanamides with phosgene was investigated and the formation of products of type **2** and the reaction mechanisms supported by spectroscopic and preparative evidence.

The disubstituted cyanamides required were prepared from the corresponding secondary amines with cyanogen bromide [2].

The Stuart ("Eugon") models of compounds **2a** and **2d** have shown that the steric hindrance between the methylene groups acting against the formation of molecule **2d** is not significant, since the alkyl parts of the diethylamino groups may rotate without considerable collision. Neither did the effect seem significant in the case of bulkier substituent groups, such as *n*-propyl-, *n*-butyl or even isopropyl.

The models revealed that the spatial arrangement of the molecule is only slightly influenced by the space requirement of groups R and R′. Steric hindrance occurred in the arrangement of the chlorine atoms. In view of the *syn-anti* isomerism at the C = N double bonds, compounds of type **2** can be assumed to occur as four (**A, B, C, D**) geometric isomers:

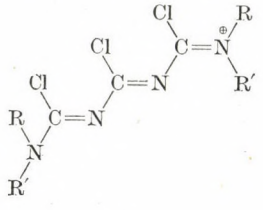

A

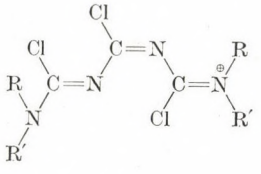

B

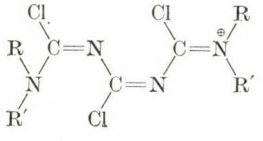

C

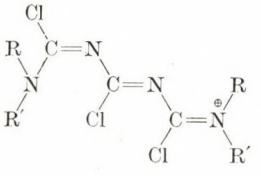

D

If the steric arrangement of the bulky chlorine atoms permits coplanarity of the double bonds, mesomerism should be considered, thus the following formula seems to be more correct than, *e.g.*, **A**;

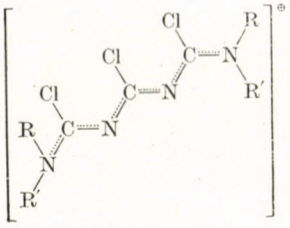

If rapid mesomeric change, *i.e.* the coplanarity of the molecule is supposed two methyl signals of equal intensity can be expected in the NMR spectrum of compound **2a**, while in the case when coplanarity cannot develop because of the collision of the chlorine atoms, three different positions of the methyl groups should be detected: the equivalent methyl groups in the dimethylamino group and the methyls of the dimethylammonium group being in cis and trans positions. Their signals may appear separately in the spectrum, *i.e.* a singlet representing six protons and a doublet each representing three protons can be expected in the spectrum.

The NMR spectrum of **2a** in deuterochloroform had two signals of equal intensity ($\delta_1 = 3.90$, $\delta_2 = 3.80$ ppm); thus the molecule has mesomer structure. Though the NMR spectrum of chloromethylenedimethylammonium chloride (**3**), prepared from dimethylformamide with phosgene with a structure analogous to that of product **2a**, contains one single methyl signal ($\delta = 4.04$ ppm) in accordance with the literature data [3] and in contrast with the well-known example of dimethylformamide; this signal is probably a doublet like in the case of **2a** if higher resolution is used.

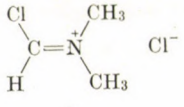

3

Thus in the NMR spectrum of **2a**, the two signals appearing at 3.90 and 3.80 ppm represent the resonance absorption of the methyl groups of the equivalent dimethylammonium groups in cis and trans positions with respect to chlorine.

The experiments carried out with respect to the above statements have confirmed the assumptions, and it has been found that diethyl-, di-*n*-propyl-, diisopropyl-, di-*n*-butyl-, and N-methyl-N-phenylcyanamide can be converted with excess phosgene into the corresponding dialkyl-[1,3,5-trichloro-5-

dialkylamino-2, 4-diazapentadiene-(2,4)-ylidene]-ammonium chlorides (**2**), irrespective of the alkyl substituents; differences occur only in the yields. In the case of dimethylcyanamide 90% yield was obtained, which decreased with increasing length of the alkyl chain in the normal series, while the reaction of di-isopropylcyanamide gave the derivate **2f** in 75% yield.

The reaction of N-methyl-N-phenylcyanamide with phosgene confirmed that the conjugation of the free electron pair of the amine nitrogen and the aryl substituent has no disturbing effect, either.

Products **2d, 2e** and **2g** were isolated as oils, while **2f** and **2h** were crystalline substances. Their structures were identified by means of spectroscopic methods, in addition to analytical examinations.

In the infrared spectra recorded in anhydrous chloroform, the most characteristic bands are those of the C = N stretching vibrations appearing at 1530—1560 cm^{-1} and 1620—1640 cm^{-1} and those of the stretching vibration of the alkyl groups found at 2850—3000 cm^{-1}.

The ultraviolet spectra of compounds **2d—2h** also confirm the correctness of structure **2.** The bands observed at 310—320 nm and at 247 nm have shapes intensities similar to those of the dimethyl derivatives **2a.**

In the NMR spectra the group of signals with a multiplicity corresponding to the alkyl groups can be found twice, showing 0.1 ppm shift as it had been observed in the case of compound **2a.**

BREDERECK and RICHTER supposed the following mechanism for the formation of compounds of type **2:**

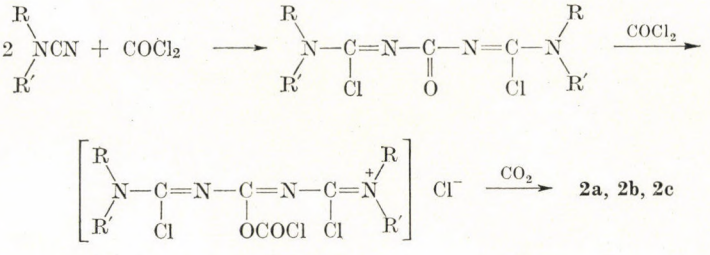

The first step of the reaction is the formation of a tetrasubstituted urea derivative, whose carbonyl group reacts then with phosgene according to the mechanism reported for tetrasubstituted urea derivatives [4] and the carbonyl oxygen is exchanged against chlorine with CO_2 evolution.

Our investigations support this reaction path. The reaction of dimethylcyanamide with phosgene in 2 : 1 mole ratio was carried out in absolute ether at 0—5 °C to obtain a white crystalline product which was identified as compound **4a** on the basis of the IR spectrum (carbonyl band at 1720 cm^{-1}) halogen content (30.2%).

This structure was also confirmed by the chemical behaviour. On the effect of water compound **5a** (N, N-bis-dimethylcarbamoyl-urea) was formed [5] with the elimination of hydrogen chloride; on the other hand, treatment with phosgene converted the product gradually into **2a**..

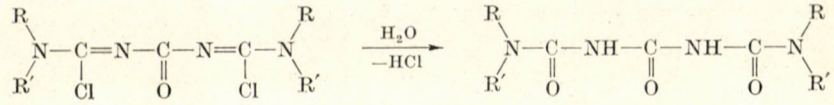

4 **5**

4a: R = R′ = CH_3— **2**

5a: R = R′ = CH_3—
5b: R + R′ = —$(CH_2)_2$—O—$(CH_2)_2$—
5c: R + R′ = —$(CH_2)_5$—
5d: R = R′ = CH_3CH_2—
5e: R = R′ = $CH_3(CH_2)_2$—
5f: R = R′ = $(CH_3)_2CH$—
5g: R = R′ = $CH_3(CH_2)_3$—
5h: R = CH_3—; R′ = C_6H_5—

Bredereck and Richter prepared **2a** in absolute dichloromethane. When isolation of the intermediate is not desired, dichloromethane should be preferred to ether, since thus both reaction steps take place in homogeneous phase.

The identical structures of the unstable compounds of type **2** obtained on the effect of excess phosgene were also confirmed by their chemical behaviour, in addition to the spectroscopic evidence. They are strongly hygroscopic substances which undergo decomposition even on the effect of the moisture content of air with the evolution of hydrochloric acid, being transformed into N, N′N-bis-dialkylcarbamoyl-urea derivatives (compounds of type **5**) which can be easily crystallized and used for identification.

On the basis of the infrared spectra it is concluded that compounds of type **5** can probably be characterized in the solid state by structure **6a** containing a hydrogen bridge.

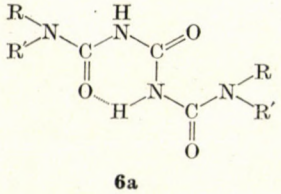

6a

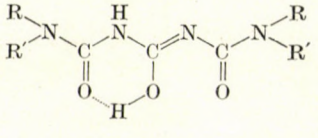

6b

In each compound, structure **6a** is indicated by the IR bands characteristic of weakly associated NH groups in the 3260—3240 cm^{-1} region and

by ν NH bands between 3200 cm^{-1} and 3000 cm^{-1} representing NH groups involved in strong (but not cyclic dimeric) association. In accordance with these, the very intense absorptions in the 1790—1740 cm^{-1} region and the weak bands between 1675 and 1660 cm^{-1} can be assigned to the ν_{as} C = O and ν_s C = O coupled vibrations of non-associated imide carbonyls, while the rather intense band in the 1650—1635 cm^{-1} region can be identified as the absorption of the carbonyl groups participating in the intramolecular hydrogen bridge. The bands found in the 3000—2850 cm^{-1} region must be due to the alkyl groups.

However, the spectral data do not exclude structure **6b**, which also contains a hydrogen bridge, since the absorptions found at 1640—1650 cm^{-1} may be due to a C = N bond.

Similarly to **2a, 2d, 2e** and **2f,** can be converted by heating into 1,3,5-triazine derivatives [5] with the elimination of alkyl halides.

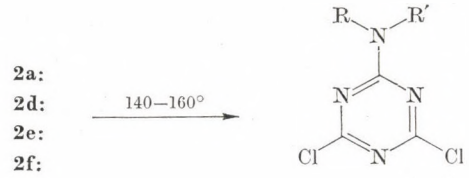

7

7a: R = R′ = CH_3—
7d: R = R′ = CH_3CH_2—
7e: R = R′ = $CH_3(CH_2)_2$—
7f: R = R′ = $(CH_3)CH$—

The 2,4-dichloro-6-alkylamino-1,3,5-triazines (**7**) are easily crystallizable products; their structures were proved by means of spectroscopic methods, in addition to elemental analytical results.

Since in nitrogen-containing aromatic compounds the presence of the nitrogen atom has such an influence on the aromatic γ (= CH) and γ CC band frequencies as if the compound were a benzene derivative carrying a substituent at the place of the nitrogen atom, 1,3,5-triazines can be regarded as trisubstituted aromatic rings. In the infrared spectra of compounds of type **7** the skeletal stretching vibrations appear in the 1600—1560 cm^{-1} and 1470—1450 cm^{-1} regions. In the 800 cm^{-1} and 790 cm^{-1} interval a strong band is found which can be attributed to the out-of-plane skeletal vibration corresponding to the 1,3,5-trisubstitution of an aromatic ring; this bond is somewhat shifted because of the presence of the two halogen atoms.

The NMR spectra shows the presence of alkyl groups in identical positions.

The structures of the compounds of type **7** obtained by heating were also verified by mass spectroscopy. Since in the future we intend to study the nucleophilic cyclization reactions of trichlorodiazapentadiene derivatives resulting in 1,3,5-triazines, the triazine derivatives prepared in the course of the present investigations were examined in detail by means of mass spectroscopy. It was expected that the evaluation of the mass spectra might provide common characteristics which would later facilitate the identification of such compounds.

All the four compounds (**7a, 7d, 7e, 7f**) give a molecular ion peak (M^+) of significant intensity; this intensity decreases with increasing length of the alkyl chain. The molecular formulas of the parent ions were confirmed by means of precise mass measurements.

Primary splitting of the parent ions and the most intense ion peaks are due to the fragmentation of the substituted amino group. The same observation was made by JÖRG *et al.* [6] in the case of a related compound Simazine.

It is common to the spectra compound that the $(M-R)^+$ ion is present, formed from the parent ion by means of homolytic alkyl radical splitting; in the case **7a** and **7d** methyl and ethyl, while from **7e** and **7f** propyl radicals are split off, respectively. The probable structure of the ion type produced is:

$(M-R)^+$

In monosubstituted aminotriazines this type of ions was not observed, but the splitting of an R—H olefin from the parent ion was detected [6, 7]. A common feature is the β-splitting of the alkyl group with respect to the amino nitrogen, resulting in ions of mass numbers M-1 (**7a**), M-1 and M-15 (**7d**), M-29 (**7e**) and M-15 (**7f**). The important fragmentation path of this ion type is the splitting off of an R—H olefin, which equally occurs in compounds **7d, 7e** and **7f.**

Special paths can be observed in the fragmentation of the dimethylamino derivative **7a**: the ion peaks of mass number 163 and 149 are due to the loss of NCH_3 and $CH_2=NCH_3$, respectively, from the parent ion. This was confirmed by accurate mass measurements and the detection of the corresponding metastable ion peaks. In the spectrum of **7a** the very intense peak of mass number 44 corresponds to the composition C_2H_6N, thus it is

a dimethylamino group; the ion of mass number 42 is obtained from this by splitting off of H_2. The fragment ion of mass number 30 corresponds to CH_4N. In the spectra of the other compounds the ions R_2N^+ analogous to the peak obtained at m/s 44 could not be observed. At the same time, the alkyl group R gives a significant ion peak in the spectra of **7e** and **7f** (m/e 43, $C_3H_7^+$) and its further fragments can also be found (m/e 41, 39).

A large number of fragment peaks due to the splitting of the triazine ring can be found in the spectra of all the four compounds. Their intensities are relatively not high, in accordance with the great stability of the skeleton. The majority of these ions is known or can be traced back to ion species resulting from the splitting of the ring, as detected in the mass spectra of amino-dichloro-s-triazine and ethylamino-dichloro-s-triazine [7]. Among them the ion at m/e 55 has the greatest intensity; this was identified as a $C_2H_3N_2$ atomic group which is supposed to have the structure $CH_2 = N - C = \overset{+}{N}H$ in the

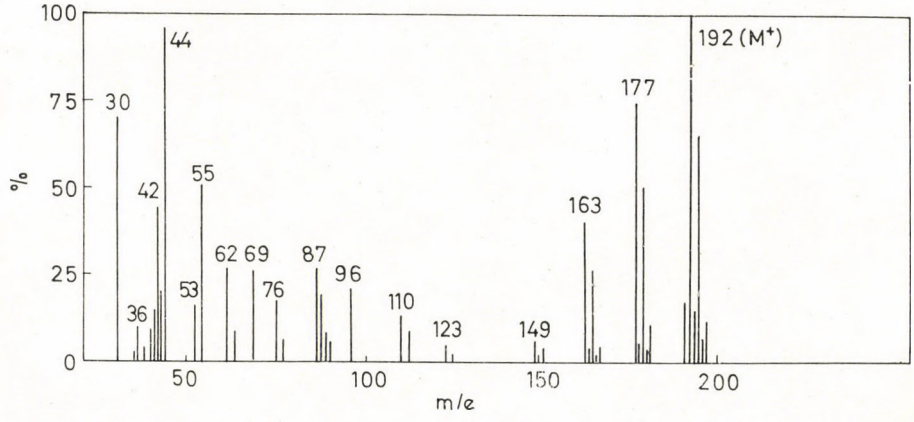

Fig. 1. Line diagram of the mass spectrum of 2,4-dichloro-6-dimethylamino-1,3,5-triazine

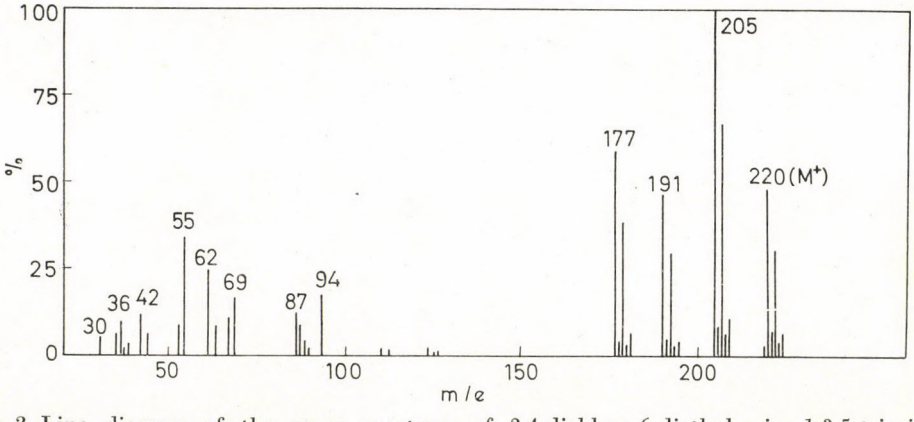

Fig. 2. Line diagram of the mass spectrum of 2,4-dichloro-6-diethylamino-1,3,5-triazine

case of compounds **7d** and **7e.** In **7a,** however, the possibility of structure $CH_3-N-C\equiv\overset{+}{N}$ should also be taken into account. In **7f** the ion with m/e 55 cannot be formed because of the branching of the alkyl chain. In each spectrum we can find the ion peak at m/e 62 ($Cl-C\equiv\overset{+}{N}H$) characteristic of chloro-substituted triazine rings and the ion peak at m/e 87 ($Cl-C\equiv\overset{+}{N}-CN$). In compounds **7d** and **7f** the ion with the formation $C_4H_4N_3$ (m/e 94) can also be attributed to the splitting of the ring; its probable structure is $CH_3-CH=$ $=N-C\equiv\overset{+}{N}-CN$. Such an ion cannot be formed from compound **7f** because of the branching structure of the alkyl group; its homologue higher by a CH_2 group, *i.e.*, the fragment ion with m/e 108 is formed here. In compound **7a** containing a dimethylamino group, the ion peak at m/e 96 appears instead

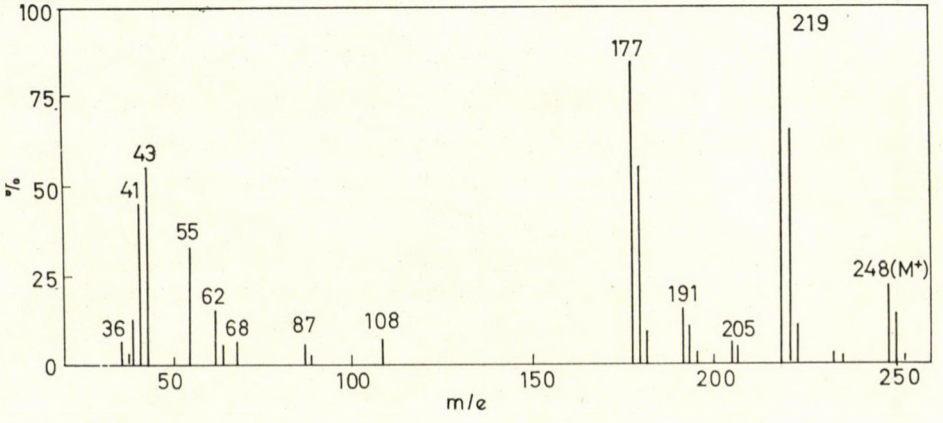

Fig. 3. Line diagram of the mass spectrum of 2,4-dichloro-6-di-*n*-propylamino-1,3,5-triazine

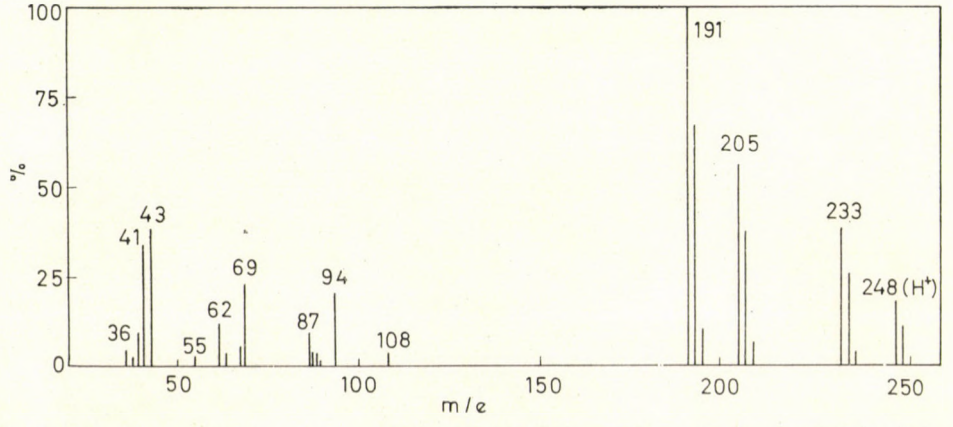

Fig. 4. Line diagram of the mass spectrum of 2,4-dichloro-6-diisopropylamino-1,3,5-triazine

of that at 94; this contains two more hydrogen atoms. The molecular formula was confirmed by means of accurate mass measurements: its probable structure is $(CH_3)_2N-\overset{+}{C}N-CN$. The line diagrams of compounds of type **7** well illustrate the above facts (Figs 1—4).

Experimental

All melting points were determined with a BÜCHI 320—388 apparatus. The NMR spectra were recorded at 60 Mc/s with a VARIAN 60 A instrument, using tetramethylsilane internal standard. The chemical shifts are given in δ ppm units.

The UV spectra were recorded with a PERKIN—ELMER 124 spectrophotometer, and a PERKIN—ELMER 237 instrument was used for recording the IR spectra.

The mass spectra were obtained with a mass spectrometer of type MS-902; the samples were introduced at 120 °C by means of a glass-ball system. The temperature of the ionization chamber was 190 °C. The accurate mass measurements were carried out with a resolution power of 16.000 with an accuracy of 2 ppm.

Dialkyl-[1,3,5-trichloro-5-dialkylamino-2,4-diazapentadien-2,4-ylidene] ammonium chloride (2) General procedure

A solution of dialkyl- or aryl-alkyl cyanamide (0.1 mole) in absolute methylene chloride was added dropwise to a solution of phosgene (0.15 mole) in absolute methylene chloride, cooled with ice under stirring; the absence of moisture must be ensured. The mixture was allowed to warm up slowly to room temperature, when a strong evolution of gas began. The solution was allowed to stand overnight, then the solvent was distilled off and the residue washed with absolute ether and dried in vacuum.

Dimethyl-[1,3,5-trichloro-5-dimethylamino-2,4-diazapentadien-2,4-ylidene] ammonium chloride (2a)

A yellow crystalline product **(2a)** (14.5 g; 99%) was obtained from phosgene (14.8 g; 0.15 mole) and dimethylcyanamide (7.0 g; 0.1 mole) in absolute methylene chloride (50 ml). The substance was strongly hygroscopic; m.p. 123—126 °C (lit. m.p. 125 °C).

$C_7H_{12}Cl_4N_4$ (239.82). Calcd. Cl 48.40. Found Cl 50.10%.

IR ($CHCl_3$): ν $CH_{aliphatic}$ 3000, 2920 cm^{-1}
ν C = N 1640, 1560 cm^{-1}
UV ($CHCl_3$): 310 nm (4.28); 247 nm (4.22)
NMR ($CDCl_3$): 3.80 (s, 6H, $-CH_3$)
3.90 (s, 6H, $-CH_3$).

Diethyl-[1,3,5-trichloro-5-diethylamino-2,4-diazapentadien-(2,4)-ylidene] ammonium chloride (2d)

A yellow oily product **(2d)** (11 g; 63%) was obtained from phosgene (14.8 g, 0.15 mole) and diethylcyanamide (9.8 g, 0.1 mole) in absolute methylene chloride (50 ml). The substance was strongly hygroscopic.

$C_{11}H_{20}Cl_4N_4$ (349.83). Calcd. Cl 41.50. Found Cl 42.30%.

IR ($CHCl_3$): ν $CH_{aliphatic}$ 2950, 2930 cm^{-1}
ν C = N 1625, 1550 cm^{-1}
UV ($CHCl_3$): 316 nm (4.32); 247 nm (4.25)
NMR ($CDCl_3$): 1.42 (t, 6H, J = 7.2 Hz, $-CH_3$)
1.55 (t, 6H, J = 7.2 Hz, $-CH_3$)
4.01 (q, 4H, J = 7.2 Hz, $-CH_2-$)
4.09 (q, 4H, J = 7.2 Hz, $-CH_2-$).

Di-n-propyl-[1,3,5-trichloro-5-di-n-propylamino-2,4-diazapentadien-(2,4)-yliden e] ammonium chloride (2e)

A yellow-brown oily product **2e** (12.1 g; 60%) was obtained from phosgene (14.8 g, 0.15 mole) and di-*n*-propylcyanamide (12.6 g, 0.1 mole) in absolute methylene chloride medium (50 ml). The substance was strongly hygroscopic.

$C_{15}H_{28}Cl_4N_4$ (405.93). Calcd. Cl 34.80. Found Cl 34.50%.

IR ($CHCl_3$): ν $CH_{aliphatic}$ 2970, 2940, 2880 cm^{-1}
ν C = N 1625, 1550 cm^{-1}
UV ($CHCl_3$): 316 nm (4.45); 247 nm (4.39),
NMR ($CDCl_3$): 1.02 (t, 6H, J = 6.7 Hz, $-CH_3$)
1.09 (t, 6H, J = 6.7 Hz, $-CH_3$)
1.42—2.28 (broad m, 8H, $-CH_2-$)
3.30—4.30 (broad m, 8H, $-CH_2-N$).

Di-isopropyl-[1,3,5-trichloro-5-diisopropylamino-2,4-diazapentadien-(2,4)-ylidene] ammonium chloride (2f)

A light yellow crystalline product (**2f**) (15.2 g; 75%) was obtained from phosgene (14.8 g, 0.15 mole) and diisopropylcyanamide (12.6 g, 0.1 mole) in absolute methylene chloride (50 ml). The substance was strongly hygroscopic, m.p. 85—86 °C.

$C_{15}H_{28}Cl_4N_4$ (405.93). Calcd. Cl 34.80. Found Cl 33.50%.

IR ($CHCl_3$): ν $CH_{aliphatic}$ 3010, 2980, 2940 cm^{-1}
ν C = N 1610, 1530 cm^{-1}
UV ($CHCl_3$): 316 nm (4.53); 248 (4.47),
NMR ($CDCl_3$): 1.51 (d, 24H, J = 6.8 Hz, $-CH_3$)
4.39 (q, 2H, J = 6.8 Hz, $>CH-$)
4.83 (q, 2H, J = 6.8 Hz, $>CH-$).

Dibutyl-[1,3,5-trichloro-5-dibutylamino-2,4-diazapentadien-(2,4)-ylidene] ammonium chloride (2g)

A brownish oily product (**2g**) (12 g; 52%) was obtained from phosgene (14.8 g, 0.15 mole) and dibutylcyanamide (15.4 g, 0.1 mole) in absolute methylene chloride (50 ml). The substance was strongly hygroscopic.

$C_{19}H_{36}Cl_4N_4$ (461.31). Calcd. Cl 30.3. Found Cl 31.2%.

IR ($CHCl_3$): ν $CH_{aliphatic}$ 2970, 2930, 2870 cm^{-1}
ν C = N 1620, 1540 cm^{-1}
UV ($CHCl_3$): 317 nm (4.51); 249 nm (4.50).

N-Phenyl-N-methyl-[1,3,5-trichloro-5-methylanilino-2,4-diazapentadien-(2,4)-ylidene] ammonium chloride (2h)

A yellowish crystalline product **2h** (14.3 g; 70%) was obtained from phosgene (14.8 g, 0.15 mole) and N-phenyl-N-methylcyanamide (13.4 g, 0.1 mole) in absolute methylene chloride (50 ml). The substance was strongly hygroscopic, m.p. 129—131 °C.

$C_{17}H_{16}Cl_4N_4$ (417.13). Calcd. Cl 33.9. Found Cl 34.1%.

IR ($CHCl_3$): ν $CH_{aromatic}$ 3040—3000 cm^{-1}
ν $CH_{aliphatic}$ 2980 cm^{-1}
ν C = N 1600, 1530 cm^{-1}
UV ($CHCl_3$): 247 nm (4.71)
NMR ($CDCl_3$): 3.66—4.10 (t, 6H, $-CH_3$)
7.4—7.8 (broad s, 10H, $-C_6H_5$).

1,5-Dimethylamino-1,5-dichloro-2,4-diazapentadien-3-one (4a)

A solution of phosgene (3.95 g, 0.04 mole) in absolute ether (15 ml) was added dropwise to a solution of dimethylcyanamide (5.6 g, 0.08 mole) in absolute ether (10 ml) cooled with ice under stirring. The absence of atmospheric moisture must be ensured. In a short time a white precipitate separated; it was filtered off after agitating for half an hour, washed with absolute ether and dried in vacuum. A white crystalline product (4.98 g; 52%) was obtained, m.p. 138—140—142 °C.

$C_7H_{12}Cl_2N_4$ (223.09). Calcd. Cl 29.7. Found Cl 30.2%.
IR (KBr): ν $CH_{aliphatic}$ 2950 cm^{-1}
ν C = O 1720 cm^{-1}
ν C = N 1650, 1640 cm^{-1}.

N,N′-bis-Dialkylcarbamoylurea (5)
General procedure

Compound **2** was allowed to stand in a crystallization dish exposed to atmospheric moisture for several days. The substance first liquefied then gradually solidified with the evolution of hydrochloric acid. Recrystallization gave a white crystalline product (**5**).

N,N′-bis-Dimethylcarbamoylurea (5a)

2a (1.0 g, 3.4 mmole) gave **5a** (0.6 g; 86.4%), m.p. 140—142 °C (lit. [5], m.p. 142 °C).
$C_7H_{14}N_4O_3$ (202.15).
IR (KBr): ν NH 3260 cm^{-1}
ν $CH_{aliphatic}$ 3000, 2940 cm^{-1}
ν C = O 1740, 1690, 1650 cm^{-1}
γ NH 750 cm^{-1}.

N,N′-bis-Diethylcarbamoylurea (5d)

2d (2 g, 5.7 mmole) gave **5d** (1.18 g; 80%). The product was recrystallized from water; m.p. 120—121 °C.
$C_{11}H_{22}N_4O_3$ (258.23). Calcd. C 51.2; H 8.55; N 21.70. Found C 50.8; H 8.45; N 21.35%.
IR (KBr): ν NH 3280 cm^{-1}
ν $CH_{aliphatic}$ 3000—2850 cm^{-1}
ν C = O 1760, 1660, 1640 cm^{-1}
γ NH 762 cm^{-1}.

N,N′-bis-di-n-Propylcarbamoylurea (5e)

2e (2 g, 4.95 mmole) gave **5**; (0.8 g; 51.0%). The product was recrystallized from a mixture of acetone and water to obtain long needles, m.p. 130—131 °C.
$C_{15}H_{30}N_4O_3$ (314.32). Calcd. C 57.02; H 9.20; N 17.92. Found C 56.72; H 9.40; N 17.90%.
IR (KBr): ν NH 3240 cm^{-1}
ν $CH_{aliphatic}$ 2960—2870 cm^{-1}
ν C = O 1760, 1680, 1650 cm^{-1}
γ NH 765 cm^{-1}

N,N′-bis-Diisopropylcarbamoylurea (5f)

2f (2 g, 4.95 mmole) gave **5f** (0.6 g; 28.8%). The product was recrystallized from water to obtain a white crystalline product, m.p. 150—152 °C.
$C_{15}H_{30}N_4O_3$ (314.32). Calcd. C 57.02; H 9.20; N 17.92. Found C 57.80; H 9.10; N 17.65%.
IR (KBr): ν NH 3240 cm^{-1}
ν $CH_{aliphatic}$ 2950, 2880 cm^{-1}
ν C = O 1760, 1665, 1640 cm^{-1}
γ NH 760 cm^{-1}.

N,N′-bis-di-n-Butylcarbamoylurea (5g)

2g (2 g, 4.33 mmole) gave **5g** (0.65 g; 40.3%). The product was recrystallized from a mixture of acetone and water to give white, long needles, m. p. 98—99 °C.
$C_{19}H_{38}N_4O_3$(370.52). Calcd.C 61.58; H 10.30; N 15.18. Found C 62.80; H 10.66; N 15.15%
IR (KBr): ν NH 3240 cm^{-1}
ν $CH_{aliphatic}$ 2950—2865 cm^{-1}
ν C = O 1760, 1680, 1640 cm^{-1}
γ NH 760 cm^{-1}.

N,N′-bis-Methylanilinocarbamoylurea (5h)

2h (2 g, 4.79 mmole) gave **5h** (1.3 g; 83.2%). The product was recrystallized from a mixture of acetone and water. A white crystalline substance was obtained, m.p. 148—149 °C.

$C_{17}H_{18}N_4O_3$ (326.34). Calcd. C 62.20; H 5.51; N 17.19. Found C 62.64; H 5.80; N 17.07%.

IR (KBr): ν NH 3240 cm^{-1}
ν $CH_{aromatic}$ 3100—3000 cm^{-1}
ν $CH_{aliphatic}$ 3000—2900 cm^{-1}
ν C = O, C = C 1790, 1680, 1660, 1600 cm^{-1}
γ NH 760 cm^{-1}.

2,4-Dichloro-6-dialkylamino-1,3,5-triazine (7)
General procedure

Product **2** was heated to 140—160 °C or to 150—170 °C on a paraffin oil bath in a round-bottomed flask equipped with a thermometer and an outlet for gases. On gradual increase of the temperature the substance melted, and a strong gas evolution started. After the evolution of the gas had ceased, the brownish product was cooled and recrystallized from aqueous methanol to obtain a white crystalline substance.

2,4-Dichloro-6-dimethylamino-1,3,5-triazine (7a)

2a (2 g, 6.82 mmole) yielded **7a** (0.95 g; 72%) after heating at 150—170 °C for 2.5 hrs. The product was recrystallized from a mixture of methanol and water, m.p. 117—118 °C (lit. [5, 8], m.p. 121—122 °C).

$C_5H_6Cl_2N_4$ (193.0). Calcd. C 31.18; H 3.15; Cl 36.74; N 29.03. Found C 31.67; H 3.43; Cl 36.62; N 29.08%.

IR (KBr): ν $CH_{aliphatic}$ 2980—2900 cm^{-1}
ν C = N 1600, 1550 cm^{-1}
γ = CH 796 cm^{-1}

NMR ($CDCl_3$): 3.25 (s, 6H, dimethylamino-CH_3).

2,4-Dichloro-6-diethylamino-1,3,5-triazine (7d)

2d (2 g, 5.74 mmole) gave **7d** (0.7 g; 55.2%) on heating at 140—145 °C for 2.5 hrs. The product was recrystallized from a mixture of methanol and water; m.p. 78—79 °C (lit. [8] m.p. 85 °C, from hexane).

$C_7H_{10}Cl_2N_4$ (221.08). Calcd. C 38.0; H 4.88; Cl 31.9; N 25.38. Found C 38.04; H 4.90; Cl 30.5; N 24.77%.

IR (KBr): ν $CH_{aliphatic}$ 3000—2890 cm^{-1}
ν C = N 1590, 1560 cm^{-1}
γ = CH 790 cm^{-1}

NMR ($CDCl_3$): 1.28 (t, 6H, J = 6.6 Hz, diethylamino—CH_3)
3.75 (q, 4H, J = 6.6 Hz, diethylamino—CH_2).

2,4-Dichloro-6-di-n-propylamino-1,3,5-triazine (7e)

2e (2 g, 4.93 mmole) was converted into **7e** (0.52 g; 42.5%) by heating at 140—145 °C for 2.5 hrs. The product was recrystallized from a mixture of methanol and water; m.p. 56—58 °C (lit. [9], m.p. 56—58 °C).

$C_9H_{14}Cl_2N_4$ (294.13). Calcd. C 43.45; H 5.68; Cl 28.40; N 22.50. Found C 43.10; H 5.55; Cl 28.80; N 22.50%.

IR (KBr): ν $CH_{aliphatic}$ 3000—2990 cm^{-1}
ν C = N 1585—1555 cm^{-1}
γ = CH 795 cm^{-1}

NMR ($CDCl_3$): 0.95 (t, 6H, J = 6.6 Hz, di-*n*-propylamino—CH_3)
1.40—2.00 (m, 4H, di-*n*-propylamino—CH_2—)
3.58 (t, 4H, J = 7.9 Hz, di-*n*-propylamino—CH_2—).

2,4-Dichloro-6-diisopropylamino-1,3,5-triazine (7f)

2f (2 g, 4.93 mmole) gave **7f** (0.62 g; 51.0%) on heating at 140—145 °C for 2.5 hrs. The product was recrystallized from a mixture of methanol and water; m.p. 103—105 °C (lit. [9] m.p. 103—105 °C).

$C_9H_{14}Cl_2N_4$ (249.13). Calcd. C 43.45; H 5.68; Cl 28.40; N 22.50. Found C 44.50; H 5.70; Cl 26.08; N 22.30%.

IR (KBr): ν $CH_{aliphatic}$ 3000—2890 cm^{-1}
ν C = N 1565 cm^{-1}
γ = CH 788 cm^{-1}

NMR ($CDCl_3$); 4.40 (d, 12H, J = 6.6 Hz, diisopropylamino—CH_3)
4.20—4.80 (m, 2H, J = 6.6 Hz, diisopropylamino—$\geqslant$CH)

REFERENCES

1. BREDERECK, K., RICHTER, R.: Ber. **99,** 2454 (1966)
2. GARBRECHT, W. L., HERBST, R. M.: J. Org. Chem. **18,** 1003 (1953)
3. MARTIN, G., MARTIN, M.: Bull. soc. chim. France **1963,** (8—9) 1637
4. EILINGSFELD, H., SEEFELDER, M., WEIDINGER, H.: Angew. Chem. **72,** 836 (1960); Ber. **96,** 2671 (1963)
5. BREDERECK, K., RICHTER, R.: Ber. **99,** 2461 (1966)
6. JÖRG, J., HOURIET, R., SPITELLER, G.: Monatsch. Chem. **97,** 1064 (1966)
7. ROSS, J. A., TWEEDY, B. G.: Org. Mass Spectrom. **3,** 219 (1970)
8. KOHAN, M. J., MUNN, G. E.: Belg. Pat. 622 057 (1963); C. A. **63,** 3075 (1965)
9. BRIT. Pat. 814 949, June 17, 1959; C.A. **54,** P. 9195.

Zoltán CSŰRÖS
Rudolf SOÓS } 1111 Budapest XI., Műegyetem rkp 3.

Ágnes ANTUS-ERCSÉNYI; 1045 Budapest IV., Tó u. 1—5.
István BITTER; 1111 Budapest XI., Műegyetem rkp 3.
József TAMÁS; 1088 Budapest VIII., Puskin u 11/13.

Acta Chimica Academiae Scientiarum Hungaricae, Tomus 76 (1), pp. 95—105 (1973)

FLAVONOIDS, XXV*

PREACTION OF 2'-OR-CHALCONE DIBROMIDE WITH AMMONIA; PREPARATION OF CHALCONE AZIRIDINE AND 3-AMINOFLAVANONE

GY. LITKEI, R. BOGNÁR and J. ANDÓ

(Institute of Organic Chemistry, L. Kossuth University, Debrecen)

Received January 24, 1972

Investigation of the bromine addition to 2'-OR-chalcone derivatives (**1**) has shown that the protective groups may be split off during this reaction depending on the substituent in ring B of the molecule, the polarity of the solvent and the character of the protective group.

2'-OR-chalcone dibromides (**2**) react with ammonia to give a flavone (when R = H), or *trans*-2-(4-R'-phenyl)-3-(2'-OR-benzoyl)-ethyleneimine (**9**) (when R = $CH_2C_6H_5$ or CH_2OCH_3), depending on the character of the protective group.

The aziridine **9** can be benzoylated to obtain the N-benzoylaziridine derivative **10**, which is converted into 2,3-*trans*-3-(N-benzoyl)-aminoflavanone (**11**) with acid.

The reaction mechanisms and the role of stereochemical factors, as well as the stereochemistry of the end products are considered, the suggestions being supported by IR and NMR spectrometric results.

As it has been known, 2'-OR chalcone epoxides (R = $CH_2C_6H_5$; CH_2—OCH_3) can be converted into various flavonoid derivatives of different states of oxidation [1—7]. Chalcone aziridines analogous to chalcone epoxides have been investigated by several authors [8—9], but the preparation of aziridines from chalcones containing a hydroxyl group at C-2' has not been studied up to now.

In 1971, we reported the preparation of *cis*- and *trans*-1-cyclohexyl-2-(4-R'-phenyl)-3-(2'-OR-benzoyl)-ethyleneimines (R = $CH_2C_6H_5$; CH_2OCH_3; R' = H; Cl; NO_2) obtained from 2'-OR-chalcone derivatives [10]. It was stated that the 3-aminoflavonoid derivative could not be prepared from the isomeric aziridine derivatives under the conditions examined. It was reported at the same time, that the reaction of 2'-hydroxychalcone with cyclohexylamine in the presence of iodine resulted in 3-(N-cyclohexyl)-aminoflavanone, 3-(N-cyclohexyl)-aminoflavone and 2-benzalcoumaranone (aurone) [10].

In the present paper, the preparation of 2'-OR-chalcone aziridines and the possibilities of their conversions are discussed. The formation of the aziridine in the presence of a 2'-hydroxy substituent was studied, and the reaction mechanisms were compared with those of the analogous *trans*-2'-OR-chalcone epoxides.

* Part XXIV: LITKEI, GY., NEUBAUER, A., BOGNÁR, R.: Magy. Kém. Foly. **78**, 359 (1972)

Preparation of 2'-OR-chalcone dibromides

Non-substituted aziridines can be obtained from the corresponding dibromides by allowing then to react with ammonia [11].

2'-Acetoxychalcone dibromide (**2b**) can be obtained from the chalcone **1b** with a calculated amount of bromine in satisfactory yield [12], but chalcones **1c, 1g** give the stable dibromide **2a** instead of dibromides **2c, 2g** expected under similar conditions; *i.e.*, the protective group is split off. This product was also obtained in the bromination of **1a** in glacial acetic medium. The same dibromide can be obtained by the condensation of *ω*-bromo-*o*-hydroxyacetophenone with benzaldehyde in glacial acetic acid containing hydrogen bromide [13].

In a similar manner, the chalcone **1d** yielded the dibromide **2i,** which proved to be identical with the dibromide obtainable from **1i** [14].

1 **2**

a: R=R'=H
b: R=$COCH_3$; R'=H
c: R=$CH_2C_6H_5$; R'=H
d: R=$CH_2C_6H_5$; R'=OCH_3
e: R=$CH_2C_6H_5$; R'=NO_2
f: R=$CH_2C_6H_5$; R'=Cl
g: R=CH_2OCH_3; R'=H
h: R=CH_2OCH_3; R'=NO_2
i: R=H; R'=OCH_3

According to our investigations, if ring B of the initial chalcone is substituted with a nitro group or chlorine, even the methoxymethyl protective group, which is otherwise unstable, is not split off during bromination. Thus, the chalcones **1e, f, h** could be converted into the dibromides **2e, f, h** with bromine in carbon tetrachloride.

Thus, the substituent in *para* position of ring B of the chalcone molecule influences significantly the stability of the protective group in the *ortho* position of ring A. A similar effect can also be observed in other reactions of chalcone derivatives [5, 6, 15].

Acetylation of **2a** results in **2b** being identical with (±)-*erythro*-2'-acetoxychalcone dibromide whose structure was proved by FISCHER and ARLT [15].

The corresponding chalcone dibromides could also be prepared by bromination with pyridinium hydrobromide perbromide ($C_5H_5\overset{+}{N}H\overset{-}{Br}_3$). In glacial acetic acid, the chalcones **1a-f** could be converted into the dibromides **2a-f** in satisfactory yields by this procedure. According to the experiments the methoxymethyl protective group is split off in the course of the reaction. Bromination in glacial acetic acid did not cause splitting off of the protective group, thus the dibromide **2c** could be obtained from **1c.**

In the course of the bromination experiments, another reaction also takes place simultaneously, in addition to the bromine addition which probably involves an ionic or radial mechanism, depending on the polarity of the solvent. In glacial acetic acid the protective group is not split off, only bromine addition occurs, while in carbon tetrachloride the protective group is split off, too.

The products obtained are (±)-*erythro*-chalcone dibromides, as shown by the NMR spectroscopic investigations, in accordance with the findings of WEBER and BROSCHE [16]. The coupling constant of the C_α—H and C_β—H doublets is 11.5 Hz.

Reaction of 2'-OR-chalcone dibromides with ammonia

The dibromides **2a, i** were made to react with methanolic ammonia resulting in flavone (**3,** R' = H) and 4'-methoxyflavone (**3,** R' = OCH_3) in satisfactory yields. The same product was obtained in the reaction with cyclohexylamine or sodium hydroxide.

Similarly, a mixture of 3-bromoflavanone isomers [17] also yielded flavone when treated with ammonia in absolute methanol.

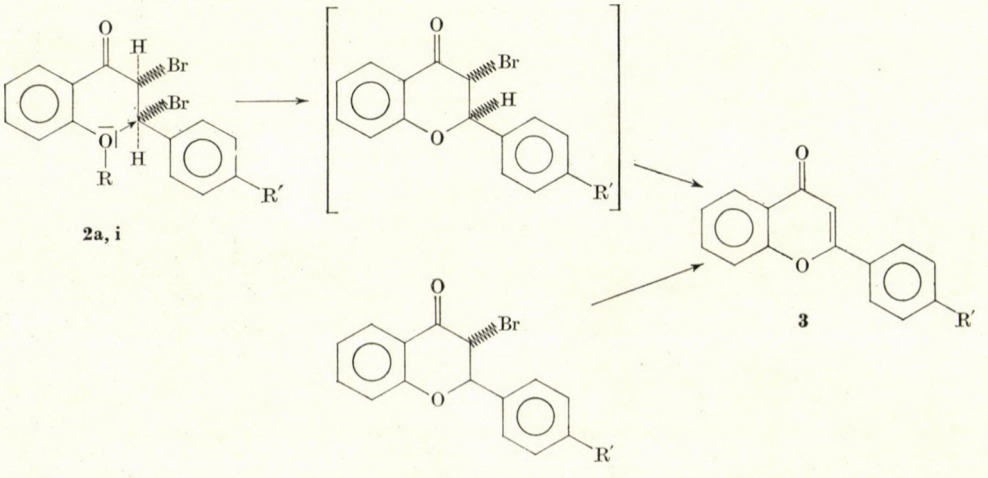

According to the experiments, the aziridine derivative probably is not formed in the course of the reaction; in the first step 3-bromoflavanone is obtained, and the subsequent *trans*-elimination of hydrogen bromide results in **3.** The formation of either the aziridine intermediate or its conversion into 3-aminoflavanone and flavone is not probable, since the reaction of 3-aminoflavanone with ammonia in methanol gave exclusively 3-aminoflavone under the experimental conditions applied.

The treatment with cyclohexylamine of **2a** in dry benzene afforded 3-cyclohexylaminoflavanone (**5**), 3-cyclohexylaminoflavone (**8**) and 2-benzalcoumaranone (**7**). A similar product was obtained from **1a** with cyclohexylamine in the presence of iodine [10]. As supposed previously, a mixture of the *cis*- and *trans*-aziridine derivatives (**4**) is the intermediate product in this reaction. The phenolate anion of the intermediate (**4**) attacks **5** at the C_α or C_β carbon atom; in the case of **7**, the attack occurs through **6.** Product **8** can be obtained from **5** in a secondary reaction [19].

2'-Benzyloxychalcone dibromide (**2c**) was allowed to react with methanolic ammonia to obtain the aziridine **9c.** No isomers were formed in the course

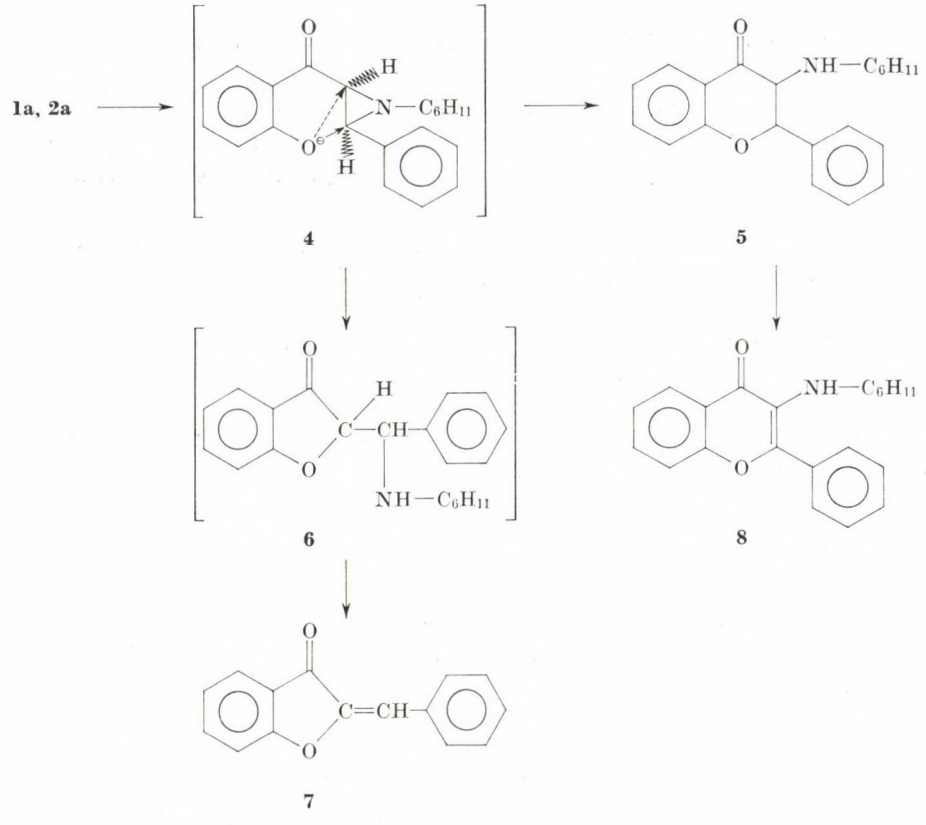

of the reaction. Under similar conditions, the dibromides *2e, f, h* yielded homogenous products **9e, f, h** in satisfactory yields. Previously, it was found that the reaction of **1c** with cyclohexylamine in the presence of iodine or that of **2c** with cyclohexylamine resulted in a mixture of *cis*- and *trans*-1-cyclohexyl-2-phenyl-3-(2'-benzyloxybenzoyl)-ethyleneimine [10, 19]. The two isomers can also be obtained from **2f** with cyclohexylamine.

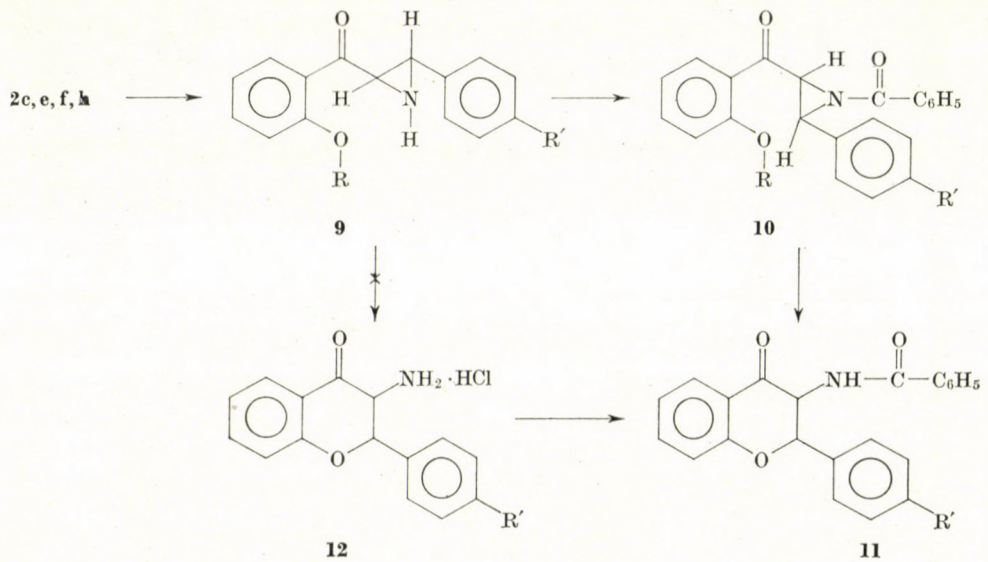

According to the spectroscopic and analytical investigations, **9c, e, f, h** were found to be *trans*-2-(4-R'-phenyl)-3-(2'-OR-benzoyl)-ethyleneimines. Thus, e.g., in **9f**, the ν_{CO} and ν_{NH} vibrations can be assigned to the bands appearing at 1659 cm^{-1} and 3228 cm^{-1}, respectively, which are characteristic of *trans*-ethyleneimine derivatives [20]. In the NMR spectrum, the complex multiplet of the aromatic protons are found at 2.17—3.07 ppm, the CH_2 singlet at 5.02 ppm, while the singlet of the C_α—H and C_β—H protons appear at 6.3 ppm and 6.9 ppm, respectively; the signal at 7.4 ppm can be assigned to N—H (τ scale). The C_α—H and C_β—H signals can be found in the region characteristic of *trans*-ethyleneimine protons [21].

The spectroscopic data of aziridines **9** are shown in Table II.

The colourless aziridine derivatives are rather unstable compounds. They decompose with discoloration when exposed to light and air. The formation of 3-amino-flavanone derivatives could not be detected on treatment with hydrochloric acid.

The N-benzoylaziridine derivatives **10** were obtained from the aziridines **9** with benzoyl chloride in absolute benzene, in the presence of triethylamine.

In the course of the reaction the opening of the ring did not occur, as it is shown by the NMR spectrum (Table IV). In the NMR spectrum, the C_α—H and C_β—H signals appear at ppm values lower than those of non-substituted derivatives.

The boiling of N-benzoylaziridines **10** with hydrochloric acid in ethanol resulted in splitting off the protective group and the formation of 3-(N-benzoyl)-aminoflavanone derivatives **11.** The structure of **11** (R' = H) was verified by benzoylation of the known compound 3-aminoflavanone (**12,** R' = H); the products obtained in the two different ways were identical.

According to our former investigations, in *cis*- and *trans*-N-cyclohexyl-aziridine derivatives the protective group is not split off with acid, only the aziridine ring is cleaved [19].

On the basis of our experimental results, the opening of the ethyleneimine ring of 2'-OR-chalcone aziridines and the splitting off of the protective group at C-2' is determined by the electronic structure of the ethyleneimine ring.

In N-benzoylaziridine derivatives the electron-withdrawing effect of the carbonyl group results in decreased electron density on the β carbon atom. This favours internal nucleophilic attack by the ethereal oxygen, similarly to the corresponding epoxides [6].

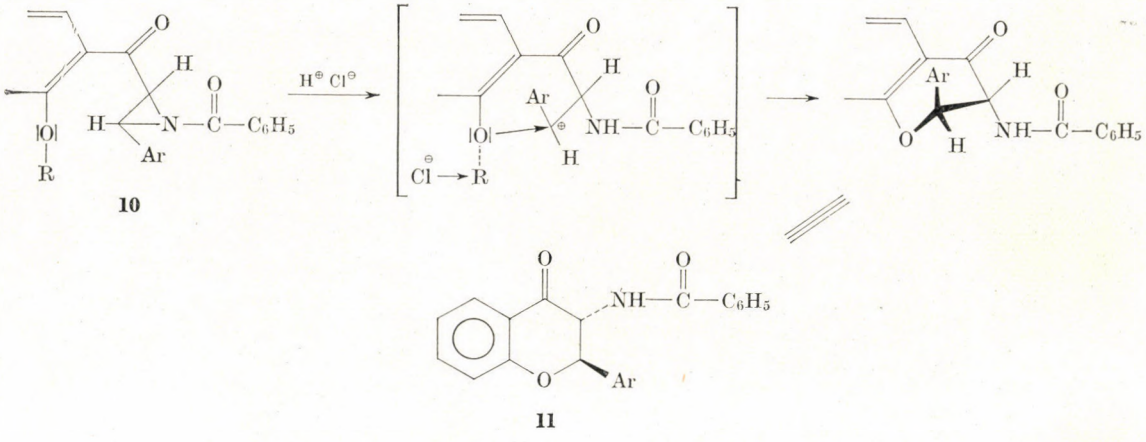

10 **11**

The protective group is split off and the aziridine ring is opened simultaneously, followed by cyclyzation after inversion of the β carbon atom, resulting in 2,3-*trans*-3-(N-benzoyl)-aminoflavanone. This concept has been confirmed by the NMR spectroscopic investigations (Table V). The 2-phenyl and 3-NH-COC_6H_5 groups are in *trans* configuration. The coupling constant of the C_2—H and C_3—H protons is in agreement with the literature data [25].

Experimental

Melting points are uncorrected. The NMR spectra were recorded with a JEOL JNM-100 MHz instrument in $CDCl_3$, the infrared spectra with a UNICAM SP 200 G spectrophotometer in KBr pellets.

2'-Hydroxychalcone dibromide (2a)

(a) Chalcone **1g** (10 g) [22] was dissolved in carbon tetrachloride (50 ml) and bromine (5.97 g) in carbon tetrachloride (20 ml) was added. Strong evolution of hydrogen bromide was observed during the reaction. After 1 hr the solvent was evaporated in vacuum at 40 °C and the residual oil crystallized from absolute ethanol to obtain 3.2 g (22%) of **2a**, m.p. 190—192 °C, (lit. [13] m.p. 192 °C).

The product prepared similarly from chalcone **1c** [1] in 37% yield had m.p. 190—191 °C.

(b) Chalcone **1a** (5.6 g) was brominated in glacial acetic acid. The crude product which separated was recrystallized from ethyl acetate to yield 3.3 g (34%) of **2a**, m.p. 190—192 °C.

(c) Chalcone **1g** (4 g) was dissolved in glacial acetic acid (35 ml) and pyridine hydrobromide perbromide (4.25 g) [23] was added to it under stirring. After 2 hrs the precipitate was filtered off and recrystallized from ethyl acetate to give 4 g (52%) of **2a**, m.p. 190—192 °C.

$C_{15}H_{12}O_2Br_2$ (384.08). Calcd. Br 41.60. Found Br 42.18%.

2'-Hydroxy-4-methoxychalcone dibromide (2i)

The chalcone **1d** (0.01 mole) was allowed to react with bromine (0.01 mole) as described above under *(a)*. The product was crystallized from glacial acetic acid to yield 46% of **2i**, m.p. 143—145 °C (lit. [14] m.p. 144—145 °C).

$C_{16}H_{14}O_3Br_2$ (414.10). Calcd. C 46.30; H 3.39; Br 38.60. Found C 46.54; H 3.52; Br 37.44%.

2'-Acetoxychalcone dibromide (2b)

(a) Dibromide **2a** (1 g) was allowed to react with a mixture of acetic anhydride (10 ml) and 70% perchloric acid (2 drops) at room temperature for 24 hrs. The product obtained on pouring the solution onto ice was crystallized from absolute ethanol to yield 0.75 g (67.5%) of **2b**, m.p. 106—108 °C.

(b) Chalcone **1b** (2.66 g) [12] was treated with pyridinium hydrobromide perbromide (3.5 g) in glacial acetic acid (35 ml) at room temperature, with stirring. The product which separated on the addition of water was crystallized from absolute ethanol to obtain 3.65 g (85%) of **2b** m.p. 107—108 °C (lit. [12] m.p. 107 °C).

$C_{17}H_{14}Br_3O_2$ (426.11). Calcd. C 48.00; H 3.29; Br 36.20. Found C 48.17; H 3.28; Br 35.14%.

2'-Benzyloxychalcone dibromide (2c)

(a) Chalcone **1c** (0.01 mole) was made to react with pyridinium hydrobromide perbromide (0.011 mole) according to the procedure described above under *(c)*. The product was crystallized from absolute ethanol to obtain 3.3 g (70%) of **2c**, m.p. 90—92 °C.

(b) Chalcone **1c** (3.14 g) was dissolved in glacial acetic acid (50 ml) and mixed with a solution of bromine (0.54 ml) in glacial acetic acid (10 ml). The product which separated on the addition of water was recrystallized from absolute ethanol to give 3.25 g (68.5%) of **2c**, m.p. 91—93 °C.

$C_{22}H_{18}O_2Br_2$ (474.19). Calcd. C 55.90; H 3.81; Br 33.70. Found C 55.94; H 3.90; Br 32.76%.

2'-Benzyloxy-4-methoxychalcone dibromide (2d)

The product obtained from **1d** with pyridinium hydrobromide perbromide was recrystallized from carbon tetrachloride to yield 83% of **2d**, m.p. 115—118 °C.

$C_{23}H_{20}O_3Br_2$ (504.22). Calcd. C 55.00; H 3.98; Br 31.70. Found C 55.34; H 4.20; Br 29.95%.

2'-Benzyloxy-4-chlorochalcone dibromide (2f)

Chalcone **1f** [6] was treated with bromine in carbon tetrachloride. The residue was recrystallized from a mixture of benzene and petroleum ether to yield 76% of **2f**, m.p. 127—128 °C. In the pyridinium hydrobromide perbromide procedure the yield was 82%; m.p. 126—128 °C.

$C_{22}H_{17}O_2Br_2Cl$ (508.64). Calcd. C 52.00; H 3.36. Found C 52.41; H 3.58%.

2'-Benzyloxy-4-nitrochalcone dibromide (2e)

Chalcone **1e** [6] was brominated in carbon tetrachloride and the product was crystallized from a mixture of benzene and petroleum ether to obtain **2e** in 88.5% yield; m.p. 138—140 °C. In the pyridinium hydrobromide perbromide procedure the yield was 88%; m.p. 138—140 °C.

$C_{22}H_{17}O_4Br_2N$ (519.19). Calcd. N 2.70; Br 30.80. Found N 2.62; Br 31.15%.

2'-Methoxymethoxy-4-nitrochalcone dibromide (2h)

The product obtained from chalcone **1h** [22] with bromine in carbon tetrachloride according to the procedure described in the previous section *(a)*, was crystallized from a mixture of ethyl acetate and petroleum ether to obtain **2h** in 45% yield; m.p. 128—130 °C.

$C_{17}H_{15}O_5Br_2N$ (473.12). Calcd. Br 33.80; N 2.96. Found Br 33.98; N 2.83%.

Flavone (3; R′ = H)

(a) The dibromide **2a** [1 g] was dissolved in absolute methanol saturated with dry ammonia (25 ml) and the mixture was kept in a refrigerator for 15 hrs. The solution was evaporated to dryness and the residue extracted with hot petroleum ether (5 × 15 ml). The crude product was crystallized from aqueous ethanol to give 0.4 g (67%) of flavone m.p. 94—96 °C (lit. [17] m.p. 95.5—97.5 °C).

(b) The dibromide **2a** (1 g) was treated with 2N NaOH solution (2.9 ml) in ethanol (50 ml) at room temperature for 30 min. The product which precipitated on the addition of water was crystallized from aqueous ethanol to yield 50% of flavone, m.p. 94—96 °C.

(c) The dibromide **2a** (1.2 g) was allowed to react with cyclohexylamine (2.5 ml) in absolute methanol (25 ml) for 24 hrs. The product which separated on the addition of water was crystallized from aqueous ethanol to yield 40% of flavone, m.p. 94—96 °C.

(d) A mixture of 3-bromoflavanone isomers [17] obtained by the bromination of flavanone (1.14 g) was allowed to react with absolute methanol (25 ml) saturated with dry ammonia for 24 hrs. Flavone was obtained in 71% yield, m.p. 94—96 °C.

These products synthetized in different ways did not show melting point depression in admixture with pure authentic flavone, and also the spectroscopic properties were identical.

4'-Methoxyflavone (3; R' = OCH_3)

The product obtained from the dibromide **2i** in 90% yield according to the previous procedure *(a)* was crystallized from methanol; m.p. 156—158 °C (lit. [24] m.p. 157—158 °C).

$C_{16}H_{12}O_3$ (252.26). Calcd. C 76.10; H 4.75; OCH_3 12.30. Found C 76.26; H 4.57; OCH_3 12.68%.

trans-2-(4-R'-Phenyl)-3-(2'-OR-benzoyl)-ethyleneimine (9c, e, f, h)

The dibromides **2c, e, f, h** (0.01 mole) were dissolved in absolute methanol saturated with dry ammonia (50 ml) and let to stand in a refrigerator for 48 hrs. The product which precipitated was crystallized from absolute ethanol. The data of the products are given in Table I, and their spectroscopic data are shown in Table II.

trans-N-Benzoyl-2-(4-R'-phenyl)-3-(2'-OR-benzoyl)-ethyleneimine (10c, e, f, h)

The ethyleneimine (**9c, e, f,** or **h**) (0.03 mole) was treated with benzoyl chloride (0.031 mole) in the presence of triethylamine in absolute benzene (25 ml) at room temperature for 24 hrs. After filtering off the salt, the benzene solution was washed with water, dried and

Table I

trans-2-(4-R'-Phenyl)-3-(2'-OR-benzoyl)-ethyleneimines **(9)**

	R'–	R–	Yield, %	M. p., °C	Cald.			Found		
					C	H	N/Cl	C	H	N/Cl
9c	H	$CH_2C_6H_5$	83	106—8	80.50	5.82	4.26	81.40	5.72	4.27
9e	NO_2	$CH_2C_6H_5$	90	116—8	70.70	4.85	7.50	70.88	4.92	7.91
9f	Cl	$CH_2C_6H_5$	80	93—4	72.80	4.96	3.87	72.53	4.55	3.92
							9.76			10.38
9h	NO_2	CH_2OCH_3	70	115—7	62.40	4.91	8.54	62.66	4.70	9.00

Table II

IR and NMR spectroscopic data of trans-2-(4-R'-phenyl)-3-(2'-OR-benzoyl)-ethyleneimines **(9)**

	IR[ζcm^{-1}]		NMR [τ]			
	$\nu_{C=O}$	ν_{NH}	Aromatic protons	CH_2	$H_\alpha + H_\beta^a$	NH
9c	1666	3237	2.19—3.28[b]	5.00[c]	6.54	7.30[d]
9e	1664	3258	1.91—2.93[b]	4.97[c]	6.50	7.24[d]
9f	1659	3228	2.17—3.07[b]	5.02[c]	6.63	7.40[d]

[a] the centre of doublet; [b] complex multiplet; [c] singlet; [d] the centre of broad singlet

concentrated to half of its original volume. The product which precipitated on the addition of petroleum ether was crystallized from absolute ethanol. The data of the products are summarized in Tables III and IV.

Table III

trans-N-Benzoyl-2-(4-R'-phenyl)-3-(2'-OR-benzoyl)-ethyleneimines **(10)**

	R'	R	Yield, %	M.p., °C	Cald.			Found		
					C	H	N	C	H	N
10c	H	$CH_2C_6H_5$	78	128—130	80.05	5.33	3.24	80.04	5.32	3.52
10e	NO_2	$CH_2C_6H_5$	80	146—148	72.90	4.62	5.85	72.74	5.27	5.97
10f	Cl	$CH_2C_6H_5$	84	135—137	74.30	4.74	2.99	74.06	4.69	3.12
10h	NO_2	CH_2OCH_3	75	103—105	66.80	4.63	6.48	66.87	4.23	6.57

3-(N-Benzoyl)-aminoflavanone (11; R′ = H)

(a) Ethyleneimine **10c** (1 g) was boiled in absolute methanol (50 ml) in the presence of conc. HCl (0.5 ml) for 1 hr. The product which separated was crystallized from ethyl acetate to give 0.4 g (50%) of the product m.p. 239—241 °C.

(b) 3-Aminoflavanone hydrochloride* (0.23 g) [18] was allowed to react with benzoyl chloride (0.12 ml) in absolute benzene (20 ml) in the presence of triethylamine (0.3 ml) at

* The authors' thanks are due to M. RÁKOSI for supplying 3-aminoflavanone hydrochloride and 3-aminoflavone samples.

Table IV

Infrared and NMR spectroscopic data of trans-N-benzoyl-2-(4-R'-phenyl)-3-(2'-OR-benzoyl)-ethyleneimines **(10)**

	IR [cm^{-1}]	NMR[τ] (*J*, Hz)			
	$\nu_{C=O}$	Aromatic protons	CH_2	$H_\alpha + H_\beta$	$O-CH_3$
10c	1670, 1686	2.02—3.10[a]	4.93[b]	5.75[c] (2.8)	
10e	1676	1.91—3.12[a]	4.97[b]	5.76[c] (2.8)	—
10f	1675, 1687	2.11—3.15[a]	4.97[b]	5.78[c] (3)	—
10h	1689	1.74—3.12[c]	5.00[b]	5.77[c] (3)	6.77[b]

[a] complex multiplet; [b] singlet; [c] centre of quartet

room temperature for 4 hrs. The substance which separated was washed with water and crystallized from a mixture of ethyl acetate and dioxane to give 0.25 g (86%) of the product, m.p. 239—241 °C.

The substances obtained in the two different ways did not show melting point depression in admixture, and their infrared spectra were also identical.

$C_{22}H_{17}O_3N$ (343.36). Calcd. C 77.00; H 4.96; N 4.08. Found C 76.58; H 4.80; N 4.08%.

3-(N-Benzoyl)-amino-4'-chloroflavanone (11; R' = Cl)

Ethyleneimine **10f** (1 g) was treated with hydrochloric acid as described above under *(a)*. The product was crystallized from a mixture of ethyl acetate and dioxane to obtain 0.4 g (50%) of the pure substance, m.p. 248—250 °C.

$C_{22}H_{16}O_3ClN$ (377.81). Calcd. C 70.00; H 4.24; N 3.71; Cl 9.40. Found C 70.15; H 4.38; N 3.87; Cl 9.28%.

3-(N-Benzoyl)-amino-4'-nitroflavanone (11; R' = NO_2)

(a) The product, prepared from **10h** according to the previous procedure *(a)* in 65% yield, had m.p. 224—225 °C.

Table V

IR and NMR spectroscopic data of 2,3-trans-3-(N-benzoyl)-amino-4'-R-flavanone **(11)**

R	IR [cm^{-1}]		NMR [τ] [*J* Hz]					
	$\nu_{C=O}$	ν_{NH}	Aromatic protons[a]	H_2^b	H_3^c	$J_{2,3}$	NH[b]	$J_{3H;NH}$
H	1647 1710	3307	2.1—2.9	4.22	4.77	12.4	1.31	8.4
NO_2	1642 1710	3324	1.70—2.86	4.04	4.71	12.4	1.23	8.6
Cl	1647 1710	3332	2.1—2.89	4.21	4.77	12.4	1.30	8.4

[a] complex multiplet
[b] centre of doublet
[c] centre of quartet

(b) The product made from **10e** in a similar way in 30% yield melted at 224—225 °C. $C_{22}H_{16}O_5N_2$ (388.37). Calcd. C 68.00; H 4.12; N 7.21. Found C 67.04; H 4.19; N 7.14%.

The infrared and NMR data of the 3-(N-benzoyl)-amino-4'-R-flavanones prepared are summarized in Table V.

*

The authors' thanks are due to Z. DINYA, A. LÉVAI, L. SZILÁGYI and S. SZABÓ for the accomplishment of the spectroscopic investigations, to É. D. RÁKOSI for the microanalyses and to Mrs. S. HAJNAL for her valuable technical assistance.

REFERENCES

1. BOGNÁR, R., STEFANOVSKI, J.: Tetrahedron **18,** 143 (1962)
2. BHRAHA, S. C., JAIN, A. C., SESHADRI, T. R.: Tetrahedron **20,** 1141 (1964); **21,** 963 (1965)
3. CHOPIN, J., DURUAL, P.: Bull. soc. chim. France **1965,** 3350
4. SHARMA, T. C., VERMA, B. L., BOKADIA, M. M.: Chem. and Ind. **1966,** 599
5. LITKEI, GY., BOGNÁR, R.: Kém. Közl. **34,** 249 (1970)
6. LITKEI, GY., BOGNÁR, R., DINYA, Z.: Acta Chim. (Budapest) **71,** 401 (1972)
7. CULLERI, W. P., DONELLY, D. M. X., KEENAN, A. K., LAVIN, T. P., MELODY, D. P., PHILBIN, E. M.: J. Chem. Soc. (C) **1971,** 2848
8. CROMWELL, N. H., BABSON, R. D., HARRIS, C. E.: J. Am. Chem. Soc. **65,** 312 (1943)
9. SOUTHWICK, P. L., CRISTMAN, D. R.: J. Am. Chem. Soc. **74,** 1886 (1952)
10. BOGNÁR, R., LITKEI, GY., SZIGETI, P.: Acta Chim. Acad. Sci. Hung. **68,** 421 (1971)
11. CROMWELL, N. H., MERCER, G. D.: J. Am. Chem. Soc. **79,** 3819 (1957)
12. FEUERSTEIN, W., KOSTANECKI, S.: Ber. **31,** 1757 (1898)
13. PENDSE, H. K., LIMAYE, S. D.: J. Progr. Chem. Sci. **2,** 70 (1955); C. Zentr. **1956,** 10712
14. PENDSE, H. K., LIMAYE, S. D.: J. Progr. Chem. Sci. **2,** 90 (1955); C. Zentr. **1956,** 10714
15. FISCHER, F., ARLT, W.: Chem. Ber. **97,** 1910 (1964)
16. WEBER, F. G., BROSCHE, K.: Tetrahedron **27,** 1435 (1971)
17. BOGNÁR, R., RÁKOSI, M., LITKEI, GY.: Acta Chim. Acad. Sci. Hung. **34,** 353 (1962)
18. BOGNÁR, R., RÁKOSI, M.: Ann. **693,** 225 (1966)
19. LITKEI, GY., BOGNÁR, R., SZIGETI, P., TRAPP, V.: Acta Chim. (Budapest) **73,** 69 (1972)
20. CROMWELL, N. H., BABURY, R. E., ADALFANG, J. L.: J. Am. Chem. Soc. **82,** 424 (1960)
21. POHLAND, A. E., BADGER, R. C., CROMWELL, N. H.: Tetrahedron Letters **48,** 4369 (1965)
22. ENEBÄCK, C.: Soc. Sci. Fenn. Comm. Phys.-Math. XXVIII, 61 (1963)
23. FIESER, L. F.: J. Chem. Ed. **31,** 291 (1954)
24. AUWERS, K., ANSCHÜTZ, L.: Ber. **54,** 1558 (1921)
25. BOGNÁR, R., CLARK-LEWIS, J. W., LIPTÁK-TŐKÉS, A., RÁKOSI, M.: Aust. J. Chem. **23,** 2015 (1970)

György LITKEI
Rezső BOGNÁR
János ANDÓ
Szerves Kémiai Intézet, 4010 Debrecen, Hungary.

Acta Chimica Academiae Scientiarum Hungaricae, Tomus 76 (1), pp. 107—112 (1973)

THE STUDY OF SOME HETEROCYCLES, XXVII

THE HALOGENATION AND NITRATION REACTIONS OF 2-(*M*-TOLYL)-4-X-THIAZOLES

I. SIMITI and M. FARKAS

(Laboratory of Organic Chemistry, Faculty of Pharmacy, Institute of Medicine and Pharmacy, Cluj)

Received March 22, 1972

In continuation of former research, the nitration and bromination of 2-(*m*-tolyl)-4-chloromethylthiazole was studied in order to establish the influence of the methyl group on the para position of the benzene ring and on position 5 of the thiazole ring.

To complete our former studies on the bromination and nitration of 2-(*p*-X-phenyl)-4-chloromethylthiazoles [1], in the present work the bromination and nitration of 2-(*m*-tolyl)-4-chloromethylthiazole was studied; unlike the former group of compounds, in this case there are two very reactive positions: position 5 of the thiazole and position 4 of the benzene ring.

The bromination of 2-(*m*-tolyl)-4-chloromethylthiazole (**I**) showed that, depending on the amount of bromine and even in the absence of a catalyst, both the monobromo derivative (**II**) (with 1.2 moles of bromine) and the dibromo derivative (**III**) (with 6 moles of bromine) can be prepared.

The position occupied by the bromine atom was established both in a synthetic way and by oxidative degradation.

The monobromo derivative (**II**) obtained by the bromination of **I** is not identical with 2-(4-bromo-3-methylphenyl)-4-chloromethylthiazole (**IV**) which we obtained by the condensation of the corresponding thioamide with dichloroacetone; thus in **II** the bromine did not enter the *para* position of the benzene ring. The acid obtained by oxidative degradation contains no bromine and its dimethyl ester is identical with dimethyl isophthalate. The IR spectrum of **II** does not show the band characteristic of the unsubstituted thiazole CH group. All these facts suggest that the bromine occupies position 5 of the thiazole ring.

The dibromo derivative (**III**) obtained by the bromination of **I** with excess bromine is identical with the compound obtained in the bromination of 2-(4-bromo-3-methylphenyl)-4-chloromethylthiazole (**IV**), and it is converted by oxidation into 4-bromoisophthalic acid. In **III** the lack of the 3075—3100 cm^{-1} band is observed, which shows that one of the bromine atoms occupies position 5 of the thiazole ring, while the other one position 4 of the benzene ring.

The experiments also prove that further bromination of the monobromo derivative **II** results in the dibromo derivative **III**.

Like in former investigations, it seems that the presence of Ag_2SO_4 facilitates bromination of the benzene ring. The bromo derivative obtained in this way has an IR spectrum identical with that of 2-(3-methyl-4-bromophenyl)-4-chloromethylthiazole (**IV**) and the mixture of the two substances gives no m.p. depression. Thus, under catalytical conditions the bromine enters position 4 of the benzene ring.

Both 2-(m-tolyl)-4-chloromethyl-5-bromothiazole (**II**) and 2-(3-methyl-4-bromophenyl)-4-chloromethyl-5-bromothiazole (**III**) can be transformed by the Sommelet reaction in the corresponding aldehydes (**V, VI**) which confirms the applicability of this reaction to the thiazole series, even if an electrophilic group is present in position 5.

The aldehyde **VI** is converted by oxidation into the corresponding acid (**VII**), which is identical with the product of the haloform reaction of *2*(-*m*-tolyl)-4-acetylthiazole when the solution is acidified without previous destruction of the excess of bromine [2].

In the bromination of 2-(*m*-tolyl)-4-carboxy-thiazolic acid a similar behaviour was found to that of 2-aryl-4-chloromethylthiazoles, *i.e.*, a small amount of bromine (1.2 mole) leads to a monobromo derivative (**VIII**) which is identical with the oxidation product of 2-(*m*-tolyl)-5-bromo-4-formylthiazolic aldehyde.

When the acid is brominated with an excess of bromine, the dibromo acid (**VII**) identical with the product of the haloform reaction, is obtained.

Thus, the carboxylic group does not influence the character of the bromination reaction.

In the nitration reactions with a mixture of sulfuric acid and nitric acid 2-(*m*-tolyl)-4-chloromethylthiazole (**I**) or 2-(*m*-tolyl)-4-hydroxy-4-chloromethyl-Δ^2-thiazole hydrochloride [3] give 2-(3-methyl-4-nitrophenyl)-4-chloromethylthiazole (**IX**) as the main product; the oxidation of the latter compound yields 4-nitroisophthalic acid.

If the nitration is effected in acetic anhydride, although the isolated main product is a dinitro derivative, chromatography shows the presence of other nitro derivatives, independently of the amount of HNO_3 used (1 or 6 moles).

Since the oxidation of this dinitro derivative results in 4-nitroisophthalic acid and its IR spectrum has no absorption band characteristic of the valence vibration of hydrogen attached to the thiazole ring, the compound must be 2-(3-methyl-4-nitrophenyl)-4-chloromethyl-5-nitrothiazole (**X**).

The nitration with HNO_3–H_2SO_4 mixture of 2-(*m*-tolyl)-4-chloromethyl-5-bromothiazole (**II**) occurs in position 4 of the benzene ring and the same product results (**XI**) as in the bromination of 2-(3-methyl-4-nitrophenyl)-4-chloromethylthiazole.

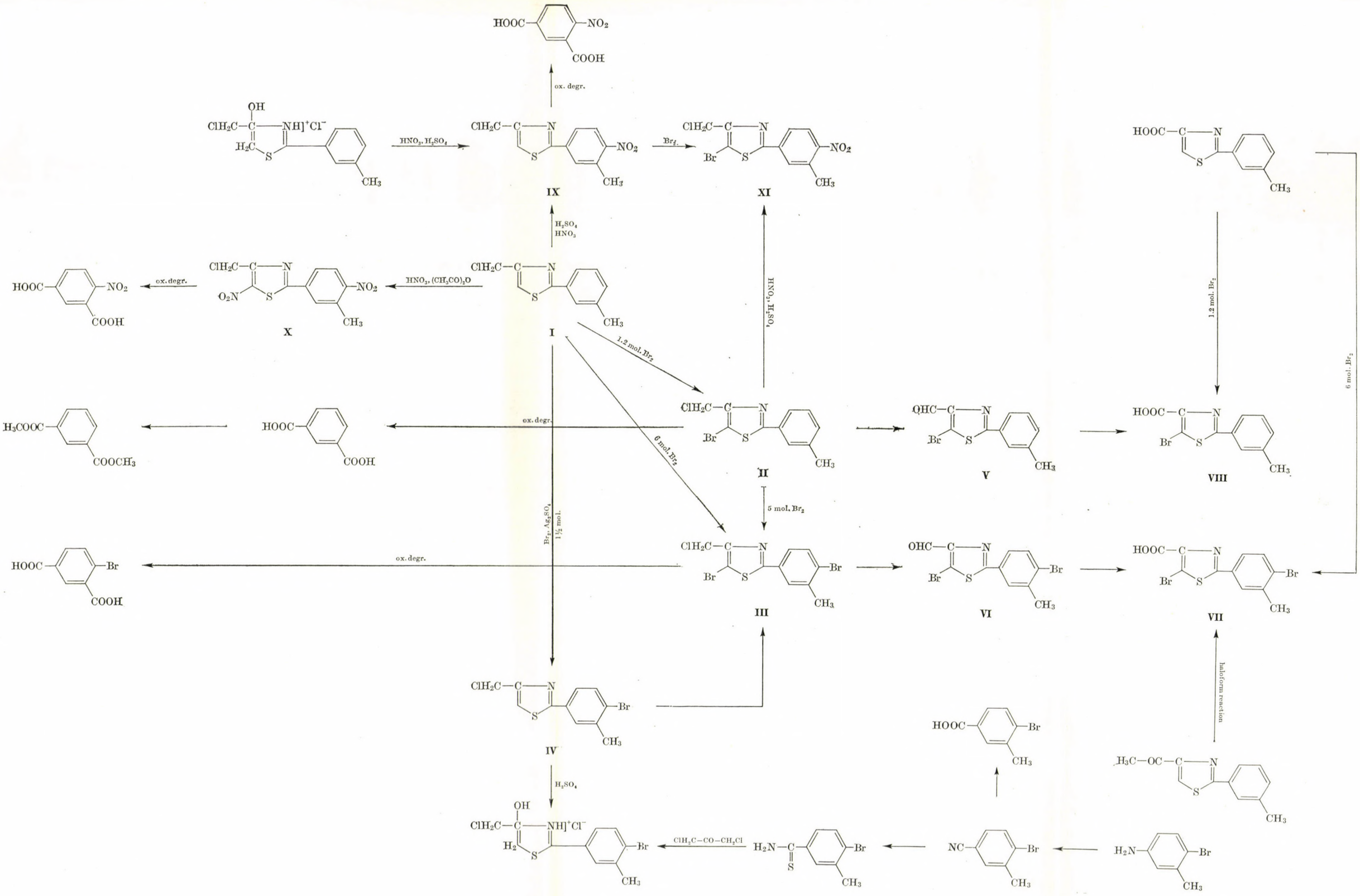
HOOC
NO2
COOH
ox. degr.
ClH2C
OH
NH]+Cl−
H2C
S
CH3
HNO3, H2SO4
IX
Br2
XI
H2SO4
HNO3
HNO3, (CH3CO)2O
O2N
X
I
1.2 mol. Br2
HNO3, H2SO4
II
6 mol. Br2
5 mol. Br2
III
Br2, Ag2SO4
1½ mol.
IV
H2SO4
ClH2C—CO—CH2Cl
H2N
NC
HOOC
H3COOC
COOCH3
OHC
V
VI
VII
VIII
1.2 mol. Br2
6 mol. Br2
haloform reaction
H3C—OC

Experimental

2-(m-Tolyl)-4-chloromethyl-5-bromothiazole (II)

To 0.003 mole of 2-(*m*tolyl)-4-chloromethylthiazole dissolved in either acetic acid or acetic anhydride, 0.0036 mole of Br_2 was added. The mixture was kept 30 min. at room temperature, then poured on ice. The isolated substance was recrystalized from aqueous alcohol and decolorized with active charcoal, m.p. 91—92 °C.

$C_{11}H_8ClBrNS$ (302.629). Calcd N 4.63. Found N 4.89%.

3-Methyl-4-bromo-benzonitrile

To a solution of 26.7 g $CuSO_4 \cdot 5H_2O$ and 6.94 g NaCl in 86 ml water there was added a solution of 6.85 g anhydrous Na_2SO_3 and 1.56 g NaOH in 43 ml water during 10 min. After sedimentation of the cuprous chloride the liquid phase was syphoned off and replaced by 43 ml of water. To this CuCl supension 13.8 g NaCN in 22 ml water was added under continuous mechanical stirring. When the precipitate dissolved completely, the solution was externally cooled with ice and 250 ml benzene was poured on its surface in order to extract the cuprous cyanide formed.

15.9 g 3-methyl-4-bromoaniline was mixed with 16.5 ml conc. HCl in the presence of ice, maintaining the temperature of the mixture at 0—5 °C. The amine was diazotized with 5.98 g $NaNO_2$ in 16.5 ml water, keeping the reaction temperature always under 5 °C. After 15 min. the solution was neutralized with about 17 g anhydrous Na_2CO_3; the pH of the solution was controlled several times for 15 min., the temperature still being maintained below 5 °C. The neutral reaction mixture was introduced gradually with continuous stirring, into the cooled benzene solution of cuprous cyanide as prepared above. The cold mixture was stirred for 30 min., then it was allowed to warm up to room temperature, but stirring was continued for another 2 hrs. It was then warmed for 30 min. at 50 °C without stirring, the benzene layer separated and the benzene removed by distillation. The solid substance which remained was recrystallized from aqueous alcohol and decolorized with charcoal; m.p. 54—54.5 °C.

C_8H_6BrN (196.052). Calcd. N 7.14. Found N 7.54%.

3-Methyl-4-bromothiobenzamide

8 g 3-methyl-4-bromobenzonitrile was dissolved in about 100 ml ethanol saturated with gaseous ammonia. With cooling H_2S was bubbled for 5 hrs through the solution. The reaction mixture was then refluxed for 1 hr and then the alcohol removed by distillation. The solid substance was recrystallized from water, m.p. 139—140 °C.

C_8H_8BrNS (230.134). Calcd. N 6.08. Found 6.23%.

2-(3-Methyl-4-bromophenyl)-4-hydroxy-4-chloromethyl-Δ^2-thiazoline hydrochloride

3.45 g 3-methyl-4-bromothiobenzamide was dissolved in 27 ml acetone and 1.8 g symodichloroacetone was added to the solution. The reaction vessel was closed and shaken until the dichloroacetone completely dissolved, then allowed to stand for 24 hrs. The crystalline substance was filtrated off and washed on the filter with a little acetone; m.p. 152—152.5 °C.

$C_{11}H_{12}Cl_2BrNOS$ (357.110). Calcd. N 3.92. Found N 4.13%.

2-(3-Methyl-4-bromophenyl)-4-chloromethylthiazole (IV)

(a) 7 ml conc. H_2SO_4 was added to 1.8 g 2-(3-methyl-4-bromophenyl)-4-hydroxy-4-chloromethyl-Δ^2-thiazoline hydrochloride. The mixture was kept 30 min. at room temperature, then poured on ice. The product was recrystallized from aqueous ethanol; m.p. 97—98 °C.

$C_{11}H_9ClBrS$ (302.63). Calcd. N 4.62. Found N 4.70%.

(b) 0.004 mole of 2-(*m*-tolyl)-4-chloromethylthiazole **I** was dissolved in 15 ml conc. H_2SO_4, and 0.002 mole of Ag_2SO_4, then, after thorough shaking of the suspension, 0.004 mole of Br_2 was added. The reaction mixture was stirred for 4 hrs and allowed to stand overnight. It was then filtered through a sintered glass filter and the filtrate poured on ice. The dried product was dissolved in warm ethanol, filtered, and the organic substance precipitated by the addition of water. The crude product was recrystallized from aqueous alcohol in the presence of decolorizing charcoal, m.p. 93—94 °C.

$C_{11}H_8ClBrNS$ (302.63). Calcd. N 4 .64. Found N 4.66%.

2-(3-Methyl-4-bromophenyl)-4-chloromethyl-5-bromothiazole (III)

(a) 0.004 mole of 2-(*m*-tolyl)-4-chloromethyl-thiazole (**I**) was dissolved in glacial acetic acid, and 0.024 mole of bromine, in glacial acetic acid, was added. After 30 min. the solution was poured on ice. The product was recrystallized from aqueous alcohol and decolorized with charcoal: m.p. 97 °C.

$C_{11}H_8ClBr_2NS$ (381.537). Calcd. N 3.67. Found N 3.91%.

(b) 0.003 mole of 2-(*m*-tolyl)-4-chloromethyl-5-bromothiazole (**II**) was dissolved in glacial acetic acid and 0.015 mole of Br_2, in glacial acetic acid, was added. After standing 30 min. at room temperature, the solution was poured on ice. The crude product was recrystallized from aqueous ethanol and decolorized with charcoal; m.p. 97—98 °C.

$C_{11}H_8ClBr_2NS$ (381.537). Calcd. N 3.67. Found N 3.87%.

(c) 0.003 mole of 2-(3-methyl-4-bromophenyl)-4-chloromethylthiazole (**IV**) was dissolved in glacial acetic acid and 0.0036 mole of Br_2 was added to the solution. After 30 min. the solution was poured on ice. The product which precipitated was recrystallized from aqueous ethanol; m.p. 98—98.5 °C.

$C_{11}H_8ClBr_2NS$ (381.537). Calcd. N 3.67. Found N 3.70%.

Hexamethylenetetramine salt of 2-(3-methyl-4-bromophenyl)-4-chloromethyl-5-bromothiazole

A solution of 1.4 g hexamethylenetetramine in 20 ml chloroform was added to 3.14 g 2-(3-methyl-4-bromophenyl)-4-chloromethyl-5-bromothiazole dissolved in 10 ml chloroform. The reaction mixture was refluxed for 1 1/2 hrs, then cooled and the hexamethylenetetramine salt was filtered off; m.p. 209—210 °C.

2-(3-Methyl-4-bromophenyl)-4-formyl-5-bromothiazole (VI)

3.3 g hexamethylenetetramine salt of 2-(3-methyl-4-bromophenyl)-4-chloromethyl-5 bromothiazole and 0.88 g hexamethylenetetramine were refluxed in 110 ml 50% acetic acid for 30 min. The solution was cooled, the crude product filtred off, and recrystallized from aqueous alcohol in the presence of decolorizing carbon; m.p. 130—130.5 °C.

$C_{11}H_7Br_2NOS$ (361.072). Calcd. N 3.88. Found N 3.87%.

2-(3-Methyl-4-bromophenyl)-4-carboxy-5-bromothiazole (VII)

(a) 0.1 g 2-(3-methyl-4-bromophenyl)-4-formyl-5-bromothiazole was thoroughly ground in a morter with 0.044 g $KMnO_4$, and mixed with the cooled solution of 0.1 g NaOH in about 4 ml water. The reaction mixture was kept for 48 hrs at room temperature with occasional stirring. It was diluted with a little hot water and filtered through a fluted filter. The filtrate was decolorized with alcohol and filtered again. The filtrate was acidified with conc. HCl and the suspension heated on a water bath until the alcohol evaporated. It was then cooled and filtered. The isolated acid was recrystallized from aqueous acetic acid, m.p. 212—212.5 °C.

$C_{11}H_7Br_2NO_2S$ (377.072). Calcd. N 3.71. Found N 3.74%.

(b) A suspension of 0.002 mole of 2-(*m*-tolyl)-4-acetylthiazole in 100 ml 2.5% NaOBr solution was vigorously shaken for about 3 hrs. The reaction mixture was filtered, the filtrate acidified with conc. HCl and let to stand at room temperature for 24 hrs. It was then filtered, and the acid recrystallized from aqueous ethanol, m.p. 207—208 °C.

$C_{11}H_7Br_2NO_2S$ (377.072). Calcd. N 3.71. Found N 3.81%.

(c) 0.005 mole of 2-(*m*-tolyl)-4-carboxythiazole was dissolved in glacial acetic acid and treated with 0.03 mole of Br_2. After 1 hr the solution was poured on ice. The crude product was recrystallized from aqueous alcohol and treated with decolorizing charcoal; m.p. 207—207.5 °C.

$C_{11}H_7Br_2NO_2S$ (377.072). Calcd. N 3.71. Found N 3.92%.

Hexamethylenetetramine salt of 2-(m-tolyl)-4-chloromethyl-5-bromothiazole

3.02 g 2-(*m*-tolyl)-4-chloromethyl-5-bromothiazole was dissolved in 10 ml chloroform and treated with 1.68 g hexamethylenetetramine in 20 ml chloroform. The solution was refluxed for 1 1/2 hrs, cooled and filtered. The isolated hexamethylenetetramine salt had m.p. 196—197 °C.

2-(m-Tolyl)-4-formyl-5-bromothiazole (V)

3.2 g hexamethylenetetramine salt of 2-(*m*-tolyl)-4-chloromethyl-5-bromothiazole and 0.99 g hexamethylenetetramine were dissolved in 110 ml 50% acetic acid and refluxed for 30 min. After cooling, the aldehyde which precipitated was recrystallized from aqueous ethanol with decolorizing charcoal; m.p. 85—85.5 °C.

$C_{11}H_8BrNOS$ (282.164). Calcd. N 4.96. Found N 4.86%.

2-(m-Tolyl)-4-carboxy-5-bromothiazole (VIII)

(a) 0.005 mole of 2-(*m*-tolyl)-4-carboxythiazole was dissolved in glacial acetic acid and 0.006 mole of Br_2 was added to the solution. It was allowed to stand 1 hr and poured on ice. The precipitate was recrystallized from aqueous ethanol with decolorizing charcoal; m.p. 192—192.5 °C.

$C_{11}H_8BrNO_2S$ (298.164). Calcd. N 4.69. Found 5.00%.

(b) 0.2 g 2-(*m*-tolyl)-4-formyl-5-bromothiazole was thoroughly ground in a mortar with 0.13 g $KMnO_4$; the mixture was treated with a cold, conc. aqueous solution of 0.2 g NaOH. The reaction mixture was stored about 24 hrs at room temperature with occasional shaking. It was then diluted with warm water and filtered through a fluted filter. If necessary, the filtrate was decolorized with alcohol, filtrated again and acidified with conc. HCl. The isolated acid was recrystallized from aqueous ethanol, in the presence of decolorizing carbon; m.p. 192—193 °C.

$C_{11}H_8BrNO_2S$ (298.164). Calcd. N 4.69. Found N 4.62%.

2-(3-Methyl-4-nitrophenyl)-4-chloromethylthiazole (IX)

(a) A cooled mixture consisting of 1.5 ml conc. H_2SO_4 and 1 ml HNO_3 (d = 1.42) was added to 0.5 g 2-(*m*-tolyl)-4-chloromethylthiazole, the temperature being kept below 60 °C. The solution was let to stand for 30 min. at 60 °C, and then poured on ice. The isolated substance was recrystallized from alcohol and decolorized with charcoal; m.p. 125—126 °C.

$C_{11}H_9ClN_2O_2S$ (268.721). Calcd. N 10.42. Found N 10.48%.

(b) 1.4 g 2-(*m*-tolyl)-4-hydroxy-4-chloromethyl-Δ_2-thiazolinehydrochloride was added in small portions into a cold nitration mixture consisting of 3.8 ml conc. H_2SO_4 and 2.6 ml HNO_3 (d = 1.42). The solution was stored at room temperature for 30 min., then poured on ice. The isolated substance was recrystallized from ethanol and decolorized with charcoal; m.p. 125 °C.

$C_{11}H_9ClN_2O_2S$ (268.721). Calcd. N 10.42 Found N. 10.44%.

2-(3-Methyl-4-nitrophenyl)-4-chloromethyl-5-nitrothiazole (X)

2.5 g 2-(*m*-tolyl)-4-chloromethylthiazole was dissolved in 30 ml acetic anhydride, the solution was filtered and 10 ml HNO_3 (d = 1.42) was added to it while maintaining the temperature below 60 °C. The mixture was allowed to stand at 60 °C for 30 min. and poured on ice. The crude product was recrystallized from aqueous ethanol and decolorized with charcoal; m.p. 151—152 °C.

$C_{11}H_8ClN_3O_4S$ (313.721). Calcd. N 13.39. Found N 13.62%.

2-(3-Methyl-4-nitrophenyl)-4-chloromethyl-5-bromothiazole (XI)

(a) A mixture of 2.0 ml conc. H_2SO_4 and 1.4 ml HNO_3 (d = 1.42) was added to 0.003 mole of 2-(*m*-tolyl)-4-chloromethyl-5-bromothiazole, the temperature being kept below 60 °C. The solution was let to stand at 60 °C for 30 min., then poured on ice. The precipitate was recrystallized from ethanol and treated with decolorizing carbon; m.p. 137—138 °C.

$C_{11}H_8ClBrN_2O_2S$ (347.629). Calcd. N 8.06. Found N 8.14%.

(b) 0.004 mole of 2-(3-methyl-4-nitrophenyl)-4-chloromethylthiazole was dissolved in glacial acetic acid, and with continuous cooling 0.0048 mole of bromine was added to the filtered solution. It was let to stand at room temperature for 30 min., then poured on ice. The crude product was recrystallized from ethanol and decolorized with charcoal; m.p. 138—139 °C.

$C_{11}H_8ClBrN_2O_2S$ (347.629). Calcd. N 8.06. Found N 8.27%.

REFERENCES

1. SIMITI, I., FARKAS, M.: Ann. (in press)
2. SIMITI, I., FARKAS, M.: Bull. soc. chim. France, **9**, 3862 (1968)
3. SIMITI, I., COMAN, M.: Rev. Roum. (in press)

I. SIMITI
Mária FARKAS
Cluj, Str. V. Babeş 41, ROMANIA.

INDEX

INORGANIC AND ANALYTICAL CHEMISTRY – ANORGANISCHE UND ANALYTISCHE CHEMIE – НЕОРГАНИЧЕСКАЯ И АНАЛИТИЧЕСКАЯ ХИМИЯ

PHYSICAL CHEMISTRY – PHYSIKALISCHE CHEMIE – ФИЗИЧЕСКАЯ ХИМИЯ

ORGANIC CHEMISTRY – ORGANISCHE CHEMIE – ОРГАНИЧЕСКАЯ ХИМИЯ

Printed in Hungary

A kiadásért felel az Akadémiai Kiadó igazgatója — Műszaki szerkesztő: Zacsik Annamária

A kézirat nyomdába érkezett: 1972. X. 21. — Terjedelem: 10.25 (A/5) ív 71 ábra, 1 melléklet

73.74139 Akadémiai Nyomda, Budapest — Felelős vezető: Bernát György

ACTA CHIMICA
ТОМ 76—ВЫП 1

РЕЗЮМЕ

Исследование состава отечественных и иностранных летучих масел, I

Комбинированый метод анализа летучих масел на основое эффективного разделения и инструментального идентифицирования компонентов

К. РЕТИ-БЕЛАФИ, Ш. ИГЛЕВСКИ, Э. КЕРЕНИ и Р. КОЛЬТА

Был разработан комбинированный метод для анализа летучих масел, основанный на эффективном разделении и инструментальном исследовании структуры компонентов. Количественный анализ производился с помощью капиллярной газовой хроматографии. С целью качественного анализа летучие масла подвергались ректификации с вращающейся вставкой, элюционной жидкофазной хроматографии, препаративной газовой хроматографии и химическому разделению. В результате были получены чистые компоненты, идентифицирование которых производилось с помощью ИК и УФ а также масс-, спектрометрии, ЯМР и на основе химических превращений. Комбинированный метод анализа иллюстрируется анализом образца, «обезментоленного» импортированного масла мяты, выделенного из Mentha arvensis.

О некоторых проблемах определения молекулярного веса методом приближенной равновесной седиментации

М. БЛАЖО и А. ЦУППОН

Были сделаны попытки исключения неопределенности в получении и обработке данных приближенной равновесной седиментации на основе ультра центрифугального метода для определения молекулярного веса полидисперсных макромолекулярных веществ в неидеальных растворах. Дифференциальное уравнение Ламме для условий Архибальда было решено нумерически, принимая во внимание зависимость диффузионного и седиментационного коэффициентов от концентрации. На основе этого решения были установлены следующие экспериментальные условия, позволяющие применение линейной экстраполяции концентрационного градиента к мениску по Шлирену

$$\frac{2D}{S\omega^2 r^2} > 0{,}05 \quad \text{и} \quad Dt > 0{,}75 \cdot 10^{-2} \text{ см}^2.$$

В случае неидеальных растворов и (или) полидисперсных смесей, наблюдаемый молекулярный вес изменяется со временем. Было найдено, что в этом случае линейная экстраполяция с учетом $t^{1/2}$ дает лучшие результаты, чем с учетом t. Использование диаграммы Траутмана для экстраполяции концентрационного градиента к исходным концентрациям, а также для определения M_z было распространено к неидеальным растворам.

Определение скорости коррозии железа в системе ацетон — вода — ацетат натрия

Й. ДЕВАИ, Р. ШЮТЦ-РАТКОВИЧ и Л. МЕСАРОШ

Были изучены кинетические параметры растворения железа в системах ацетон — вода — ацетат натрия различных составов. Вследствие относительно высокого сопротивления растворов, поляризационные кривые снимались с помощью потенциостата, снабженного автоматической компенсирующей установкой, пригодной для исключения поляризации сопротивления. На основе экспериментальных данных были определены наклоны прямых Тафеля, которые использовались для определения плотности тока коррозии.

Было установлено, что величины a и b не зависят от концентрации ацетона и уменьшаются с увеличением концентрации иона ацетата.

Плотности коррозионного тока уменьшаются с увеличением концентрации ацетона и увеличиваются с увеличением концентрации иона ацетата.

Совместное определение ионов металлов с помощью полярографии сверхгармонического переменного тока

Й. ДЕВАИ, Т. ГАРАИ, Б. ПАЛАДИ-ФЕНЕШ, Л. МЕСАРОШ и САЕД САБЕТ АБД ЭЛЬ РЕХИМ

Метод полярографии второго и третьего гармонических компонентов переменного тока применялся для совместного определения таких полярографически обратимых пар деполяризаторов, разница потенциалов полуволны которых меньше 200 мв. На основе результатов было установлено, что — в противоположность полярографии основного гармонического переменного тока — в данном случае совместное определение может быть осуществлено успешно в интервале концентраций, зависящих от природы деполяризаторов, даже и для разности потенциалов полуволны, равной 40 мв.

Определение константы скорости реакции переноса с помощью анализа гармонической компоненты тока, возникающего под влиянием переменного напряжения синусоидной формы

Й. ДЕВАИ, Т. ГАРАИ и Л. МЕСАРОШ

Был разработан метод определения константы скорости реакции переноса с помощью измерения второй и третьей гармонической компонент переменного тока, возникающего на электроде, поляризованном переменным током небольшой амплитуды и синусоидной формы, суперпонированным на напряжение постоянного тока. Константа скорости реакции переноса может быть определена на основе сравнения экспериментальных данных с рассчитанными на ЭВМ.

Равновесие в системе ацетон—вода

М. ШИМОНИ, Ю. КАРДОШ и А. НЕСМЕИ

Приводятся две простые равновесные модели для интерпретации химических сдвигов в спектрах ЯМР систем вода — ацетон. Первая модель применима в широком интервале концентраций: $0,9 > x_{H_2O} > 0,02$ и в свою основу включает сольватационный обмен, в котором любая из молекул является активным участником. Константы равновесия, определенные с помощью трех различных резонансных методов, равны 0,62 (вода H^1) 2,04 (карбонильный O^{17}) и 1,32 (карбонильный C^{13}). Расхождения в значениях константы, вероятно, вызваны тем, что сольватация типа вода-вода доминирует над сольватацией типа вода-ацетон. Вторая модель кажется применимой для интервала $0,14 > x_{H_2O} > 0$ и основана на ступенчатом образовании водородной связи между ацетоном и водой, с пренебрежением взаимодействия вода — вода. Так как во второй модели учитываются три индивидуальных водных состояния, то вторая модель является неопределенной и может быть решена лишь при введении произвольных констант равновесия.

Ацилирование дизамещенных цианамидов фосгеном, I

Получение и некоторые реакции производных 1,3,5-трихлор-2,4-диазапентадиена

З. ЧЮРЁШ, Р. ШООШ, А. АНТУШ-ЭРЧЕНИ, И. БИТТЕР и Й. ТАМАШ

Были исследованы строение и механизм образования хлористого диалкил-[1,3,5-трихлор-5-диалкиламино-2,4-диазапентадиен-(2,4)-илиден]-аммония при взаимодействии

цианамидов с фосгеном. Спектроскопически была доказана структурная аналогия с хлористым хлорметилендиалкиламмонием. Были изучены реакции полученных продуктов, протекающие под влиянием воды и тепла, и было идентифицировано строение получаемых в данных реакциях продуктов.

Флавоноиды, XXV

Реакция 2′-ОР-халкондибромида с аммиаком: получение халкон-азиридина и 3-аминофлаванона

ДЬ. ЛИТКЕИ, Р. БОГНАР и Й. АНДО

При исследовании присоединения брома к производным 2′-ОР-халкона (**1**) было установлено, что в зависимостиот заместителя *B*-кольца, полярности растворителя и природы защитной группы, наряду с присоединением брома происходит отщепление защитной группы.

Дибромиды 2′-ОР-халкона (**2**), реагируя с аммиаком, дают, в зависимости от природы защитной группы, либо флавон (если R = H), либо *транс*-2-(4-Р'-фенил)-3-(2′-ОР-бензоил)-этиленимин (**9**) (если R = $CH_2C_6H_5$ или CH_2OCH_3).

Азиридин *9* бензоилируется до N-бензоилазиридинового производного (**10**); при обработке последнего кислотой был получен 2,3-*транс*-3 (N-бензоил)-аминофлаванон (**11**).

Излагаются представления относительно механизма реакций, стерических условий протекания реакций, а также стереохимии конечных продуктов, которые основываются на данных ИК и ЯМР спектроскопических исследований.

Изучение некоторых гетероциклов, XXVII

Исследование галогенирования и нитрования 2-(м-толил)-4-Х-тиазолов

И. ШИМИТИ и М. ФАРКАШ

Продолжением предыдущей работы является настоящее исследование нитрования и бромирования 2-(м-толил)-4-хлорметитиазола с целью изучения эффекта метильной группы в пара-положении бензольного кольца и в положении 5 тиазольного кольца.

ATLAS OF THERMOANALYTICAL CURVES III

TG-, DGT-, DTA-curves measured simultaneously

edited by G. LIPTAY

This series, whose third volume is presented here, supplies a great want. Up to now the various results obtained by different thermoanalytical methods and instruments could not be compared with one another, owing to difference in experimental conditions. Now the two most frequently used thermoanalytical methods, differential thermoanalysis (DTA) and thermogravimetry (TG) have been completed by the derivative thermogravimetric curves (DTG); thus the thermal behaviour of different materials can be examined simultaneously on the same sample. — This third volume, similarly to the second, contains a collection of the thermal analysis diagrams of a wide range of materials obtained from various sources, such as inorganic and organic compounds, synthetic organic materials, minerals, rocks, coals, etc.

In English • Approx. 100 pages • Cloth

AKADÉMIAI KIADÓ Budapest HEYDEN and SONS Ltd. London

A co-edition — distributed in the socialist countries by Kultura, Budapest, in all other countries by Heyden and Sons Ltd., London

ASCORBINOMETRIC TITRATIONS

by L. ERDEY and GY. SVEHLA

It was at the and of the fourties that L. Erdey and his research team began to deal with ascorbimetric titrations. This book gives an account of the principle and system of their research method, and describes in detail the results achieved between 1949 and 1965. In the course of time, a number of researchers joined in continuing the author's and his co-workers' pioneering work in the field of ascorbimetric titrations, opening up new vistas of industrial applications of this method. The book will be helpful to analytical chemists who already use this titration method, or want to explore its possibilities in their daily laboratory work.

In English • Approx. 150 pages • Cloth

AKADÉMIAI KIADÓ
Budapest

RECENT FLAVONOID RESEARCH

edited by R. BOGNÁR, V. BRUCKNER and CS. SZÁNTAY

(Recent Developments in the Chemistry of Natural Carbon Compounds 5)

This new volume of the series deals with a branch of organic chemistry which has great traditions in Hungary. The material of the book consists of two parts: it contains the lectures held at the 3rd Hungarian Bioflavonoid Symposium, and it gives a survey and summary of Hungarian chemical research on flavonoids from 1950 till today.

In English • Approx. 130 pages • Cloth

ASSIGNMENTS FOR VIBRATIONAL SPECTRA OF 700 BENZENE DERIVATIVES

by GY. VARSÁNYI

Infrared spectra are very effective means of identification and differentiation of chemical substances. The book lists 700 benzene derivatives, denoting the structural units repsonsible for various vibrational modes, i.e. for the bands observed with a given intensity at a certain wave-number. With the aid of these data it becomes possible to analyse the structure of benzene derivatives other than those listed in the book, assigning the bands to known structural units or to determine the new constitutional features of the compound from the intensities and wave-numbers of the spectral bands observed.

In English • Approx. 640 pages • 100 illustrations • 350 spectra • 700 structural formulas • 800 tables • Cloth

AKADÉMIAI KIADÓ
Publishing House of the Hungarian Academy of Sciences
Budapest

The Acta Chimica publish papers on chemistry, in English, German, French and Russian.

The Acta Chimica appear in volumes consisting of four parts of varying size, 4 volumes being published a year.

Manuscripts should be addressed to

Acta Chimica
Budapest 112/91 Műegyetem

Correspondence with the editors should be sent to the same address.

The rate of subscription is $ 24.00 a volume.

Orders may be placed with "*Kultúra*" Foreign Trade Company for Books and Newspapers (1389 Budapest 62, P.O.B. 149 Account No. 218-10-990) or with representatives abroad

---

Les Acta Chimica paraissent en français, allemand, anglais et russe et publient des mémoires du domaine des sciences chimiques.

Les Acta Chimica sont publiés sous forme de fascicules. Quatre fascicules seront réunis en un volume (4 volumes par an).

On est prié d'envoyer les manuscrits destinés à la rédaction à l'adresse suivante:

Acta Chimica
Budapest 112/91 Műegyetem

Toute correspondance doit être envoyée à cette même adresse.

Le prix de l'abonnement est de $ 24,00 par volume.

On peut s'abonner à l'Entreprise pour le Commerce Extérieur de Livres et Journaux «*Kultúra*» (1389 Budapest 62, P.O.B. 149 Compte-courant N°. 218-10-990) ou à l'étranger chez tous les représentants ou dépositaires.

«*Acta Chimica*» издают трактаты из области химической науки на русском, французском, английском и немецком языках.

«*Acta Chimica*» выходят отдельными выпусками разного объема. 4 выпуска составляют один том. 4 тома публикуются в год.

Предназначенные для публикации рукописи следует направлять по адресу:

Acta Chimica
Budapest 112/91 Műegyetem

По этому же адресу направлять всякую корреспонденцию для редакции.

Подписная цена — $ 24,00 за том.

Заказы принимает предприятие по внешней торговле книг и газет «*Kultúra*» (1389 Budapest 62, P.O.B. 149 Текущий счет № 218-10-990) или его заграничные представительства и уполномоченные.

Reviews of the Hungarian Academy of Sciences are obtainable at the following addresses:

ALBANIA

Drejtorija Qändrone e Pärhapjes
dhe Propagandimit të Librit
Kruga Konferenca e Päzes
Tirana

AUSTRALIA

A. Keesing
Box 4886, GPO
Sydney

AUSTRIA

GLOBUS
Höchstädtplatz 3
A-1200 Wien XX

BELGIUM

Office International de Librairie
30, Avenue Marnix
1050 Bruxelles
Du Monde Entier
162, Rue du Midi
1000 Bruxelles

BULGARIA

HEMUS
11 pl Slaveikov
Sofia

CANADA

Pannonia Books
2, Spadina Road
Toronto 4, Ont.

CHINA

Waiwen Shudian
Peking
P. O. B. 88

CZECHOSLOVAKIA

Artia
Ve Smečkách 30
Praha 2
Poštovní Novinová Služba
Dovoz tisku
Vinohradská 46
Praha 2
Mad'arská Kultura
Václavské nám. 2
Praha I
SLOVART A. G.
Gorkého
Bratislava

DENMARK

Ejnar Munksgaard
Nörregade 6
Copenhagen

FINLAND

Akateeminen Kirjakauppa
Keskuskatu 2
Helsinki

FRANCE

Office International de Documentation
et Librairie
48, rue Gay-Lussac
Paris 5

GERMAN DEMOCRATIC REPUBLIC

Deutscher Buch-Export und Import
Leninstraße 16
Leipzig 701
Zeitungsvertriebsamt
Fruchtstraße 3—4
1004 Berlin

GERMAN FEDERAL REPUBLIC

Kunst und Wissen
Erich Bieber
Postfach 46
7 Stuttgart S.

GREAT BRITAIN

Blackwell's Periodicals
Oxenford House
Magdalen Street
Oxford
Collet's Subscription Import
Department
Dennington Estate
Wellingsborough. Northants.
Robert Maxwell and Co. Ltd.
4—5 Fitzroy Square
London W. I

HOLLAND

Swetz and Zeitlinger
Keizersgracht 471—478
Amsterdam C.
Martinus Nijhof
Lange Voorhout 9
The Hague

INDIA

Hind Book House
66 Babar Road
New Delhi I

ITALY

Santo Vanasia
Via M. Macchi 71
Milano
Libreria Commissionaria Sansoni
Via La Marmora 45
Firenze
Techna
Via Cesi 16
40135 Bologna

JAPAN

Kinokuniya Book-Store Co. Ltd.
826 Tsunohazu 1-chome
Shinjuku-ku
Tokyo
Maruzen and Co. Ltd.
P. O. Box 605
Tokyo-Central

KOREA

Chulpanmul
Phenjan

NORWAY

Tanum-Cammermeyer
Karl Johansgt 41—43
Oslo I

POLAND

RUCH
ul. Wronia 23
Warszawa

ROUMANIA

Cartimex
Str. Aristide Briand 14—18
Bucureşti

SOVIET UNION

Mezhdunarodnaya Kniga
Moscow G—200

SWEDEN

Almquist and Wiksell
Gamla Brogatan 26
S—101 20 Stockholm

USA

F. W. Faxon Co. Inc.
15 Southwest Park
Westwood, Mass. 02090
Stechert Hafner Inc.
31. East 10th Street
New York, N. Y. 10003

VIETNAM

Xunhasaba
19, Tran Quoc Toan
Hanoi

YUGOSLAVIA

Forum
Vojvode Mišića broj 1
Novi Sad
Jugoslovenska Knjiga
Terazije 27
Beograd

23. V. 1973 Index: 26.007

ACTA CHIMICA

ACADEMIAE SCIENTIARUM HUNGARICAE

ADIUVANTIBUS

V. BRUCKNER, GY. DEÁK, K. POLINSZKY,
E. PUNGOR, G. SCHAY, Z. G. SZABÓ

REDIGIT

B. LENGYEL

TOMUS 76 FASCICULUS 2

AKADÉMIAI KIADÓ, BUDAPEST

1973

ACTA CHIM. (BUDAPEST) ACASA 76 (2) 113–219 (1973)

ACTA CHIMICA

A MAGYAR TUDOMÁNYOS AKADÉMIA KÉMIAI TUDOMÁNYOK OSZTÁLYÁNAK IDEGEN NYELVŰ KÖZLEMÉNYEI

SZERKESZTI

LENGYEL BÉLA

TECHNIKAI SZERKESZTŐK

DEÁK GYULA és HARASZTHY-PAPP MELINDA

Az Acta Chimica német, angol, francia és orosz nyelven közöl értekezéseket a kémiai tudományok köréből.

Az Acta Chimica változó terjedelmű füzetekben jelenik meg, egy-egy kötet négy füzetből áll. Évente átlag négy kötet jelenik meg.

A közlésre szánt kéziratok a szerkesztőség címére (Budapest 112/91 Műegyetem) küldendők.

Ugyanerre a címre küldendő minden szerkesztőségi levelezés. A szerkesztőség kéziratokat nem ad vissza.

Megrendelhető a belföld számára az „Akadémiai Kiadó"-nál (1363 Budapest Pf 24. Bankszámla 215-11488), a külföld számára pedig a „Kultúra" Könyv- és Hírlap Külkereskedelmi Vállalatnál (1389 Budapest 62, P.O.B. 149 Bankszámla: 218-10-990) vagy annak külföldi képviseleteinél és bizományosainál.

Die Acta Chimica veröffentlichen Abhandlungen aus dem Bereiche der chemischen Wissenschaften in deutscher, englischer, französischer und russischer Sprache.

Die Acta Chimica erscheinen in Heften wechselnden Umfanges. Vier Hefte bilden einen Band. Jährlich erscheinen 4 Bände.

Die zur Veröffentlichung bestimmten Manuskripte sind an folgende Adresse zu senden:

Acta Chimica
Budapest 112/91 Műegyetem

An die gleiche Anschrift ist auch jede für die Redaktion bestimmte Korrespondenz zu richten. Abonnementspreis pro Band: $ 24,00.

Bestellbar bei dem Buch- und Zeitungs-Außenhandels-Unternehmen »*Kultúra*« (1389 Budapest 62, P.O.B. 149 Bankkonto Nr. 212-10-990) oder bei seinen Auslandsvertretungen und Kommissionären.

Acta Chimica Academiae Scientiarum Hungaricae, Tomus 76 (2), pp. 113—119 (1973)

SEPARATION OF ANTIPYRINE DERIVATIVES BY ION EXCHANGE CHROMATOGRAPHY

J. GAÁL and J. INCZÉDY*

(Institute of General Chemistry, Technical University, Budapest)

Received September 6, 1971

An ion exchange chromatographic method has been developed for the separation of antipyrine, 4-aminoantipyrine and dimethylaminoantipyrine. The optimum conditions of the separation and the eluent composition were determined by calculations. The protonation constants, ion exchange equilibrium constants, and the kinetic parameters required for the calculations have been determined separately.

It has been shown [1] that the optimum composition of the eluent for the separation of organic bases can be predicted by calculation if the protonation constants of the bases and the ion exchange constants of the protonated bases are known.

Now a method was developed for the separation of antipyrine (A), 4-aminoantipyrine (AA) and dimethylaminoantipyrine (pyramidon, (DAA)) on a macroporous cation exchange resin column using the previously reported calculation methods.

Since in the literature we could find protonation constant data only for antipyrine [2] and dimethylaminoantipyrine [3], the protonation constants of all bases were determined in solutions containing 20% ethanol (ionic strength: 10^{-2}). The protonation constant of antipyrine was determined by the photometric method, while those of the other two bases by the potentiometric method. The constants obtained are listed in Table I.

For the calculation of the ion exchange constants of the protonated bases relative to sodium ion, distribution measurements were carried out using the

Table I

Protonation constants of the bases in 20% alcohol solution (20 °C)

Base	Method used	lg K_1	lg K_2
Antipyrine	photom.	1.38	
4-aminoantipyrine	pH-metric	3.96	
Dimethylaminoantipyrine	pH-metric	4.92	1.44

* Present adresse: Institute of Analytical Chemistry, University for Chemical Engineering, Veszprém, Hungary

static, batch method. The distribution coefficients of the bases on the sodium-form resin were determined from 20% ethanolic solutions of different pH, but of constant sodium ion concentration. Plotting the experimental distribution coefficients against the pH, Eq. (1) was fitted to the points, and the K^x values (*i.e.* the ion exchanges constants) were calculated. Since the amount of the base was kept low relative to the amount of sodium ions, the following equation could be used in the calculations:

$$D_w = K^x \frac{Q}{[Na^+]} \left(\frac{[H^+]K}{1 + [H^+]K} \right) \tag{1}$$

where D_w denotes the weight distribution coefficient, K the first protonation constant of the base, Q the capacity of the resin (mequ/g) while K^x is the ion exchange constant of the protonated base. Since the measurements were carried out with solutions of pH larger than 2, where the diprotonated form of DAA was practically absent, only the first protonation constants of the bases were used in the calculation.

The calculated K^x values are collected in Table II.

Table II

Ion exchange equilibrium constants of the protonated base cation relative to sodium ion (Lewatit S−100; 20 °C)

Base	K^x_{BH-Na}
Antipyrine	0.57
4-aminoantipyrine	(0.32)
Dimethylaminoantipyrine	0.25

Elution measurements using ion exchange columns were also carried out for the determination of volume distribution coefficients. Since the elution peaks obtained at room temperature were found to broaden, the dynamic measurements were performed at 60° C. The volume distribution coefficients obtained from elution data at various pH were converted to weight distribution coefficients, and compared with those obtained by static measurements at room temperature. The conversion was made using the following relation:

$$\frac{D}{\sigma} = D_w \tag{2}$$

where D and the D_w are the volume and weight distribution coefficients, respectively, while σ is the column density (g of dry resin in 1 ml of the column).

The calculated weight distribution coefficients obtained in two different series of experiments under different conditions are shown in Fig. 1. The deviation between the corresponding curves is not significant.

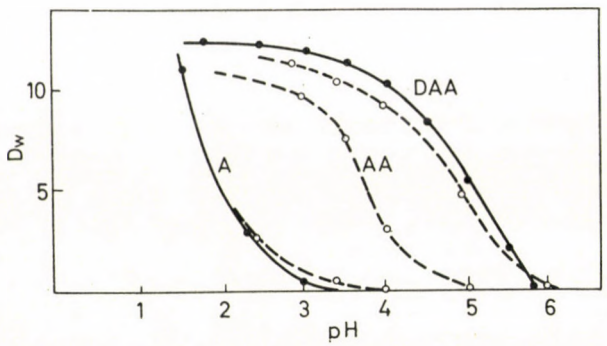

Fig. 1. Weight distribution coefficients of the bases at constant sodium ion concentration ($10^{-1}M$) and at various pH of the solution. ——— static measurements (20 °C); — — — elution measurements (60 °C)

It has been shown [4] that the best separation of two successively running components can be obtained if an eluent is used, for which the ratio of $(D + a)$ values for the two components has a maximum (a is the void fraction of the column). The optimum ratio for the separation of A from AA was found to occur at pH 3.60, while that for the separation of AA from DAA at pH 4.40. Therefore the separation of the three bases was performed with an eluent of constant sodium ion concentration, with its pH changing stepwise from 3.6 to 4.4.

To obtain information on the necessary size of the column, first the plate height of the column was calculated from the elution curves using GLUECK AUF's [5] equation

$$h = \frac{L}{8\left(\frac{v_{\max}}{\beta}\right)^2}, \tag{3}$$

where h denotes the plate height (cm), L the length of the column used (cm), $v_{\max}$ the total eluent volume (ml), and β the band width (ml) for $c_{\max} \times 0.368$.

The h value for A was found to be the largest: 5.11 cm, while those for AA and DAA, were 0.58 and 0.61 cm, respectively, under the given conditions (60 °C; flow rate: 0.028 cm/sec). For the investigation of the peculiar behaviour of A, the inner diffusion coefficients of the bases were calculated. Assuming that under the given conditions the mass transfer was controlled mainly by particle diffusion, according GLUECKAUF [5], h can be expressed as:

$$h = 1.64\, r + \frac{D}{(D+a)^2}\,\frac{0.142\, r^2 F}{d_r}, \tag{4}$$

where r denotes the radius of the resin particle, a is the void fraction of the

resin column, F the linear velocity of the eluent (cm/sec), and d_r the inner diffusion coefficient (cm²/sec).

Using the above equation d_r can be calculated.

At the same time kinetic measurements were also made to determine the diffusion coefficients of the bases in question. The agreement found between the values obtained in two different ways was very convincing. Antipyrine, in spite its small molecular weight, excelled in low diffusivity.

The expected behaviour of antipyrine may be explained partly by its lower protonation constant. Thus in solutions of medium pH only a very small fraction of the base is present as cation. However, at lower pH values, where the ion exchange process is appreciable, the loading of the resin is quite different from that observed in solutions of higher pH.

The diffusion coefficients obtained are summarized in Table III.

Table III

Calculated inner diffusion coefficients of the bases (Lewatit S—100; 60 °C)

Base	From elution data cm²/sec	From kinetic measurements cm²/sec
Antipyrine	8.15×10^{-8}	7.93×10^{-8}
4-aminoantipyrine	2.99×10^{-7}	
Dimethylaminoantipyrine	2.50×10^{-7}	2.25×10^{-7}

The column length necessary for quantitative separation was calculated using the following formula [6]:

$$N > 2\pi \left[\frac{\frac{D_2 + a}{D_1 + a} + 1}{\frac{D_2 + a}{D_1 + a} - 1} \right]^2, \qquad (5)$$

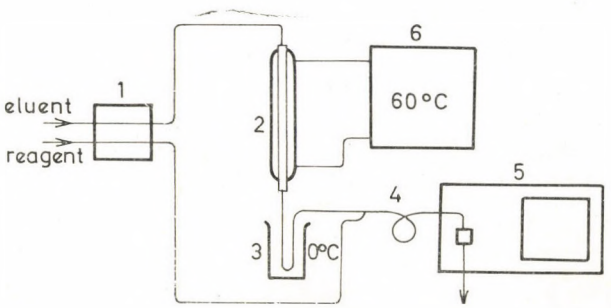

Fig. 2. Chromatographic apparatus for the separation of antipyrine derivatives. *1* peristaltic pump; *2* ion exchange column with heating jacket; *3* cooler; *4* mixing coil; *5* photometer; *6* thermostat

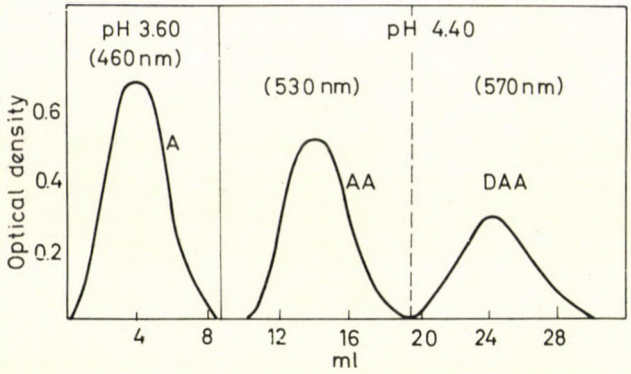

Fig. 3. Separation of antipyrine (A), 4-amino-antipyrine (AA) and dimethylaminoantipyrine (DAA). Ion exchange column: Lewatit S—100 (0.2—0.4 mm) 6.5×187 mm. Flow rate: 33 ml/hr; Eluent: sodium acetate–acetic acid buffer; $[Na^+] = 10^{-1}M$; 60 °C

where D_1 and D_2 are the volume distribution coefficients of the two successive species, N is the required number of theoretical plates of the column.

Using the optimum column, flowing rate and elution composition, the separation of the three bases was realized. The feeding of the column and the continuous, automatic detection of the separated species in the effluent were carried out with an apparatus of our own design (see Fig. 2).

The chromatogram of the separation is shown in Fig. 3.

Experimental

Reagents. In all experiments a.g. reagents were used.

The commercially available bases (antipyrine, 4-aminoantipyrine, pyramidon) were dissolved in ethanol, treated with charcoal and crystallized after filtration. The alcohol containing stock solutions were prepared from the purified substances.

Ion exchange resin. Commercially available Lewatit SP—100 resin was sieved and the fraction with the particle size of 0.2—0.4 mm was treated with acid and alkali in the usual way, then converted to the sodium-form and washed with deionized water and finally extracted in a Soxleth apparatus with 96% ethanol. The extracted resin was dried at room temperature and stored in a glass bottle. The capacity of the resin was determined by the usual method [7] and found to be 4.98 mequ/g of air dried resin. The column density of the resin was $\sigma = 0.365$.

Instruments. The quantitative determination of the bases was made with a Spektromom 201 (MOM, Hungary) spectrophotometer; the estimation of the bases in the visible range was carried out with iron(III) sulfate as reagent and a Spekol (Carl Zeiss, GDR) photometer. The pH was measured with a Universal

pH meter (RADELKIS, Hungary) for feeding the column automatically in the column experiments, a Peripump (KUTESZ, Hungary) peristaltic pump was used.

Determination of the protonation constant of antipyrine. The optical densities of the solutions of various pH, containing 4×10^{-5} M antipyrine and 20% alcohol, were measured at 260 nm on the spectrophotometer and the log K value was calculated by the usual method [8].

Determination of the protonation constants by pH-metric titration. 10 ml of 10^{-1} M alcoholic stock solution was diluted with water to 45 ml and titrated against standard 0.2 M hydrochloric acid. Nitrogen was bubbled through the solution during titration; the pH was measured using glass and calomel electrodes. From the data obtained the log K values were calculated.

Determination of the distribution coefficients by static method. A 0.25 g air dried, pretreated resin sample of the sodium form was weighed in a glass stoppered bottle. The solution of various pH containing 10^{-1} M sodium chloride and 10^{-3} M base, investigated in 20% ethanol/water mixture, were prepared from known portions of stock solutions. The pH was adjusted by addition of dilute hydrochloric acid, and the solution filled up to 50 ml in volumetric flask. The concentration of sodium ions was kept constant at 10^{-1} M in all experiments. 25 ml of the solution prepared was pipetted to the resin sample and, after closing the bottle, it was allowed to stand for 24 hrs with periodic shaking for equilibration. After equilibration, a part of both the original and the equilibrated solutions were analyzed for the base content spectrophotometrically. At the same time the pH of the equilibrated solution was also measured. The optical densities of the antipyrin solutions were measured at 230 nm, while those of pyramidon at 270 nm after the addition of hydrochloric acid. The concentration was determined using calibration graphs, then the weight distribution coefficient (D_w) of the bases was calculated:

$$D_w = \frac{\text{mmol base/g air dried resin}}{\text{mmol base/ml solution}}. \qquad (6)$$

Elution experiments. For elution experiments an ion exchange column of size 6.5×72 mm was prepared from the pretreated sodium-form resin. The column was heated with a heating jacket and kept at 60 °C. The column was equilibrated with the eluent before the elution experiment, then 0.25 ml of the stock solution (containing 10^{-1} M base) was poured onto the resin column and the elution was carried out with the eluent of the desired pH but of constant sodium ion concentration. The eluents were sodium acetate–acetic acid buffers of constant sodium ion concentration, containing also 20% ethanol. They were fed to the column by means of a peristaltic pump at a rate of 33 ml/hour. The effluent was cooled first in an ice bath (see Fig. 2) then the iron(III) sulfate

reagent (0.5% cryst. iron(III) ammonium sulfate and 0.2 *M* hydrochloric acid) was added at a rate of 43.8 ml/hour. After mixing, the optical density of the solution was measured in a flow-through cell at 460 (antipyrine), 530 (4-aminoantipyrine), or 570 nm (pyramidone). From the data obtained elution graphs were constructed and the peak eluent volumes (v_{max}, ml) determined. The volume distribution coefficient was also calculated [5]:

$$D = \frac{v_{max}}{X} - a, \tag{7}$$

where X is the column volume (ml), a is the void fraction of the column.

Separation of bases. According to calculations, a resin column of 187 nm length is required for quantitative separation of the bases if eluents of pH 3.60 and pH 4.4 are used. Therefore, a column of size 6.5×187 nm was prepared, kept at 60 °C and the mixture of the three bases (40 μmol A; 20 μmol AA and 50 μmol DAA) was poured onto the column and the elution was carried out using the apparatus shown in Fig. 2.

Kinetic measurements. 100 ml of a test solution containing 10^{-4} *M* base and 20% ethanol was prepared, the temperature adjusted to 20 or 60 °C; 0.365 g of hydrogen-form resin was then added to the vigorously stirred solution. Time to time 1 or 2.5 ml samples were taken by a pipette and the base content of the solution determined by means of the spectrophotometric method. From the data obtained kinetic curves were constructed and the half reaction time established. For calculation of the diffusion coefficient the following equation was used [9]:

$$t_{1/2} = 0.030 \frac{r^2}{d_r}, \tag{8}$$

where $t_{1/2}$ is the half reaction time, r is the mean radius of the resin particles (cm).

REFERENCES

1. INCZÉDY, J.: Acta Chim. (Budapest) **69,** 265 (1971)
2. MILLER, G. E., BARNEYEE, N. C., STONE, C. M.: J. Pharmacol. Exp. Theor., **151,** 245 (1967)
3. KOLTHOFF, M., BOSCH, W.: Rec. Trav. Chim. Pay-Bas, **48**
4. INCZÉDY, J., KLATSMÁNYI-GÁBOR, P., ERDEY, L.: Acta Chim. Acad. Sci. Hung., **61,** 261 (1969)
5. GLUECKAUF, E.: Soc. Chem. Ind. (London), **34,** (1954)
6. INCZÉDY, J.: J. Chromatog., **50,** 112 (1970)
7. INCZÉDY, J.: Analytical applications of ion exchangers. Pergamon Press, Oxford 1966
8. INCZÉDY, J.: Komplex egyensúlyok analitikai alkalmazása. Műszaki Könyvkiadó, Budapest, 1970
9. BARRER, R. M.: Diffusion in and through solids. Cambridge Press, 1941

János INCZÉDY
Judit GAÁL
Veszprém, Schönherz Z. u. 12. Hungary.

Acta Chimica Academiae Scientiarum Hungaricae, Tomus 76 (2), pp. 121—139 (1973)

UNTERSUCHUNG DER CHEMISCHEN ZUSAMMENSETZUNG VON BITUMINA AUS ROMASCHKINO UND ALGYÖ, I

TRENNUNG DER BITUMINA IN VERBINDUNGSGRUPPEN MIT HOMOGENER CHEMISCHER STRUKTUR

L. ZALKA

(Donau-Mineralölwerke, Százhalombatta)

Eingegangen am 1. Oktober 1971

Das Ziel der experimentellen Arbeit war die Untersuchung der chemischen Zusammensetzung und Struktur von Bitumina aus Romaschkino und Algyő. Nach einem neu entwickelten Verfahren wurden die Bitumina in Fraktionen mit relativ homogener chemischer Struktur zerlegt. Es wurde die Elementarzusammensetzung und das Molekulargewicht der einzelnen Fraktionen bestimmt und ihre UV-, IR- und NMR-Spektra wurden aufgenommen.

Das Trennverfahren umfaßt folgende Operationen: Abscheidung der Asphaltene mit *n*-Hexan, Trennung des Maltenteiles durch Flüssigkeitschromatographie an Silikagel, fraktionierte Kristallisation, Trennung der *n*-Paraffine durch Adduktbildung mit Harnstoff, Molekulardestillation und zuletzt Trennung der Aromaten gemäß der Zahl der Ringe durch Flüssigkeitschromatographie an mit Pikrinsäure präpariertem Adsorbens.

Das Bitumen ist ein Produkt äußerst komplizierter Zusammensetzung des Erdöls. In den durch verschiedene technologische Verfahren (Destillation, Extraktion, Blasen) gewonnenen Bitumina sind diejenigen Bestandteile des Erdöls enthalten, deren Zusammensetzung am kompliziertesten und deren Molekulargewicht am höchsten ist. Im Bitumen konzentrierte sich — in den hochmolekularen Komponenten eingebaut — auch der überwiegende Teil der im Erdöle befindlichen Heteroatome.

Die rheologischen und mechanischen Eigenschaften des Bitumens sind stark abhängig von seiner chemischen und kolloidchemischen Struktur. Wegen der verwickelten chemischen Struktur beschränkte man sich lange Zeit hindurch auf die Untersuchung der physikalischen Eigenschaften. In den letzten Jahrzehnten wurde jedoch eine tiefere chemische Deutung der physikalischen Eigenschaften des Bitumens immer dringender notwendig. Forschungen dieser Art werden durch das Ausbreiten neuer Trennungsmethoden und instrumenteller analytischer Untersuchungen für die Prüfung von Bitumina wesentlich erleichtert. Da es sich um ein äußerst kompliziertes Vielkomponentensystem handelt, wird die Isolierung charakteristischer Verbindungsgruppen angestrebt, wobei die Trennungsverfahren immer mehr verfeinert werden. Ein kurzer Überblick über die Entwicklung der Gruppenanalyse des Bitumens sowie seiner Trennung in mehr oder minder einheitliche Verbindungsgruppen

zeigt, daß mehr und mehr zusammengesetzte Trennschemen entwickelt und modernere analytische Methoden zur Feststellung der chemischen Bestandteile angewendet wurden.

Verfahren zur Trennung von Bitumina

Die eingehende Untersuchung der Bitumina durch Fraktionieren mit selektiven Lösungsmitteln begann im Jahre 1916 mit der Arbeit von MARCUSSON [1]. Er prüfte die Zusammensetzung natürlicher und aus Erdöl stammender Bitumina. Die unlöslichen Bestandteile des Bitumens wurden mit Leichtbenzin gefällt und die schwereren Komponenten wurden aus der Benzinlösung an Fullererde adsorbiert. Letztere wurde dann mit Schwefelkohlenstoff extrahiert. Die auf diese Weise erhaltenen Stoffe bezeichnete MARCUSSON als Harze. Eine weitere Fraktionierung der an Fullererde nicht adsorbierten Öle führte MARCUSSON nicht durch. Er entwickelte auch ein Verfahren zur quantitativen Bestimmung der im Bitumen enthaltenen Asphaltogensäuren und Asphaltogensäureanhydride. Nach dem in 1931 entwickelten Verfahren von PÖLL [2] wurden die Asphaltene mit Petroläther gefällt und die Lösung mit Fullererde behandelt. Der adsorbierte Teil, das sog. Ölharz, wurde mit Chloroform extrahiert. Aus dem nicht adsorbierten Teil der Lösung wurde der Petroläther abdestilliert und auf diese Art der ölige Teil des Bitumens erhalten. Die vorangehend mit Petroläther gefällten Asphaltene wurden in Chloroform gelöst und anschließend mit Fullererde behandelt. Durch Extraktion des adsorbierten Teils mit Pyridin wurden die Asphaltharze erhalten. Der in Pyridin unlösliche Teil wurde mit einem Gemisch aus Pyridin und Schwefelkohlenstoff (1:1) extrahiert. Den so gewonnenen Teil nannte PÖLL Hartasphalt. HOIBERG und GARRIS [3] trennten die Bitumina in fünf Fraktionen. Die Asphaltene wurden mit Hexan gefällt und aus dem in Hexan gelösten Teil wurden durch fraktionierte Fällung mit verschiedenen Lösungsmittelgemischen vier Fraktionen abgesondert, und zwar Hartharze, Weichharze, Öle und Ceresine.

Eine verfeinerte und wirksame Trennmethode wurde von O'DONNEL entwickelt [4]. Er trennte die Asphaltene mit Isopentan ab und trennte dann die Maltene durch Molekulardestillation in 10 Fraktionen. Die Destillate wurden auf Silikagel chromatographisch in gesättigte Verbindungen, aromatische Verbindungen und Harze zerlegt. Die gesättigte Fraktion wurde entparaffiniert und das erhaltene Paraffin durch Adduktbildung mit Harnstoff, das Öl durch Thermodiffusion in weitere Fraktionen getrennt. Die aromatische Verbindungen wurden durch Chromatographieren auf Aluminiumoxid in mono- und bicyklische Fraktionen getrennt. Durch Oxydation dieser Fraktionen ließen sich die Schwefelverbindungen in Sulfone überführen. Aus den Molekulardestillaten wurden die polaren Stickstoff- und Schwefelverbindungen durch Behandeln mit Quecksilberchlorid entfernt (Abb. 1).

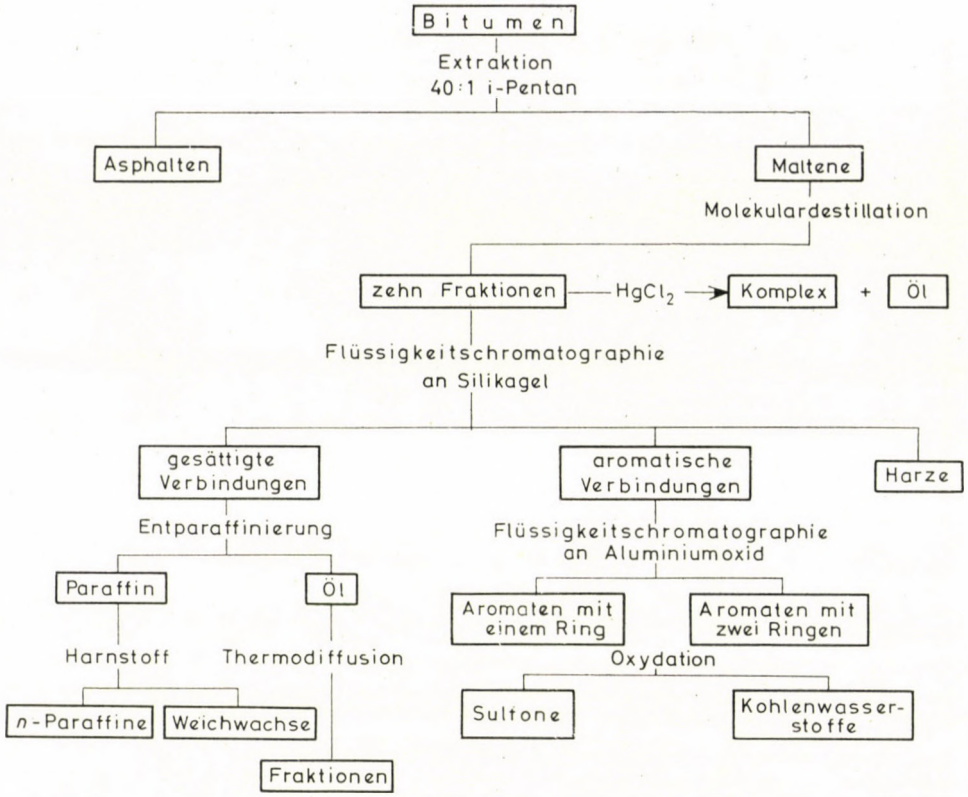

Abb. 1

BESTOUGEFF und BARGMAN [5, 6] befaßten sich ebenfalls eingehend mit der chemischen Zusammensetzung der Bitumina. Nach ihrem Verfahren wurden die Asphaltene mit *n*-Heptan gefällt, der Maltenteil entparaffiniert und durch Destillation, fraktionierte Fällung und Flüssigkeitschromatographie auf Silikagel und Aluminiumoxid in Verbindungsgruppen getrennt. Die Asphaltene ließen sich endlich durch fraktionierte Fällung in drei Fraktionen trennen. Die genannten Verfasser entwickelten auch ein Verfahren zur Trennung der im Bitumen vorkommenden Schwefelverbindungen. KLEINSCHMIDT [7] untersuchte die Veränderung der chemischen Zusammensetzung von Bitumina im Laufe von Alterungsvorgängen. Diese Veränderungen wurden durch Gruppenanalyse verfolgt. Die Asphaltene wurden mit *n*-Pentan gefällt und die Lösung in einer mit Fullererde beschickten Säule chromatographiert. Als selektive Lösungsmittel wurden *n*-Pentan, Methylenchlorid und Methyläthylketon verwendet. Die erhaltenen Fraktionen wurden als wasserhelles Öl, dunkles Öl und Asphaltharz bezeichnet. CHELTON und TRAXLER [8] chromatographierten die nach der Fällung der Asphaltene mit Pentan erhaltene Malten-

lösung in einer mit Silikagel gefüllten Säule. Die Säule wurde mit Methylcyclohexan, Benzol und i-Butanol eluiert und das benzolische Eluat auf Magnesiumsilikat erneut chromatographiert. Die Asphaltene wurden aus der benzolischen Lösung durch Zugabe steigender Methanolmengen fraktioniert gefällt (Abb. 2). TRAXLER und SCHWEYER [9] entwickelten ein Verfahren zur Zerlegung des Bitumens in drei Bestandteile. Zuerst wurde das Bitumen mit Butanol-1 behandelt, wodurch ein Niederschlag erhalten wurde, der die Asphaltene und eine geringe Menge an Harzen enthielt. Dieser wurde als asphaltischer Teil bezeichnet. Die in Butanol löslichen Bestandteile wurden in heißem Aceton gelöst. Nach dem Abkühlen der Lösung auf —23,3° wurden die von den Verfassern als gesättigte Verbindungen bezeichneten Substanzen ausgeschieden. In der acetonischen Lösung verblieben die ungesättigten Öle, die als cyklische Verbindungen bezeichnet wurden. Mit Hilfe der auf diese Weise bestimmten drei Gruppen stellten die Verfasser die Zusammensetzung der Bitumina im

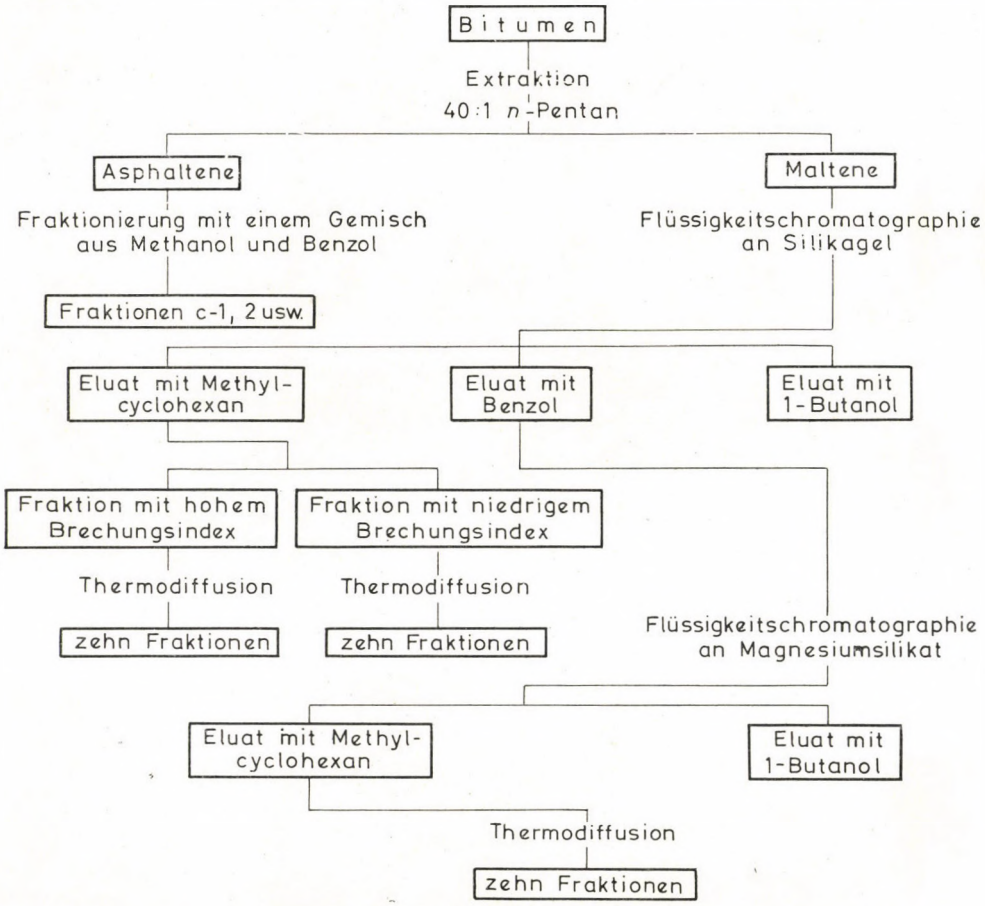

Abb. 2

Dreieckdiagramm dar und folgerten aus ihrer Lage im Diagramm auf ihre Eigenschaften. BOYD und MONTGOMERY [10] extrahierten die löslichen Teile eines bitumenhaltigen Sandes aus Athabasca mit *n*-Pentan und anschließend die Asphaltene mit Tetrachlorkohlenstoff. Der Extrakt wurde an Fullererde chromatographiert. Als Eluenten wurden Pentan, Tetrachlorkohlenstoff, Benzol, Chloroform und Methanol verwendet.

Die Gruppenzusammensetzung des Bitumens aus Romaschkino wurde von mehreren Verfassern untersucht. PRINZLER und Mitarbeiter [11] untersuchten die Gruppenzusammensetzung eines Destillationsrückstandes aus Romaschkino durch Flüssigkeitschromatographie auf Silikagel. Die Paraffine und Naphthene wurden mit Petroläther, die Ölharze mit einem Gemisch aus Benzol und Petroläther 1:1, die Asphaltharze mit Aceton und schließlich die Asphaltene mit Pyridin eluiert. Die Paraffine und Naphtene enthaltende Fraktion wurde erneut chromatographiert, wobei eine Paraffin/Naphten-Fraktion und eine monoaromatische Fraktion erhalten wurde. Die Paraffine wurden durch Adduktbildung mit Harnstoff in Normalparaffine und verzweigte Paraffine getrennt. HRAPIA [12] befaßte sich ebenfalls mit der Gruppenanalyse des Bitumens aus Romaschkino. Er trennte die Asphaltene mit Pentan ab und trennte dann die Maltene durch Molekulardestillation und Chromatographie in 360 Fraktionen. Der C_A-, C_P- und C_N-Gehalt der einzelnen Fraktionen wurde durch Strukturgruppenanalyse bestimmt. Die Maltene wurden durch Molekulardestillation in 12 Fraktionen getrennt und dann jede einzelne Fraktion durch Chromatographie an Aluminiumoxid in weitere 30 Fraktionen zerlegt. Als Elutionsmittel ließen sich Benzin 60/70, Benzol und ein Gemisch aus Benzol und Methanol verwenden.

LEIBNITZ und PAPP [13] trennten ein Bitumen aus Nagylengyel durch Chromatographie an Aluminiumoxid in 32 Fraktionen, deren Strukturgruppenzusammensetzung ebenfalls bestimmt wurde. Sie bestimmten die Anzahl und Verteilung der Naphtenringe und der aromatischen Ringe in den einzelnen Fraktionen. CORBETT [14, 15] trennte die Bitumina in vier Gruppen, wobei er sich der Elutions-Adsorptionschromatographie bediente. Nach dem Abscheiden der Asphaltene erhielt er mittels Chromatographie eine gesättigte Fraktion, eine aus Naphthenen und Aromaten bestehende Fraktion und eine aromatische Fraktion. Zur Bestimmung der durchschnittlichen chemischen Zusammensetzung verwendete er die densitometrische Methode von VAN KREVELEN. Die Asphaltene wurden mit *n*-Heptan gefällt. Die Maltenlösung wurde in einer mit Aluminiumoxid gefüllten Säule chromatographiert. Als Elutionsmittel wurden *n*-Heptan, Benzol, Benzol–Alkohol (1 : 1) und zuletzt Trichloräthylen verwendet (Abb. 3). MIDDLETON [16] trennte schwere Erdölfraktionen, darunter auch Bitumina mittels Flüssig–Fest–Gradientenelutionschromatographie an Aluminiumoxid. Die Probe wurde vorher an einem Teil der Säulefüllung adsorbiert. Die Elutionsmittel, die eine optimale Trennung

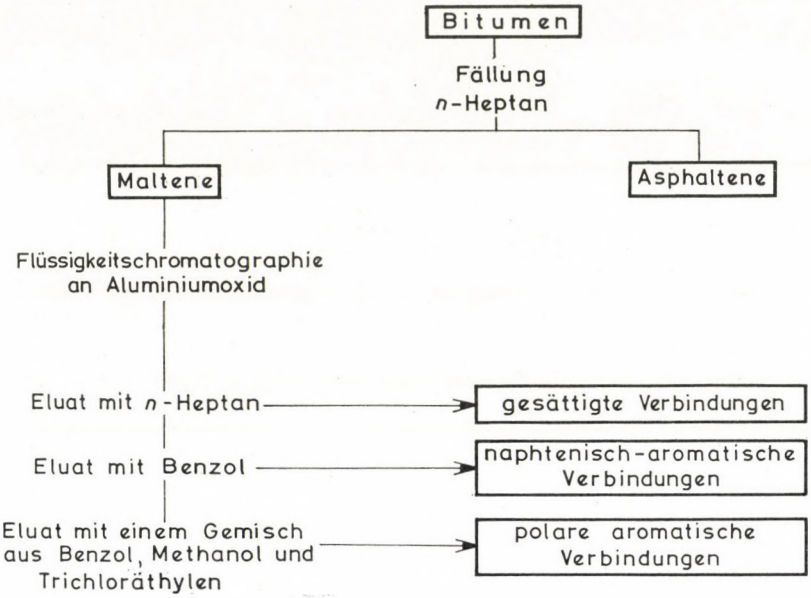

Abb. 3

ermöglichten, wurden experimentell bestimmt. Das Gradientenelutionssystem bestand aus fünf Lösungsmitteln, und zwar *n*-Pentan, *n*-Hexan, Dichlormethan, Tetrahydrofuran und Methanol. Es wurden folgende Fraktionen erhalten: gesättigte Verbindungen, mono- und diaromatisches Öl, polyaromatisches Öl, Weichharz, Hartharz und Asphaltene. Das Eluat wurde kontinuierlich durch UV-Spektroskopie kontrolliert und die Fraktionen auf Grund dieser Ergebnisse geschnitten.

In der Sowjetunion entwickelte SERGIENKO [17] ein Verfahren zur Zerlegung von Bitumina. Dabei wurden die Asphaltene mit *n*-Pentan gefällt und die Maltenlösung an Silikagel chromatographiert. Als Elutionsmittel wurden Petroläther, Tetrachlorkohlenstoff, Benzol, Aceton und ein Gemisch aus Alkohol und Benzol verwendet.

In Ungarn befaßten sich NYÚL, MÓZES und ZAKAR [18—21] im Ungarischen Erdöl- und Erdgas-Forschungsinstitut mit der Untersuchung der Gruppenzusammensetzung von Bitumina. Nach einem ihrer Verfahren werden die Bitumina in drei Komponenten, und zwar in Asphaltene, ölige sowie harzige Bestandteile getrennt. Die Asphaltene werden mit leichtem Benzin abgeschieden und anschließend die harzigen Bestandteile an Fullererde adsorbiert. Durch Extraktion der Fullererde wird die Harzkomponente erhalten. Der ölige Teil bleibt in der Benzinlösung. Nach einer anderen Methode der genannten Verfasser werden die Asphaltene mit *n*-Hexan abgetrennt und die Maltenlösung an weitporigem Silikagel chromatographiert. Der ölige Teil wird

mit *n*-Hexan, die Ölharze mit Benzol und die Asphaltharze mit Chloroform–Aceton (1:1) eluiert. Dieses zweite Verfahren liefert wesentlich besser reproduzierbare Werte als die erste Methode.

L. VAJTA und Zs. VAJTA [22—24] fanden die Methode von TRAXLER und SCHWEYER am günstigsten und verwendeten sie in ihren ausgedehnten Bitumenuntersuchungen. Ihrer Meinung nach ist diese Methode zum Vergleich verschiedener Bitumina sehr gut reproduzierbar und die Trennung einfach durchführbar.

Aus dem Gesagten zeigt sich, daß die anfänglich für die Gruppenanalyse von Bitumina eingeführte Perkolation mit aktivierter Fullererde und die danach folgende selektive Extraktion im weiteren durch die einfachere und besser reproduzierbare Ergebnisse liefernde Elutions–Flüssigkeitschromatographie abgelöst wurde. Als Adsorbens wird weitporiges Silikagel oder aktiviertes Aluminiumoxid verwendet. Da praktisch Säulen beliebiger Größe gebaut werden können, die dabei leicht zu handhaben sind, stieg die Menge des auf einmal trennbaren Bitumens an, wodurch eine Reihe weiterer Trennungen ermöglicht wurde. Zur Desorption der drei wichtigsten Bestandteilgruppen — gesättigte Verbindungen, Ölharze bzw. Asphaltharze — werden Lösungsmittel mit steigender Polarität verwendet: Elutionsmittel für die gesättigten Verbindungen sind Leichtbenzinfraktionen oder reine gesättigte aliphatische Kohlenwasserstoffe kleiner Kohlenstoffatomzahl, für Ölharze wird meistens Benzol als Elutionsmittel eingesetzt, während Asphaltharze durch stark polare Verbindungen wie Methylalkohol, Pyridin, Aceton, Chloroform, bzw. deren Gemische eluiert werden. Vor der chromatographischen Trennung werden die Asphaltene meistens abgetrennt. Die Menge der gefällten Asphaltene hängt weitgehend von dem verwendeten Lösungsmittel ab. Die in der Lösung verbleibenden Maltene werden chromatographiert, gegebenenfalls noch vor dem Chromatographieren durch Molekulardestillation in Fraktionen getrennt. Die gesättigte Verbindungen enthaltenden Fraktionen werden in einigen Fällen bei tiefen Temperaturen (−30. . .−50°) entparaffiniert und das erhaltene Paraffin durch Adduktbildung mit Harnstoff in Hart- und Weichparaffine getrennt. Der ölige Maltenteil kann auch durch Thermodiffusion [4, 8, 25] zerlegt werden.

Herstellung von Bitumenfraktionen mit homogener chemischer Struktur

Der überwiegende Teil der in der Literatur veröffentlichten Trennverfahren für Bitumina ermöglicht nur die Bestimmung der Gruppenzusammensetzung, liefert jedoch keine Fraktionen, deren Zusammensetzung genügend homogen wäre, um die chemische Struktur klären zu können.

Über das Bitumen aus dem Romaschkinoer Erdöl stehen ebenfalls nur Gruppenzusammensetzungsangaben zur Verfügung. Eine ausführlichere Unter-

suchung des Bitumens von Algyő wurde bisher überhaupt nicht durchgeführt.

In unserer Arbeit wurde ein Trennverfahren entwickelt, das die Herstellung von zur Klärung der Struktur geeigneten Fraktionen mit homogener Struktur ermöglicht. Daneben wurde eine Kombination der analytischen Methoden ausgearbeitet, wodurch eine tiefgehende strukturelle Charakterisierung der Fraktionen durchgeführt werden kann.

Ziel unserer Arbeit war auch der Vergleich der Struktur von Bitumina, die aus Erdölen verschiedener Herfkunft und mittels verschiedener Technologien hergestellt worden sind.

Bei der Entwicklung des Trennverfahrens wurden die verschiedenen Trennmethoden derart kombiniert, daß das Ziel der Herstellung von Bitumenfraktionen mit relativ homogener chemischer Struktur so weit wie möglich angenähert werden konnte. Das Schema des entwickelten Trennverfahrens ist in Abb. 4 dargestellt.

Der erste Schritt war die Abscheidung der Asphaltene. Die von den übrigen Bestandteilen des Bitumens hinsichtlich des Molekulargewichtes, der Löslichkeit und der chemischen Struktur wesentlich abweichenden Asphaltene werden wegen ihrer charakteristischen Eigenschaften und wegen ihrer wichtigen Rolle im Aufbau des Bitumens zweckmäßig gesondert behandelt und untersucht.

Der erste Schritt in der Trennung der Maltene war die Elutions–Flüssigkeitschromatographie. Dabei wurden vier charakteristische, voneinander in sämtlichen Eigenschaften abweichende Fraktionen erhalten. Diese sind die folgenden:

1. paraffinisches Öl,
2. naphtenisch-aromatisches Öl,
3. Ölharz,
4. Asphaltharz.

Die weiteren Trennungsschritte dienten zur Absonderung von Verbindungsgruppen noch einheitlicherer Zusammensetzung innerhalb der oben genannten Fraktionen. Die Fraktionen 1—3 wurden bei —30°C entparaffiniert, wodurch die Paraffine von den verzweigten, hauptsächlich Naphten- und aromatische Ringe enthaltenden Verbindungen getrennt wurden. Aus den Paraffinen wurden durch Adduktbildung mit Harnstoff die hochmolekularen geradkettigen oder nur wenig verzweigten Paraffine abgesondert. Danach wurden sämtliche bis dahin erhaltenen Fraktionen durch Molekulardestillation ihrer Molekülgröße entsprechend in zwei Fraktionen getrennt. Als letzte Trennungsoperation folgte die Trennung der aromatischen Fraktionen nach ihrer Ringzahl durch Flüssigkeitschromatographie. Dadurch wurden wertvolle Informationen über die Zahl und Art der nicht kondensierten und kondensierten aromatischen Ringsysteme erhalten.

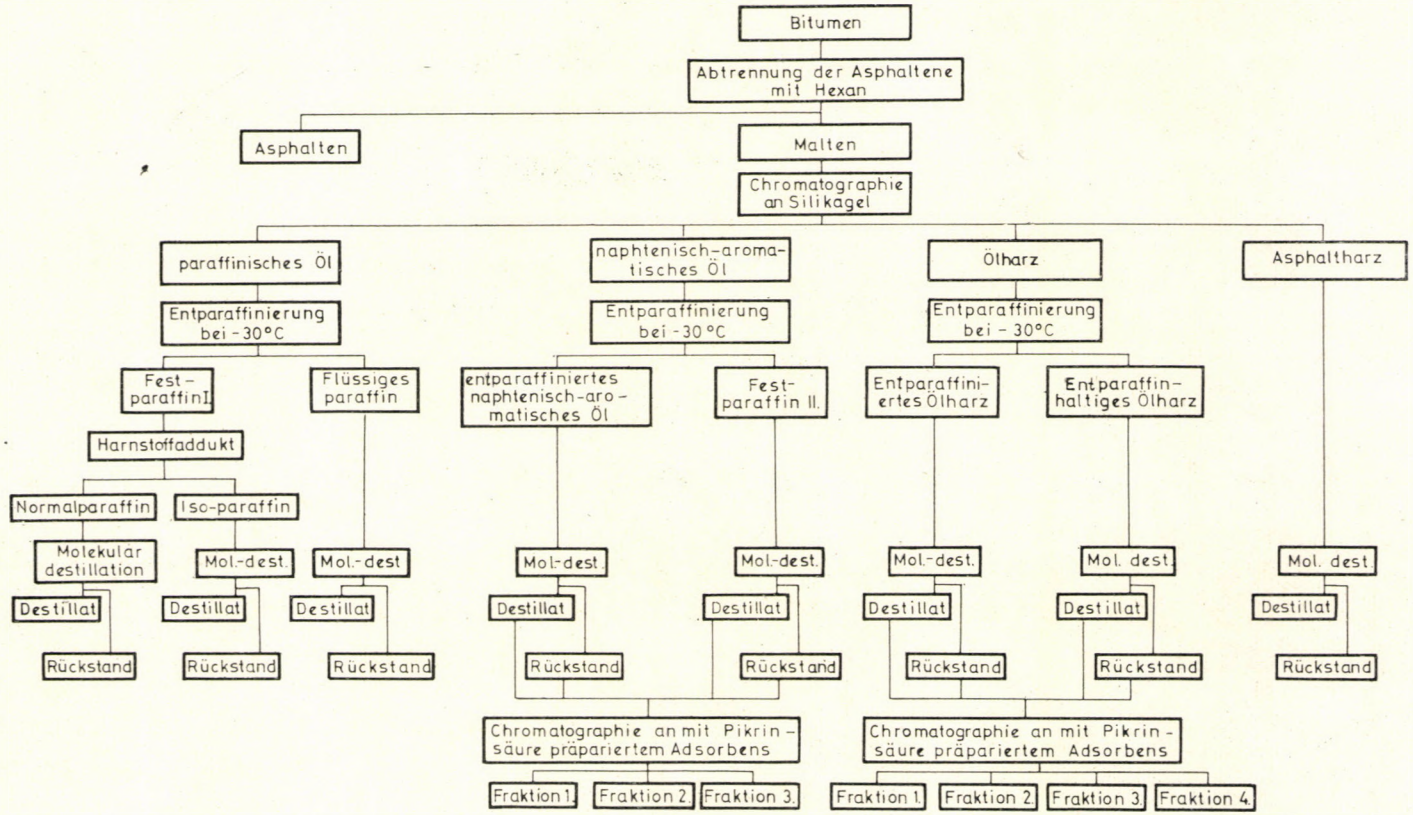
Bitumen
Abtrennung der Asphaltene mit Hexan
Asphalten
Malten
Chromatographie an Silikagel
paraffinisches Öl
naphtenisch-aromatisches Öl
Ölharz
Asphaltharz
Entparaffinierung bei -30°C
Entparaffinierung bei -30°C
Entparaffinierung bei -30°C
Fest-paraffin I.
Flüssiges paraffin
entparaffiniertes naphtenisch-aromatisches Öl
Fest-paraffin II.
Entparaffiniertes Ölharz
Entparaffinhaltiges Ölharz
Harnstoffaddukt
Normalparaffin
Iso-paraffin
Molekular destillation
Mol.-dest.
Mol.-dest.
Mol-dest.
Mol-dest.
Mol.-dest.
Mol. dest.
Mol. dest.
Destillat
Destillat
Destillat
Destillat
Destillat
Destillat
Destillat
Rückstand
Rückstand
Rückstand
Rückstand
Rückstand
Rückstand
Rückstand
Chromatographie an mit Pikrinsäure präpariertem Adsorbens
Chromatographie an mit Pikrinsäure präpariertem Adsorbens
Fraktion 1.
Fraktion 2.
Fraktion 3.
Fraktion 1.
Fraktion 2.
Fraktion 3.
Fraktion 4.

Abb. 4

Bei den Endfraktionen wurde das Molekulargewicht und die Elementarzusammensetzung bestimmt und die chemische Struktur der einzelnen Fraktionen mit IR-, UV- und NMR-Spektroskopie untersucht.

Es wurden vier Bitumenproben untersucht:

1. Romaschkinoer Extraktbitumen,
2. Romaschkinoer Destillationsbitumen,
3. Romaschkinoer geblasenes Bitumen,
4. Algyőer Extraktbitumen.

Das Romaschkinoer und Algyőer Extraktbitumen wurde im Entbituminierbetrieb der Donau- Mineralölwerke, Százhalombatta hergestellt. Das Destillationsbitumen wurde im AV-II-Betrieb desselben Unternehmens verfertigt. Das geblasene Bitumen wurde im Versuchsreaktor des Ungarischen Erdöl- und Erdgas-Forschungsinstituts aus Romaschkinoer Gudron (Erweichungspunkt 43 °C) hergestellt. Einige charakteristische Eigenschaften der Bitumina sind in Tab. I zusammengestellt.

Tabelle I

Charakteristische Eigenschaften einiger Bitumina aus Romaschkino and Algyő

Eigenschaft	Bitumen aus Romaschkino			Extraktbitumen aus Algyő
	Extr.	Destill.	Geblas.	
Erweichungspunkt, (»Ring und Ball«-Methode), °C	54	50	50	47
Penetration bei 25 °C, 1/10 mm	31	59	134	nicht meßbar
Duktilität bei 25 °C, mm	1000	1000	600	nicht meßbar
Brechpunkt nach Fraass, °C	+2	−10	−18	−25
Paraffingehalt, Gew.%	1,44	2,09	2,26	3,43
Dichte bei 25 °C, g/ml	1,0288	1,0125	0,9997	0,9705
Conradson-Zahl, Gew.%	20,7	21,0	17,1	13,0
Flammpunkt nach Marcusson, °C	345	349	331	346
Elementaranalyse:				
C, %	85,2	85,2	85,1	87,6
H, %	10,3	10,3	10,7	11,7
S, %	3,6	3,1	3,2	0,8
O, %	1,0	1,4	1,5	0,4
Molekulargewicht	860	880	770	850

Elutions-Flüssigkeitschromatographie

Mit Rücksicht auf die Anzahl der geplanten, nacheinander folgenden Trennungsoperationen wurde eine verhältnismäßig große Probenmenge von etwa 1 kg Bitumen verarbeitet. Um die Arbeit zu beschleunigen, projektierten und bauten wir eine große chromatographische Säule mit hoher Leistung (Abb. 5). Darin sind fünf Säulen mit Längen von je 2500 mm in Reihe geschaltet. Der Durchmesser der ersten Säule beträgt 80 mm, der Durchmesser der übrigen vier Säulen 40 mm. Die gesamte Länge der Säule beträgt 12 500

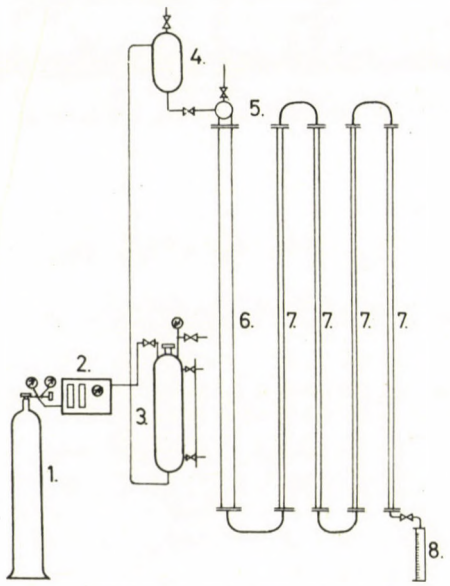

Abb. 5. Einrichtung zur Chromatographie von Bitumina. *1* — Stickstoff-Flasche; *2* — Druckregler; *3* — Lösungsmittelbehälter; *4* — Zwischengeschaltetes Gefäß; *5* — Schauglas; *6* — Säule mit 80 mm Durchmesser; *7* — Säule mit 40 mm Durchmesser; *8* — Sammelgefäß

mm. Um eine gleichmäßige Temperatur zu sichern, wurde im Kühlmantel der Säulen Wasser von 25 °C in Zirkulation gehalten. Die Maltenlösung, bzw. die Elutionsmittel wurden in den mit einem Niveauanzeiger versehenen Lösungsmittelbehälter *3* eingeführt und daraus mittels Stickstoffdruck *1* über ein dazwischengeschaltetes Gefäß *4* auf die Säule *6* geleitet. Der Stickstoffdruck wurde durch einen Druckregler *2* auf den gewünschten Wert (im allgemeinen unterhalb 0,5 atü) eingestellt. Die Entnahmegeschwindigkeit des Eluats betrug 500 ml/h. Die Säule war mit 12 kg weitporigem Silikagel (Korngröße 0,1—0,5 mm) gefüllt.

Nach dem Abscheiden der Asphaltene mit *n*-Hexan wurde die Lösung der Maltene in *n*-Hexan auf die Säule aufgegeben. Die Säulenbelastung betrug

4—6% auf Malten bezogen. Zur Benetzung der Säule wurde *n*-Hexan, als Elutionsmittel wurden *n*-Hexan, Benzol und Aceton verwendet. Die Lösungsmittel wurden vorangehend mit Molekularsieb entwässert. Bei der Elution mit *n*-Hexan wurden zwei Fraktionen erhalten: ein paraffinisches Öl und ein naphtenisch-aromatisches Öl. Die Erscheinung des naphtenisch-aromatischen Öles wurde durch den Farbumschlag des Eluats nach Blaß-Zitronengelb angezeigt. Die Grenze zwischen den beiden Fraktionen wurde auch refraktometrisch überwacht. Die Ölharze wurden mit Benzol eluiert, die Asphaltharze mit Aceton. Die prozentuelle Verteilung der erhaltenen insgesamt fünf Fraktionen ist in Tab. II zusammengestellt.

Tabelle II

Gruppenzusammensetzung von Bitumina aus Romaschkino und Algyő

Fraktion		Bitumen aus Romaschkino			Extraktbitumen aus Algyő
		Extr.	Destill.	Geblas.	
Paraffinisches Öl,	Gew.%	9,2	11,1	19,1	31,3
Naphtenisch-aromatisches Öl,	Gew.%	3,0	4,9	6,6	5,3
Ölharz,	Gew.%	61,4	55,4	44,9	43,5
Asphaltharz,	Gew.%	13,0	12,0	11,1	13,5
Asphaltenteil,	Gew.%	10,2	13,4	15,0	6,1
Verlust,	Gew.%	3,2	3,2	3,3	0,3

Ein Vergleich der verschiedenen Romaschkinoer Bitumina zeigt einen wesentlichen Unterschied in der Gruppenzusammensetzung des Extraktbitumens und des Destillationsbitumens. Das erstere enthält weniger Öl und mehr Harz. Diese Abweichung ergibt sich aus der unterschiedlichen Herstellungstechnologie und wirkt sich auch auf die Verwendbarkeit des Bitumens aus. Der höhere Asphaltengehalt, der verhältnismäßig geringe Harzgehalt und der hohe Ölgehalt des Romaschkinoer geblasenen Bitumens zeigt an, daß das unter milden Umständen durchgeführte Blasen in erster Reihe die Umsetzung der Harze in Asphaltene und in wesentlich geringerem Maße die Umsetzung des Öles in Harz bewirkte. Einige analytische Angaben der auf chromatographischem Weg erhaltenen Fraktionen sind in Tab. III zusammengefaßt. Das Molekulargewicht der Fraktionen steigt vom paraffinischen Öl bis zu den Asphaltenen gleichmäßig an. Auch der Schwefelgehalt steigt an, während der Sauerstoffgehalt den maximalen Wert in der Asphaltharzfraktion erreicht. Das Gewichts- bzw. Atomverhältnis C : H steigt von den gesättigten Verbindungen in Richtung der Asphaltene an.

Tabelle III

Molekulargewicht, Elementaranalyse, Kohlenstoffgehalt in aromatischer, paraffinischer und naphtenischer Bindung der bei der chromatographischen Trennung von Bitumenproben erhaltenen Fraktionen

Probe	Fraktion	Mol. Gew.	Elementaranalyse, Gew.%				Verhältnis C : H		IR-Spektrometrie		
			C	H	S	O	in Gewicht	in Atomzahl	C_A	C_P	C_N
1	2	3	4	5	6	7	8	9	10	11	12
Romaschkinoer Extraktbitumen	Ausgangsbitumen	860	85,2	10,3	3,6	1,0	8,3	0.69	+	+	+
	Paraffinisches Öl	637	86,3	13,8	—	—	6,2	0,52	—	64,3	35,7
	Naphtenisch-aromatisches Öl	726	85,4	12,9	1,8	—	6,6	0,55	12,4	65,3	22,3
	Ölharz	840	85,6	10,4	3,3	1,0	8,2	0,69	32,6	55,8	11,6
	Asphaltharz	1160	83,5	11,2	3,8	2,3	7,4	0,62	+	+	+
	Asphaltenteil	3540	85,7	8,1	4,0	2,0	10,5	0,88	+	+	+
Romaschkinoer Dest.-Bitumen	Ausgangsbitumen	880	85,2	10,3	3,1	1,4	8,2	0,69	+	+	+
	Paraffinisches Öl	622	86,2	13,9	—	—	6,2	0,52	—	66,8	33,2
	Naphtenisch-aromatisches Öl	775	85,2	12,9	1,6	—	6,6	0,55	11,5	61,4	27,1
	Ölharz	764	84,5	9,9	4,1	1,3	8,5	0,70	42,5	48,1	9,4
	Asphaltharz	1100	82,1	9,6	3,7	4,8	8,5	0,70	+	+	+
	Asphaltenteil	3200	85,9	7,2	4,4	2,0	11,9	0,90	+	+	+
Romaschkinoer geblasenes Bitumen	Ausgangsbitumen	770	85,1	10,7	3,2	1,5	7,9	0,66	+	+	+
	Paraffinisches Öl	584	86,0	13,9	—	—	6,2	0,51	—	63,2	36,8
	Naphtenisch-aromatisches Öl	698	85,7	12,7	1,7	—	6,7	0,56	12,2	69,6	18,2
	Ölharz	751	84,4	9,7	3,4	2,5	8,7	0,72	36,4	56,6	7,0
	Asphaltharz	980	80,8	9,6	3,4	5,7	8,4	0,70	+	+	+
	Asphaltenteil	3540	85,2	7,9	4,1	2,3	10,8	0,99	+	+	+
Algyőer Extraktbitumen	Ausgangsbitumen	850	87,6	11,7	0,8	0,4	7,4	0,62	+	+	+
	Paraffinisches Öl	707	85,8	14,2	—	—	6,0	0,50	—	85,7	14,3
	Naphtenisch-aromatisches Öl	732	86,1	13,3	0,8	—	6,4	0,54	13,9	83,9	2,2
	Ölharz	730	87,6	10,2	1,2	1,3	8,6	0,72	42,4	57,6	—
	Asphaltharz	1140	85,9	10,6	3,2	2,7	8,1	0,68	+	+	+
	Asphaltenteil	2800	87,3	9,1	1,4	1,6	9,6	0,80	+	+	+

Aus dem IR-spektroskopisch bestimmten Anteil des aromatisch, paraffinisch und naphtenisch gebundenen Kohlenstoffgehaltes der einzelnen Fraktionen kann festgestellt werden, daß der paraffinisch gebundene und hauptsächlich der naphtenisch gebundene Kohlenstoffgehalt mit zunehmendem Molekulargewicht der Fraktionen abnimmt, während ihr Aromatengehalt zunimmt. Dieser Befund weist auf eine wesentliche Änderung der Molekülstrukturen hin.

Entparaffinierung

Aus den durch Elutionschromatographie erhaltenen Fraktionen wurden die kristallisierbaren Paraffine durch Lösungsmittel-Entparaffinierung bei −30 °C abgeschieden. Die Entparaffinierung des paraffinischen Öles und des naphtenisch-aromatischen Öles war leicht durchführbar. Aus dem Ölharz wurden die Bestandteile paraffinischen Charakters bereits schwerer abgeschieden, jedoch ließen sich auch hier wesentliche Mengen an bei −30 °C kristallisierenden Bestandteilen herstellen. Aus dem Asphaltharz wurde erwartungsgemäß kein filtrierbarer Niederschlag erhalten. Die Materialbilanz der Entparaffinierung der vier Proben ist in Tab. IV, das Molekulargewicht und der aromatisch, paraffinisch und naphtenisch gebundene Kohlenstoffgehalt ist in Tab. V und VI gezeigt.

Tabelle IV

Festparaffingehalt verschiedener Fraktionen von Bitumina aus Romaschkino und Algyő

Probe	Paraffinisches Öl				Naphtenisch-aromatisches Öl				Ölharz			
	Flüssiges Paraffin, Ausbeute, Gew.%		Festparaffin I, Ausbeute, Gew.%		Paraffinfreies Öl, Ausbeute, Gew.%		Festparaffin II, Ausbeute Gew.%		Paraffinfreies Öl, Ausbeute, Gew.%		Paraffinhaltiges Ölharz, Ausbeute, Gew.%	
	a	b	a	b	a	b	a	b	a	b	a	b
Romaschkinoer Extraktbitumen	14,1	1,30	85,9	7,90	60,1	1,80	39,9	1,20	91,9	56,7	8,1	5,0
Romaschkinoer Dest.-bitumen	16,7	1,85	83,3	9,25	55,9	2,74	44,1	2,16	93,1	51,6	6,9	3,8
Romaschkinoer geblasenes Bitumen	53,2	10,14	46,8	8,96	73,1	4,82	27,0	1,78	91,3	41,0	8,7	3,9
Algyőer Extraktbitumen	15,2	4,7	84,8	26,6	53,7	2,85	46,3	2,45	88,6	38,6	11,4	4,9

a = auf die Operation bezogen
b = auf das Bitumen bezogen

Tabelle V

Molekulargewicht und Verteilung des Kohlenstoffgehaltes bei den paraffinischen und naphtenisch-aromatischen Ölfraktionen von Bitumina aus Romaschkino und Algyő

Probe	Paraffinisches Öl							
	Flüssiges Paraffin				Festparaffin I			
	Mol.-gew.	C_A	C_P	C_N	Mol.-gew.	C_A	C_P	C_N
Romaschkinoer Extraktbitumen	550	—	52,2	47,8	755	—	80,2	19,8
Romaschkinoer Dest.-bitumen	598	—	52,1	47,9	720	—	83,7	16,3
Romaschkinoer geblasenes Bitumen	577	—	57,1	42,9	670	—	89,8	10,2
Algyőer Extraktbitumen	585	—	60,3	39,7	773	—	91,8	8,2

Probe	Naphtenisch-aromatisches Öl							
	Paraffinfreies Öl				Festparaffin II			
	Mol.-gew.	C_A	C_P	C_N	Mol.-gew.	C_A	C_P	C_N
Romaschkinoer Extraktbitumen	644	15,1	59,5	25,4	810	10,5	89,5	—
Romaschkinoer Dest.-bitumen	747	13,4	59,5	27,1	842	10,2	87,1	2,7
Romaschkinoer geblasenes Bitumen	623	15,5	54,5	30,0	770	11,0	89,0	—
Algyőer Extraktbitumen	710	18,2	63,6	18,2	940	10,7	89,2	—

Tabelle VI

Molekulargewicht und Verteilung des Kohlenstoffgehaltes bei den Ölharzfraktionen von Bitumina aus Romaschkino und Algyő

Probe	Ölharz							
	entparaffiniert				paraffinhaltig			
	Mol.-gew.	C_A	C_P	C_N	Mol.-gew.	C_A	C_P	C_N
Romaschkinoer Extraktbitumen	760	34,5	47,4	18,1	990	20,7	79,3	—
Romaschkinoer Dest.-bitumen	690	44,0	43,0	13,0	1140	28,2	71,2	—
Romaschkinoer geblassenes Bitumen	742	38,5	53,4	8,1	1240	23,1	76,9	—
Algyőer Extraktbitumen	715	47,8	52,2	—	970	26,3	73,7	—

Die Menge des aus paraffinischen und naphtenisch-aromatischen Ölfraktionen erhaltenen festen Paraffins liegt bei Romaschkinoer Bitumina um 10% (auf Bitumen bezogen), während sie beim Algyőer Extraktbitumen fast 30% erreicht. Dies ist das Mehrfache des mit den üblichen Methoden bestimmten Paraffingehaltes. Der aus dem Ölharz abgesonderte paraffinische Teil kann jedoch nicht als Gemisch reiner Paraffin-Kohlenwasserstoffe betrachtet werden, sondern es handelt sich um Verbindungen, in denen lange Paraffinketten an aromatische Ringe gebunden sind.

Bei allen drei Fraktionen ist das Molekulargewicht des festen Teiles wesentlich höher als das Molekulargewicht des entparaffinierten Teiles. Der Naphtenringgehalt ist am höchsten im entparaffinierten Teil des paraffinischen Öles, wesentlich geringer im entparaffinierten naphtenisch-aromatischen Öl und äußerst niedrig im entparaffinierten Ölharz. Dagegen liegen Naphtenringstrukturen im paraffinischen Teil des naphtenisch-aromatischen Öles und des Ölharzes praktisch nicht vor. Dieser Befund zeigt, daß die Naphtenringe größtenteils nicht mit paraffinischen Seitenketten verbunden sind, sondern an aromatische Ringe gebunden vorliegen.

Naphtenringe mit langen Seitenketten bilden einen wesentlichen Teil der gesättigten Ölfraktionen.

Abtrennung der Normalparaffine

Die aus der paraffinischen Ölfraktion der Bitumina stammende Festparaffinfraktion I wurde mittels Adduktbildung mit Harnstoff in Normal- und Isoparaffine getrennt.

Die Probe wurde in warmem Benzol gelöst und der in Methanol gelöste Harnstoff bei 50 °C unter Rühren dazu gegeben. Die Adduktbildung setzte sofort ein, wobei ein dichter weißer Niederschlag gebildet wurde. Nach einstündigem Rühren wurde das Addukt abfiltriert, mit Benzol gewaschen und das Benzol vom kristallinen Addukt abgedampft. Die Zersetzung des Adduktes ließ sich auf die übliche Weise durchführen.

Die aus der naphtenisch-aromatischen Ölfraktion stammende Festparaffinfraktion II wurde ebenfalls auf die oben beschriebene Weise behandelt, wobei jedoch nur ein äußerst geringer Teil an Normalparaffinen erhalten wurde. Wahrscheinlich wird die Adduktbildung durch die mit den langen Paraffinketten verbundenen aromatischen oder naphtenischen Ringe gehindert.

Wir fanden, daß etwa eine Hälfte der Festparaffinfraktion I aus Normal- oder in geringerem Maße verzweigten Paraffin-Kohlenwasserstoffen besteht, während der mit Harnstoff kein Addukt bildende Teil Kettenverzweigungen bzw. Naphtenringe enthält. Das Molekulargewicht und die Verteilung der Kohlenstoffatome bei der Festparaffinfraktion I sind in Tab. VII zusammengestellt.

Tabelle VII

Molekulargewicht und Verteilung des Kohlenstoffgehaltes bei den aus der Festparaffinfraktion I gewonnenen Normal- und Isoparaffinen

Probe	Festparaffin I							
	Normalparaffin				Isoparaffin			
	Mol.-gew.	C_A	C_P	C_N	Mol.-gew.	C_A	C_P	C_N
Romaschkinoer Extraktbitumen	855	—	100,0	—	657	—	60,8	39,2
Romaschkinoer Dest.-bitumen	829	—	100,0	—	674	—	62,0	38,0
Romaschkinoer geblasenes Bitumen	780	—	100,0	—	612	—	80,7	19,3
Algyőer Extraktbitumen	790	—	100,0	—	640	—	80,6	19,4

Molekulardestillation

Die nach den oben beschriebenen Operationen erhaltenen Fraktionen wurden der Molekulardestillation unterworfen, wobei die bereits gewissermaßen als homogen betrachtbaren Fraktionen nach dem Molekulargewicht in engere Fraktionen zerlegt werden konnten. Aus jeder einzelnen Fraktion wurden zwei weitere Fraktionen erhalten, das Destillat und der Rückstand. Sämtliche Destillationen wurden bei 10^{-6} Torr (am Stutzen gemessen) durchgeführt. Die Temperatur war bei Ölfraktionen 220—230 °C, bei Harzen 250—270 °C. Das Molekulargewicht der erhaltenen Destillate war ziemlich ähnlich (zwischen 500 und 600), obwohl die Ausgangsfraktionen sowohl hinsichtlich des Molekulargewichtes als auch der Zusammensetzung große Unterschiede aufwiesen. Das Molekulargewicht und die Menge des Destillationsrückstandes war selbstverständlich in hohem Maße verschieden, je nach der Zusammensetzung der Ausgangsfraktion.

Trennung der aromatischen Verbindungen nach der Ringzahl

Die weitere Trennung der durch Molekulardestillation erhaltenen Fraktionen des naphtenisch-aromatischen Öles und des entparaffinierten Ölharzes nach der Zahl der aromatischen Ringe wurde an mit Pikrinsäure präpariertem Adsorbens mittels Flüssigkeitschromatographie durchgeführt. Das Prinzip des Verfahrens besteht darin, daß Verbindungen mit einem, zwei oder mehreren aromatischen Ringen — infolge der unterschiedlichen Stabilität ihrer mit Pikrinsäure gebildeten Komplexe — durch Elutionschromatographie getrennt werden können [26, 27].

Zur Trennung wurde ein mit Pikrinsäure präparierter Aluminiumsilikat-Krackkatalysator verwendet. Die chromatographische Säule war eine 1000 mm

lange Glasröhre mit 12 mm innerem Durchmesser, umgeben von einem Temperiermantel aus Glas. Die Säulenbelastung betrug 0,5—1,7%. Die Elutionsbedingungen waren die folgenden:

— Gesättigte Verbindungen und einen aromatischen Ring enthaltende Verbindungen: bei 20 °C; Elutionsmittel: aromatenfreies Benzin mit einem Siedebereich von 60—120 °C;

— Verbindungen mit zwei aromatischen Ringen: bei 40 °C; Elutionsmittel: Tetrachlorkohlenstoff;

— Verbindungen mit mehreren aromatischen Ringen: bei 60 °C; Elutionsmittel: Tetrachlorkohlenstoff;

— Rückstand: bei 40 °C; Elutionsmittel: Aceton.

Nach diesem Verfahren gelang es, aus den meisten Fraktionen weitere Fraktionen zu erhalten, die die Verbindungen mit einheitlicher Struktur in konzentriertem Zustand enthielten, wodurch die analytische Untersuchung der Struktur der letzteren Verbindungen wesentlich erleichtert wurde.

Molekulargewicht und Elementarzusammensetzung

Zur Molekulargewichtsbestimmung der Bitumenfraktionen wurde die thermoosmometrische Methode gewählt. Im Falle eines entsprechend gewählten Lösungsmittels erwies sich diese Methode als geeignet sowohl für Fraktionen höchsten als auch geringsten Molekulargewichtes. Ein wichtiger Vorteil der Methode ist, daß nur geringe Substanzmengen erforderlich sind. Als Lösungsmittel wurden Tetrachlorkohlenstoff und Chloroform verwendet. Die Molekulargewichte und die Elementarzusammensetzungen der wichtigeren Fraktionen sind in Tab. III zusammengefasst.

Das erläuterte Verfahren zur Trennung von Bitumina ermöglicht die Trennung der Bitumenproben in 32 Fraktionen, deren chemische Zusammensetzung einzeln charakteristisch und bis zu einem gewissen Grade gleichartig ist. Nach jeder Trennungsoperation wurde sowohl bezüglich der Operation als auch der Bitumenprobe eine volle Materialbilanz zusammengestellt. Auf diese Weise konnte die Richtung der Konzentrierung der einzelnen Verbindungsgruppen verfolgt und auf dieser Grundlage der nächste Trennungsschritt gewählt werden. Neben der quantitativen Auswertung wurde selbstverständlich auch eine laufende qualitative Kontrolle durchgeführt, in erster Linie durch Spektrometrie. Die Elementarzusammensetzung und das Molekulargewicht der wichtigeren Intermediär- und Endfraktionen wurden bestimmt und ihre UV-, IR- und NMR-Spektren ebenfalls aufgenommen. Dadurch wurde ein näherer Einblick in die durchschnittliche chemische Zusammensetzung der einzelnen Fraktionen erhalten. Dieser Teil unserer Arbeit sowie der Vergleich der chemischen Struktur der verschiedenen Bitumina soll in unserem nächster Artikel behandelt werden.

LITERATUR

1. MARCUSSON, J.: Angew. Chem., **29,** 346 (1916)
2. PÖLL, H.: Petroleum, **28,** 36 (1932)
3. HOIBERG, A. J., GARRIS, W. E.: Ind. Eng. Chem. Anal. Ed., **16,** 294 (1944)
4. O'DONNEL, G.: Anal. Chem., **23,** 894 (1951)
5. BESTOUGEFF, M.: Proc. Third World Petr. Congress, Section VI., 116 (1951)
6. BESTOUGEFF, M., BARGMAN, D.: Fourth World Petr. Congress, Section V/B, Paper 1.213 (1955)
7. KLEINSCHMIDT, L. R.: J. Res. Nat. Bur. Stand., **54,** 163 (1955)
8. CHELTON, H. M., TRAXLER, R. N.: Fifth World Petr. Congress, Section V, Paper 19.247 (1959)
9. TRAXLER, R. N.: Asphalt. Reinhold Publishing Co., New York, 1961
10. BOYD, M. I., MONTGOMERY, D. S.: Fuel, **41,** 335 (1962)
11. PRINZLER, H., KLIMKE, R., DORN, N.: Chem. Techn. , **14,** 739 (1962)
12. HRAPIA, H.: Erdöl u. Kohle, **18,** 689 (1965)
13. LEIBNITZ, E., HRAPIA, H., PAPP, J.: Chem. Techn., **16,** 737 (1964)
14. CORBETT, L. W.: Anal. Chem., **36,** 1967 (1964)
15. CORBETT, L. W.: Anal. Chem., **41,** 576 (1969)
16. MIDDLETON, W. R.: Anal. Chem., **39,** 1839 (1967)
17. SERGIENKO, S. R.: Wysokomolekuljarnye soedinenija nefti. Gostoptechisdat, Moskau, 1959
18. NYÚL, GY., MÓZES, GY., ZAKAR, P.: Berichte des Instituts MÁFKI, Nr. 132., Veszprém, 1957
19. MÓZES, GY., ZAKAR, P.: Berichte des Instituts MÁFKI, Nr. 270., Veszprém, 1962
20. ZAKAR, P.: Bitumen zsebkönyv. Műszaki Könyvkiadó, Budapest, 1961
21. CSIKÓS, R., MÓZES, GY., ZAKAR, P.: A fúvatott bitumen. Műszaki Könyvkiadó, Budapest, 1965
22. VAJTA, L., VAJTA-KRÁLIK, Zs.: Acta Chim. Acad. Sci. Hung., **46,** 391 (1965)
23. VAJTA, L., VAJTA, Zs.: Acta Chim. Acad. Sci. Hung., **50,** 407 (1966)
24. VAJTA, L.: Per. Polytechn. Chem. Eng. **11,** 209 (1967)
25. GARDNER, R. A., HARDMAN, H. F., JONES, A. L., WILLIAMS, R. B.: Chem. Eng. **4,** 155 (1959)
26. BÁLINT, T.: MÁFKI Közl. **3,** 223 (1962)
27. BÁLINT, T.: MÁFKI Közl. **5,** 15 (1964)

Lajos ZALKA; Százhalombatta 3. Pf. 1. Ungarn.

Acta Chimica Academiae Scientiarum Hungaricae, Tomus 76 (2), pp. 141–165 (1973)

UNTERSUCHUNG DER CHEMISCHEN ZUSAMMENSETZUNG VON BITUMINA AUS ROMASCHKINO UND ALGYŐ, II

UNTERSUCHUNG DER BITUMENFRAKTIONEN MIT HOMOGENER CHEMISCHER STRUKTUR

L. Zalka,* K. Bélafi-Réthy** und E. Kerényi**

Eingegangen am 1. Oktober 1971

Die nach den in der ersten Mitteilung beschriebenen Trennverfahren gewonnenen Bitumenfraktionen mit homogener chemischer Struktur wurden mittels UV- und IR-Spektroskopie, NMR-Spektrometrie und mit sonstigen Methoden untersucht. Durch Anwendung dieser, für Bitumenuntersuchungen neu entwickelten oder adaptierten Methoden und durch die Summierung der erhaltenen Ergebnisse gelang es, über Einzelheiten der chemischen Struktur der verhältnismäßig homogenen Fraktionen Angaben zu erhalten. Diese ermöglichten die Feststellung der strukturellen Merkmale der traditionellen Bitumenfraktionen; es konnten strukturelle Unterschiede bei Bitumina verschiedener Herkunft nachgewiesen und einige Abweichungen in der Struktur geklärt werden, die durch die Herstellungstechnologie der Bitumina bedingt sind.

Die Zusammensetzung bzw. Struktur von Bitumina ist trotz ihrer vielseitigen Verwendung verhältnismäßig wenig bekannt. Dieser Umstand erschwert die Charakterisierung der Bitumensorten und die Feststellung von Zusammenhängen zwischen der Qualität und den technologischen Parametern der Bitumenherstellung bzw. den anwendungstechnischen Parametern den Bitumenverwendung. Durch die Entwicklung von wirksamen Methoden zur Erforschung der Struktur, neben der Einführung von wirksamen Trennverfahren, können die genannten Zusammenhänge mehr und mehr angenähert werden.

Bekannte Methoden zur Strukturuntersuchung von Bitumina

Infolge der allgemeinen Verbreitung der Ultraviolett- und Infrarotspektroskopie und der Kernresonanzspektrometrie konnten diese Methoden auch zur Untersuchung von Bitumina angewendet werden. Die spektroskopisch erhaltenen Angaben trugen wesentlich zur genaueren Aufklärung der Kohlenwasserstoffstruktur der Bitumina bei.

Die spektroskopische Untersuchung von Bitumina begann vor etwa anderthalb Jahrzehnten, als Ergebnis der Ausdehnung der für Erdölprodukte kleinen Molekulargewichts entwickelten Methoden auf Produkte hohen Mole-

**Donau- Mineralölwerke, Százhalombatta und ** Ungarisches Erdöl- und Erdgas-Forschungsinstitut, Veszprém*

kulargewichts, darunter auf Bitumina. Ein Teil der Mitteilungen über Bitumenanalyse beschränkte sich auf den Vergleich der Spektren von Bitumina verschiedener Herkunft und auf deren qualitative Charakterisierung [1, 2].

Später suchten FISCHER und SCHRAM [3] bereits Zusammenhänge zwischen der Menge der mit den sogenannten traditionellen Methoden bestimmten Strukturgruppen und dem IR-Spektrum. Sie fanden einen engen Zusammenhang zwischen dem nach dem ndM-Verfahren bestimmten aromatisch bzw. paraffinisch gebundenen Kohlenstoffgehalt und der Intensität der Banden des IR-Spektrums bei 1600 cm^{-1} bzw. 730 cm^{-1}. Dadurch ergab sich die Möglichkeit, den aromatisch bzw. paraffinisch gebundenen Kohlenstoffgehalt der Ölfraktion von Bitumina durch IR-Spektroskopie zu bestimmen.

CHELTON und Mitarbeiter [4] berichteten bereits über die quantitative Bestimmungsmöglichkeit von Kohlenwasserstoffgruppen, die ohne instrumentelle Untersuchungen nicht erfaßbar sind. Sie fanden einen Zusammenhang zwischen dem IR-Spektrum und der durchschnittliche Menge der Methyl- und Methylengruppe n pro Molekül. Ähnliche Ergebnisse erhielten auch BOYD und Mitarbeiter [5].

SMITH und Mitarbeiter [6] untersuchten die anwendungstechnische Eigenschaften von Bitumina in Abhängigkeit von der Struktur und suchten einen Zusammenhang zwischen der Struktur der Kohlenstoffkette und der Wetterbeständigkeit des Bitumens.

KNOTNERUS [7] beschäftigte sich mit der chromatographischen Fraktionen einiger Bitumina und bestimmte die Anzahl der CH_3-, CH_2-, NH-, SO- und CO-Gruppen im durchsch nittlichen Molekül aufgrund des IR-Spektrums.

Durch die Entwicklung der NMR-Spektreometrie wurde die Erkenntnis der Kohlenwasserstoffstruktur von Bitumina durch wertvolle Angaben erweitert. Es ergab sich die Möglichkeit der Bestimmung der genauen Verteilung der Wasserstoffatome in der Kohlenwasserstoffkette.

CHAMBERLAIN und Mitarbeiter [8, 9, 10] charakterisierten die gesättigten und aromatischen Fraktionen von Bitumina — neben anderen physikalischen Kennwerten — durch die auf NMR-spe ktrometrischen Weg bestimmte Wasserstoffverteilung.

Die gemeinsame Auswertung der IR-spektroskopischen Daten und der durch NMR bestimmten Wasserstoffverteilung lieferte ausführliche Informationen über die Kohlenwasserstoffketten von Bitumina [11—13].

MIDDLETON [14] verwendete die Möglichkeiten der instrumentellen Analyse zur Ergänzung der Ergebnisse der wirksamen Trennung von Bitumina.

Die wichtigsten Angaben aus der Fachliteratur der spektrometrischen Analyse von Bitumina sind in Tab. I zusammengestellt.

Diese Angaben beziehen sich überwiegend entweder auf einzelne Bitumenfraktionen oder auf das ursprüngliche Bitumen. Diejenigen Forscher, die einzelne Fraktionen untersuchten, verzichteten auf eine umfassende strukturelle

Tabelle I

Methoden zur IR-spektroskopischen Analyse von Bitumina in der Fachliteratur

Lit.-hinweis	Spektralbereich, cm^{-1}	Lösungsmittel	Schichtdicke, cm	Ergebnis	Vorbereitungsoperationen
[1]	5000—1250	Tetrachlorkohlenstoff	0,0018	qualitative Analyse	—
		i-Oktan	0,01		
[2]	5000—1250	Tetrachlorkohlenstoff	0,05	qualitative Analyse	Flüssigkeitschromatographie
	2500—700		0,01		
[3]	2000—700	Dekalin	0,01	qualitative Analyse	Flüssigkeitschromatographie an Al_2O_3
	1610		0,01	$C_A\%$	
	720		0,01	$C_P\%$	
[4]	3300—2780	Tetrachlorkohlenstoff	0,015		Flüssigkeitschromatographie an Silikagel, Thermodiffusion
	2960			CH_3	
	2920			CH_2	
	1600			$C_A\%$	
[5]	3000—700	Tetrachlorkohlenstoff	0,015	qualitative Analyse	Flüssigkeitschromatographie an Fullererde bzw. Silikagel
	2960			CH_3	
	2920			CH_2	
	1380			CH_3	
[6]	3000—700	Tetrachlorkohlenstoff	0,01	qualitative Analyse	Originalbitumen
		Schwefelkohlenstoff	0,01		
	2920			CH_2	
	1380			CH_3	
	720			CH_2	
[7]	4000—700	Tetrachlorkohlenstoff	0,01	qualitative Analyse	Flüssigkeitschromatographie
			0,005		
	3480			NH	
	1720			CO	
	1460			CH_2	
	1380			CH_3	
	1035			SO	
[11]	4000—700		0,01	qualitative Analyse	Molekulardestillation, Flüssigkeitschromatographie
	3600			OH	
	3480			NH	
	1740—1655			CO	
	1600			Aromaten	
[13]	4000—700	Schwefelkohlenstoff	0,005	qualitative Analyse	Flüssigkeitschromatographie
			0,01		
	1720			C=O	
	1610			Aromaten	
	1380			CH_3	
	720			CH_2	

Charakterisierung der Bitumina, während jene Verfasser, die sich mit dem Gesamtbitumen befaßten, wegen der komplizierten Zusammensetzung nur zu einem oberflächlichen, durchschnittlichen Bild über die Struktur gelangen konnten.

Zur Untersuchung der Bitumenfraktionen verwendete Methoden

In unserer Arbeit wurden vor der ausführlichen Strukturuntersuchung unserer Bitumenproben verschiedener Herkunft und verschiedener Herstellungstechnologie wirksame Trennungsoperationen durchgeführt, wodurch hinsichtlich ihrer Struktur ziemlich homogene Fraktionen erhalten wurden. Über das Trennverfahren wurde im ersten Teil unserer Mitteilung berichtet [15].

Die durchschnittliche Molekülstruktur der aus den Bitumenproben erhaltenen engen Fraktionen wurde einerseits durch UV-, IR- und NMR-Spektrometrie, anderseits durch Bestimmung der Elementarzusammensetzung und des durchschnittlichen Molekulargewichts untersucht. Das Ziel der Bitumenuntersuchungen war die Charakterisierung der Struktur bzw. Zusammensetzung des Gesamtbitumens aufgrund der Daten der Fraktionen mit homogener Struktur.

Die Methoden der spektrometrischen Analysen wurden durch die Weiterentwicklung der früher ausgearbeiteten bzw. der von der Literatur übernommenen Prüfmethoden erhalten.

Die zur Untersuchung des Aromatengehalts von Erdöldestillaten durch BÁLINT entwickelte UV-Absorptionsmethode wurde auf die Untersuchung der Bitumenfraktionen ausgedehnt. Dadurch konnte der Gehalt an Aromaten mit einem zwei und mehr Ringen bei den für Verbindungen mit verschiedenen Ringzahlen charakteristischen Wellenlängen von 2000 Å, 2300 Å und 2600 Å bestimmt werden. Die spezifischen Extinktionskoeffizienten der einzelnen Aromatentypen sind — bei einer Kalibrierung mit auf chromatographischem Wege getrennten Aromatenkonzentraten aus schweren Destillaten — allein vom durchschnittlichen Molekulargewicht des Erdölproduktes abhängig. Folglich konnte die quantitative Bestimmung der aromatischen Kohlenwasserstofftypen in schweren Erdölprodukten, in Kenntnis des durchschnittlichen Molekulargewichts der zu untersuchenden Probe durchgeführt werden. Zur Ausarbeitung der Methode wurden die aus schweren Erdölprodukten durch Flüssigkeitschromatographie gewonnenen aromatischen Fraktionen verwendet, demzufolge enthalten die so bestimmten Konzentrationswerte außer dem entsprechenden Aromatentyp auch die bei der chromatographischen Trennung mitlaufenden z. B. schwefelhaltigen Verbindungsgruppen. Die Genauigkeit der Methode wird auf etwa $\pm 5\%$ geschätzt.

Die Messungen wurden mit einem automatisch registrierenden UV-Spektrophotometer der Firma Perkin-Elmer (Typ 137 UV) durchgeführt. Die

Spektren wurden im Bereich zwischen 1900 Å und 3000 Å registriert. Als Lösungsmittel wurde aromatenfreies Benzin verwendet. Die Schichtendicke in der Küvette betrug 0,1 cm. In Abb. 1 wird das UV-Spektrum einer Bitumenprobe gezeigt; die drei Meßpunkte sind bezeichnet.

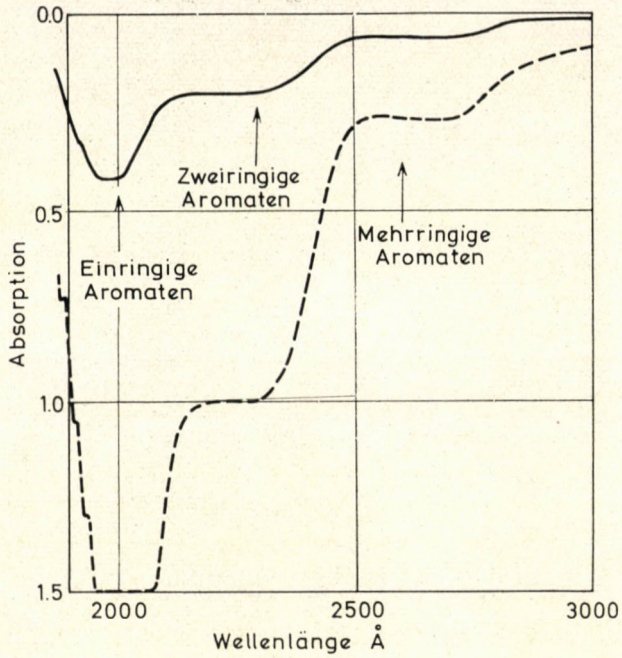

Abb. 1. UV-Spektrum der Ölharzfraktion des Romaschkinoer Extraktbitumens. (——— 0,15 g/l, ——— 0,62 g/l; Schichtdicke 0,1 cm)

Der aromatisch, paraffinisch und naphtenisch gebundene Kohlenstoffgehalt der Bitumenproben wurden durch IR-Absorptions-Spektrophotometrie gemessen. Der Zusammenhang zwischen den auf verschiedene Weise gebundenen Kohlenstoffgehalten und dem IR-Spektrum wurde von BRANDES [17, 18] festgestellt; später ließ sich dieser Zusammenhang bei Bitumina verwenden [3]. Dabei wurde der paraffinisch gebundene Kohlenstoffgehalt durch Intensitätsmessung der Bande bei 720, bzw. 730 cm^{-1} (Pendelschwingung der $-CH_2$-Gruppen), der aromatisch gebundene Kohlenstoffgehalt durch Intensitätsmessung der Bande bei 1610 bzw. 1600 cm^{-1} (Schwingung des aromatischen Ringes) bestimmt. Der naphtenisch gebundene Kohlenstoffgehalt wurde aus dem Unterschied zwischen dem Gesamtkohlenstoffgehalt und der Summe des paraffinisch und aromatisch gebundenen Kohlenstoffgehaltes berechnet. Die Spektren wurden nach der sog. Grundlinienmethode ausgewertet. Das IR-Spektrum einer Bitumenprobe im benötigten Spektralbereich von 1900 cm^{-1}

bis 660 cm^{-1}, unter Bezeichnung der Meßpunkte, ist in Abb. 2 dargestellt. Der Fehler der Methode beträgt nach unseren Erfahrungen kaum mehr als der für Erdöldestillate bestimmte Messfehler der ursprünglichen ndM-Methode und kann auf höchstens 3—4% geschätzt werden.

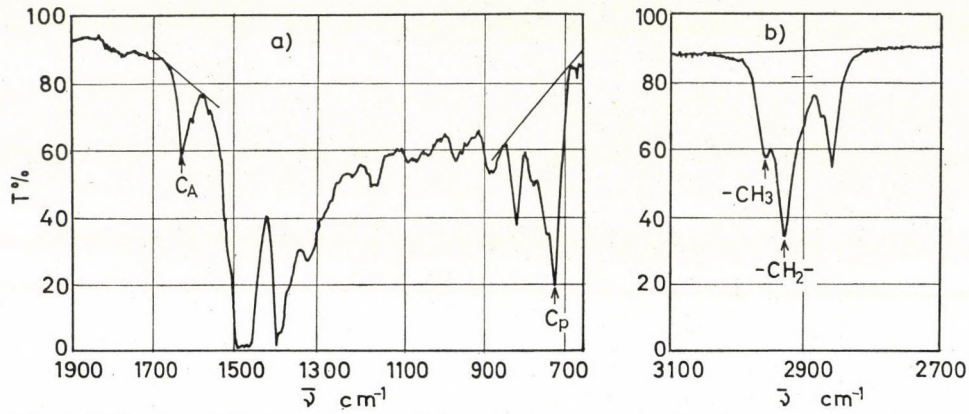

Abb. 2. Teile des IR-Spektrums der Ölfraktion des naphtenisch-aromatischen Teiles aus Romaschkinoer Extraktbitumen, zur Bestimmung der Werte C_A%, C_P%, n_{CH_3} und n_{CH_2}. *a)* Schichtdicke 0,01 cm; *b)* Schichtdicke 0,01 cm; 15,2 g/l

Die Anzahl der Methyl- und Methylengruppen im durchschnittlichen Molekül der Bitumenproben wurde — nach einer im Institut »MÁFKI« früher entwickelten und jetzt auf Bitumina ausgedehnten Methode — ebenfalls durch IR-Spektroskopie gemessen [19]. Die Bestimmung beruht auf der Intensitätsmessung der antisymmetrischen Valenzschwingungsbande bei 2960 cm^{-1} für Methylgruppen bzw. 2930 cm^{-1} für Methylengruppen. Das Spektrum der Lösungen der Bitumenproben wurde im Bereich zwischen 3100 und 2700 cm^{-1} bei Konzentrationen von 20 g/l registriert. Die Meßgenauigkeit wird mit Rücksicht auf das hohe durchschnittliche Molekulargewicht auf $\pm 1-2$ Gruppen geschätzt. In Abb. 2 ist auch der Valenzschwingungsbereich der Methyl- und Methylengruppen bei einer untersuchten Bitumenfraktion gezeigt. Die IR-Spektren wurden mit einem Gerät UR 20 der Firma Carl Zeiss Jena aufgenommen. Es wurden Prismen aus NaCl und Küvetten mit einer Schichtdicke von 0,012 cm verwendet.

Die NMR-Spektrometrie ermöglicht die quantitative Bestimmung der verschiedene Gruppen bildenden Wasserstoffatome und dadurch der verschiedenen Strukturgruppen. In unserer Arbeit wurden die einzelnen Strukturgruppen — in guter Übereinstimmung mit anderen Methoden — auf der Integralkurve der Spektren innerhalb der in Tab. II angeführten Grenzen gemessen.

Abb. 3 zeigt das NMR-Spektrum einer Bitumenprobe, unter Bezeichnung der bestimmten Gruppen. Die Messungen wurden mit einem 60 MHz Protonresonanz-Spektrometer VARIAN Type T-60 durchgeführt. Es wurden 10—20%ige Lösungen in Tetrachlorkohlenstoff bei 30° untersucht; als innerer Standard wurde Tetramethylsilan verwendet. Die Spektren wurden im Bereich von 0—8 ppm, d. h. 0—500 Hz registriert, unter gleichzeitiger Aufnahme der Integralkurve.

Tabelle II

Spektralbereiche zur Auswertungen der NMR-Spektren von Bitumenfraktionen

Bindungstyp des Wasserstoffs	Chemische Verschiebung (δ), ppm
$-CH_3$	0,7—1,2
$-CH_2-$	1,2—1,4
$>CH-$	1,4—1,8
$Ar-CH_3$	1,8—2,6
$Ar-CH_2-$	2,6—3,2
$Ar-H$	6,6—8,0

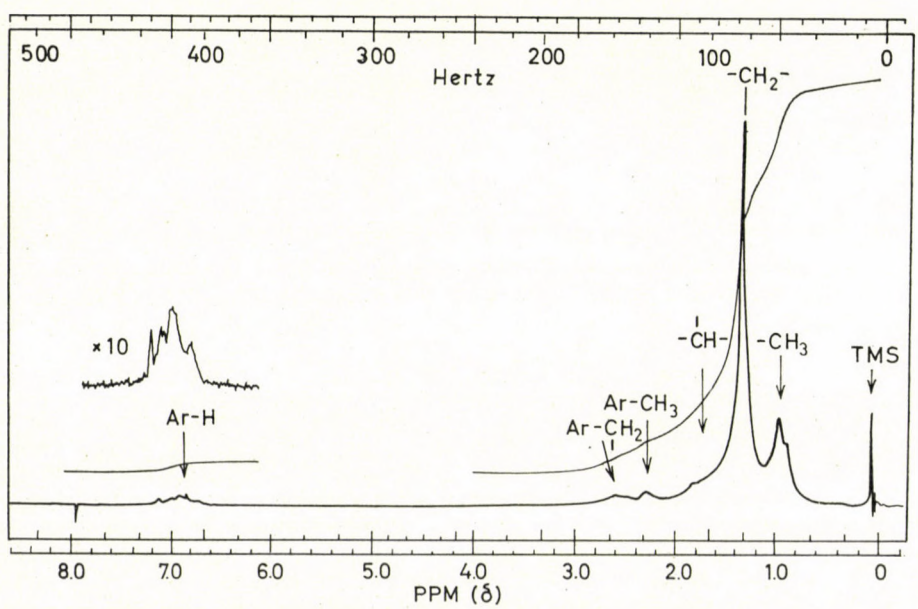

Abb. 3. Naphtenisch-aromatischer Teil aus Algyőer Extraktbitumen: NMR-Spektrum der einringigen Fraktion aus dem Destillat der Ölfraktion

Die Bestimmung der Elementarzusammensetzung der Bitumenproben wurde nach den traditionellen Methoden durchgeführt. Kohlenstoff und Wasserstoff wurde nach PREGL bestimmt, mittels gravimetrischer Messung des gebildeten Kohlendioxids und Wassers.

Zur Schwefelbestimmung wurde die Methode von SCHÖNIGER verwendet. Die Probe wurde in Sauerstoff verbrannt und die entstandenen Sulfationen mit einer Maßlösung aus Bariumperchlorat in Gegenwart von Thorin als Indikator titriert.

Der Sauerstoffgehalt wurde durch die Methode von UNTERZAUCHER bestimmt. Der gebundene Sauerstoff der Probe wird dabei zu Kohlenmonoxid umgesetzt, letzteres mit Jodpentoxid zu Kohlendioxid oxydiert und das freiwerdende Jod titrimetrisch bestimmt.

Zur Bestimmung des durchschnittlichen Molekulargewichts der Bitumenfraktionen erwies sich die thermoosmometrische Methode als am besten geeignet [21, 22]. Die Messungen wurden mit dem KNAUERschen Dampfdruckosmometer unter Anwendung von Lösungen in Tetrachlorkohlenstoff bei Konzentrationen von 0,1 Mol/l durchgeführt. In einigen Fällen, als die Trennung mit keiner wesentlichen Veränderung des Molekulargewichtes verbunden war, wurde das Molekulargewicht der getrennten Fraktionen als identisch mit dem Molekulargewicht der Ausgangsfraktion angenommen.

Zusammensetzung der Bitumenfraktionen

Wie bereits erwähnt, wurden vor den Zusammensetzungs- bzw. Strukturuntersuchungen wirksame Trennungsoperationen durchgeführt, die bereits hinsichtlich der Zusammensetzung und der Struktur gewisse Aufklärungen lieferten [15]. Zunächst wurden die Ausgangsproben entasphalteniert, anschließend mittels Flüssigkeitschromatographie in Fraktionen getrennt, die paraffinhaltigen Fraktionen bei $-30°$ entparaffiniert und einer Adduktbildung mit Hanrstoff unterworfen und endlich die Fraktionen mittels Molekulardestillation und Flüssigkeitschromatographie an präparierten Säulen in weitere Fraktionen mit verhältnismäßig homogener Zusammensetzung zerlegt.

Die vier untersuchten Bitumenarten waren Romaschkinoer Extraktbitumen, Destillationsbitumen und geblasenes Bitumen bzw. Algyőer Extraktbitumen. Im weiteren werden die Ergebnisse der Untersuchungen einzelner charakteristisch homogener Fraktionen vorgeführt.

Die gesättigten Kohlenwasserstoffkomponenten der Bitumenproben sind hauptsächlich in der nach der Entparaffinierung der chromatographisch gewonnenen paraffinischen Ölfraktion erhaltenen Normalparaffinfraktion und flüssigen Paraffinfraktion enthalten. Um sie zu charakterisieren, werden die Analysen des Molekulardestillationsrückstandes im weiteren ausführlicher behandelt.

Im Molekulardestillationsrückstand der *Normalparaffinfraktion des paraffinischen Ölteiles* sind die geradkettigen Normalparaffin-Kohlenwasserstoffe, d. h. die Bitumenbestandteile mit einfachster Struktur konzentriert. Die Versuchsergebnisse dieser Fraktion sämtlicher Bitumenproben sind in Tab. III angeführt.

Tabelle III

Ergebnisse der Untersuchungen des Destillationsrückstandes aus der Normalparaffinfraktion des paraffinischen Öles

Methode	Geprüfte Größe	Herkunft des Bitumens			
		Romaschkinoer			Algyőer Extrakt
		Extrakt	Destill.	Geblas.	
IR	$C_A\%$	0	0	0	0
	$C_P\%$	100,0	100,0	100,0	100,0
	$C_N\%$	0	0	0	0
	n_{CH_3}	4,0	5,8	2,8	4,2
	n_{CH_2}	56,8	50,7	53,6	57,3
NMR	n_{CH}	2,2	4,9	2,4	3,2
	n_{CH_2}	57,2	49,8	54,2	57,4
	n_{CH_3}	4,2	6,3	2,9	4,6
Dampfdruck-Osmometrie	$\overline{MG}$	892	854	820	912
Menge der Fraktion, auf das Bitumen bezogen, Gew.%		2,8	4,5	1,1	10,3
Annähernde Bruttoformel		$C_{64}H_{130}$	$C_{61}H_{123}$	$C_{59}H_{120}$	$C_{65}H_{132}$

In den Tabellen, die die Versuchsergebnisse der Bitumenfraktionen enthalten, wurden die Meßmethode, die Meßergebnisse und die daraus berechneten Größen angegeben. Die Erklärung der in den Tabellen befindlichen Abkürzungen ist wie folgt:

$C_A\%$ — prozentuelle Menge der aromatisch gebundenen Kohlenstoffatome
$C_P\%$ — prozentuelle Menge der paraffinisch gebundenen Kohlenstoffatome
$C_N\%$ — $100 - (C_A + C_P)$ = prozentuelle Menge der naphtenisch gebundenen Kohlenstoffatome
n_{CH_3} — Anzahl der Methylgruppen pro durchschnittliches Molekül
n_{CH_2} — Anzahl der Methylengruppen pro durchschnittliches Molekül
n_{CH} — Anzahl der Methingruppen pro durchschnittliches Molekül
n_{Ar-H} — Anzahl der an Kohlenstoffatome der aromatischen Ringen gebundenen Wasserstoffatome pro durchschnittliches Molekül
n_{Ar-CH_2} — Anzahl der an Kohlenstoffatome der aromatischen Ringen gebundenen Methylengruppen pro durchschnittliches Molekül

n_{Ar-CH_3} — Anzahl der an Kohlenstoffatome der aromatischen Ringen gebundenen Methylgruppen pro durchschnittliches Molekül

Einringig — Gehalt der Probe an Aromaten mit einem Ring, in Gew.%

Zweiringig — Gehalt der Probe an Aromaten mit zwei Ringen, in Gew.%

Mehrringig — Gehalt der Probe an Aromaten mit mehreren Ringen, in Gew.%

$\overline{MG}$ — durchschnittliches Molekulargewicht der Probe

n_C — $\overline{MG} \cdot \frac{C\%}{100 \times 12}$ = Anzahl der Kohlenstoffatome im durchschnittlichen Molekül

n_{C_A} — $n_C \frac{C_A\%}{100}$ = Anzahl der aromatisch gebundenen Kohlenstoffatome im durchschnittlichen Molekül

nC_P — $n_C \frac{C_P\%}{100}$ = Anzahl der paraffinisch gebundenen Kohlenstoffatome im durchschnittlichen Molekül

nC_N — $n_C \frac{C_N\%}{100}$ = Anzahl der naphtenisch gebundenen Kohlenstoffatome im durchschnittlichen Molekül

n_S — $\overline{MG} \cdot \frac{S\%}{100 \times 32}$ = Anzahl der Schwefelatome im durchschnittlichen Molekül

n_C — $\overline{MG} \cdot \frac{O\%}{100 \times 16}$ = Anzahl der Sauerstoffatome im durchschnittlichen Molekül

— — wurde nicht untersucht

Die Bruttoformeln der Fraktionen wurden aus den Ergebnissen der Elementaranalyse und dem Molekulargewicht, oder aus der spektrometrisch bestimmten Gruppenzusammensetzung und dem Molekulargewicht berechnet.

Aus Tab. III geht hervor, daß der paraffinisch gebundene Kohlenstoffgehalt bei sämtlichen vier untersuchten Bitumenfraktionen 100% beträgt; dies ist ein Beweis für die Wirksamkeit der Trennung und für die Homogenität der Fraktion. Die Anzahl der Verzweigungen pro durchschnittliches Molekül beträgt 2—4; dies beweist, daß eine hohe Anreicherung der geradkettigen oder wenig verzweigten Paraffine erreicht wurde. Die aus dem Molekulargewicht und aus den spektroskopischen Daten berechnete Bruttoformel der Fraktionen stimmt annähernd mit der Formel der Paraffine überein.

Es war überraschend, daß die untersuchten Bitumina einen hohen Gehalt an annähernd normalen Paraffinen aufweisen. In den verschiedenen Romaschkinoer Bitumina erreicht die Menge der Normalparaffine 3—5%, im Algyőer Bitumen etwa 15%.

Die Analysenergebnisse des Destillationsrückstandes der *paraffinischen Ölfraktion* sind in Tab. IV angegeben. Im Falle sämtlicher Ausgangsbitumina ist diese Fraktion aromatenfrei und die Menge der paraffinisch und naphtenisch gebundenen Kohlenstoffatome ist fast gleich; allein bei der entsprechenden Fraktion des Algyőer Bitumens ist die Menge der paraffinisch gebundenen Kohlenstoffatome bemerkbar höher.

Die Romaschkinoer Fraktionen enthalten pro durchschnittliches Molekül vier Naphtenringe, während beim Algyőer Bitumen drei Naphtenringe gefunden wurden. In Übereinstimmung damit war auch der Verzweigungsgrad der Kohlenstoffketten bei der Algyőer Bitumenfraktion geringer: gegenüber den

Tabelle IV

Ergebnisse der Untersuchungen des Destillationsrückstandes aus der flüssigen Paraffinfraktion des paraffinischen Öles

Methode	Geprüfte Größe	Herkunft des Bitumens			
		Romaschkinoer			Algyőer Extrakt
		Extrakt	Destill.	Geblas.	
IR	C_A	0	0	0	0
	C_P	54,3	52,4	52,7	61,1
	C_N	45,7	47,6	47,3	38,9
	n_{CH_3}	7,7	8,0	7,0	7,4
	n_{CH_2}	26,6	30,9	30,6	31,0
NMR	n_{CH}	11,3	10,5	10,7	8,6
	n_{CH_2}	25,7	31,1	29,5	30,4
	n_{CH_3}	7,1	7,6	7,0	7,1
Dampfdruck-Osmometrie	$\overline{MG}$	620	690	660	644
Menge der Fraktion, auf das Bitumen bezogen, Gew.%		0,74	1,04	1,74	3,16
Annähernde Bruttoformel		$C_{44}H_{84}$	$C_{49}H_{95}$	$C_{47}H_{91}$	$C_{46}H_{91}$

durchschnittlich 11 Methingruppen bei den Romaschkinoer Fraktionen fanden wir hier etwa 9. Einige mögliche Strukturvarianten des Destillationsrückstandes der flüssigen Paraffinfraktionen des paraffinischen Öles sind in Abb. 4 dargestellt.

Die *Ölfraktion* des flüssigkeitschromatographisch abgetrennten *naphtenisch-aromatischen Teiles* enthielt — neben einem geringen Gehalt an gesättigten Kohlenwasserstoffen — einen wesentlichen Teil der ein- und zweiringigen aromatischen Bestandteile der Proben. Die ein- und zweiringigen Fraktionen, hergestellt durch Flüssigkeitschromatographie aus dem Destillat und dem Rückstand der Molekulardestillation, wurden eingehender untersucht. Der ein- und zweiringige Aromatengehalt dieser Fraktionen erreicht zwar nicht das 100%, jedoch gelang es, infolge der 60—90% igen Anreicherung der einzelnen Aromatentypen, ein klares Bild über die durchschnittliche Molekülstruktur dieser etwa 3—4% der Bitumenproben ausmachenden Fraktionen zu erhalten.

Die *einringigen Fraktionen des Destillats und des Rückstands* wichen voneinander allein in der Länge der an den aromatischen Ring gebundenen Alkylketten ab; die Substitutionsverhältnisse des aromatischen Ringes und die Struktur der Alkylkette waren dagegen fast gleich. Die diesbezüglichen Ergeb-

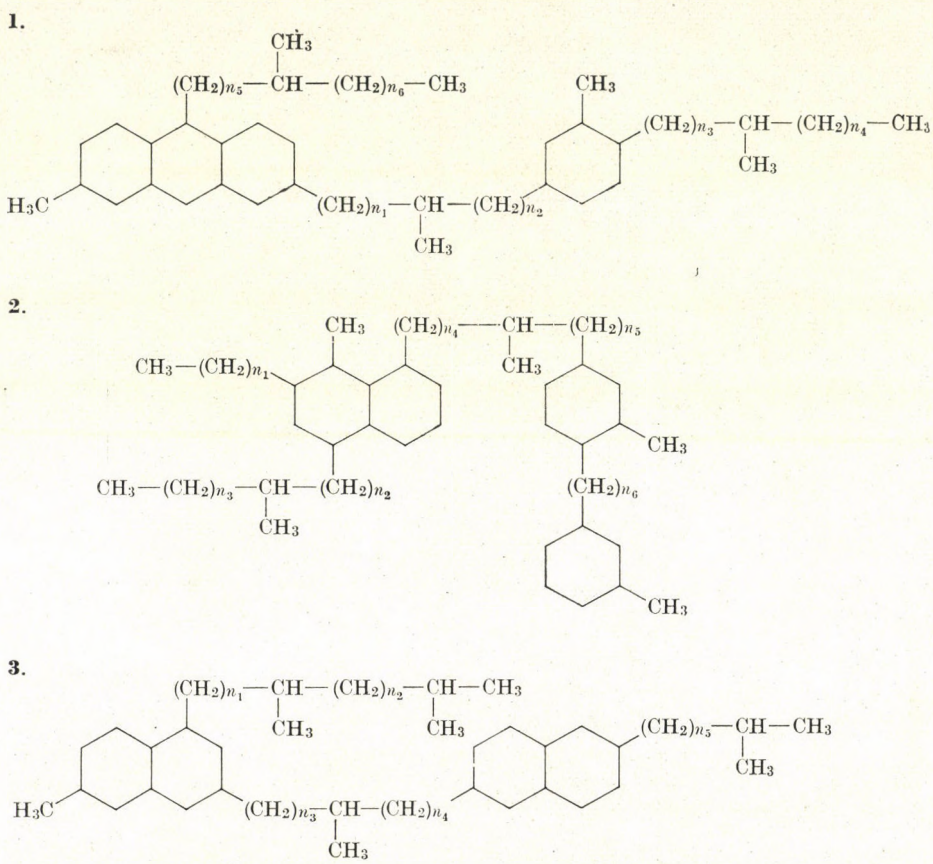

Abb. 4. Paraffinischer Ölteil aus Romaschkinoer Extraktbitumen: einige Strukturvarianten des Destillationsrückstandes der Ölfraktion ($\Sigma n = 26$)

nisse unserer Untersuchungen sind in Tab. V und VI enthalten. Die Ergebnisse zeigen eine durchschnittlich 3 bis 4fache Substitution des aromatischen Ringes an. Die Zahl der unmittelbar an den aromatischen Ring gebundenen Methylgruppen war bei beiden Fraktionen zwischen 1 und 2, während die Zahl der längeren Alkylketten 2 bis 3 betrug. Die Kohlenstoffskelettstruktur der Seitenketten, d. h. die Zahl der Verzweigungen und der Naphtenringe liegt zwischen den bei den Normalparaffin- und paraffinischen Ölfraktionen des paraffinischen Öles beobachteten Werten.

Der Schwefelgehalt der Fraktionen lag zwischen 0,8 und 1,6%, woraus sich ein Wert von etwa 0,3 Schwefelatomen pro durchschnittliches Molekül ergibt, d. h. es muß sich in jedem dritten Molekül ein Schwefelatom befinden. Drei mögliche Varianten der Molekülstruktur, die die einringige Fraktion gemeinsam charakterisieren, sind in Abb. 5 dargestellt.

Tabelle V

Ergebnisse der Untersuchung der einringigen Fraktion aus dem Destillat der Ölfraktion des naphtenisch-aromatischen Teiles

Methode	Geprüfte Größe	Herkunft des Bitumens			
		Romaschkinoer			Algyőer Extrakt
		Extrakt	Destill.	Geblas.	
IR	$C_A\%$	16,2	17,0	14,6	12,1
	$C_P\%$	59,3	58,2	59,4	67,4
	$C_N\%$	24,5	24,8	26,0	20,5
	n_{CH_2}	22,3	25,2	21,0	27,4
	n_{CH_3}	5,9	6,8	6,2	6,2
NMR	n_{CH}	6,0	6,3	8,5	6,2
	n_{CH_2}	20,8	22,14	19,2	24,5
	n_{CH_3}	4,7	4,9	6,2	5,5
	n_{Ar-H}	2,5	2,4	2,8	2,3
	n_{Ar-CH_2}	2,5	2,9	2,1	2,7
	n_{Ar-CH_3}	1,7	1,4	1,2	1,0
UV	Einringig	76,0	77,4	77,9	69,9
	Zweiringig	2,5	4,2	7,1	8,7
	Mehrringig	0,2	0,4	—	—
Dampfdruck-Osmometrie	$\overline{MG}$	583	614	603	650
Chemische Analyse	C%	86,4	86,0	85,9	87,0
	H%	12,5	12,7	12,1	12,7
	S%	1,6	1,4	1,0	0,8
Berechnete Werte	n_C	42,0	44,0	43,2	47,1
	nC_A	6,8	7,5	6,3	5,7
	nC_P	24,9	25,6	25,7	31,7
	nC_N	10,3	10,9	11,2	9,7
	n_S	0,3	0,3	0,2	0,2
	n_O	—	—	—	—
Menge der Fraktion auf das Bitumen bezogen, Gew.%		0,34	0,44	2,23	1,06
Annähernde Bruttoformel		$C_{42}H_{73}S_{0,3}$	$C_{44}H_{78}S_{0,3}$	$C_{43}H_{73}S_{0,2}$	$C_{47}H_{82}S_{0,2}$

Tabelle VI

Ergebnisse der Untersuchung der einringigen Fraktion aus dem Destillationsrückstand der Ölfraktion des naphtenisch-aromatischen Teiles

Methode	Geprüfte Grösse	Herkunft des Bitumens			
		Romaschkinoer			Algyőer Extrakt
		Extrakt	Destill.	Geblas.	
1.	2.	3.	4.	5.	6.
IR	$C_A\%$	10,3	12,2	13,4	12,3
	$C_P\%$	62,9	64,3	59,4	69,3
	$C_N\%$	26,8	23,5	27,2	18,4
	n_{CH_2}	37,6	37,0	37,8	44,2
	n_{CH_3}	9,0	9,2	8,0	7,0
NMR	n_{CH}	11,5	7,9	11,2	8,7
	n_{CH_2}	36,9	33,3	34,4	40,8
	n_{CH_3}	9,7	7,0	9,2	6,6
	n_{Ar-H}	1,6	2,8	1,6	2,2
	n_{Ar-CH_2}	2,9	3,0	2,3	2,5
	n_{Ar-CH_3}	1,6	1,7	1,6	1,1
UV	Einringig	63,5	69,3	62,5	60,4
	Zweiringig	5,7	3,8	8,8	13,5
	Mehrringig	0	0	0	0
Dampfdruck-Osmometrie	$\overline{MG}$	890	823	853	910
Chemische Analyse	C%	86,2	86,0	86,7	86,6
	H%	13,1	13,2	12,7	13,0
	S%	1,0	0,9	0,8	1,3
	O%	—	—	—	—
Berechnete Werte	n_C	63,9	59,0	61,6	65,7
	n_{C_A}	6,6	7,2	8,3	8,1
	n_{C_P}	40,2	37,9	36,6	45,5
	n_{C_N}	17,1	13,9	16,7	12,1
	n_S	0,3	0,2	0,2	0,4
	n_O	—	—	0,2	—
Menge der Fraktion auf das Bitumen bezogen, Gew.%		0,47	0,70	0,74	1,29
Annähernde Bruttoformel		$C_{64}H_{117}S_{0,3}$	$C_{59}H_{108}S_{0,2}$	$C_{62}H_{108}S_{0,2}O_{0,2}$	$C_{67}H_{118}S_{0,4}$

1.

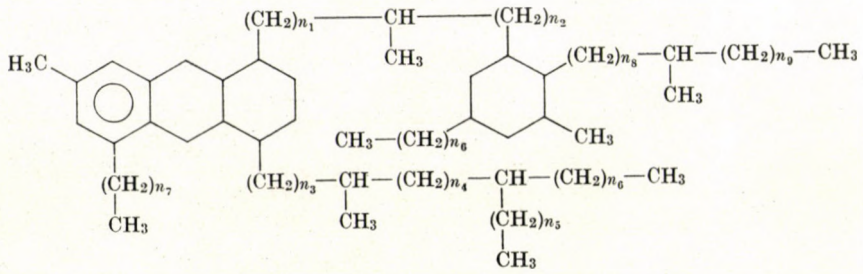

2.

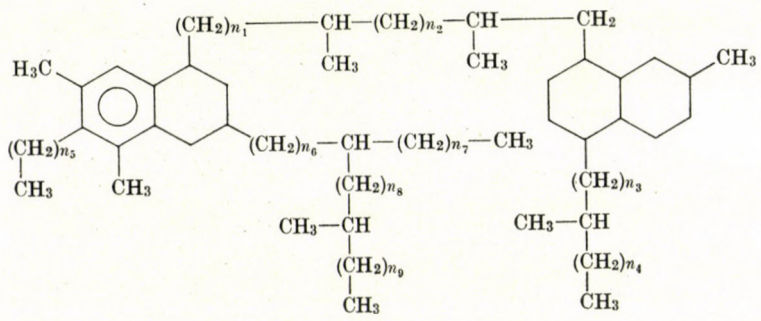

3.

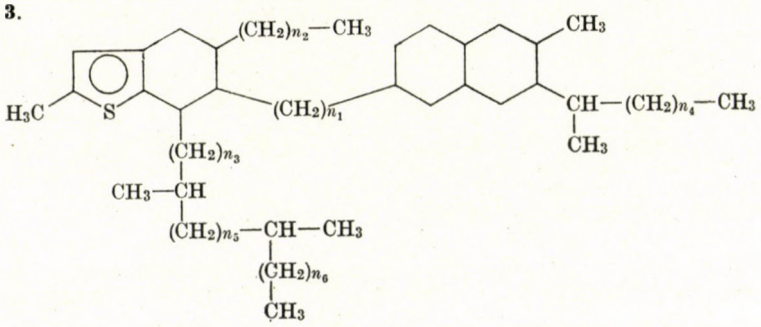

Abb. 5. Naphtenisch-aromatischer Teil aus Romanischkinoer Extraktbitumen: einige Strukturvarianten der einringigen Fraktion aus dem Destillationsrückstand der Ölfraktion ($\Sigma n = 38$)

Die Herstellung reiner *zweiringiger Fraktionen* war ein schwieriges Problem; das Konzentrat war sowohl durch einringige als auch durch mehrringige Aromaten verunreinigt. Die Wirksamkeit der chromatographischen Trennung wurde in diesem Fall außer durch die Gegenwart von Komponenten mit hohem Molekulargewicht auch durch den hohen Gehalt an Heteroatomen vermindert. Die Ergebnisse unserer Untersuchungen sind in Tab. VII und VIII zusammengefaßt.

Ähnlich wie bei den einringigen Fraktionen und in Übereinstimmung mit dem Unterschied im Molekulargewicht, wichen die aus dem Destillat und aus

Tabelle VII

Ergebnisse der Untersuchung der zweiringigen Fraktion aus dem Destillat der Ölfraktion des naphtenisch-aromatischen Teiles

Methode	Geprüfte Größe	Herkunft des Bitumens			
		Romaschkinoer			Algyőer Extrakt
		Extrakt	Destill.	Geblas.	
1.	2.	3.	4.	5.	6.
IR	C_A%	18,6	18,4	18,4	21,3
	C_P%	60,4	61,7	65,3	60,2
	C_N%	21,5	19,9	17,7	18,5
	n_{CH_2}	21,5	23,2	24,6	28,6
	n_{CH_3}	5,5	5,6	5,3	5,9
NMR	n_{CH}	6,2	6,6	5,3	6,7
	n_{CH_2}	20,4	20,7	21,2	25,1
	n_{CH_3}	3,7	4,8	5,4	6,2
	n_{Ar-H}	2,9	1,8	2,8	2,1
	n_{Ar-CH_2}	3,1	3,0	4,3	3,7
	n_{Ar-CH_3}	1,0	1,0	0,9	0,8
UV	Einringig	4,2	0,8	1,3	12,2
	Zweiringig	51,5	65,8	54,1	66,1
	Mehrringig	11,5	1,6	15,5	0
Dampfdruck Osmometrie	$\overline{MG}$	583	614	603	650
Chemische Analyse	C%	84,3	83,3	83,1	85,9
	H%	12,5	12,0	12,1	12,8
	S%	3,9	3,8		
	S%	3,9	3,8	3,8	1,1
	O%	—	—	1,0	—
Berechnete Werte	n_C	41,0	42,6	41,8	46,5
	nC_A	7,6	7,8	6,2	9,9
	nC_P	24,8	26,3	27,3	28,0
	nC_N	10,0	8,5	7,4	8,6
	n_S	0,7	0,8	0,7	0,2
	n_O	—	—	—	—
Menge der Fraktion, auf das Bitumen bezogen, Gew.%		0,16	0,08	0,72	0,21
Annähernde Bruttoformel		$C_{41}H_{73}S_{0,7}$	$C_{43}H_{74}S_{0,8}$	$C_{42}H_{73}S_{0,7}O_{0,4}$	$C_{47}H_{83}S_{0,2}$

Tabelle VIII

Ergebnisse der Untersuchung der zweiringigen Fraktion aus dem Destillationsrückstand der Ölfraktion des naphtenisch-aromatischen Teiles

Methode	Geprüfte Größe	Herkunft des Bitumens			
		Romaschkinoer			Algyőer Extrakt
		Extrakt	Destill.	Geblas.	
1.	2.	3.	4.	5.	6.
IR	C_A%	11,8	16,7	17,6	16,4
	C_P%	62,6	64,3	59,7	63,1
	C_N%	25,6	19,0	22,7	20,5
	n_{CH_2}	36,8	34,4	33,8	39,6
	n_{CH_3}	5,8	8,8	7,9	6,2
NMR		9,6	8,4	10,9	10,6
	n_{CH_2}	32,8	31,3	34,5	36,2
	n_{CH_3}	4,6	5,9	7,0	5,2
	n_{Ar-H}	3,8	1,3	2,5	2,8
	n_{Ar-CH_2}	2,8	3,6	3,8	4,5
	n_{Ar-CH_3}	1,6	2,9	1,7	0,7
UV	Einringig	0	0	0	0
	Zweiringig	38,7	57,8	56,9	41,5
	Mehrringig	21,8	9,0	9,5	5,1
Dampfdruck-- Osmometrie	$\overline{MG}$	890	823	835	910
Chemische Analyse	C%	84,7	84,1	84,6	84,8
	H%	11,9	12,1	11,4	11,9
	S%	3,4	2,8	2,7	1,4
	O%	—	0,9	0,5	0,7
Berechnete Werte	n_C	62,8	57,7	60,1	64,3
	n_{C_A}	7,3	9,6	10,6	10,5
	n_{C_P}	39,3	37,1	35,9	40,6
	n_{C_N}	16,7	11,0	13,6	13,2
	n_S	0,9	0,7	0,7	0,4
	n_O	—	0,5	0,3	0,4
Menge der Fraktion auf das Bitumen bezogen, Gew.%		0,28	0,39	0,48	0,22
Annähernde Bruttoformel		$C_{63}H_{106}S_{0,9}$	$C_{58}H_{100}S_{0,7}O_{0,5}$	$C_{60}H_{97}S_{0,7}O_{0,3}$	$C_{64}H_{108}S_{0,4}O_{0,4}$

dem Destillationsrückstand gewonnenen zweiringigen Fraktionen voneinander allein hinsichtlich der Länge der an den aromatischen Ring gebundenen Alkylketten ab. Die Substitutionsverhältnisse der Ringe und die Struktur der Alkylketten war annähernd gleich.

Die Substitution der aromatischen Ringe war durchschnittlich 5- bis 6fach; davon waren nur 1—2 Substituenten Methylgruppen. Bei der Destillatfraktion enthielten die längeren Alkylsubstituenten neben durchschnittlich 10—15 Methylgruppen 1—2 Naphtenringe und 5—6 Methingruppen, d. h. Verzweigungen. Bei der Rückstandfraktion war die Länge der Alkylsubstituenten selbstverständlich höher, jedoch ohne wesentliche Abweichungen in den Proportionen.

Es wurden keine wesentlichen Unterschiede zwischen dem Aufbau der Bestandteile in den zweiringigen Fraktionen verschiedener Herkunft gefunden.

1.

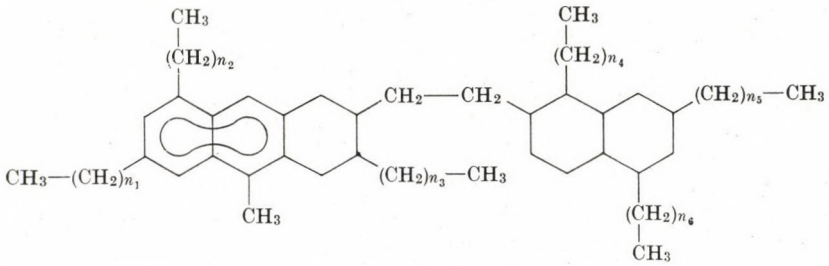

2.

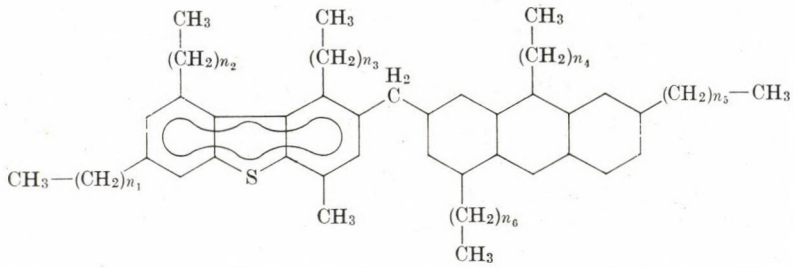

3.

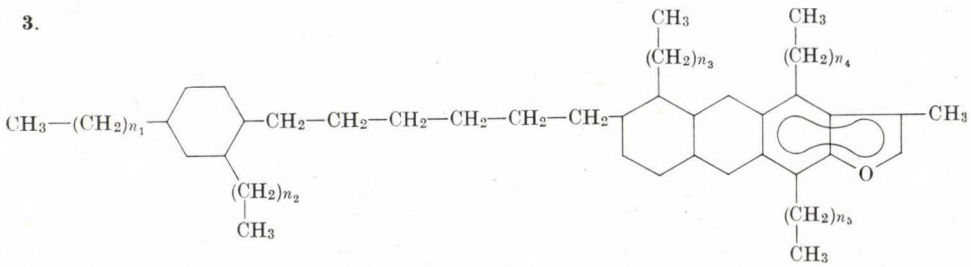

Abb. 6. Naphtenisch-aromatischer Teil aus Algyőer Extraktbitumen: einige Strukturvarianten der zweiringigen Fraktion aus dem Destillationsrückstand der Ölfraktion ($\Sigma n = 36$)

Erwähnenswert ist allein der abweichende Schwefelgehalt: die aus Romaschkinoer Bitumina erhaltenen Fraktionen enthalten pro durchschnittliches Molekül fast ein Schwefelatom, während die Algyőer Fraktionen nur ein halbes Schwefelatom enthalten. Einige Strukturvarianten für die aus der Ölfraktion des naphtenisch-aromatischen Teiles gewonnenen zweiringigen Fraktionen sind in Abb. 6 dargestellt.

Die Ölharzfraktion repräsentiert einen beträchtlichen Teil der untersuchten Bitumina. Eine Trennung der Fraktion in homogenere Fraktionen konnte — wie übrigens zu erwarten war — mit den verwendeten Operationen nicht erreicht werden. Vermutlich enthalten die Komponenten des Ölharzes innerhalb eines Moleküls Einheiten mit verschiedener Ringzahl. Demzufolge konnte nur eine geringe Anreicherung bei den Trennungsoperationen erhalten werden. Zur Charakterisierung der Ölharzfraktion werden deshalb in den Tab. IX und X die Versuchsergebnisse des Destillationsrückstands des »entparaffinierten« Ölharzes (dieser Rückstand macht den überwiegenden Teil der Fraktion aus) sowie des Destillationsrückstandes der »paraffinhaltigen« Fraktion angegeben.

Auffallend ist der hohe aromatisch gebundene Kohlenstoffgehalt der Fraktionen. Dieser beträgt in der »paraffinhaltigen« Fraktion 3—4 aromatische Ringe pro druchschnittliches Molekül, in der »entparaffinierten« Fraktion 4—5 Ringe. An die mehrfach kondensierten aromatischen Ringsysteme schließen sich bei beiden Fraktionen durchschnittlich 5—7 Wasserstoffatome, 5—6 Methylengruppen und 2—3 Methylgruppen an. Eine Ausnahme bilden die entsprechenden Fraktionen des Algyőer Bitumens, wo der Substitutionsgrad der aromatischen Ringsysteme etwas geringer ist, als bei den Fraktionen aus den Romaschkinoer Bitumina.

In der aus dem Ölharz erhaltenen »paraffinhaltigen« Fraktion konnten keine naphtenisch gebundenen Kohlenstoffatome nachgewiesen werden. Die Ringanalyse der »entparaffinierten« Fraktion des Algyőer Extraktbitumens konnte wegen dem hohen Gehalt an aromatisch gebundenem Kohlenstoff nicht durchgeführt werden. In den Fraktionen Romaschkinoer Herkunft zeigte die Ringanalyse, daß die Anzahl der aromatischen Ringe etwa 2 bis 3mal höher ist als die der Naphtenringe.

Das Kohlenstoffskelett der an aromatische bzw. Naphtenringe gebundenen Alkylketten ist sowohl bei der »paraffinhaltigen« als auch bei der »entparaffinierten« Fraktion durchschnittlich 5—6mal verzweigt; zugleich ist die Zahl der Methylengruppen, d. h. die Länge der Seitenketten in der »paraffinhaltigen« Fraktion wesentlich höher.

Die chemischen Analysen ergaben in den Algyőer Fraktionen pro durchschnittliches Molekül 1 Schwefelatom und 1,5—2 Sauerstoffatome, in den Romaschkinoer Fraktionen 3—4 Schwefelatome und ungefähr ein Sauerstoffatom. Unsere mit Pyrolyse verbundenen gaschromatographischen Unter-

Tabelle IX

Ergebnisse der Untersuchung des Destillationsrückstandes aus dem entparaffinierten Ölharz

Methode	Geprüfte Größe	Herkunft des Bitumens			
		Romaschkinoer			Algyőer Extrakt
		Extrakt	Destill.	Geblas.	
1.	2.	3.	4.	5.	6.
IR	C_A%	33,7	39,7	41,6	47,6
	C_P%	45,9	42,9	46,2	*
	C_N%	20,4	17,4	12,2	*
	n_{CH_2}	29,2	27,5	38,2	29,7
	n_{CH_3}	7,5	8,2	11,6	6,7
NMR	n_{CH}	8,6	7,0	9,8	6,8
	n_{CH_2}	27,1	22,9	29,9	23,6
	n_{CH_3}	5,6	5,9	6,8	3,8
	n_{Ar-H}	4,9	4,8	5,6	7,2
	n_{Ar-CH_2}	5,9	4,8	5,6	4,1
	n_{Ar-CH_3}	2,4	1,9	3,8	1,6
UV	Einringig	33,4	25,0	33,8	13,2
	Zweiringig	16,7	11,9	14,7	17,2
	Mehrringig	38,2	39,1	37,1	37,2
Dampfdruck-Osmometrie	$\overline{MG}$	997	834	1100	806
Chemische Analyse	C%	85,3	83,5	84,4	86,6
	H%	10,4	10,1	10,1	10,3
	S%	3,8	3,8	3,7	1,2
	O%	0,6	1,1	1,9	1,9
Berechnete Werte	n_C	70,9	58,0	77,4	58,2
	nC_A	23,9	23,0	32,2	27,7
	nC_P	32,5	24,9	35,8	*
	nC_N	14,5	10,1	9,5	*
	n_S	1,2	1,0	1,3	0,3
	n_O	0,4	0,6	1,3	1,0
Menge der Fraktion auf das Bitumen bezogen, Gew.%		42,9	40,4	19,6	20,8
Annähernde Bruttoformel		$C_{71}H_{104}S_{1,2}O_{0,4}$	$C_{58}H_{84}S_{1,0}O_{0,6}$	$C_{77}H_{111}S_{1,3}O_{1,3}$	$D_{58}H_{83}S_{0,3}O_{1,0}$

* Wegen des hohen Aromatengehaltes gelang es nicht, die Angaben zu bestimmen

Tabelle X

Ergebnisse der Untersuchung des Destillationsrückstandes aus der »paraffinhaltigen« Fraktion des Ölharzes

Methode	Geprüfte Größe	Herkunft des Bitumens			
		Romasckinoer			Algyőer Extrakt
		Extrakt	Destill.	Geblas.	
1.	2.	3.	4.	5.	6.
IR	C_A	21,9	32,1	24,0	25,0
	C_P	78,1	67,9	76,0	75,0
	C_N	0	0	0	0
	n_{CH_2}	59,2	51,0	66,2	53,4
	n_{CH_3}	5,9	6,2	8,6	5,7
NMR	n_{CH}	8,8	9,1	14,4	9,2
	n_{CH_2}	49,6	46,2	57,8	48,4
	n_{CH_3}	4,5	4,5	6,2	4,4
	n_{Ar-H}	6,3	6,1	7,2	3,8
	n_{Ar-CH_2}	6,1	5,2	5,0	3,8
	n_{Ar-CH_3}	1,6	2,0	2,4	1,5
UV	Einringig	19,7	25,7	14,7	10,2
	Zweiringig	15,0	15,9	20,9	24,6
	Mehrringig	20,3	24,6	23,8	52,5
Dampfdruck-Osmometrie	$\overline{MG}$	1100	1190	1475	1110
Chemische Analyse	C%	85,2	83,3	85,1	87,3
	H%	12,1	11,1	11,7	11,8
	S%	2,7	3,1	2,9	0,9
	O%	—	1,1	1,3	1,4
Berechnete Werte	n_C	78,1	82,6	104,6	80,8
	n_{C_A}	17,1	26,5	25,1	20,2
	n_{C_P}	61,0	56,1	79,5	60,6
	n_{C_N}	0	0	0	0
	n_S	0,9	1,2	1,3	0,3
	n_O	—	0,8	1,2	1,0
Menge der Fraktion auf das Bitumen, Gew.%		4,65	3,4	3,1	4,41
Annähernde Bruttoformel		$C_{78}H_{133}S_{0,9}$	$C_{83}H_{132}S_{102}O_{0,8}$	$C_{105}H_{173}S_{1,3}O_{1,2}$	$C_{81}H_{131}S_{0,3}O_{1,0}$

suchungen zeigten, daß der Schwefel größtenteils in Form von Thiophenderivaten bzw. Benzothiophenderivaten vorliegt. In den Pyrolyseprodukten konnte die Gegenwart von Benzothiophen nachgewiesen und die Gegenwart von Thiophen mit hoher Wahrscheinlichkeit vermutet werden.

Die Bindungsverhältnisse der Sauerstoffatome ließen sich durch unsere bisherigen Arbeiten noch nicht eindeutig aufklären. Die Bande mittlerer Intensität im Valenzschwingungsbereich der C=O-Gruppe weist darauf hin, daß nicht alle durch die chemische Analyse bestimmten Sauerstoffatome (1—2 pro durchschnittliches Molekül) in C=O-Bindungen vorliegen können. Es kann angenommen werden, daß ein Teil der Sauerstoffatome pseudoaromatische Ringe bildet, die sich ähnlich verhalten wie die aromatischen und die schwefelhaltigen pseudoaromatischen Verbindungen.

1.

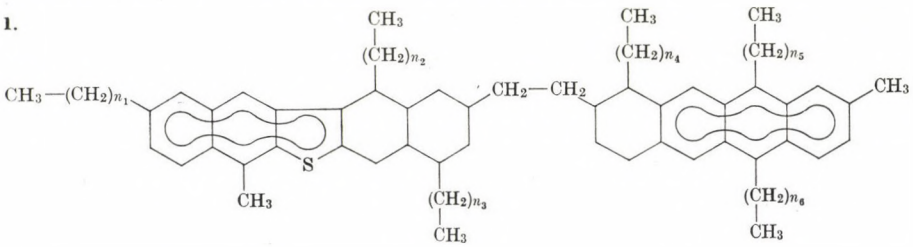

2.

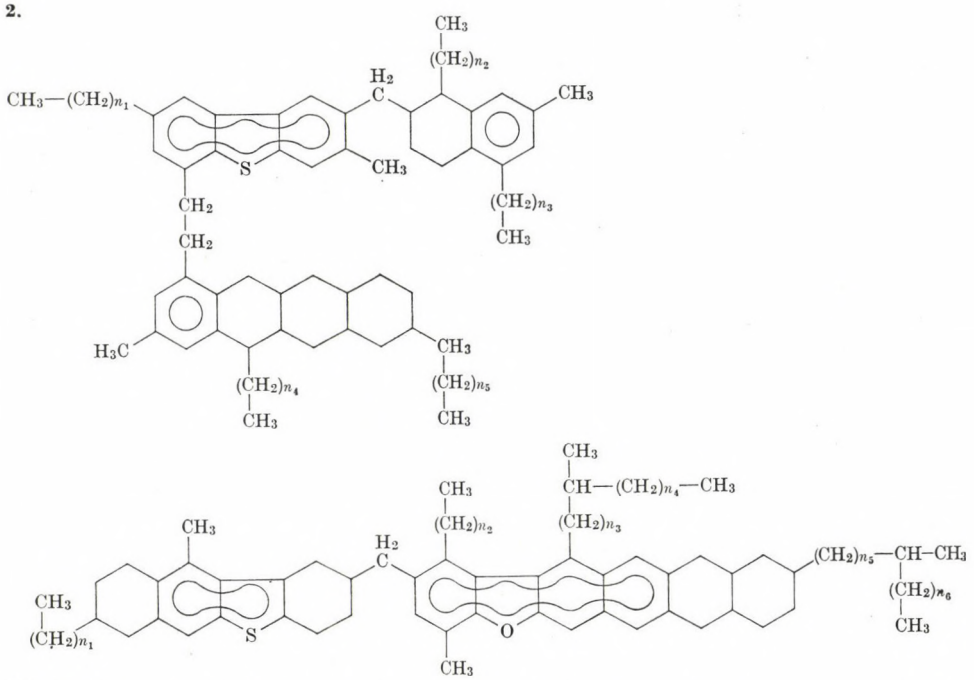

Abb. 7. Einige Strukturvarianten des Destillationsrückstandes des »entparaffinierten« Ölharzes aus Romaschkinoer Extraktbitumen (Σ n = 30)

Einige Varianten der durchschnittlichen Struktur der »paraffinhaltigen« und »entparaffinierten« Fraktion des Ölharzes sind in Abb. 7 dargestellt.

Die Asphaltharzfraktionen machen etwa 10% der Bitumenproben aus und bestehen den Erwartungen entsprechend aus Verbindungen mit hohem durchschnittlichen Molekulargewicht und hohem Gehalt an Heteroatomen.

Bei der spektrometrischen Untersuchung der Asphaltharzfraktionen stellte es heraus, daß diese Methoden zu deren Untersuchung nicht oder nur teilweise geeignet sind, da die Zusammensetzung und Struktur der Asphaltharze recht wesentlich von denen der Ölfraktionen abweichen. Die Fehler bei den UV-Absorptionsmethoden und bei den IR-spektrometrischen Gruppenanalysen sind vermutlich durch den hohen Gehalt an Heteroatomen (4% Schwefel, 2,6% Sauerstoff) bedingt. Die Elementarzusammensetzung, das durchschnittliche Molekulargewicht und die mittels den NMR-Spektren bestimmte Protonenverteilung ist in Tab. XI angegeben.

Aufgrund der qualitativen Auswertung der IR-Spektren konnte festgestellt werden, daß ein Teil des bedeutenden Sauerstoffgehaltes des Asphalt-

Tabelle XI

Ergebnisse der Untersuchung der Asphaltharzfraktion

Methode	Geprüfte Größe	Herkunft des Bitumens			
		Romaschkinoer			Algyőer Extrakt
		Extrakt	Destill.	Geblas.	
NMR	n_{CH}	13,9	8,3	6,3	9,0
	n_{CH_2}	29,9	25,8	25,7	33,3
	n_{CH_3}	9,1	7,9	10,3	6,7
	n_{Ar-H}	6,5	4,4	7,3	5,5
	n_{Ar-CH_2}	7,0	5,7	5,6	5,1
	n_{Ar-CH_3}	3,1	2,2	3,5	2,5
Dampfdruck-Osmometrie	$\overline{MG}$	1160	1100	980	1140
Chemische Analyse	C%	83,5	82,1	80,8	85,9
	H%	11,2	9,6	9,6	10,6
	S%	3,8	3,7	3,4	3,2
	O%	2,3	4,8	5,7	2,7
Menge der Fraktion auf Bitumen bezogen, Gew.%		13,0	12,0	11,1	13,5
Annähernde Bruttoformel		$C_{81}H_{130}S_{1,4}O_{1,6}$	$C_{73}H_{106}S_{1,3}O_{3,3}$	$C_{66}H_{94}S_{1,0}O_{3,5}$	$C_{82}H_{124}S_{0,5}O_{1,9}$

harzes in Form von C=O-Bindungen vorliegt. Im Valenzschwingungsbereich der C=O-Gruppe (1750—1650 cm^{-1}) wurden zwei Banden beobachtet, von denen die Bande höherer Frequenz (1700 cm^{-1}) der an ein aliphatisches Kohlenstoffatom gebundenen Karbonylgruppe entspricht, während die Bande bei 1660 cm^{-1} einer mit einem aromatischen Ring in konjugierter Position befindlichen Karbonylgruppe zugeordnet werden konnte. Das IR-Spektrum der Asphaltharzfraktion, die aus der Romaschkinoer Destillationsbitumenprobe erhalten wurde, ist in Abb. 8 dargestellt.

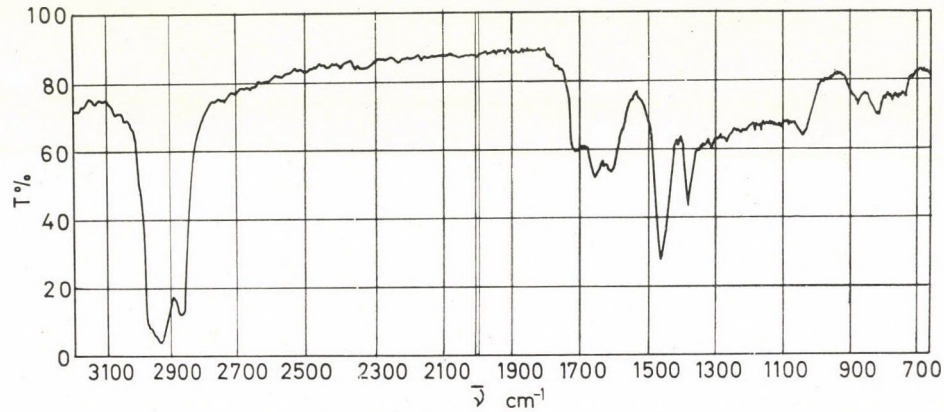

Abb. 8. IR-Spektrum der Asphaltharzfraktion aus Romaschkinoer Destillationsbitumen (KBr-Tablette, 3,2 mg)

Die im vorliegenden Teil unserer Arbeit behandelten Analysenmethoden erwiesen sich als unzulänglich bei der Strukturuntersuchung der Asphaltenfraktion. Demgemäß wurden andere Untersuchungsmethoden verwendet, um ein Bild über die Struktur des Asphaltens zu gewinnen. Über diese Versuchsergebnisse wird in einer späteren Mitteilung berichtet.

Schlußfolgerungen

Aufgrund der Ausbeuten und Strukturanalysendaten der aus vier Bitumenproben verschiedener Herkunft gewonnenen Fraktionen können einige Bemerkungen über die Zusammensetzung der Bitumina gemacht werden:

1. Die Ausbeute an verschiedenen Fraktionen mit homogener Struktur zeigt typische Abweichungen bei den Bitumenproben verschiedener Herkunft. So kann aufgrund der Mengenverhältnisse der Fraktionen ein entschiedener Unterschied einerseits zwischen den Extraktbitumina aus Algyő und Romaschkino und andererseits zwischen aus Romaschkino stammenden, jedoch mit verschiedenen Technologien hergestellten Bitumina nachgewiesen werden.

2. Infolge der Eigenart der angewendeten wirksamen Trennungsoperationen wurden keine wesentlichen Unterschiede in der Zusammensetzung bzw. Struktur der erhaltenen analogen Fraktionen aus den verschiedenen Bitumina gefunden. Die in den Trennungsoperationen erhaltenen Fraktionen erwiesen sich zugleich als ziemlich homogen in ihrer chemischen Struktur und unterschieden sich voneinander charakteristisch.

3. Trotz der Ähnlichkeit der analogen Fraktionen aus Ausgangsmaterialien verschiedener Herkunft konnten zwischen diesen geringere Unterschiede nachgewiesen werden. So wurden z. B. in den Fraktionen des Algyőer Bitumens gegenüber den Fraktionen Romaschkinoer Herkunft im allgemeinen weniger Verzweigungen und naphtenische bzw. aromatische Ringsysteme gefunden.

*

Die spektrometrischen Analysen und sonstigen Untersuchungen der Bitumenfraktionen wurden im Ungarischen Erdöl- und Erdgas-Forschungsinstitut, die Elementaranalysen zum größten Teil am Institut für organische Chemie der Eötvös-Loránd-Universität durchgeführt. Es sei an dieser Stelle den wissenschaftlichen Mitarbeitern Frau Dr. H. MEDZIHRADSZKY und Frau B. MARKÓ-MONOSTORY für die Elementaranalysen und Herrn M. KÁNTOR für die pyrolysegaschromatographischen Untersuchungen gedankt. Endlich möchten die Verfasser den Donau- Mineralölwerken für die finanzielle Unterstützung der experimentellen Arbeit ihren Dank aussprechen.

LITERATUR

1. SCHWEYER, H. E.: Anal. Chem., **30,** 205 (1958)
2. TRAXLER, R. N., SCHWEYER, H. E.: Oil Gas J., **52,** 158 (1953)
3. FISCHER, K. A., SCHRAM, A.: Erdöl u. Kohle, **12,** 368 (1959)
4. CHELTON, H. M., TRAXLER, R. N.: 5th World Petr. Congr. Section V, Paper 19 (1959)
5. BOYD, M. J., MONTGOMERY, D. S.: Fuel, **41,** 335 (1962)
6. SMITH, C. D., SCHUETZ, C. C., HODGSON, R. S.: Bitumen, Teere, **1966,** 436
7. KNOTNERUS, J.: Erdöl u. Kohle, **23,** 341 (1970)
8. CHAMBERLAIN, N. F., NEUREITER, N. P., SAUNDERS, R. K., WILLIAMS, R. B.: 5th World Petr. Congr. Section V, Paper 8 (1959)
9. WILLIAMS, R. B., CHAMBERLAIN, N. F.: 6th World Petr. Congr. Section V, Paper 17 (1963)
10. CHAMBERLAIN, N. F.: 7th World Petr. Congr. Section V, Paper 12 (1967)
11. HELM, R. N., PETERSSEN, J. C.: Erdöl u. Kohle, **22,** 37 (1969)
12. NICKSIC, S. W., JEFFRIES-HARRIS, H. J.: Inst. Petr. **54,** 532, 107 (1968)
13. GARDNER, R. A., HARDMAN, H. F., JONES, A. L., WILLIAMS, R. B.: J. Chem. Eng. Data, **4,** 155 (1959)
14. MIDDLETON, W. R.: Anal. Chem., **39,** 1839 (1967)
15. ZALKA, L.: Acta Chim. (Budapest), **76,** 121 (1973)
16. BÁLINT, T.: Acta Chim. Acad. Sci. Hung., **31,** 17 (1962); **35,** 391 (1963)
17. BRANDES, G.: Brennst. Chem., **37,** 263 (1956)
18. BRANDES, G.: Erdöl u. Kohle, **11,** 700 (1958)
19. BÉLAFI, K., BOR, GY.: MÁFKI Közl. **6,** (1965)
20. MÁZOR, L.: Szerveskémiai analízis II. Mennyiségi elem-analízis. Műszaki Könyvkiadó, Budapest, 1962
21. SIMON, W.: Chimia (Schweiz), **19,** 544 (1965)
22. SIMON, W., CLERC, J. T., BUHNER, R. E.: Microchem. J., **10,** 495 (1966)

Lajos ZALKA; Százhalombatta 3. Pf. 1. Ungarn

Katalin BÉLAFI-RÉTHY
Ervin KERÉNYI } Veszprém, Wartha V. u. 1—3, Ungarn.

Acta Chimica Academiae Scientiarum Hungaricae, Tomus 76 (2), pp. 167—177 (1973)

UNTERSUCHUNG DER ZUSAMMENSETZUNG VON EINHEIMISCHEN UND AUSLÄNDISCHEN ÄTHERISCHEN ÖLEN, II

ANALYSE EINES UNGARISCHEN PFEFFERMINZÖLES

K. Bélafi-Réthy,* S. Iglewski,* E. Kerényi* und R. Kolta**

Eingegangen am 14. Februar 1972

Die qualitative und quantitative Zusammensetzung des ungarischen Pfefferminzöles wurde mit einer für die Analyse von ätherischen Ölen entwickelten kombinierten Methode untersucht. Im Öl wurden mittels Kapillar-Gaschromatographie 38 Komponenten nachgewiesen, deren Anteil einzeln mehr als 0,01 Gew.% beträgt; darunter betrug die Menge von 24 Komponenten jeweils mindestens 0,1 Gew.%. Nach einer wirksamen Trennung konnten mittels spektrometrischer Methoden die wesentlichen Komponenten: α-Pinen, β-Pinen, Limonen, 1,8-Cineol, *p*-Cymol, 2,6-Dimethyloktan-2-ol, 3,7-Dimethyl--1,7-oktadien-3-ol (Linalool), Menthon, Menthofuran, Isomenthon 3,7-Dimethyl-1,6-oktadien-3-ol (Linalool), Menthylacetat, Neomenthol, Neoisomenthol, Caryophyllen, Menthol, Isomenthol, Piperiton und Calamenen identifiziert werden. Unter den in Spuren vorliegenden Begleitkomponenten wurden β-Myrcen, Isopulegol, Menthylisovalerianat und ε-Cadinen gefunden. Die quantitative Zusammensetzung des Pfefferminzöles wurde gaschromatographisch bestimmt. Die Menge der identifizierten Komponenten betrug mehr als 98,6% der untersuchten Probe.

Über die Zusammensetzung des Öles der ungarischen, zum Mitcham-Typ gehörenden Pfefferminze (Mentha piperita Huds. var. officinalis forma rubescens Camus) stehen nur wenig Angaben zur Verfügung; allein die Hauptkomponenten und deren Konzentrationen sind bekannt [1]. Auch die in jüngster Zeit im Betrieb für Kosmetik und Haushaltschemie durchgeführten gaschromatographische sowie die im Heilpflanzenforschungsinstitut durchgeführten dünnschichtchromatographischen Untersuchungen beschränkten sich auf die Trennung und Identifizierung der Hauptkomponenten [2].

Literaturangaben über die Zusammensetzung der Pfefferminzöle

Abgesehen vom ungarischen Öl befassen sich verhältnismäßig viele Veröffentlichungen mit der Zusammensetzung der Pfefferminzöle [3]; die untersuchten ätherischen Öle stammten jedoch aus Pflanzen verschiedener Varietäten und Formen, die in verschiedenen Gegenden angebaut und meistens zu verschiedenen Zeitpunkten geerntet wurden. Das Ziel der Analysen war außer der eingehenden Kenntnis des Pfefferminzöles [z. B. 4, 5, 16] in einigen Fällen ein Vergleich des Öles aus Pflanzen verschiedener Art, Varietät und Form

**Ungarisches Erdöl- und Erdgas-Forschungsinstitut, Veszprém und **Betrieb für Kosmetik und Haushaltschemie*

[z. B. 6, 7] oder die Beobachtung der pflanzenphysiologischen Veränderungen und der Biosynthese der Komponenten [z. B. 8, 9].

Über die Zusammensetzung der Pfefferminzöle wurden ziemlich viele Angaben angehäuft [1, 4, 10]. Eine Literaturübersicht der im Öl der Mentha piperita gefundenen Komponenten liegt in Tabelle I vor. Die Angaben stammen teils aus chemischen Untersuchungen, teils aus gaschromatographischen und dünnschichtchromatographischen Bestimmungen und zum Teil auch aus spektrometrischen Analysen. Abgesehen von den letzteren Methoden liefern die erwähnten Methoden bei der qualitativen Analyse unbekannter Substanzen oft irreführende Feststellungen; daher ist es möglich, daß die Tabelle viele falsche Angaben enthält. Die Zusammensetzung der Öle der in verschiedenen Gegenden angebauten verschiedenen Varietäten und Formen können charakteristische Abweichungen aufweisen; folglich sind die in der Fachliteratur vorhandenen Angaben auch in dieser Hinsicht nur als Möglichkeiten aufzufassen.

Wegen der Unsicherheit der Literaturangaben über die Pfefferminzöle und in Ermangelung von Angaben über die Zusammensetzung des einheimischen hochwertigen Pfefferminzöles erschien es uns wichtig, eine genaue und ausführliche Analyse des ungarischen Pfefferminzöles durchzuführen.

Analytische Methode

In der vorangegangenen Mitteilung [17] wurde ausführlich über die von uns entwickelte Methode zur Bestimmung der Zusammensetzung von ätherischen Ölen berichtet. Bei der Analyse des ungarischen Pfefferminzöles wurde ein vereinfachter Analysengang angewendet. Zur Isolierung der reinen Komponenten wurden nur Flüssigkeitschromatographie und präparative Gaschromatographie angewendet und bei der Identifizierung der Komponenten wurde außer den spektrometrischen Methoden nur Hydrierung in Anspruch genommen.

Bei der quantitativen Analyse der Probe wurde der Chromatograph P-AID/F der Firma Carlo Erba teils mit gefüllter Säule, teils mit Kapillarsäule verwendet. Die Analyse wurde auf Grund der Aufnahmen des Pfefferminzöles und seiner flüssigkeitschromatographischen Fraktionen durchgeführt. Bei zusammenfallenden Komponenten stützten wir uns auf die spektrometrischen Untersuchungen.

Die Kohlenwasserstoffe und ihre sauerstoffhaltigen Derivate wurden durch Flüssigkeitschromatographie an Silikagel unter Anwendung von *n*-Hexan und Methanol als Elutionsmittel getrennt. Zur Grobpräparierung der Komponenten wurde das Gerät Fractovap P der Firma Carlo Erba, zur Feinpräparierung eine abgeänderte Form des analytischen Gaschromatographen GCHF 18 der Firma W. Giede angewendet.

Die IR-Spektren der reinen oder angereicherten Komponenten und ihrer hydrierten Produkte wurden mit einem Gerät UR-10 der Firma Carl Zeiss Jena aufgenommen; die Massenspektren wurden mit einem Massenspektrometer ZEME MI 1305, die NMR-Spektern mit einem Gerät ZKR-60 der Firma Zeiss erhalten. Die Auswertung der Spektren beruhte auf der Untersuchung der Spektren von Modellverbindungen, auf dem Vergleich mit bekannten Spektren und auf den Zusammenhängen zwischen den Spektren und der Struktur.

Versuchsergebnisse

Das Kapillar-Gaschromatogramm des untersuchten aus der Balaton-Gegend stammenden Pfefferminzöles ist in Abb. 1 gezeigt. Das Kapillar-Gaschromatogramm der durch Flüssigkeitschromatographie erhaltenen, lö-

Tabelle I

In Pfefferminzöl gefundene Komponenten aufgrund der Literatur

Kohlenwasserstoffe

Monoterpene

α-Pinen	[1, 4, 11]
β-Pinen	[11, 13]
Limonen	[1, 11]
Dipenten	[1, 4]
γ-Terpinen	[1, 12]
α-Phellandren	[1, 4]
Camphen	[1, 12]
Δ^3-*p*-Menthen	[1]
o-Cymol	[12, 13]
p-Cymol	[11, 12]
β-Myrcen	[11, 12]

Sesquiterpene

γ-Cadinen	[1, 4]	Cubenen	[5]
ε-Cadinen	[5]	Ylangen	[5]
δ-Cadinen	[5]	α-Burbonen	[5]
Caryophyllen	[1, 4]	β-Burbonen	[5]
Aromadendren	[4]	S-Guajazulen	[14]
β-Elemen	[5]	Humulen	[5]
α-Muurolen	[5]	ε-Bulgaren	[5]
γ-Muurolen	[5]	α-Maalien	[5]
ε-Muurolen	[5]	Bicycloelemen	[5]
Chalamenen	[5]		

Kohlenwasserstoffderivate

Alkohole

Menthol	[z.B. 1]	Neomenthol	[1, 4]
Thymol	[1, 4]	Carvacrol	[1, 4]
n-Amylalkohol	[1, 4]	i-Amylalkohol	[1, 4]
Hexenol	[1, 4]	Oktanol	[1]
Äthylamylcarbinol	[1, 4]	β-Bethulenol	[1]
tr.-Sabinenhydrat	[1, 4]	Chlovandiol	[1]
Caryophyllenalkohol	[1]		

Aldehyde

Acetaldehyd	[1, 4]	i-Butyraldehyd	[12]
i-Valeraldehyd	[1, 4]	Benzaldehyd	[4]
Phenylacetaldehyd	[15]	Furfurol	[1]
tr.-2-Hexenal	[12]		

Ketone

Menthon	[z.B. 1]	Äthylamylketon	[15]
Piperiton	[1, 4]	Isomenthon	[1, 4]
Jasmon	[1, 4]	Pulegon	[1, 4]
Methylamylketon	[1]	Aceton	[1, 4]
3-Methylcyclohexanon	[1, 4]	i-Pulegon	[4]

Säuren und Ester

Essigsäure	[1, 4]	i-Valeriansäure	[1, 4]
Menthylacetat	[z.B. 1]	Menthylisovalerianat	[1,4]
Hexenylphenylacetat	[1]	Äthylamylcarbinolacetat	[15]

Sonstige Sauerstoffverbindungen

Cineol (Eucalyptol)	[1, 4, 11, 12]	Menthofuran	[1, 4, 11]

Sonstige Verbindungen

Dimethylsulfid [1, 4]

sungsmittelfreien Kohlenwasserstoff-Fraktion ist in Abb. 2, die Aufnahme der lösungsmittelfreien Kohlenwasserstoffderivat-Fraktion in Abb. 3 dargestellt. Die Analysen wurden in 50 m langen, mit Carbowax-1000 benetzten Kapilla-

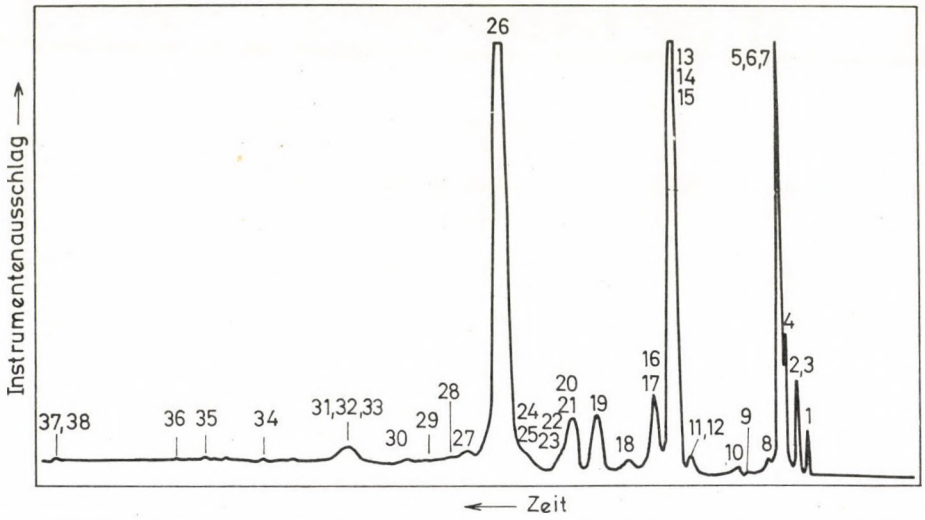

Abb. 1. Gaschromatogramm des ungarischen Pfefferminzöles
Gerät: Carlo Erba P-AID/F;
Säule: 50 m lange Kapillare, mit Carbowax-1000 benetzt. Temperatur: 125 °C; Trägergas: Argon, Trägergasgeschwindigkeit: 1,6 ml/min

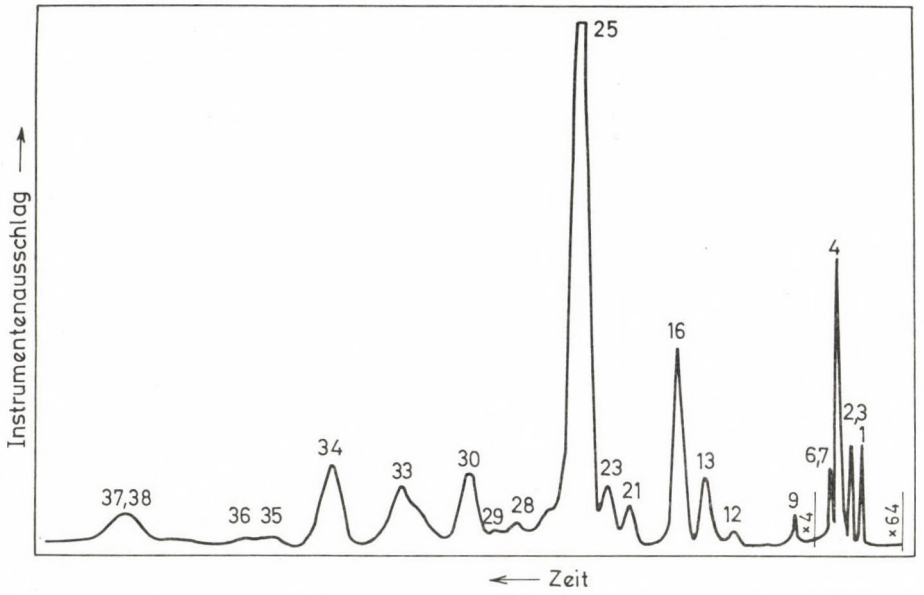

Abb. 2. Gaschromatogramm der Kohlenwasserstoff-Fraktion des ungarischen Pfefferminzöles
Versuchsbedingungen wie in Abb. 1

ren, bei 125 °C und einer Trägergasgeschwindigkeit von 1,6 ml/min, mit Argon als Trägergas durchgeführt. Die nachweisbaren Komponenten wurden in den Abbildungen aufgrund der flüssigkeitschromatographischen, gaschromatographischen und spektrometrischen Befunde mit Nummern versehen. Die Angaben über die qualitative und quantitative Zusammensetzung ließen sich auf diese Nummern beziehen. Aus den Abbildungen ist ersichtlich, daß zwei Hauptkomponenten und — ohne weitere selektive Konzentrierungsoperationen — insgesamt 38 Komponenten in der Probe nachgewiesen werden konnten.

Über die Ergebnisse der Reinigung der einzelnen Komponenten, über die Spektrumaufnahmen der reinen oder angereicherten Fraktionen (bzw. ihrer hydrierten Produkte) und über die Methode der Identifizierung gibt Tab. II eine Übersicht. Die durch Hydrierung hergestellten Verbindungen sind in der Tabelle mit 1/a, 3/a, 4/a bezeichnet. Die Konzentrate der Komponenten wurden als rein betrachtet, wenn keine oder nur geringe Verunreinigungen nachgewiesen werden konnten. Sie wurden als angereichert betrachtet, wenn sie die zu bestimmende Komponente in einer zur Identifizierung ausreichenden Kon-

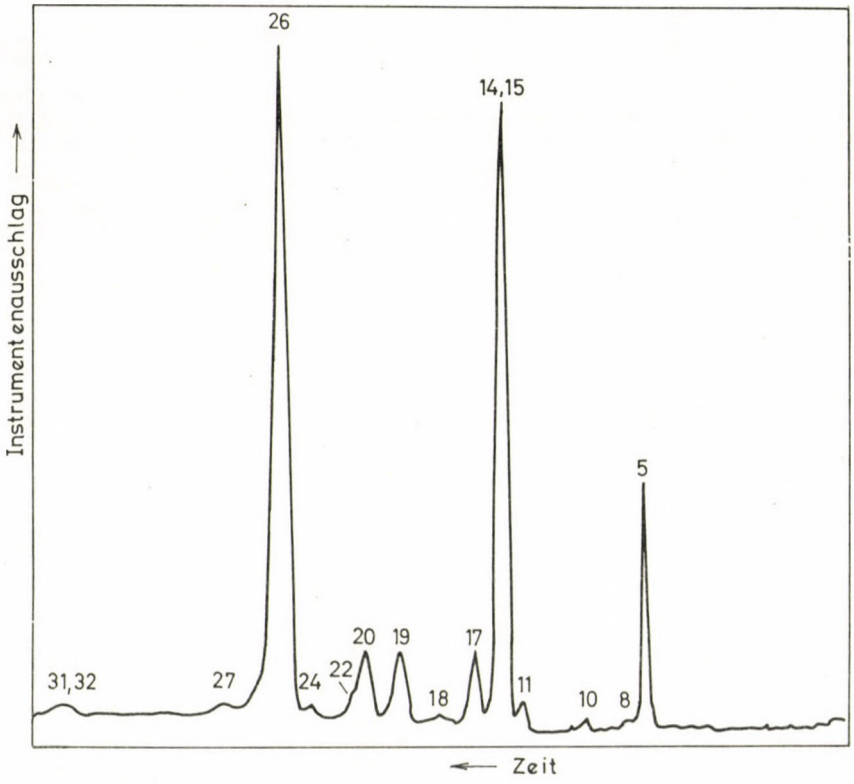

Abb. 3. Gaschromatogramm der Kohlenwasserstoffderivat-Fraktion des ungarischen Pfefferminzöles
Versuchsbedingungen wie in Abb. 1

Tabelle II

Trennung und Identifizierung der Komponenten des ungarischen Pfefferminzöles

Nr.	Relative Retention	Reinigung		Spektrum			Identifizierung			Komponente
		rein	angereichert	IR	Massen-	NMR	Modellverbindung	Bekanntes Spektrum	Zuordnung der Spektrumbanden	
1	81	+		+	+	+	+	[21]	+	α-Pinen
1/a	—	+		+				[22]	+	Pinan
2	91		+	+				[21]	+	β-Pinen
3	91	+		+	+			[18]	+	β-Myrcen
3/a	—	+		+					+	2,6-Dimethyloktan
4	100	+		+	+	+		[21]	+	Limonen
4/a		+		+				[22]	+	*p*-Menthan
5	104	+		+	+		+	[21]	+	1,8-Cineol
6	104	+		+	+			[22]	+	*p*-Cymol
7	104									Kohlenwasserstoff
8	115									Kohlenwasserstoffderivat
9	132									Kohlenwasserstoff
10	140		+	+	+				+	2,6-Dimethyl-oktan-2-ol
11	179	+		+	+		+	[21]	+	3,7-Dimethyl-1,7-oktadien-3-ol (Linalool)
12	179									Sesquiterpen
13	191									Sesquiterpen
14	191	+		+	+			[19]	+	Menthon
15	191		+	+				[21]	+	Menthofuran
16	208									Sesquiterpen
17	208	+		+	+			[19]	+	Isomenthon
18	228		+	+	+		+		+	3,7-Dimethyl-1,6-oktadien-3-ol (Linalool)
19	253	+		+	+			[19]	+	Menthylacetat
20	273	+		+				[20]	+	Neomenthol
21	273									Sesquiterpen
22	290		+	+				[21]	+	Isopulegol
23	290									Sesquiterpen
24	307		+	+				[20]	+	Neoisomenthol
25	307		+	+				[21]	+	Caryophyllen
26	330	+		+			+	[20]	+	Menthol
27	356		+	+				[20]	+	Isomenthol
28	372									Sesquiterpen
29	383									Sesquiterpen
30	403									Sesquiterpen
31	450	+		+	+			[21]	+	Piperiton
32	450		+	(Abb. 4)			+		+	Menthylisovalerianat
33	450									Sesquiterpen
34	518									Sesquiterpen
35	563									Sesquiterpen
36	587									Sesquiterpen
37	741		+	+				[23]	+	Chalamenen
38	741		+	+				[23]	+	ε-Cadinen

Tabelle III

Quantitative Zusammensetzung des ungarischen Pfefferminzöles

Nr.	Komponenten			Menge				
				Monoterpene	Sesquiterpene	Alkohole	Oxoverbindungen	Sonstige Sauerstoffverbindungen
1 2		α-Pinen β-Pinen		0,4 0,7				
4 5	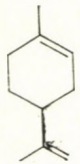	Limonen 1,8-Cineol	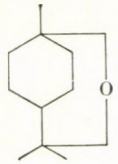	1,2				6,5
6 8	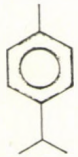	p-Cymol Kohlenwasserstoffderivat	—	0,5				0,2
10 11	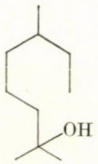	2,6-Dimethyloktan-2-ol 3,7-Dimethyl-1,7--oktadien-3-ol	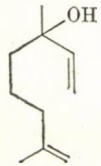			0,7 0,9		

14 15		Menthon Menthofuran					23,6	2,6
16 17	—	Sesquiterpen Isomenthon			0,2		3,1	
18 19		3,7-Dimethyl-1,6--oktadien-3-ol Menthylacetat				1,4		4,4
20 24		Neomenthol Neoisomenthol				3,9 0,3		
25 26		Caryophyllen Menthol			1,1	44,2		

Tabelle III (Fortsetzung)

Nr.	Komponenten			Menge				
				Monoterpene	Sesquiterpene	Alkohole	Oxoverbindungen	Sonstige Sauerstoffverbindungen
27 30	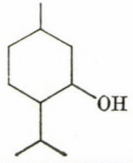	Isomenthol Sesquiterpen	—		0,1		1,8	
31 33	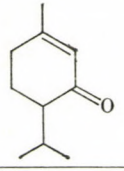	Piperiton Sesquiterpen	—		0,1		1,2	
34 37	—	Sesquiterpen Chalamenen	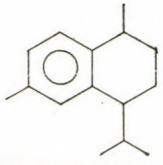		0,1 0,1			
				2,8	1,7	53,2	27,9	13,7

zentration enthielten. Im Laufe der Analysen strebten wir außer der Identifizierung auch die Untersuchung der Spektren von weniger bekannten reinen Komponenten an, diese sind in der Tabelle angeführt. Die zur Identifizierung verwendeten Modellverbindungen wurden teils durch den Betrieb für Kosmetik und Haushaltschemie zu Verfügung gestellt, teils im Ungarischen Erdöl- und Erdgas-Forschungsinstitut hergestellt. Bei den Fällen von Identifizierungen aufgrund bekannter Spektren wurden die entsprechenden Literaturhinweise in der Tabelle angegeben. Als Beispiel für in der Fachliteratur unbekannte Spektren ist in Abb. 4 das Spektrum des Menthylisovalerianats dargestellt. Das IR-Spektrum der ausreichend angereicherten Probe wurde in einer Küvette mit Kaliumbromid-Fenster und einer Schichtdicke von 0,0020 cm aufgenommen.

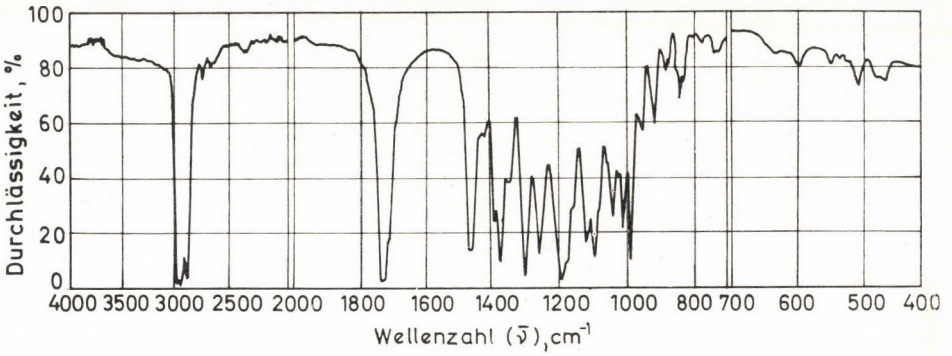

Abb. 4. IR-Spektrum des Menthylisovalerianats
Gerät: Zeiss UR-10; Schichtdicke; 0,020 mm

Die Raumstruktur der meisten identifizierten Komponenten war aufgrund der Literaturangaben oder unserer Versuchsergebnisse eindeutig; sonst wurde die Konformation der Komponenten nicht untersucht.

Die quantitative Zusammensetzung des ungarischen Pfefferminzöles ist in Tab. III angegeben. Hier sind nur Komponenten angeführt, deren Anteil 0,1 Gew.% erreicht. Die Mengen wurden nach Verbindungsgruppen summiert. Im ungarischen Pfefferminzöl befinden sich in nachweisbarem, jedoch 0,1 Gew.% nicht erreichenden Mengen β-Myrcen, Isopulegol, Menthylisovalerianat, ε-Cadinen und einige andere, nicht näher untersuchte Sesquiterpene.

In Übereinstimmung mit den Literaturangaben wurden als Hauptkomponenten des ungarischen Pfefferminzöles Menthol und Menthon gefunden. In beachtlichen Mengen sind auch das für Pfefferminzöl charakteristische Menthofuran sowie Limonen, 1,8-Cineol, Isomenthon, Neomenthol, Menthylacetat, Piperiton und Caryophyllen vorhanden. In Übereinstimmung mit anderen Untersuchungen konnten zuletzt α-Pinen, β-Pinen, β-Myrcen und ein Oktanol-

Isomer nachgewiesen werden. Da wir uns nicht mit der Untersuchung von in äußerst geringen Mengen vorhandenen Komponenten befaßten, kam es nicht zum Nachweis einiger Monoterpene sowie Alkohol-, Aldehyd- und Ketonderivate. Es ist jedoch beachtenswert, daß das als bedeutende Komponente betrachtete Pulegon nach unseren Untersuchungen nicht nachweisbar war. Dagegen stellten wir — im Gegensatz zur Fachliteratur — fest, daß im Pfefferminzöl geringe Mengen an zweierlei sonst bekannten Oktadienol-Isomeren (alle beide sind in der Fachliteratur als Linalool genannt), sowie beachtliche Mengen an Neoisomenthol und Isomenthol vorhanden sind. Die Menge der identifizierten Komponenten machte mehr als 98,6% des ätherischen Öles aus.

LITERATUR

1. Gildemeister, E., Hoffmann, F.: Die ätherischen Öle. Band VII, Akademie Verlag, Berlin, 1961
2. Unveröffentlichte Daten
3. Anal. Chem. **35,** (5) 39 R (1963); **37,** (5) 46 R (1965); **39,** (5) 47 R (1967); **41,** (5) 40 R (1969); **43,** (5) 45 R (1971)
4. Hefendehl, F. W.: Planta Medica, **10,** 179 (1962)
5. Vlahov, R., Holub, M., Ognjanov, I., Herout, V.: Coll. Czechoslov. Chem. Comm., **32,** 808 (1967)
6. Handa, K. L., Smith, D. M., Nigam, I. C., Levi, L.: J. Pharm. Sci., **53,** 1407 (1964)
7. Sticher, O., Flück, H.: Pharm. Acta. Helv., **43,** 411 (1968)
8. Battaile, J., Loomis, W. D.: Biochim. Biophys. Acta (Amsterdam), **51,** 545 (1961)
9. Rothbächer, H.: Pharmazie, **23,** 389 (1968)
10. Guenther, R.: The essential oils. Volume I—III. Nostrand Co., New York, 1949
11. Ettre, L. S., Purell, J. E., Billeb, K.: J. Chrom., **24,** 355 (1966)
12. McCarty, W. C., Venkatramana Bhat, K., Roscoe, Ch. W., Vischer, L.: J. Pharm. Sci., **52,** 1005 (1963)
13. Ognjanov, I., Vlahov, R.: Compl. Rend. Acad. Bulg., **14,** 459 (1961)
14. Katsuhara, J., Yamasaki, H.: Kigyo Kagaku Sasshi, **70,** 343 (1967)
15. Ognjanov, J., Vlahov, R.: Parfumery Essential Oil Record, **56,** 370 (1965)
16. Rotbacher, H., Suteu, F., Kraus, A.: Planta Medica, **15,** 344 (1967)
17. Bélafi-Réthy, K., Iglewski, St., Kerényi, E., Kolta, R.: Acta Chim. (Budapest), **76,** 1 (1973)
18. Ahlog, G., Seibl, J., Kováts, E.: Liebigs Ann. Chem., **675,** 83 (1964)
19. Gildemeister, E., Hoffmann, F.: Die ätherischen Öle. Band II. Akademie Verlag, Berlin, 1960
20. Mignal, S., Farnow, H., Porsch, F.: Dragoco Berichte, **6,** 182 (1962)
21. Bellanoto, J., Hidalgo, A.: Infrared analysis of essential oils. Heyden Son Ltd, London, 1971
22. Infrared Spectral Data of the American Petroleum Institute. Research Project 44, 1956
23. Pliva, J., Horák, M., Herout, V., Sarm, F.: Die Terpene. Sammlung der Spektren und physikalischen Konstanten. Teil I, Akademie Verlag, Berlin, 1960

Katalin Bélafi-Réthy
Stanislaw Iglewski
Ervin Kerényi
} 8200 Veszprém, Wartha V. u. 1—3. Ungarn

Rezső Kolta; 1113 Budapest, Bocskai út 90.

Acta Chimica Academiae Scientiarum Hungaricae, Tomus 76 (2), pp. 179—182 (1973)

XENON DIFLUORIDE AS AN ANALYTICAL REAGENT, II*

DETERMINATION OF CHROMIUM

A. SCHNEER-ERDEY and K. KOZMUTZA

(Research Group for Inorganic Chemistry of the Hungarian Academy of Sciences, Department for General and Inorganic Chemistry of the Eötvös Loránd University, Budapest)

Received February 14, 1972

Xenon difluoride which can be easily dosed and safely used, oxidises in weakly acid medium at about 100 °C in 25 minutes chromium(III) to chromate. This can be used for the iodometric determination of 1—20 mg chromium. The accuracy of the method is low. However, 20 ng—0.001 mg chromium can be determined photometrically with good accuracy.

Usually chromium is determined by the oxidation of chromium(III) to chromium(VI), and the latter is measured gravimetrically, volumetrically or photometrically. Thus the chromium content of steels, alloys, minerals, electroplating baths, tanning liquors, dilute aqueous solutions (reactor water) can be measured [2—4]. Oxidation can be performed both in acid and alkaline media. In the alkaline medium several oxidising agents, (*e.g.* H_2O_2 or Br_2) can be used whereas in acid medium peroxidisulfate and silver ions are applied.

The chromium content of samples to be decomposed is converted to chromate by alkaline oxidative fusion. On leaching with water and filtering chromium can be separated from many of the accompanying elements.

In our preliminary communication [5] we have reported that chromium (III) can be oxidised in acid solution with xenon difluoride to chromium(VI). It has been found, however, that in strongly acid and in close to neutral solutions the oxidation is not quantitative and it does not preceed with a satisfactory rate. Also it has been established that the material of the vessel and large quantity of xenon fluoride do not affect the reaction.

In view of all these, it seemed expedient to investigate more extensively those conditions, under which xenon fluoride might be used as an oxidising agent for the determination of chromium. A micro method for the determination of chromium has been considered since xenon fluoride can be used even in highly dilute solutions.

The reaction is the following:

$$2\ Cr^{3+} + 3\ XeF_2 + 8\ H_2O \rightleftharpoons 3\ Xe \uparrow + 2\ CrO_4^{2-} + 6\ F^- + 16\ H^+$$

* For Part I see [1]

It can be calculated from the well known pH dependence of the redox potential of the Cr(III)/Cr(VI) system [6] that xenon difluoride (redox potential, E = 2.2 V [7]), is able to oxidise chromium(III) to chromium(VI) in acid media. The redox couple, Cr^{3+}/CrO_4^{2-} has a redox potential of +1.36 V at pH=0. The hydrolysis of xenon difluoride gives the following products:

$$XeF_2 + H_2O \rightarrow Xe\uparrow + 2\,HF + \tfrac{1}{2}\,O_2$$

Between pH 4 and 9 the rate of decomposition of xenon difluoride is the lowest [8]. The half time of the hydrolysis is about 7 hours. In alkaline medium the rate of the reaction is very high. Thus all our experiments were performed in acid media between pH 0 and 3.2. The pH of the aqueous chromium alum ($KCr(SO_4)_2 \cdot 12\,H_2O$) solution is 3.15.

First the oxidation of chromium(III) was investigated at different pH values. For this reason about 70 measurements were carried out in the pH range from 0 to 3.15 in the following way:

About 1.6 g of pulverised alum was weighed, dissolved in distilled water and the solution diluted to 1 litre. Then 5.00 ml was withdrawn and the chromium content determined iodometrically. 5.00 ml of the stock solution corresponds after oxidation to 4.80 ml of 0.01 *n* $Na_2S_2O_3$, so contained 0.8319 mg of chromium.

Data plotted in Fig. 1 show only the lowest and heighest values of our results obtained at identical pH values. These two data are connected with a continuous line, so that also the scattering of the measurements can be evaluated from the figure. It can be seen that the measurements (about 30) carried out between pH 0 and 1.5 do not give satisfactory results. With increasing pH however, both the accuracy and the reproducibility of the results improved.

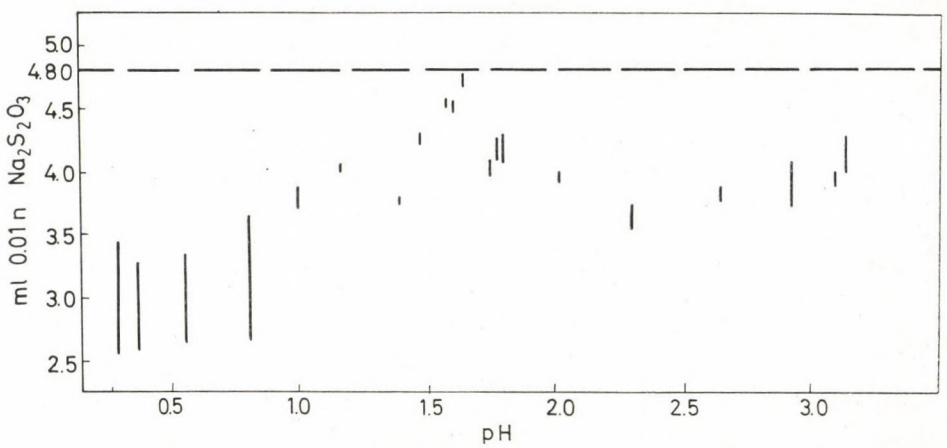

Fig. 1. The measure of the oxidation as a function of the pH

It is also observable that the best results were obtained between pH 1.5 and 1.7. It follows from the data of Fig. 1 that at pH 1.65 the oxidation is presumably complete, and this may give a basis for the determination of chromium.

Procedures

a) Volumetric method

Into a titration flask, a sample containing 1—20 mg of chromium is introduced. The solution is adjusted to pH 1.65. 10—200 mg of xenon difluoride is added, the mixture is allowed to stand for 5 minutes, then placed on a water bath for 25 minutes. During this time, the oxidation of chromium-(III) to chromate is complete, the excess of xenon difluoride is decomposed, and the gaseous decomposition products (Xe, O_2) are removed from the solution. After cooling, 40 ml of 2 *N* hydrochloric acid and some solid potassium iodide are added to the yellow solution, and iodine is titrated with 0.1 or 0.01 *N* standard sodium thiosulfate solution.

Attempts were made to measure the chromium content of industrial tanning liquors, but owing to melasse used for the reduction of bichromate, substantially more reagent was consumed for the oxidation than the calculated value. Thus, the use of the rather expensive xenon difluoride is not justified in this case.

For the determination of small amount of chromium photometry is the most suitable method. Diphenylcarbazide was applied as a reagent; sensitivity: 1.6 ng chromium/cm^2 [4]. 1—100 ng/ml chromium was determined using this reagent. For this purpose, a known amount of chromium alum was dissolved in a volumetric flask, the pH of the solution was adjusted with sulphuric acid, and after dilution, a solution containing 831.9 ng/ml of Cr was obtained.

b) Photometric method

To 1—4 ml of a chromium solution a few grains (not more than 0.1 mg) of xenon difluoride are added (chromium in 1 mg of alum is oxidised with 0.508 mg of xenon difluoride to chromate). To this colourless mixture 10 ml of 2 *N* sulfuric acid and 4 ml of freshly prepared 0.15 per cent diphenylcarbazide solution in ethanol are added in a 50-ml volumetric flask, and the intensive violet solution is diluted to the mark with water. Then the solution is measured on a Hilger H 700 spectrophotometer at 540 nm using a 1 cm cell. The chromium content is obtained from a calibration curve. 830 $\pm$ 50 ng/cm^3 of chromium has been found in the solution.

It can be concluded that xenon difluoride is a satisfactory oxidising agent for the determination of small quantities of chromium. Under the ex-

perimental conditions used by us, the procedure cannot be considered as an accurate analytical method for the determination of more than 1 mg of chromium.

*

The authors are indebted to Dr. Peter GRÓZ, Chemical Department of the Central Research Institute for Physics for giving us the xenon difluoride preparation.

REFERENCES

1. ERDEY-SCHNEER, A., KOZMUTZA, K.: Magy. Kém. Foly. **77,** 97—99 (1971); Acta Chim. Hung. **69,** 9—13 (1971)
2. ERDEY, L.: A kémiai analízis súly szerinti módszerei (Gravimetric methods of chemical analysis) Akadémiai Kiadó, Budapest, 1960
3. FRESENIUS-JANDER: Handbuch d. analytischen Chemie. Teil 3, Bd. VI b α, Springer Verlag, Berlin, Göttingen, Heidelberg, 1958
4. SANDELL, E. B.: Colorimetric determination of traces of metals. Interscience Publ. New York, London 1959
5. ERDEY-SCHNEER, A., KOZMUTZA, K.: Magy. Kém. Foly. **75,** 378 (1969); Acta Chim. Hung. **61,** 235 (1969)
6. Analytical Pocket Book 3rd ed. p. 366. Műszaki Kiadó, Budapest, 1966
   POURBAIX, M.: Atlas of electrochemical equilibria in aqueous solution, p. 257—259. Pergamon Press, Oxford, 1966
7. APPELMAN, E. H., MALM, I. G.: J. Am. Chem. Soc. **86,** 2297 (1967)
8. BECK, M., DÓZSA, L.: Magy. Kém. Foly. **73,** 522 (1967)

Anna SCHNEER-ERDEY
Kornélia KOZMUTZA
} 1088 Budapest, Múzeum krt. 6—8.

Acta Chimica Academiae Scientiarum Hungaricae, Tomus 76 (2), pp. 183—192 (1973)

SOME CHEMICAL REACTIONS OF THE ELECTRODE GAP AND THEIR ROLE IN SPECTROCHEMICAL ANALYSIS, XI

SEPARATION OF THE REACTIONS OCCURRING IN THE ANODE AND CATHODE SPACES. THE METHOD OF SEPARATION

Z. L. SZABÓ and L. PÖPPL

(Department of Inorganic and Analytical Chemistry, L. Eötvös University, Budapest)

Received February 28, 1972

A method has been devised for the separate quantitative determination of carbon dioxide formed in the anode and cathode spaces. A suitable gas cell has been designed from which the gas mixture can be selectively removed during burning of the arc by suction through bore holes in the two electrodes. Optimum conditions for the application of this technique have been established; under these, the gaseous reaction products from the two electrode spaces can be measured separately with an error of 3.6% in the separation.

In former communications [1—10] we reported on the chemical reactions of polarized A.C. arcs burning between a rotated aluminium electrode and carbon or copper counter-electrodes, on the effect of these reactions and on their dependence on the experimental conditions. In these studies we utilized the data of spectral analysis [1, 2], as well as the gas chromatographic [3—6] and gas-titrimetric [7—10] results relevant to changes in the gas phase. Thus we determined the consumption of oxygen or carbon dioxide by the arc, and the production of carbon dioxide, carbon monoxide and nitrogen oxide as a function of various parameters. These processes were found to be redox reactions, the extent of which depends also on the polarity of the electrode. A deeper study of the phenomena inevitably required a method for the separation and separate determination of the gaseous products of stationary, standard anodes and cathodes, even if both are made of the same substance, *e.g.* carbon. The separation of the gas spaces by suction proved to be an adequate way to accomplish this.

A carbon–aluminium electrode pair was used in our exploratory tests. Carbon electrodes, even under experimental conditions to be discussed later, produce a considerable amount of carbon dioxide in an oxygen-containing atmosphere, whose determination can be carried out with relative ease and rapidity. As we intended to utilize also emission spectral data and, since, owing to its large heat of oxidation, aluminium is a good model substance, we decided to use aluminium electrodes. According to our hypothesis, the carbon dioxide generated in the arc will be derived from the carbon side only and with

an efficient separation, no carbon dioxide (or only negligible amounts) will be obtained from the aluminium side.

The first tests were carried out in air. In these, besides carbon dioxide, some carbon monoxide, nitrogen oxide and aluminium oxide, and a small amount of cyanogen were formed. Nitrogen oxide and dicyan interfere with the acidimetric determination of carbon dioxide. Therefore, after the optimum conditions had been established, a mixture composed of 20% oxygen and 80% argon was used to demonstrate the adequate separation efficiency.

Apparatus and Method

The electrode support shown in Fig. 1 was designed for these studies. In essence, this is an exchangeable, 50 mm high glass or quartz tube with a volume of 13 to 25 cm^3. Lateral gas inlet and outlet tubes were mounted on the cells. The interchangeable cell types are shown in Fig. 2. At the top and the bottom these cells were covered with stainless steel plates pressed firmly to

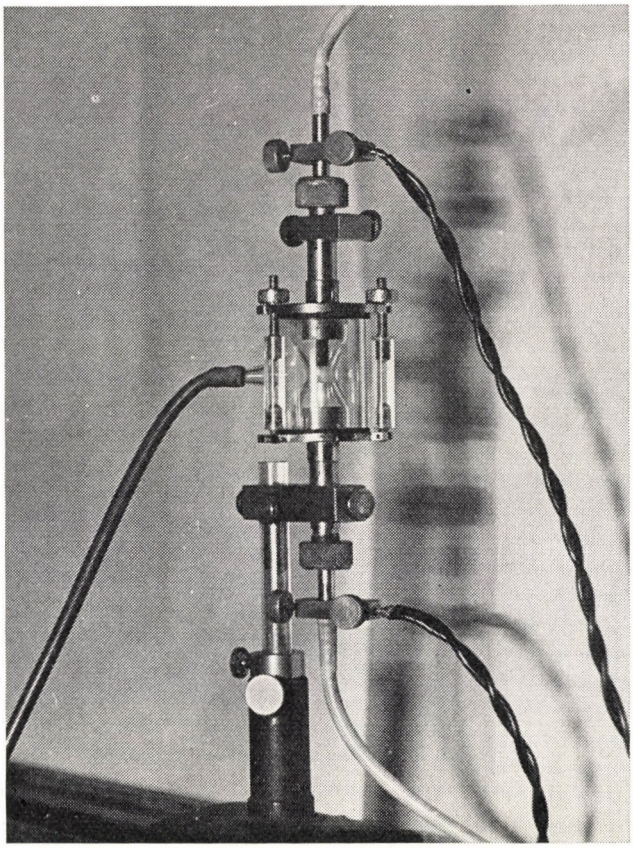

Fig. 1. Electrode stand with gas cell

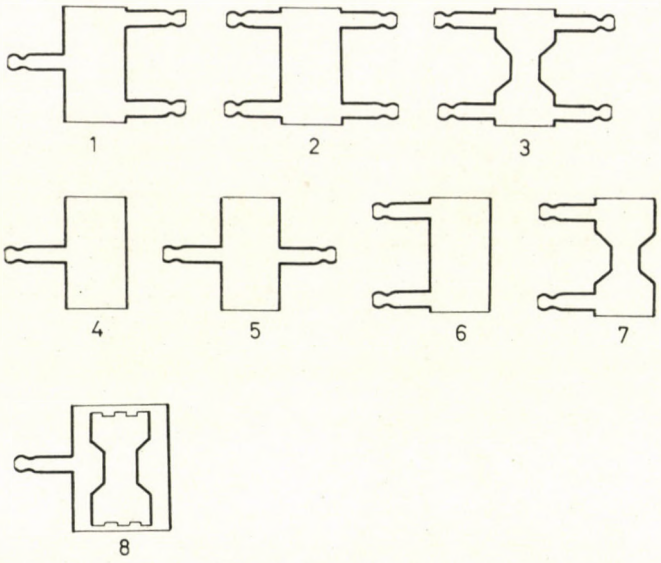

Fig. 2. Gas cell types

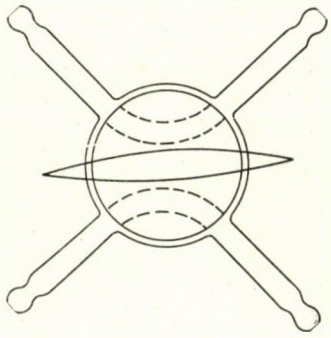

Fig. 3. Four-way stopcock

the cells by Lucite insulated screws. Rubber rings between the cell-ends and the steel plates served as sealing gaskets. Steel tubes, with a conical opening at one end, served as the electrode holders; the rod shaped electrodes were fixed by pushing into these conical wells. The electrode holder steel tubes were mounted through rubber gaskets into the end plates of the cells. Two evacuated flasks, 600 cm^3 each, were used to maintain the gas flow, and also served as reactors for gas analysis and as titration vessels [7]. For the control of gas flow rate, glass capillaries of the same dimensions were inserted into both gas lines. By varying the inner diameter (from 0.3 to 0.4 mm) and the length (from 20 to 100 mm) of these capillaries, various flow rates could be selected: these remained practically constant over the short time of the used arc generation.

The communication line between the flasks and the cell was ensured by rubber tubing and a four-way stopcock (Fig. 3). The capillaries were placed between the cell and the four-way stopcock. A steady gas flow was maintained by an overpressure of a few cm H_2O, from a mercury-sealed gasometer. Between gasometer and cell, a water-sealed bubble-tube could be inserted to show the gas flow. The device complete with cell No. 8, is shown in Fig. 4.

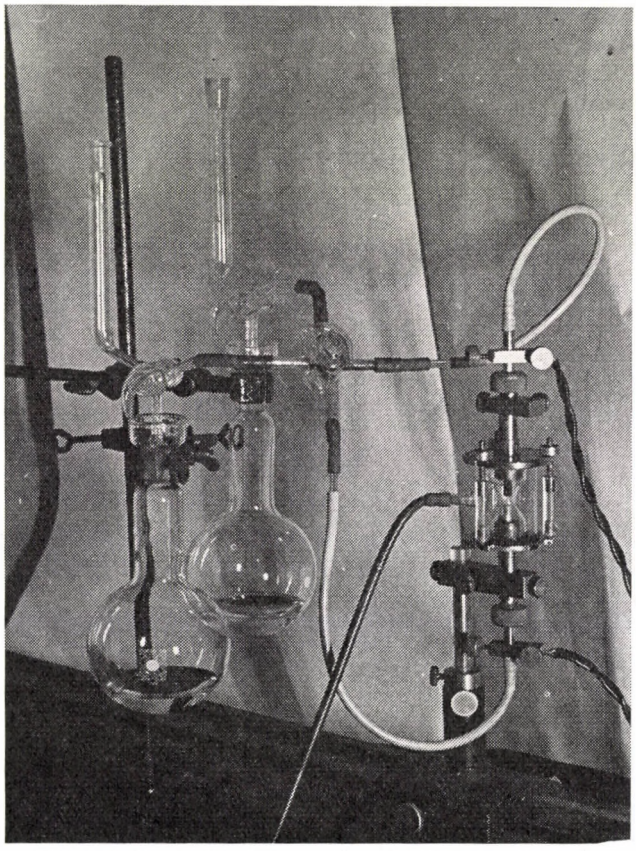

Fig. 4. Gas cell with reaction flasks assembled

Experimental conditions

Excitation: By an arc generator controlled also in the arc circuit (constructed by O. SZAKÁCS [11]).

Mains voltage 220 V.

Ignition at maximum voltage.

Control and polarization: by Thyratron valves and a Feussner motor, simultaneously.

Number of discharges: 50 sec^{-1} (0 + 1 arcs).

Average current: 12 A (short-circuit current in a complete period: 25 A).

Burning time of the arc: 8 sec.

Electrode pair. Normal, standard shape RW-II carbon electrode, diameter 6 mm, length 20 mm and 99.99% pure aluminium electrode.

Distances between the electrodes were 3, 5, and 8 mm, from test to test.

5 ml pentane was poured into each of the two 600 cm^3 flasks and, according to the amount of carbon dioxide expected, 5.00 to 25.00 cm^3 0.1*N* $Ba(OH)_2$ solution was allowed to flow underneath the pentane. After dilution with 50 cm^3 of boiled-out, hot distilled water, the flasks were evacuated with a water pump and cooled to room temperature. Then the apparatus was assembled. The gas cell and the connection tubing were flushed with carbon dioxide-free air from the gasometer, the flasks were short-connected with the four-way stopcocks, then the stop-cocks of the flasks were opened. Through an appropriate turning of the four-way stop-cock, the suction into the two flasks was brought to effect simultaneously and after about one second the arc was switched on for eight seconds. Suction was continued until the pressure in the flasks became equal to the atmospheric. The carbon dioxide content of the gas samples thus captured was determined according to a method described earlier [7].

Discussion

Based on earlier considerations, we supposed that a successful separation of the gases in the anode space from those in the cathode space would depend on the volume and shape of the gas cell, on the distance between the electrodes and on the rate of gas flow. Therefore, experiments were carried out first to establish the optimum values for these parameters. In early tests we used glass cells No. 1 and 2 (*cf.* Fig. 2), of about 25 cm^3 capacity each, and electrodes 5 and 8 mm apart. The gas flow rate at both exit ports was 910 $cm^3\ min^{-1}$. This value was chosen on the basis of the following considerations. In preliminary work we found that during the 8 sec burning time in air, the electric arc with an upper carbon anode (a.c. polarized excitation with a current of 12 A) produces 10 cm^3 of carbon dioxide. In the most unfavourable, but unlikely case that this carbon dioxide would form in 1/4 of the 8 sec burning time (a 0 + 1 arc ignited at peak voltage), *i.e.* in 2 sec, which would amount to a production of 300 cm^3 carbon dioxide per minute, the complete removal by suction would require a threefold amount of gas, *i.e.* 900 $cm^3\ min^{-1}$ at both sides of the electrodes.

The results obtained with an electrode gap of 8 mm and a 12 A arc are shown in Table I. All results are mean values of five parallel tests. Apart from some exceptions, single values deviate by less than 5% from the mean.

The separation ratio is defined as the amount of carbon dioxide from the carbon side divided by that from the aluminium side.

Table I

Effect of gas inlet position in the case of compact electrodes

Cell No.	CO_2 found (cm^3)			Separation ratio
	Carbon side	Aluminium side	Total	
1	3.66	1.43	5.09	2.6
2	3.58	0.87	4.45	4.1

Apparently owing to the more uniform flow of the gas, a better separation can be achieved with cell No. 2. The total amount of carbon dioxide produced is less because of direct cooling of the electrode by the gas stream. The substantial amount of carbon dioxide found on the aluminium side suggests that the flow and suction patterns in the cell do not ensure satisfactory separation.

In the following we used electrodes of the same size as before but each with a 2 mm bore drilled along its longitudinal axis; through this hole the gas was removed by suction from and into the flasks. This hole seemed suitable in so far as it did not cause a further pressure drop in the gas streams that pass the 0.4 mm capillaries used as flow regulators. As the gas cell, the 25 cm^3 glass vessel No. 4 (*cf.* Fig. 2) was used; into this, carbon dioxide-free air from the gasometer was fed through a lateral tube at the middle part of the cell. We employed an upper carbon anode and a lower aluminium cathode; this arrangement was adhered to in further work. Here too, a 5 mm gap between the electrodes was first tested. The results are:

carbon dioxide from the carbon side	4.88 cm^3
carbon dioxide from the aluminium side	1.40 cm^3
total carbon dioxide recovered	6.28 cm^3
separation ratio	3.5

As compared to previous results, these data do not show any substantial improvement in separation efficiency. Only the amount of carbon dioxide did increase owing to the fact that the drilled electrodes had smaller masses thus became more strongly incandescent in the arc. The poor separation was due to mixing by diffusion and convection, therefore, some improvement was expected from an increase of the electrode gap, though this would affect also plasma conditions. So tests were made both with a smaller (3 mm) and a greater gap (8 mm). With a 10 mm gap, the constant burning of the arc was impeded. The pertinent results together with the above data are shown in Table II.

Upon increasing the electrode gap, the amount of carbon dioxide produced also increases, owing to the change in the same direction of the amount of energy conveyed into the arc gap. The separation efficiency is also improved

Table II

Effect of the length of the electrode gap

Electrode gap	CO_2 found (cm^3)			Separation ratio
	Carbon side	Aluminium side	Total	
3 mm	2.99	1.10	4.09	2.7
5 mm	4.88	1.40	6.28	3.5
8 mm	7.95	2.21	10.16	3.6

since over a greater distance, gas exchange occurs to a smaller degree. Here the difference in this respect between the 5 mm and 8 mm gaps was not quite as pronounced as in subsequent tests, where we expected a stronger effect under other experimental conditions.

By using smaller cells, we tried to further reduce mixing of the gas. In a 17 cm^3 cell of the same shape as before (No. 4) but with electrodes 8 mm apart, separation became, in fact, better:

carbon dioxide from the carbon side	8.12 cm^3
carbon dioxide from the aluminium side	1.75 cm^3
total carbon dioxide recovered	9.87 cm^3
separation ratio	4.6

The total amount of carbon dioxide was essentially the same as before.

We also checked whether the gas flow rate used was sufficient for the removal of the carbon dioxide formed. By changing the dimensions of the capillaries acting as "valves" between the cell and the reactor flasks we obtained the results shown in Table III. For comparison, the above data are again included.

Table III

Effect of gas flow rate

Flow rate, $cm^3\ min^{-1}$	CO_2 found (cm^3)			Separation ratio
	Carbon side	Aluminium side	Total	
2×500	7.08	1.91	8.99	3.7
2×910	8.12	1.75	9.87	4.6
2×1100	8.58	2.23	10.81	3.8

This table shows that with the increase of air supply, the total amount of carbon dioxide formed increases in proportion to the enhanced oxygen supply. The separation efficiency passes through a maximum because at higher gas velocities, the stronger mixing effect brings more carbon dioxide over the aluminium electrode. This phenomenon can be observed visually: the arc burns at, and flares out from the electrode side away from the lateral feed-inlet tube. Using cell No. 5 (*cf.* Fig. 2) with gas inlets at two sides, the mixing effect is even stronger and the separation ratio drops to about 3.

The placing of the gas inlet farther from the middle part of the plasma seemed to be a better solution. Therefore, we tested the 17 cm^3 cell No. 6 (*cf.* Fig. 2) with electrode gaps of 5 and 8 mm. The results are shown in Table IV.

A further but still insufficient improvement can be noted. Also it is obvious that an 8 mm gap should be employed.

Also the bores through the electrodes were expected to affect the results. The corresponding data are collected in Table V; they show again that if the mass (wall thickness) of the electrode is decreased, the carbon electrode, owing to more intense incandescence, produces more carbon dioxide. From the viewpoint of gas removal and gas flow patterns, the 3 mm bore ensures the least mixing in cell No. 6. This finding was utilized in further tests.

We attempted to further increase the efficiency of separation by suppressing the mixing of the gas. By constricting the middle part of the cell to 10 mm and modifying the way of the air feed, a satisfactory arrangement was found. The results with cells Nos. 7, 3 and 8 (*cf.* Fig. 2) are shown in Table VI. These

Table IV

Results of tests with cell No. 6

Electrode gap	CO_2 found (cm^3)			Separation ratio
	Carbon side	Aluminium side	Total	
5 mm	6.28	1.23	7.51	5.1
8 mm	10.22	1.74	11.96	5.9

Table V

Effect of the hole diameter through the electrode

Bore diameter, mm	Thickness of electrode wall, mm	CO_2 found (cm^3)			Separation ratio
		Carbon side	Aluminium side	Total	
2.0	2.0	10.22	1.74	11.96	5.9
3.0	1.5	13.72	2.03	15.75	6.8
4.0	1.0	14.50	3.20	17.70	4.5

Table VI

Results with cells constricted at their middle heights

Cell	CO_2 found cm^3			Separation ratio
	Carbon side	Aluminium side	Total	
No. 7	10.31	1.06	11.37	9.7
No. 3	12.30	1.77	14.07	6.9
No. 8	10.61	0.85	11.46	12.5

three cells were made of quartz since glass was prone to cracking when so close to the arc. The capacity of cells No. 3 and 7 was 17 cm^3 each, the same as that of the inner compartment of cell No. 8.

Results with cell No. 7 showed that the constriction at the middle part of a cell did enhance separation as expected. However, the reduced mixing in the gas phase retards oxidation since the electrode side lying farther from the point of air intake is poorly supplied with oxygen. The two-sided air feed in cell No. 3 furnishes ample oxygen but again separation is worse owing to the more intense turbulence. The best separation was achieved with the double-wall gas cell No. 8. The advantage of this type of cell consists in the uniform supply of air entering at its top and bottom through six 1.5×2.0 mm holes arranged in a circle. Thus the one-sided burning of the arc is avoided, and the mixing of the gases from the anode and cathode spaces is reduced.

As already mentioned, in an arc that burns in air, a parallel reaction produces also nitrogen oxide which, by its reaction with barium hydroxide, interferes with the acidimetric determination of carbon dioxide. Nitrogen oxide is chiefly formed within the plasma [10], therefore, its removal by suction yields nearly equal amounts from both electrode side as confirmed by direct tests. The nitrogen oxide amounts to a few tenths of a cm^3 from each side and, though this hardly affects the accuracy of carbon dioxide determinations for the carbon side, it is nearly equal to the amount of carbon dioxide passed over to the aluminium side. Therefore, the results discussed up to now are to be regarded as relative values only. The true separation ratio in cell No. 8 was expected to be about 2 times higher. This was checked by the use of this latter cell and the results with a feed mixture of 20% oxygen and 80% argon have confirmed this assumption. The experimental conditions were as follows:

Excitation: A.C. polarized arc,
Burning time: 8 sec,
Ignition: at peak voltage,
Number of discharges: 0 + 1,
Type of cell: No. 8,
Electrode pair: upper carbon anode, lower aluminium cathode,
Electrode gap: 8 mm,
Hole drilled along the longitudinal axis of the electrodes: 3 mm in diameter,
Mean current: 13 A (short-circuit current over the entire period: 27 A),
Gas atmosphere: 20% O_2 + 80% Ar,
Gas flow rate: 2×910 cm^3 min^{-1}.

The results:

CO_2 from the carbon electrode side:	7.16 cm^3,
CO_2 from the aluminium electrode side:	0.27 cm^3,

Total CO_2 found	7.43 cm^3,
Separation ratio:	26.5.

This ratio shows that only 3.6% of the total carbon dioxide formed in the arc passed over to the aluminium side. Thus the systematic error of this separation method under the given experimental conditions is 3.6%.

A further study of this method and its applications will be described in a forthcoming paper.

REFERENCES

1. SZABÓ, Z. L., SZAKÁCS, O.: Acta Chim. (Budapest), **73,** 115 (1972)
2. SZABÓ, Z. L., TÖRÖK, T.: Acta Chim. (Budapest), **73,** 125 (1972)
3. SZABÓ, Z. L., TROMLER, J., LÁNYI, K. TH. I., TÓTH, I.: Acta Chim. (Budapest), **73,** 135 (1972)
4. SZABÓ, Z. L., TÓTH, I.: Acta Chim. (Budapest), **73,** 257 (1972)
5. SZABÓ, Z. L., TÓTH, I.: Acta Chim. (Budapest), **73,** 267 (1972)
6. SZABÓ, Z. L., TÓTH, I.: Acta Chim. (Budapest), **73,** 275 (1972)
7. SZABÓ, Z. L., TÓTH, I.: Acta Chim. (Budapest), **73,** 363 (1972)
8. SZABÓ, Z. L., TÓTH, I.: Acta Chim. (Budapest), **73,** 373 (1972)
9. SZABÓ, Z. L., TÓTH, I.: Acta Chim. (Budapest), **73,** 387 (1972)
10. SZABÓ, Z. L., TÓTH, I.: Acta Chim. (Budapest), **75,** 217 (1973)
11. SZAKÁCS, O.: Proc. of the Coll. Spectr. Intern., p. 997, Debrecen, 1967

Zoltán László SZABÓ
László PÖPPL
1088 Budapest, Múzeum krt. 4/b.

Acta Chimica Academiae Scientiarum Hungaricae, Tomus 76 (2), pp. 193—199 (1973)

SOME CHEMICAL REACTIONS OF THE ELECTRODE GAP AND THEIR ROLE IN SPECTROCHEMICAL ANALYSIS, XII

SEPARATION OF THE REACTIONS IN THE ANODE AND CATHODE SPACES. EFFECT OF THE DIRECTION OF GAS FLOW, OF THE POLARITY AND POSITION OF THE ELECTRODES

Z. L. SZABÓ and L. PÖPPL

(Institute of Inorganic and Analytical Chemistry, L. Eötvös University, Budapest)

Received February 28, 1972

A study of our separation method has shown that the amount of carbon dioxide formed, and the possibility of separation depend on the polarity of the electrodes and on their position. The primary effect must be ascribed to the direction of the gas stream (to or from the anode), it being modified by the upwards convection of hot gases. From a comparison of data referring to air and to a mixture of argon and oxygen, information about the nitrogen-oxygen reactions can be obtained.

In the preceding paper [1] of this series we have reported on a method developed for the separate study of the gaseous reaction products formed simultaneously in the anode and in the cathode spaces. For a further study of the method, and of the phenomena involved, it was necessary to examine the effects of the direction of gas flow, of the upward convection of hot gases, of the polarity of the carbon electrode and of its position. In these tests carbon dioxide free air or a mixture of 20% oxygen and 80% argon were used.

Effects of the Direction of Gas Flow, and of the Upward Convection of Heat

The electrode holder, already described [1], was used with a gas cell. The gas cell was a glass tube 50 mm in length, with an inner diameter of 24 mm, its volume being about 22 cm^3. The experimental conditions were as follows.

Excitation: Polarized A.C. arc excitation.

Ignition at peak voltage.

Discharge number: 0 + 1.

Average current: 12 A (short circuit current in a complete period: 25 A).

Electrode pair: RW—II type carbon electrodes 6 mm in diameter and 20 mm long, each with a 2 mm hole drilled along its longitudinal axis.

Electrode gap: 5 mm.

Air flow rate: 910 $cm^3\ min^{-1}$.

The gap and hole dimensions previously stated as optimum values we decreased to the above values in order to avoid overheating the electrodes

and thus make the variations in the small amounts of carbon dioxide formed more noticeable. The two carbon electrodes were placed so that alternately the upper and the lower one could be used as the anode. The air was introduced through the hole of the lower electrode and exhausted through that of the upper electrode, or the other way round. Thus four possible variants were realized. The carbon dioxide formed in the arc discharges was determined by titrimetric gas analysis as described previously [2]; the results shown in Table I represent mean values of five tests.

The differences between the values shown are due to three effects, *viz.* to the CO_2-removing and O_2-supplying effect of the gas stream, to the heating and convection effect of the gases moving upwards, and to the cooling effect of the gas stream. The last is, perhaps, of secondary importance since the gas flow rates were the same in all four cases thus the cooling effect could not have been very different from case to case. If the data of Table I are arranged in increasing order, it becomes apparent that a decisive role can be attributed to the circumstance whether, through the electrode hole, the air flow removes carbon dioxide from the more strongly heated anode space which, therefore, produces more carbon dioxide and replenishes it with oxygen-rich gas, or thə air flow carries the carbon dioxide containing gas to the surface and into ths hole of the anode. This effect is modified by the upward flow of heat in so far ae

Table I

Effect of the direction of gas flow

Gas introduced through	CO_2 (cm^3) found	
	upper carbon anode	lower carbon anode
lower electrode	7.6	9.5
upper electrode	8.3	7.8

Table II

Effect of the direction of gas flow

Direction of gas flow relative to the anode		Direction of upward heat flow relative to the anode	Total of negative signs	CO_2 found (cm^3)
−	−	−	3	9.3
−	−	+	2	8.3
+	+	−	1	7.8
+	+	+	0	7.6

it either helps the removal of carbon dioxide or works against it. If the direction of CO_2-containing air flowing away from the anode is marked by a minus sign whereas that of the flow towards the anode by a plus sign, and, for the purposes of illustration, the gas flow with the stronger effect is given a two-fold weight relative to the ascending flow of heat, then we obtain the same sequence as that of the experimental values (Table II).

These results have been verified by tests in a cell provided with a lateral tube at its middle height (*cf.* previous paper, Fig. 2, cell No. 1). Here the air was admitted in two streams each through one of the holes in the electrodes and removed through the lateral tube, or this direction of flow was reversed. The gas flow rate way adjusted to 910 $cm^3\ min^{-1}$ per electrode to allow comparisons. The data for the four possible cases are shown in Table III.

Table III

Effects of the position (polarity) of the electrode and of the direction of gas flow

Air introduced through	CO_2 (cm^3) found	
	upper carbon anode	lower carbon anode
electrodes	11.8	10.1
lateral tube	10.7	9.8

The results in Table III show that, for electrodes arranged similarly, more carbon dioxide is always formed at electrodes through the holes of which oxygen is being supplied. This reveals that near the front surface of the electrode some oxidation takes place also in the hole, and the more oxygen is carried by the gas, the more carbon dioxide is produced. If the supply stream passes through the plasma, it becomes depleted in oxygen and enriched with carbon dioxide when arriving at the comparatively cooler parts of the electrode hole. This would further decrease the reactivity which is small already. If an oxygen-rich gas mixture enters the hole, appreciable oxidation may occur even at sites of very low reactivity. To this effect will be added the heating of the upper electrode by ascending hot gases.

Separation of the Electrode Spaces Studied by Varying the Position and Polarity of the Carbon Electrode

In possession of the above facts and of the optimum conditions of separation [1], we studied how the amount of carbon dioxide and the efficiency of separation depend on the polarity and position of the carbon electrode in the case of carbon–aluminium electrode pair. Thus, in comparison to previous ex-

perimental conditions, the electrode material was changed, the electrode gap was fixed at 8 mm, and electrodes with 3 mm holes were used. Two series of tests were carried out, one with excitation in carbon dioxide free air (Table IV) and one with excitation in a mixture of 20% oxygen and 80% argon (Table V). As for the position and polarity of the carbon electrode, here also four variants could be realized.

In air, as known, also nitrogen oxide is formed which falsifies the results of the acidimetric determination of carbon dioxide. This interference is considerable and causes greater relative errors in the analyses on the aluminium side. Consequently, the experimental results obtained in air are to be regarded as indicative only, however, they do not influence the direction of the effects studied, but reduce the "apparent efficiencies" of the separations.

From separate consideration of Tables IV and V, the following conclusions can be drawn.

Table IV

Effect of the position and polarity of the carbon electrode in air

Position and polarity of the carbon electrode	CO_2 found (cm^3)			Separation ratio*
	carbon side	aluminium side	total	
upper, anode	10.6	0.85	11.5	12.5
lower, anode	9.6	0.82	10.4	11.7
upper, cathode	2.68	0.56	3.24	4.8
lower, cathode	2.36	0.71	3.07	3.3

* The separation ratio is the quotient of the amounts of carbon dioxide from the two electrodes [1].

Table V

Effect of the position and polarity of the carbon electrode in a gas mixture of 20% oxygen and 80% argon

Position and polarity of the carbon electrode	CO_2 found (cm^3)			Separation ratio*
	carbon side	aluminium side	total	
upper, anode	7.2	0.27	7.5	26.5
lower, anode	6.2	0.35	6.6	17.8
upper, cathode	1.51	0.19	1.70	7.9
lower, cathode	1.18	0.32	1.50	3.7

* The separation ratio is the quotient of the amounts of carbon dioxide from the two electrodes [1].

As already found in earlier experiments [2—4], a carbon anode produces more carbon dioxide than does a carbon cathode in the same position, because the anode is heated more strongly and the positive polarity favours oxidation reactions.

Owing to the upward flow of heat, if polarities are the same, it is always the upper carbon electrodes that is heated to incandescence and is oxidized to a greater degree.

Ascending hot gases not only heat the upper electrode but, through convection of gases, carry part of the carbon dioxide formed upwards and this considerably affects the separation efficiency. It is the quantity of carbon dioxide carried over to the aluminium side in which this causes the relatively greater difference, as unequivocally shown by the data pertinent to aluminium electrodes of the same polarity but different positions.

The degree of separation depends also on the amount of carbon dioxide formed: when this is greater, the separation ratio also increases. However, the relationship is not linear, which suggests that certain parts of the electrode surface are not exposed to the convection (chiefly the inner side of the hole and, on the cylinder surface, areas farther from the front surface of the electrode) and, on the other hand, that carbon dioxide is formed not only on the surface of the electrode.

On comparing the amounts of carbon dioxide formed in the two kinds of gas atmosphere it is apparent that in air anodic polarization produces 1.56 (1.54 and 1.58) times and cathodic polarization 2.0 (1.93 and 2.05) times more carbon dioxide than in the oxygen–argon mixture with the same percentage of oxygen in it as in air. Since the flow rate and oxygen content of the two gas mixtures were the same, the cause of this difference must be sought in the behaviour of the other reaction partner, *i.e.* the carbon electrode, in differences of the physical character of the gas atmosphere and in the state of the plasma. On arc excitation in oxygen–argon mixtures the evaporation of aluminium is less intense than in air and, therefore, at equal currents the mean temperature of the plasma is higher in oxygen–argon mixtures and the spectrum is more spark-like [8, 3]. In the same way, the destruction of the carbon electrode material should be less. Taking into account the poor heat conductivity of argon, the precondition of this is, of course, that the electrode-cooling effect of the gas should be of minor importance. The experimental data support this. The data and the separation ratios shown indicate also that most of the carbon dioxide is formed on the surface of the carbon electrode and only a smaller part of it in the plasma sheath (aureole). Other authors [6] have found that in the presence of nitrogen oxide a greater number of oxygen atoms is produced by the arc. Consideration of this finding prompts the suggestion that also the reaction here discussed is partially controlled by the amount of atomic oxygen present. In the anodic case when the carbon electrode gets appreciably incan-

descent and carbon dioxide formation is more extensive, the effect of the gas atmosphere is smaller, in accord with the circumstance that, on more intense evaporation, the side-effects gradually loose their importance [4, 7].

From the factors of 1.56 and 2.0 for the deviation in the formation of total carbon dioxide, an approximate calculation gives the actual efficiency of separation also for the cases when air is used in the cell. Disregarding the differences in physical and chemical effects due to the different gas atmospheres, and considering the absolute amount of mass transfer by diffusion and convection to be proportional to the amount of carbon dioxide formed, as a first approximation we may use the factors 1.56 and 2.0 for a calculation of the values to be expected in air from values noted for the aluminium side in the oxygen–argon mixture. In this way the following results are obtained:

Table VI

Separation ratios calculated and found

Position and polarity of the carbon electrode	Separation ratio	
	in the oxygen--argon mixture	calculated for air
upper, anode	26.5	25.5
lower, anode	17.8	17.4
upper, cathode	7.9	7.5
lower, cathode	3.7	3.7

upper anode: 0.42 cm^3 carbon dioxide,
lower anode: 0.55 cm^3 carbon dioxide,
upper cathode: 0.36 cm^3 carbon dioxide,
lower cathode: 0.64 cm^3 carbon dioxide.

With these values we can calculate the separation ratios, disregarding the few tenths of a cubic centimeter of nitrogen oxide in the side of the carbon electrode which accompany also the greater amounts of carbon dioxide. In this way the values presented in Table VI are obtained; they agree fairly well with the results found in tests with the oxygen–argon mixture.

Some informative data for the nitrogen–oxygen reaction can also be obtained from the separation ratios in argon–oxygen mixtures and from the values noted for the two electrode sides in air. Though previous findings [5] suggest that nitrogen oxide production is not the same on the carbon and the aluminium sides, as a simplifying assumption we considere these to be equal.

Now, dealing with the aluminium side only, we obtain (showing the lower aluminium cathode instead of the corresponding upper carbon anode):

lower cathode: 0.86 cm^3 nitrogen oxide,
upper cathode: 0.54 cm^3 nitrogen oxide,
lower anode: 0.40 cm^3 nitrogen oxide,
upper anode: 0.20 cm^3 nitrogen oxide.

It is of interest to note that the total amount (1.06 cm^3) of nitrogen oxide calculated for the lower aluminium cathode and upper aluminium anode agrees quite well with the total amount (0.94 cm^3) of nitrogen oxide calculated for the upper cathode and lower anode, and the average value of the four data is 0.50 cm^3. This value agrees well with our single direct measurement according to which, on the carbon anode side 0.51 cm^3, and on the aluminium cathode side 0.62 cm^3, altogether 1.13 cm^3, of nitrogen oxide was formed. However, these findings may only serve as a starting point for a further and more detailed study of the oxygen–nitrogen reaction.

REFERENCES

1. SZABÓ, Z. L., PÖPPL, L., Acta Chim. (Budapest), **76,** 183 (1973)
2. SZABÓ, Z. L., TÓTH, I.: Acta Chim. (Budapest), **73,** 363 (1972)
3. SZABÓ, Z. L., TÓTH, I.: Acta Chim. (Budapest), **73,** 373 (1972)
4. SZABÓ, Z. L., TÓTH I.: Acta Chim. (Budapest), **73,** 387 (1972)
5. SZABÓ, Z. L., TÓTH. I.: Acta Chim. (Budapest), **75,** 217 (1973)
6. TAGGART, F. K. Mc.: Plasma Chemistry in Electrical Discharges, Elsevier Publ. Co. Inc., New York 1967
7. SZABÓ, Z. L., TÓTH, I.: Acta Chim. (Budapest), **73.** 267 (1972)
8. SZABÓ, Z. L., TÓTH, I.: Acta Chim. (Budapest), **73,** 257 (1972)

Zoltán László SZABÓ
László PÖPPL
1088 Budapest, Múzeum krt. 4/b.

Acta Chimica Academiae Scientiarum Hungaricae, Tomus 76 (2), pp. 201—205 (1973)

ZUR BESTIMMUNG VON RESTGEHALTEN (BASISVERUNREINIGUNGEN) IN DER EMISSIONSSPEKTRALANALYSE

G. HAUPTMANN, M. HAUPTMANN und G. JÄGER

(VEB Petrolchemisches Kombinat Schwedt, Kombinatsbetrieb Zeitz, Direktionsbereich Forschung)

Eingegangen am 10. April 1972

Nach einem kurzen Überblick über Methoden, die aus der Literatur bekannt sind, wird auf ein Verfahren von KEREKES-CSÉTI näher eingegangen. Es wird eine Empfehlung gegeben, in welchem Fällen graphische oder rechnerische Verfahren anzuwenden sind.

1. Überblick über bekannte Verfahren

Im Gegensatz zu »gewöhnlichen« spektroskopischen Arbeiten zeichnet sich die Restgehaltbestimmung durch die Besonderheit aus, daß eine größere Zahl von Meßwerten (Einwaagen, Schwärzungs- oder Intensitätsmessungen) zu einem Ergebnis führt, das in einer einzigen Konzentrationsangabe besteht. Dies bedingt eine notwendige Verflechtung mit mathematischen Methoden. Will man zusätzlich zum eigentlichen Ergebnis Angaben über die mögliche Fehlerhaftigkeit bzw. über die Vertrauenswürdigkeit haben, so steigt der mathematische Aufwand rasch an, und es ist nicht immer leicht, die Vor- und Nachteile bestimmter Verfahren zu erkennen.

Generell kann man die in der Literatur [1—15] beschriebenen Verfahren in graphische und numerische unterteilen. Da graphische Verfahren den Vorteil der Anschaulichkeit haben, ist es kein Zufall, daß das erste bekannte Verfahren [1] ein graphisches ist. Auch der Zeitpunkt der Veröffentlichung (1938) ist nicht ganz zufällig; in den dreißiger Jahren führten sich emissionsspektralanalytische Methoden als Routinemethoden ein.

PIERCE und NACHTRIEB [2] wiesen darauf hin, daß der Restgehalt zu hoch bestimmt würde, wenn die Untergrundintensität unberücksichtigt bliebe.

Die erste umfangreichere Arbeit stammt von GATTERER [3]. Hier wird deutlich der Grundgedanke des Additionsverfahrens ausgesprochen, daß man zur Restkonzentration, die bestimmt werden soll, Zusätze in der gleichen Größenordnung zufügen muß, um einen deutlichen Effekt zu erzielen, wobei jedoch die Wirkung der Restkonzentration noch merklich und somit meßbar sein muß. Es werden sodann zwei graphische Verfahren geschildert, von denen das eine nur auf Schwärzungsmessungen beruht (ohne Kenntnis der Anstiege der Schwärzungskurve und der Eichkurve; der Anstieg der Eichkurve wird im Verlauf des Verfahrens bestimmt); das zweite basiert (wegen des nicht ganz

gradlinigen Verlaufs der Schwärzungskurven) auf der Konstruktion der Schwärzungskurve mit Hilfe eines Stufenfilters. Beide Verfahren sind auch rein rechnerisch anwendbar.

Von EICHHOFF und MAINKA [4] werden die Additionsverfahren als leitprobenfreie Verfahren schlechthin empfohlen. Der Begriff »leitprobenfrei« scheint uns jedoch nicht zweckmäßig, weil man darunter nur das Arbeiten mit Haupteichkurven verstehen sollte. Die gleiche Arbeit [4] enthält eine Weiterentwicklung des Verfahrens von GATTERER [3] und einen Versuch zur Berechnung des Fehlers der Restgehaltbestimmung, der allerdings nicht die gewünschte Übereinstimmung mit dem Experiment ergab.

Von ADDINK [5] wird darauf hingewiesen, daß das Additionsverfahren nur dann angewandt werden darf, wenn das zu bestimmende Element aus der Probe unter den gewählten Bedingungen in gleicher Weise verdampft und angeregt wird wie aus der zugefügten Menge.

Wegen seiner Einfachheit wurde von uns versuchsweise das (numerische) Verfahren von KEREKES-CSÉTI [13] auf ein praktisches Problem angewandt. Dabei stellte sich heraus, daß es (wie alle numerischen Verfahren) Voraussetzungen erfordert, die nicht immer erfüllbar sind, worauf hier kurz eingegangen werden soll. (Es wird aus Gründen der Verständlichkeit nicht genau die Nomenklatur der Autorin verwendet).

2. Bemerkungen zum Verfahren von Kerekes-Cséti

Das Verfahren basiert auf folgenden Überlegungen: Wenn c_x die zu bestimmende Restkonzentration darstellt, c_1 bis c_3 die (in bekannter Menge zugegebenen) Zusätze, ΔS_1 bis ΔS_3 die entsprechenden Schwärzungsdifferenzen zwischen Analysen- und Vergleichslinie, u und v den Anstieg bzw. das absolute Glied der Gleichung für den geraden Teil der Eichkurve, so gibt

$$\Delta S_1 = u \log (c_1 + c_x) + v \tag{1a}$$

$$\Delta S_2 = u \log (c_2 + c_x) + v \tag{1b}$$

$$\Delta S_3 = u \log (c_3 + c_x) + v \tag{1c}$$

Durch Subtraktion, Division und Umformung kann man daraus erhalten

$$\left(1 + \frac{c_2 - c_1}{c_x + c_1}\right)^a = 1 + \frac{c_3 - c_1}{c_x - c_1} \tag{2}$$

wobei

$$a = \frac{\Delta S_3 - \Delta S_1}{\Delta S_2 - \Delta S_1} \tag{2a}$$

ist.

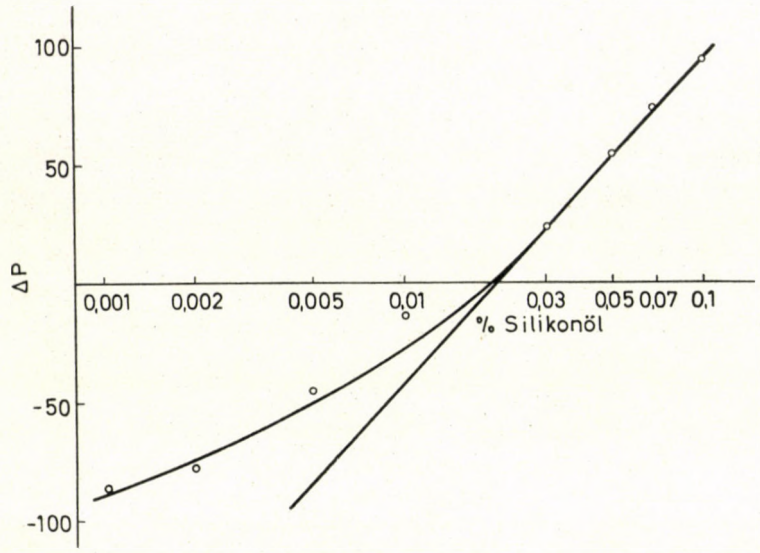

Abb. 1. Restgehaltbestimmung nach DUFFENDACK und WOLFE ($c_x = 0{,}0037\%$)

Wenn $c_2 \leqq 2c_1$ ist, so daß der Ausdruck $c_2 - c_1/c_x + c_1 < 1$ bleibt, so kann die linke Seite der Gleichung 2 in Reihe entwickelt werden. Vernachlässigt man die Glieder von höherer Ordnung als zwei, so erhält man

$$c_x = \frac{1}{2} \frac{a(a-1)(c_2-c_1)^2}{c_3 - c_1 - a(c_2-c_1)} - c_1 . \tag{3}$$

In der Arbeit [13] wird sodann mathematisch begründet, daß der Fehler für c_x bei $c_1 : c_2 : c_3 = 1 : 2 : 3$ und bei $a = 1{,}6$ am kleinsten ist.

Wir möchten dem hinzufügen, daß sich bei Einhaltung des Verhältnisses $c_1 : c_2 : c_3 = 1 : 2 : 3$ die Gleichung 3 vereinfachen läßt zu

$$c_x = c_1 \left[\frac{a(a-1)}{2(2-a)} - 1 \right]. \tag{4}$$

Man arbeitet also trotz des vorausgehenden mathematischen Aufwandes nach einer auffallend einfachen Gleichung. Während nun aber die Forderung $c_1 : c_2 : c_3 = 1 : 2 : 3$ leicht erfüllbar ist, liegt ein Nachteil des Verfahrens darin, daß die Größe a, deren Wert nur von den Schwärzungen der Analysen- und Vergleichslinien in den Spektrogrammen der drei Proben abhängt, eben nicht immer gleich 1,6 sein wird. Eine Änderung der Anregungs-, Aufnahme- und Entwicklungsbedingungen oder die Variierung anderer Parameter wie z. B. der Vergleichsintensität, wodurch evtl. der Wert $a = 1{,}6$ annähernd erreich-

bar wäre, bedeuten aber Eingriffe in das spektrochemische Verfahren, die unzulässig sind, weil dadurch u. U. der Fehler der Messungen stark ansteigen kann. Es ist auch anzunehmen, daß schon geringfügige Abweichungen vom Idealwert 1,6 beträchtliche Fehler verursachen, da man schon für alle Werte $a \geqq 2$ physikalisch sinnlose Ergebnisse erhält, wovon man sich anhand von Gleichung 4 leicht überzeugen kann. Einen schwer abschätzbaren, starken Einfluß hat auch die Wahl von c_1, durch die festgelegt wird, welcher Abschnitt der Eichkurve benutzt wird. Nach unserer Erfahrung erhält man für c_x zu niedrige Werte, wenn c_1 zu klein gewählt wird und zu große Werte, wenn c_1 zu groß gewählt wird.

Die Problematik sei abschließend an einem Beispiel demonstriert: Zur Herstellung von Eichproben für die spektrochemische Bestimmung von Silikonöl in Mineralölen [16] stand uns zeitweise kein absolut silikonölfreies Mineralöl zur Verfügung. Zur Bestimmung der »Basisverunreinigung« wandten wir das (graphische) Verfahren von DUFFENDACK und WOLFE [1] und das (numerische) Verfahren von KEREKES-CSÉTI [13] an. Nach dem graphischen Verfahren (siehe die Abbildung) ergibt sich eine Basisverunreinigung von 0,0037%.

Beim numerischen Verfahren ist das Ergebnis jedoch stark davon abhängig, in welchem Konzentrationsbereich man arbeitet. Wählt man z. B. $c_1 = 0{,}001\%$, so sind

$$\begin{aligned} c_1 &= 0{,}001\% \qquad \Delta P_1{}^* = -87 \\ c_2 &= 0{,}002\% \qquad \Delta P_2 \;\; = -72 \\ c_3 &= 0{,}003\% \qquad \Delta P_3 \;\; = -62 \end{aligned}$$

Nach Gleichung 2a ergibt sich $a = 1{,}67$, nach Gleichung 3 oder 4 erhält man $c_x = 0{,}00069\%$.

Wählt man $c_1 = 0{,}005\%$, so sind

$$\begin{aligned} c_1 &= 0{,}005\% \qquad \Delta P_1 = -48 \\ c_2 &= 0{,}010\% \qquad \Delta P_2 = -25 \\ c_3 &= 0{,}015\% \qquad \Delta P_3 = \;\; -\;\; 9 \end{aligned}$$

Nach Gleichung 2a ergibt sich $a = 1{,}70$, nach Gleichung 3 oder 4 erhält man $c_x = 0{,}0049\%$.

Wählt man $c_1 = 0{,}01\%$, so sind

$$\begin{aligned} c_1 &= 0{,}01\% \qquad \Delta P_1 = -25 \\ c_2 &= 0{,}02\% \qquad \Delta P_2 = \;\; 3 \\ c_3 &= 0{,}03\% \qquad \Delta P_3 = \;\; 23 \end{aligned}$$

* Es wurde mit der $P_{1/2}$-Transformation gearbeitet. Die P-Werte der Analysenlinie sind in bezug auf den Untergrund korrigiert.

Nach Gleichung 2a ergibt sich $a = 1{,}72$, nach Gleichung 3 oder 4 erhält man $c_x = 0{,}012\%$.

Es zeigt sich, daß man nur im mittleren Konzentrationsbereich ein Ergebnis erhält, das dem Ergebnis nach dem Verfahren von DUFFENDACK und WOLFE nahekommt.

3. Schlußfolgerungen

Wie schon von GATTERER [3] vor längerer Zeit erwähnt wird, ist bei der Anwendung numerischer Verfahren zur Restgehaltsbestimmung die Gefahr besonders groß, daß bestimmte Voraussetzungen (z. B. konstanter Anstieg für Schwärzungs- und Eichkurve) nicht ausreichend erfüllt sind, was bei Nichtbeachtung zu falschen Ergebnissen führt. Diese Erfahrung bestätigte sich auch bei der Anwendung eines neueren numerischen Verfahrens [13].

Es ist deshalb zu empfehlen, bei der erstmaligen Ausführung einer Restgehaltbestimmung, bzw. falls solche Bestimmungen selten durchzuführen sind, unbedingt ein graphisches Verfahren zu verwenden. Vor der Anwendung rechnerischer Verfahren ist genau zu prüfen, ob alle Voraussetzungen dafür erfüllt sind.

LITERATUR

1. DUFFENDACK, O. S., WOLFE, R. A.; Industrial and Engineering Chem. (An. Ed.) **10,** 161 (1938)
2. PIERCE, W. C., NACHTRIEB, N. H.: dito **13,** 774 (1941)
3. GATTERER, A.: Spectrochim. Acta **1,** 513 (1941)
4. EICHHOFF, H. J., MAINKA, E.: Mikrochim. Acta 1955, 298
5. ADDINK, N. W. H.: Mikrochim. Acta 1955, 703
6. CSÉTI, S.: Acta Chim. Acad. Sci. Hung. **10,** 307 (1956)
7. ROSENDAHL, F.: Spectrochim. Acta **10,** 201 (1957)
8. THIEME, O.: Chem. Technik **11,** 151 (1959)
9. RUBINSTEJN, R. N.: Zavod. Labor. **25,** 308 (1959)
10. NALIMOV, V. V.: Zavod. Labor. **27,** 861 (1961)
11. PLŠKO, E., PROKS, J.: Acta Chim. Acad. Sci. Hung. **30,** 267 (1962)
12. TÖRÖK, T.: Chemia Analytyczna **7,** 47 (1962)
13. KEREKES-CSÉTI, S.: Acta Chim. Acad. Sci. Hung. **35,** 377 (1963)
14. PLŠKO E. Acta Chim. Acad. Sci. Hung. **41,** 373 (1964)
15. TÖRÖK T.: Acta Chim. Acad. Sci. Hung. **49,** 11 (1966)
16. HAUPTMANN, G., KEIL, G., EBERHARDT, E., Schmierstoffe und Schmierungstechnik **29,** 38 (1968)

Gerhart HAUPTMANN
Marianne HAUPTMANN
Günter JÄGER

VEB Petrolchemisches Kombinat Schwedt
VEB Kombinatsbetrieb Zeitz 49 Zeitz 2 DDR.

Acta Chimica Academiae Scientiarum Hungaricae, Tomus 76 (2), pp. 207—215 (1973)

ON THE DIELECTRIC RELAXATION OF *n*-PENTANOL IN THE LIQUID PHASE

J. Liszi

(Department of Physical Chemistry, University of Veszprém, and Electrochemical Researc Group, Hungarian Academy of Sciences, Veszprém)

Received January 24, 1972

The dielectric relaxation of *n*-pentanol has been investigated in the liquid phase between −60°C and +60 °C within the frequency range from 300 kHz to 250 MHz. In this frequency range, the first absorption region of *n*-pentanol is exhibited, for which the value of Cole-Davidson's α parameter was found to be 0.5. The average enthalpy of activation is 6.7 kcal/mole. The enthalpy of activation of *n*-alcohols has been correlated to the number of carbon atoms *(n)*;

$$\Delta H^*(\text{kcal/mole}) = 7.72 \ln n + 1.35$$

The change of the enthalpy of activation with the number of carbon atoms allows to conclude that relaxation in this frequency domain is caused by molecular units.

The investigation of dielectric properties gives often valuable informations on the structure of liquids [1]. In the course of these investigations both the statical dielectric constant [2—4] and dielectric relaxation processes [5—7] are made use of. References cited above indicate that small electric field strengths are applied in general recently, however, attention has been directed also to the investigation of dielectric saturation [8, 9].

There are only a few publication, which report on the investigation of the dielectric properties of liquid alcohols in a relatively broad temperature and frequency range.

In the present paper the complex dielectric constant on *n*-pentanol is studied in the temperature range from −60 °C to +60 °C in the frequency domain from 300 kHz to 250 MHz. The Cole—Davidson [1] α-parameter and the Arrhenius activation energy [1] were determined for n-pentanol and a relationship was found between the number of carbon atoms of aliphatic alcohols and the activation energy of their relaxation processes.

Results

n-Pentanol A.G., was distilled on a column of 20 theoretical plates, and the middle fraction (b.p. 138 °C, a refractive index $n_D(20) = 1.4100$) was used for the investigations. Special thermostated cells, made of stainless steel, were used. Measurements were carried out by the bridge method. Specification of the bridges used are listed in Table I.

Table I

Bridge	Frequency range
Dielectric coefficient and loss factor testing set, Tr—9701	300 kHz $\leq$
Siemens, Scheinwiederstandsmessbrücke, Rel. 3 R 277	1 MHz $\leq$
Radelkis Universal Dielectrometer, Type: OH—301	3 MHz
Wayne Kerr, V.H.F. Admittance bridge, Type B 901	50—250 MHz

With the first three bridges listed in Table I, the static dielectric constant has been measured. (At 3 MHz frequency, there was a deviation from the static dielectric constant only below —40 °C). Our results are shown in Tables II and III, and Figs 1 and 2. Denotations used in the tables and the figures are as follows:

t — temperature (°C), ε°—static dielectric constant,
ε' — the real part of the complex dielectric constant,
ε'' — the imaginary part of the complex dielectric constant.

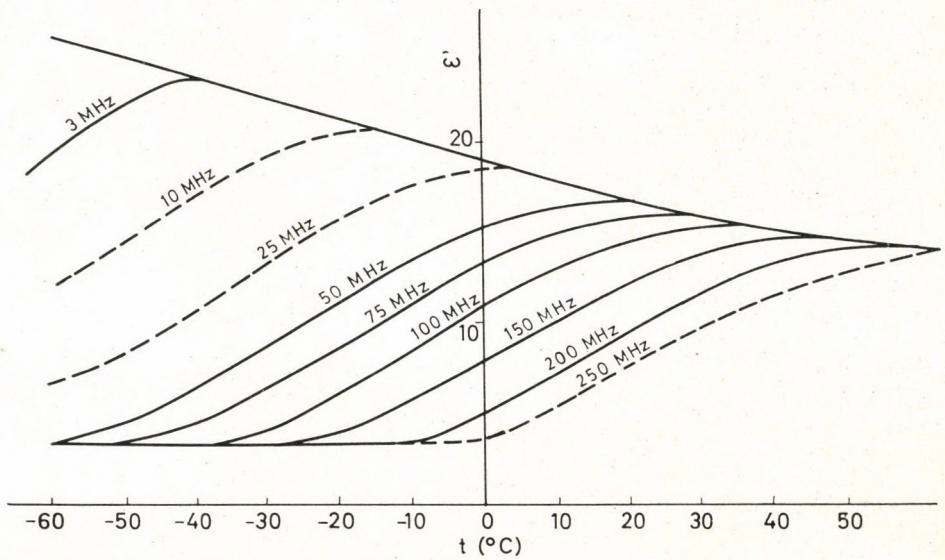

Fig. 1. The real part of the dielectric constant of *n*-pentanol as a function of frequency and temperature

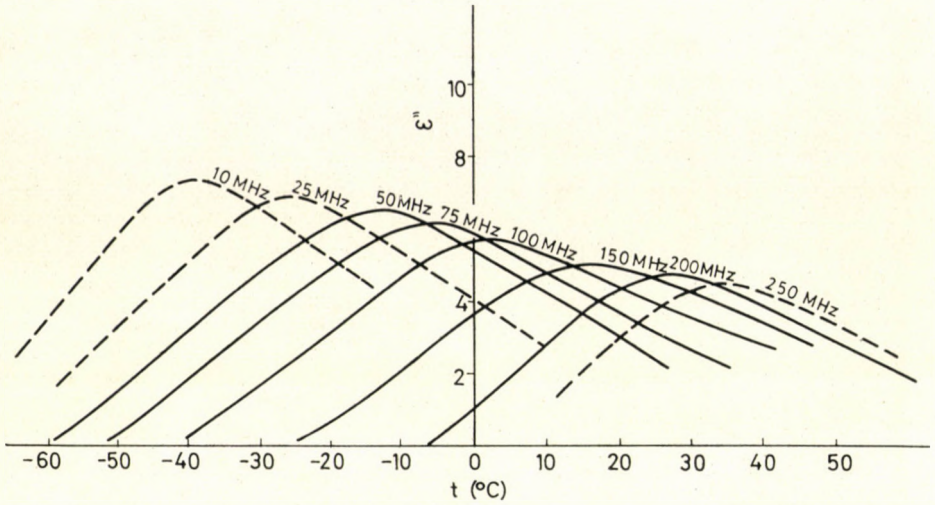

Fig. 2. The imaginary part of the dielectric constant of *n*-pentanol as a function of frequency and temperature

The complex dielectric constant (ε^*) can be expressed as follows

$$\varepsilon^* = \varepsilon' - j\varepsilon'' \tag{1}$$

where j is the imaginary unit. Data listed in Table II were obtained by the graphical interpolation of a great number of data. The dielectric constant has been determined a temperature intervals of 2° C, but for the sake of briefness, values are given only per 10 °C intervals.

In Figs 1 and 2 dotted lines represent calculated values.

Discussion

The classical theory of DEBYE [1], gives the following relationship between the complex dielectric constant frequency:

$$\frac{\varepsilon'' - n^2}{\varepsilon^\circ - n^2} = \frac{1}{1 + j\omega\tau}. \tag{2}$$

In Eq. (2) ε° is the static dielectric constant, ω the angular frequency, τ the macroscopic relaxation time, n^2 the square of the refractive index referred to infinite wavelength, which includes the effect of electron and atomic polarisation, but is independent of the orientation polarisation. Eq. (2) is not valid for associative liquids, particularly for those composed of molecules containing hydroxy groups. (The deformation of the "Debye semicircle" [1] can be

Table II

The dielectric constant of n-pentanol as a function of temperature

t(°C)	ε°
60	14.0
50	14.4
40	15.2
30	15.8
20	16.8
10	18.0
0	19.1
−10	20.1
−20	21.4
−30	22.5
−40	23.7
−50	25.2
−60	26.6

Table III

The dielectric constant on n-pentanol as a function of temperature and frequency

t(°C)	50 MHz		75 MHz		100 MHz		150 MHz		200 MHz	
	ε'	ε''	ε'	ε''	ε'	ε''	ε'	ε''	ε'	ε''
60	14.0	—	14.0	—	14.0	—	14.0	—	14.8	1.8
50	14.4	—	14.4	—	14.4	—	14.4	—	14.0	2.8
40	15.2	—	15.2	—	15.2	2.8	14.6	3.4	13.2	3.9
30	15.8	—	15.8	2.7	15.3	3.6	13.8	4.3	11.6	4.6
20	16.8	3.0	15.8	3.7	14.4	4.4	12.2	4.9	9.6	4.3
10	16.4	4.3	14.9	4.8	13.0	5.3	10.1	4.8	7.2	2.8
0	15.4	5.4	13.4	5.9	10.9	5.7	8.0	3.7	5.0	1.0
−10	13.6	6.4	11.1	6.0	8.5	4.7	5.8	2.1	3.6	—
−20	11.2	6.1	8.7	4.9	6.1	3.1	3.9	0.7	3.4	—
−30	8.6	4.8	6.4	3.4	4.0	1.7	3.4	—	3.4	—
−40	6.5	3.1	4.4	1.8	3.4	0.2	3.4	—	—	—
−50	4.6	1.5	3.6	0.3	—	—	—	—	—	—
−60	3.5	0.1	3.4	—	—	—	—	—	—	—

noticed.) For substances of this kind, COLE and DAVIDSON [10] recommended the following equation:

$$\frac{\varepsilon^* - n^2}{\varepsilon^\circ - n^2} = \frac{1}{(1 + j\omega\tau)^\alpha} \tag{3}$$

where $0 < \alpha \leqslant 1$ is an empirical constant. In the case of $\alpha = 1$, Eq. (3) is reduced to Eq. (2). On introducing the denotation $\omega\tau = \Phi$, the racionalisation of Eq. (3) gives the following expressions:

$$\frac{\varepsilon' - n^2}{\varepsilon^\circ - n^2} = \cos^\alpha \Phi \cos \alpha\Phi \tag{4}$$

$$\frac{\varepsilon''}{\varepsilon^\circ - n^2} = \cos^\alpha \Phi \sin \alpha\Phi. \tag{5}$$

In the coordinate system $\varepsilon''/\varepsilon^\circ - n^2$ *vs.* $\varepsilon' - n^2/\varepsilon^\circ - n^2$ the so called reduced COLE—DAVIDSON diagram is obtained, which for $\alpha = 1$ is a semicircle, and if $\alpha < 1$, the shape of the diagram differs from semicircular, and this difference is the more marked, the greater is the deviation of α from the unity. The reduced COLE—DAVIDSON diagram of *n*-pentanol is shown in Fig. 3. In the system investigated $\alpha = 0.5$. This is to be considered as an average value, since α decreases slightly with increasing temperature, and at -50 °C a value by about 10 per cent higher has been obtained than at $+50$ °C.

In knowledge of α, and using Eqs (4) and (5) the macroscopic relaxation time as the function of temperatures could be calculated. The results are presented in Table IV. Data in Table IV represent averages of relaxation times, calculated from the experimental results obtained at various frequencies. At a

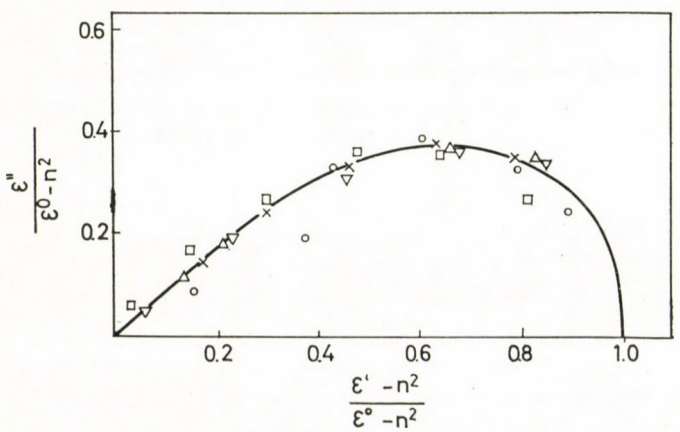

Fig. 3. The reduced COLE—DAVIDSON diagram of *n*-pentanol
50 MHz 75 MHz 100 MHz
150 MHz 200 MHz

given temperature, the error of experimental data caused an uncertainty of about 6 per cent in the calculated relaxation time.

Table IV

Macroscopic relaxation time as a function of temperature

t(°C)	$\tau \cdot 10^8$(sec)
30	0.31
20	0.53
10	0.93
0	1.41
−10	1.93
−20	3.10
−30	4.70

Dielectric relaxation is a process requiring activation energy. The temperature dependence of relaxation can be described with good approximation by the so called Arrhenius equation

$$\tau = A \exp\left\{\frac{\Delta H^*}{RT}\right\} \tag{6}$$

where ΔH^* is the enthalpy of activation. The preexponential coefficient, A, comprises the entropy of activation, the moment of inertia of the molecule and the temperature (see *e.g.* [1] and [11]), so that it cannot be considered in principle as constant. However, practically it is constant in a rather broad temperature interval. The temperature dependence of A is analysed extensively *e.g.* in Ref. [1]. Fig. 4 shows the $\log \tau$ *vs.* $1/T$ plot. The enthalpy of activation is 6.7 kcal/mole. This value is almost the same as the energy of the hydrogen bond [12], which permits certain considerations on the mechanism of dielectric relaxation.

For liquid monovalent aliphatic alcohols it is customary to distinguish three dielectric relaxation regions [13, 14]. The first is the absorption belonging to a broad, relatively low region of frequency. The second and third absorption regions belong to considerably narrower and higher frequencies [21]. In our work, the first absorption region of *n*-pentanol has been investigated. The second absorption region arises presumably from the rotation of the monomer molecules or the —OR group (where R denotes a hydrocarbon), while the third absorption region may be caused by the rotation of the —OH group around the C=O bond [7]. No unequivocal explanation has been given so far for the first absorption region. This absorption region disappears gradually,

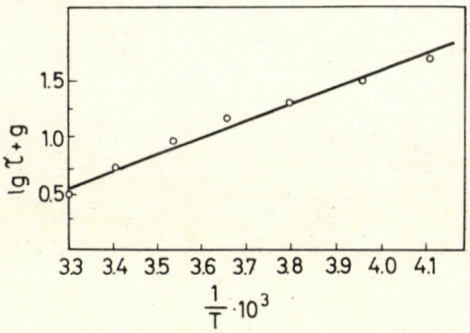

Fig. 4. lg τ *vs.* 1/T plot for the calculation of the enthalpy of activation

when the alcohol is diluted with an apolar solvent [15—17]. Its other characteristic feature is that the relaxation time belonging to it increases gradualy with the number of carbon atoms of the *n*-alcohols.

We tried to correlate the activation enthalpy values with the number of carbon atoms. The enthalpies of activation are given in Table V.

Table V

Alcohol	Δ H*(kcal)mole	Ref.
Methanol	3.66	[1]
Ethanol	3.67	[1]
n-Propanol	5.00	[1]
n-Butanol	5.96	[18]
n-Pentanol	6.7	present work
n-Heptanol	7.9	[19]

In Fig. 5 the enthalpy of activation is plotted as a function of the logarithm of the carbon atom number. According to the figure, enthalpy of activation changes linearly with the logarithm of the number of carbon atoms. This relationship is not valid for methanol, the first member of the homologus series. The equation of the straight line in Fig. 5 is the following:

$$\Delta H^* = 7.72 \lg n + 1.35$$

where n is the number of carbon atoms. Such regular change in the enthalpy of activation [7] with increasing carbon number indicates that relaxation is caused by molecular units. In principle, three possibilities should be considered:

1. Chain associates are formed, and the relaxation of the associates is measured in the absorption region investigated. In this case, the broadness of the absorption band should change considerably with a change in temperature,

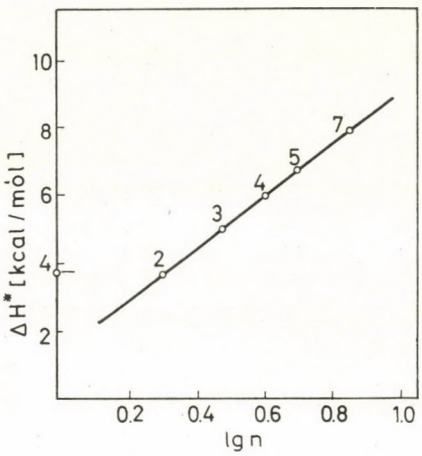

Fig. 5. The enthalpy of activation of *n*-alcohols as a function of the logarithm of the number of carbon atoms

since equilibrium is shifted with increasing temperature towards the smaller associates. Fig. 2 does not show such tendency.

2. It is assumed [2] that strongly polar cyclic tetramers are formed, and these cause the relaxation. This assumption would explain the monotonic change of the enthalpy of activation with the number of carbon atoms, and it agrees well with the experimental finding that this type of relaxation disappears in the dilute solutions of *n*-alcohols in apolar solvents. In this case namely, the association equilibrium is shifted by the dilution towards the monomeric alcohol, the first absorption region disappears gradually, and the second region becomes decisive.

3. In view of the fact that the enthalpy of activation of the relaxation is almost identical with the energy of the hydrogen bond, a mechanism, which inclused the breaking of the hydrogen bonds and the rotation of the monomers cannot be excluded. In this case, the relatively low relaxation frequency were to be explained by the assumption that the breaking of the hydrogen bonds is a slower process than the rotation of the monomeric alcohol molecules. In dilute solutions with apolar substances, the association equilibrium is shifted towards the formation of the monomeric molecules, and the first absorption region gradually disappears by dilution.

Investigations reported in this publication support the explanations 2 and 3. The exact mechanism of relaxation, however, still awaits for clarification.

REFERENCES

1. HILL, N., PRICE, A. H., WAUGHAN, W. E., DAVIES, M.: Dielectric Properties and Molecular Behaviour. Van Nostrand Reinhold Co. London, New York, Toronto, Melbourne 1969
2. FRÖHLICH, H.: Theory of Dielectrics. Clarendon Press, Oxford, 1949
3. HUYSKENS, P., GILLEROT, G., ZEEGERS-HUYSKENS, TH.: Bull. soc. Chim. Belge **72,** 666 (1963)
4. BAHE, L. W., DANNHAUSER, W.: J. Phys. Chem. **40,** 3058 (1964)
5. Molecular Relaxation Processes. Lectures delivered and synopses of papers read at the Chemical Society Symposium, Aberystwyth 7—9 July 1965. Academic Press, London, New York 1966
6. DANIEL, V. V.: Dielectric Relaxation. Academic Press, London, New York 1967
7. CROSSLEY, J.: Dielectric Relaxation and Molecular Structure in Liquids. Roy. Inst. Chem. Rev. **4** (1) 70 (1971)
8. MALECKI, J.: Acta Phys. Polonica **29,** (1) 45 (1966)
9. MALECKI, J.: Acta Phys. Polonica **28** (6) 891 (1965)
10. DAVIDSON, D. W., COLE, R. H.: J. Chem. Phys. **18,** 1417 (1951)
11. BAUER, E.: Cah. Phys. **20,** 1 (1944)
12. PIMENTAL, G. C., MCCLELLAN, A. L.: The Hydrogen Bond. W. H. Freeman and Company. San Francisco and London 1960
13. GARG, S. K., SMYTH, C. P.: J. Phys. Chem. **69,** 1294 (1965)
14. BROT, C., MAGAT, M.: J. Chem. Phys. **39,** 841 (1963)
15. YOHARI, G. P., SMYTH, C. P.: J. Am. Chem. Soc. **91,** 6215 (1969)
16. MORIAMEZ, M., LEBURN, A.: Archs. Sci. Genève **13,** 40 (1960)
17. DENNEY, D. J., RING, J. W.: J. Chem. Phys. **39,** 1268 (1963)
18. RIZK, H. A., YOUSSEF, N. : Z. Physik. Chem. (Leipzig) **244** (3—4) 165 (1970)
19. MIDDELHOEK, J., BÖTTCHER, C. J. F.: Molecular Relaxation Processes, p. 69 Academic Press, 1966
20. BORDEWIJK, P., BÖTTCHER, C. J. F.: J. Phys. Chem. **73,** 3255 (1969)
21. BARBENZA, G. H., CALDERWOOD, JH.: J. Phys. D., Appl. Phys. **4,** 525 (1971)

János LISZI; 8200 Veszprém, Schönherz Z. u. 12. Hungary.

RECENSIONES

Progress in Drug Research

Vol. 15.

Ed. by E. Jucker, Birkhäuser Verlag, Basel, 1972. 395 pages

Similarly to the former volumes of the series, it was the editor's intention to include in this monograph papers interesting for both pharmaceutical chemists and pharmacologists. In view of this endeavour and considering the actuality and skilful treatment of the problems discussed in the individual chapters, this new volume of the well-known series may command considerable interest. The book consist of the following chapters;

Ayurvedic Medicine — Past and Present (by S. SHARMA); The Psychotomimetric Agents (by S. COHEN); Pharmacology of Clinically Useful Beta-Adrenergic Blocking Drugs (by A. M. KAROW Jr., M. W. RILEY and R. P. AHLQUIST); On the Understanding of Drug Potency (by Y. M. MCFARLAND); Stoffwechsel von Arzneimitteln als Ursache von Wirkungen, Nebenwirkungen und Toxizität (by O. WINTERSTEINER); Cyclopropane Compounds of Biological Interest (by A. BURGER) and Drug Action and Assay by Microbial Kinetics (by E. R. GARETT).

Index for Vol. 12—15, Subject Index for the whole series, as well as Author and Papers Indices are also included in the book.

GY. DEÁK

William G. DAVIES: *Introduction to Chemical Thermodynamics*

The author of this book, published by Saunders, is a professor at St. Mary's College, South-Bend (Indiana). He has aimed at introducing university freshmen to the thermodynamics of chemical equilibria in a clear and descriptive way, primarily bearing in mind the molecular structure of matter. In his view the feelings of the vast majority of students can only be "hostile" towards thermodynamics, when presented merely as abstract concepts. The book aims at throwing light on the nature of chemical equilibria, but it is not its intention to give a complete chemical thermodynamic picture, and so it does not deal, for example, with a theoretical explanation of reversibility, or with the thermodynamics of machines.

The author has also strived, using the minimum amount of mathematics, to describe as many concepts as possible on a molecular basis, and in so doing makes a point of ensuring that his findings should be strictly exact.

The book is divided into 11 chapters, which are followed by a summary of the fundamental physical concepts, tables and solutions to problems. At the end of each chapter are found problems requiring in part simple calculation, and in part merely qualitative consideration. The individual chapters are:

1.	Equilibrium and probability	22 pages
2.	Population of energy levels	27 pages
3.	Energy level spacings	22 pages
4.	Competition of energy level sets	15 pages
5.	Internal energy	29 pages
6.	Entropy	29 pages
7.	Energy and entropy in action	15 pages
8.	Enthalpy	19 pages
9.	Entropy increase and free enthalpy decrease	28 pages
10.	Ideal gases	18 pages
11.	Free enthalpy and equilibrium	40 pages
		264 pages

1. Equilibrium and probability. In the introduction chemical reactions are characterized by "upwards" and "downwards" tendencies (affinity). Equilibrium is defined as the most probable state. The example is treated throughout of how equal numbers of hydrogen and deuterium atoms may be distributed among the molecular species they can form. It shows how the gradation of the probability increases with the rise in the number of particles.

2. Population of energy levels. In this chapter the microstates of a few particles are defined for a given energy content, and the number of microdistributions belonging to a given macrodistribution is calculated by induction. The Boltzmann factor is introduced without proof, and the properties of exponential distribution are illustrated on numerical examples.

3. Energy level spacings. Starting from the wave nature of particles and from the de Broglie equation, the energy of a particle closed in a one-dimensional potential box is deduced, and hence the translational energy level spacings are characterized. The same formula is used to calculate the orders of magnitude of the rotational and vibrational energy level spacings too, by substituting the atomic distance and the vibrational amplitude into the dimensions of the box.

4. Competition of energy level sets. The author considers the population at various temperatures of two energy level sets, in which the energies of the ground level and the energy level intervals differ. He establishes that at low temperature the difference in the ground levels is the decisive factor, whereas at high temperature it is the difference in the energy level intervals. He already mentions at this stage that thermodynamics characterizes the former by the difference in internal energy, and the latter by the difference in entropy.

5. Internal energy. The internal energy is defined as the average energy of an energy level set. The macroscopic state of the system, the change of the state due to an external effect, the work of volume change and the heat are also defined. The equation of the first law is given and explained. Next follows the Hess theorem and a method of calculating the energy changes in chemical reactions with the use of the bond energies.

6. Entropy. The maximum thermodynamic probability (Boltzmann probability) is interconnected with the temperature and the density of the energy levels. Entropy is defined as $k \ln W$, and the additivity of entropy is established on the basis of the product of the partial probabilities. The author discusses in detail how the standard entropies of some simple molecules depend on the moment of inertia and on the frequencies of the normal vibrations. The *principle* of calculating the absolute entropy from molecular parameters is described, but the relations are not deduced, and only the expression for the translational entropy is given. From the change in the thermodynamic probability upon the action of heat, the macroscopic expression for the entropy change is deduced. In order to avoid the concept of reversibility, it is noted merely that the expression is valid only in the state of Boltzmann distribution.

7. Energy and entropy. A detailed treatment is given of the "low energy in action — high entropy rule". Concrete numerical data are used to illustrate how equilibrium is established at various temperatures between chemical substances of different energies and entropies. A separate treatment is given to simple nitrogen compounds, equilibria between single and double bonds, and dissociations.

8. Enthalpy. The problems of compression and expansion work and heat measured at constant pressure are discussed on an experimental basis. The change of enthalpy is defined as the heat transfer at constant pressure (work other than that of volume change is not mentioned). The heat of formation is defined. It is established that the general observations referring to the energy can be correlated to the enthalpy too, and in this way attention is drawn to the importance tabulated heats of formation.

9. Entropy increase and free enthalpy decrease. From the spontaneous increase in the probability the increasing tendency of the entropy is established. This is referred to as the second law of thermodynamics. The definition of free enthalpy is arrived at via the elimination of the environment at constant pressure. Since the concept of reversibility was not introduced earlier either, no explanation is given as to why one may use the *real* heat and temperature of the *system* in considering the entropy change of the environment. The condition of equilibrium is defined as the state of minimum free enthalpy. Special discussions are given to the water–ice equilibrium, the $NO_2 - N_2O_4$ equilibrium and the dependence of the yield on the normal free enthalpy difference. The free enthalpy of formation is defined. In conclusion it is stated that the free enthalpy cannot be given such a molecular interpretation as the energy or entropy.

10. Ideal gases. A study is made of the energy, enthalpy and entropy changes in the isothermal expansion of perfect gases. The probability quotients can be unambiguously interrelated with the volume quotients and thus the logarithm of the latter with the entropy change. The expression for the free enthalpy of gases is arrived at by means of the entropy of gases. The isothermal mixing of perfect gases is discussed in a similar way.

11. Free enthalpy and equilibrium. On the basis of the preceding chapter it is first shown how to calculate the vapour pressure of a pure liquid from the free enthalpy difference of the liquid and vapour states. The author then turns to the chemical equilibrium between two volatile substances, to epuilibrium between two gases, and generalizes the relation for gaseous equilibrium between several components. The equilibrium constant is explained, and its calculation illustrated on numerical examples. A detailed treatment is given of how the free enthalpy of formation can be estimated from bonding considerations. Finally general statements are made on the relation between normal free enthalpy difference and yield. Equilibrium reactions in condensed phases are not dealt with.

The author emphasizes in the introduction that he does not strive for completeness or exactness. The book undoubtedly gives an interesting view, and can be considered as a very noteworthy enterprise, especially if its content is regarded as a *preliminary* study for exact thermodynamics. It gives many useful ideas, and even some which it does not employ its elf. For example, in the same way as it treats the probability conditions of the mixing of perfect gases, it would be possible to avoid the definition of thermodynamic probability and the Stirling formula too, if the concept of the probability of a single microdistribution were introduced, this being the reciprocal of the thermodynamic probability. The author is undoubtedly right in that such a method of treatment presents thermodynamics to the university student in a more favourable way. It is also possible perhaps to combine this method of instruction with a more exact treatment. I should welcome the appearance of a Hungarian *translation* of this book.

G. VARSÁNYI

INDEX

INORGANIC AND ANALYTICAL CHEMISTRY — ANORGANISCHE UND ANALYTISCHE CHEMIE
НЕОРГАНИЧЕСКАЯ И АНАЛИТИЧЕСКАЯ ХИМИЯ

PHYSICAL CHEMISTRY — PHYSIKALISCHE CHEMIE — ФИЗИЧЕСКАЯ ХИМИЯ

Printed in Hungary

A kiadásért felel az Akadémiai Kiadó igazgatója — Műszaki szerkesztő: Zacsik Annamária

[A kézirat nyomdába érkezett: 1972. X. 19. — Terjedelem: 9,8 (A/5) ív, 32 ábra

73.74244 Akadémiai Nyomda Budapest — Felelős vezető: Fernát György

ACTA CHIMICA

ТОМ 76—ВЫП. 2

РЕЗЮМЕ

Разделение производных антипирина с помощью ионообменной хроматографии

Й. ГААЛ и Й. ИНЦЕДИ

Был разработан метод хроматографического разделения антипирина, 4-аминоантипирина и диметиламиноантипирина (Пирамидона) на мактропористой катионообменной колонке. Оптимальность условий разделения и состава проявителя была установлена на основе констант равновесия (константа протонирования, константа ионообменного равновесия), а также на основе кинетических данных, определенных ранее.

Исследование химического состава рамашкиновых и альдёвских битумов, I

Разделение битумов на группы соединений с характерным химическим составом

Л. ЗАЛКА

Целью исследований было изучение химического состава и строения рамашкинских и альдёвских битумов. С помощью нового метода битумы были разделены на фракции с относительно гомогенным химическим строением. Для отдельных фракций были определены элементарный состав и молекулярный вес. Далее эти фракции были исследованы с помощью УФ, ИК и ЯМР спектроскопических методов.

Метод разделения заключается в следующем: отделение асфальтенов н.-гексаном, М-26 н фракции жидкофазной хроматографией на силикагеле, фракционированная кристаллизация, отделение н. парафинов с образованием карбамидного аддукта, молекулярная дестилляция и разделение ароматических продуктов по числу членов цикла с помощью жидкофазной хроматографии на адсорбенте, обработанном пикриновой кислотой.

Исследование химического состава рамашкиновых и альдёвых битуменов, II

Исследований фракций с характерным химическим строением

Л. ЗАЛКА, Е. КЕРЕНИ и К. БЕЛАФИ

Фракции битуменов с характерным химическим строением, изолированные согласно методу, описанному в предыдущем сообщении, были исследованы методами ИК, УФ и ЯМР спектроскопий, а также другими методами. С помощью исследований, разработанных и примененных для битуменовых фракций, а также их обобщения, удалось получить подробные сведения относительно химического строения сравнительно гомогенных фракций. Приводимые данные позволяют определение параметров химического строения битуменовых фракций и различий в строении битуменов различного происхождения, а также различий, обусловленных технологическими условиями.

Исследование состава отечественным и иностранных летучих масел, II

Анализ масла отечественной перичной мяты

К. РЕТИ-БЕЛАФИ, Ш. ИГЛЕВСКИ, Э. КЕРЕНИ и Р. КОЛТА

С помощью нового комбинированного метода исследования летучих масел, был изучен качественный и количественный состав масла отечественной перичной мяты. На основе данных капиллярной газовой хроматографии было установлено, что масло венгерской перичной мяты содержит 38 компонентов в количестве, превышающем 0,01%, среди которых 24 компонента находились в количествах больших или равных 0,1%. После эффективного разделения среди важных компонентов были идентифицированы спектроскопическим путем следующие соединения: α-пинен, β-пинен, лимулен 1,8-цинеол, п-цимол, 2,6-диметилоктан-2-ол, 3,7-диметил-1,7-октадиен-3-ол (линалоол), ментон, ментофуран, изоментон, 3,7-диметил-1,6-октадиен-3-ол (линалоол), ментилацетат, неоментол, неоизоментол, кариофиллен, ментол, изоментол, пиперитон и каламенен. В сопровождающих компонентах, присутствующих лишь в виде следов, были найдены β-мирцен, изопулегол, ментилизовалерианат и ε-кадинен. Количественный состав масла перичной мяты был определен с помощью газовой хроматографии. Общее количество идентифицированных веществ в изученных образцах превышало 98,6% от всего веса образца.

Дифторид ксенона как аналитический реагент, II

измерение содержания хрома

А. ШНЕР-ЭРДЕИ и К. КОЗМУТЦА

Легко порционируемый и надежно используемый XeF_2 в слабо кислой среде, при температуре около 100°C, за 25 минут окисляет Cr(III) до хромата. На основе этого, Cr в количестве 1—20 мг может быть определен приближенно волюметрическим методом, а в количествах 20 нг — 0,001 мг — фотометрическим методом.

Некоторые химические реакции в электродных щелях и их роль в спектрохимическом анализе, XI

Разделение реакций в анодном и катодном пространствах. Метод разделения

З. Л. САБО и Л. ПЁППЛ

Был разработан метод раздельного измерения количеств двуокиси углерода, образующихся в анодном и катодном пространствах. Были сконструированы такие газовые ячейки, в которых газовая смесь отсасывалась через ходы в электродах во время горения дуги. Были установлены оптимальные условия метода, что касается разделения, которые позволяют измерение газовых продуктов в электродных пространствах. Погрешность разделения в двух пространствах 3,6%.

Некоторые химические реакции в электродных щелях и их роль в спектрохимическом анализе, XII

Разделение анодных и катодных реакций. Роль направления потока газа, полярности и расположения электродов

З. Л. САБО и Л. ПЁППЛ

Рассматривая данный метод разделения, было установлено, что количество образующейся двуокиси углерода, а также возможность разделения зависит от полярности и расположения электрода. Первостепенную роль здесь играет направление потока газа по отношению к углеродному аноду, т. е. в направлении к нему или от него. Это влияние модифицировано тепловым потоком, движущимся вверх. При сравнении данных, относящихся к воздуху и смеси аргона с кислородом, можно получить сведения относительно роли газовой атмосферы и реакции азота с кислородом.

Определение остаточного содержания (основных примесей) в эмиссионном спектральном анализе

Г. ХАУПТМАНН, М. ХАУПТМАНН и Г. ЕГЕР

После короткого рассмотрения известных в литературе методов, был подробно рассмотрен метод Керекеша—Чети. Были сделаны предложения относительно того, в каких случаях может быть применен графический, а в каких случаях — расчетный методы.

Диэлектрическая релаксация н-пентанола в жидкой фазе

Й. ЛИСИ

Диэлектрическая релаксация н-пентанола была изучена в интервале частот 300 кгц — 250 МГц и в интервале температур —60 — +60°С. В этом интервале частот наблюдается первая область дисперсии. Согласно полученным результатам, величина параметра α по Коль-Давидсону в первой области дисперсии равна 0,5. Величина аррениусовской энтальпии активации равна 6,7 ккал/моль. Была изучена зависимость энтальпии активации от числа атомов углерода (n) н-спиртов, и было найдено следующее выражение:

$$\Delta H^* \text{ (ккал/моль)} = 7{,}72 \lg n + 1{,}35$$

Это регулярное изменение энтальпии активации свидетельствует о том, что релаксация, наблюдаемая в данном интервале частот, вызвана молекулярными звеньями.

RECENT FLAVONOID RESEARCH

edited by R. BOGNÁR, V. BRUCKNER and CS. SZÁNTAY

(Recent Developments in the Chemistry of Natural Carbon Compounds 5)

This new volume of the series deals with a branch of organic chemistry which has great traditions in Hungary. The material of the book consists of two parts: it contains the lectures held at the 3rd Hungarian Bioflavonoid Symposium, and it gives a survey and summary of Hungarian chemical research on flavonoids from 1950 till today.

In English • Approx. 130 pages • Cloth

ASSIGNMENTS FOR VIBRATIONAL SPECTRA OF 700 BENZENE DERIVATIVES

by GY. VARSÁNYI

Infrared spectra are very effective means of identification and differentiation of chemical substances. The book lists 700 benzene derivatives, denoting the structural units repsonsible for various vibrational modes, i.e. for the bands observed with a given intensity at a certain wave-number. With the aid of these data it becomes possible to analyse the structure of benzene derivatives other than those listed in the book, assigning the bands to known structural units or to determine the new constitutional features of the compound from the intensities and wave-numbers of the spectral bands observed.

In English • Approx. 640 pages • 100 illustrations • 350 spectra • 700 structural formulas • 800 tables • Cloth

AKADÉMIAI KIADÓ
Publishing House of the Hungarian Academy of Sciences
Budapest

ATLAS OF THERMOANALYTICAL CURVES III

TG-, DGT-, DTA-curves measured simultaneously

edited by G. LIPTAY

This series, whose third volume is presented here, supplies a great want. Up to now the various results obtained by different thermoanalytical methods and instruments could not be compared with one another, owing to difference in experimental conditions. Now the two most frequently used thermoanalytical methods, differential thermoanalysis (DTA) and thermogravimetry (TG) have been completed by the derivative thermogravimetric curves (DTG); thus the thermal behaviour of different materials can be examined simultaneously on the same sample. — This third volume, similarly to the second, contains a collection of the thermal analysis diagrams of a wide range of materials obtained from various sources, such as inorganic and organic compounds, synthetic organic materials, minerals, rocks, coals, etc.

In English • Approx. 100 pages • Cloth

AKADÉMIAI KIADÓ Budapest HEYDEN and SONS Ltd. London

A co-edition — distributed in the socialist countries by Kultura, Budapest, in all other countries by Heyden and Sons Ltd., London

ASCORBINOMETRIC TITRATIONS

by L. ERDEY and GY. SVEHLA

It was at the end of the fourties that L. Erdey and his research team began to deal with ascorbimetric titrations. This book gives an account of the principle and system of their research method, and describes in detail the results achieved between 1949 and 1965. In the course of time, a number of researchers joined in continuing the author's and his co-workers' pioneering work in the field of ascorbimetric titrations, opening up new vistas of industrial applications of this method. The book will be helpful to analytical chemists who already use this titration method, or want to explore its possibilities in their daily laboratory work.

In English • Approx. 150 pages • Cloth

AKADÉMIAI KIADÓ
Budapest

The Acta Chimica publish papers on chemistry, in English, German, French and Russian.

The Acta Chimica appear in volumes consisting of four parts of varying size, 4 volumes being published a year.

Manuscripts should be addressed to

Acta Chimica
Budapest 112/91 Műegyetem

Correspondence with the editors should be sent to the same address.

The rate of subscription is $ 24.00 a volume.

Orders may be placed with "*Kultúra*" Foreign Trade Company for Books and Newspapers (1389 Budapest 62, P.O.B. 149 Account No. 218-10-990) or with representatives abroad

---

Les Acta Chimica paraissent en français, allemand, anglais et russe et publient des mémoires du domaine des sciences chimiques.

Les Acta Chimica sont publiés sous forme de fascicules. Quatre fascicules seront réunis en un volume (4 volumes par an).

On est prié d'envoyer les manuscrits destinés à la rédaction à l'adresse suivante:

Acta Chimica
Budapest 112/91 Műegyetem

Toute correspondance doit être envoyée à cette même adresse.

Le prix de l'abonnement est de $ 24,00 par volume.

On peut s'abonner à l'Entreprise pour le Commerce Extérieur de Livres et Journaux «*Kultúra*» (1389 Budapest 62, P.O.B. 149 Compte-courant N°. 218-10-990) ou à l'étranger chez tous les représentants ou dépositaires.

«*Acta Chimica*» издают трактаты из области химической науки на русском, французском, английском и немецком языках.

«*Acta Chimica*» выходят отдельными выпусками разного объема. 4 выпуска составляют один том. 4 тома публикуются в год.

Предназначенные для публикации рукописи следует направлять по адресу:

Acta Chimica
Budapest 112/91 Műegyetem

По этому же адресу направлять всякую корреспонденцию для редакции.

Подписная цена — $ 24,00 за том.

Заказы принимает предприятие по внешней торговле книг и газет «*Kultúra*» (1389 Budapest 62, P.O.B. 149 Текущий счет № 218-10-990) или его заграничные представительства и уполномоченные.

Reviews of the Hungarian Academy of Sciences are obtainable at the following addresses:

ALBANIA

Drejtorija Qändrone e Pärhapjes
dhe Propagandimit të Librit
Kruga Konferenca e Päzes
Tirana

AUSTRALIA

A. Keesing
Box 4886, GPO
Sydney

AUSTRIA

GLOBUS
Höchstädtplatz 3
A-1200 Wien XX

BELGIUM

Office International de Librairie
30, Avenue Marnix
1050 Bruxelles
Du Monde Entier
162, Rue du Midi
1000 Bruxelles

BULGARIA

HEMUS
11 pl Slaveikov
Sofia

CANADA

Pannonia Books
2, Spadina Road
Toronto 4, Ont.

CHINA

Waiwen Shudian
Peking
P. O. B. 88

CZECHOSLOVAKIA

Artia
Ve Smečkách 30
Praha 2
Poštovní Novinová Služba
Dovoz tisku
Vinohradská 46
Praha 2
Mad'arská Kultura
Václavské nám. 2
Praha 1
SLOVART A. G.
Gorkého
Bratislava

DENMARK

Ejnar Munksgaard
Nörregade 6
Copenhagen

FINLAND

Akateeminen Kirjakauppa
Keskuskatu 2
Helsinki

FRANCE

Office International de Documentation
et Librairie
48, rue Gay-Lussac
Paris 5

GERMAN DEMOCRATIC REPUBLIC

Deutscher Buch-Export und Import
Leninstraße 16
Leipzig 701
Zeitungsvertriebsamt
Fruchtstraße 3—4
1004 Berlin

GERMAN FEDERAL REPUBLIC

Kunst und Wissen
Erich Bieber
Postfach 46
7 Stuttgart S.

GREAT BRITAIN

Blackwell's Periodicals
Oxenford House
Magdalen Street
Oxford
Collet's Subscription Import
Department
Dennington Estate
Wellingsborough. Northants.
Robert Maxwell and Co. Ltd.
4—5 Fitzroy Square
London W. 1

HOLLAND

Swetz and Zeitlinger
Keizersgracht 471—478
Amsterdam C.
Martinus Nijhof
Lange Voorhout 9
The Hague

INDIA

Hind Book House
66 Babar Road
New Delhi 1

ITALY

Santo Vanasia
Via M. Macchi 71
Milano
Libreria Commissionaria Sansoni
Via La Marmora 45
Firenze
Techna
Via Cesi 16
40135 Bologna

JAPAN

Kinokuniya Book-Store Co. Ltd.
826 Tsunohazu 1-chome
Shinjuku-ku
Tokyo
Maruzen and Co. Ltd.
P. O. Box 605
Tokyo-Central

KOREA

Chulpanmul
Phenjan

NORWAY

Tanum-Cammermeyer
Karl Johansgt 41—43
Oslo 1

POLAND

RUCH
ul. Wronia 23
Warszawa

ROUMANIA

Cartimex
Str. Aristide Briand 14—18
Bucureşti

SOVIET UNION

Mezhdunarodnaya Kniga
Moscow G—200

SWEDEN

Almquist and Wiksell
Gamla Brogatan 26
S—101 20 Stockholm

USA

F. W. Faxon Co. Inc.
15 Southwest Park
Westwood, Mass. 02090
Stechert Hafner Inc.
31. East 10th Street
New York, N. Y. 10003

VIETNAM

Xunhasaba
19, Tran Quoc Toan
Hanoi

YUGOSLAVIA

Forum
Vojvode Mišića broj 1
Novi Sad
Jugoslovenska Knjiga
Terazije 27
Beograd

30. V. 1973

Index: 26.007

ACTA CHIMICA

ACADEMIAE SCIENTIARUM HUNGARICAE

ADIUVANTIBUS

V. BRUCKNER, GY. DEÁK, K. POLINSZKY,
E. PUNGOR, G. SCHAY, Z. G. SZABÓ

REDIGIT

B. LENGYEL

TOMUS 76 FASCICULUS 3

AKADÉMIAI KIADÓ, BUDAPEST

1973

ACTA CHIM. (BUDAPEST) ACASA 76 (3) 221–337 (1973)

ACTA CHIMICA

A MAGYAR TUDOMÁNYOS AKADÉMIA KÉMIAI TUDOMÁNYOK OSZTÁLYÁNAK IDEGEN NYELVŰ KÖZLEMÉNYEI

SZERKESZTI

LENGYEL BÉLA

TECHNIKAI SZERKESZTŐK

DEÁK GYULA és HARASZTHY-PAPP MELINDA

Az Acta Chimica német, angol, francia és orosz nyelven közöl értekezéseket a kémiai tudományok köréből.

Az Acta Chimica változó terjedelmű füzetekben jelenik meg, egy-egy kötet négy füzetből áll. Évente átlag négy kötet jelenik meg.

A közlésre szánt kéziratok a szerkesztőség címére (Budapest 112/91 Műegyetem) küldendők.

Ugyanerre a címre küldendő minden szerkesztőségi levelezés. A szerkesztőség kéziratokat nem ad vissza.

Megrendelhető a belföld számára az „Akadémiai Kiadó"-nál (1363 Budapest, Pf. 24. Bankszámla 215 11 488), a külföld számára pedig a „Kultúra" Könyv- és Hírlap Külkereskedelmi Vállalatnál (1389 Budapest 62, P. O. B. 149. Bankszámla: 218 10990) vagy annak külföldi képviseleteinél és bizományosainál.

Die Acta Chimica veröffentlichen Abhandlungen aus dem Bereiche der chemischen Wissenschaften in deutscher, englischer, französischer und russischer Sprache.

Die Acta Chimica erscheinen in Heften wechselnden Umfanges. Vier Hefte bilden einen Band. Jährlich erscheinen 4 Bände.

Die zur Veröffentlichung bestimmten Manuskripte sind an folgende Adresse zu senden:

Acta Chimica
Budapest 112/91 Műegyetem

An die gleiche Anschrift ist auch jede für die Redaktion bestimmte Korrespondenz zu richten. Abonnementspreis pro Band: $ 24.00.

Bestellbar bei dem Buch- und Zeitungs-Außenhandels-Unternehmen »*Kultúra*« (1389 Budapest 62, P. O. B. 149. Bankkonto No. 218 10990) oder bei seinen Auslandsvertretungen und Kommissionären.

Acta Chimica Academiae Scientiarum Hungaricae, Tomus 76 (3), pp. 221—228 (1973)

PHOTOMETRIC MICRODETERMINATION OF ALUMINIUM WITH ARSENAZO III

V. MIKHAYLOVA

(Department of Chemistry, University of Sofia, Sofia 26, Bulgaria)

Received October 15, 1971

Aluminium forms a violet 1 : 1 complex with Arsenazo III in the pH range 2—8. The absorption spectrum of the complex reveals two peaks, at 550 and 583 nm, the maximum absorbance being reached at pH 4.

The molar absorptivity is 19 800 ± 200 at pH 3.5 and 23 500 ± 200 at pH 5.0; the corresponding spectrophotometric sensitivity is 0.0014 μg Al · cm^{-2} and 0.0011 μg Al · cm^{-2} for $A = 0.001$.

Beer's law is followed in the range of 0.01—0.60 μg Al · ml^{-1} at pH 3.5. The reaction has been applied for the photometric microdetermination of aluminium in calcite. The sensitivity of the reaction, as determined by statistical methods, is 0.01 μg Al · ml^{-1}.

The photometric determination of small quantities of aluminium by recommended methods is complicated because of the ability of aluminium to form hydroxo complexes which are kinetically inert. At pH 1 only negligible amounts of hydroxo complexes are formed, but at higher pH values their amounts are already considerable and this complexation competes with, and retards, the development of the colour reaction.

The use of organic azo-compounds containing an arsonic group as photometric reagents for aluminium is favoured by the fact that Al^{3+} reacts readily with the $-AsO(OH)_2$ group in moderately acidic media. For this reason these reactions proceed rapidly and are sensitive. An illustration of these reactions is that of Al^{3+} with Arsenazo I [1, 2].

The use of Arsenazo III (1,8-dihydroxynaphthalene-3,6-disulfonic acid-2,7bis [(azo-2)-phenylarsonic acid]) as photometric reagent for Al^{3+} has not been studied in detail. Moreover SAVVIN [3] has indicated that the molar absorptivity of the Al^{3+}-Arsenazo III complex is $\varepsilon = 0$. However, in our previous work [4] it has been shown that there is complexation between Al^{3+} and Arsenazo III. The investigation of this reaction with regard to its analytical application is the subject of the present work.

Experimental

Reagents

Arsenazo III solution. A 10^{-4} *M* aqueous solution was prepared by weighing the reagent (Fluka), and standardized by spectrophotometric titration with 4.10×10^{-5} *M* thorium(IV) at $\lambda = 600$ nm and pH 3.1. The Arsenazo III concentration found was 7.45×10^{-5} *M*.

Aluminium(III) nitrate (Schering—Kahlbaum, p.a.). A 10^{-2} *M* solution was checked complexometrically by back-titration with zinc, with xylenol orange as indicator. Solutions of lower concentrations were prepared by dilution with water.

Reagent grade $Ca(NO_3)_2$, $Cd(NO_3)_2 \cdot 6H_2O$, $CuSO_4 \cdot 5H_2O$, KSCN, $MgSO_4 \cdot 7H_2O$, $Mn(NO_3)_2 \cdot H_2O$, $Na_2SiO_3 \cdot 8H_2O$, $Ni(NO_3)_2 \cdot 6H_2O$, $ZnSO_4 \cdot 7H_2O$ were used to prepare solutions of various ions.

Buffer solutions pH 2—8 were prepared from analytical grade reagents as described by KOLTHOFF [5].

Apparatus

Absorption spectra were recorded with a Specord UV—VIS spectrophotometer (Zeiss). Spectrophotometric measurements were performed with a Zeiss Universal Spectrophotometer VSU—1. Photometric determinations were carried out with a FEK—56 photometer (USSR). For pH measurements a pH-meter (Z. Seibold, type GLD) with a glass electrode was used.

Result and Discussion

Aluminium(III)-Arsenazo III complex formation

In order to find the optimal pH for complex formation, the reaction of aluminium(III) with Arsenazo III was carried out in the pH range of 2—8. Arsenazo III was found to form violet complexes with Al^{3+} in this pH range. The absorption spectra (Fig. 1) show that at pH 3 the complex formation is already considerable and the maximum absorbance is achieved at pH 4. The complex spectra have two well defined peaks at 550 nm and 583 nm. At pH > 5 the absorption maximum at 550 nm decreases and in more alkaline media the

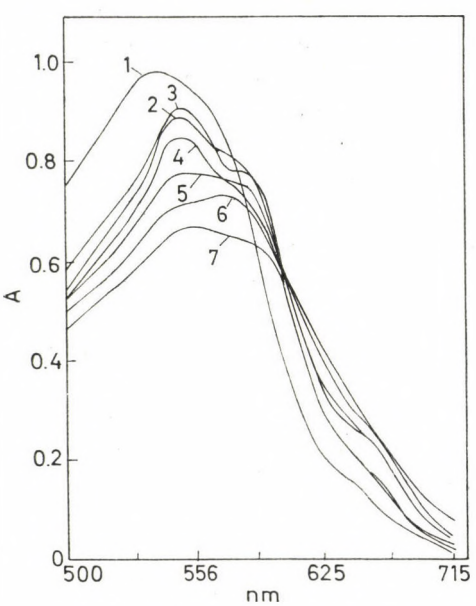

Fig. 1. Dependence of the absorption spectrum on the acidity $C_{Al} = 1.20 \times 19^{-4} M$, $C_{\text{Arsenazo III}} = 1.49 \times 10^{-5} M$; Arsenazo III curve (1) pH 5.1; aluminium-Arsenazo III curves, pH: (2) 3.1, (3) 4.0, (4) 5.1, (5) 5.5, (6) 6.1, (7) 7.8

two peaks collapse into one broad band. It is very likely that at about pH 5, the Al^{3+}-Arsenazo III complex begins to add OH^- groups, *i.e.* hydrolysis takes place accompanied by the decrease of the absorbance. In the present case buffer solutions (biphthalate–hydrochloric acid, biphthalate–alkali and boric acid–alkali buffers) were used to maintain the required pH.

If, however, the excess acid is neutralized with sodium hydroxide, the spectra do not have two maxima even at pH 4, their shape being the same as that observed at pH $>$ 5. Seemingly, the local excess of alkali is unavoidable, the hydrolysis starts in more acidic media, resulting in a decrease of the absorbance.

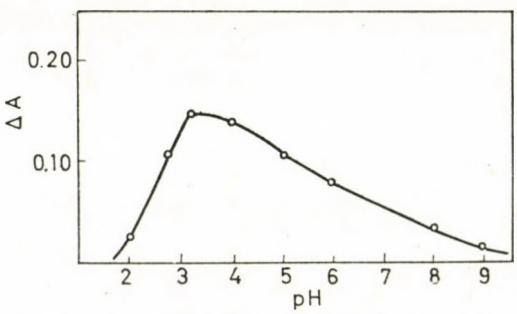

Fig. 2. Difference between the absorbances of the complex and the reagent at 600 nm

Because of the fact that an absorption maximum of Arseno III (λ_{max} = = 540 nm) is close to that of its aluminium complex, it is practically not possible to measure on the wavelength range corresponding to maximum absorbance of the complex. The difference between the absorbance of the reagent and that of the complex was found to be the greatest at λ = 600 nm in the pH range of 3—4 (Fig. 2).

Composition of the complex

As reported by SAVVIN [3], Arsenazo III usually forms 1 : 1 complexes with di- and trivalent cations. The composition of the Al^{3+}-Arsenazo III complex was checked by means of several methods: the continuous variation method applied in the same way as in the case of the calcium–calcon complex [6], the mole ratio method, the method of straight line of ASMUS [7] and by the BENT—FRENCH method [8].

The data shown in Table I were used for calculating the quantities required by the last three methods.

The results obtained by the methods applied are shown in Figs 3, 4, 5, 6. A 1 : 1 complex composition was proved.

Table I

V_R ml	0.70	1.00	1.50	2.00	3.00	4.00
$C_R \times 10^5$	0.35	0.50	0.75	1.00	1.50	2.00
A	0.054	0.077	0.114	0.152	0.222	0.296
ΔA	0.022	0.033	0.048	0.063	0.091	0.124
5.00	6.00	7.00	8.00	9.00	10.00	11.00
2.50	3.00	3.50	4.00	4.50	5.00	5.50
0.362	0.424	0.487	0.540	0.593	0.642	0.690
0.145	0.152	0.159	0.164	0.169	0.175	0.181

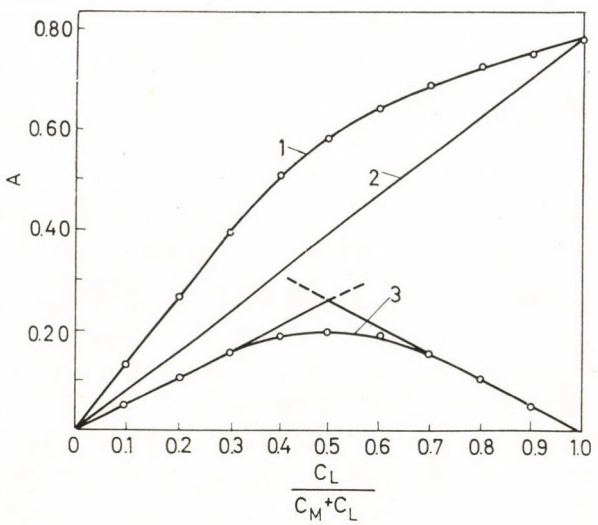

Fig. 3. Continuous variations study for the determination of the complex composition. $\lambda = 600$ nm, pH = 3.9, $C_L + C_M = 2.98 \times 10^{-5}\ M$. 1 — absorbance of complex and ligand, 2 — absorbance of ligand, 3 — absorbance of complex

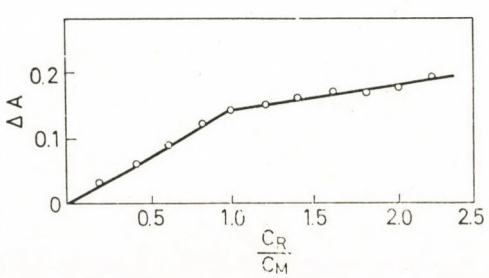

Fig. 4. Mole ratio method $C_M = 2.5 \times 10^{-5}\ M$

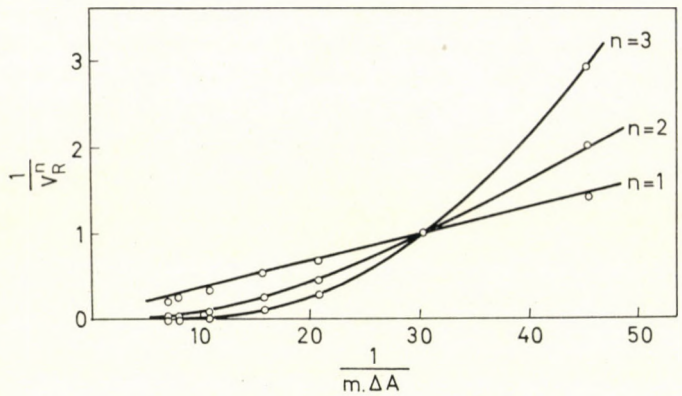

Fig. 5. Method of straight line of Asmus. $C_M = 2.50 \times 10^{-5}\ M$, V_R — volume of Arsenazo III, $m_{\Delta A} = \frac{\Delta A}{l}$, $l = 1$ cm, $n = \frac{L}{M}$ ratio

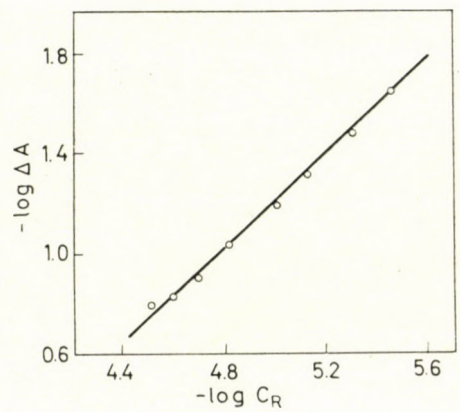

Fig. 6. Bent-French method. $C_M = 2.50 \times 10^{-5}\ M$, the slope = 1.0

Concentration of metal in all the cases is $C_M = 2.50 \times 10^{-5}\ M$. ΔA is the difference between the absorbances of the complex and the reagent at 600 nm, $l = 1$ cm.

pH = 3.9 (biphthalate buffer).

Sensitivity of the reaction

The molar absorptivity of the complex was determined at various acidities in the pH range of 3.5—6.2.

For each pH value, series of solutions were made with the reagent to metal mole ratio equal or greater than 3 and their absorbance was measured with a VSU—1 instrument $\lambda = 600$ nm. The molar absorptivity was deter-

mined by applying a least squares procedure to the $\Delta A = \varepsilon cl$ straight line (Table II).

Table II

Molar absorptivity of the aluminium–Arsenazo III complex at 600 nm

pH	3.5	3.9	4.5	5.0	5.5	6.2
$\varepsilon \times 10^{-4}$ (1 mol^{-1} cm^{-1})	1.98	1.98	2.14	2.35	2.33	2.10

The values of ε were calculated at pH 5.0 and pH 3.5 and were found to be $\varepsilon = 23\,500 \pm 200$ and $\varepsilon = 19\,800 \pm 200$, respectively. The sensitivity, as defined by Sandell, is 0.0011 μg Al cm^{-2} at pH 5.0 and 0.0014 μg Al cm^{-2} at pH 3.5.

From the optical characteristics of the aluminium(III)-Arsenazo III complex it is obvious that this compound can be used for analytical purposes. The experimental conditions depend upon the composition of the material to be analyzed. As reported in a previous paper [4], the selectivity of the reaction is greater in more acidic media. On the other hand, in acidic media the reaction sensitivity decreases. The experiments carried out with various ions show that a pH of 3.5 is suitable regarding both sensitivity and selectivity.

The interference by various foreign ions was studied at pH 3.5 (acetate buffer) in solutions containing 10 μg Al^{3+} per 25 ml volume.

The results are listed in Table III, where b is the maximum amount of the ion in 25 ml, which does not yet interfere.

Table III

Interference of foreign ions

Ion	Cu^{2+}	Ca^{2+}	Ni^{2+}	Co^{2+}	Mn^{2+}	Zn^{2+}	Mg^{2+}	Cd^{2+}	SiO_3^{2-}	SCN^-
b, μg	5	10	60	170	200	540	700	800	120	2900

The ions Fe(II), Fe(III), Ag(I), Ti(III), interfer seriously, as well as F^-, $C_2O_4^{2-}$, $C_4H_4O_6^{2-}$, $C_2H_5O_7^{3-}$ do at concentrations of 2—4 μg.

Photometric determination of aluminium(III)

The recommended procedure for the determination of microamounts of aluminium(III) is as follows.

Procedure. Into a 25 ml volumetric flask are added 10.0 ml of $7.45 \times \times 10^{-5}$ M Arsenazo III, 5.0 ml buffer solution of pH 3.5 (biphthalate or acetate) and the corresponding volume of a 1.82×10^{-4} M aluminium(III)

solution. The violet colour develops immediately and persists for 2 hours. The photometric measurements were performed with an FEK—56 photometer (red filter) in 30 nm cells against a reagent blank treated in the same way. The order of mixing the reagents is not important at pH 3.5. If, however, the reaction is used in more alkaline media, the buffer should be added in solution after mixing the reagents.

At 600, mm (red filter) and pH 3.5 the absorbance of the complex follows Beer's law in the range 0.01—0.60 μg Al ml^{-1}.

The method described was applied to the determination of aluminium-(III) in calcite.

Analysis of calcite

The sample (0.3—0.5 g) was decomposed by fusion with 2.5 g sodium carbonate in a platinum crucible and dissolved in about 30 ml of 5% hydrochloric acid. The precipitation of aluminium and iron was carried out as follows. 1—2 drops of concentrated hydrogen peroxide were added, then the excess of peroxide was destroyed by gentle boiling. Precipitation with 20% pyridine was made in the presence of Methyl Red indicator. The solution was heated on a water bath to coagulate the precipitate, filtered and washed with a 0.5% solution of pyridine and 3% ammonium chloride.

The separation of aluminium(III) from iron(III) was carried out by means of the thiocyanate method followed by the extraction of thiocyanate iron complexes with amyl alcohol. The precipitate was dissolved in 3 ml 6N hydrochloric acid and 10 ml of 20% potassium thiocyanate was added. The complexes of iron(III) were removed by 4—5 extractions with amyl alcohol. The aqueous solution obtained was evaporated and the excess of thiocyanate

Table IV

Determination of aluminium in calcite

N°	Calcite taken (g)	Aliquote (ml)	Aluminium found* (% Al_2O_3)
1	0.3024	3	0.14
2	0.3056	5	0.13
3	0.4025	3	0.13
4	0.4025	5	0.14
5	0.5009	3	0.12
6	0.5002	3	0.13

* Average of 3 determination from separate aliquots
Average value of Al = 0.13% Al_2O_3
Standard deviation = $\pm$ 0.01% Al_2O_3

destroyed with 3 ml conc. nitric acid. The solution was evaporated to dryness. The residue was dissolved in water and collected in a 100 ml volumetric flask. The aliquots of this solution were used for the photometric determination of aluminium by the recommended procedure. The aluminium contents were calculated from a calibration curve plotted for the range of 0.10—0.60 μg Al · ml^{-1}. The results obtained for calcite are shown in Table IV.

By statistical methods [9], the sensitivity of the reaction at pH 3.5 was found to be 0.01 μg Al · ml^{-1}.

REFERENCES

1. KUZNETSOV, V. I., GOLUBTSOVA, R. B.: Zav. Lab., **21,** 1422 (1955)
2. GOLUBTSOVA, R. B.: Zh. Anal. Khim., **12,** 420 (1957)
3. SAVVIN, S. B.: Arsenazo III. p. 43. Atomizdat, Moscow 1966
4. MIKHAYLOVA, V., ILKOVA, P.: Anal. Chim. Acta, **53,** 194 (1971)
5. KOLTHOFF, I. M.: Acid-Base Indicators. Academic Press, New York, 1937
6. HILDEBRAND, G., REILLEY, C.: Anal. Chem., **29,** 258 (1957)
7. ASMUS, E.: Z. Anal. Chem., **178,** 104 (1960)
8. BENT, A., FRENCH, C.: J. Amer. Chem. Soc., **63,** 569 (1941)
9. DOERFEL, K.: Beurteilung von Analysenverfahren und Ergebnissen. Springer-Verlag, Berlin, 1962

Veselina MIKHAYLOVA; Sofia 26, Anton Ivanov Str. 1. Bulgaria.

Acta Chimica Academiae Scientiarum Hungaricae, Tomus 76 (3), pp. 229—242 (1973)

DER KATALYTISCHE EINFLUSS EINIGER KOBALT(III)-KOMPLEXE AUF DIE OXIDATION VON JODID DURCH PEROXODISULFAT

H. BARTELT und M. SCHNEIDER

Sektion Chemie der Humboldt-Universität zu Berlin, 108 Berlin, Bunsenstr. 1, DDR

Eingegangen am 20 Juli 1972

Es wurde der katalytische Einfluß der Co(III)-Komplexionen

$[Co\ a_6]^{3+}$, $[Co\ en_3]^{3+}$, $[Co\ pn_3]^{3+}$, $[Co\ chn_3]^{3+}$ und $[Co\ phan_3]^{3+}$

auf die Redoxreaktion zwischen $S_2O_8^{2-}$ und J^- untersucht.

In Gegenwart der Co(III)-Komplexe vergrößert sich die Reaktionsanfangsgeschwindigkeit um den Faktor 10 . . . 200 je nach Art des Komplexes. Diese Zahlen gelten für eine Co(III)-Komplex-Konzentration von $1 \cdot 10^{-3}$ *M* und

$$[S_2O_8^{2-}]_0 = 5 \cdot 10^{-4}\ M, \quad [J^-]_0 = 2{,}5 \cdot 10^{-3}\ M.$$

Die Katalysewirkung steigt, wenn das Konzentrationsverhältnis Komplex : Redoxpartner vergrößert wird. (vorgelagertes Gleichgewicht).

Bis auf $[Co\ phan_3]^{3+}$ unterscheiden sich die Komplexe nur wenig in ihrer katalytischen Wirkung.

Aus der Beeinflussung der Reaktionsanfangsgeschwindigkeit durch Zugabe von Cl^- wurde eine Beziehung zur angenäherten Berechnung der Stabilitätskonstanten für die outer-sphere-Komplexe zwischen Co(III)-Komplex und Cl^- abgeleitet.

1. Einleitung

Die Reaktion

$$S_2O_8^{2-} + 2\,J^- \rightarrow 2\,SO_4^{2-} + J_2 \qquad (1)$$

wurde bereits von KING und JACOBS [1], INDELLI und AMIS [2] sowie von INDELLI und PRUE [3] untersucht. Es ist bekannt, daß diese Reaktion nach einem Zeitgesetz 1. Ordnung bezüglich beider Reaktionspartner verläuft.

Die Geschwindigkeitskonstante 2. Ordnung wurde von INDELLI und AMIS [2] bei einer Ionenstärke von $J = 6{,}75 \cdot 10^{-3}$ und einer Temperatur von 25 °C zu $k = 1{,}310 \cdot 10^{-3}$ l.Md$^{-1} \cdot$ sec^{-1} bestimmt.

Da die Reaktion (1) zwischen gleichsinnig geladenen Ionen abläuft, ist der relativ langsame Reaktionsablauf verständlich. Im geschwindigkeitbestimmenden Schritt müssen die Abstoßungskräfte überwunden werden.

Bei Anwesenheit von Komplexkationen wie z. B. $[Co(NH_3)_6]^{3+}$ nimmt die Geschwindigkeit der Reaktion (1) stark zu. Diese Katalysewirkung ist durch eine outer-sphere-Komplexbildung zwischen Reaktionspartner und Komplexkation zu erklären [4, 5].

Unter outer-sphere-Komplexbildung versteht man die Anlagerung von Liganden in der zweiten (äußeren) Sphäre an ein Komplexion:

$$[Co(NH_3)_6]^{3+} + S_2O_8^{2-} \rightleftharpoons \{[Co(NH_3)_6] \cdot S_2O_8\}^{+}. \qquad (2)$$

Für den Vorgang der outer-sphere-Komplexbildung, der abhängig ist von der Art und der Konzentration der Ionen [6, 7, 8], gilt das MWG [9]. Die Einstellung des Gleichgewichtes erfolgt sehr schnell [10]. Die Stabilitätskonstanten der outersphere-Komplexe sind relativ klein und liegen im Bereich $\lg K = 0{,}5 \ldots 4$. Es können mehrere Liganden in der äußeren Sphäre angelagert werden, so daß sich mehrere Stabilitätskonstanten angeben lassen.

Zur Erklärung der outer-sphere-Komplexe müssen vorrangig elektrostatische Kräfte betrachtet werden. Einige experimentelle Ergebnisse [11, 12] zeigen aber, daß man weitere Kräfte berücksichtigen muß.

Die Katalysewirkung der Komplexkationen auf die Reaktion (1) läßt sich im wesentlichen durch die folgenden Vorstellungen deuten:

a) Durch die outer-sphere-Komplexbildung nach (2) wird ein Reaktionspartner im outer-sphere-Komplex gebunden, der eine positive Gesamtladung trägt. Für die katalytisch ablaufende Reaktion fallen damit die elektrostatischen Abstoßungskräfte weg und es resultiert eine Verringerung der Aktivierungsenergie.

b) Eine weitere Möglichkeit der katalytischen Wirkung ist die der Elektronenvermittlung zwischen den Redoxpartnern durch den inner-sphere-Komplex. Dieser Mechanismus setzt die gleichzeitige Bindung beider Reaktionspartner im outer-sphere-Komplex voraus. Das ist jedoch prinzipiell möglich. NILKOLASEV und BECK [5] konnten z. B. die bevorzugte Existenz eines $\{[Fe\ phan_3]S_2O_8J\}$- outer-sphere-Komplexes nachweisen.

Es ist anzunehmen, daß $S_2O_8^{2-}$ und J^- die äußere Sphäre in *trans*-Stellung besetzen. Zwischen Liganden in trans-Stellung wurde von CHATT und Mitarbeitern [13] eine elektronische Wechselwirkung festgestellt. Hierbei dient der inner-sphere-Komplex als Elektronenvermittler.

In dieser Arbeit sollen einige Co(III)-Komplexe bezüglich ihrer katalytischen Wirkung auf die Reaktion (1) untersucht werden. Dabei soll festgestellt werden, ob die Reihenfolge der outer-sphere-Komplexstabilität der Co(III)-Komplexkationen identisch ist mit der Folge der gemessenen Reaktionsgeschwindigkeiten.

Aus der Literatur sind, wenn man die unterschiedlichen experimentellen Bedingungen berücksichtigt, nur wenig gut vergleichbare outer-sphere-Komplexstabilitätskonstanten von Co(III)-Komplexkationen bekannt. Die zu Vergleichzwecken in dieser Arbeit geeigneten Literaturwerte sind in Tabelle I zusammengefaßt.

Tabelle I

Outer-sphere-Komplexstabilitätskonstanten (β_{01}) von einigen Co(III)-Komplexen

Ligand	Komplexkationen $[Co\ a_6]^{3+}$	$[Co\ en_3]^{3+}$	$[Co\ pn_3]^{3+}$	$[Co\ phan_3]^{3+}$	Lit.
Cl^-	1,48	1,72	1,60		[14]
Br^-	1,66	1,32			[15]
J^-	1,23	0,93			[15]
SO_4^{2-}	3,30	3,23			[16]
SO_4^{2-}	3,56	3,45	3,76		[14]
SO_4^{2-}	3,26	3,10			[17]
J^-				1,69	[18]

Für die experimentellen Untersuchungen wurden folgende Komplexe verwendet:

1. $[Co\ a_6]Cl_3$ — a = NH_3
2. $[Co\ en_3]Cl_3 \cdot 3H_2O$ — en = Äthylendiamin
3. $[Co\ pn_3]Cl_3$ — pn = 1,2 Diaminopropan
4. $[Co\ chn_3]Cl_3 \cdot 1H_2O$ — chn = *trans*-1,2-Diaminocyclohexan
5. $[Co\ phan_3]Cl_3 \cdot 7H_2O$ — phan = 1,10-Phenanthrolin

Diese Komplexe sind sehr stabil. Die Bruttostabilitätskonstanten der Komplexkationen sind in Tabelle II zusammengestellt. Hierbei wurden die aus der Literatur nicht bekannten Co(III)-Komplexstabilitätskonstanten berechnet nach (3).

$$E^0_{\text{kompl.}} = E^0_{\text{hydr.}} = \frac{RT}{nF} \ln \frac{\beta_{III}}{\beta_{II}} \tag{3}$$

Tabelle II

Bruttostabilitätskonstanten der verwendeten Co(III)-Komplexe

Komplexe	β_{III}	β_{II}	$E^0_{\text{kompl.}}$ [mV] gegen GKE
$[Co\ a_6]^{3+}$	34,36 [25]	5,11 [25]	−183 [7]
$[Co\ en_3]^{3+}$	48,69 [25]	13,82 [25]	−495 [26]
$[Co\ pn_3]^{3+}$	50,34	14,72 [28]	−503 [27]
$[Co\ chn_3]^{3+}$	50,90	15,22 [30]	−515 [26]
$[Co\ phan_3]^{3+}$	45,55	19,90 [31]	+ 86 [29]

β_{II}, β_{III} = Bruttostabilitätskonstanten der Co(II)- und Co(III)-Komplexe
$E^0_{hydr.}$ = Standardredoxpotential des hydratisierten Redoxsystems
$E^0_{hydr.}$ = 1,84 V[19,20]
$E^0_{kompl.}$ = Standardredoxpotential des Redoxsystems der Komplexionen

2. Experimentelles

2.1 *Herstellung der Komplexverbindungen*

Zur Präparation der Komplexe $[Co\ a_6]Cl_3$, $[Co\ en_3]Cl_3 \cdot 3H_2O$ und $[Co\ pn_3]Cl_3$ wurden oft erprobte Standardmethoden angewendet [32, 33, 34]. Die Verbindungen $[Co\ chn_3]Cl_3 \cdot 1H_2O$ und $[Co\ phan_3]Cl_3 \cdot 7H_2O$ wurden einmal aus $[Co\ a_5\ Cl]Cl_2$ sowie aus $Na_3[Co(CO_3)_3] \cdot 3H_2O$ [21] hergestellt. Beide Ausgangsverbindungen eignen sich gut zur Herstellung der Aminkomplexe.

Die erhaltenen Co(III)-Komplexverbindungen wurden (bis auf eine einmalige Umkristallisation bei $[Co\ pn_3]Cl_3$) mindestens zweimal umkristallisiert. Für alle Arbeiten wurde bidestilliertes Wasser verwendet.

Bei der Herstellung, der Lagerung und dem Gebrauch der benutzten Co(III)-Komplexsalze wurde ihre Lichtempfindlichkeit [22, 23] berücksichtigt.

2.2 *Bestimmung der Reaktionsgeschwindigkeit*

Der Ablauf der Reaktion (1) wurde photometrisch über die Jodkonzentration verfolgt. Hierzu war eine sehr empfindliche und stabilisierte Apparatur erforderlich, da sehr kleine Jodkonzentrationen (ca. 10^{-7} *M*) zu messen waren. Den Aufbau der Apparatur zeigt Abb. 1.

Die Anfangsgeschwindigkeit der Reaktion wurde bestimmt, indem die Zeit gemessen wurde, die bis zum Erreichen einer sehr geringen Jodkonzentration ($5 \cdot 10^{-6}$ *M* J_2) erfordlich war. Die Anfangsgeschwindigkeit ergibt sich dann zu

$$v_0 = \frac{\Delta C_{S_2O_8}\,2-}{\Delta t} \tag{4}$$

mit $\Delta C_{S_2O_7}\ 2- = \Delta C_{J_2} = 5 \cdot 10^{-6}\ M$.

Die entsprechenden Jodkonzentrationen wurden durch Eichkurven ermittelt. Hierbei wurde die jeweilige Konzentration an KJ und dem Co(III)-Komplexsalz berücksichtigt.

Die Messungen wurden bei einer Wellenlänge von 350 nm durchgeführt. Bei den Messungen mit $[Co\ phan_3]^{3+}$ mußte mit 400 nm gemessen werden, da die Eigenabsorption des Komplexes bei 350 nm zu hoch ist.

Bei den Reaktionen in Gegenwart des $[Co\ phan_3]^{3+}$-Komplexes trafen z. T. Störungen durch eine sehr geringe kolloidale Trübung auf, die wahrschein-

lich auf eine CT-Komplexbildung des freien Jods mit dem π-System des Phenanthrolins zurückzuführen ist [24]. Dieses Verhalten wurde jedoch bei der Aufstellung der Eichkurven berücksichtigt.

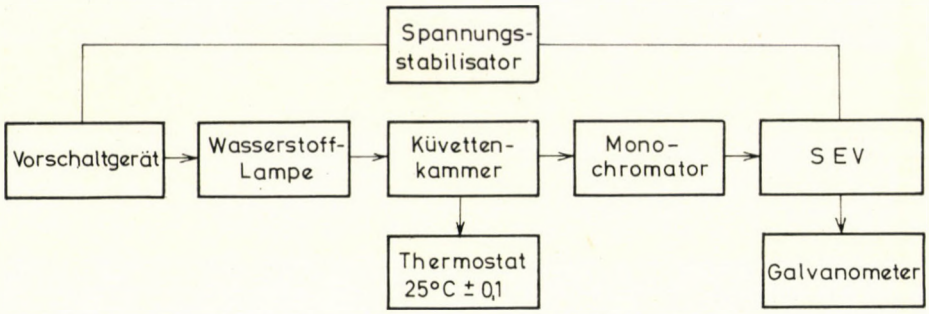

Abb. 1. Schematischer Aufbau der Meßapparatur

Bei allen Messungen betrug die Konzentration an Co(III)-Komplex $1 \cdot 10^{-3}$ *M*.

Die Meßtemperatur war 25 °C.

3. Meßergebnisse

3.1 *Reaktion ohne Komplexzusatz*

Zur Prüfung der Apparatur wurde die Reaktion (1) zunächst ohne Komplexsalz gemessen.

Bei den Konzentrationen $[J^-]_0 = 2{,}5 \cdot 10^{-3}\,M$ und $[S_2O_8^{2-}]_0 = 5 \cdot 10^{-4}\,M$ ergab sich eine Anfangsgeschwindigkeit von

$$v_0 = 8{,}35 \cdot 10^{-8}\ M \cdot \text{min}^{-1}.$$

Die Geschwindigkeitskonstante 2. Ordnung ergibt sich mit

$$k = \frac{v_0}{C^0_{S_2O_8}\,2- \cdot C^0_{J^-}} \tag{5}$$

zu $k = 1{,}11 \cdot 10^{-3}\ 1 \cdot \text{Mol}^{-1} \cdot \text{sec}^{-1}$
$= 6{,}66 \cdot 10^{-2}\ 1 \cdot \text{Mol}^{-1} \cdot \text{min}^{-1}$.

Dieser Wert stimmt mit den Literaturangaben [2] gut überein.

3.2 *Variation der $S_2O_8^{2-}$ - und J^--Konzentration*

Diese Messungen wurden nur mit $[Co\ en_3]^{3+}$ als Katalysator durchgeführt. Sie sollten dazu dienen, einen Überblick über die Verhältnisse beim katalytischen Ablauf der Reaktion (1) zu vermitteln.

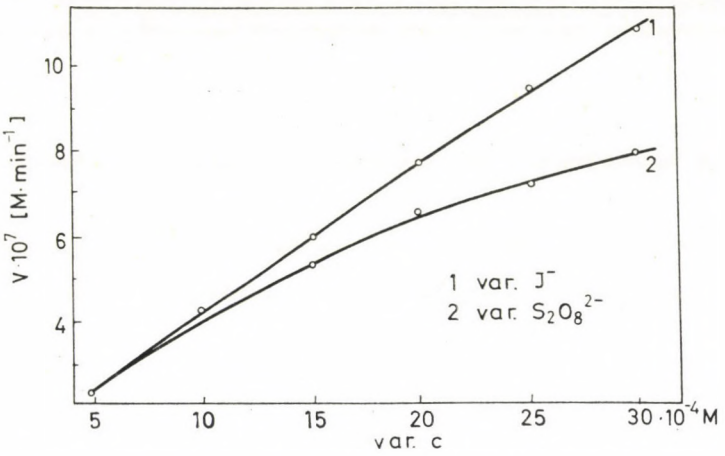

Abb. 2. Änderung der Anfangsgeschwindigkeit bei Variation von $C^0_{S_2O_8}2-$ und C^0_J
Bei Variation von $C^0_{S_2O_8}2-$: $C^0_J = 5 \cdot 10^{-4}\ M$
Bei Variation von $C^0_{J^-}$: $C^0_{S_2O_8}2- = 5 \cdot 10^{-4}\ M$

Die Totalkonzentrationen $C^0_{S_2O_8}2-$ und C^0_J — wurden im Bereich $5 \cdot 10^{-4}$... $30 \cdot 10^{-4}\ M$ variiert. Dabei wurde jeweils die Konzentration eines Reaktionspartners bei $5 \cdot 10^{-4}\ M$ konstant gehalten.

Die erhaltenen Anfangsgeschwindigkeiten in Abhängigkeit von der Ausgangskonzentration der Reaktionspartner sind in Tab. III zusammengefaßt und in Abb. 2 graphisch dargestellt.

Tabelle III

Änderung der Anfangsgeschwindigkeiten bei Variation der Konzentration der Reaktionspartner

$C^0_{S_2O_8}2-[M]$	v_0 $[M \cdot min^{-1}]$	$C^0_{J^-}$ $[M]$	v_0 $[M \cdot min^{-1}]$
$5 \cdot 10^{-4}$	$2{,}31 \cdot 10^{-7}$	$5 \cdot 10^{-4}$	$2{,}28 \cdot 10^{-7}$
$10 \cdot 10^{-4}$	$4{,}22 \cdot 10^{-7}$	$10 \cdot 10^{-4}$	$4{,}25 \cdot 10^{-7}$
$15 \cdot 10^{-4}$	$5{,}30 \cdot 10^{-7}$	$15 \cdot 10^{-4}$	$5{,}92 \cdot 10^{-7}$
$20 \cdot 10^{-4}$	$6{,}52 \cdot 10^{-7}$	$20 \cdot 10^{-4}$	$7{,}58 \cdot 10^{-7}$
$25 \cdot 10^{-4}$	$7{,}15 \cdot 10^{-7}$	$25 \cdot 10^{-4}$	$9{,}33 \cdot 10^{-7}$
$30 \cdot 10^{-4}$	$7{,}85 \cdot 10^{-7}$	$30 \cdot 10^{-4}$	$10{,}70 \cdot 10^{-7}$
$C^0_{J^-} = 5 \cdot 10^{-4}\ M$		$C^0_{S_2O_8}2- = 5 \cdot 10^{-4}\ M$	

3.3 *Zugabe von KCl*

Hält man die Ausgangskonzentration der Reaktionspartner sowie des Co(III)-Komplexes konstant und setzt KCl zu, so sinken die Reaktionsgeschwindigkeiten.

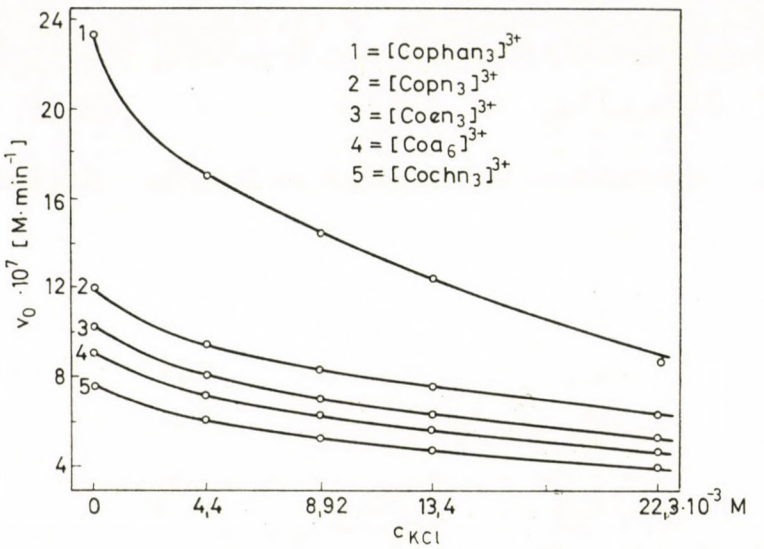

Abb. 3. Einfluß der KCl-Konzentration auf die Anfangsgeschwindigkeit
$C^0_{S_2O_8}2- = 5 \cdot 10^{-4}\ M$ (bei $[Co\ phan_3]^{3+}$ ist $C^0_{S_2O_8}2- = 5 \cdot 10^{-5}\ M$)
$C^0_J = 2{,}5 \cdot 10^{-3}\ M$

Die Cl^--Konzentration wurde im Bereich $C^0_{Cl} = 0 \ldots 22{,}3 \cdot 10^{-3}\ M$ variiert.

Die konstanten Totalkonzentrationen der Reaktionspartner waren:

$C^0_{S_2O_8}2- = 5 \cdot 10^{-4}\ M$ (bei $[Co\ phan_3]^{3+}$: $C^0_{S_2O_8^{2-}} = 5 \cdot 10^{-5}\ M$)
$C_{J-} = 5 \cdot 10^{-3}\ M$.

Die Co(III)-Komplexkonzentration betrug immer $1 \cdot 10^{-3}\ M$.

Die Reaktion mit $[Co\ phan_3]^{3+}$ als Katalysator verlief so schnell, daß hier die Peroxodisulfatkonzentration auf $5 \cdot 10^{-5}\ M$ verringert werden mußte. Das ist bei einem Vergleich der Reaktionsgeschwindigkeiten zu beachten.

Die graphische Auftragung der Anfangsgeschwindigkeiten in Abhängigkeit von der KCl-Konzentration zeigt Abb. 3. Die Meßwerte sind in Tabelle IV zusammengefaßt.

Tabelle IV

Einfluß der KCl-Konzentration auf die Anfangsgeschwindigkeit v_0

$C^0_{Cl^-}$ [M]	$[Co\ a_6]^{3+}$	$[Co\ en_3]^{3+}$	$[Co\ pn_3]^{3+}$	$[Co\ chn_3]^{3+}$	$[Co\ phan_3]^{3+}$
0	9,02	10,18	11,90	7,66	23,26
$4{,}46 \cdot 10^{-3}$	7,22	8,06	9,45	6,08	16,95
$8{,}92 \cdot 10^{-3}$	6,31	7,01	8,35	5,32	14,39
$13{,}40 \cdot 10^{-3}$	5,66	6,31	7,61	4,76	12,50
$22{,}30 \cdot 10^{-3}$	4,70	5,24	6,31	3,96	8,66

$C^0_{S_2O_8}{}^{2-} = 5 \cdot 10^{-4}\,M$ (bei $[Co\ phan_3]^{3+}$ ist $C^0_{S_2O_8}{}^{2-} = 5 \cdot 10^{-5}\,M$)

$C^0_{J^-} = 2{,}5 \cdot 10^{-3}\,M$

Geschwindigkeitswerte in $M \cdot \min^{-1} \cdot 10^7$.

4. Diskussion der Meßergebnisse

4.1 *Zur Kinetik der katalytischen Reaktion zwischen Peroxodisulfat und Jodid*

Bei der katalytisch ablaufenden $S_2O_8^{2-}/J^-$-Reaktion ist dem geschwindigkeitbestimmenden Schritt das Gleichgewicht der outer-spere-Komplexbildung vorgelagert.

Die langsame nichtkatalytische Parallelreaktion kann vernachlässigt werden.

Folgende outer-sphere-Komplexgleichgewichte sind möglich, dargestellt am Beispiel des $[Co\ en_3]^{3+}$:

$$[Co\ en_3]^{3+} + S_2O_8^{2-} \overset{K_1}{\rightleftharpoons} \{[Co\ en_3]S_2O_8\}^+ \tag{6}$$

$$[Co\ en_3]^{3+} + J^- \overset{K_2}{\rightleftharpoons} \{[Co\ en_3]J\}^{2+} \tag{7}$$

$$\{[Co\ en_3]S_2O_8\}^+ + J^- \overset{K_3}{\rightleftharpoons} \{[Co\ en_3]S_2O_8J\} \tag{8}$$

$$\{[Co\ en_3]J\}^{2+} + S_2O_8^{2-} \overset{K_4}{\rightleftharpoons} \{[Co\ en_3]S_2O_8J\} \tag{9}$$

Von den ebenfalls möglichen höheren outer-sphere-Komplexen wie z. B. $\{[Co\ en_3]J_2\}^+$ oder $\{[Co\ en_3](S_2O_8)_2\}^-$ soll hier vereinfachend abgesehen werden.

Aus den Gleichgewichten (6) ... (9) ergeben sich folgende Realisationsmöglichkeiten:

$$\{[Co\ en_3]S_2O_8\}^+ + J^- \overset{k_1}{\rightleftharpoons} \text{Produkte} \tag{10}$$

$$\{[\text{Co en}_3]\text{J}\}^{2+} + \text{S}_2\text{O}_8^{2-} \overset{k_2}{\rightleftharpoons} \text{Produkte} \tag{11}$$

$$\{[\text{Co en}_3]\text{S}_2\text{O}_8\text{J}\} \overset{k_3}{\rightleftharpoons} \text{Produkte} \tag{12}$$

Bei der Formulierung der Geschwindigkeitsgesetze für die katalytisch ablaufende Reaktion wurde von der Annahme ausgegangen, daß analog zum nichtkatalytischen Ablauf (1) am geschwindigkeitbestimmenden Schritt ein $S_2O_8^{2-}$- und ein J^--Ion beteiligt ist.

Für die Reaktionen (10) . . . (12) ergeben sich dann mit den Gleichgewichten (6) . . . (9) die Geschwindigkeitsgleichungen:

$$\begin{aligned} v_1 &= k_1 \left[\{[\text{Co en}_3]\text{S}_2\text{O}_8\}^+\right] [\text{J}^-] \\ v_1 &= k_1 K_1 [\text{Co en}_3^{3+}] [\text{S}_2\text{O}_8^{2-}] [\text{J}^-] \end{aligned} \tag{13}$$

$$\begin{aligned} v_2 &= k_2 \left[\{[\text{Co en}_3]\text{J}\}^{2+}\right] [\text{S}_2\text{O}_8^{2-}] \\ v_2 &= k_2 K_2 [\text{Co en}_3^{3+}] [\text{J}^-] [\text{S}_2\text{O}_8^{2-}] \end{aligned} \tag{14}$$

$$\begin{aligned} v_3 &= k_3 \left[\{[\text{Co en}_3]\text{S}_2\text{O}_8\text{J}\}\right] \\ v_3 &= k_3 K_1 K_3 [\text{Co en}_3^{3+}] [\text{S}_2\text{O}_8^{2-}] [\text{J}^-] \end{aligned} \tag{15}$$

Die Gesamtgeschwindigkeit ist dann:

$$v = v_1 + v_2 + v_3.$$

Erfahrungsgemäß ist $K_1 \gg K_2$, so daß man vereinfachen kann zu

$$v = v_1 + v_3.$$

Es soll nun untersucht werden, welchen Beitrag v_3 zur Gesamtgeschwindigkeit leiste. Bei den für diesen Reaktionsweg entscheidenden outer-sphere-Komplexgleichgewicht (8) muß es sich um ein Gleichgewicht mit relativ kleiner Bildungskonstante K_3 handeln. Dies ergibt sich aus dem fast linearen Anstieg der Reaktionsgeschwindigkeit bei Änderung der J^--Konzentration (Abb. 2).

Die Größenordnung der festgestellten Beeinflussung der Reaktionsgeschwindigkeit durch Cl^--Zusatz (vergleiche Abschnitt 3.3) spricht jedoch dafür, daß der outer-sphere-Komplex (8) nicht geschwindigkeitbestimmend ist: Chloridionen bilden meist geringfügig stabilere outer-sphere-Komplexe als Jodidionen. Die Messungen zeigen aber, daß eine Senkung der Reaktionsgeschwindigkeit von etwa 50% erst bei einer Cl^--Konzentration eintritt, die zehnmal größer als die J^--Konzentration ist. Dies deutet darauf hin, daß durch die Chloridionen ein Komplex verdrängt wird, der stabiler als der entsprechende J^--Komplex (8) sein muß.

Aus den geschilderten Zusammenhängen kann geschlossen werden, daß die Reaktionsgeschwindigkeit vorwiegend durch v_1 bestimmt wird.

Damit gilt:

$$v \approx v_1.$$

Wegen der relativ schwachen outer-sphere-Komplexbildung der Jodidionen läßt sich (bei den hier vorliegenden Konzentrationsverhältnissen) die Gleichgewichtskonzentration durch die Totalkonzentration ersetzen:

$$[J^-] \approx [J^-]_0.$$

Man erhält:

$$v \approx v_1 = k_1[\{[Co\ en_3]S_2O_8\}^+]\ [J^-]_0 \qquad \text{oder}$$

$$v \approx v_1 = k_1 K_1[Co\ en_3^{3+}]\ [S_2O_8^{2-}]\ [J^-]_0. \tag{16}$$

4.2 *Zugabe von KCl*

Die Zugabe von KCl verringert die Reaktionsgeschwindigkeit, da die Chloridionen selbst outer-sphere-Komplexe bilden und dadurch die Konzentration des »katalytisch aktiven« Komplexes gesenkt wird.

Die Größe der Wechselwirkung zwischen den outer-sphere-Komplexen wird bestimmt durch das Verhältnis der Stabilitätskonstanten und der Konzentrationen.

Neben den vorhandenen Gleichgewichten wird das outer-sphere-Komplexgleichgewicht der Chloridionen wirksam:

$$[Co\ en_3]^{3+} + Cl^- \overset{K_5}{\rightleftharpoons} \{[Co\ en_3]Cl\}^{2+}. \tag{17}$$

Die Reaktionsgeschwindigkeit wird bei höheren Chlorid-Konzentrationen durch die Gleichgewichte (6) und (17) bestimmt.

Für die Konzentration des »katalytisch aktiven« Komplexes (6) gilt dann:

$$[\{[Co\ en_3]S_2O_8\}^+] = [Co\ en^{3+}]_0 - [\{[Co\ en_3]Cl\}^{2+}]. \tag{18}$$

Entsprechend den Gleichgewichten (6) und (17) gilt:

$$K_1 = \frac{[\{[Co\ en_3]\,S_2O_8\}^+]}{[Co\ en_3^{3+}]\ [S_2O_8^{2-}]}$$

$$K_5 = \frac{[\{[Co\ en_3]\ Cl\}^{2+}]}{[Co\ en_3^3]\ [Cl^-]}, \quad [Co\ en_3^3] = \frac{[\{[Co\ en_3]\ Cl\}^{2+}]}{K_5[Cl^-]}.$$

Durch Substitution von $[Co\,en_3^{3+}]$ in (18) erhält man:

$$[\{[Co\,en_3]\,S_2O_8\}^+] = [Co\,en_3^{3+}]_0 - \frac{[\{[Co\,en_3]\,Cl\}^{2+}]}{[Cl^-]\,K_5} - [\{[Co\,en_3]\,Cl\}^{2+}]. \quad (19)$$

Die Gleichgewichte (6) und (17) sind über die Gleichgewichtskonzentration $[Co\,en_3^{3+}]$ gekoppelt.

Damit ergibt sich:

$$\frac{[\{[Co\,en_3]\,Cl\}^{2+}]}{K_5\,[Cl^-]} = \frac{[\{[Co\,en_3]\,S_2O_8\}^+]}{K_1\,[S_2O_8^{2-}]}$$

$$[\{[Co\,en_3]\,Cl\}^{2+}] = \frac{K_5\,[Cl^-]\,[\{[Co\,en_3]\,S_2O_8\}^+]}{K_1\,[S_2O_8^{2-}]}\,. \quad (20)$$

Nach Einsetzen von (20) in (19) erhält man:

$$[\{[Co\,en_3]\,S_2O_8\}^+] = [Co\,en_3^{3+}]_0 - \frac{[\{[Co\,en_3]\,S_2O_8\}^+]}{K_1\,[S_2O_8^{2-}]} - \frac{K_5\,[Cl^-]\,[\{[Co\,en_3]\,S_2O_8\}^+]}{K_1\,[S_2O_8^{2-}]}$$

und nach Umformung:

$$\frac{1}{[\{[Co\,en_3]\,S_2O_8\}^+]} = \frac{1+K_1\,[S_2O_8^{2-}]}{[Co\,en_3^{3+}]_0\,K_1\,[S_2O_8^{2-}]} + \frac{K_5\,[Cl^-]}{[Co\,en_3^{3+}]_0\,K_1\,[S_2O_8^{2-}]}\,. \quad (21)$$

Eine wesentliche Vereinfachung tritt ein, wenn in Gleichung (21) die Gleichgewichtskonzentrationen $[Cl^-]$ und $[S_2O_8^{2-}]$ durch die bekannten Totalkonzentrationen $[Cl^-]_0$ und $[S_2O_8^{2-}]_0$ ersetzt. Diese Näherung ist bei Cl^- unproblematisch, da hier nur relativ schwache outer-sphere-Komplexe gebildet werden.

Bei $S_2O_8^{2-}$ dagegen wird diese Vereinfachung nur bei hohen Chloridkonzentrationen annähernd zutreffen, da hier die Gleichgewichtskonzentration der $S_2O_8^{2-}$-Ionen zunimmt.

Nach Einführung der Näherungen

$$[Cl^-] \approx [Cl^-]_0$$

$$[S_2O_8^{2-}] \approx [S_2O_8^{2-}]_0 \quad \text{(bei höheren } Cl^-\text{-Konzentrationen)}$$

erhält man:

$$\frac{1}{[\{[Co\,en_3]\,S_2O_8\}^+]} = \frac{1+K_1\,[S_2O_8^{2-}]_0}{[Co\,en_3^{3+}]_0\,K_1\,[S_2O_8^{2-}]} + \frac{K_5\,[Cl^-]_0}{[Co\,en_3^{3+}]_0\,K_1\,[S_2O_8^{2-}]_0}\,. \quad (22)$$

Da die Reaktionsgeschwindigkeit der Konzentration des »katalytisch aktiven« Komplexes (6) direkt proportional ist, sollte eine graphische Auftragung $1/v_0$ gegen $[Cl^-]_0$ entsprechend der Gleichung (22) eine Gerade ergeben. Dies ist bei höheren Cl^--Konzentrationen auch der Fall. (Abb. 4).

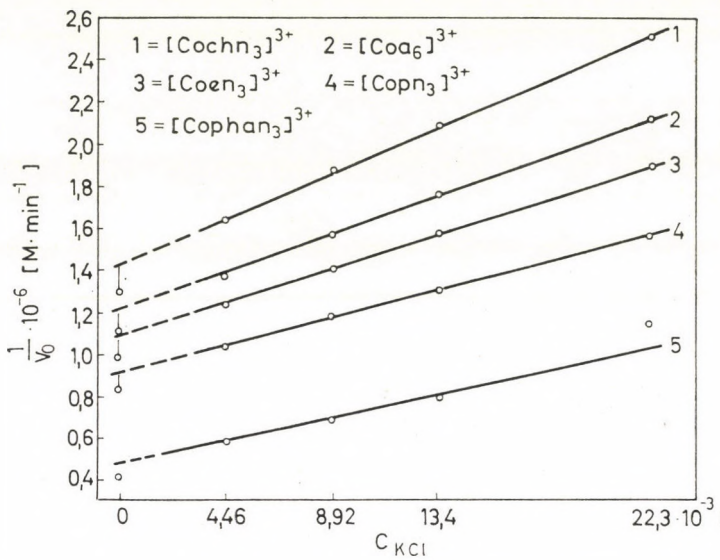

Abb. 4. Abhängigkeit der reziproken Anfangsgeschwindigkeit von der KCl-Konzentration
$C^0_{S_2O_8}{}^{2-} = 5 \cdot 10^{-4}\ M$ (bei $[Co\ phan]^{3+}$ ist $C^0_{S_2O_8}{}^{2-} = 5 \cdot 10^{-5}\ M$)
$C^0_J = 2{,}5 \cdot 10^{-3}\ M$

Durch Berücksichtigung von (13) ergibt sich der direkte Zusammenhang mit $1/v_0$:

$$\frac{1}{v_0} = \frac{1 + K_1[S_2O_8^{2-}]_0}{[Co\ en_3^{3+}]_0\,[S_2O_8^{2-}]_0\,[J^-]_0\,k_1\,K_1} + \frac{K_5\,[Cl^-]_0}{[Co\ en_3^{3+}]_0\,[S_2O_8^{2-}]_0\,[J^-]_0\,k_1\,K_1}\,. \qquad (23)$$

Aus dem Ordinationsabschnitt der Geraden (23) erhält man für K_1:

$$K_1 = \frac{1}{[S_2O_8^{2-}]_0\left\{\frac{1}{v_0}[Co\ en_3^{3+}]_0\,[J^-]_0\,k_1 - 1\right\}}\,. \qquad (24)$$

Ohne Kenntnis von k_1 kann man aus (24) keinen numerischen Wert für K_1 oder für k_1K_1 erhalten.

Aus dem Anstieg m der Geraden (23) ergibt sich eine Beziehung für K_5:

$$K_5 = m \cdot [Co\ en_3]_0[S_2O_8^{2-}]_0\,[J^-]_0 k_1 K_1. \qquad (25)$$

Die nach dem Einsetzen der experimentellen Werte in (24) und (25) erhaltenen Ausdrücke für k_1K_1 und K_5 sind in Tabelle V zusammengestellt.

Tabelle V

Ausdrücke für k_1 K_1 und K_5 bei den verwendeten Co(III)-Komplexen

Komplex	$k_1 K_1$	K_5
$[Co\ a_6]^{3+}$	$656 + 0{,}328\ K_1$	$32{,}8 + 0{,}0164\ K_1$
$[Co\ en_3]^{3+}$	$729 + 0{,}364\ K_1$	$33{,}1 + 0{,}0165\ K_1$
$[Co\ pn_3]^{3+}$	$852 + 0{,}426\ K_1$	$30{,}6 + 0{,}0153\ K_1$
$[Co\ chn_3]^{3+}$	$550 + 0{,}276\ K_1$	$33{,}3 + 0{,}0167\ K_1$
$[Co\ phan_3]^{3+}$	$16\,700 + 0{,}835\ K_1$	$49{,}7 + 0{,}00248\ K_1$

Setzt man für K_1 in Anlehnung an bekannte Stabilitätskonstanten für SO_4^{2-}-outer-sphere-Komplexe einen Wert von etwa 10^3 ein, so ergeben sich für K_5 Ergebnisse, die mit den Literaturwerten gut übereinstimmen.

Dies kann jedoch nur als Hinweis dienen, da die genauen K_1-Werte nicht bekannt sind.

4.3 *Zur katalytischen Aktivität der verwendeten Co(III)-Komplexe*

Mit Ausnahme von $[Co\ phan_3]^{3+}$ unterscheiden sich die Komplexe nur wenig in ihrer katalytischen Wirkung. Die Anfangsgeschwindigkeit der Reaktion ist zehnmal größer als beim nichtkatalytischen Ablauf.

Die Reaktionsgeschwindigkeit in Gegenwart von $[Co\ phan_3]^{3+}$ ist dagegen (bei vergleichbaren Konzentrationsbedingungen) etwa um den Faktor 20 gegenüber den anderen Komplexen vergrößert. Diese hohe Geschwindigkeit ist nicht durch eine etwas höhere outer-sphere-Komplexstabilität zu erklären. Es ist anzunehmen, daß hier die Teilgeschwindigkeit v_3 (15) einen größeren Beitrag zur Gesamtgeschwindigkeit leistet. Die Fähigkeiten des Phenanthrolin-π-Systems zur Elektronenübertragung können hierbei wirksam werden.

Der Elektronenaustausch bei der katalytisch ablaufenden Reaktion kann demnach in verschiedener Weise erfolgen:

Einmal über den Co(III)-Komplex als Elektronenvermittler und zum anderen nach einem Mechanismus analog zum nichtkatalytischen Ablauf.

Im letzten Fall besteht die Katalysewirkung der outer-sphere-Komplexbildung nur in der Aufhebung der elektrostatischen Abstoßung bei Annäherung der Reaktionspartner.

Abgesehen vom $[Co\ phan_3]^{3+}$-Komplex scheint der Elektronenaustausch über den inner-sphere-Komplex nur einen geringen Anteil zu haben.

LITERATUR

1. KING, V., JACOBS, M.: J. Am. Chem. Soc. **53,** 1704 (1931)
2. INDELLI, A., AMIS, E. S.: J. Am. Chem. Soc. **82,** 332 (1960)
3. INDELLI, A., PRUE, J. E.: J. Chem. Soc. **107** (1959)
4. BECK, M. T.: Coord. Chem. Rev., **3,** 91 (1968)
5. BECK, M. T.: Vortragsberichte zum Symposium Koordinationschemie der Übergangselemente. Jena, 1969, Sektion C. p. 1
6. SUTIN: Ann. Rev., Phys. Chem. **17,** 119 (1966)
7. BARTELT, H., LANDAZURY, S.: J. Electroanal. Chem. **22,** 105 (1969)
8. BARTELT, H.: Electrochim. Acta **16,** 307 (1971)
9. LINHARD, M.: Z. Elektrochem. **50,** 224 (1944)
10. ELDER, R., PETRUCCI, S.: Inorg. Chem. **9,** 19 (1970)
11. LARSSON, R., NORMAN, B.: J. Inorg. Nucl. Chem. **28,** 1291 (1966)
12. LARSSON, R., JOHANNSON, L.: Proc. Symp. Coord. Chem. Tihany. Akadémiai Kiadó, Budapest, 1965, p. 43
13. CHATT, J., DUNCANSON, L. A., SHAW, B. L., VENANZI, L.: Disc. Faraday Soc. **26,** 131 (1958)
14. JENKINS, J. L., MONK, C. B.: J. Chem. Soc. **68** (1951)
15. EVANS, M. G., NANCOLLAS, G. H.: Trans. Faraday Soc. **49,** 363 (1953)
16. TANAKA, N., YAMADA, A.: Z. Anal. Chem. **224,** 117 (1967)
17. TANAKA, N., KOBAYASHI, Y., KAMADA, M.: Bull. Chem. Soc. Japan **40,** 12 (1967)
18. ILCHEVA, L., BECK, M. T.: Proc. Symp. Coord. Chem., Debrecen, 1970, Akadémiai Kiadó, Budapest, p. 89
19. LAMB, A. B., LARSON, A. T.: J. Am. Chem. Soc. **42,** 2024 (1920)
20. NOYES, A. A., DEAHL, T. G.: J. Chem. Soc. **59,** 1337 (1937)
21. BAUER, H. F., DRINKARD, W. G.: J. Am. Chem. Soc. **82,** 5031 (1960)
22. KLEIN, D., MOELLER, C. W.: Inorg. Chem. **4,** 394 (1965)
23. MANFRIN, M., VARANI, G., MOGGI, L., BALZANI, V.: Mol. Photochem. **1** (4), 387 (1969)
24. GUTMANN, B.: Chemistry in Britain **7,** 102 (1971)
25. BJERRUM, J.: Metalamine Formation in Aqueous Solution, 1941, reprinted 1957. P. Haase and Son, Copenhagen, p. 251
26. BARTELT, H.: J. Electroanal. Chem. **27,** 447 (1970)
27. BARTELT, H., SKILANDAT, H.: J. Electroanal. Chem. **24,** 207 (1970)
28. EDWARDS, L. J.: Dissert. University of Michigan, 1950
29. BARTELT, H.: Elektrochim. Acta **16,** 629 (1971)
30. BERTSCH, C., FERNELIUS, W. C., BLOCK, P.: Pennsylvania State Univ., Conhart No. AT (30—1) — 907, 1956
31. ANDERREGG, G.: Helv. Chim. Acta **46,** 2397 (1963)
32. BJERRUM, J., MCREYNOLDS, J. P.: Inorg. Syntheses, Vol. 2, p. 62, New York, McGraw-Hill, 1946
33. FERNELIUS: Inorg. Syntheses, Vol. 2, p. 221, New York, McGraw-Hill, 1946
34. DWYER, F. P., SARGESON, A. M., JAMES, L. B.: J. Am. Chem. Soc. **86,** 590 (1964)

H. BARTELT
W. SCHNEIDER } 108 Berlin, Bunsenstr. 1. DDR.

Acta Chimica Academiae Scientiarum Hungaricae, Tomus 76 (3), pp. 243—268 (1973)

INFRARED SPECTRA OF 1,2,3,5-TETRASUBSTITUTED BENZENE DERIVATIVES, II*

G. VARSÁNYI and P. SOHÁR

(Department of Physical Chemistry, Technical University, Budapest and Research Institute for Pharmaceutical Chemistry, Budapest)

Received April 5, 1972

A detailed interpretation is given of the infrared spectra of thirty-five 1,2,3,5-tetrasubstituted benzene derivatives containing so-called light atoms (atomic weight less than 20) in positions 2 and 5 and so-called heavy atoms (atomic weight greater than 20) in positions 1 and 3. Correlations were established between the intensity and frequency of the spectral bands, and the influence of substituents on the electron distribution. The coupling of certain vibrations having identical symmetry was demonstrated and the association structure of the individual compounds was established.

Introduction

The subject of this paper is the interpretation of the infrared spectra of 1,2,3,5-tetrasubstituted benzene derivatives characterized by the general formula **A**. Here, the atom of the substituents in positions 2 and 5, directly bonded to the aromatic ring, is a light atom (atomic weight less than 20) and the substituents in positions 1 and 3, respectively, are halogen atoms (atomic weight greater than 20) identical in all of the compounds. The thirty five compounds investigated are listed in Table I.

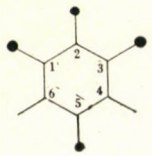

A

Similarly to Part I [1], the normal vibrations are divided into two groups [2]. The first group consists of vibrations of the aromatic ring (Fig. 1) with a possible contribution from the bonds connecting the substituents with the ring; the second group comprises the internal vibrations of the substituents. The ring vibrations are indicated according to WILSON's numbering [3] of the normal vibrations of benzene and discussed in nine groups. These are as follows:

Tangential skeletal vibrations;
radial skeletal vibrations;
out-of-plane skeletal vibrations;

* Part I: VARSÁNYI, G., SOHÁR, P.: Acta Chim. (Budapest) **74**, 315 (1972).

Table I

Compound	R	R′	X
I	OH	COOH	Cl
II	OH	COOH	Br
III	OMe	COOH	Cl
IV	OEt	COOH	Br
V	O-Allyl	COOH	Cl
VI	OAc	COOH	I
VII	OH	COOMe	Cl
VIII	OH	COOMe	Br
IX	NH_2	COOMe	Cl
X	OH	$CONH_2$	Br
XI	OMe	$CONH_2$	Cl
XII	OMe	$CONH_2$	Br
XIII	OEt	$CONH_2$	Br
XIV	O-*n*Pr	$CONH_2$	Br
XV	O-Allyl	$CONH_2$	Cl
XVI	O-Allyl	$CONH_2$	Br
XVII	OMe	CONHMe	Br
XVIII	O-Allyl	CONHMe	Br
XIX	OMe	CO—NHOH	Cl
XX	OMe	COCl	Cl
XXI	OMe	COCl	Br
XXII	OMe	CHO	Cl
XXIII	OMe	Ac	Cl
XXIV	OMe	CH=NOH	Cl
XXV	OMe	CN	Br
XXVI	OMe	$C{=}NHNH_2$	Cl
XXVII	OMe	$C{=}NHNH_2$	Br
XXVIII	OMe	C=NHNHOH	Cl
XXIX	OMe	C=NHNHOH	Br
XXX	OMe	$CSNH_2$	Br
XXXI	OH	NO_2	Br
XXXII	OMe	NO_2	Br
XXXIII	OMe	$CH_2N^+H_3{+}Cl^-$	Cl
XXXIV	OMe	NH_2	Cl
XXXV	OMe	NH_2	Br

C—H stretching vibrations;
in-plane bending C—H vibrations;
out-of-plane C—H vibrations;
C—Q stretching vibrations;
in-plane bending C—Q vibrations;
out-of-plane C—Q vibrations.

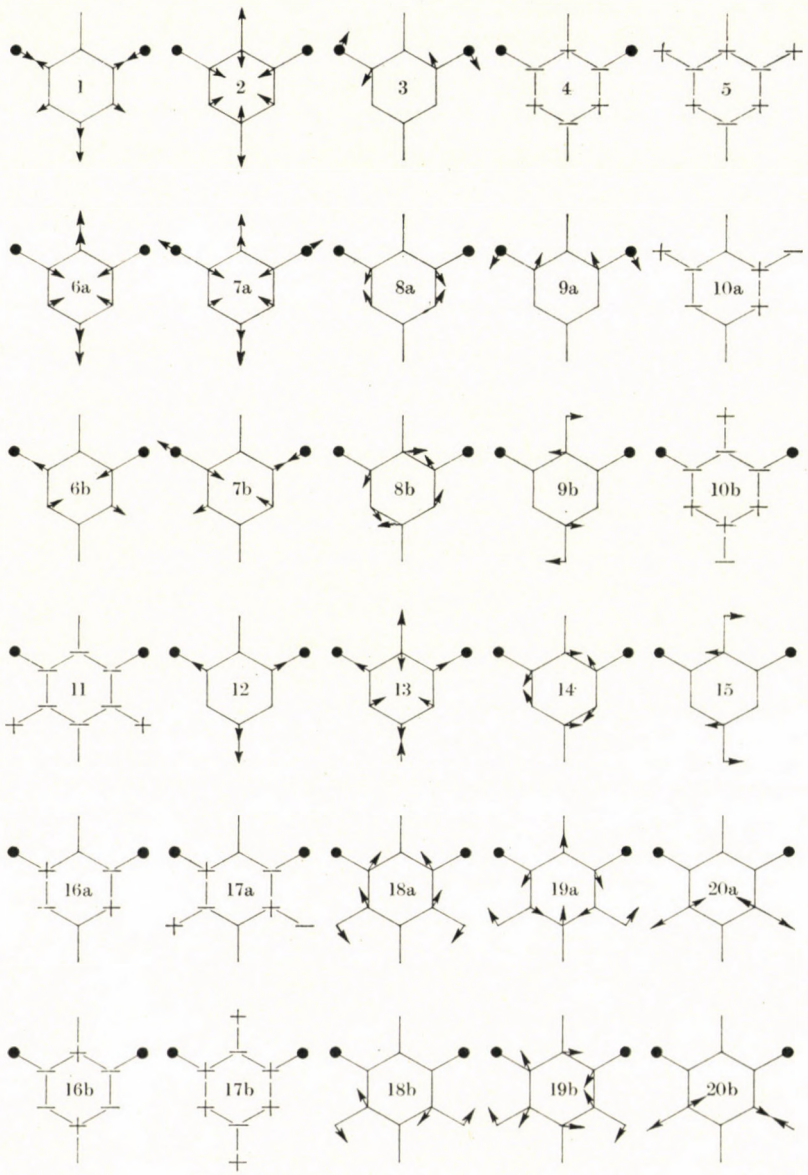

Fig. 1. Normal vibrations of benzene

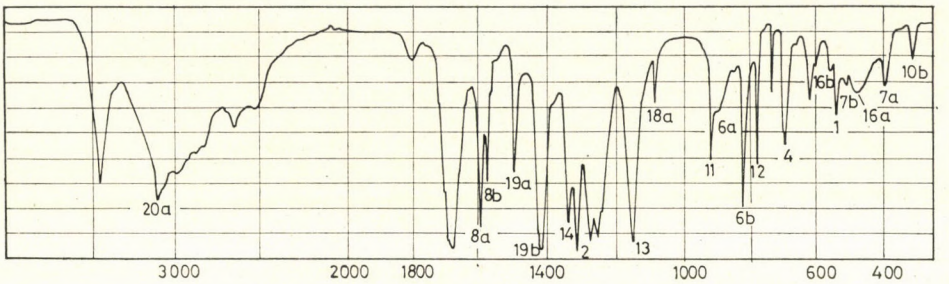

Fig. 2. 3,5-dichloro-4-hydroxybenzoic acid (I)

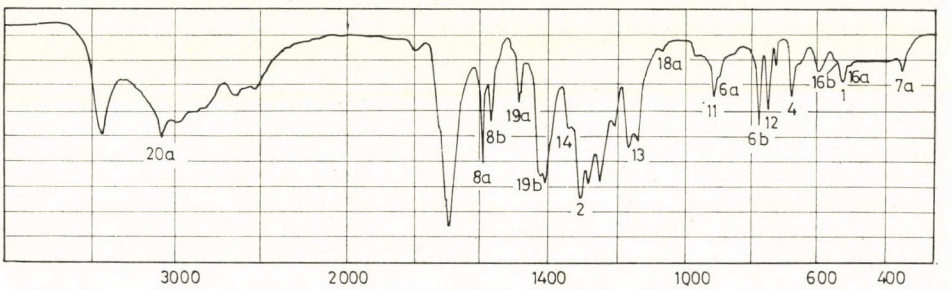

Fig. 3. 3,5-dibromo-4-hydroxybenzoic acid (II)

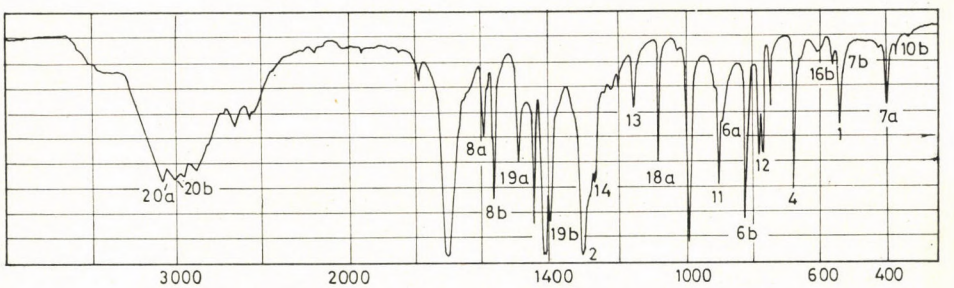

Fig. 4. 3,5-dichloro-4-methoxybenzoic acid (III)

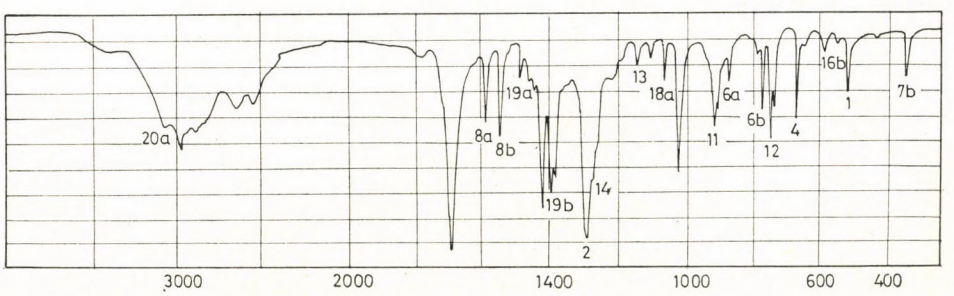

Fig. 5. 3,5-dibromo-4-ethoxybenzoic acid (IV)

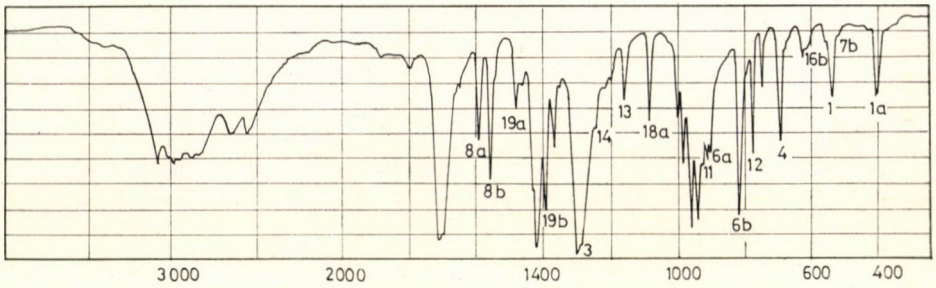

Fig. 6. 3,5-dichloro-4-allyloxybenzoic acid **(V)**

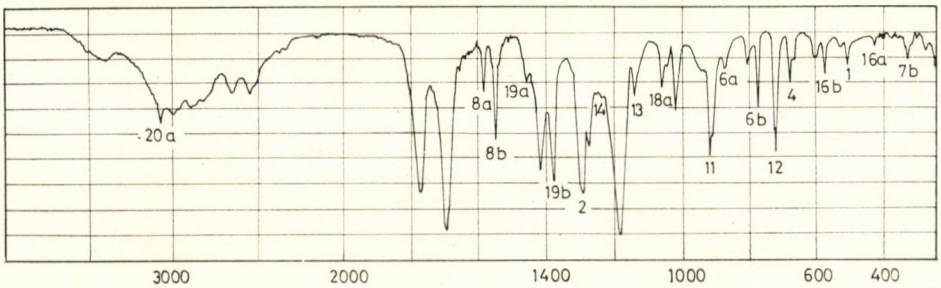

Fig. 7. 3,5-diiodo-4-acetoxybenzoic acid **(VI)**

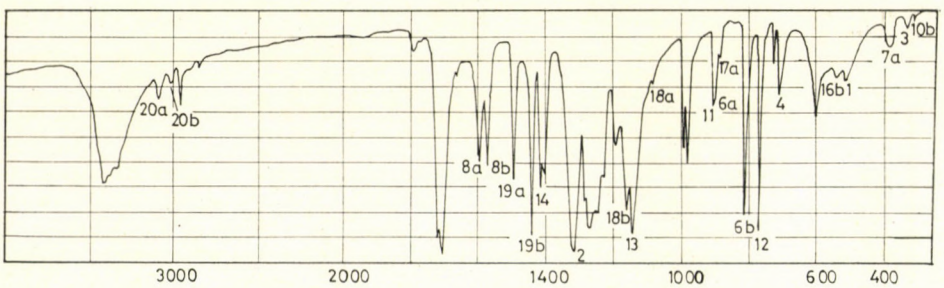

Fig. 8. Methyl 3,5-dichloro-4-hydroxybenzoate **(VII)**

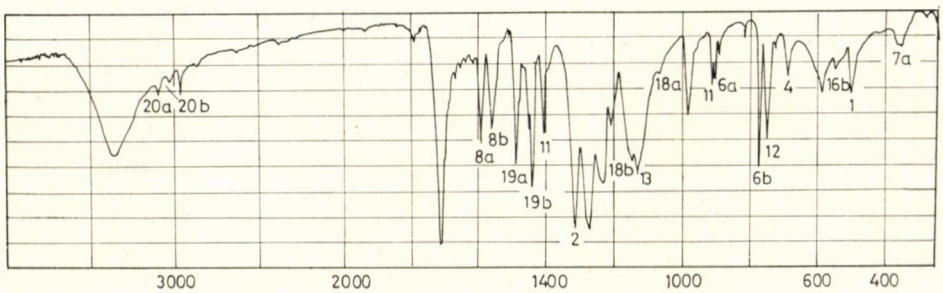

Fig. 9. Methyl 3,5-dibromo-4-hydroxybenzoate **(VIII)**

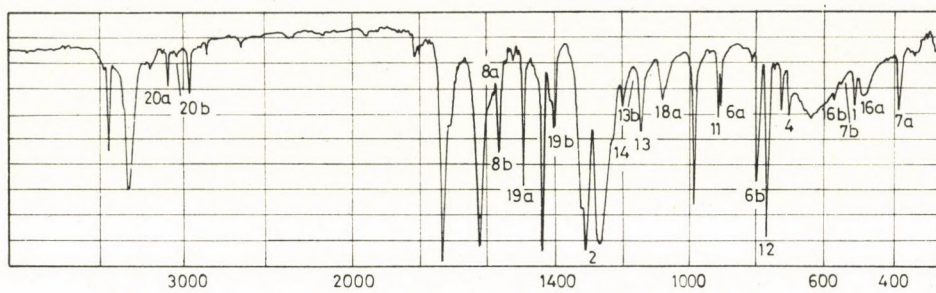

Fig. 10. Methyl 3,5-dichloro-4-aminobenzoate **(IX)**

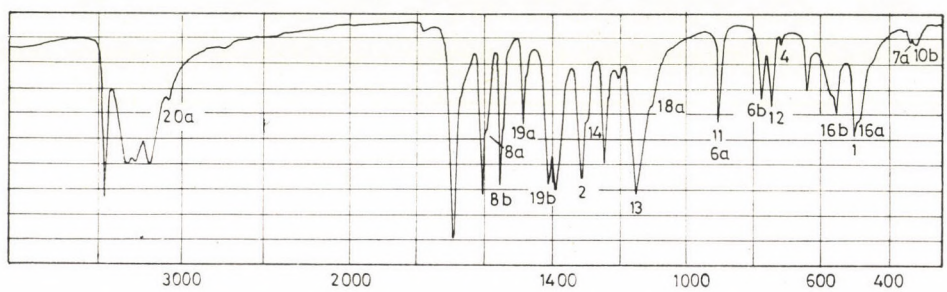

Fig. 11. 3,5-dibromo-4-hydroxybenzoic acid amide **(X)**

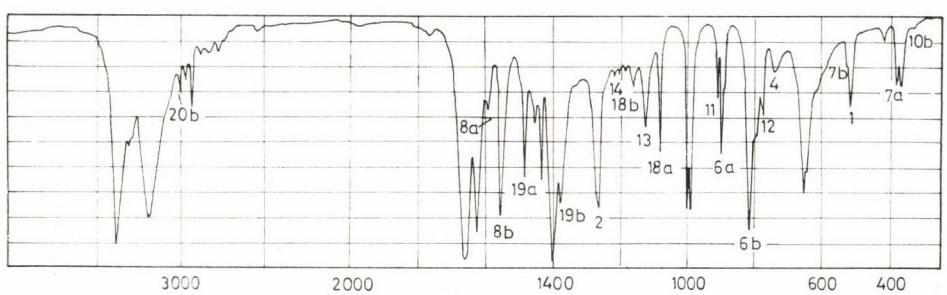

Fig. 12. 3,5-dichloro-4-methoxybenzoic acid amide **(XI)**

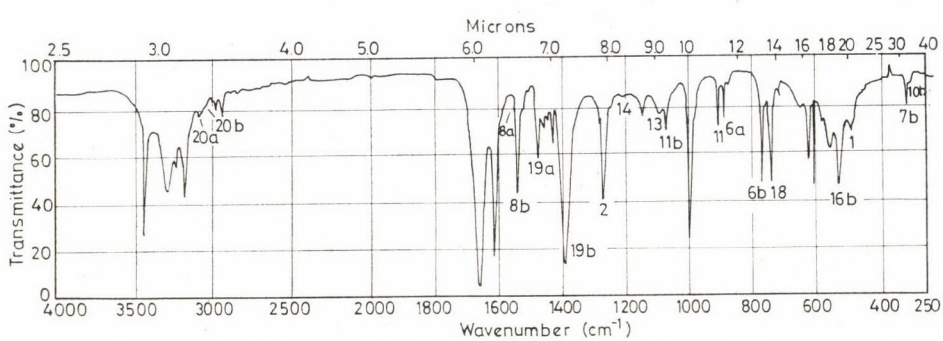

Fig. 13. 3,5-dibromo-4-methoxybenzoic acid amide **(XII)**

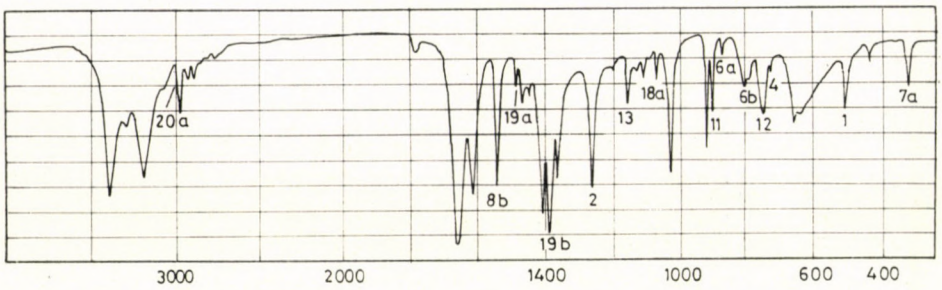

Fig. 14. 3,5-dibromo-4-ethoxybenzoic acid amide **(XIII)**

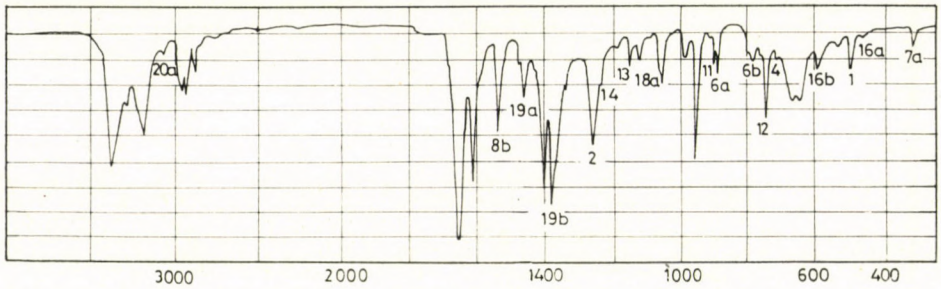

Fig. 15. 3,5-dibromo-4-*n*-propoxybenzoic acid amide **(XIV)**

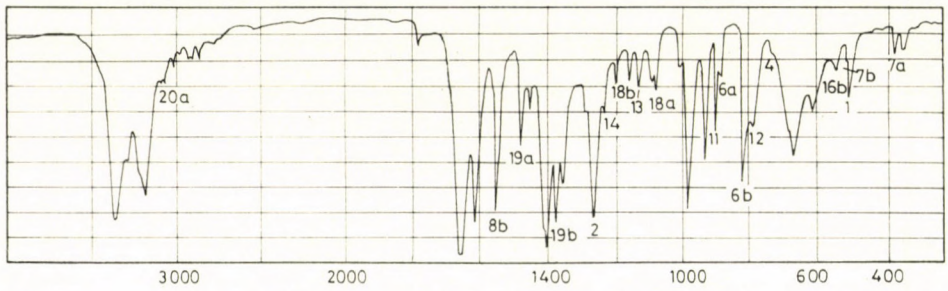

Fig. 16. 3,5-dichloro-4-allyloxybenzoic acid amide **(XV)**

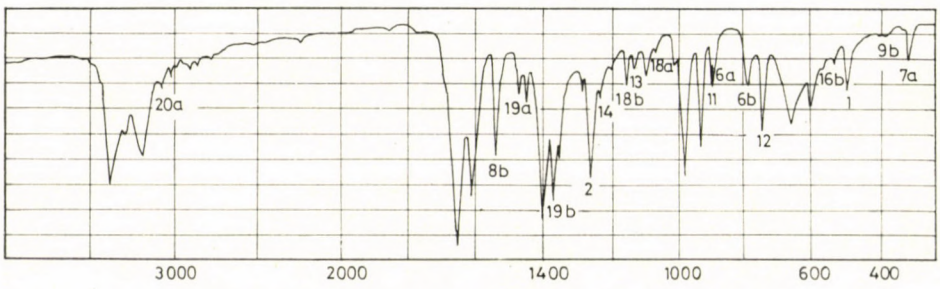

Fig. 17. 3,5-dibromo-4-allyloxybenzoic acid amide **(XVI)**

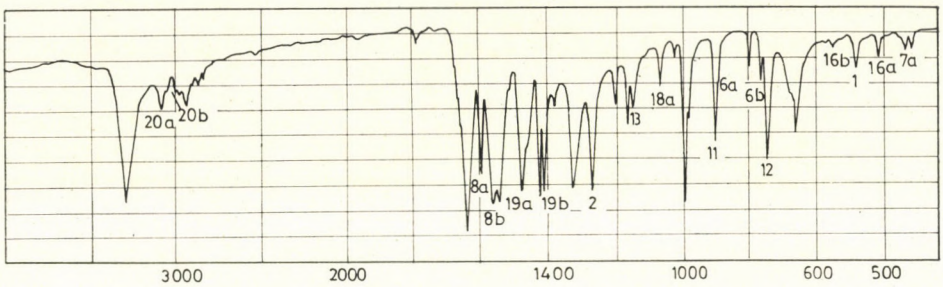

Fig. 18. 3,5-dibromo-4-methoxybenzoic acid N-methylamide (**XVII**)

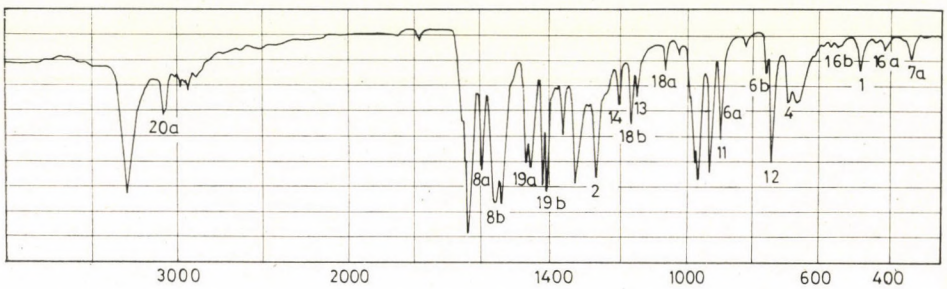

Fig. 19. 3,5-dibromo-4-allyloxybenzoic acid N-methylamide (**XVIII**)

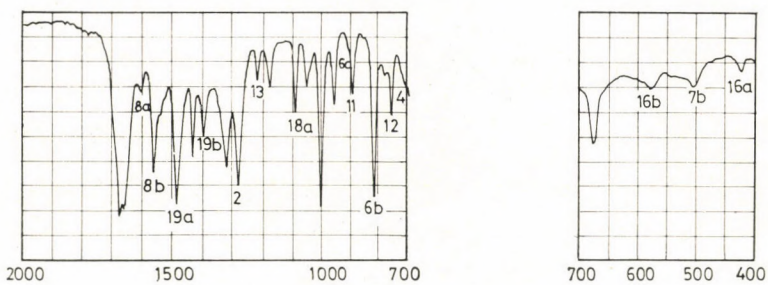

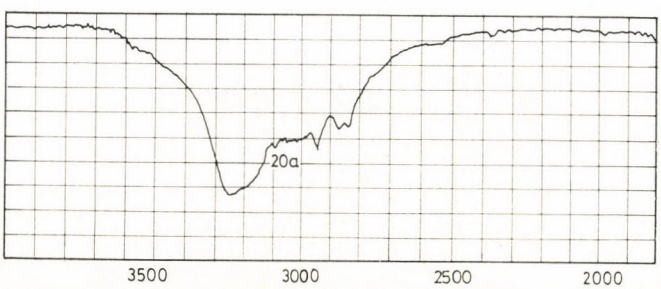

Fig. 20. 3,5-dichloro-4-methoxybenzohydroxamic acid (**XIX**)

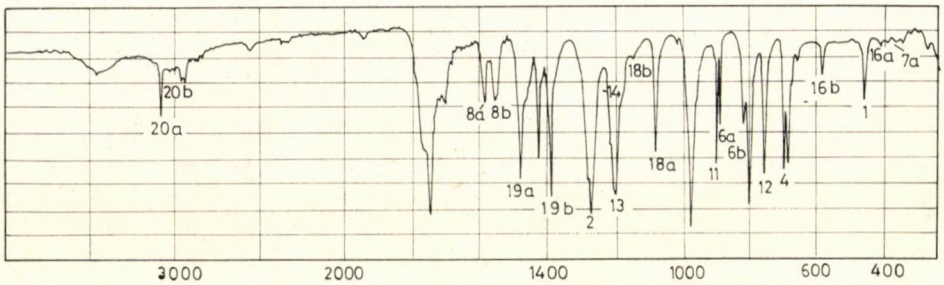

Fig. 21. 3,5-dichloro-4-methoxybenzoyl chloride (**XX**)

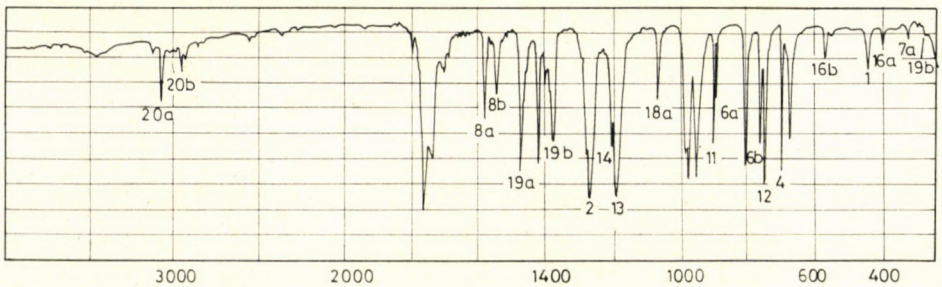

Fig. 22. 3,5-dibromo-4-methoxybenzoyl chloride (**XXI**)

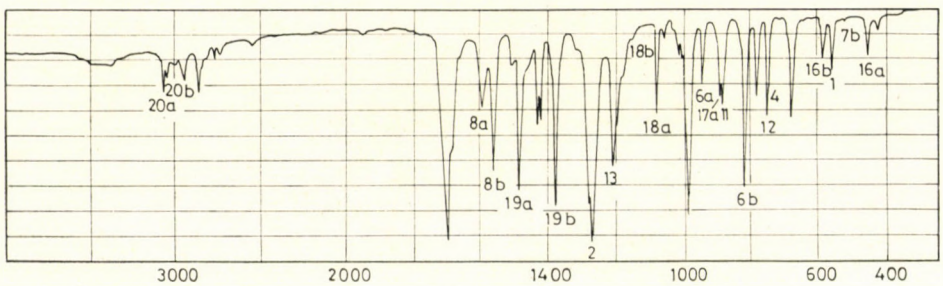

Fig. 23. 3,5-dichloro-4-methoxybenzaldehyde (**XXII**)

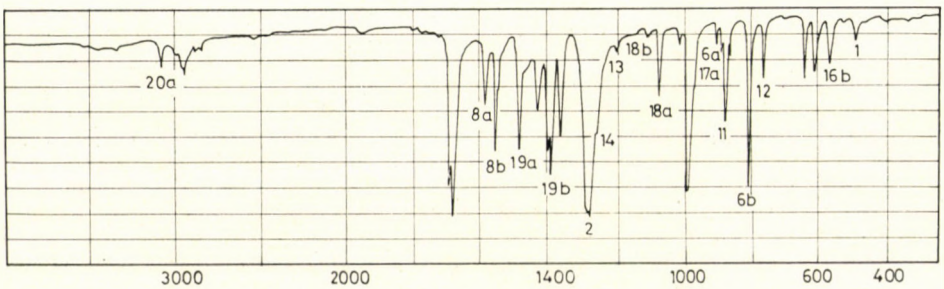

Fig. 24. 3,5-dichloro-4-methoxyacetophenone (**XXIII**)

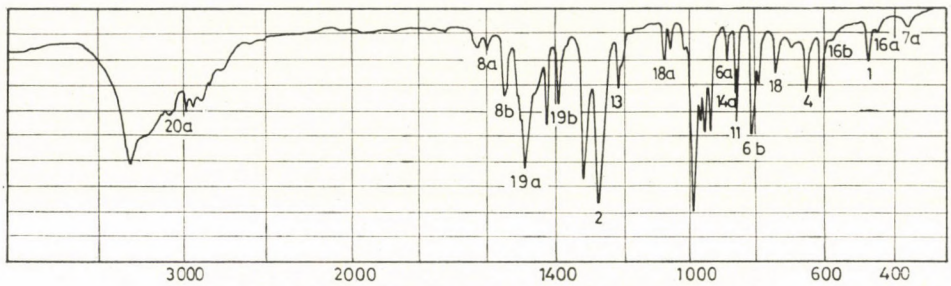

Fig. 25. 3,5-dichloro-4-methoxybenzaldoxime (**XXIV**)

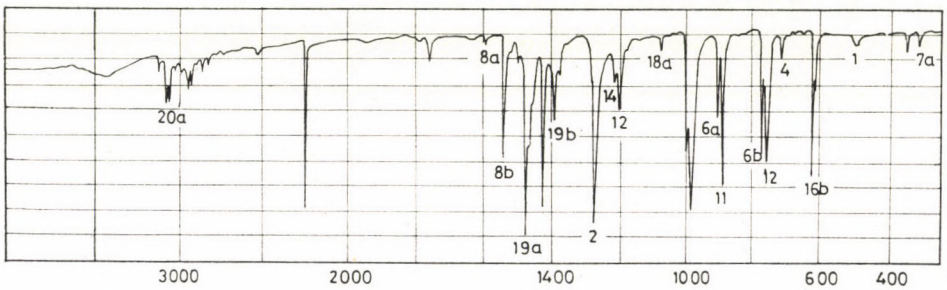

Fig. 26. 3,5-dibromo-4-methoxybenzonitrile (**XXV**)

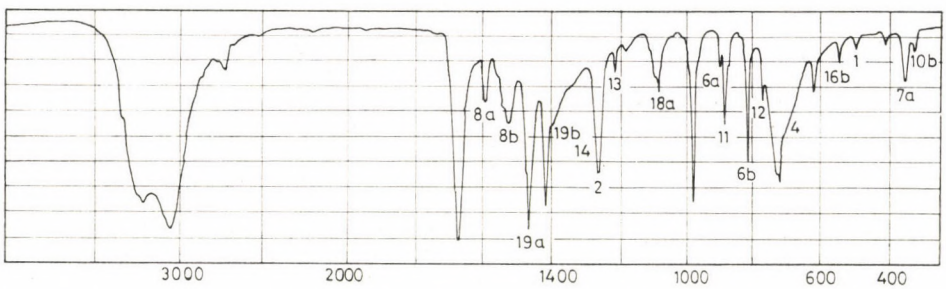

Fig. 27. 3,5-dichloro-4-methoxybenzamidine (**XXVI**)

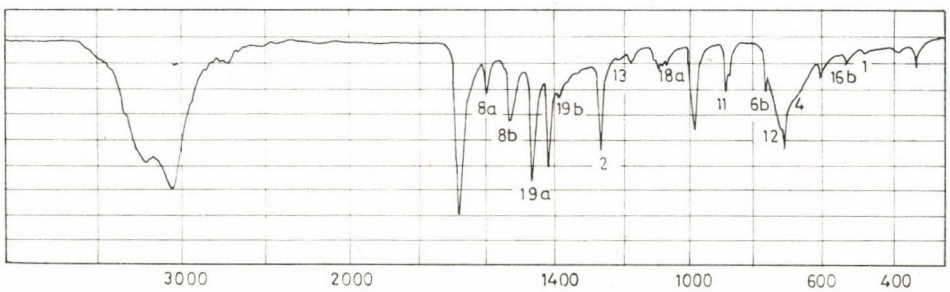

Fig. 28. 3,5-dibromo-4-methoxybenzamidine (**XXVII**)

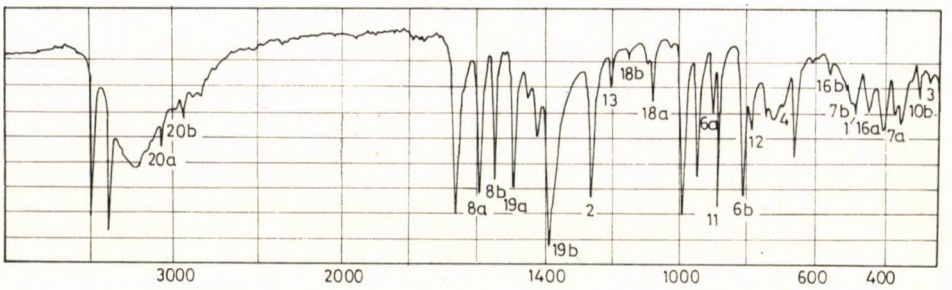

Fig. 29. 3,5-dichloro-4-methoxybenzamidoxime (**XXVIII**)

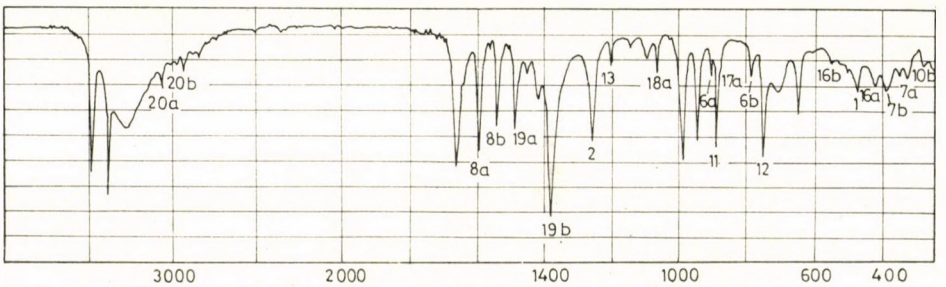

Fig. 30. 3,5-dibromo-4-methoxybenzamidoxime (**XXIX**)

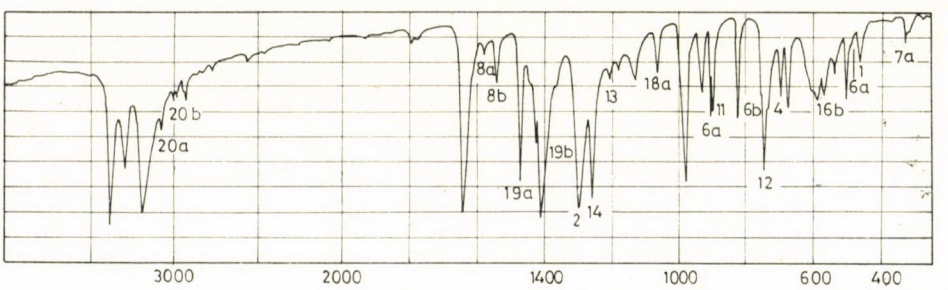

Fig. 31. 3,5-dibromo-4-methoxybenzoic acid thioamide (**XXX**)

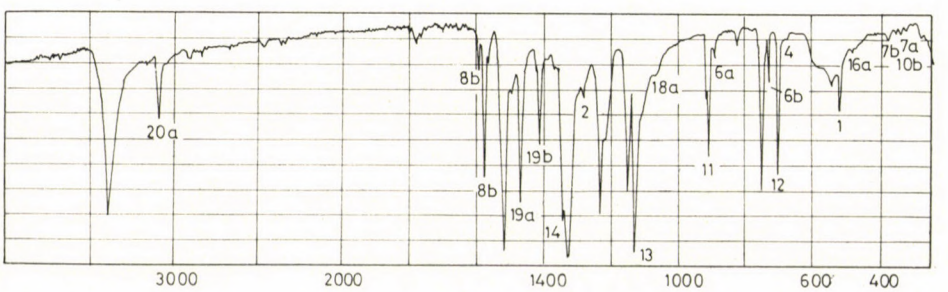

Fig. 32. 3,5-dibromo-4-hydroxynitrobenzene (**XXXI**)

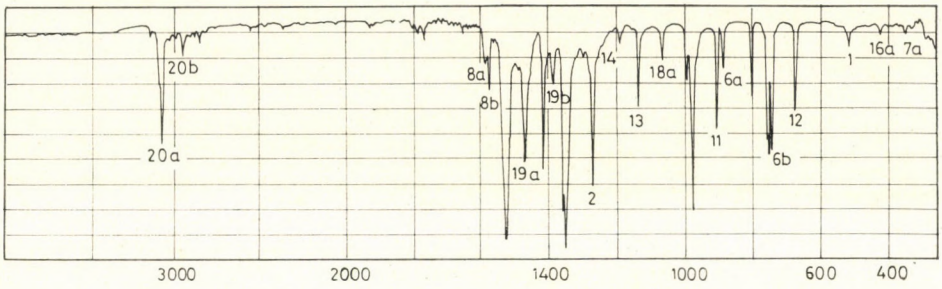

Fig. 33. 3,5-dibromo-4-methoxynitrobenzene (**XXXII**)

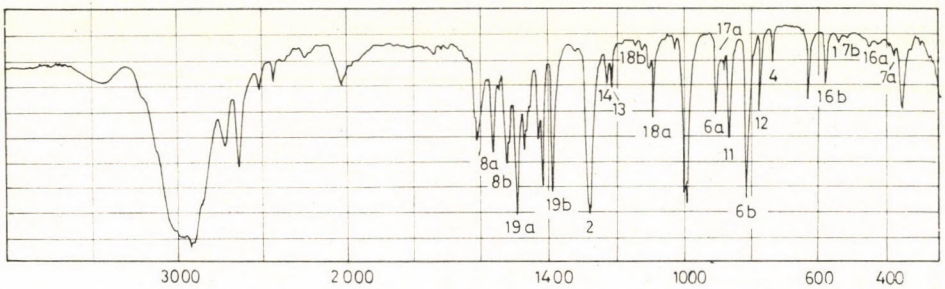

Fig. 34. 3,5-dichloro-4-methoxybenzylamine hydrochloride (**XXXIII**)

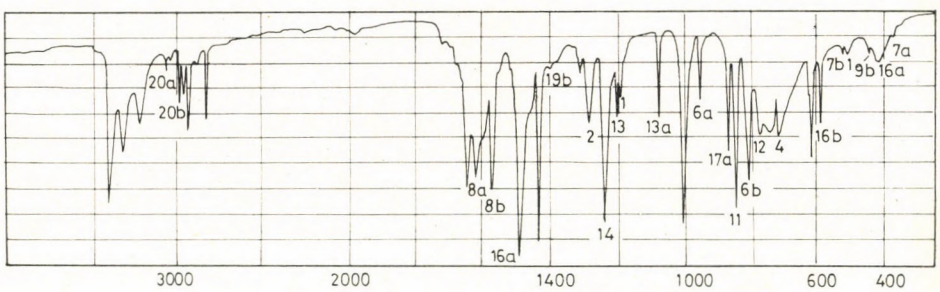

Fig. 35. 3,5-dichloro-4-methoxyaniline (**XXXIV**)

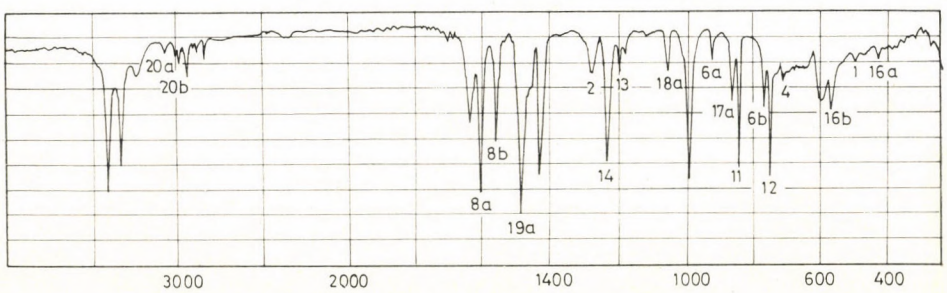

Fig. 36. 3,5-dibromo-4-methoxyaniline (**XXXV**)

Here, Q means the first atom of substituent. The usual signs are employed to distinguish the individual vibration types[4].

Experimental

The spectra were taken in KBr pellets by means of a Perkin—Elmer 457 spectrometer, with the exception of **XIX** which was examined by using a UR-10 (Zeiss, Jena) spectrometer. The spectra are shown in Figs 2—36. Beside the individual bands, the numbers of the corresponding aromatic normal vibrations are also shown in the Figures.

Discussion

1. *Tangential skeletal vibrations* (**8, 14, 19**)

The frequency of skeletal vibration **8a** is relatively insensitive towards the substituents. The band is strong, except for acid amides (**X**—**XVIII**), thioamide (**XXX**), benzylamine hydrochloride (**XXXIII**), hydroxamic acid (**XIX**) and the nitro derivatives (**XXXI**, **XXXII**). The frequency interval is 1575—1600 cm^{-1}, independently of the halogen substituent. In the spectra of the two anisidines (**XXXIV**, **XXXV**) the frequency is higher and also different for the chloro and bromo derivative (1613 and 1598 cm^{-1}, respectively).

The frequency of skeletal vibration **8b** is substantially more sensitive to the substituents. The values observed are as follows.

Carboxylic acids: 1570 (**I**), 1560 (**II**), 1557—1558 (**III**, **V**), 1545 (**VI**) and 1538 cm^{-1} (**IV**).

Esters: 1561 (**VII**), 1568 (**IX**) and 1555 cm^{-1} (**VIII**).

Acid amides: 1555 (**XVII**, **XVIII**) 1551—1553 (**XI**, **XV**), 1550 (**X**), 1539 (**XIV**), 1536 (**XII**), 1536 (**XVI**) and 1534 cm^{-1} (**XIII**).

The frequencies of nitro derivatives **XXXI** and **XXXII** are anomalously high because of the coupling with the $\nu_{as}NO_2$ vibration. The band is always strong.

The band of vibration **14** appears between 1200 and 1260 cm^{-1} and, in general, it is weak. However, it is found above 1330 cm^{-1} in the spectra of compounds containing a phenolic hydroxyl group (**I**, **II**, **X**, **XXXI**), as a consequence of coupling with the βOH vibration; it is even shifted beyond 1400 cm^{-1} and appears with a much greater intensity in methyl esters **VII** and **VIII**.

The band of vibration **19a** is nearly always strong. The intensity of this band is medium in the bromo derivatives of acids and acid amides and weak in the only iodo compound (**VI**). The frequency is sensitive to all substituents to a small extent. The bands of the chlorophenols are at 1493 cm^{-1} (**I**) and 1490 cm^{-1} (**VII**), respectively; the frequency interval of bromophenols (**II**, **VIII** and **X**) is 1476—1483 cm^{-1}. An exception is compound **XXXI**, where the

band appears at 1446 cm^{-1} in the spectrum. The frequency range of the chloroanisoles (**III, XI, XIX, XX, XXII, XXIII, XXIV, XXVI, XXVIII** and **XXXIV**) is 1476—1484 cm^{-1}. In this group, amidine **XXVI** shows an anomalously low frequency (1469 cm^{-1}) while the oxime and amidoxime vibrate with anomalous high frequencies (1490 and 1492 cm^{-1}, respectively). The frequency region of bromoanisoles **XII, XVII, XXI, XXV, XXVII, XXIX, XXX, XXXII** and **XXXV** is 1470—1479 cm^{-1}. Here again, the frequencies of the band of amidine **XXVII** and nitro compound **XXXII** (1463 and 1464 cm^{-1}, respectively) are anomalously low, however, the frequency of the band of amidoxime **XXIX** (1486 cm^{-1}) is anomalously high. The frequency of vibration **8b** is also very low in the spectra of the amidines. In iodo compound **VI**, the band appears at 1452 cm^{-1}.

The band of vibration **19b** is similarly strong. Exceptions are the spectra of amidines (**XXVI, XXVII**) and anilines (**IX, XXXIV, XXXV**), where this band is very weak. The frequency interval of phenols (**I, II, VII, VIII, X** and **XXXI**) is 1407—1420 cm^{-1} (insensitive to halogens). Methyl esters (**VII** and **VIII**) show an anomalously high frequency (1434—1438 cm^{-1}). Here, the only exceptions are the N-methylamides (**XVII, XVIII**) (1410 cm^{-1}), in consequence of the strong coupling with the amide III band of secondary amides.

2. *In-plane bending C—Q vibrations* (**3, 9, 15**)

The vibrations **3, 9a, 9b** and **15** belonging here show low frequencies and therefore cannot be identified.

3. *In-plane bending C—H vibrations* (**18**)

The features of vibrations **18a** depend to a small extent upon the halogen substituent: in the spectra of the 2,6-dichloro derivatives, both the frequency and the intensity of the corresponding band are higher (*i.e.* the amplitude is larger). The frequency interval is 1075—1095 cm^{-1} in the spectra of chloro derivatives, 1055—1080 cm^{-1} in bromo derivatives and 1054 cm^{-1} in that of the iodo compound.

The band of vibration **18b** is generally weak and cannot be identified in many cases. The frequency interval is 1143—1163 cm^{-1}.

4. *Radial skeletal vibration* (**1, 6, 12**)

The symmetry of normal vibration **1** is trigonal. The substituent in position 2 and the carbon atom attached to it vibrate with a smaller amplitude. Therefore, the vibration is less sensitive to the substituent in position 2. Its frequency is the highest in the spectrum of aldehyde (**XXII**) (553 cm^{-1}) and lowest in those of the two acid chlorides (**XX, XXI**) (462 and 441 cm^{-1}, re-

spectively). The frequencies of the bromo derivatives are generally lower by 15 cm^{-1} than those of the chloro derivatives. The larger masses of substituents X cause a further decrease in frequency by 15 cm^{-1} in the iodo compound (**VI**). Remarkably, the frequencies of anilines (**XXXIV**—**XXXV**) are medium. Presumably, in consequence of the +M effect of the primary amino group, the carbon-halogen bond is stronger (and more rigid) and thereby frequency **1** is somewhat decreased.

Skeletal vibration **6a** is strongly coupled with stretching vibration **7a** of identical phase for both halogens. As a result of coupling, the band of vibration **6a** appears at wavenumbers higher than 860 cm^{-1}. The difference between the halogens has little influence on the frequency, similarly to the higher frequency components of such coupled halogen vibrations. Exceptions are the two aniline compounds (**XXXIV** and **XXXV**) where, as mentioned above, the carbon-halogen bonds are stronger and, therefore, the frequency splitting **6a**—**7a** is greater (frequency of **6a** is higher) and a greater difference exists between frequencies of the chloro and bromo derivative (952—925 cm^{-1}). The frequency changes periodically with the mass of substituent in position 2. Namely, a frequency minimum (870 and 865 cm^{-1}, respectively) appears in the case of an ethoxy substituent (**IV**, **XIII**). The frequency is also decreased (to 868 cm^{-1}) by a 2-acetoxy group (**VI**). The frequency is anomalously high in aldehyde (**XXII**) (944 cm^{-1}) and in the anilines (**IX**: 903 cm^{-1}, **XXXIV**: 952 cm^{-1}, **XXXV**: 925 cm^{-1}).

Skeletal vibration **6b** is also strongly coupled with the carbon-halogen stretching vibration **7b**. The frequency interval of the bromo derivatives is 750—785 cm^{-1}, that of the chloro compounds falls between 800 and 820 cm^{-1}. The frequencies of nitro derivatives (**XXXI** and **XXXII**) are anomalously low (725—740 cm^{-1}). In general, the band is intense. Exceptions are the amides of ethers containing more than one carbon atom (**IV**, **V**, **XIII**—**XVI**, **XVIII**).

The substituent in position 2 exerts practically no influence on breathing vibration **12**, except on that of the nitro compounds (**XXXI**, **XXXII**) where a significant decrease in the frequency (697 and 670 cm^{-1}) is observed. The frequencies of the bromo derivatives are lower by about 30 cm^{-1} (730—755 cm^{-1}) than those of the corresponding chloro compounds (760—790 cm^{-1}). In addition to the nitro derivatives, the frequency of the aldehyde (**XXII**) is anomalously low (746 cm^{-1}), which can be explained by coupling with the βCO vibration. The frequency of iodo compound **VI** is also anomalously low (716 cm^{-1}). The band is generally intense.

5. *C—Q stretching vibrations* (**2**, **7**, **13**)

Normal vibration **2** is the identical-phase C—Q stretching vibration of the substituents in positions 2 and 5. Accordingly, it is not sensitive to chang-

ing of the halogen. The frequency interval of the majority of methoxy derivatives is 1255—1280 cm^{-1}. The frequencies of carboxylic acids (**I—VI**) and esters (**VII—IX**) are anomalously high (1285—1310 cm^{-1}) because of coupling with the νC—O(H) and νC—O types, respectively, of ester vibrations. The frequency of the thioamide (**XXX**) (1297 cm^{-1}) is also high, under influence of the νC=S vibration. The frequencies of the compounds containing a phenolic hydroxyl group are generally higher than those of anisoles, other phenol ethers have lower frequencies. An exception is nitrophenol **XXXI**, because of coupling with the $\nu_s NO_2$ vibration.

Normal vibration **7a** is mainly an identical-phase carbon-halogen stretching vibration, however, to a lesser degree it has also features of a radial skeleton vibration. The frequency range of νCCl vibrations is 360—400 cm^{-1}, that of νCBr vibrations is 310—340 cm^{-1}. The band is generally weak. The frequency of the carboxylic acids is the highest.

The νCBr frequencies are sensitive also to the substituent in position 2. Thus, the range of vibration **7a** is 335—355 cm^{-1} in the dibromophenols.

Normal vibration **7b** is predominantly the opposite-phase carbon-halogen stretching vibration with some skeletal vibration character. The interval of the νCCl frequency is narrow: 500—525 cm^{-1}. The νCBr frequency depends upon the substituent in position 2 similarly as does vibration **6a** (a minimum is found for ethyl ethers **IV** and **XIII**: 346 cm^{-1}). In general, the band is weak with a frequency interval of 380—400 cm^{-1}. The frequency of the C—I stretching vibration is 328 cm^{-1} (**VI**).

Vibration **13** is the opposite-phase stretching vibration of the substituents in positions 2 and 5. The halogen atom exerts no influence on the frequency. On the basis of frequencies, the compounds can be divided into two groups. The frequency is lower than 1160 cm^{-1} for carboxylic acids, esters, amides, N-methylamides and nitro compounds, and higher than 1190 cm^{-1} for all other substances. The band has anomalously low frequencies (1122 and 1087 cm^{-1}, respectively) for two anisic acid amides (**XI, XII**). The band intensity is medium or strong except for acetophenone (**XXIII**), amidines (**XXVI, XXVII**) and hidroxyamidines (**XXVIII, XXIX**).

6. *CH stretching vibrations* (**20**)

The band of $\nu C_{Ar}H$ vibrations **20a** and **20b** is in general of weak or medium intensity and in many cases it cannot be identified. The frequency range of vibration **20a** is 3060—3100 cm^{-1}, that of vibration **20b** 2995—3045 cm^{-1}.

7. *Out-of-plane skeletal vibrations* (**4, 16**)

The frequency and intensity of vibration **4** is quite characterless. Irrespective of the halogens, the vibration shows a high frequency in acid amides,

as a result of coupling with the amide V and amide VI vibrations. In the spectrum of benzylammonium chloride (**XXXIII**), the frequency (738 cm^{-1}) is similarly increased by coupling with the $\delta_{as}NH_3$ vibration.

The band of vibration **16a** is found between 400 and 500 cm^{-1}; it is generally weak and difficult to identify. In the case of single-atom substituents, this vibration would be forbidden in the infrared region.

In the out-of-plane skeletal vibration **16b**, halogens participate to a small degree since they exert nearly no influence on the frequency. The band is mostly weak, except for nitrile (**XXV**), where it is strong. The frequency interval is 530—560 cm^{-1}. Anomalously high frequency bands are observed in the spectrum of propyl ether (**XIV**), acetoxy derivative (**VI**) and nitrile (**XXV**). Presumably, the high frequency is caused by coupling with the internal out-of-plane vibrations of the long side-chains and with the γCN vibration, respectively. In the latter case, the band appears at 618 cm^{-1}.

8. *Out-of-plane C—Q vibrations* (**10, 5, 17b**)

Vibrations **5** and **17b** show low frequencies and are outside the measuring range.

The frequencies of vibrations **10a** and **10b** are also low, however, the frequency of vibration **10b** may accidentally lie above 300 cm^{-1}. In consequence of the above facts, the weak bands that appear in some spectra in the region under discussion, should be only conditionally assigned to vibrations **10** or **9**.

9. *Out-of-plane CH vibrations* (**11, 17a**)

The band of vibration **11** is always strong, except for ethyl and propyl ethers (**IV, XIII, XIV**). The frequency can be given by using the formula (1) of the preceding paper [1]. The Platt moments given there can be completed on the basis of the compounds studied in the present paper as follows: COCl —35, $CONHCH_3$ —34, $CSNH_2$ —30, CONHOH —20, C=NHNHOH —20, $C{=}NHNH_2$ —18, $COCH_3$ —12, $CH_2NH_2 \cdot HCl$ 0, CH=NOH +2, Cl +4.5, Br +4.5, I +5, NH_2 +14. The parameters given in the preceding paper [1], furthermore, the frequencies calculated and measured are summarized in Table II.

Vibration **17a** in the point-group C_{2v} is inactive in the infrared. However, it can be identified in some spectra as a result of the solid state of the substance and the asymmetry of the substituents, mainly in the spectra of compounds with positive or low negative Platt moments with an amino group in position 5, the band may be strong. On the basis of Formula (1) of the preceding paper [1], the frequencies measured and calculated are as follows.

Table II

Compound	M	M_m	m	Calculated (cm^{-1})	Experimental (cm^{-1})
I	−32	9	1	907,5	912
II	−32	9	1	907,5	908
III	−32	9	1	907,5	899
IV	−32	9	1	907,5	902
V	−32	9	1	907,5	913
VI	−31	10	1	906	906
VII	−29	9	1	904,5	904
VIII	−29	9	1	904,5	907
IX	−29	9	1	904,5	912
X	−23	9	1	898,5	896
XI	−23	9	1	898,5	907
XII	−23	9	1	898,5	900
XIII	−23	9	1	898,5	896
XIV	−23	9	1	898,5	899
XV	−23	9	1	898,5	897
XVI	−23	9	1	898,5	899
XVII	−25	9	1	900,5	901
XVIII	−25	9	1	900,5	900
XIX	−11	9	1	886,5	887
XX	−26	9	1	901,5	900
XXI	−26	9	1	901,5	903
XXII	−10	9	1	885,5	883
XXIII	− 3	9	1	878,3	879
XXIV	+11	11	3	860,5	860
XXV	−11	9	1	886,5	883
XXVI	− 9	9	1	884,5	884
XXVII	− 9	9	1	884,5	886
XXVIII	−11	9	1	886,5	885
XXIX	−11	9	1	886,5	886
XXX	−21	9	1	896,5	896
XXXI	−36	9	1	911,5	903
XXXII	−36	9	1	911,5	905
XXXIII	+ 9	9	3	863,5	864
XXXIV	+23	23	3	842,5	843
XXXV	+23	23	3	842,5	842

Table III

Compound	Calculated (cm^{-1})	Experimental (cm^{-1})
XXII	899	890
XXIII	896	893
XXIV	885	881
XXXIII	887	883
XXXIV	875	856
XXXV	875	860

The frequency intervals of thirty ring vibrations are given in Table IV

Table IV

Numbering of ring vibration [3]	Frequency (cm^{-1})	Numbering of ring vibration [3]	Frequency (cm^{-1})
1	440—555	**11**	840—915
2	1255—1310	**12**	716—790*
3	<300	**13**	1085—1220
4	665—740	**14**	1200—1260×
5	<300	**15**	<300
6a	865—955	**16a**	400—500
6b	725—820	**16b**	530—620
7a	310—400	**17a**	855—895
7b	325—525▽	**17b**	<300
8a	1575—1615	**18a**	1050—1100+
8b	1530—1580	**18b**	1140—1165
9a	<300	**19a**	1450—1495
9b	<300	**19b**	1370—1440
10a	<300	**20a**	3060—3100
10b	<300	**20b**	2995—3045

▽ 500—525 in 1,3-dichloro compounds
380—400 in 1,3-dibromo compounds
328 in 1,3-diiodo compound **VI**
* 760—790 in 1,3-dichloro compounds
730—755 in 1,3-dibromo compounds
716 in 1,3-diiodo compound **VI**
× 1330—1415 in phenols
\+ 1075—1095 in 1,3-dichloro compounds
1055—1080 in 1,3-dibromo compounds
1054 in 1,3-diiodo compound **VI**

II. Vibrations of the side-chain

1. *Methyl group.* All types of vibration appear in the frequency range [5] of the aliphatic methyl groups. Frequencies of the methoxy group, however, should be dealt with separately. The $\nu_s CH_3$ band is generally found between 2820 and 2850 cm^{-1}, but between 2855 and 2862 cm^{-1} in the spectra of nitro compounds (**XXXI** and **XXXII**), aldehyde (**XXII**) and nitrile (**XXV**). The $\delta_s CH_3$ vibration results generally in a very weak band between 1274 and 1308 cm^{-1} for chloro derivatives and between 1286 and 1327 cm^{-1} for bromo compounds. Therefore, the vibration is less coupled with vibration pair **19** in the bromo derivatives, clearly because the larger bromine atoms force the methoxy group more strongly out of plane of the ring.

The band of the $\delta^{+}_{as} CH_3$ vibration is strong in the case of a methoxy group. The band of the component with lower frequency is found between 1413 and 1438 cm^{-1} for chloro derivatives and between 1413 and 1426 cm^{-1} for bromo derivatives, however, in the latter case it is always at a wavenumber lower by 5—10 cm^{-1} than in the corresponding chloro compound.

The band of the $\delta^{-}_{as} CH_3$ vibration is even stronger. Both vicinal halogen atoms force the methoxy group out of the plane and, therefore, the frequency is anomalously low for all methoxy derivatives. It is interesting, however, that the frequency is hardly influenced by differences in the halogens. In some cases the frequency is split as a result of Fermi resonance. The frequency interval is generally 965—1003 cm^{-1}.

2. *The vibrations of saturated methylene and methine groups* usually result in weak bands which cannot be identified in all cases.

3. *Characteristic bands of the allyl group* (**V**, **XV**, **XVI**, **XVIII**)

$\nu_{as} CH_2$: 3068—3082 (medium); νCH: 3018—3020 (weak);
$\nu_s CH_2$: 2980—2990 (weak); $\beta_s CH_2$: 1410—1427 (strong);
γCH: 978—980 (strong); $\gamma_s CH_2$: 927—941 (strong);
$\gamma_{as} CH_2$: 595—615 cm^{-1} (medium).

4. *νC—C vibrations.* This band appears at 975 cm^{-1} in the spectrum of acetophenone (**XXIII**), as a shoulder of the $\delta^{-}_{as} CH_3$ band.

5. *νC—O and νO—C coupled vibrations.* The C—O stretching vibration of the carboxylic group appears always as an intense band between 1270 and 1285 cm^{-1}. Sometimes, it partly coalesces with the band of the ring vibration **2**.

The νO—C type group vibration of the methoxy group is always strongly coupled with the $\delta^{-}_{as} CH_3$ vibration. The arithmetic mean of the frequencies is 1093—1095 cm^{-1} in one group of chloro derivatives (benzylamine hydrochloride, aldehyde, acid chloride, acid, aniline) and 1086—1087 cm^{-1} in the other group (acid amide, hydroxamic acid, oxime, amidine). In the spectrum of dibromoaniline (**XXXV**), it is 1086 cm^{-1} while in the other bromo deriva-

tives 1081—1083 cm^{-1}. The degree of splitting is greater, the stronger electron acceptor is the substituent in position 5. The wavenumbers of splitting are: COCl 227, NO_2 214, CHO 211, COOH 210, C=NHNH$_2$ 200—209, CSNH$_2$ 204, CN 197, CH=NOH 195, $CH_2NH_2 \cdot HCl$ 193, CONH$_2$ 190, NH$_2$ 185—190, CONHOH and $CONHCH_3$ 174 cm^{-1}.

νC—C—C, νC—O—C and νO—C—C vibrations. The frequency interval of both coupled stretching vibrations of the ester group falls between 977—986 and 1264—1268 cm^{-1}, respectively. The first interval depends somewhat on the halogen substituents too because the frequencies of the chloro derivatives (**VII**, **IX**) are 983 and 986 cm^{-1}, respectively. All the bands are very intense.

Two bands arise from stretching vibrations of the ethoxy group: a strong band at 912—916 cm^{-1} and a medium one at 1104—1112 cm^{-1}. Stretching frequencies of the propoxy group in compound **XIV** are 800 (shoulder), 952 (strong) and 1125 cm^{-1} (medium). These frequencies are lower than those found in the spectrum of 4-*n*-propoxy-3,5-dimethoxybenzoic acid described in the preceding paper [1] (denoted there as **IV**) (820, 964, 1130 cm^{-1}), however, in compound **XIV**, instead of methoxy groups there are bromine atoms adjacent to the propoxy group.

The stretching frequencies of the acetoxy group are as follows: 914 (strong) and 1182 cm^{-1} (very strong). In the foregoing paper, as acetoxy group was present in compounds **V** and **XV**. The frequency was 944 and 1182 cm^{-1} when the acetoxy group was sterically hindered by two vicinal methoxy groups. However, when one of the vicinal positions was free, the band appeared at 957 and 1205 cm^{-1}. In compound **VI** of the present series, the acetoxy group is located between two iodine atoms and thereby by low frequency is justified.

6. *Carbonyl bands.* The νC=O frequencies of the carboxyl group are found between 1680 and 1710 cm^{-1}. A dimeric structure develops for each of the six acids (**I**—**VI**), but the dimeric form is looser in the case of an allyloxy or methoxy group in position 2; the frequency is lower than 1695 cm^{-1} in all other cases. The band is of course very intense. The frequency of the ester carbonyl group is 1707 cm^{-1} in the case of a hydroxyl group in position 4, and 1731 cm^{-1} in case of a primary amino group in position 4. However, when chlorine atoms are in vicinity of the hydroxyl group, a further carbonyl band appears at 1718 cm^{-1}. (Simultaneously, the νOH band is doubled.)

The frequency is 1664 cm^{-1} in the spectrum of hydroxamic acid (**XIX**); 1681—1690 in that of acetophenone (**XXIII**); 1694 in that of aldehyde (**XXII**); and 1746 and 1762 cm^{-1} in those of acid chlorides. The latter difference in frequency can be explained by the fact that the electronegativity of the chlorine atom in the acid chloride group is decreased by the chlorine atoms in positions 2 and 6 relative to the bromine atoms and, therefore, the C—Cl bond order increases, and the C=O one decreases (the frequencies are 682 and 1746 cm^{-1}). The corresponding frequencies are 669 and 1762 cm^{-1} in the

bromo derivative. The band splitting cannot be explained by Fermi resonance in the spectrum of the acetophenone for a considerable difference exists between intensities of both bands and, on the other hand, the γC=O band is also split. Instead, two types of conformation may be suggested in the solid phase. The frequency is 1771 cm^{-1} in the acetoxy group.

The βC=O band appears between 718 and 745 cm^{-1} in the case of a carboxyl group, it lies above 740 cm^{-1} when a methoxy or an allyloxy group occupies position 2, and it is lower than 732 cm^{-1} in other cases. The position of the band is 722—724 cm^{-1} in the ester group, 773 in the hydroxamic acid, 777 in the aldehyde, 803—804 in the acid chloride and 866 cm^{-1} in the ketone. The band shows medium or weak intensity.

The γC=O band appears between 645 and 655 cm^{-1} in the carboxyl group, except for the allyloxy derivative, and at 672 cm^{-1} in the spectrum of the allyloxybenzoic acid (**V**). The band is usually weak. The γC=O band of the ester group is very weak and cannot be identified in any spectrum.

The frequencies of other compounds containing a carbonyl group are as follows: CHO (**XXII**): 673; $COCH_3$ (**XXIII**): 610 and 640 (two conformations?); COCl: 640 (**XX**) and 653 (**XXI**), respectively; CONHOH (**XIX**): 675 cm^{-1}. The bands are always weak.

7. *Hydroxyl bands.* The phenolic νOH frequencies lie at 3445—3455 cm^{-1} in acids, at 3340 and 3355 cm^{-1} in esters and at 3392 cm^{-1} in nitro compounds. An additional band appears at 3420 cm^{-1} in 3,5-dichloro-4-carbomethoxyphenol (**VII**). The intermolecular bonding of the phenolic hydroxyl groups is probable in acids. In esters and in nitro derivative **XXXI**, a weak hydrogen bond is formed with the carbonyl or nitro group, respectively. The other band in compound **VII** presumably corresponds to the internal O—H . . . Cl bond because it is absent from the spectrum of the bromo derivative (**VIII**). The band at 3420 cm^{-1} may conceivably correspond to the phenolic dimer similarly to the acids not realized in the bromo derivative because of steric hindrance. This is to be rejected because bromine atoms do not impede the formation of the dimer in the acids. In those cases, however, the carboxylic dimers would orientate the molecules in a different way (OH opposite to OH). In the only acid amide derivative (**X**) containing a phenolic hydroxyl group, the band appears at 3462 cm^{-1}.

The frequency of the phenolic βOH band is 1245 and 1252 cm^{-1}, respectively, in the two acids, and 1244 and 1225 cm^{-1}, respectively, in the two esters (the hydrogen bond is weaker in the dibromo derivative). However, an additional band is found in compound **VII** at 1191 cm^{-1}, according to the weak O—H . . . Cl bond. The band is observed at 1233 cm^{-1} in nitrophenol **XXXI**, and at 1242 cm^{-1} in hydroxybenzamide **X**. The band is strong in all cases. The γOH band appears at 612 and 592 cm^{-1}, respectively, in the two acids (**I, II**), at 595 and 580 cm^{-1}, respectively, in the two esters (**VII, VIII**),

at 565 cm^{-1} in amide **X**, and at 600 cm^{-1} in nitrophenol (**XXXI**). The band is rather strong and always very diffuse.

The νOH bands of the carboxyl groups of the six carboxylic acids appear 2500 and 3100 cm^{-1} as dimeric structures showing several maxima. The βOH band is always intense between 1405 and 1416 cm^{-1}. The γOH band is always diffuse and, therefore, in some cases it is observed as a shoulder between 900 and 940 cm^{-1}.

The frequency of the νOH band lies at 3240 cm^{-1} in the spectrum of hydroxamic acid (**XIX**) and is very strong and very diffuse; it lies at 3328 cm^{-1} in oxime (**XXIV**) and is strong; it appears at 3245 and 3280 cm^{-1}, respectively, in amidoximes (**XXVIII** and **XXIX**) being strong and very diffuse. The dimeric bond is weaker in compound **XXIX** as indicated by the higher frequency. The βOH bands are very weak and cannot be usually identified. The γOH band of amidoximes appears close to 400 cm^{-1}; in the spectrum of **XXIX**, it overlaps with the band of vibration **7b**.

8. *NH vibrations.* In the spectra of the three aniline derivatives (**IX**, **XXXIV**, **XXXV**) the bands of NH_2 stretching vibrations show two kinds of structure. When the primary amino group lies near to the ester group of another molecule (**IX**), the $\nu_{as}NH_2$ band is found at 3440 and $\nu_s NH_2$ at 3332 cm^{-1}, the latter being stronger. When the amino group is near to the identical group of another molecule, a hydrogen bond is formed, too, but no uniform structure is present. Therefore, two $\nu_s NH_2$ bands appear and in this case, the $\nu_{as}NH_2$ band is the strongest. The frequencies of the latter are 3400 and 3415 cm^{-1}, respectively; those of the former ones are 3225 and 3320 as well as 3235 and 3338 cm^{-1}, respectively. The hydrogen bond is weaker in the dibromo derivative as a result of steric factors. The $\beta_s NH_2$ frequencies of aniline derivatives are the following: 1618 cm^{-1} in the ester; 1637 and 1631 cm^{-1} in the anisidines (the hydrogen bond is weaker in the latter case). The $\gamma_s NH_2$ bands are diffuse between 600 and 630 cm^{-1}, while a weaker, very diffuse absorption appears in the spectrum of both anisidines at wavenumber above 700 cm^{-1}.

The mean value of the NH_2 stretching frequencies of the amide group is 3268—3308 cm^{-1}. The position of both hydrogen atoms in the dimeric structure is most symmetric in the hydroxy derivative (**X**) and most asymmetric in the methoxydibromo derivative (**XII**). The splitting between the frequencies of the antisymmetrical and symmetrical stretching vibrations is the weakest in the former and the strongest in the latter case. It can be concluded from the extensive splitting that neither of the two bands can be assigned in this case to the antisymmetrical and symmetrical vibration form, they should rather be considered to be a free and a bound NH stretching vibration.

In the N-methylbenzamide group (**XVII**, **XVIII**), the νNH frequency lies at 3296—3300 cm^{-1}, a fact showing that the dimeric structure is looser than that in the unsubstituted amides, since the bound νNH frequency is just as

high as the mean value in the free amides. On the other hand, the dimeric structure is stronger in the amidines which is supported by the mean frequency lying at 3140—3145 cm^{-1}. In these compounds, the $\nu(=NH)$ band of the imino group can be identified as a shoulder at 3350 cm^{-1}. In the amidoximes, two νNH bands appear at 3488—3490 and at 3390—3392 cm^{-1}. From the diffuse νOH band appearing beside these, the conclusion can be drawn that the amide hydrogens are not involved in hydrogen bonds. Therefore, the higher frequency can be assigned to the νNH vibration.

From the bending vibration bands of the amino groups, only those of a few out-of-plane vibrations are identifiable (the amide bands will be discussed separately). Thus, in the spectra of amidines, the $\gamma_s NH_2$ vibration gives a strong and diffuse band at 705—710 cm^{-1}. In the spectra of amidoximes, the $\gamma(=NH)$ band is identifiable as an intense absorption at 660 and 648 cm^{-1}.

In compound **XXXIII**, the frequency of the ammonium group are as follows: $\nu_{as}N^+H_3$ 2940 cm^{-1} (very strong, very diffuse); $\nu_s N^+H_3$ 2630 and 2712 cm^{-1} (medium and strong, respectively); δ^+_{as} N^+H_3 1607 cm^{-1} (strong) and $\delta_{as}N^+H_3$ 627 cm^{-1} (strong).

9. *CN stretching vibrations.* The $\nu C{\equiv}N$ band appears at 2245 cm^{-1} in the spectrum of nitrile (**XXV**).

The $\nu C{-}N$ frequencies of amidines (**XXVI** and **XXVII**) are 1101—1102 cm^{-1}. The bands are very weak. In the same spectra, the $\nu C{=}N$ band is found in the form of a very strong maximum at 1676 cm^{-1}. In the spectra of amidoximes (**XXVIII** and **XXIX**), the band of the latter vibration is similarly very intense at 1664 and 1659 cm^{-1}, respectively.

The stretching frequencies of the CNO chain of hydroxamic acid (**XIX**) lie at 952 cm^{-1} (strong) and at 1340 cm^{-1} (shoulder, partly covered by the $\delta_s CH_3$ band of the methoxy group). In the spectrum of the oxime (**XXIV**) the stretching vibrations of the $C{=}N{-}O$ chain can be better separated into $C{=}N$ and $N{-}O$ stretching vibrations. The strong band at 1630 cm^{-1} can be assigned to the former one, and the medium intensity band at 957 cm^{-1} to the latter one. The frequencies of the CNO chain of amidoximes are as follows: 946 and 943 cm^{-1} (strong and very strong, respectively); 1100 and 1098 cm^{-1} (weak and medium).

The bending frequencies of the $C{=}N$ bond are also identifiable in the spectra of amidines and amidoximes. The $\beta C{=}N$ band lies at 722—725 cm^{-1} in the spectra of chloro derivatives, at 708—711 cm^{-1} in those of the bromo derivatives; the band is very intense in the spectra of amidines, medium in those of amidoximes. The $\gamma C{=}N$ band appears at 622—623 cm^{-1} in those of bromo derivatives. The intensity is medium in the spectra of amidines and weak in those of amidoximes.

The mean frequency of the νNH_2 vibrations of compound **XXX** is 3268 cm^{-1}, *i.e.*, it is identical with that of acid amides but somewhat less than that

of amides of methoxy acids. The $\beta_s NH_2$ (amide II) band appears at 1642 cm^{-1}, $\beta_{as} NH_2$ at 823 cm^{-1}, $\gamma_s NH_2$ at 591 cm^{-1}, each in the form of a strong maximum. The νNH band at 3290 cm^{-1} and the γNH band at 675 cm^{-1} may correspond to the hydrogen of the primary amino group which participates in the cyclic dimeric association: or perhaps to the tautomeric thioiminohydrine form. Three further bands of the thioamide group appear at 930 cm^{-1} (strong), at 1136 cm^{-1} (νC=S, medium, broad) and at 1409 cm^{-1} (very strong). The γC=S band shows medium intensity at 505 cm^{-1}.

10. *Vibrations of the nitro group.* $\nu_s NO_2$: 1325 and 1348 cm^{-1} (very strong); $\nu_{as} NO_2$: 1514 and 1519 cm^{-1} (very strong); $\beta_s NO_2$: 820 and 802 cm^{-1} (medium); $\beta_{as} NO_2$: 543 and 547 cm^{-1}, $\gamma_s NO_2$: 746 and 750 cm^{-1} (strong). Because of hydrogen bonding, the $\nu_s NO_2$ frequency in nitrophenol (**XXXI**) is lower than in nitroanisol (**XXXII**). The difference in frequencies of the scissoring vibrations can be explained by the fact that to a certain extent this accompanies the vibration of the skeleton, too, and thus the difference between the masses of the hydroxyl and methoxy groups is reflected in the frequency.

11. *Amide vibrations.* The amide I vibration of the unsubstituted amides appears as an intense maximum at 1659 cm^{-1}, and at 1690 cm^{-1} in the only hydroxy derivative. This supports the former finding for the νNH_2 vibrations that the carbonyl group occupies here a quasi-symmetric position between the two hydrogen atoms of the amino group. The amide II frequency of the primary amides is 1608—1620 cm^{-1}, and 1604 cm^{-1} for the hydroxy derivative (**X**), since — according to the above considerations — the N—H . . . O angle here deviates the most strongly from 180°. The amide II frequency of secondary amides is 1537—1538 cm^{-1}.

The amide III band of the primary amides is observed between 1389 and 1405 cm^{-1} and it is invariably strong. This band lies at 1387 cm^{-1} in the spectrum of compound **X**. The low frequency is caused by coupling with vibration **19b** which, in turn, is sensitive to mass and appears, therefore, at wavenumbers above 1400 cm^{-1} in the presence of a hydroxyl substituent and at wavenumbers below 1400 cm^{-1} in case of other substituents. The amide III frequency of secondary amides is 1327—1328 cm^{-1}.

The amide IV vibration gives a far weaker band and, in several cases, it cannot be identified. The frequency interval is 783—797 cm^{-1}, and 798 cm^{-1} in secondary amide **XVII**. The frequency range of the group vibration amide V, being mostly γC=O in character, is 641—673 cm^{-1} in the spectrum of primary amides, however, it is 633 cm^{-1} in the spectrum of compound **X**. As mentioned above, the carbonyl group is located between two hydrogen atoms in this latter substance. In secondary amides, the band is found at 655 and 666 cm^{-1} with a medium intensity. The amide VI vibration, being mostly of the $\gamma_s NH_2$ type (but of γNH type in secondary amides) appears at 615—635 cm^{-1} in the presence of a saturated ether group in position 2, and at 652—661

cm^{-1} in the case of an allyloxy substituent. (The $\gamma C=O$ frequency of the allyloxybenzoic acid (**V**) is also anomalously high.) This vibration cannot be identified in the spectrum of compound **X**. Similarly, it cannot be unambiguously identified in the spectrum of secondary amides.

*

The authors are indebted to Prof. K. LEMPERT and Dr. B. ÁGAI (Technical University, Budapest) and Drs L. FARKAS, E. KASZTREINER and G. SZILÁGYI (Research Institute for Pharmaceutical Chemistry) for supplying samples of the substances investigated in this and in our previous [1] paper, and to A. FÜRJES for the useful technical assistance.

REFERENCES

1. VARSÁNYI, G., SOHÁR, P.: Acta Chim. (Budapest) **74**, 315 (1972)
2. VARSÁNYI, G.: Vibrational Spectra of Benzene Derivatives. Academic Press, New York, London, 1969
3. WILSON, E. B.: Phys. Rev., **45**, 706 (1934)
4. SOHÁR, P., HOLLY, S., VARSÁNYI, G.: Kémiai Közlemények, **31**, 197 (1969)
5. HOLLY, S., SOHÁR, P.: Infrared Spectroscopy. Műszaki Kiadó, Budapest, 1968

György VARSÁNYI; 1111 Budapest, Budafoki út 8b.
Pál SOHÁR; 1045 Budapest, Szabadságharcosok útja 47—49.

Acta Chimica Academiae Scientiarum Hungaricae, Tomus 76 (3), pp. 269—286 (1973)

REPRODUCIBILITY OF THE ADSORPTION CAPACITY DETERMINED FROM ADSORPTION EXCESS ISOTHERMS OF LIQUID MIXTURES

G. FÓTI, L. G. NAGY and G. SCHAY*

(Department of Physical Chemistry, Technical University, Budapest and
**Central Research Institute for Chemistry of the Hungarian Academy of Sciences, Budapest)*

Received May 2, 1972

The reproducibility of the determination of adsorption capacity and specific surface excess has been investigated on a binary liquid mixture–solid adsorbent system. It has been found that the scattering of the values of the specific surface excess is, to a smaller extent, due to the uncertainty of the method applied for determining the variation of the composition of the liquid phase, and, to a greater extent, due to the inhomogeneity of the adsorbent. On the basis of the adsorption of benzene–*n*-heptane mixtures, the adsorption capacity of silica gel, chosen as model, has been determined both by the extrapolation method of SCHAY and NAGY, and by the generalized EVERETT representation. Confidence intervals of the values obtained have been estimated for both cases. An adsorption capacity value of 2.02 $\pm$ 4.25% mmol benzene/g of adsorbent has been obtained by the first method, and 2.03 $\pm$ 3.81% by the second, at the statistical probability level of 95%, in very good agreement with the result of BET surface area determination.

Introduction

It is known that in certain cases the adsorption capacity of an adsorbent may be determined from the adsorption of binary liquid mixtures on the surface of a solid adsorbent, used the functional relationship between the specific surface excess and the equilibrium composition of the homogeneous solution phase [1].

The specific surface excess, referred to unit mass of the adsorbent, can be given by the following equation:

$$n_i^\sigma = \frac{N_0}{m}(x_{i,0} - x_i) = n_{m,i}^s - n_m^s x_i \qquad (1)$$

where n_i^σ is the specific adsorption of the mixture (mmol/g adsorbent),
m is the mass of the adsorbent (g),
N_0 is the total amount of liquid mixture (mmol),
$x_{i,0}$ is the mole fraction of the ith component in the mixture before adsorption,
x_i is the mole fraction of the ith component in the homogeneous phase at equilibrium,
$n_{m,i}^s$ is the amount of the ith component in the adsorption monolayer (mmol/g),
n_m^s is the total material content of the adsorption layer (mmol/g).

It can be seen from the equation that in order to determine the adsorption capacity values, directly not measurable, on the right hand side of the equation, the amounts of the phases should be known and the composition change of the liquid phase, taking place until the equilibrium is reached, should be determined.

In our former studies [2] dealing with the reproducibility of adsorption capacity determinations it has already been assumed, and this permissible assumption will also be made here, that random errors occurring in the determination of phase amounts by mass measurements can be neglected in comparison with the scatter of the change in the mole fractions determined by refractive index measurements. Consequently, the investigation of the reproducibility of surface excess can be limited to the study of the standard deviation of concentration change, and to the determination of the increase of scatter due to inhomogeneities in the adsorbent.

If the n_i^σ *vs.* x_1 relation, *i.e.*, the surface excess isotherm, is known, a direct route is available for the determination of adsorption capacity in cases, when the adsorption isotherm can be regarded as linear in a sufficiently wide range. According to Eq. (1), the constants describing the linear section of the curve can be identified as the material content of the adsorption phase ("extrapolation method" of SCHAY and NAGY).

In certain cases also the so-called generalized EVERETT representation is suitable for the determination of adsorption capacity:

$$\frac{x_1 x_2}{n_1^\sigma} = \frac{1}{n^s_{m,1,0}} \left(\frac{\beta}{\alpha - 1} + \frac{\alpha - \beta}{\alpha - 1} x_1 \right) \tag{2}$$

where $n^s_{m,1,0}$ denotes the total monomolecular capacity of the adsorbent expresses in mmol/g for component 1,

$\beta = \dfrac{a_{m,2}}{a_{m,1}}$ is the substitution ratio *i.e.*, the ratio of the molar surface areas, and

α is the separation factor of the adsorption $\left(= \dfrac{x_1^s}{x_2^s} \dfrac{x_2}{x_1} \right)$.

If $\alpha \geqslant \beta, 1$ (first of all in the case of type II excess isotherms), the $x_1 x_2 / n_1^\sigma$ *vs.* x_1 EVERETT representation practically yields a straight line passing through the origin.

Consequently, the determination of the adsorption capacity and its reproducibility is, in both methods, equivalent to the evaluation of the parameters (and their confidence intervals) of the linear section that gives the best fit to the values calculated from the experimental results with inherent random errors.

1. Reproducibility of the determination of concentration change

Since the composition of the liquid phase is generally determined by refractive index measurements, the scatter of concentration data depends first of all on the uncertainty of this measurement, and on the random error of the calibration diagram or multiplication factor (k) used for the calculation of mole fraction changes from measured refractive index differences:

$$\Delta x = k\Delta n \tag{3}$$

$$(sd)_{\Delta x} = \pm k\Delta n \sqrt{\frac{(sd)_k^2}{k^2} + \frac{(sd)_{\Delta n}^2}{(\Delta n)^2}} \tag{4}$$

i.e.,

$$(sd)_{\Delta x}\,\%^2 = (sd)_k\,\%^2 + (sd)_{\Delta n}\,\%^2. \tag{5}$$

This last relation can also be written as

$$(sd)_{\Delta x}\% = c(sd)_{\Delta n}\,\%\,, \tag{6}$$

where two special cases can be mentioned that will occur several times in the following discussion:

$$c = 1, \text{ if } (sd)_k = 0, \text{ and}$$

$$c = \sqrt{2}, \text{ if } (sd)_k\,\% = (sd)_{\Delta n}\,\%.$$

The first case, in fact, implies that a relation, free of random errors, is known between the composition and the refractive index, whereas in the second case the use of a mole fraction *vs.* refractive index calibration diagram is assumed that has been obtained by refractive index measurements of similar reproducibility.

The scatter of the measured data can be substantially reduced, and this procedure may be necessary not only in the case of refractive index measurements, by applying the criterion of CHAUVENET [3], which has been successfully used in the practice of radiation chemistry and nuclear measurements. According to the procedure, measured data are subjected to a test for 'correctness', and the data that do not pass the test are discarded.

The CHAUVENET *criterion* can be given in the following form:

A measurement is acceptable if

$$|\bar{n} - n_i|_{\max} \leq \left(\frac{z}{10} + 1\right) |sd| \tag{7}$$

if $3 < z < 11$, and otherwise

$$\lim_{z \to 200} (\bar{n} - n_i)_{\max} \leq 3\,|sd| \tag{8}$$

where $|sd|$ denotes the absolute value of the standard deviation of the measurements,

$\bar{n}$ is the arithmetic mean value of the measured data,

n_i is the result of the individual measurements,

z is the number of measurements.

The scatter of concentration change values was calculated from the refractive index data given in Table I.

Table I

The scatter of refractive index measurements

Liquid mixture: benzene–*n*-heptane
Apparatus: differential refractometer
10^{-4} change in mole fraction equiv. to 1.2 divisions, *i.e.*, $k = \Delta x/\Delta n = 8.33 \times 10^{-5}$ mole fr/div
Selection on the basis of the CHAUVENET criterion

Table Ia

	n_1	Δn_1	$(\Delta n_1)^2$	Δn_1	$(\Delta n_1)^2$	Δn_1	$(\Delta n_1)^2$
1.	640.5	−0.6	0.36	−0.3	0.09	−0.1	0.01
2.	642.0	0.9	0.81	1.2	1.44	—	—
3.	641.0	−0.1	0.01	0.2	0.04	0.4	0.16
4.	640.3	−0.8	0.64	−0.5	0.25	−0.3	0.09
5.	643.0	1.9	3.61	—	—	—	—
6.	641.0	−0.1	0.01	0.2	0.04	0.4	0.16
7.	640.0	−1.1	1.21	−0.8	0.64	−0.6	0.36
		+0.1	6.65	0.0	2.50	−0.2	0.78

$\bar{n}_1 = 641.1$ 1. $(sd) = \pm 1.06$
$1.7 \times 1.06 = 1.80$
Upon discarding value No. 5
$\bar{n}_1 = 640.8$

2. $(sd) = \pm 0.71$
$1.6 \times 0.71 = 1.13$
Upon discarding value No. 2
$\bar{n}_1 = 640.6$

1. $(sd) = \pm 0.44$
$1.5 \times 0.44 = 0.66$
All values acceptable

The variation of the refractive index is

$$\Delta n = \bar{n}_1 - \bar{n}_2 - \text{corr}$$

where the correction term is equal to the difference between $\bar{n}_1^0$ and $\bar{n}_2^0$, which have been determined simultaneously with the measurement of n_1 and n_2, from a mixture of unchanged composition.

The results are summarized in Table II.

It is clear from the data that the scatter can be substantially reduced by the CHAUVENET selection.

Table Ib

	n_2	Δn_2	$(\Delta n_2)^2$	Δn_2	$(\Delta n_2)^2$
1.	212.0	−0.1	0.01	0.3	0.09
2.	212.5	0.4	0.16	0.8	0.64
3.	211.0	−1.1	1.21	−0.7	0.49
4.	211.5	−0.6	0.36	−0.2	0.04
5.	214.0	1.9	3.61	—	—
6.	212.0	−0.1	0.01	0.3	0.09
7.	211.5	−0.6	0.36	−0.2	0.04
		−0.2	5.72	+0.3	1.39

$\bar{n}_2 = 212.1$

1. $(sd) = \pm 0.97$
   $1.7 \times 0.97 = 1.65$
   Upon discarding value No. 5
   $\bar{n}_2 = 211.7$

2. $(sd) = \pm 0.53$
   $1.6 \times 0.53 = 0.85$
   All values acceptable

Table Ic

	n_1^0	Δn_1^0	$(\Delta n_1^0)^2$	Δn_1^0	$(\Delta n_1^0)^2$
1.	330.0	−0.6	0.36	−0.3	0.09
2.	330.0	−0.6	0.36	−0.3	0.09
3.	330.0	2.4	5.76	—	—
4.	330.0	−0.6	0.36	−0.3	0.09
5.	331.0	0.4	0.16	0.7	0.49
6.	329.0	−1.6	2.56	−1.3	1.69
7.	331.5	0.9	0.81	1.2	1.44
		0.3	10.37	−0.3	3.89

$\bar{n}_1^0 = 330.6$

1. $(sd) = \pm 1.31$
   $1.7 \times 1.31 = 2.23$
   Upon discarding value No. 3
   $\bar{n}_1^0 = 330.3$

2. $(sd) = \pm 0.88$
   $1.6 \times 0.88 = 1.41$
   All values acceptable

It is also noted here that the absolute value of the standard deviation of refractive index change, as is shown by the corrected scatter of the individual refractive index measurements, is not in a characteristic functional relationship with the composition, therefore, the application of the constant value $(sd)_{\Delta n} = \pm 1.25$ in the whole composition range appears to be justified in calculating the scatter of concentration change (see below).

Table Id

	n_2^0	Δn_2^0	$(\Delta n_2^0)^2$	Δn_2^0	$(\Delta n_2^0)^2$
1.	341.0	0.3	0.09	0.5	0.25
2.	341.0	0.3	0.09	0.5	0.25
3.	340.0	−0.7	0.49	−0.5	0.25
4.	340.0	−0.7	0.49	−0.5	0.25
5.	340.0	−0.7	0.49	−0.5	0.25
6.	342.0	1.3	1.69	—	—
7.	341.0	0.3	0.09	0.5	0.25
		0.1	3.43	0.0	1.50

$\bar{n}_2^0 = 340.7$

1. $(sd) = \pm 0.75$
   $1.7 \times 0.75 = 1.28$
   Upon discarding value No. 6
   $\bar{n}_2^0 = 340.5$

2. $(sd) = \pm 0.55$
   $1.6 \times 0.55 = 0.88$
   All values acceptable

Table II

Scatter of refractive index change and mole fraction change data

	Without correction	Corrected by the Chauvenet method
$\bar{n}_1$	641.1±1.06	640±0.44
$\bar{n}_2$	212.1±0.97	211.7±0.53
$\bar{n}_1^0$	330.6±1.31	330.3±0.88
$\bar{n}_2^0$	340.7±0.75	340.5±0.55
Δn	439.1	439.1
$(sd)_{\Delta n}$	±2.07	±1.25
$(sd)_{\Delta n}$%	±0.47%	±0.28%
$(sd)_{\Delta x}$ % $c = 1$	±0.47%	±0.28%
$(sd)_{\Delta x}$ % $c = \sqrt{2}$	±0.66%	±0.40%

2. Scatter of the specific surface excess values

The calculations on the reproducibility of adsorption capacity and the measured specific surface excess are demonstrated by the detailed analysis of the data given in Table III.

Measurements were carried out at eight different equilibrium liquid compositions; for each of them seven adsorption excess values, y_{ij}, were determined, and two values that deviated most from the average were discarded in each

Table III

Summary of data on liquid mixture adsorption isotherms

Mixture: benzene(1)–*n*-heptane(2)
Adsorbent: silica gel — 360 m^2/g $\pm$ 5% (BET — N_2)
Liquid/adsorbent ratio: $L/m = 5$ (g/g)
Temperature: 25 $\pm$ 1 °C
Simplified notations: $x_{1,i} = x_i$

$$n^{\sigma}_{i,ij} = y_{ij} \text{ (mmol/g)}$$

$$\frac{1}{n}\sum_{j=1}^{n} y_{ij} = y_i \text{ (mmol/g)}$$

i	j	x_i	y_{ij}	Δy_{ij}	$(\Delta y_{ij})^2$	$(sd)_{y_i}$	$(sd)_{yi}(\%)$	$\frac{x_i(1-x_i)}{y_i}$
1	1	0.022	1.41	—0.03	0.0009			
	2		1.39	—0.05	0.0025			
	3		1.49	0.05	0.0025			
	4		1.48	0.03	0.0009			
	5		1.45	0.01	0.0001			
			$y_i = 1.44$	0.01	0.0069	$\pm$0.041	$\pm$2.85	0.0149
2	1	0.098	1.66	0.03	0.0009			
	2		1.61	—0.02	0.0004			
	3		1.59	—0.04	0.0016			
	4		1.66	0.03	0.0009			
	5		1.63	0.00	0.0000			
			$y_i = 1.63$	0.00	0.0038	$\pm$0.031	$\pm$ 1.90	0.0542
3	1	0.223	1.46	—0.06	0.0036			
	2		1.55	0.03	0.0009			
	3		1.50	—0.02	0.0004			
	4		1.53	0.01	0.0001			
	5		1.58	0.06	0.0036			
			$y_i = 1.52$	0.02	0.0086	$\pm$0.047	$\pm$3.07	0.1140
4	1	0.363	1.37	0.08	0.0064			
	2		1.22	—0.07	0.0049			
	3		1.29	0.00	0.0000			
	4		1.30	0.01	0.0001			
	5		1.27	—0.02	0.0004			
			$y_i = 1.29$	0.00	0.0118	$\pm$0.053	$\pm$4.10	0.1792
5	1	0.471	1.02	—0.04	0.0016			
	2		1.03	—0.03	0.0009			
	3		1.11	0.05	0.0025			
	4		1.07	0.01	0.0001			
	5		1.09	0.03	0.0009			
			$y_i = 1.06$	0.02	0.0060	$\pm$0.039	$\pm$ 3.65	0.2350

Table III. cont.

i	j	x_i	y_{ij}	Δy_{ij}	$(\Delta y_{ij})^2$	$(sd)_{y_i}$	$(sd)_{y_i}(\%)$	$\frac{x_i(1-x_i)}{y_i}$
6	1	0.555	0.90	0.00	0.0000			
	2		0.96	0.06	0.0036			
	3		0.90	0.00	0.0000			
	4		0.84	−0.06	0.0036			
	5		0.89	−0.01	0.0001			
			$y_i = 0.90$	−0.01	0.0073	±0.043	± 4.78	0.2742
7	1	0.675	0.60	−0.03	0.0009			
	2		0.69	0.06	0.0036			
	3		0.63	0.00	0.0000			
	4		0.58	−0.05	0.0025			
	5		0.66	0.03	0.0009			
			$y_i = 0.63$	0.01	0.0079	±0.044	± 7.06	0.3482
						±0.066	±10.6	
8	1	0.819	0.33	−0.04	0.0016			
	2		0.41	0.04	0.0016			
	3		0.41	0.04	0.0016			
	4		0.35	−0.02	0.0004			
	5		0.36	−0.01	0.0001			
			$y_i = 0.37$	0.01	0.0053	±0.036	± 9.85	0.4010
						±0.054	±14.8	

set. The remaining five values, given above, have satisfied the CHAUVENET criterion in every case as can be seen from the comparison of columns 5 and 7 of the Table.

It should be noted here that in two sets, belonging to the highest benzene concentrations ($i = 7$ and $i = 8$) the liquid to adsorbent ratio was 10/3 (g/g). In order to render the scatter values belonging to different liquid compositions comparable, the lower values of $(sd)_{y_{7,8}}$ and $(sd)_{y_{7,8}}\%$ standard deviations obtained from the measured adsorption excess values were recalculated for the phase ratio of 5 g/g, at which the other data were determined. In these cases two data can be found in the Table. The recalculation is based on the assumption that the scatter of the specific adsorption excess is determined by the random error of refractometric measurements alone. As will be discussed below, this assumption is incorrect, *i.e.*, the scatter has been overestimated by this correction. The true value is between the original and the corrected one, being much closer to the original value.

Considering that in the whole composition range the measurements were carried out at the same phase ratio (and the data obtained under different

conditions were approximately corrected), it may be expected that the absolute value of the standard deviation of the specific surface excess should be independent of the composition. The values of $(sd)_{n_1^\sigma}$ in column 7 of Table III, indeed, scatter only randomly around an average value of about $\pm$ 0.045. Consequently, the percent deviation, $(sd)_{n_1^\sigma}\%$, of the measured value (see column 8 of Table III) is, obviously, the function of the composition, and the trend of this function is qualitatively opposite to that of the $n_1^\sigma - x_1$ excess isotherm (see Fig. 1). It should be noted that the validity of the following

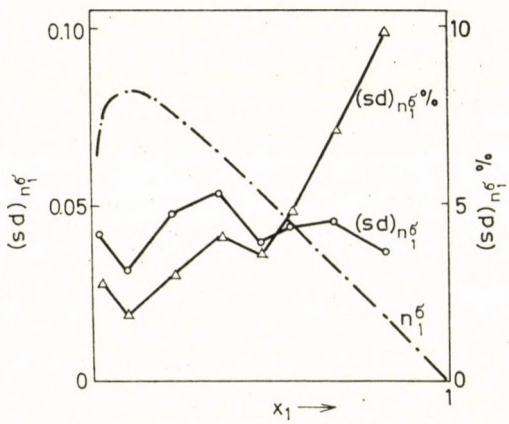

Fig. 1. Deviations of n_1^σ values measured in the benzene (1) – *n*-heptane (2) – silica gel system as a function of the composition

regression analysis is bound to the condition that the isotherm is determined at a constant liquid mixture to adsorbent ratio, or more precisely, that $(sd)_{n_1^\sigma}$ is constant, which follows from the constant ratio of phases.

As a further step, the random errors of the specific surface excess, arising from the scattering of refractive index data, have been evaluated for the individual points of the above isotherm. The calculations were based on the following relations:

$$n_1^\sigma = \frac{N_0}{m} \Delta x_1 = \frac{N_0}{m} k \Delta n \tag{9}$$

$$(sd)_{n_1^\sigma}\% = (sd)_{\Delta x_1}\% = c\,(sd)_{\Delta n}\% = c\,(sd)_{\Delta n} \frac{kN_0/m}{n_1^\sigma} 100\,. \tag{10}$$

In the equations it is assumed that the phase ratio, N_0/m, is not a stochastic variable, *i.e.*, the standard deviation of mass measurements is zero. It is noted that the phase ratio ($L/m = 5$, and 10/3 g mixture/g adsorbent) should be substituted in mol mixture/g adsorbent units (N_0/m). In the calculation the average molecular weight of the original liquid mixture (before the adsorption) should be used.

The calculations were performed with a value of $(sd)_{\Delta n} = \pm 1.25$, obtained from refractive index data satisfying the Chauvenet criterion, so there is ground for the comparison of the calculated $(sd)_{n_1^\sigma}\%$ values and the percent scatter of the measured surface excess values (see Table III), which also satisfy the above criterion.

Table IV shows the percent standard deviation of the specific surface excess, $(sd)_{n_1^\sigma}\%$, as a function of the equilibrium mole fraction of the liquid phase, x_1.

Table IV

The deviation of specific surface excess, $(sd)_{n_1^\sigma}$ %

x_1	Values calculated from $(sd)_{\Delta n}$		Based on measured n_1^σ data
	$(sd)_k = 0$	$(sd)_k\% = (sd)_{\Delta n}\%$	
0.022	±0.37%	±0.52%	±2.85%
0.089	±0.33%	±0.47%	±1.90%
0.223	±0.36%	±0.51%	±3.07%
0.363	±0.44%	±0.63%	±4.10%
0.471	±0.55%	±0.78%	±3.65%
0.555	±0.68%	±0.96%	±4.78%
0.675	±0.98%	±1.38%	±7.06—10.6%
0.819	±1.72%	±2.43%	±9.85—14.8%

It is apparent from the data that the actually observed deviations of the specific surface excess are 4 to 9 times higher than the calculated values; in other words, the random error of refractive index determination may be responsible only for 10 to 20% of the deviation of results. The greater part of the scatter and, consequently, of the uncertainty of the final results, *i.e.*, the adsorption capacity and specific surface area, must be attributed to the application of the so-called multi-sample isotherm determination technique.

It follows from the nature of the 'multi-sample' isotherm determination method that each specific surface excess value measured, n_1^σ, arises from a different portion of the adsorbent. Consequently, the homogeneity of the adsorbent and representative sampling are of basic importance in the measurement. It is obvious, however, that with a certain probability, depending on the nature of the adsorbent and its dispersity, samples of adsorption capacity far different from the average value are also obtained, so sampling errors may strongly affect the reproducibility. In the case of the silica gel used in our experiments this effect increased the scatter of the individual points of the isotherm by a factor of 5 to 10 as compared to the scatter caused by the uncertainty of refractive index measurements.

3. Least squares approximation of the linear section of the surface excess isotherms and of the Everett representation [4]

In the following the curve fitting procedure and the estimation of the confidence intervals of the parameters obtained will be discussed. Some assumptions are made:

The values of mole fractions $x_{1,i}$ are defined quantities *(i.e.,* $(sd)_{x_{1,i}} = 0$), whereas the corresponding measured surface excess values, $n^{\sigma}_{1,ij}$, are treated as random variables of normal distribution, having the same variance for all $x_{1,i}$. The mean expectation value of $n^{\sigma}_{1,i}$ is a linear function of the equilibrium concentration, $x_{1,i}$.

Let this linear function be represented by the following equation:

$$y = B_0 + B_1 x \tag{11}$$

In the SCHAY—NAGY method for the measurement of adsorption capacity the actual form of the equation is

$$n_1^{\sigma} = n^s_{m,1} - n^s_m x_1 \tag{1}$$

whereas in the generalized EVERETT representation it takes the following form:

$$\frac{x_1 x_2}{n_1^{\sigma}} = \frac{1}{n^s_{m,1,0}} \frac{\beta}{\alpha - 1} + \frac{1}{n^s_{m,1,0}} \frac{\alpha - \beta}{\alpha - 1} x_1 . \tag{2}$$

Now the expectation values of the constants B_0 and B_1, and their estimated confidence intervals should be determined. Using the method of least squares, the regression line of form

$$Y = d_0 + d_1 x \tag{12}$$

has the following parameters:

$$d_1 = \frac{\Sigma (x_i - \bar{x})(y_i - \bar{y})}{\Sigma (x_i - \bar{x})^2} \tag{13}$$

and

$$d_0 = \bar{y} - d_1 \bar{x} \tag{14}$$

where regression parameters d_0 and d_1 are estimates for B_0 and B_1. The extent of deviation of the measured data from the estimated regression line is characterized by the 'square of residuals':

$$(sd)^2_{yx} = \frac{\Sigma (y_i - Y_i)^2}{n - 2} \tag{15}$$

where n is the number of $x_i - y_i$ pairs.

If it is assumed that the random variables, y_i, are of normal distribution, the estimates for d_0 and d_1 form a two-dimensional normal distribution, and their estimated quadratic error can be given by

$$(sd)^2_{d_0} = (sd)^2_{yx} \frac{\Sigma x_i^2}{n\Sigma(x_i - \bar{x})^2} \tag{16}$$

and

$$(sd)^2_{d_1} = \frac{(sd)^2_{yx}}{\Sigma(x_i - \bar{x})^2} \,. \tag{17}$$

If the above conditions are fulfilled, it can be proved that the confidence limits of constants B_0 and B_1 obey the so called t-distribution of STUDENT, so the confidence intervals can be given as

$$\begin{aligned} d_0 - t_A(sd)_{d_0} \leq \mathrm{B}_0^{A\%} \leq d_0 + t_A(sd)_{d_0} \\ d_1 - t_A(sd)_{d_1} \leq B_1^{A\%} \leq d_1 + t_A(sd)_{d_1} \end{aligned} \tag{18}$$

where t_A denotes the critical value of a t-distribution of $n - 2$ degree of freedom, at a statistical probability level of $A\%$.

The parameters of the linear section of the x_1x_2/n_1^σ *vs.* x_1 EVERETT representation, and their confidence intervals can also be approximated by the above method. It should be noted, however, that the procedure is less justified in this case, since the quadratic error of the x_1x_2/n_1^σ function does depend on the composition at a constant liquid mixture to adsorbent ratio. As it is known, in this representation a well defined linear section appears only for type II (and transition type I—II) n_1^σ *vs.* x_1 excess isotherms, so the above calculation procedure is demonstrated on the model of benzene–*n*-heptane–silica gel system. This system has a pure type II isotherm, which has already been studied in connection with investigations on the scatter of the surface excess, n_1^σ. This choice gives the opportunity for a direct comparison of the results obtained by the extrapolation method of SCHAY and NAGY and from the generalized EVERETT representation.

It is further noted that the model calculations do not take into account that the lines to be fitted should pass through a given, fixed point (in the extrapolation method $n_1^\sigma = 0$ at $x_1 = 1$, and in the EVERETT representation $x_1x_2/n_1^\sigma = 0$ at $x_1 = 0$). Consequently, the calculations yield two parameters. Now, if $B_0 \approx -B_1$ is obtained from the linear section of the n_1^σ *vs.* x_1 function, or if $B_0 \approx 0$ is obtained from the linear section of the x_1x_2/n_1^σ *vs.* x_1 function, this proves that the excess isotherm is really of type II.

For the sake of simplicity, in the following demonstration of the calculation process the independent variable $x_{i,1}$ is denoted by x_i, and the corresponding average of the function $n_{1,i}^\sigma$ (or $x_{1,i}x_{2,i}/n_{1,i}^\sigma$) is denoted by y_i.

3.1 *The method of* SCHAY *and* NAGY

Eight points of the isotherm were chosen for demonstration purposes (Table III and Fig. 2). Three points, corresponding to the lowest benzene concentrations, are in the nonlinear range, the remaining points fall on the linear

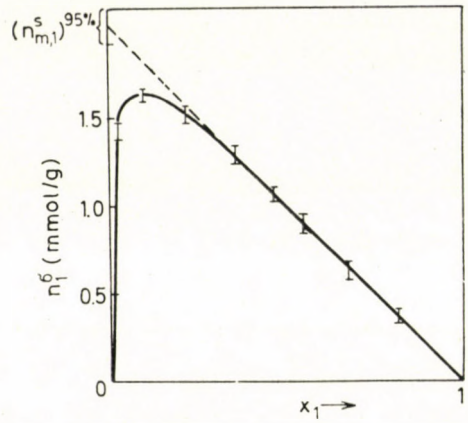

Fig. 2. n_1^σ *vs.* x_1 excess isotherm of the benzene (1) – *n*-heptane (2) – silica gel system; $(n^s_{m,1})^{95\%} = 2.02 \pm 4.25\%$ (from 5 measured points)

section of the isotherm. In the regression analysis given below (see also Table V) only these latter points are taken into account.

Table V

Regression analysis for the SCHAY—NAGY *method*

Table Va

i	x_i	Δx_i	$(\Delta x_i)^2$	y_i	Δy_i	$\Delta x_i \cdot \Delta y_i$
4	0.363	$\pm$0.2136	0.0456	1.29	0.44	$\pm$0.0940
5	0.471	$\pm$0.1056	0.0111	1.06	0.21	$\pm$0.0222
6	0.555	$\pm$0.0216	0.0004	0.90	0.05	$\pm$0.0011
7	0.675	0.0984	0.0097	0.63	−0.22	$\pm$0.0216
8	0.819	0.2424	0.0588	0.37	−0.48	$\pm$0.1163
Σ	$\bar{x} = 0.5766$	0.0000	0.1256	$\bar{y} = 0.85$	0.00	$\pm$0.2552

$$d_1 = -\frac{0.2552}{0.1256} = -2.03$$

$$d_0 = 0.850 + 2.03 \times 0.5766 = 0.850 + 1.170 = 2.02$$

$$(sd)^2_{yx} = \frac{7.67 \times 10^{-4}}{3} = 2.56 \times 10^{-4}$$

$$(sd)^2_{d_1} = \frac{2.56 \times 10^{-4}}{0.1256} = 20.4 \times 10^{-4}$$

$$(sd)^2_{d_0} = 20.4 \times 10^{-4} \frac{1.7878}{5} = 7.28 \times 10^{-4}$$

$$B_1 = -2.03 \pm 4.52 \times 10^{-2}$$

$$B_0 = 2.02 \pm 2.70 \times 10^{-2} = 2.02 \pm 1.34\% = n^s_{m,1}$$

$$-B_1 - B_0 = 0.01 \pm 5.26 \times 10^{-2} = 0.01 \pm 526\% = n^s_{m\,2}$$

Table Vb

i	Y_i	$y_i - Y_i$	$(y_i - Y_i)^2 \cdot 10^6$	x_i^2
4	1.283	0.007	49	0.1317
5	1.070	−0.010	100	0.2218
6	0.893	0.007	49	0.3080
7	0.650	−0.020	400	0.4556
8	0.357	0.013	169	0.6707
Σ	4.253	−0.003	767	1.7878

3.2 *Generalized* EVERETT *method*

3.2.1. Regression analysis by taking into account all the eight points of the isotherm (see Table VIa, b)

Table VI

Regression analysis for the generalized EVERETT *method*

Table VIa

i	x_i	Δx_i	$(\Delta x_i)^2$	y_i	Δy_i	$\Delta x_i \cdot \Delta y_i$
1	0.022	−0.381	0.1452	0.0149	−0.1877	0.0714
2	0.098	−0.305	0.0929	0.0542	−0.1484	0.0453
3	0.223	−0.180	0.0324	0.1140	−0.0886	0.0159
4	0.363	−0.040	0.0016	0.1792	−0.0234	0.0009
5	0.471	0.068	0.0046	0.2350	0.0324	0.0022
6	0.555	0.152	0.0231	0.2742	0.0716	0.0109
7	0.675	0.272	0.0739	0.3482	0.1456	0.0396
8	0.819	0.416	0.1730	0.4010	0.1984	0.0826
Σ	$\bar{x} = 0.403$	−0.008	0.5467	$\bar{y} = 0.2026$	−0.0001	0.2688

Table VIb

i	Y_i	$y_i - Y_i$	$(y_i - Y_i)^2 \cdot 10^8$	x_i^2
1	0.0150	−0.0001	1	0.0005
2	0.0515	0.0027	729	0.0096
3	0.1139	0.0001	1	0.0497
4	0.1827	−0.0035	1 225	0.1317
5	0.2360	−0.0010	100	0.2218
6	0.2770	−0.0028	784	0.3080
7	0.3372	0.0110	12 100	0.4556
8	0.4075	−0.0065	4 225	0.6707
Σ	1.6208	−0.0001	19 165	1.8476

$$d_1 = \frac{0.2688}{0.5467} = 0.492$$

$$d_0 = 0.2026 - 0.492 \times 0.403 = 0.2026 - 0.1983 = 0.0043$$

$$(sd)^2_{yx} = \frac{1.9165 \times 10^{-4}}{6} = 3.194 \times 10^{-5}$$

$$(sd)^2_{d_1} = \frac{3.194 \times 10^{-5}}{0.5467} = 5.84 \times 10^{-5}$$

$$(sd)^2_{d_0} = 5.84 \times 10^{-5} \frac{1.8476}{6} = 1.35 \times 10^{-5}$$

$$B_1 = 0.492 \pm 7.65 \times 10^{-3}$$

$$B_0 = 0.0043 \pm 3.68 \times 10^{-3} = 0.0043 \pm 85.5\%$$

$$\frac{1}{B_1} = 2.03 \pm 3.16 \times 10^{-2} = 2.03 \pm 1.55\ \% = n^s_{m,1,0}$$

since $$B_0 = \frac{1}{n^s_{m,1,0}} \frac{\beta}{\alpha - 1} \approx 0, \quad i.e. \quad \alpha \approx \infty,$$

therefore,

$$B_1 = \frac{1}{n^s_{m,1,0}} \frac{\alpha - \beta}{\alpha - 1} = \frac{1}{n^s_{m,1,0}} .$$

3.2.2. Regression analysis by taking into account five arbitrarily chosen points (Tables VIc, d)

Table VIc

i	x_i	Δx_i	$(\Delta x_i)^2$	y_i	Δy_i	$\Delta x_i \cdot \Delta y_i$
1	0.022	−0.420	0.1764	0.0149	−0.2077	0.0872
3	0.223	−0.219	0.0479	0.1140	−0.1086	0.0238
5	0.471	0.029	0.0008	0.2350	0.0124	0.0004
7	0.675	0.233	0.0543	0.3482	0.1256	0.0293
8	0.819	0.377	0.1421	0.4010	0.1784	0.0673
Σ	$\bar{x} = 0.442$	0.000	0.4215	$\bar{y} = 0.2226$	0.0001	0.2080

Table VId

i	Y_i	$y_i - Y_i$	$(y_i - Y_i)^2 \cdot 10^8$	x_i^2
1	0.0155	−0.0006	36	0.0005
3	0.1146	−0.0006	36	0.0497
5	0.2369	−0.0019	361	0.2218
7	0.3227	0.0255	65 025	0.4556
8	0.4085	−0.0075	5 625	0.6707
Σ	1.0982	0.0149	71 083	1.3983

$$d_1 = \frac{0.2080}{0.4215} = 0.493$$

$$d_0 = 0.2226 - 0.493 \times 0.442 = 0.2226 - 0.2179 = 0.0047$$

$$(sd)^2_{yx} = \frac{7.1083 \times 10^{-4}}{3} = 2.369 \times 10^{-4}$$

$$(sd)^2_{d_1} = \frac{2.369 \times 10^{-4}}{0.4215} = 5.62 \times 10^{-4}$$

$$(sd)^2_{d_0} = 5.62 \times 10^{-4} \frac{1.3983}{5} = 1.57 \times 10^{-4}$$

$$B_1 = 0.493 \pm 2.37 \times 10^{-2}$$

$$B_0 = 0.0047 \pm 1.25 \times 10^{-2} = 0.0047 \pm 266\%$$

$$\frac{1}{B_1} = 2.03 \pm 9.78 \times 10^{-2} = 2.03 \pm 4.82\% = n^s_{m,1,0}$$

from consideration similar to the above.

As the results indicate, the monomolecular adsorption capacity values determined by the two different methods are in excellent agreement, the

difference of about 0.5 per cent being substantially lower than the standard deviations. This agreement, although indirectly, indicates in itself that the n_1^σ *vs.* x_1 excess isotherm is of type II. It can also be seen that in the x_1x_2/n_1^σ *vs.* x_1 representation the deviation of the points falling on the curved section of the n_1^σ *vs.* x_1 isotherm ($i = 1$, 2 and 3), which points cannot be taken into account in the extrapolation method, is also within the limits of the random scatter of the results around the line determined by the rest of the points (Fig. 3). This

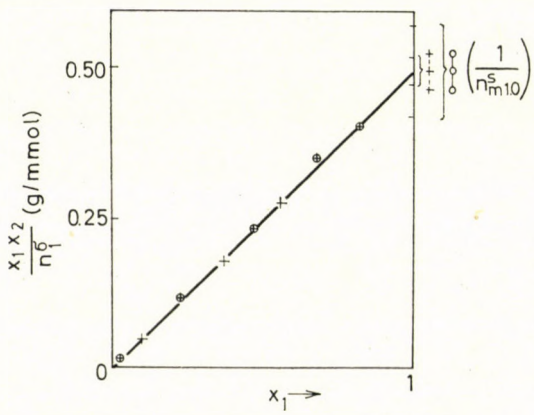

Fig. 3. $\frac{x_1 x_2}{n_1^\sigma}$ *vs.* x_1 plot for the benzene (1) – *n*-heptane (2) – silica gel system; $\left(\frac{1}{n^s_{m,1,0}}\right)^{95\%} =$ $= 0.492 \pm 3.81\%$ + —— + —— + (from 8 measured points), and $= 0.493 \pm 15.3\%$ ○ — — ○ —— ○ (from 5 measured points)

fact indicates that even in this range the separation constant, α, is much higher than unity, or than β. The fact that the absolute values of $n^s_{m,2}(= -B_1 - B_0)$ determined by the SCHAY—NAGY method, and those of

$$\frac{1}{n^s_{m,1,0}} \quad \frac{\beta}{\alpha - 1} \; (= B_0)$$

obtained in the EVERETT representation are very close to zero, proves unambiguously that the n_1^σ *vs.* x_1 excess isotherm is indeed of type II. This is even more convincing if one takes into account that standard deviations are close to, or in certain cases many times exceed 100%.

On the basis of Table VII, which summarizes the results of the calculations and lists the absolute values of the monomolecular adsorption capacity, $n^s_{m,1}$, and the specific surface area of the adsorbent, a^s, as well as their standard deviations at statistical probability levels of 80, 90, 95 and 99%, enables one to compare the specific surface area values obtained by the SCHAY—NAGY method and by the EVERETT method, and to compare both with the BET

Table VII

Deviations of the adsorption capacity

Method of surface area determination	No. of measured data	$n^s_{m,1}$ (mmol benzene/g)	a^s (m^2/g)	Statistic probability			
				80%	90%	95%	99%
SCHAY—NAGY	5	2.02	363.6	(*sd*)%: ±2.19	± 3.15	± 4.25	± 7.82
Generalized	8	2.03	365.4	(*sd*)%: ±2.24	± 3.03	± 3.81	± 5.78
EVERETT	5	2.03	365.4	(*sd*)%: ±7.87	±11.3	±15.3	±28.1
BET—N_2			360 ±5%				

surface area obtained from the nitrogen gas adsorption isotherm. The agreement is very good in every case. If the results of the two calculations by the EVERETT method are compared, it turns out that the reduction of the number of experimental data, particularly at higher statistical probability levels, considerably increases the deviation.

REFERENCES

1. NAGY, L. Gy., SCHAY, G.: Magy. Kém. Foly. **77**, 113 (1971)
2. FÓTI, Gy., NAGY, L. Gy., SCHAY, G.: Magy. Kém. Foly. **77**, 479 (1971)
3. OVERMAN, R. T., CLARK, H. M.: Radioisotope Techniques. McGraw-Hill, New York, 1960
4. FELIX, M., BLÁHA, K.: Mathematical Statistics in Chemical Industry (in Hungarian). Műszaki Kiadó, Budapest, 1964

György FÓTI
Lajos György NAGY } 1111 Budapest, Budafoki út 8.

Géza SCHAY; 1025 Budapest, Pusztaszeri út 57/69.

Acta Chimica Academiae Scientiarum Hungaricae, Tomus 76 (3), pp. 287—294 (1973)

NITROPHENOLS, II.*
THE REACTIVITY OF 5-NITROHYDROXYHYDROQUINONE ETHERS

SYNTHESIS OF 3-SUBSTITUTED DERIVATIVES

A. F. ABOULEZZ and W. S. EL-HAMOULY
(National Research Centre, Dokki, Cairo, Egypt)

Received January 17, 1972

The formation of 6-hydroxy-3-methoxy-5-nitro-2-hydroxybenzyl alcohol methylene ether affords evidence for the reactivity of the 3-position in the 1-methyl ether of 5-nitrohydroxyhydroquinone. The 3-substituted phenylthioacetic and phenylacetic acids fail to undergo lactonization.

In a previous work [1], the behaviour of 2,4-dihydroxy-1-methoxy-5-nitrobenzene (**I**) towards chlorination, chloromethylation and Mannich condensation was reported. It was suggested that the products carry the new substituent in the 3-position, and the present communication provides additional supporting evidence. This was sought, *inter alia*, by transformation of the substituent to a carboxyl-containing group to find out if it is capable of lactonization.

3-Chloro-2,4-dihydroxy-1-methoxy-5-nitrobenzene (**II**), previously obtained by chlorination of **I**, reacts with thioglycollic acid in alkaline medium to give 2,6-dihydroxy-3-methoxy-5-nitrophenylthioacetic acid (**III**). Methylation of **II** with diazomethane affected both hydroxyl groups giving 3-chloro-5-nitro-1,2,4-trimethoxybenzene (**IV**). The latter compound failed to react with thioglycollic acid, but the action of alkali caused demethylation of the group *para* to the nitro group yielding 3-chloro-1,4-dimethoxy-2-hydroxy-5-nitrobenzene (**V**). The structure of **V** was supported by its preparation from 1,4-dimethoxy-2-hydroxy-5-nitrobenzene (**VI**) by chlorination with sulfuryl chloride. This reagent introduced the halogen in the same position in 1,2-dimethoxy-4-hydroxy-5-nitrobenzene (**VII**), and had the additional effect of demethylating the methoxyl group *para* to the nitro group, giving **II**.

The activity of the 3-position in **I** was also demonstrated by another series of reactions starting from 2,4-dihydroxy-1-methoxy-5-nitro-3-piperidinomethylbenzene (**VIII**) obtained by Mannich condensation [1]. Reaction with potassium cyanide gave 3-cyanomethyl-2,4-dihydroxy-1-methoxy-5-nitrobenzene (**IX**) as the main product, in addition to bis(2,6-dihydroxy-3-methoxy-5-nitrophenyl)methane (**X**) and 2,6-dihydroxy-3-methoxy-5-nitrophenylethyl

* Part I, Acta Chim. Acad. Sci. Hung. **42**, 41 (1964)

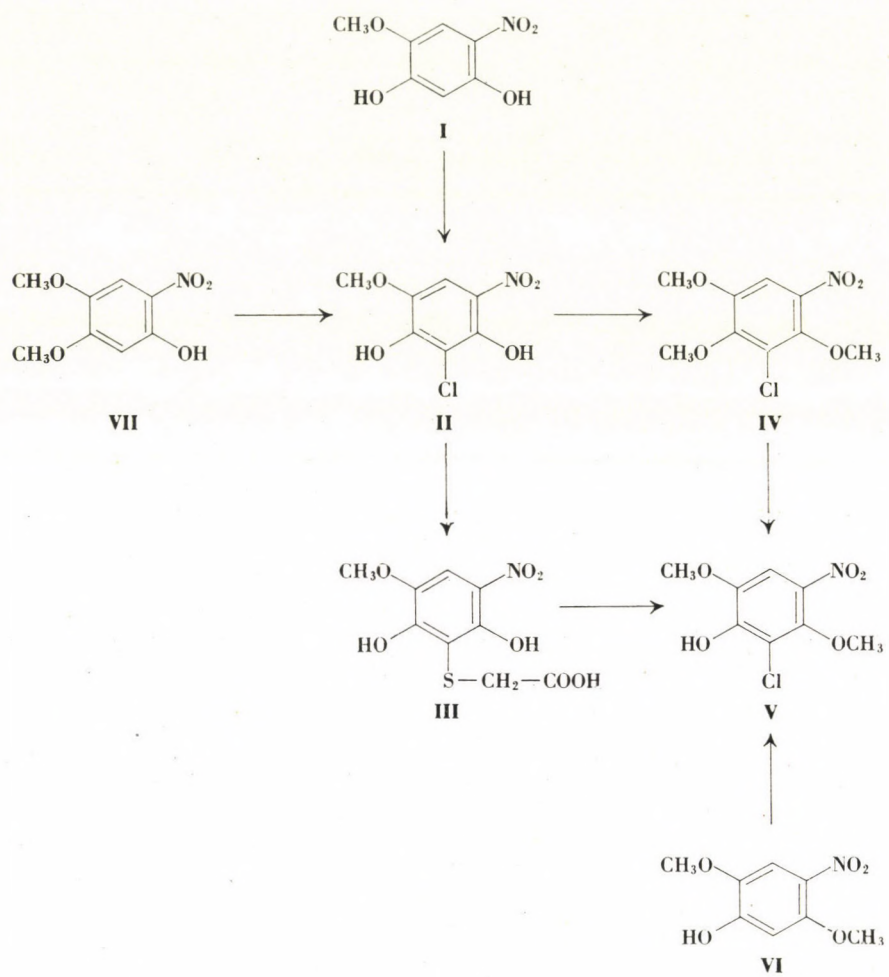

acetate (**XI**) as by-products. Methylation of **X** with diazomethane gave bis(5-nitro-2,3,6-trimethoxyphenyl)methane (**XII**). The NMR spectrum of the compound **XII** contained a singlet at δ 7.51 for the hydrogen proton at C-4, a singlet at δ 4.25 due to the two protons of the methylene group, three singlets at δ 3.92, δ 3.85 and δ 3.72, due to the protons of the three CH_3O groups attached to C-2, C-5 and C-6. Alkaline hydrolysis of both **IX** and **XI** gave the same 2,6-dihydroxy-3-methoxy-5-nitrophenylacetic acid (**XIII**) from which an acid chloride (**XIV**) was prepared; both the methyl ester (**XV**) and the ethyl ester (**XI**) were made by the action of methanol and ethanol, respectively, on **XIV**. Treatment of **XV** with diazomethane afforded methyl 5-nitro-2,3,6-trimethoxyphenylacetate (**XVI**), from which the free acid (5-nitro-2,3,6-trimethoxyphenylacetic acid, **XVII**) was obtained by saponification. These reac-

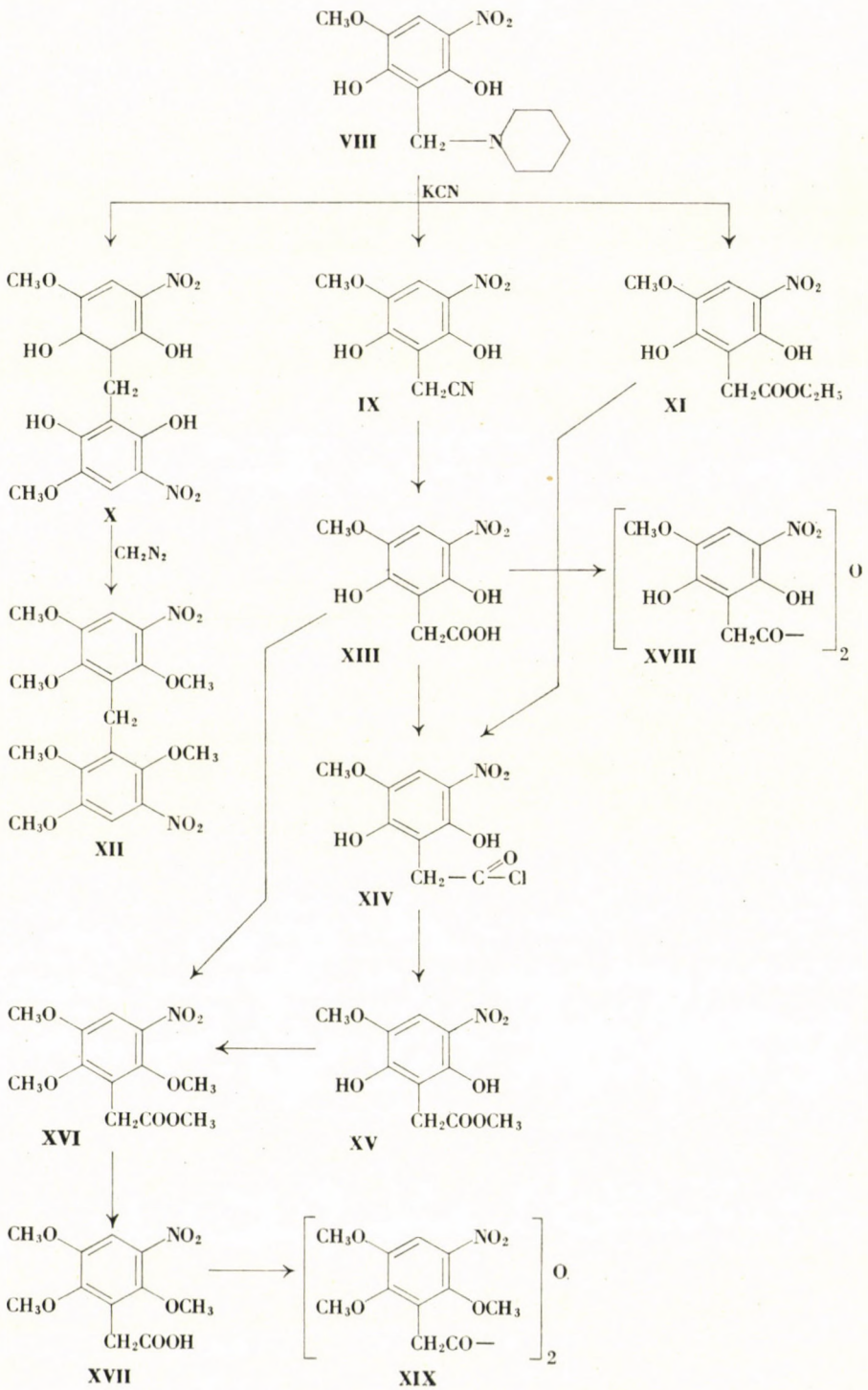
VIII
KCN
IX
XI
X
CH_2N_2
XII
XIII
XVIII
XIV
XVI
XV
XVII
XIX

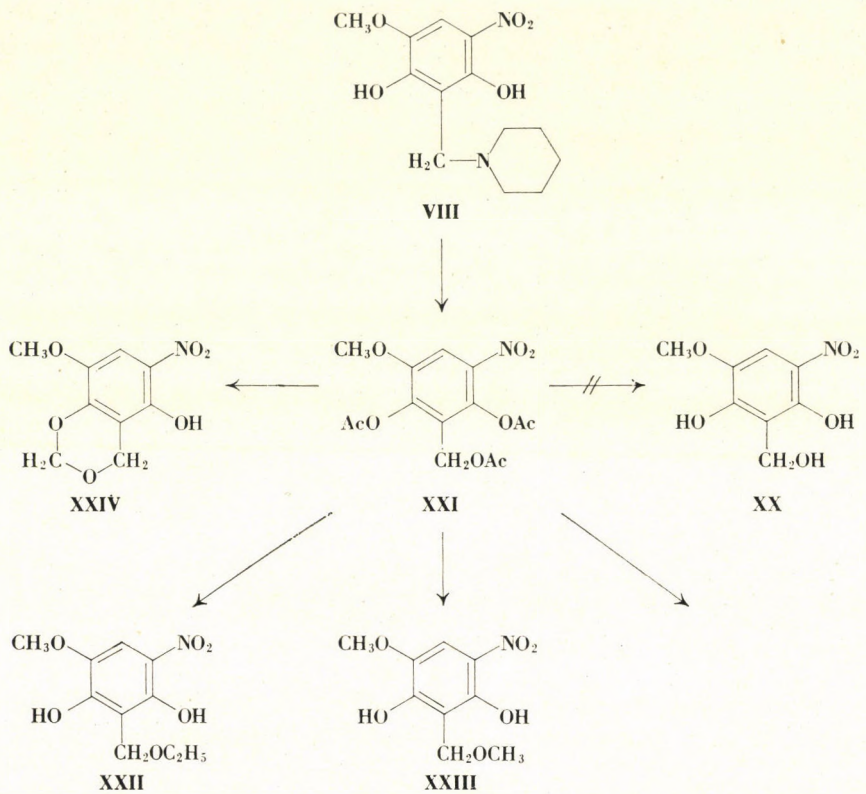

tions are in agreement with structure **III** in showing that no lactone formation has occurred. Moreover, the possibility of location of the acetic acid group *ortho* to the nitro group was dismissed on the basis of the reaction of the two free acids **XIII** and **XVII** with acetic anhydride, whereby the corresponding anhydrides, **XVIII** and **XIX**, resulted and not the acetylanthranils [2].

In an attempt to obtain 2,6-dihydroxy-1-methoxy-5-nitrobenzyl alcohol (**XX**), the piperidinomethyl derivative **VIII** was treated with acetic anhydride, and the product (2,6-diacetoxy-3-methoxy-5-nitrobenzyl acetate, **XXI**) was saponified with alkali; surprisingly, no trace of **XX** resulted but, instead, a compound was obtained which was identical with the diphenylmethane derivative (**X**). The hydrolysis of **XXI** with hydrochloric acid in ethyl or methyl alcohol gave 2,6-dihydroxy-3-methoxy-5-nitrobenzyl ethyl (or methyl) ether (**XXII** and **XXIII**). Treatment of **XXI** with paraformaldehyde in acidic medium afforded a compound for which the structure of 6-hydroxy-3-methoxy-5-nitro-2-hydroxybenzyl alcohol methylene ether (**XXIV**) is now proposed. The NMR spectrum of compound **XXIV** has a singlet at δ 3.91 for the three protons of the CH_3O group, two singlets at δ 7.18 and δ 5.41 for the two CH_2 groups and two

singlets at δ 7.18 and 7.50, one for the hydrogen proton at C-4 and the other for the (OH) proton. The reaction leading to this product provides evidence for the reactivity of the 3-position in **I** despite the absence of ability of the obtained *o*-hydroxyphenylacetic acid (**XIII**) and *o*-hydroxyphenylthioacetic acid (**III**) to undergo lactonization.

Experimental

2,6-Dihydroxy-3-methoxy-5-nitrophenylthioacetic acid (III)

A mixture of 3-chloro-2,4-dihydroxy-1-methoxy-5-nitrobenzene (**II**; 0.88 g), methanol (20 ml), aqueous sodium hydroxide solution (5%, 20 ml) and thioglycollic acid (80%, 1.2 ml) were refluxed on a steam bath for 4 hrs. The reaction mixture was concentrated to half its volume, cooled and acidified with dilute hydrochloric acid. The precipitate was filtered off and crystallized from methanol; if only a little or no precipitate was formed, the acidic solution was extracted with chloroform, dried, evaporated to dryness and the residue crystallized from methanol to give **III** m.p. 196 °C; yield, 95%.

$C_9H_9NO_7S$ (275.23). Calcd. C 39.29; H 3.27; N 5.09; S 11.67.
Found C 39.22; H 3.40; N 4.87; S 12.15%.

3-Chloro-5-nitro-1,2,4-trimethoxybenzene (IV)

An ethereal solution of diazomethane, prepared from nitrosomethylurea (2 g), was added to 3-chloro-2,4-dihydroxy-1-methoxy-5-nitrobenzene (**II**; 0.88 g) suspended in ether. The mixture was allowed to stand 2 hrs at room temperature and then kept overnight in a refrigerator. After evaporation of the ether, the residue was crystallized from methanol to give **IV** (0.9 g) m.p. 104 °C.

$C_9H_{10}ClNO_5$ (247.63). Calcd. C 43.63; H 4.04; Cl 14.34.
Found C 43.28; H 4.04; Cl 13.67%.

3-Chloro-1,4-dimethoxy-2-hydroxy-5-nitrobenzene (V)

(a) A solution of the chloronitrotrimethoxybenzene (**IV**, 1 g) and potassium hydroxide (4 g) in methanol (50 ml) was refluxed on a steam bath for 2 hrs. The solution was concentrated and diluted with water, filtered from any unreacted material, and acidified with hydrochloric acid. The resulting precipitate was collected by filtration and crystallized from methanol to give **V** (0.6 g) m.p. 154 °C.

$C_8H_8NO_5$ (233.61). Calcd. C 41.12; H 3.45.
Found C 41.19; H 3.60%.

(b) To a suspension of 1,4-dimethoxy-2-hydroxy-5-nitrobenzene (**VI**, 0.5 g) in dry ether (20 ml), freshly distilled sulfuryl chloride (2 ml) was added. The mixture was refluxed gently on a steam bath for 2 hrs. The solvent was evaporated and the residue was recrystallized from methanol to give **V** in quantitative yield, m.p. 154 °C.

3-Chloro-2,4-dihydroxy-1-methoxy-5-nitrobenzene (II)

1,2-Dimethoxy-4-hydroxy-5-nitrobenzene (**VII**) was treated with sulfuryl chloride as described above to give **II** in quantitative yield, m.p. 190 °C. Mixed melting point determination with an authentic sample gave no depression.

Action of potassium cyanide on 2,4-dihydroxy-1-methoxy-5-nitro-3-piperidinomethylbenzene

A mixture of 2,4-dihydroxy-1-methoxy-5-nitro-3-piperidino-methylbenzene (**VIII**, 11.5 g), ethyl alcohol (120 ml) and a solution of potassium cyanide (15 g) in water (20 ml) was heated and stirred under reflux for 8 hrs. The reaction mixture was concentrated to half of its volume, diluted with water, and acidified with hydrochloric acid. The resulting precipitate was filtered off and treated with boiling ethanol to leave an alcohol-insoluble material (0.46 g), which was bis(2,6-dihydroxy-3-methoxy-5-nitrophenyl)methane (**X**), m.p. 275 °C

(decomp.; from dioxan). The alcohol-soluble part was concentrated and cooled to give 3-cyanomethyl-1,4-dihydroxy-1-methoxy-5-nitrobenzene (**IX**; 3.9 g), m.p. 216 °C (from alcohol). The mother liquor was diluted with water, when 2,6-dihydroxy-3-methoxy-5-nitrophenylethyl acetate (**XI**; 3.1 g) separated; m.p. 185 °C (from aqueous ethanol).

Compound **X**:	$C_{15}H_{14}N_2O_{10}$	(382.28).	Calcd. C 47.12; H 3.69; N 7.32.
			Found C 47.51; H 4.06; N 7.38%.
Compound **IX**:	$C_9H_8N_2O_5$	(224.17).	Calcd. C 48.22; H 3.57; N 12.55.
			Found C 48.33; H 3.66; N 11.99%.
Compound **XI**:	$C_{11}H_{13}NO_7$	(271.22).	Calcd. C 48.71; H 4.79; N 5.16.
			Found C 48.98; H 4.98; N 5.13%.

Bis(5-nitro-2,3,6-trimethoxyphenyl)methane (XII)

A sample of **X** (0.5 g) was methylated with diazomethane as described above for **IV**. **XII** was obtained and had m.p. 135—6 °C (from methanol).

$C_{19}H_{22}N_2O_{10}$ (649.55). Calcd. C 52.05; H 5.06; N 6.39.
Found C 52.65; H 5.16; N 7.21%.

2,6-Dihydroxy-3-methoxy-5-nitrophenylacetic acid (XIII)

The 3-cyanomethyl derivative (**IX**; 6.7 g) or the ethyl acetate derivative (**XI**; 8.1 g) was added to a 20% solution of potassium hydroxide (15 ml) in ethanol (10 ml). The mixture was refluxed for 8 hrs. After evaporation of most of the alcohol, the cooled solution was acidified with dilute hydrochloric acid. **XIII** precipitated; it was filtered off, washed with a little cold water, dried and crystallized from ethyl acetate; the product had m.p. 233—4 °C, yield 80—95%.

$C_9H_7NO_7$ (241.15) Calcd. C 44.44; H 3.7.
Found C 44.46; H 3.9%.

2,6-Dihydroxy-3-methoxy-5-nitrophenylacetic acid methyl (or ethyl) ester (XV and XI)

To a suspension of **XIII** (0.78 g) in carbon disulfide (30 ml), thionyl chloride (3 ml) was added. The mixture was heated under reflux until **XIII** completely dissolved. The solution was then evaporated to dryness in vacuum to leave the acid chloride **XIV**, which was directly converted to the esters **XIV** and **XI** by crystallization from methyl or ethyl alcohol. **XI** had m.p. 185 °C and it was identical with the compound prepared previously. Compound **XV** melted at 190 °C.

$C_{10}H_{11}NO_7$ (257.2). Calcd. C 46.92; H 4.31.
Found C 46.88; H 4.40%.

Methyl 5-nitro-2,3,6-trimethoxyphenylacetate (XVI)

An ethereal solution of diazomethane prepared from nitrosomethylurea (4 g) was added to **XIII** (or **XV**) (0.5 g) suspended in dry ether (10 ml). The mixture was stored in a refrigerator overnight. After evaporation of the ether, the residue was crystallized from aqueous methanol to give **XVI** in 85% yield; m.p. 50 °C.

$C_{12}H_{15}NO_7$ (285.25). Calcd. C 50.52; H 5.30.
Found C 50.48; H 5.37%.

5-Nitro-2,3,6-trimethoxyphenylacetic acid (XVII)

The above ester (**XVI**; 0.5 g) was saponified for a day at room temperature with a 5% aqueous solution of potassium hydroxide (10 ml) containing few drops of alcohol. The resulting clear solution was then acidified with dilute HCl. The free acid **XVII** separated as crystals; m.p. 134 °C (from benzene–petroleum ether); the yield was nearly quantitative.

$C_{11}H_{13}NO_7$ (271.22). Calcd. C 48.71; H 4.8; N 5.16.
Found C 48.53; H 5.0; N 5.13%.

Bis(2,6-diacetoxy-3-methoxy-5-nitrophenylacetic) anhydride (XVIII)

2,6-Dihydroxy-3-methoxy-5-nitrophenylacetic acid (**XIII**; 0.5 g) was refluxed with excess acetic anhydride (15 ml) for 2 hrs. After removal of the reagent in vacuum, **XVIII** separated and it was crystallized from ethyl acetate to obtain 0.3 g, m.p. 207 °C.

$C_{26}H_{24}N_2O_{17}$ (636.47). Calcd. C 49.21; H 3.77; N 4.40.
Found C 49.17; H 3.68; N 4.18%.

Bis (5-nitro-2,3,6-trimethoxyphenylacetic) anhydride (XIX)

Compound **XVII** (0.5 g) was treated in the same manner as described above. **XIX** was then crystallized from benzene–petroleum ether to obtain 0.36 g, m.p. 125 °C.

$C_{22}H_{22}N_2O_{13}$ (522.42). Calcd. C 50.37; H 4.58; N 5.34.
Found C 50.15; H 4.65; N 5.0%.

2,6-Diacetoxy-3-methoxy-5-nitrobenzyl acetate (XXI)

A mixture of 2,4-dihydroxy-1-methoxy-5-nitro-3-piperidinomethylbenzene (**VIII**; 2 g), sodium acetate (0.2 g) and acetic anhydride (10 ml) was refluxed for 2 hrs. The reaction mixture was evaporated and the residue recrystallized from ethyl acetate to give **XXI** (1.45 g). Recrystallization from benzene–petroleum ether gave m.p. 114 °C.

$C_{14}H_{15}NO_9$ (341.24). Calcd. C 49.56; H 4.40.
Found C 49.59; H 4.58%.

Alkaline hydrolysis of XXI

Compound **XXI** (0.5 g) was treated with a 20% aqueous sodium hydroxide solution (10 ml) for 24 hrs at room temperature. The solution was then filtered and acidified with dilute hydrochloric acid, the resulting precipitate was filtered off, washed with water, dried and crystallized from dioxan ethanol to give **X** (0.2 g) m.p. 275 °C (decomp.).

2,6-Dihydroxy-3-methoxy-5-nitrobenzyl ethyl (or methyl) ether (XXII and XXIII)

Compound **XXI** (0.5 g) was dissolved in the appropriate alcohol (ethanol or methanol) and the solution was treated with 1 ml of conc. HCl. The mixture was then refluxed on a steam bath for 1 hr. After evaporation of the solvent, the residue was dissolved in benzene, filtered from the impurities and then petroleum ether was added to the filtrate. On cooling, a crystalline substance (**XXII** or **XXIII**, according to the alcohol used) was obtained in satisfactory yield. The ethyl ether (**XXII**) had m.p. 130 °C.

$C_{10}H_{13}NO_6$ (243.21). Calcd. C 49.50; H 5.35.
Found C 49.32; H 5.52%.
The methyl ether (**XXIV**) melted at 117 °C (lit. (1) m.p. 117 °C).

6-Hydroxy-3-methoxy-5-nitro-2-hydroxybenzyl alcohol methylene ether (XXIV)

A mixture of the triacetate **XXI** (0.5 g), acetic acid (10 ml), conc. HCl (3 ml) and paraformaldehyde (0.2 g) was refluxed for 3 hrs. The mixture was evaporated under reduced pressure to dryness, and the residue crystallized from methanol to give **XXIV** (0.39 g). A second recrystallization from dioxan–alcohol (1 : 8) gave an a analytical sample, m.p. 192—3 °C.

$C_9H_9NO_6$ (227.17). Calcd. C 47.58; H 3.99; H 6.17.
Found C 47.65; H 4.13; N 6.28%.

*

The authors' thanks are expressed to Mr. MAHER EL-SOUKARY, Petroleum Department, for the NMR analyses.

REFERENCES

1. ABOULEZZ, A. F., ZAYED, S. M. A. D., EL-HAMOULY, W. S.: Acta Chim. Acad. Sci. Hung. **42**, 41 (1964)
2. GORDON, N. WALKER: J. Am. Chem. Soc. **77**, 6698 (1955)

A. F. ABOULEZZ
W. S. EL-HAMOULY
National Research Centre Tahreer Street, Dokki, Cairo, Egypt.

Acta Chimica Academiae Scientiarum Hungaricae, Tomus 76 (3), pp. 295—297 (1973)

SYNTHESIS OF COMPOUNDS WITH POTENTIAL FUNGICIDAL ACTIVITY

SH. A. SHAMS EL-DINE and O. CLAUDER

(Institute of Organic Chemistry, Semmelweis Medical University, Pharmaceutical Faculty, Budapest)

Received March 6, 1972

Twelve new alkyl esters of 1,3,4-thiadiazol-(5-methyl-1,3,4-thiadiazol or 5-trifluoromethyl-1,3,4-thiadiazol)-2-yl dithiocarbamic acid were synthesized, where the alkyl group is methyl, ethyl, *n*-propyl or carbethoxymethyl. The compounds were prepared to be tested for their fungicidal activity.

It is well known that dithiocarbamates are active against fungi, especially human dermatophytes [1]. Several compounds containing the dithiocarbamate group have been synthesized [2, 3] and the mechanism of their fungicidal action [4] as well as their structure-activity relationship studied [5, 6].

On the other hand it has been reported that compounds containing sulfur as a member of the ring have antifungal activity. Among such sulfur-containing nuclei are thiazoles [7], benzothiazoles [8], 1,2,4-dithiazoles [9], 1,2,4- [10] and 1,3,4-thiadiazoles [11, 12], benzothiadiazoles [13] and 1,3,4-oxathiazoles [14]. More recently salts and esters of 1,3-thiazol-2-yl dithiocarbamic acid were synthesized and described to have fungicidal activity against phytophthora and piricularia [15, 16]. Thus the idea of synthesizing some compounds containing both the thiadiazole ring and the dithiocarbamate moiety seemed reasonable in the hope that these compounds may have fungicidal properties.

The compounds were synthesized via the following route:

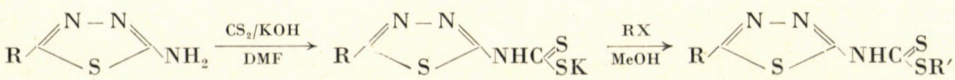

I—III **IV—VI** **VII—XVIII**

(R=H, CH_3, CF_3; R'=CH_3, C_2H_5, *n*-C_3H_7 or $CH_2CO_2C_2H_5$)

This route is similar to the method described in the recent literature [16] with slight modification in the process of separation of the products. The antifungal testing of these new compounds is in progress.

Table I

Groups R,R′, percentage yields, the melting points and microanalytical data of the products are given in the following table

Comp. No.	R	R′	Yield %	M.p., °C	Microanalysis				
					Molecular formula	C%		H%	N%
VII	H	CH_3	85	189—91	$C_4H_5N_3S_3$	Calcd.	25.11	2.64	21.87
						Found	25.46	2.90	21.94
VIII	H	C_2H_5	87	165—7	$C_5H_7N_3S_3$	Calcd.	29.25	3.44	20.47
						Found	29.24	3.60	20.42
IX	H	C_3H_7	90	172—4	$C_6H_9N_3S_3$	Calcd.	32.85	4.15	19.16
						Found	32.94	4.30	19.43
X	H	$CH_2CO_2C_2H_5$	85	162—4	$C_7H_9N_3O_2S_3$	Calcd.	31.92	3.45	15.95
						Found	31.80	3.56	16.10
XI	CH_3	CH_3	85	195—7	$C_5H_7N_3S_3$	Calcd.	29.25	3.44	20.47
						Found	29.20	3.51	20.31
XII	CH_3	C_2H_5	90	159—61	$C_6H_9N_3S_3$	Calcd.	32.85	4.15	19.16
						Found	32.84	4.20	19.28
XIII	CH_3	C_3H_7	90	160—1	$C_1H_{11}N_3S_3$	Calcd.	36.02	4.76	18.00
						Found	35.87	4.90	18.35
XIV	CH_3	$CH_2CO_2C_2H_5$	85	144.5—5.5	$C_8H_{11}N_3O_2S_3$	Calcd.	34.64	4.01	15.15
						Found	34.50	4.20	14.99
XV	CF_3	CH_3	85	224—6	$C_5H_4F_3N_3S_3$	Calcd.	23.16	1.59	16.21
						Found	23.05	1.93	16.60
XVI	CF_3	C_2H_5	88	203—4.5	$C_6H_6F_3N_3S_3$	Calcd.	26.36	2.22	15.38
						Found	26.22	2.05	15.70
XVII	CF_3	C_3H_7	90	199—201	$C_7H_8F_3N_3S_3$	Calcd.	29.26	2.81	14.63
						Found	29.03	2.96	15.18
XVIII	CF_3	$CH_2CO_2C_2H_5$	87	149—51	$C_8H_8F_3N_3O_2S_3$	Calcd.	29.89	2.51	13.08
						Found	29.67	2.70	12.90

Experimental

All m.p.-s are uncorrected.

Potassium 1,3,4-thiadiazol-(5-methyl-1,3,4-thiadiazol or 5-trifluoro-methyl-1,3,4-thiadiazol)2-yl dithiocarbamates (IV—VI)

0.05 mole of 2-amino-1,3,4-thiadiazole (2-amino-5-methyl- or 2-amino-5-trifluoro-methyl-1,3,4-thiadiazole) (**I— III**) was dissolved in 30 ml dimethylformamide. To this solution there was added 2.85 g potassium hydroxide followed by the gradual addition of 3 ml carbon disulfide during 15 min so that the temperature of the reaction mixture did not rise above 35 °C; it was then allowed to stand 1 hr. Chloroform was added gradually with shaking, and the yellowish crystals of the potassium salt that separated were filtered off and washed with chloroform.

Group R, the melting points and the percentage yields of the products are listed below:

Comp. No.	R	M.p., °C	Yield, %
IV	H	246— 50° (decomp.)	88
V	CH_3	215— 20° (decomp.)	85
VI	CF_3	240— 45° (decomp.)	85

Esters of 1,3,4-thiadiazol-(5-methyl-1,3,4-thiadiazol or 5-trifluoro-methyl-1,3,4,thiadiazol)-2-yl dithiocarbamic acid (VII—XVIII)

0.005 mole of the potassium 1,3,4-thiadiazol-(5-methyl-1,3,4-thiadiazol or 5-trifluoro-methyl-1,3,4-thiadiazol)-2-yl dithiocarbamate (**IV—VI**) was refluxed with 20 ml absolute methanol and then 0.006 mole of an alkyl halide (CH_3I, C_2H_5Br, n-C_3H_7Br or $ClCH_2CO_2C_2H_5$) was added gradually. The reaction mixture was refluxed for 5—10 min, poured on excess water and the precipitate that separated was filtered off; it was washed with water and recrystallized from aqueous alcohol.

REFERENCES

1. Kligman, A. M., Rosenzweig, W.: J. Invest. Dermatol. **10,** 59 (1948)
2. Zsolnai, T.: Arzneim. Forsch. **18,** 1319 (1968)
3. Kuehle, E., Holtschmidt, H., Grewe, F., Kaspers, H.: Brit. Pat. 1,097,237: C. A. **69,** 10111 (1968)
4. Gancheva, I., Selkostop: Nauka (Sofia) **7,** 45 (1968)
5. Sehra, K. B., Trivedi, P. K.: Labdev (Kanpur, India) No. 3 (3), 153 (1965)
6. Weuffen, W., Martin, D.: Pharmazie **21,** 686 (1966)
7. Giri, S., Shukla, S. C.: Indian J. Appl. Chem. **29,** 80 (1966)
8. Edelson, E., Haskin, A. H.: Arch. Dermatol. and Syphilol. **66,** 244 (1952)
9. Allen, R. E., Shelton, R. S., Van Campen, M. G.: J. Am. Chem. Soc. **76,** 1158 (1954)
10. Noguchi, T., Hashimoto, Y., Mori, T., Kano, S., Miyazaki, K.: Yakugaku Zasshi, **88,** 1437 (1968)
11. Landquist, J. K.: Brit. Pat. 1, 028, 152: C. A. **65,** 2273 (1966)
12. Pianka, M.: J. Sci. Food Agr. **19,** 502 (1968)
13. Van Daalen, J. J., Daams, J., Koopman, H., Tempel, H.: Rec. trav. Chim. Pays-Bas **86,** 1159 (1967)
14. Muhlbauer, E., Weiss, W.: Brit. Pat. 1,079,348: C. A. **68,** 69000 (1968)
15. Farbenfabriken Bayer A. G.: Fr. Pat. 2,003,102: C. A. **72,** 100684 (1970)
16. Farbenfabriken Bayer A. G.: Fr. Pat. 2,003,118: C. A. **72,** 100683 (1970)

Sh. A. Shams El-Dine; University of Alexandria, Pharmaceutical Faculty, Alexandria.

Otto Clauder; 1092 Budapest, Hőgyes E. u. 7.

Acta Chimica Academiae Scientiarum Hungaricae, Tomus 76 (3), pp. 299—316 (1973)

KINETIC STUDIES ON THE PREPARATION OF 1-PHENYL-1,4-DIHYDRO-3(2*H*)-ISOQUINOLINONE AND ITS 4-ALKYL DERIVATIVES BY MEANS OF AMIDOALKYLATION INVOLVING CYCLIZATION

Gy. Deák, K. Gáll-Istók, Zs. Kálmán and J. Haskó-Breuer

(Research Institute for Experimental Medicine, Hungarian Academy of Sciences, Budapest)

Received May 2, 1972

Kinetic studies were carried out on the reactions of phenylacetonitriles and phenylacetic amides carrying alkyl substituent(s) in the α-position with benzaldehyde, in polyphosphoric acid, yielding 4-alkyl-1-phenyl-1,4-dihydro-3(2*H*)-isoquinolinones. IR spectrometric and gas chromatographic methods were used for concentration determination. It has been found that the space requirement of the alkyl substituent(s) has a considerable influence on the reaction rate. Comparison of the constants and the half-life periods indicate that the hydration of nitriles and the cyclization reactions probably proceed by similar mechanisms.

Of the heterocyclic carbonyl compounds, lactamtype derivatives of quinoline and isoquinoline have been relatively little investigated so far. The compounds can be classified into three types, according to the position of the nitrogen and oxygen atoms in the ring: 3,4-dihydro-2(1H)-quinolinone (hydrocarbostyril), 3,4-dihydro-1(2*H*)-isoquinolinone (hydroisocarbostyril) and 1,4-dihydro-3(2*H*)-isoquinolinone. In the literature there are almost no data in connection with the last compound; its 1-aryl derivatives were successfully prepared [1] by the reaction of aromatic aldehydes with arylacetonitriles in polyphosphoric acid (PPA) medium. When this reaction was extended to the synthesis of derivatives carrying alkyl substituent(s) in position 4, the reaction conditions required (time, temperature) were found to be strongly dependent on the number and nature (straight- or branched-chain structure) of the alkyl groups. Since investigations on the hydration of nitriles in PPA led to similar observations, kinetic studies seemed to be promising. Therefore, in the present work such studies were carried out on the hydration of nitriles and the preparation of isoquinolinone from the nitrile or acid amide; the comparison of the kinetic curves and the rate constants was expected to yield information on the mechanism of the amidoalkylation reaction involving cyclization.

According to former investigations [1], the synthesis of the parent substance and certain derivatives substituted in the nucleus can be carried out starting with either the aromatic nitrile or acid amide:

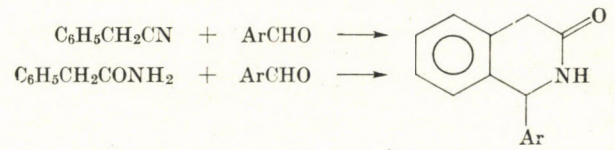

In the course of the reaction, benzyl cyanide is assumed to produce an intermediate ion (denoted by **I**) stabilized by charge delocalization; it is then converted into the end-product in an aromatic S_E reaction:

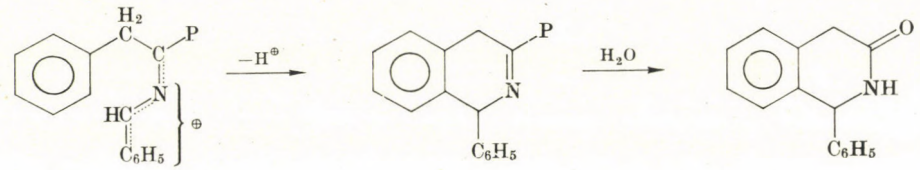

I

(HP = polyphosphoric acid)

When starting from the acid amide, benzylidene-bis-(phenylacetamide) is formed first, and this yields the end-product through an intermediate ionic state similar to **I**:

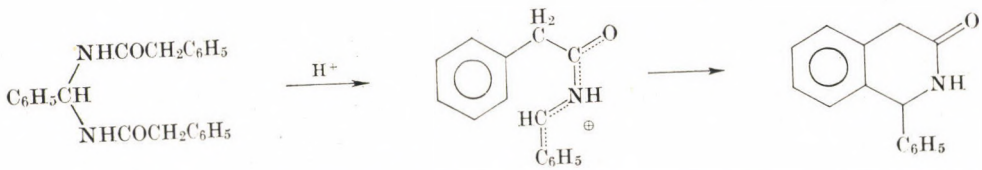

Considering that, according to our results, conversion of the bis-amide into the product is such a rapid reaction that no bis-amide can be detected in the reaction mixture, the determination of the following compounds in the presence of one another was necessary in the kinetic studies planned.

Starting material(s)	Compound to be determined
Nitrile	Nitrile
Nitrile + aldehyde	Nitrile, aldehyde and product
Acid amide + aldehyde	Aldehyde + product

The first task was the development of suitable analytical methods.

Nitriles and aldehydes were successfully determined quantitatively by means of gas chromatography. The sample taken from the polyphosphoric acid solution was made neutral with 2% sodium hydroxide, then the aldehyde and nitrile were separated from the rest by steam distillation. Since autooxidation of benzaldehyde under the conditions of the distillation would cause a

large error, a few crystals of hydroquinone were added to the solution to be distilled, and the operation was carried out in nitrogen atmosphere. The end of the distillation was decided by treating one droplet of the distillate with iodine vapours on a glass plate coated with a Kieselgel layer. When no dark spot was observed, the distillation was finished. The aqueous distillate was repeatedly extracted with chloroform, the combined extracts were dried and examined by gas chromatography. Calibration curves were used for quantitative determination. In order to check the reliability of the method, the starting materials and the product were dissolved in polyphosphoric acid in amounts corresponding to different stages of the progress of the reaction, and gas chromatographic analysis was accomplished after the isolation procedure applied. On the basis of these investigations the method seemed to be satisfactory for the present purposes.

A solid residue was obtained in the distilling flask after the steam distillation; this consisted of the product, the by-product (acid amide) and an inorganic salt. The solution containing a precipitate was made alkaline (pH 9), then cooled to —20 °C for 3 hr, the solid was filtered off and dried; it was then suitable for the determination of the isoquinolinone content. IR spectroscopy was selected for this determination. The IR spectra of 1-phenyl-1,4-dihydro-3(2*H*)-isoquinolinone (Spectrum 1) and phenylacetamide (Spectrum 2) were compared and the bands at 1320 cm^{-1} and 1355 cm^{-1} were found to be suitable for differentiating between the two compounds, since these bands are absent from the spectrum of phenylacetamide. Differences exist, of course in the 700—600 cm^{-1} range, too, but the bands in this interval do not seem suitable for quantitative analytical purposes. Although the Amide I band appears at 1670 cm^{-1} and 1645 cm^{-1} in the spectra of the isoquinolinone derivative and phenylacetamide, respectively, the bands are too broad and cannot be used for quantitative determination of the two compounds in the presence of each other.

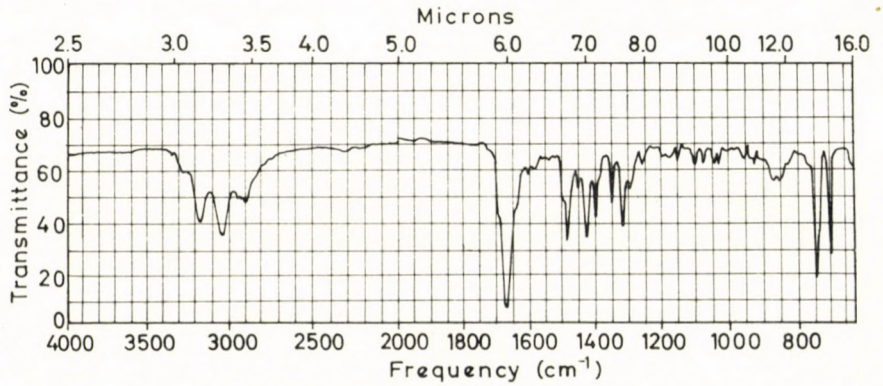

Spectrum 1. IR spectrum of 1-phenyl-1,4-dihydro-3(2*H*)-isoquinolinone (in KBr)

Spectrum 3 was recorded on a 50—50% (w/w) mixture of the isoquinolinone derivative and phenylacetamide.

In this spectrum the bands most characteristic of the isoquinolinone and of phenylacetamide are those appearing at 1320, 1350, 1400, 1485, 1665 cm^{-1} and 1420, 1640 cm^{-1}, respectively.

Spectrum 4 is the infrared spectrum of an experimental sample. The reaction was carried out between benzyl cyanide and benzaldehyde in polyphosphoric acid (1 : 1.5) at 70 °C for 120 min.

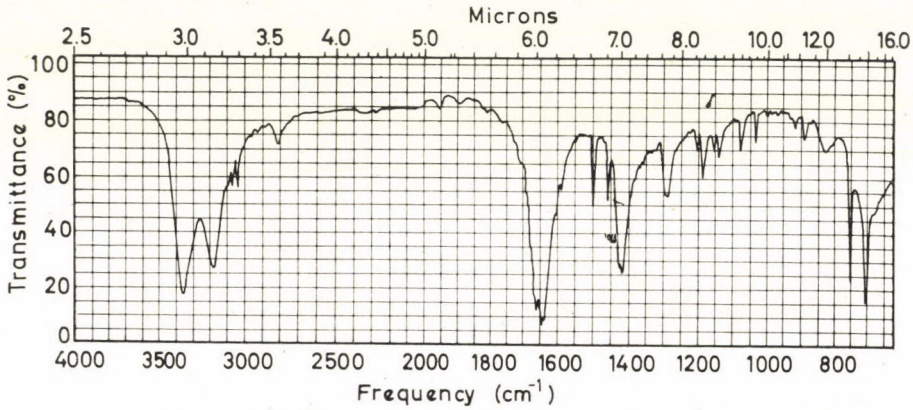

Spectrum 2. IR spectrum of phenylacetamide (in KBr)

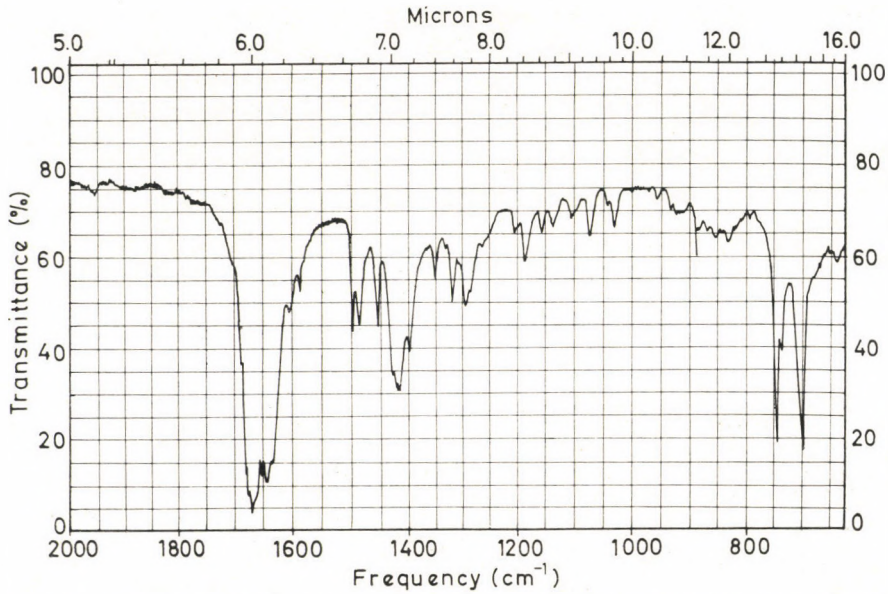

Spectrum 3. IR spectrum of a 1 : 1 mixture of 1-phenyl-1,4-dihydro-3(2*H*)-isoquinolinone and phenylacetamide (in KBr)

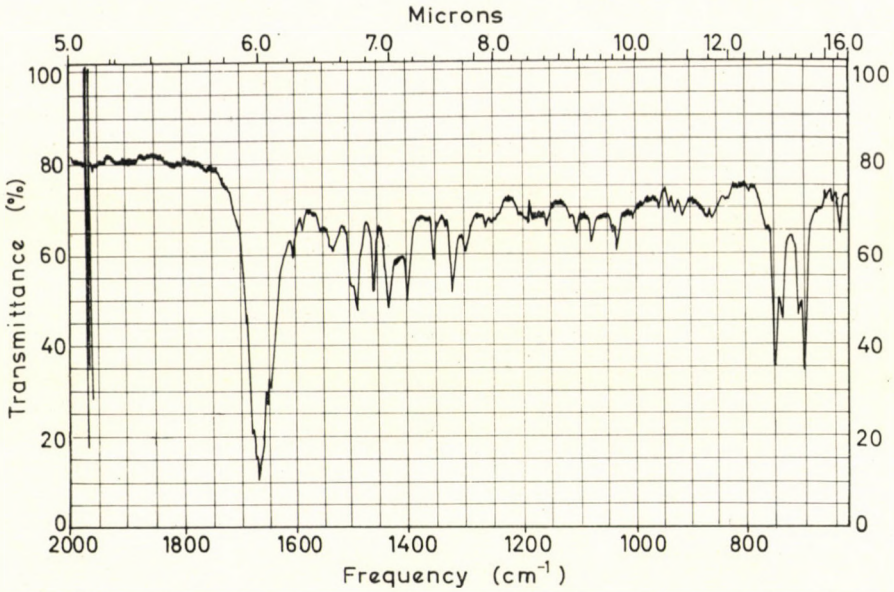

Spectrum 4. IR spectrum of the product of the reaction of benzaldehyde and benzyl cyanide in PPA (in KBr)

Comparing Spectra 4 and 3, it is striking that the bands characteristic of the isoquinolinone derivative (1665, 1485, 1400, 1350 and 1320 cm^{-1}) are the stronger ones, in accordance with the preparative experiments.

In the further work, the band appearing at 1350 cm^{-1} was used for the determination of the isoquinolinone derivative content of the samples, using a calibration diagram.

As mentioned in the introductory part, the hydration of benzyl cyanide derivatives carrying alkyl substituent(s) in the α-position, accomplished in polyphosphoric acid, and the reaction with benzaldehyde of nitriles and of the acid amides obtained from them were investigated. For these measurements the preparation of the following nitriles and acid amides was required:

$$C_6H_5C(R^1,R^2)X$$

X = CN or $CONH_2$

R^1	R^2	Name
H	H	Benzyl cyanide
H	CH_3	α-phenylpropionic nitrile (amide)
CH_3	CH_3	α-phenylisobutyric nitrile (amide)
H	iPr	α-phenylisovaleric nitrile (amide)
CH_3	iPr	α-phenyl-α-methylisovaleric nitrile (amide)
H	*n*Bu	α-phenylcaproic nitrile (amide)

Two methods were used for the preparation of the phenylacetonitriles substituted in the α-position. α-Phenylpropiononitrile was prepared according to the method of MAKOSZA [2] using methyl iodide for alkylation in the presence of benzyltriethylammonium chloride which prevents disubstitution. The other nitriles were obtained as described by TARANKO [3], in dimethyl sulfoxide solution.

Hydrogen peroxide hydration of the nitriles was attempted in order to prepare the acid amides. This proved to be successful except for the case of α-phenyl-α-methylisovaleramide; the nitrile corresponding to this compound could not be hydrated with either hydrogen peroxide or in polyphosphoric acid medium, even if rather vigorous conditions were applied. The reactions of the other nitriles were effected under identical conditions. The highest yield (71%) was obtained for α-phenylpropionamide, the lowest (35%) for α-phenylisobutyramide which has two methyl substituents in the α-position.

α-Phenylisovaleramide carrying only one alkyl substituent in the α-position, as well as the hexanamide could be prepared in higher yields (41% and 49%, respectively).

Comparing the IR spectra of the acid amides and the isoquinolinone derivatives prepared from them (Spectra 5—14), the following bands were found to be suitable for quantitative measurements:

1-phenyl-1,4-dihydro-4-methyl-3(2*H*)-isoquinolinone	1355 cm^{-1}
1-phenyl-1,4-dihydro-4,4-dimethyl-3(2*H*)-isoquinolinone	1350 cm^{-1}
1-phenyl-1,4-dihydro-4-isopropyl-3(2*H*)-isoquinolinone	1285 cm^{-1}
4-butyl-1-phenyl-1,4-dihydro-3(2*H*)-isoquinolinone	1360 cm^{-1}

In the case of 1-phenyl-1,4-dihydro-4-isopropyl-4-methyl-3(2*H*)-isoquinolinone the method could not be applied, since no band undisturbed by that of the corresponding amide could be found in the spectrum.

In order to check the method, 1 : 1 mixture were prepared from the amide–lactam pairs, and the lactam contents were determined from the IR spectra. Although the error of the method is relatively high (3—5%) as compared with other analytical procedures, it seemed satisfactory for the present purpose.

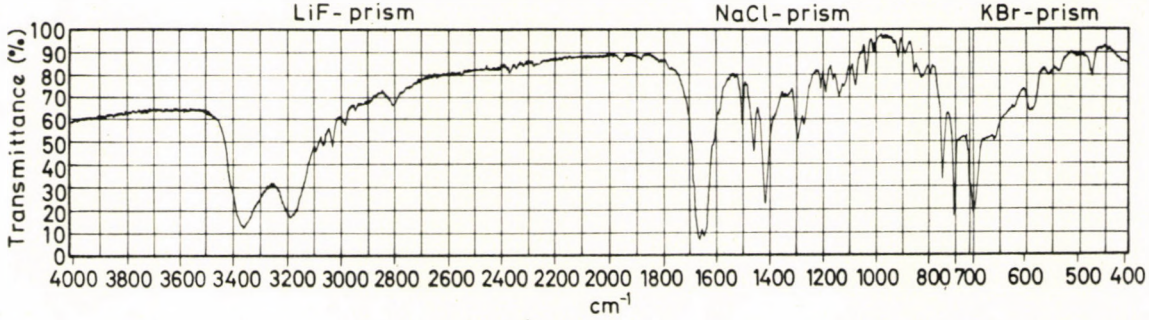

Spectrum 5. IR spectrum of α-phenylpropionamide (in KBr)

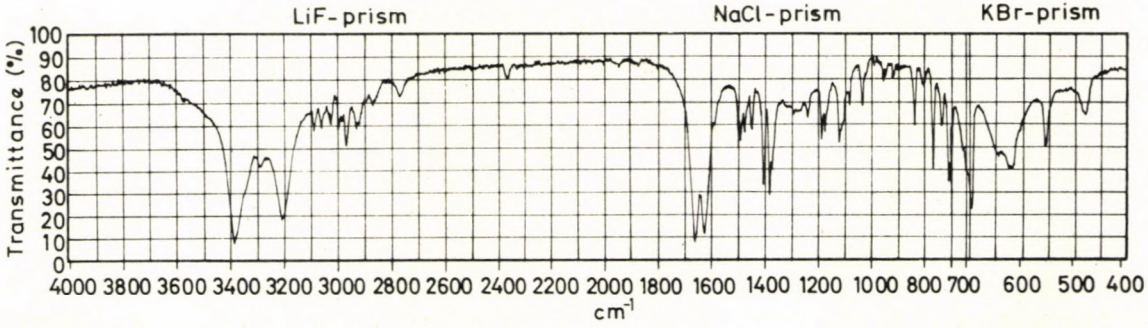

Spectrum 6. IR spectrum of α-phenylisobutyramide (in KBr)

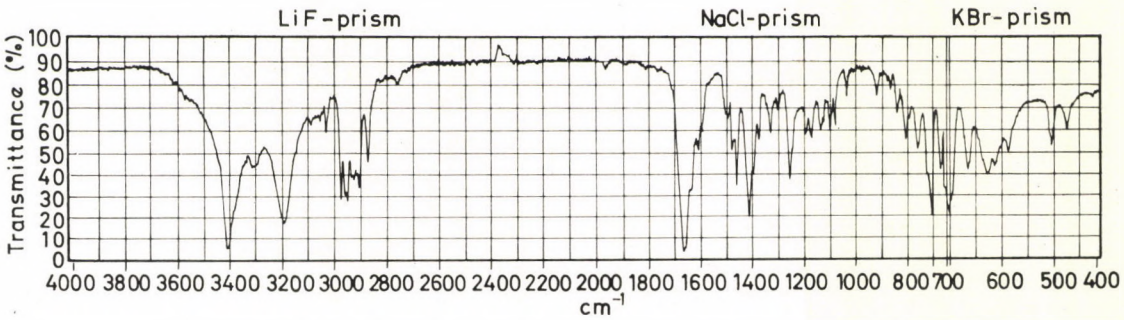

Spectrum 7. IR spectrum of α-phenylisovaleramide (in KBr)

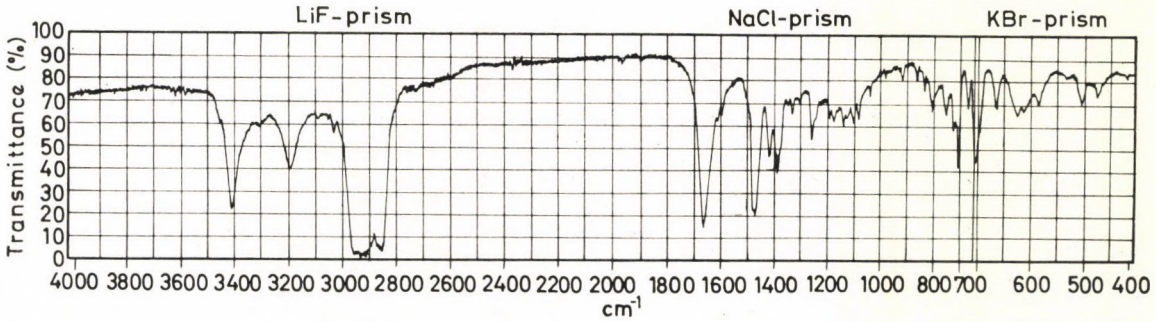

Spectrum 8. IR spectrum of α-phenyl-α-methylisovaleramide (in KBr)

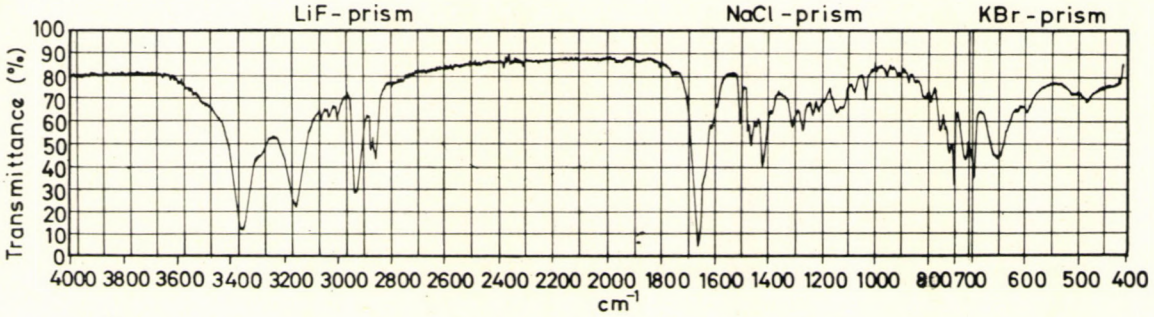

Spectrum 9. IR spectrum of α-phenylhexanamide (in KBr)

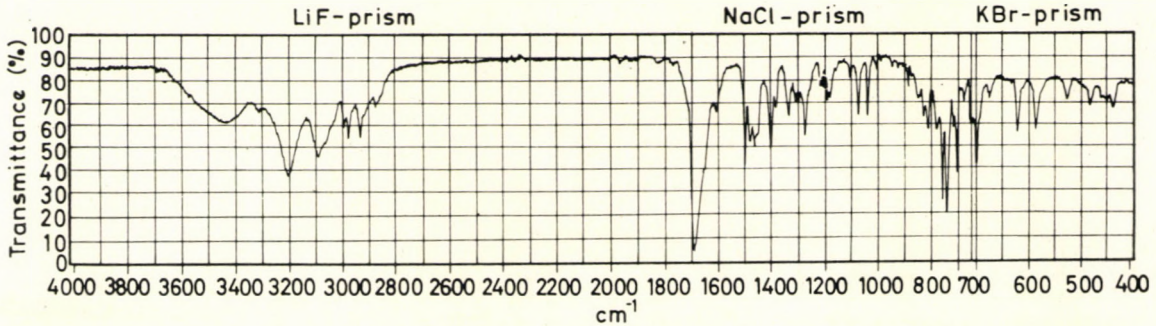

Spectrum 10. IR spectrum of 1-phenyl-1,4-dihydro-4-methyl-3(2*H*)-isoquinolinone (in KBr)

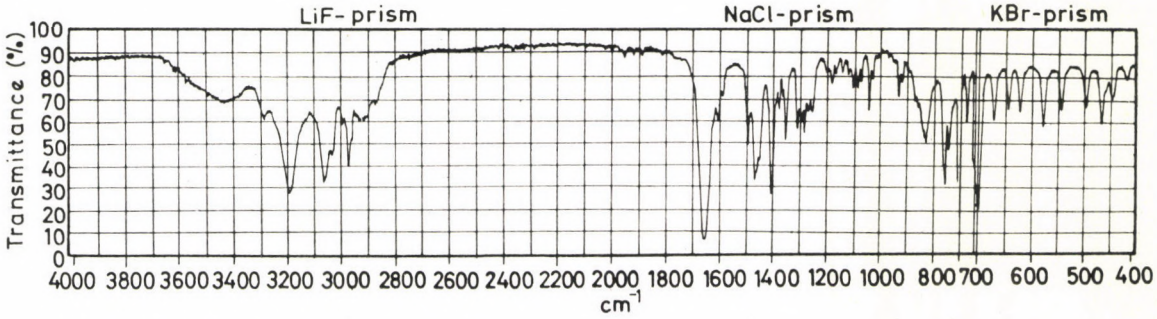

Spectrum 11. IR spectrum of 1-phenyl-1,4-dihydro-4,4-dimethyl-3(2*H*)-isoquinolinone (in KBr)

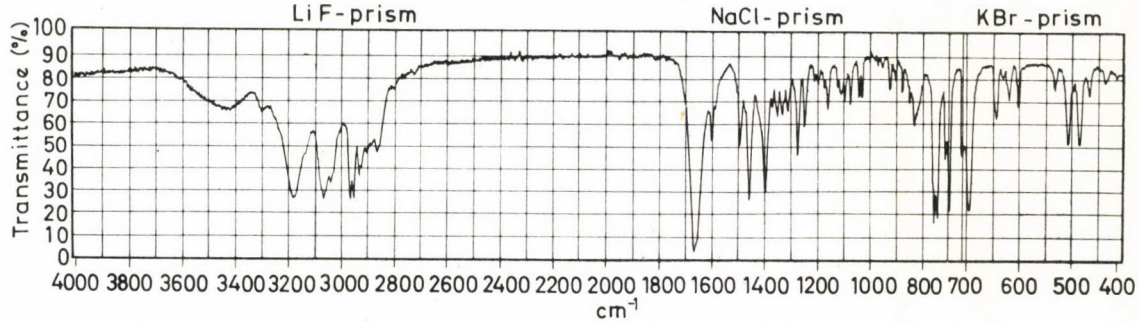

Spectrum 12. IR spectrum of 1-phenyl-1,4-dihydro-4-isopropyl-3(2*H*)-isoquinolinone (in KBr)

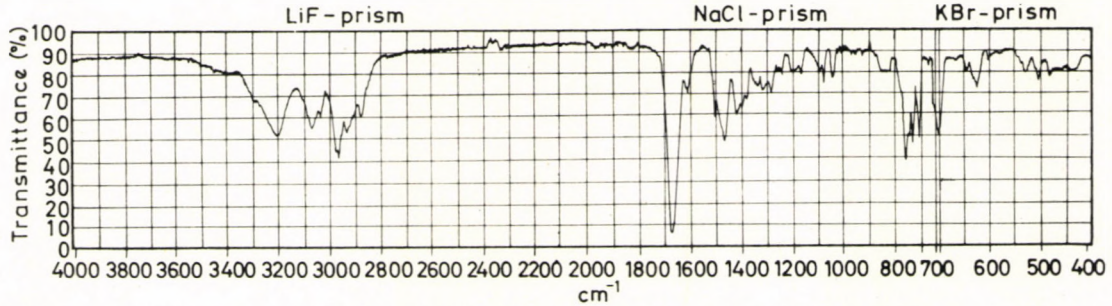

Spectrum 13. IR spectrum of 1-phenyl-1,4-dihydro-4-isopropyl-4-methyl-3(2*H*)-isoquinolinone (in KBr)

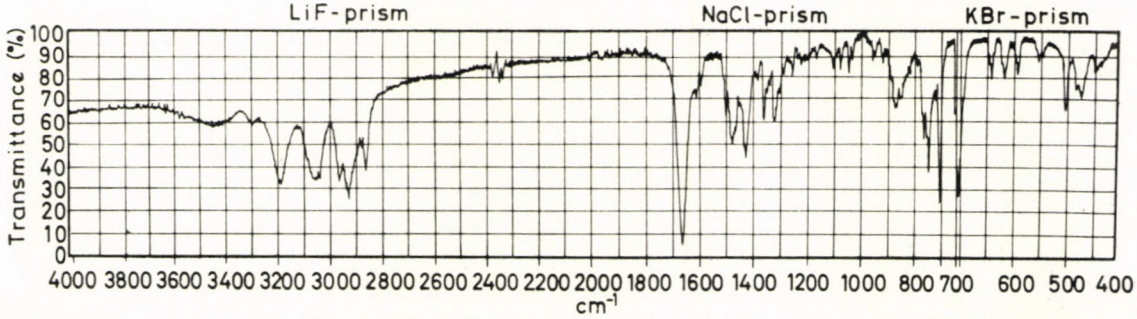

Spectrum 14. IR spectrum of 4-butyl-1-phenyl-1,4-dihydro-3(2*H*)-isoquinolinone (in KBr)

Kinetic measurements

The kinetic measurements were made under standard conditions (100 °C, in polyphosphoric acid of 1 : 1 composition, nitrogen stream). For easier comparison of the results, 1 : 1 mole ratios of the nitrile : aldehyde and amide : aldehyde were used, at nearly identical mole/l concentrations.

Each experimental series was repeated, and in the case of satisfactory agreement the results of the parallel measurements were plotted on the same concentration (c) *vs.* time (t) diagram. The curves constructed in this way were used in the calculation of the kinetic parameters.

In the first series the hydration of nitriles was studied (see Fig. 1 for the parent compound). In the measurement of the rate of hydration, the reac-

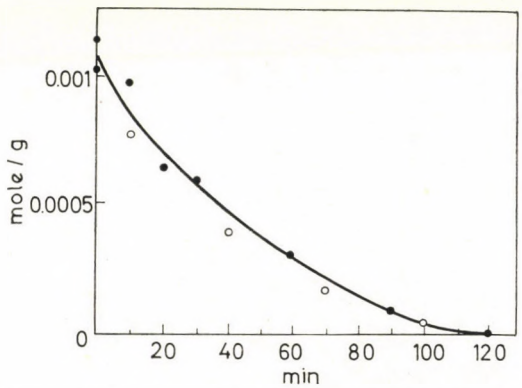

Fig. 1. Reaction of benzyl cyanide in PPA at 100 °C; $C_0 = 1.09 \times 10^{-3}$ mole/g

tion was supposed to follow first-order kinetics. This assumption seems to be confirmed by the fact that graphical representation of the ln c values as a function of time gave a linear relationship for all nitriles (see Fig. 2 for the parent compound). The rate constants calculated from the slope of the lines are summarized in Table I.

According to the measurements, hydration brought about by PPA is a time-reaction. It is known that earlier the hydration of nitriles catalyzed by mineral acids was represented by the following scheme:

$$R{-}C{\equiv}N + HCl \rightleftharpoons R{-}\underset{\displaystyle Cl}{\underset{|}{C}}{=}NH \xrightarrow{H_2O} R{-}\underset{\displaystyle OH}{\underset{|}{C}}{=}NH \longrightarrow OHR{-}\underset{\displaystyle NH_2}{\underset{|}{C}}{=}O$$

In the former scheme the slowest, rate-determining step would be the rupture of the carbon–halogen bond. Recently, Oláh *et al.* [4] have shown that the following salt-like compound

$$R{-}C{\equiv}N + HCl \rightleftharpoons R{-}\overset{\oplus}{C}{\equiv}NHCl^{\ominus}$$

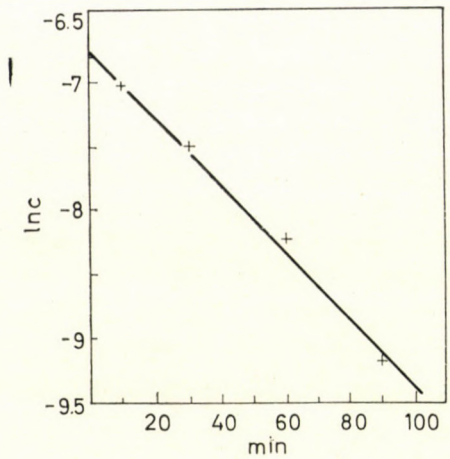

Fig. 2. Reaction of benzyl cyanide in PPA at 100°C

Table I

Hydration of nitriles to amides in 1 : 1 polyphosphoric acid at 100 °C

Nitrile	$k_1 \cdot 10^2$ min	Half-life, min
Benzyl cyanide	2.63	26.0
α-Phenylpropiononitrile	2.00	34.5
α-Phenylisobutyronitrile	1.80	36.0
α-Phenylisovaleronitrile	1.64	42.0
α-Phenyl-α-methylisovaleronitrile	0.25	240.0
α-Phenylhexanenitrile	insoluble	

is formed under the experimental conditions applied by them. This salt-like compound would then yield the amide with water in the rate-determining slow step:

$$R—C\overset{\oplus}{\equiv}NH + H_2O \longrightarrow RCONH_2 + H^{\oplus}$$

Thus, if such a salt-like compound were formed also with PPA, the slow step would be the reaction with water in this case, too, since protonation is an instantaneous reaction. This is inconsistent, however, with the fact that the reaction of the PPA solution with ice-water yields the amide immediately. Still it can be supposed that the nitrile and PPA (which has acid anhydride character) give compound *b* shown in the following scheme:

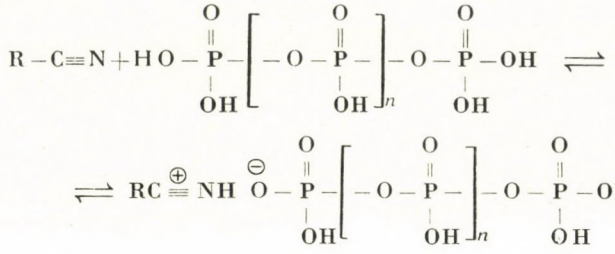

a)

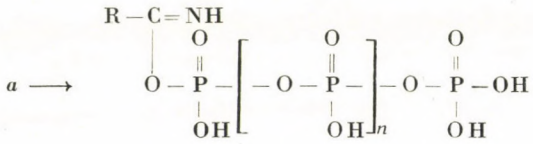

b)

Formally, compound *b* can be regarded as the imino derivative of the mixed anhydride of the corresponding RCOOH carboxylic acid and polyphosphoric acid, which, in accordance with its anhydride character, can rapidly react with water:

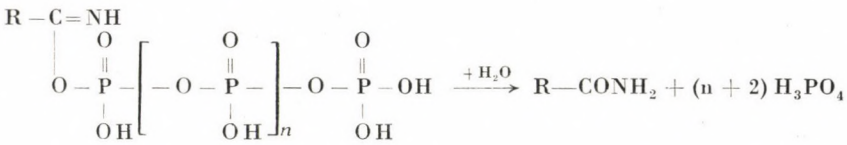

b)

According to the former statements, the rate-determining step can only be the formation of compound *b*, since the latter should rapidly transform into the product when acted upon by water.

The rate constants obtained for the nitriles well agree with the results of the preparative experiments, namely, that the alkyl groups in the α-position may have a considerable influence on the rate of the reaction.

The reaction takes place most readily with non-substituted benzyl cyanide; a somewhat lower rate is observed with the derivatives carrying methyl, dimethyl or isopropyl substituents in the α-position. A significant change appears in the case of α-phenyl-α-methylisovalerionitrile, since its conversion is very low even in 360 min.

On the basis of the rate constants and half-life periods, the following order is obtained for the reactivity of nitriles: benzyl cyanide $>$ α-phenylpropionitrile $\approx$ α-phenylisobutyronitrile $\approx$ α-phenylisovaleronitrile $\geqslant$ α-phenyl-α-methylisovaleronitrile.

On the basis of the mechanism outlined above, the rate-determining step of the reaction is the formation of a carbon-oxygen bond. This means that the P^- anion (HP = polyphosphoric acid) has to approach the carbon atom of the nitrile group of benzyl cyanide. During the establishment of the bond, the state of hybridization and, together with this, the valence orientation of this C atom is altered; the *sp* hybrid transforms into an sp^2 hybride. It can be supposed that the presence of alkyl groups in the α-position, particularly the simultaneous presence of isopropyl and methyl, affect unfavourably both the accessibility of the carbon atom and the change of the valence angle. In other words, the activation energy of the reaction is increased. An examination of the Stuart-Briglieb models of the compounds supports this hypothesis: proximity of the groups having great space requirements makes the actual part of the molecule very crowded, the carbon atom of the nitrile group is greatly hindered, and the cyanoalkyl group practically cannot rotate.

In the next measurement series the condensation reaction between nitriles and benzaldehyde was studied measuring the variation in the concentrations of the starting materials (nitrile, aldehyde) and of the product (lactam). In Figs 3 and 4 the data of the reactions taking place with benzyl cyanide and its derivative carrying an isopropyl substituent in the α-position, are shown; kinetic curves of similar character were obtained with the other nitriles, too.

In PPA the hydration of nitriles should also be taken into account in addition to the reaction of the nitrile with benzaldehyde; thus two simultaneous reactions take place, and therefore the results of measurement cannot be used for the calculation of rate constants. Consequently, the kinetic curves were evaluated only qualitatively and the half-life periods were determined from the curves (Table II).

The kinetic curves and half-life periods clearly show that nitriles always react more rapidly than benzaldehyde does. This can be attributed to the occurrence of two simultaneous reactions.

A comparison of the data in Table II and I gives the same result: the nitrile is consumed faster in the presence of benzaldehyde than in its absence. The order of the half-life periods of the nitriles is essentially identical with that obtained in the case of hydration; α-methyl-α-phenylisovaleronitrile reacts again very slowly. This indicates that the rate-determining step in the hydration and condensation reactions of nitriles depends on the substituent in the α-position in an identical way.

Since, according to the preparative experiments, acid amides also react with benzaldehyde, the possibility of a consecutive reaction between the acid amide (or its precursor) formed from a nitrile and benzaldehyde should also be taken into account. If the rate of this reaction is not higher than that of the main reaction, it has no disturbing effect. Therefore, the reactions of benz-

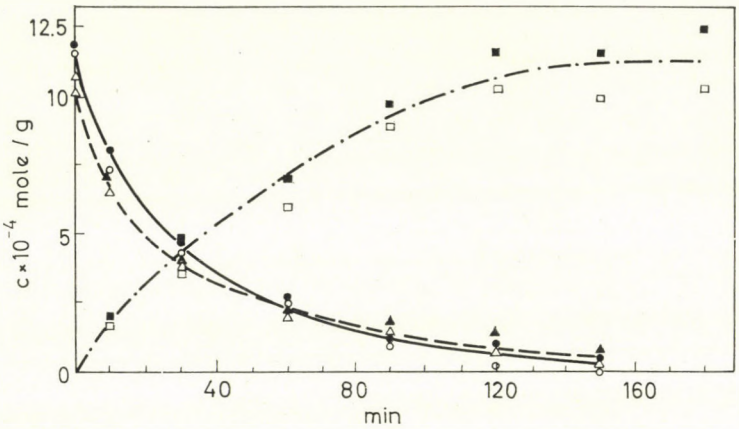

Fig. 3. Reaction of benzyl cyanide and benzaldehyde in PPA at 100°C
○ benzyl cyanide, $C_0 = 1.18 \times 10^{-3}$ mole/g
△ benzaldehye $C_0 = 1.04 \times 10^{-3}$ mole/g
□ 1-phenyl-1,4-dihydro-3(2H)-isoquinolinone

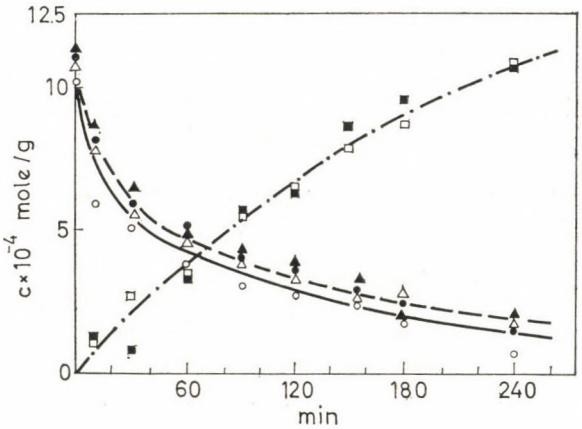

Fig. 4. Reaction of α-phenylisovaleronitrile and benzaldehyde in PPA at 100°C
○ α-phenylisovaleronitrile, $C_0 = 1.07 \times 10^{-3}$ mole/g
△ benzaldehyde, $C_0 = 1.11 \times 10^{-3}$ mole/g
□ 1-phenyl-1,4-dihydro-4-isopropyl-3(2H)-isoquinolinone

aldehyde with the acid amides formed from the nitriles were also investigated. In these experiments the benzaldehyde consumption and the formation of the isoquinoline derivative were measured. Since, as mentioned above, the accuracy of the determination of the concentration of isoquinolinone (IR spectroscopic method) is lower than that of the gas-chromatographic measurements applied for benzaldehyde, the scattering of the points regarding the former is greater, but still significant.

Table II

Reaction of nitriles and benzaldehyde in 1 : 1 polyphosphoric acid at 100 °C

Nitrile	Half-life periods		
	Benzaldehyde	Nitrile $T_{1/2}$, min	Isoquinolinone
Benzyl cyanide	24	19	40
α-Phenylpropionitrile	36	28	42
α-Phenylisobutyronitrile	41	32	48
α-Phenylisovaleronitrile	44	37	83
α-Phenyl-α-methylisovaleronitrile	320	216	—*

* Not measured in lack of a suitable analytical method.

In Figs 5 and 6 the data regarding the condensation of phenylacetamide and α-phenylisovaleramide with benzaldehyde are shown.

The reaction of α-phenylhexanamide could also be studied, since in this case solubility problems did not occur.

Since only one reaction is to be considered in this case, the determination of the kinetic order of the reaction and the rate constants was attempted. On the basis of theoretical considerations, a second-order reaction was assumed; the plot of the reciprocal value of the concentrations as a function of time gave a straight line (for the reaction of α-phenylhexanamide, see Fig. 7).

The rate constants calculated from the correlation $1/c = k\tau + 1/c_0$ are listed in Table III.

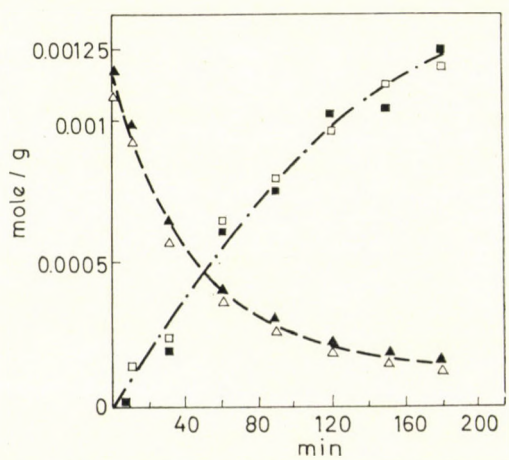

Fig. 5. Reaction of phenylacetamide and benzaldehyde in PPA at 100°C
△ benzaldehyde, $C_0 = 1.13 \times 10^{-3}$ mole/g
□ 1-phenyl-1,4dihydro-3(2*H*)-isoquinolinone

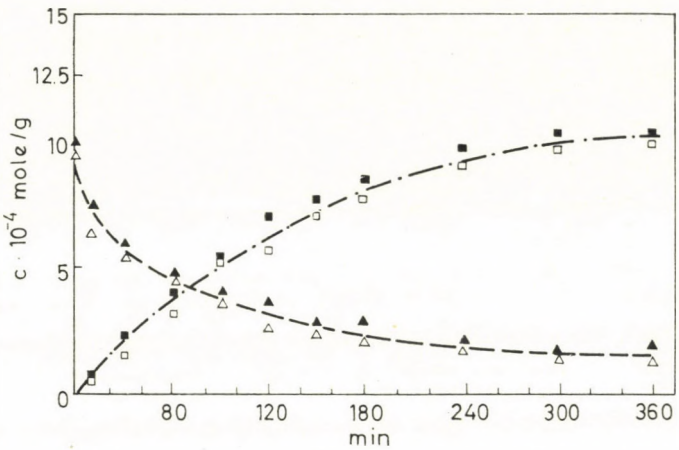

Fig. 6. Reaction of α-phenylhexanamide in PPA at 100°C
△ benzaldehyde, $C_0=0.97\times10^{-3}$ mole/g
□ 4-butyl-1-phenyl-1,4dihydro-3(2*H*)-isoquinolinone

It can be seen from the table that the order of the rate constants is identical with that obtained in the hydration of nitriles and in the reaction of nitriles with benzaldehyde. It is interesting to point out the significant effect exerted by the α-butyl group on the reactivity of the acid amide group. Comparing the data in Tables II and III, it can be seen that the amide reacts somewhat more rapidly than the corresponding nitrile, but this difference in the rates can be neglected in evaluating the reaction of nitriles.

Comparing the rate constants and half-life periods of the three reactions (*i.e.*, hydration of nitriles, and the reactions with benzaldehyde of nitriles and acid amides), it can be supposed that the reactions proceed by analogous mechanisms.

Table III

Reaction of phenylacetamide and its derivatives substituted in the 1-position with benzaldehyde in 1 : 1 PPA at 100 °C

Acid amide	k, g/mole · min	Half-life of the amide, $T_{1/2}$, min
Phenylacetamide	30.4	36
α-Phenylpropionamide	29.6	38
α-Phenylisobutyramide	24.5	43
α-Phenylisovaleramide	22.5	43
α-Phenylhexanamide	18.0	49

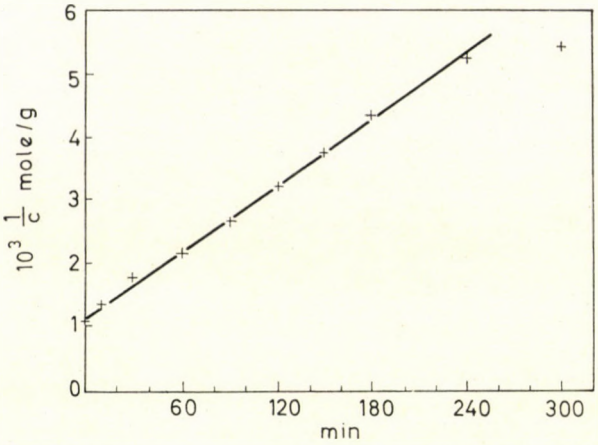

Fig. 7. Reaction of α-phenylhexanamide and benzaldehyde in PPA at 100°C

Experimental

a) Materials

The nitriles were prepared according to the methods of MAKOSZA [2] and TARANKO [3]; elemental analysis, IR spectra and gas chromatography were used for checking their purity.

The amides were synthesized as described by VASILIU [5]; the respective nitrile was hydrated in the presence of H_2O_2 in alcoholic solution at pH 8.

The synthesis of isoquinolinone derivatives will be published in a forthcoming paper [6].

Polyphosphoric acid was also prepared by us by mixing phosphorus pentoxide and 85% phosphoric acid in 1 : 1 weight ratio and heating the mixture to 100 °C for 4 hr, with stirring; moisture should be carefully excluded.

b) Kinetic measurements

The reactions were carried out in a cylindrical glass apparatus (Fig. 8), immersed into a thermostated oil bath, equipped with a magnetic stirrer. Polyphosphoric acid was weighed into this, heated to 100 °C and maintained at this temperature for 20 min while the passing of a stream of dry nitrogen was started through it. Then calculated amounts of the reaction components and a few crystals of hydroquinone were added. Samples of nearly identical weight, withdrawn with a calibrated pipette, were cooled rapidly, weighed and analyzed according to the procedure described.

Gas-liquid chromatography was performed in an Aerograph A-600-C chromatograph, equipped with a hydrogen flame ionization detector. A coiled stainless steel column of 1/8″ o.d. and 5 ft long was used. The column was packed with acid-washed Chromasorb W, 80—100 mesh, coated with 3% SE—30 (Applied-Science). The chromatography was performed isothermally at 150 °C. The carrier gas was nitrogen at a flow rate of 25 ml/min.

The calibration curves used in the quantitative measurements were obtained with solutions prepared from known amounts of nitriles and aldehydes. Owing to the good separation and sharpness of the gas chromatographic peaks, the peak heights were used for calibration.

The lactam content of the samples was determined on the basis of the IR spectra, by means of a calibration curve. For its construction a sample series was prepared consisting of 750 mg of KBr and 1—5 mg of pure isoquinolinone derivative each. After homogenization, 650.0 mg of the individual samples was compressed for precisely 1 min under a pressure of 200 atm, after evacuation. In this way pellets of identical and constant cross-section were obtained. The spectra were recorded in the preselected region containing the bands chosen for measurement, then the log I_0/I values were calculated according to the base-line method. Plotting these values as a function of the lactam concentration of the sample, a linear correlation was obtained up to about 3.5—4 mg/pellet concentration. The IR spectra were recorded with a Zeiss UR—10 spectrophotometer, with a slit width of 4.

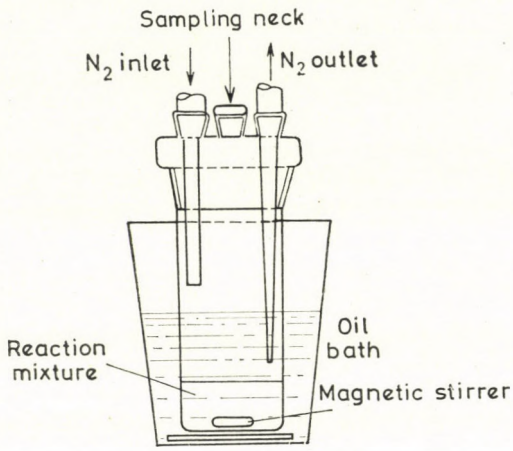

Fig. 8. Apparatus designed for the kinetic measurements

REFERENCES

1. Csűrös, Z., Deák, Gy., Hoffman, I., Török-Kalmár, A.: Acta Chim. Acad. Sci. Hung. **60,** 177 (1964)
2. Makosza, M., Serafinowa, B.: Rocz. Chem. **39,** 1401 (1965); C. A. **64,** 17474g
3. Tarankó, L. B., Perry, R. H.: J. Org. Chem. **34,** 226 (1969)
4. Oláh, G. A., Kiovsky, E.: J. Am. Chem. Soc. **90,** 4666 (1968)
5. Vasiliu, Gh.: Rev. Chem. **18,** 259 (1967); C. A. **67,** 108408m
6. Deák, Gy., Froyen, P., Gáll-Istók, K., Møller, J.: (in press)

Gyula Deák
Klára Gáll-Istók
Zuzsa Kálmán
Judit Haskó-Breuer

1083 Budapest, Szigony u. 43.

Acta Chimica Academiae Scientiarum Hungaricae, Tomus 76 (3), pp. 319—333 (1973)

MULTICOMPONENT COPOLYMERIZATION

ON SOME SPECIAL CASES OF TERPOLYMERIZATION EQUATION

Cr. SIMIONESCU, N. ASANDEI and I. NEGULESCU
(P. Poni Institute of Macromolecular Chemistry, Jassy, Romania)

Received April 15, 1971

The validity of the ALFREY—GOLDFINGER equations for the calculation of the composition of terpolymers from known reactivity ratios was confirmed by numerous authors in the last years. For the special cases of one or more components being not homopolymerizable but copolymerizable with the other partners, equations have been proposed in which one factor, R, must be determined experimentally if the reactivity ratios are known from binary copolymerization experiments.

In this paper the system acrylonitrile–acrilic acid-4-vinylcyclohexene and acrylonitrile–maleic anhydride-4-vinylcyclohexene are examined. Important changes are found in the factor R owing to the influence of the penultimate unit, solvent effects, etc., therefore, the proposed equations for the special cases give different results depending on the reaction conditions. An average value of the factor R is proposed, so that the solutions of the terpolymerization equations for special cases should approximate the real composition as closely as possible.

In addition, the terpolymer compositions calculated by the simplified HAM's equations are compared with the values calculated from the ALFREY—GOLDFINGER equations and the experimental values for systems involving one or more monomers with very low self-propagation rates.

Introduction

The first theoretical and experimental investigations on multicomponent copolymers were carried out in the late 1940's, in the 1950's few papers on this subject were published but since 1960 the literature devoted to them has been increasing rapidly.

The practical importance of multicomponent copolymers, especially terpolymers, is growing continuously. The addition, in a small amount, of a third component to a binary copolymer may result in certain properties (solubility, vulcanizability, adhesivity, dyeability, etc.), different from those of the copolymers consisting of only two monomers, which make it suitable for particular applications.

Relationships between the composition of a terpolymer and that of the corresponding monomer have been proposed for the first time by ALFREY and GOLDFINGER [1]. The theory of copolymerization of vinyl monomers developed

* Presented in part at the IUPAC International Symposium on Macromolecular Chemistry, Budapest, 1969

by these authors was subsequently extended to *n*-component systems by WALLING and BRIGGS [2] and by SKEIST [3] to allow the calculation of the composition *vs.* conversion curves.

Experimental verifications for low conversion three-component systems were also reported.

According to ALFREY and GOLDFINGER, the well known terpolymerization equations are [1]:

$$d[M_1] : d[M_2] : d[M_3] = m_1 : m_2 : m_3 =$$

$$= [M_1]\left\{\frac{[M_1]}{r_{31}r_{21}} + \frac{[M_2]}{r_{21}r_{23}} + \frac{[M_3]}{r_{31}r_{23}}\right\}\left\{[M_1] + \frac{[M_2]}{r_{12}} + \frac{[M_3]}{r_{13}}\right\}:$$

$$: [M_2]\left\{\frac{[M_1]}{r_{12}r_{31}} + \frac{[M_2]}{r_{12}r_{32}} + \frac{[M_3]}{r_{32}r_{13}}\right\}\left\{[M_2] + \frac{[M_1]}{r_{21}} + \frac{[M_3]}{r_{23}}\right\}:$$

$$: [M_3]\left\{\frac{[M_1]}{r_{13}r_{21}} + \frac{[M_2]}{r_{23}r_{12}} + \frac{[M_3]}{r_{13}r_{23}}\right\}\left\{[M_3] + \frac{[M_1]}{r_{31}} + \frac{[M_2]}{r_{32}}\right\},$$

where $r_{ij} = K_{ii}/K_{ij} \neq 0$, the amounts in square brackets represent concentrations in the monomer mixture, *m*'s are the monomer concentrations in the terpolymer and K_{ij} are the rate constants of nine elementary reactions constructed from the combinations of three polymer radicals and three monomers.

ALFREY and GOLDFINGER [4] have shown that these equations cannot be employed if the system contains one or more components that do not undergo homopolymerization, *i.e.* reaction with a growing chain ending in a monomer unit of their own type, *e.g.* diethyl maleate, crotonic acid, etc.; if monomer M_i is of such type, then $K_{ii} = 0$ and all the $r_{ij} = 0$. For the case of three monomers, three cases can be found:

1) Monomer M_3 does not homopolymerize ($K_{33} = 0$) but can copolymerize with M_1 and M_2 ($K_{31} \neq 0$, $K_{32} \neq 0$).

2) Monomer M_2 and M_3 cannot homopolymerize ($K_{22} = K_{33} = 0$, $r_{21} = r_{23} = r_{31} = r_{32} = 0$), but can copolymerize with one another and with M_1.

3) Monomers M_2 and M_3 can neither homopolymerize, nor copolymerize with one another ($K_{22} = K_{33} = K_{23} = K_{32} = 0$).

Our attention was focused on the first two cases, therefore, we decided to choose the system acrylonitrile(1)–acrylic acid(2)-4-vinylcyclohexene(3) for the first case and the system acrylonitrile(1)–maleic anhydride(2)-4-vinylcyclohexene(3) for the second.

Experimental

The solvent and monomers were distilled under reduced pressure in order to free them from inhibitor and were stored at −10 °C. Acrylic acid could be stored as a solid for several days in this way, but dioxan was always freshly distilled before use. Commercial azobis(isobutyronitrile) used in these experiments was purified by recrystallization twice from ether.

Mixtures of the monomers of different composition and the solvent (the mole ratio of solvent to monomer mixture was 1 :1) were introduced into glass ampoules and 1% (based on the monomer mixture) of azobis(isobutyronitrile) was added.

The ampoules were sealed under a slight nitrogen pressure after evacuating and filling with nitrogen for several times. They were then kept in a water bath thermostated at 60 ± ± 0.1 °C and turned over for the time necessary to obtain a conversion of a few per cent; the time required for this increased with increasing 4-vinylcyclohexene content in the monomer mixture. The contents of the ampoules were added dropwise to methanol containing hydroquinone under slight stirring. The copolymers were collected by filtration and after prolonged washing with methanol were dried under high vacuum for 24 hrs. The conversion was calculated from the weight of polymer obtained from a known amount of reaction mixture. The oxygen, nitrogen and carbon content of the copolymer samples were then determined by elemental analysis.

Results and Discussion

A. Monomer M_3 does not homopolymerize, but can copolymerize with M_1 and M_2.

In possession of experimental data the question arises of how they can best be used to estimate the parameters of interest.

Table I

Experimental data for the system acrylonitrile(1)–acrylic acid(2)

No.	Solvent	Feed composition (mole fr.) $[M_1]$	Feed composition (mole fr.) $[M_2]$	Copolymer yield (%)	N (%)	Copolymer composition (mole fr.) m_1	Copolymer composition (mole fr.) m_2
1	Benzene	0.670	0.330	2.95	13.50	0.587	0.413
2		0.744	0.256	5.33	15.33	0.653	0.347
3		0.816	0.184	1.48	17.60	0.731	0.269
4		0.855	0.145	0.50	18.78	0.770	0.230
5	Bulk	0.754	0.246	1.28	14.43	0.621	0.379
6		0.820	0.180	2.35	16.71	0.701	0.299
7		0.862	0.138	1.71	18.26	0.753	0.247
8		0.912	0.088	3.77	20.55	0.827	0.173

The runs with the lowest conversion in each of the respective series were considered (Tables I—III). FINEMAN—ROSS [5] plots were used to determine the reactivity ratios in the usual manner, *e.g.*, in Figs 1—3, F/f (f—1) is plotted against F^2/f, where F is the initial mole ratio of the two monomers in the feed and f is the same ratio in the copolymer.

The dependence of the results on the polarity of the solvents is not surprising because for some systems containing one or two polar monomers (acrylic acid–acrylonitrile, acrylic acid–methyl methacrylate, acrylonitrile–styrene), different reactivity ratios for different solvents were reported [6—8].

In the cases where all the monomers can homopolymerize, binary copolymerization experiments are sufficient for determining the necessary ratios

Table II

Experimental data for the system 4-vinylcyclohexene(1)–acrylic acid(2)

No.	Solvent	Feed composition (mole fr.)		Copolymer yield (%)	C + H (%)	Copolymer composition (mole fr.)	
		$[M_1]$	$[M_2]$			m_1	m_2
1	Benzene	0.664	0.336	3.25	62.37	0.109	0.891
2		0.769	0.231	2.18	64.80	0.148	0.852
3		0.843	0.157	0.93	65.52	0.162	0.838
4		0.854	0.146	1.20	65.68	0.164	0.836
5	Dioxan	0.614	0.386	1.07	62.62	0.111	0.889
6		0.741	0.259	5.35	65.00	0.152	0.848
7		0.865	0.135	4.50	66.58	0.180	0.820
8		0.882	0.118	3.80	66.92	0.185	0.815
9	Bulk	0.651	0.349	0.82	60.65	0.080	0.920
10		0.776	0.224	1.06	62.95	0.119	0.881
11		0.872	0.128	1.15	65.38	0.158	0.842
12		0.908	0.102	0.42	66.08	0.167	0.833

Table III

Experimental data for the system 4-vinylcyclohexene(1)–acrylonitrile(2)

No.	Solvent	Feed composition (mole fr.)		Copolymer yield (%)	N (%)	Copolymer composition (mole fr.)	
		$[M_1]$	$[M_2]$			m_1	m_2
1	Benzene	0.678	0.322	4.00	18.08	0.184	0.816
2		0.756	0.244	2.38	16.20	0.236	0.764
3		0.853	0.147	3.82	14.76	0.292	0.708
4		0.911	0.089	2.15	13.98	0.313	0.687
5	Dioxan	0.659	0.341	0.96	20.19	0.130	0.870
6		0.743	0.257	5.30	18.60	0.178	0.822
7		0.844	0.116	1.65	13.83	0.321	0.679
8		0.898	0.102	3.10	13.08	0.334	0.666
9	Bulk	0.672	0.328	3.66	20.40	0.126	0.873
10		0.744	0.256	2.16	18.91	0.160	0.840
11		0.843	0.157	5.56	16.70	0.231	0.769
12		0.893	0.107	2.97	14.93	0.288	0.712

and subsequently the terpolymer composition, no terpolymerization experiment being required for this purpose.

It was already reported [9—10] that 4-vinylcyclohexene reacts with free alkyl radicals; on reacting with azobis(isobutyronitrile), 4-vinylcyclo-

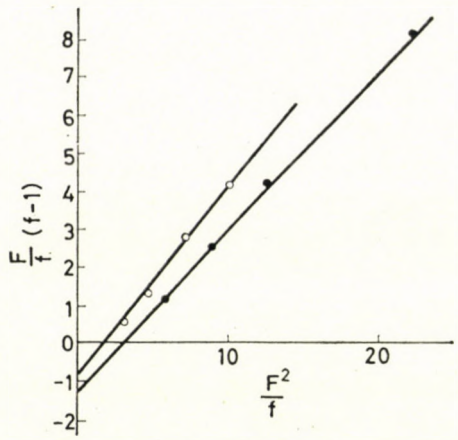

Fig. 1. FINEMAN—ROSS plots and reactivity ratios for the copolymerization of acrylonitrile(1) with acrylic acid(2);
(◯) copolymerization in benzene at 60 °C; $r_1 = 0.48$, $r_2 = 0.75$
(◯) copolymerization in bulk at 60 °C; $r_1 = 0.43$, $r_2 = 1.25$
copolymerization in dioxan at 60 °C; $r_1 = 1.06$, $r_2 = 1.25$ [6]

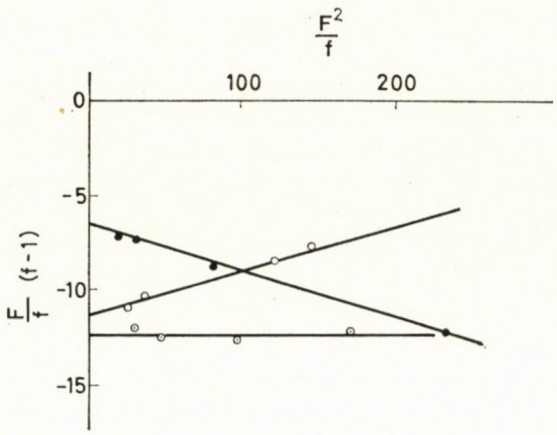

Fig. 2. FINEMAN—ROSS plots and reactivity ratios for the copolymerization of 4-vinylcyclohexene(1) with acrylonitrile(2):
(◯) copolymerization in benzene at 60 °C; $r_1 = -0.025 \pm 0.025$, $r_2 = 6.5$
(◯) copolymerization in dioxan at 60 °C; $r_1 = 0.020 \pm 0.020$, $r_2 = 11.4$
(◯) bulk copolymerization at 60 °C; $r_1 = 0.000$, $r_2 = 12.4$

hexene forms 1-cyanoisopropyl-4-vinylcyclohexene as the main product [11] and for this reason this monomer cannot homopolymerize by a radical mechanism with azobis(isobutyronitrile) as initiator. For our first system, acrylonitrile(1)–acrylic acid(2)–4-vinylcyclohexene(3), instead of classical equations (1), the following equations are valid [4]:

$$d[M_1] : d[M_2] : d[M_3] = m_1 : m_2 : m_3 =$$

$$= [M_1]\left\{R\frac{[M_1]}{r_{21}} + \frac{[M_2]}{r_{21}} + \frac{[M_3]}{r_{23}}\right\}\left\{[M_1] + \frac{[M_2]}{r_{12}} + \frac{[M_3]}{r_{13}}\right\}:$$

$$:[M_2]\left\{R\frac{[M_1]}{r_{12}} + \frac{[M_2]}{r_{12}} + \frac{[M_3]}{r_{13}}\right\}\left\{[M_2] + \frac{[M_1]}{r_{21}} + \frac{[M_3]}{r_{23}}\right\}: \qquad (2)$$

$$:[M_3]\left\{\frac{[M_1]}{r_{13}r_{21}} + \frac{[M_2]}{r_{12}r_{23}} + \frac{[M_3]}{r_{13}r_{23}}\right\}\{R[M_1]+[M_2]\},$$

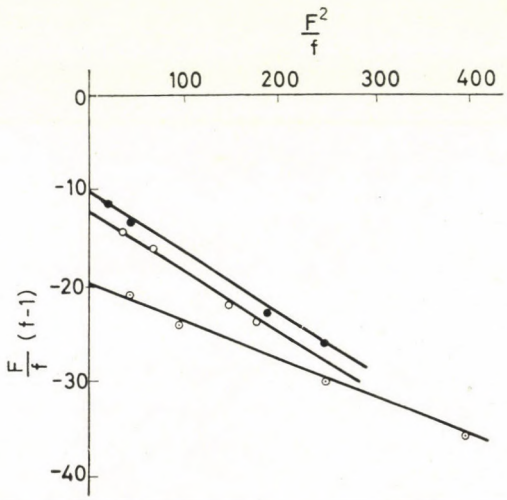

Fig. 3. FINEMAN—ROSS plots and reactivity ratios for the copolymerization of 4-vinylcyclohexene(1) with acrylic acid(2);
(○) copolymerization in benzene at 60 °C; $r_1 = -0.061 \pm 0.061$, $r_2 = 12.0$
(○) copolymerization in dioxan at 60 °C; $r_1 = -0.065 \pm 0.065$, $r_2 = 10.0$
(○) bulk copolymerization at 60 °C; $r_1 = -0.045 \pm 0.045$, $r_2 = 19.3$

where $R = K_{31}/K_{32}$; r_{12}, r_{21}, r_{13} and r_{23} are known from binary copolymerization experiments. A single terpolymerization experiment gives R and its value must be constant (in a given system).

However, the R value may change similarly to the reactivity ratios with temperature, solvent, etc., and there may be an effect of nonterminal units on the reactivity of polymer radicals.

As shown by BARB [12], if the penultimate unit exerts a detectable effect, a ternary copolymer would have a composition somewhat different from that calculated on the basis of copolymerization data for pairs of monomers (deviation up to 5 mole per cent); it may be noted that electrostatic effects due to nonterminal monomer units should be dependent on the dielectric properties of the medium. For our system, in the copolymerization of acrylo-

nitrile(1) with 4-vinylcyclohexene(3), penultimate effects occur with the reactivity ratios of $r_{13} = 5.47$ and $r'_{13} = 17.21$ for copolymerization in benzene and $r_{13} = 9.95$; $r'_{13} = 20.00$ for bulk copolymerization, determined by BARB's method [12] (see Figs 4, 5).

With the reactivity ratios determined under various conditions (feed composition, solvent) the R values shown in Table IV. are obtained. In Table V, terpolymer compositions calculated with different R factors are compared with the experimental results; owing to the scatter of the values obtained, an average R factor is proposed, $R_m = -0.69$, so that the solution of terpolymerization equations (2) for this special case should approximate the real composition as closely as possible.

If in the simplified equations of HAM [13], Eqs (4) and (3), M_3 is the component with vanishing self propagation rate, *i.e.*, $K_{33} = 0$, $r_{31} = r_{32} = 0$, then Eq. (3) remains unaltered because the ratio of $m_1 : m_2$ does not depend

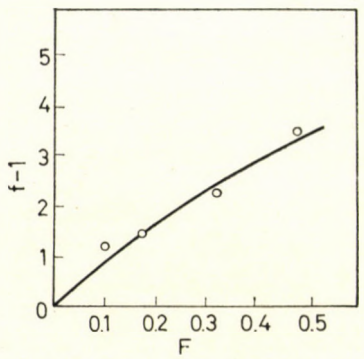

Fig. 4. Copolymerization of acrylonitrile and 4-vinylcyclohexene in benzene at 60 °C. Plot according to BARB's equation

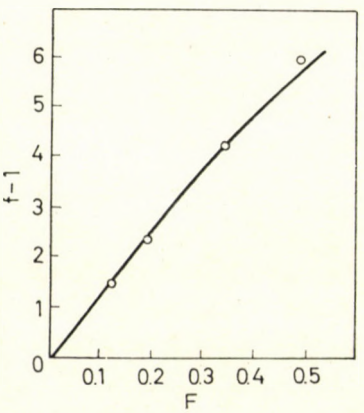

Fig. 5. Bulk copolymerization of acrylonitrile and 4-vinylcyclohexene at 60 °C. Plot according to BARB's equation

Table IV

Values of R factor for different solvents calculated by means of ALFREY–GOLDFINGER's *Eqs (2)*

Solvent	Reactivity ratios	Feed composition (mole %)	Experimental copolymer composition (mole %)	Factor R
Benzene	$r_{12} = 0.48$ $r_{21} = 0.75$ $r_{13} = 6.50$ $r_{23} = 12.0$	$[M_1] = 24.84$ $[M_2] = 24.84$ $[M_3] = 50.32$	$m_1 = 41.47$ $m_2 = 55.92$ $m_3 = 2.61$	$R_1 = -0.88$
Benzene	$r_{12} = 0.48$ $r_{21} = 0.75$ $r_{13} = 6.50$ $r_{23} = 12.0$	$[M_1] = 40.14$ $[M_2] = 19.51$ $[M_3] = 40.35$	$m_1 = 54.10$ $m_2 = 38.03$ $m_3 = 7.87$	$R_2 = -0.53$
Dioxan	$r_{12} = 1.06$ $r_{21} = 0.92$ $r_{13} = 11.4$ $r_{23} = 10.3$	$[M_1] = 41.20$ $[M_2] = 19.62$ $[M_3] = 39.18$	$m_1 = 54.94$ $m_2 = 34.98$ $m_3 = 10.08$	$R_3 = -0.59$
Bulk	$r_{12} = 0.43$ $r_{21} = 1.25$ $r_{13} = 12.4$ $r_{23} = 19.3$	$[M_1] = 24.75$ $[M_2] = 24.82$ $[M_3] = 50.43$	$m_1 = 37.38$ $m_2 = 59.25$ $m_3 = 3.39$	$R_4 = -0.77$

on the addition to M_3. However, as K_{33} approaches zero, Eq. (4) may be modified by multiplying the numerator and denominator by r_{32}, becoming in the limit [14]:

$$\frac{m_1}{m_2} = \frac{[M_1]}{r_{21}}\left(\frac{[M_2]}{r_{12}} + [M_1] + \frac{[M_3]}{r_{13}}\right) \Big/ \frac{[M_2]}{r_{12}}\left(\frac{[M_1]}{r_{21}} + [M_2] + \frac{[M_2]}{r_{23}}\right) \tag{3}$$

$$\frac{m_1}{m_3} = \frac{[M_1]}{r_{31}}\left(\frac{[M_3]}{r_{13}} + [M_1] + \frac{[M_2]}{r_{12}}\right) \Big/ \frac{[M_3]}{r_{13}}\left(\frac{[M_1]}{r_{31}} + [M_3] + \frac{[M_2]}{r_{32}}\right). \tag{4}$$

Hence:

$$\frac{m_1}{m_3} = [M_1]R\left(\frac{[M_3]}{r_{13}} + [M_1] + \frac{[M_2]}{r_{12}}\right) \Big/ \frac{[M_3]}{r_{13}}\left([M_1]R + [M_2]\right) \tag{5}$$

where:

$R = K_{31}/K_{32}$; m_i, $[M_i]$, r_{ij} and K_{ij} have the same meaning as in the usual terpolymerization equations (1).

On comparing the ALFREY—GOLDFINGER equations (2) with Eqs (3, 5) obtained by HAM for the same case, it is evident that in the simplified equations the ratio m_1/m_2 is independent of the factor R; this independence has a nega-

Table V

Comparison between the experimental values of the composition of terpolymers and those calculated by means of ALFREY–GOLDFINGER's *Eqs (2) with different R values and* $R_m = -0.69$

Solvent	Feed composition (mole %)	Copolymer composition (mole %)					
		Experimental	Calculated with R_1	Calculated with R_2	Calculated with R_3	Calculated with R_4	Calculated with R_m
Benzene	$[M_1] = 24.84$	$m_1 = 41.47$	$m_1 = 41.47$	$m_1 = 42.73$	$m_1 = 42.65$	$m_1 = 42.75$	$m_1 = 42.69$
	$[M_2] = 24.84$	$m_2 = 55.92$	$m_2 = 55.92$	$m_2 = 51.36$	$m_2 = 52.35$	$m_2 = 51.13$	$m_2 = 51.83$
	$[M_3] = 50.32$	$m_3 = 2.61$	$m_3 = 2.61$	$m_3 = 5.91$	$m_3 = 5.00$	$m_3 = 6.12$	$m_3 = 5.48$
Dioxan	$[M_1] = 41.20$	$m_1 = 54.94$	$m_1 = 64.55$	$m_1 = 65.99$	$m_1 = 54.94$	$m_1 = 61.15$	$m_1 = 63.55$
	$[M_2] = 19.62$	$m_2 = 34.98$	$m_2 = 28.56$	$m_2 = 28.94$	$m_2 = 34.98$	$m_2 = 30.42$	$m_2 = 27.63$
	$[M_3] = 39.18$	$m_3 = 10.08$	$m_3 = 6.89$	$m_3 = 5.07$	$m_3 = 10.08$	$m_3 = 8.42$	$m_3 = 8.82$
Bulk	$[M_1] = 24.75$	$m_1 = 37.38$	$m_1 = 42.65$	$m_1 = 39.69$	$m_1 = 39.33$	$m_1 = 37.38$	$m_1 = 40.43$
	$[M_2] = 24.82$	$m_2 = 59.23$	$m_2 = 54.43$	$m_2 = 56.05$	$m_2 = 56.24$	$m_2 = 59.23$	$m_2 = 55.56$
	$[M_3] = 50.43$	$m_3 = 3.39$	$m_3 = 2.92$	$m_3 = 4.26$	$m_3 = 4.43$	$m_3 = 3.39$	$m_3 = 4.01$

tive effect on the calculation of terpolymer composition because the data obtained experimentally and used for the calculation of the factor R with Eq. (5) and calculated again with Eqs (3, 5), are not the same; this discrepancy does not appear in the case of the ALFREY—GOLDFINGER equations(2).

The values of the R factor calculated by means of the simplified Eq. (5) are presented in Table VI.

Table VI

Values of the R factor calculated by means of simplified equation (5)

Solvent	Feed composition (mole %)	Experimental copolymer composition (mole %)	Factor R
Benzene	$M_1 = 24.84$ $M_2 = 24.84$ $M_3 = 50.32$	$m_1 = 41.47$ $m_2 = 55.92$ $m_3 = 2.61$	$R_1 = -3.18$
Benzene	$M_1 = 40.11$ $M_2 = 19.54$ $M_3 = 40.35$	$m_1 = 54.10$ $m_2 = 38.03$ $m_3 = 7.87$	$R_2 = 0.47$
Dioxan	$M_1 = 41.20$ $M_2 = 19.62$ $M_3 = 39.18$	$m_1 = 54.94$ $m_2 = 34.98$ $m_3 = 10.08$	$R_3 = 0.20$
Bulk	$M_1 = 24.75$ $M_2 = 24.82$ $M_3 = 50.43$	$m_1 = 37.38$ $m_2 = 59.23$ $m_3 = 3.39$	$R_4 = 1.08$

In Table VII, terpolymer compositions calculated from Eqs (3, 5) are compared with the experimental results and with the values obtained by means of the ALFREY—GOLDFINGER equations (2).

The underlined data show the copolymer composition which would correspond to the experimental values after recalculation with the values of factor R, implicitly calculated from the respective experimental data. It is difficult in these cases to propose an average R factor analogous with R_m of the ALFREY—GOLDFINGER Eqs (2), owing to the scatter of the values obtained.

Since in the copolymerization of the binary system acrylonitrile-4-vinylcyclohexene penultimate effects occur, Eqs (3, 5), can be rearranged, with HAM's indications [14], to yield:

$$\frac{m_1}{m_2} = \frac{\dfrac{[M_1]}{r_{21}}\left(\dfrac{[M_2]}{r_{12}} + \dfrac{\dfrac{[M_3]}{r'_{13}(r_{13}\cdot[M_1]/[M_3]+1)}}{r'_{13}\cdot[M_1]/[M_3]+1} + [M_1]\right)}{\dfrac{[M_2]}{r_{12}}\left(\dfrac{[M_1]}{r_{12}} + [M_2] + \dfrac{[M_3]}{r_{23}}\right)} \tag{6}$$

Table VII

Comparison between the experimental values of the composition of terpolymers obtained in different solvents and those calculated by means of the ALFREY–GOLDFINGER*'s Eqs (2) or simplified Eqs (3, 5) with different R values*

Solvent	Feed composition (mole %)	Copolymer composition (mole %)					
		Experimental	Calculated from Eqs (2) with R_m	with R_1	Calculated with R_2	from Eqs (3, 5) wtih R_3	with R_4
Benzene	$[M_1] = 24.84$	$m_1 = 41.47$	$m_1 = 42.69$	$m_1 = 39.06$	$m_1 = 35.93$	$m_1 = 32.81$	$m_1 = 37.40$
	$[M_2] = 24.84$	$m_2 = 55.92$	$m_2 = 51.83$	$m_2 = 58.47$	$m_2 = 53.74$	$m_2 = 49.17$	$m_2 = 55.99$
	$[M_3] = 50.32$	$m_3 = 2.61$	$m_3 = 5.48$	$m_3 = 2.47$	$m_3 = 10.33$	$m_3 = 18.02$	$m_3 = 6.61$
Benzene	$[M_1] = 40.11$	$m_1 = 54.10$	$m_1 = 56.63$	$m_1 = 57.88$	$m_1 = 55.66$	$m_1 = 52.31$	$m_1 = 56.47$
	$[M_2] = 19.51$	$m_2 = 38.03$	$m_2 = 33.98$	$m_2 = 38.61$	$m_2 = 36.82$	$m_2 = 34.90$	$m_2 = 37.67$
	$[M_3] = 40.35$	$m_3 = 7.87$	$m_3 = 9.39$	$m_3 = 3.51$	$m_3 = 8.02$	$m_3 = 12.79$	$m_3 = 5.86$
Dioxan	$[M_1] = 41.20$	$m_1 = 54.94$	$m_1 = 63.55$	$m_1 = 68.93$	$m_1 = 66.05$	$m_1 = 62.98$	$m_1 = 67.45$
	$[M_2] = 19.62$	$m_2 = 34.98$	$m_2 = 27.33$	$m_2 = 27.87$	$m_2 = 26.71$	$m_2 = 25.47$	$m_2 = 27.27$
	$[M_3] = 39.18$	$m_3 = 10.08$	$m_3 = 8.82$	$m_3 = 3.20$	$m_3 = 7.24$	$m_3 = 11.55$	$m_3 = 5.28$
Bulk	$[M_1] = 24.75$	$m_1 = 37.38$	$m_1 = 40.43$	$m_1 = 25.65$	$m_1 = 24.96$	$m_1 = 23.57$	$m_1 = 25.28$
	$[M_2] = 24.82$	$m_2 = 59.23$	$m_2 = 55.56$	$m_2 = 73.49$	$m_2 = 71.73$	$m_2 = 67.55$	$m_2 = 72.42$
	$[M_3] = 50.43$	$m_3 = 3.39$	$m_3 = 4.01$	$m_3 = 0.86$	$m_3 = 3.67$	$m_3 = 8.88$	$m_3 = 2.30$

$$\frac{m_1}{m_3} = \frac{[M_1]R\left(\dfrac{[M_3]}{\dfrac{r'_{13}(r_{13}\cdot[M_1]/[M_3]+1)}{r'_{13}\cdot[M_1]/[M_3]+1}} + [M_1] + \dfrac{[M_2]}{r_{12}}\right)}{\dfrac{[M_3]}{\dfrac{r'_{13}(r_{13}\cdot[M_1]/[M_3]+1)}{r'_{13}\cdot[M_1]/[M_3]+1}}([M_1]\,R+[M_2])} \quad (7)$$

With these equations other values of the factor R were obtained; thus, $R_{\mathrm{I}} = = 0.0175$ (corresponding to R_1 from Eqs (3, 5)) and $R_{\mathrm{III}} = 0.0059$ (corresponding to R_3 from the same equations). The experimental and calculated results are compared in Table VIII.

Table VIII

Comparison of terpolymer compositions calculated by means of Eqs (6, 7) with the experimental values

Solvent	Feed composition (mole %)	Copolymer composition (mole %)		
		Experimental	Calculated from Eqs (6, 7)	
			with R_{I}	with R_{II}
Benzene	$[M_1] = 24.84$	$m_1 = 41.47$	$m_1 = 36.91$	$m_1 = 36.76$
	$[M_2] = 24.84$	$m_2 = 55.92$	$m_2 = 60.76$	$m_2 = 60.57$
	$[M_3] = 50.32$	$m_3 = 2.61$	$m_3 = 2.33$	$m_3 = 2.66$
Bulk	$[M_1] = 24.75$	$m_1 = 37.38$	$m_1 = 24.80$	$m_1 = 24.43$
	$[M_2] = 24.82$	$m_2 = 59.23$	$m_2 = 74.47$	$m_2 = 73.35$
	$[M_3] = 50.43$	$m_3 = 3.39$	$m_3 = 0.73$	$m_3 = 2.22$

The independence of the m_1/m_2 ratio of the R values has also a negative effect, this fact being better observed, as below, in the case of bulk copolymerization, but the results are improved relative to those obtained with Eqs (3, 5).

B. Monomers M_2 and M_3 cannot homopolymerize ($K_{22} = K_{33} = 0$), ($r_{21} = r_{23} = r_{31} = r_{32} = 0$) but can copolymerize with one another and with M_1.

For this case, ALFREY—GOLDFINGER [4] proposed the following equations:

$$\frac{m_1}{m_2} = \frac{[M_1](R_2R_3[M_1]+R_2[M_2]+R_3[M_3])\left([M_1] + \dfrac{[M_2]}{r_{12}} + \dfrac{[M_3]}{r_{13}}\right)}{[M_2]\left(R_3\dfrac{[M_1]}{r_{12}} + \dfrac{[M_2]}{r_{12}} + \dfrac{[M_3]}{r_{13}}\right)(R_2[M_1] + [M_3])} \quad (8)$$

$$\frac{m_1}{m_3} = \frac{[M_1](R_2R_3[M_1]+R_2[M_2]+R_3[M_3]) + \left([M_1]\dfrac{[M_2]}{r_{12}} + \dfrac{[M_3]}{r_{13}}\right)}{[M_3]\left(R_2\dfrac{[M_1]}{r_{13}} + \dfrac{[M_2]}{r_{12}} + \dfrac{[M_3]}{r_{13}}\right)(R_3[M_1]+[M_2])} \quad (9)$$

where $R_2 = K_{21}/K_{23}$, and $R_3 = K_{31}/K_{32}$. In principle, a single terpolymerization experiment is enough to determine R_2 and R_3, provided r_{12} and r_{13} are known. The simplified HAM's equations (3, 5) become [14]:

$$\frac{m_1}{m_2} = \frac{[M_1]\,R_2'\left([M_1] + \dfrac{[M_2]}{r_{12}} + \dfrac{[M_3]}{r_{13}}\right)}{\dfrac{[M_2]}{r_{12}}([M_1]\,R_2' + [M_3])} \tag{10}$$

$$\frac{m_1}{m_3} = \frac{[M_1]\,R_3'\left([M_1] + \dfrac{[M_2]}{r_{12}} + \dfrac{[M_3]}{r_{13}}\right)}{\dfrac{[M_3]}{r_{13}}([M_1]\,R_3' + [M_2])} \tag{11}$$

where $R_2' = K_{21}/K_{23}$, $R_3' = K_{31}/K_{32}$.

For illustration, the system acrylonitrile(1)-*p*-dioxene(2)–maleic anhydride(3) has been chosen, using IWATSUKI and YAMASHITA's data [15].

For the cases where in the feed *p*-dioxene and maleic anhydride were in the 1 : 1 mole ratio, their incorporation into the copolymer was assumed to be in the same ratio [15]; for the other cases, only $(m_2 + m_3)$ was estimated by deducing the amount of acrylonitrile from the polymer. Taking thus the system: $[M_1] = 78.69$, $[M_2] = 10.98$, $[M_3] = 10.33$. $m_1 = 87.00$, $m_2 = 6.50$, $m_3 = 6.50$, with reactivity ratios $r_{12} = 5.9$ [15], $r_{13} = 6.0$ [16], the following values for R were obtained, $R_2 = 0.0795$, $R_3 = 0.0394$ (calculated from Eqs (8, 9) and $R_2' = 0.0566$, $R_3' = 0.0543$ [calculated from Eqs (10, 11)].

In Table IX the terpolymer composition calculated from the simplified Eqs (10, 11) are compared with the experimental data and with the values obtained from Eqs (8, 9).

The compositions calculated according to the simplified Eqs (10, 11) show as good in agreement with the experimental values as those calculated by means of the ALFREY—GOLDFINGER Eqs (8, 9). In the cases in which the agreement between experimental values and the compositions given by the ALFREY—GOLDFINGER Eqs (8, 9) is rather poor, the compositions given by the simplified Eqs (10 11,) are also rather erratic.

With the average values of R_2, R_3, R_2' and R_3' these estimates are probably in a better agreement with the real compositions, more so as the authors have observed solvent effects in the above terpolymerization, some of which are considered to be due to the equilibrium complex formation between *p*-dioxene and maleic anhydride; as a consequence of this complex, IWATSUKI and YAMASHITA suggest that this terpolymerization consists not only of the nine elementary reactions assumed in the usual theory of terpolymerization.

Table IX

Comparison of the experimental terpolymer compositions with those calculated by means of ALFREY–GOLDFINGER's *Eqs (8, 9) and simplified Eqs (10, 11)*

Feed composition (mole %)	Copolymer composition (mole %)		
	Experimental	Calculated from Eqs (8, 9)	Calculated from Eqs (10, 11)
$[M_1] = 10.00$	$m_1 = 3.30$	$m_1 = 2.20$	$m_1 = 1.98$
$[M_2] = 45.00$	$m_2 = 48.35$	$m_2 = 50.00$	$m_2 = 48.37$
$[M_3] = 45.00$	$m_3 = 48.35$	$m_3 = 47.80$	$m_3 = 49.65$
$[M_1] = 50.10$	$m_1 = 52.70$	$m_1 = 42.56$	$m_1 = 41.15$
$[M_2] = 25.10$	$m_2 = 23.65$	$m_2 = 29.23$	$m_2 = 29.14$
$[M_3] = 24.80$	$m_3 = 23.65$	$m_3 = 28.21$	$m_3 = 29.71$
$[M_1] = 51.60$	$m_1 = 69.70$	$m_1 = 68.29$	$m_1 = 63.65$
$[M_2] = 43.30$	$m_2 + m_3 =$	$m_2 = 19.85$	$m_2 = 21.45$
$[M_3] = 5.10$	$= 30.30$	$m_3 = 11.86$	$m_3 = 14.90$
$[M_1] = 50.10$	$m_1 = 60.50$	$m_1 = 41.95$	$m_1 = 41.92$
$[M_2] = 20.20$	$m_2 + m_3 =$	$m_2 = 28.95$	$m_2 = 28.18$
$[M_3] = 29.70$	$= 39.50$	$m_3 = 29.12$	$m_3 = 29.90$

For the cases in which penultimate effects are observed for only one of the two possible binary combinations (M_1, M_2 and M_1, M_3), Eqs (10, 11) become:

$$\frac{m_1}{m_2} = \frac{[M_1]\,R_2''\left([M_1] + \dfrac{[M_2]}{r_{12}} + X\right)}{\dfrac{[M_2]}{r_{12}}\,(M_1 R_2'' + M_3)} \tag{12}$$

$$\frac{m_1}{m_3} = \frac{[M_1)\,R_3''\left([M_1] + \dfrac{[M_2]}{r_{12}} + X\right)}{X([M_1]\,R_3'' + [M_2])} \tag{13}$$

where

$$X = \frac{\dfrac{[M_3]}{r_{13}'(r_{13}' \cdot [M_1]/[M_3] + 1)}}{r_{13}' \cdot [M_1]/[M_3] + 1}\,. \tag{14}$$

For the illustration, the system acrylonitrile(1)-maleic anhydride (2)–4-vinylcyclohexene(3) was chosen, with copolymerization in benzene. The reactivity ratios in this case are: $r_{12} = 6.0$ [16], $r_{13} = 6.5$, from the terminal model, and $r_{12} = 6.0$, $r_{13} = 5.47$, $r_{13}' = 17.24$, from the penultimate model. Taking an initial feed composition ($[M_1] = 20.25$, $[M_2] = 39.91$, $[M_3] =$

= 38.84) and the copolymer composition corresponding to it ($m_1 = 24.43$, $m_2 = 38.69$, $m_3 = 36.88$), the values of the factor R are as follows: $R_2 = 0.4137$, $R_3 = 0.1567$ (calculated from Eqs (8, 9); $R_2 = 0.2615$, $R_3 = 0.3026$ (calculated from Eqs (10, 11)) and $R_2'' = 0.3375$, $R_{33}'' = 0.0018$ (calculated from Eqs (12, 13)).

The calculated and experimental results for another feed composition are compared in Table X.

Table X

Comparison of the experimental terpolymer composition with those calculated by means of ALFREY—GOLDFINGER's *Eqs (8, 9), the* HAM *Eqs (10, 11) and the modified* HAM *Eqs (12, 13)*

Feed composition (mole %)	Copolymer composition (mole %)			
	Experimental	Calculated Eqs (8, 9)	Calculated Eqs (10, 11)	Calculated Eqs (12, 13)
$[M_1] = 23.38$	$m_1 = 25.79$	$m_1 = 27.82$	$m_1 = 30.61$	$m_1 = 36.25$
$[M_2] = 46.02$	$m_2 = 49.28$	$m_2 = 34.60$	$m_2 = 34.49$	$m_2 = 43.40$
$[M_3] = 30.60$	$m_3 = 24.93$	$m_3 = 37.58$	$m_3 = 34.40$	$m_3 = 20.40$

Certainly both in the first and second cases ALFREY—GOLDFINGER equations with the penultimate modifications can be constructed. But when ALFREY—GOLDFINGER's Eqs (2) or (8, 9) and the simplified Eqs (3, 5) or (10, 11) show a good consistency in the results, the problem may be appreciably simplified by utilizing, instead of the ALFREY—GOLDFINGER equation, the simplified expression (6, 7) or (12, 13) due to HAM as a basis.

REFERENCES

1. ALFREY, T., GOLDFINGER, G.: J. Chem. Phys., **12**, 322 (1944)
2. WALLING, G., BRIGGS, E. R.: J. Amer. Chem. Soc., **67**, 1774 (1945)
3. SKEIST, J.: J. Amer. Chem. Soc., **68**, 1781 (1946)
4. ALFREY, T., GOLDFINGER, G.: J. Chem. Phys., **14**, 115 (1946)
5. FINEMAN, N., ROSS, S. D.: J. Polymer Sci., **5**, 259 (1950)
6. HERMA, H., ULBRICHT, J.: Faserforsch. Textiltechn., **16**, 387 (1965); **16**, 335 (1965)
7. KERBER, R.: Makromol. Chem., **96**, 30 (1966)
8. KERBER, R.: Makromol. Chem., **100**, 290 (1967)
9. SHELTON, J. R., HENDERSON, J. N.: J. Org. Chem., **26**, 2185 (1961)
10. SHELTON, J. R., CHAMP, A.: J. Org. Chem. **28**, 1393 (1963)
11. BORCHERT, E. E.: Dissert. Abstr., **25**, 3482 (1965)
12. BARB, W. G.: J. Polymer Sci., **11**, 117 (1953)
13. HAM, G. E.: J. Polymer Sci., **A2**, 2753 (1964)
14. HAM, G. E.: J. Polymer Sci., **A2**, 4191 (1964)
15. IWATSUKI, S., YAMASHITA, Y.: Makromol. Chem., **89**, 205 (1965)
16. YOUNG, R. S.: J .Polymer Sci., **54**, 411 (1961)

Cristofor I. SIMIONESCU
N. ASANDEI
I. NEGULESCU

Iași, Str. Universității Nr. 16, Romania.

RECENSIONES

M. A. BROWN: *X-ray Methods*

Merrow Publ. Co., Ltd., Watford (England), 1971, pp. 58

The idea of this booklet is a good one — to give newcomers to the subject (*e.g.* undergraduates) or even experts in different fields of chemistry a brief description of the basic principles and the manifold applications of X-rays in science. It is comprised of eight chapters. The first is an introduction to the production, absorption, scattering, diffraction, monochromatisation, intensity recording and measurement of X-rays. The second presents various methods (absorption, emission, fluorescence and diffraction) of quantitative analysis provided by X-rays to chemistry. The other six, equally short (3—5 pages) chapters give the essentials of the following subjects: qualitative analysis, preferred orientation and its effect upon different X-ray techniques, particle size determination, measurement of degree of crystallinity in polymers, microradiography, etc. It should be welcomed that the author omitted discussing the X-ray structure determination, planning to publish a separate monograph on this comprehensive subject.

The highly condensed text with clear drawings helps to form fundamental thoughts on quite diverse problems in which only one thing is common: the usage of X-rays. In order to serve this goal, it would have been worth-while to present properly detailed practical examples after each independent item.

It is a pleasure to recomend this booklet to everyone who is seeking a popular short survey of various applications of X-rays in chemistry.

A. KÁLMÁN

Topics in Current Chemistry; Volume 28. π-Complexes of Transition Metals

Springer Verlag, Berlin—Heidelberg—New York, 1972, 181 p.

This volume of the series is devoted to some diverse aspects of the chemistry of transition metal π-complexes in which olefins, acetylenes and unsaturated cyclic systems act as ligands. Owing to the large amount of information now available on metal π-complexes, the contents of the book can obviously cover only some special problems of current interest in this field of chemistry.

The first chapter (39 pp, 129 refs) is a contribution by G. HÄFELINGER (Lehrstuhl für Organische Chemie der Universität Tübingen, G. F. R.) and is entitled "Theoretical Considerations for Cyclic $(pd)_\pi$ Systems". This is a fully theoretical paper based on the MO treatment of cyclic molecules containing heteroatoms whose *d* orbitals may participate in the formation of the delocalized π molecular orbitals. Examples of such systems which are of interest to the chemist working with transition metal complexes are the transition metal chelates of diimines.

The second chapter (43 pp. 173 refs) written by J. TSUJI (Basic Research Laboratory, Toray Industries Inc., Kamakura, Japan) on "Organic Synthesis by Means of Transition

Metal Complexes" treats some general patterns of organic reactions using transition metal complexes mainly in the form of catalysts although stoichiometric transformations constitute a significant part too. The review is based on the reactions of noble metal complexes and seeks to deal with the rather complex reaction sequences as a succession of simple fundamental reactions like oxidative addition, metal–metal bond cleavage, insertion reactions, etc.

The paper by L. D. PETTIT (Department of Inorganic and Structural Chemistry, The University, Leeds, U. K.) and D. S. BARNES (Department of Chemistry, The University, Keele, Staffs., U. K.) on "The Stability and Structures of Olefin and Acetylene Complexes of Transition Metals" constitutes the third chapter (54 pp. 153 refs). This review does not attempt to give a comprehensive survey of all known olefin and acetylene complexes, but restricts itself to stability data and characteristic structures, both of which furnish some information about the nature of bonding in these compounds. The emphasis laid on numerical values of stability is to be welcomed, since — in contrast to other types of co-ordination compounds — the thermodynamic data on transition metal π-complexes are rather scanty.

The last section (40 pp. 166 refs) is a contribution by H. WERNER (Anorganisch-chemisches Institut der Universität Zürich, Switzerland) entitled "Ringliganden-Verdrängungsreaktionen von Aromaten-Metall-Komplexen" which treats the substitution of C_5H_5 ligands (or their derivatives) in transition metal complexes. This reaction has not been reviewed before at all since these ligands are usually firmly bound and other ligands (if present) are substituted more easily. The mechanism of these reactions is not yet clear and the author proposes a new general scheme which is based on the electrophilic attack of the new ligand.

All chapters are up-to-date and cover the literature up to 1971. This book is a useful addition to the bookshelf of the chemist working in transition metal chemistry, although a somewhat more oriented selection of the topics and thus a restriction to a more limited part of π-complex chemistry would have been advantageous.

L. MARKÓ

D. W. van KREVELEN: *Properties of Polymers*

Correlations with chemical structure

With the collaboration of P. J. HOFTYZER

Elsevier Publ. Co., Amsterdam—London—New York, 1972; with 126 illustrations and 98 tables

The enormous development of the industry requires information about the properties of new high polymers whose physical properties have never been investigated or measured experimentally. The design of manufacturing and processing equipment as well as the application and use of the final products require considerable knowledge of the processed materials.

VAN KREVELEN's book aims at providing methods for the estimation of the most important properties of high polymers in solid, liquid and dissolved states in cases where experimental data are not available.

Using the chemical constitution of the repeating unit, it is shown that a number of quantities have additive properties — within certain limits of precision — so these quantities can be calculated in a simple manner from group contributions or increments and each functional group in the high polymer molecule actually performs a function which is reflected in the properties.

The book is written for specialists working on practical problems in the field of macromolecules, for chemical engineers who are often forced to execute designs without having enough data at disposal and who look in vain for numerical values of the quantities needed under the conditions of the process, for manufacturers and polymer technologists who try to get a better insight into the relationships in their branch and for all who are interested in the correlation between chemical structure and properties.

The book consists of six main parts, which are as follows:

Part I: Introduction: Polymers and additive properties.
Part II: Thermophysical Properties: Volumetric, calorimetric, cohesive and adhesive properties as well as transition temperatures.
Part III: Properties in Fields of Force: Behaviour of Polymers in mechanical and electromagnetic fields of force.

Part IV: Transport Properties: Transport of heat, momentum and matter, heat conductivity, viscosity, diffusivity.

Part V: Physical and Chemical Change: Crystallization, orientation, degradation as well as thermochemical properties.

Part VI: Retrospect: Correlations and interrelations between physical properties.

Tables of the properties of polymers enhance the value of the book as a reference work.

There are but a few slight inaccuracies in the book, as for instance: the molar refractive index (Mn) was introduced first by EISENLOHR *(c.f.* Ber. **53,** 1746, 2053 (1920), **54,** 299 (1921); **57,** 1808 (1924)) and not by VOGEL. The results of the Soviet and other socialist researchers are — with the exception of the works of EXNER — not treated so as it would be desirable. Nevertheless, owing to its content the book will undoubtedly win high acclaim among macromolecular chemists. It may be recommended to specialists of high polymers as well as chemical engineers and technologists.

I. GÉCZY

INDEX

Printed in Hungary

A kiadásért felel az Akadémiai Kiadó igazgatója — Műszaki szerkesztő: Zacsik Annamária

A kézirat nyomdába érkezett: 1972. XI. 2. — Terjedelem: 10,50 (A/5 ív) 82 ábra.

73.74292 Akadémiai Nyomda, Budapest — Felelős vezető: Bernát György

ACTA CHIMICA

ТОМ 76—ВЫП. 3

РЕЗЮМЕ

Фотометрическое определение алюминия с помощью Арсеназо III

В. МИХАЙЛОВА

Алюминий образует с Арсеназо III при pH = 2—8 фиолетовый комплекс с составом 1 : 1. Абсорбционный спектр комплекса обладает двумя пиками при 550 и 583 мμ с максимальной абсорбцией при pH = 4.

Молярное светопоглощение при pH = 5 равно 18 800 ± 200 и 23 500 ± 200. Соответствующие спектрофотометрические чувствительности равны 0,0014 μгAl · см$^{-2}$ и 0,0011 μг Al · см$^{-2}$ при A = 0,001.

Закон Бэра соблюдается в интервале 0,01—0,60 μг Al · мл$^{-1}$ при pH = 3,5. Реакция может быть использована для фотометрического микроаналитического определения алюминия в кальците. Чувствительность реакции равна 0,01 μг Al · мл$^{-1}$, используя статистические методы.

Каталитическое влияние некоторых комплексов кобальта III на окисление йодида пероксидисульфатом

Х. БАРТЕЛЬТ и М. ШНЕЙДЕР

Было изучено каталитическое влияние следующих комплексных ионов $[Co(a)_6]^{+3}$, $[Co(en)_3]^{+3}$, $[Co(pn)_3]^{+3}$ $[Co(chn)_3]^{+3}$ и $[Co(chn)_3]^{+3}$ $[Co(phen)_3]^{+3}$ на реакцию $S_2O_8^{-2}$ и I^-.

Начальная скорость реакции в присутствии комплексов Co(III) возрастает в зависимости от природы комплексов в 100 . . . 200 раз. Эти значения справедливы для концентраций [комплекс Co(III)] = 10^{-3}M, $[S_2O_8^{-2}]_0 = 5 \cdot 10^{-4}$ M и $[I^-]_0 = 2{,}5 \cdot 10^{-3}$ M.

Каталитическое влияние возрастает при увеличении концентрации редоксного партнера комплекса (предварительное равновесие). Каталитические влияния комплексов, за исключением $[Co(phen)_3]^{+3}$, лишь слегка различаются.

Исходя из изменения начальной скорости под влиянием добавления хлоридных ионов, было выведено уравнение расчета констант устойчивости комплексов типа внешней сферы, образованных между комплексным ионом Co(III) и Cl^-.

Инфракрасные спектры 1,2,3,5-тетразамещенных бензола, II

ДЬ. ВАРШАНИ и П. ШОХАР

Приводится подробный анализ ИК спектров 35 различных 1,2,3,5- тетразамещенных производных бензола, в которых в положениях 2 и 5 находятся легкие атомы (атомный вес меньше 20), а в положениях 1,3 — тяжелые атомы (атомный вес больше 20). Были определены зависимости между интенсивностями полос спектров, а также их частот и влиянием заместителей на распределение электронов. Указывается на перекрывание некоторых колебаний одинаковой симметрии, а также было установлено строение ассоциатов отдельных соединений.

Воспроизводимость адсорбционной емкости, определенной из избыточной адсорбционной изотермы смеси жидкостей

ДЬ. ФОТИ, Л. ДЬ. НАДЬ и Г. ШАЙ

Была исследована возможность воспроизводимости данных по избытку удельной поверхности и адсорбционной емкости в системе двухкомпонентной смеси жидкостей с твердым адсорбентом. Причиной разброса данных по избытку удельной поверхности является, в основном, неоднородность адсорбента, а также, но в меньшей степени, ненадежность метода, применяемого для измерения изменения состава жидкой фазы. Адсорбционная емкость силикагеля, выбранного в качестве модели, была определена на основе данных адсорбции из смеси жидкостей бензол — н-гептан и как с помощью экспраполяционного метода Шай-Надя, так и с помощью обобщенного выражения Эверетта. В обоих случаях оценивался интервал надежности полученных значений. Для величины емкости с помощью первого метода было получено значение $2{,}02 \pm 4{,}25\%$, а с помощью второго метода: $2{,}03 \pm 3{,}81\%$ ммоля бензола/г адсорбента при 95%-ной статистической надежности, что находится в хорошем согласии с результатами определения поверхности методом БЕТ.

Нитрофенолы, II

Реактивность эфиров 5-интрогидроксигидрохинона. Синтез 3-замещенных производных

А. Ф. АБУЛЕЗЗ и В. С. ЭЛЬ-ХАМУЛИ

Образование метиленового эфира 6-гидрокси 3-метокси-5-нитро-2-оксибензилового спирта доказывает реактивность позиции 3 в 1-метиловом эфире 5-гидрокси-гидрохинона, несмотря на то, что 3-замещенная фенилтиоуксусная и фенилуксусная кислоты не способны на лактонизацию.

Синтез соединений, вероятно обладающих фунгицидальной активностью

Ш. А. ШАМС ЭЛЬ-ДИНЕ и О. КЛАИДЕР

Были синтезированы 12 новых алкильных эфиров 1,3,4-тиадиазоль-, 5-метил-1,3,4-тиадиазоль- и 5-трифторметил-1,3,4-тиадиазоль-2-ил-дитиокарбаминовой кислоты. В качестве алкильных групп служили метильная, этильная, н-пропильная и карбетоксиметильная. Эти соединения были приготовлены для пробы их фунгицидальной активности.

Кинетическое исследование получения 1-фенил-1,4-дигидро-3(2H)-изохинолина и его 4-алкильных производных с помощью циклизирующего амидоалкилирования

ДЬ. ДЕАК, К. ГАЛЛ-ИШТОК, Ж. КАЛМАН и Ю. ХАШКО-БРОЙЕР

Было проведено кинетическое исследование реакции нитрилов фенилуксусной кислоты или амидов, содержащих в α-положении алкильный заместитель или заместители, с бензальдегидом в полифосфорной кислоте, приводящей к образованию 4-алкил-1-фенил-1,4-дигидро-3(2*H*)-изохинолинов. Для определения концентрации были использованы ИК спектрометрический и газовохроматографический методы. Было установлено, что заполнение пространства алкильными заместителями оказывает важное влияние на скорость реакции. На основе сравнения констант скоростей и времен полураспада можно полагать, что гидратация нитрилов и реакции циклизации протекают на основе подобных механизмов.

Многокомпонентная сополимеризация. Об уравнениях тройной сополимеризации в некоторых специфических случаях

К. СИМИОНЕСКУ, Н. АСАНДЕИ и И. НЕГУЛЕСКУ

Справедливость уравнений Альфрея—Гольдфингера для расчета составов терполимеров на основе известных отношений реактивностей являлась предметом многочисленных статей в последние годы. Для специфических случаев, когда один или более компенентов не способны к гомополимеризации, но сополимеризуются с другими партнерами, были предложены уравнения, в которых один из факторов R должен быть определен экспериментально, если отношения реактивностей известны из исследований бинарной сополимеризации.

Были изучены системы акрилонитрил — акриловая кислота — 4-винилциклогексен и акрилонитрил — малеиновый ангидрид — 4-винилциклогексен. Было найдено, что значительные изменения в факторе R являются результатом влияния предпоследнего члена, эффекта растворителя и т. д. Таким образом, предлагаемые для специфических случаев уравнения дают различные результаты, зависящие от условий реакции. Предлагается введение среднего значения фактора R, так что решение уравнений тройной сополимеризации для специфических случаев дает наилучшее приближение для действительного состава.

Помимо этого, составы терполимера, рассчитанные с помощью упрощенных уравнений Хэма, сравниваются с величинами, рассчитанными с помощью уравнений Альфрея-Гольдфингера, а также с экспериментальными величинами для систем, содержащих один или более мономеров с очень низкой скоростью собственного роста цепи.

The Acta Chimica publish papers on chemistry in English, German, French and Russian.

The Acta Chimica appear in volumes consisting of four parts of varying size, 4 volumes being published a year.

Manuscripts should be addressed to

Acta Chimica
Budapest 112/91 Műegyetem

Correspondence with the editors should be sent to the same address.

The rate of subscription is $ 24.00 a volume.

Orders may be placed with "*Kultúra*" Foreign Trade Company for Books and Newspapers (1389 Budapest 62, P. O. B. 149. Account No. 218 10990) or with representatives abroad.

Les Acta Chimica paraissent en français, allemand, anglais et russe et publient des mémoires du domaine des sciences chimiques.

Les Acta Chimica sont publiés sous forme de fascicules. Quatre fascicules seront réunis en un volume (4 volumes par an)

On est prié d'envoyer les manuscrits destinés à la rédaction à l'adresse suivante:

Acta Chimica
Budapest 112/91 Műegyetem

Toute correspondance doit être envoyée à cette même adresse.

Le prix de l'abonnement est de $ 24.00 par volume.

On peut s'abonner à l'Entreprise pour le Commerce Extérieur de Livres et Journaux «*Kultúra*» (1389 Budapest 62, P. O. B. 149. Compte-courant No. 218 10990) ou à l'étranger chez tous les représentants ou dépositaires.

«*Acta Chimica*» издают трактаты из области химической науки на русском, французском, английском и немецком языках.

«*Acta Chimica*» выходят отдельными выпусками разного объема. 4 выпуска составляют один том. 4 тома публикуются в год.

Предназначенные для публикации рукописи следует направлять по адресу:

Acta Chimica
Budapest 112/91 Műegyetem

По этому же адресу направлять всякую корреспонденцию для редакции.

Подписная цена — $ 24.00 за том.

Заказы принимает предприятие по внешней торговле книг и газет «*Kultúra*» (1389 Budapest 62. P. O. B. 149. Текущий счет № 218 10990) или его заграничные представительства и уполномоченные.

Reviews of the Hungarian Academy of Sciences are obtainable at the following addresses:

ALBANIA
Drejtorija Qändrone e Pärhapjes dhe Propagandimit të Librit
Kruga Konferenca e Päzes
Tirana

AUSTRALIA
A. Keesing
Box 4886, GPO
Sydney

AUSTRIA
GLOBUS
Höchstädtplatz 3
A-1200 Wien XX

BELGIUM
Office International de Librairie
30, Avenue Marnix
Bruxelles 5
Du Monde Entier
5, Place St.-Jean
Bruxelles

BULGARIA
HEMUS
11 pl Slaveikov
Sofia

CANADA
Pannonia Books
2, Spadina Road
Toronto 4, Ont.

CHINA
Waiwen Shudian
Peking
P. O. B. 88

CZECHOSLOVAKIA
Artia
Ve Směčkách 30
Praha 2
Poštovní Novinová Služba
Dovoz tisku
Vinohradská 46
Praha 2
Mad'arska Kultura
Václavské nám. 2
Praha 1
SLOVART A. G.
Gorkého
Bratislava

DENMARK
Ejnar Munksgaard
Nörregade 6
Copenhagen

FINLAND
Akateeminen Kirjakauppa
Keskuskatu 2
Helsinki

FRANCE
Office International de Documentation et Librairie
48, rue Gay-Lussac
Paris 5

GERMAN DEMOCRATIC REPUBLIC
Deutscher Buch-Export und Import
Leninstraße 16
Leipzig 701
Zeitungsvertriebsamt
Fruchtstraße 3—4
1004 Berlin

GERMAN FEDERAL REPUBLIC
Kunst und Wissen
Erich Bieber
Postfach 46
7 Stuttgart S.

GREAT BRITAIN
Blackwell's Periodicals
Oxenford House
Magdalen Street
Oxford
Collet's Subscription Import Department
Dennington Estate
Wellingsborough. Northants.
Robert Maxwell and Co. Ltd.
4—5 Fitzroy Square
London W. 1

HOLLAND
Swetz and Zeitlinger
Keizersgracht 471—487
Amsterdam C.
Martinus Nijhof
Lange Voorhout 9
The Hague

INDIA
Hind Book House
66 Babar Road
New Delhi 1

ITALY
Santo Vanasia
Via M. Macchi 71
Milano
Libreria Commissionaria Sansoni
Via La Marmora 45
Firenze
Techna
Via Cesi 16.
40135 Bologna

JAPAN
Kinokuniya Book-Store Co. Ltd.
826 Tsunohazu 1-chome
Shinjuku-ku
Tokyo
Maruzen and Co. Ltd.
P. O. Box 605
Tokyo-Central

KOREA
Chulpanmul
Phenjan

NORWAY
Tanum-Cammermeyer
Karl Johansgt 41—43
Oslo 1

POLAND
Ruch
ul. Wronia 23
Warszawa

ROMANIA
Cartimex
Str. Aristide Briand 14—18
Bucureşti

SOVIET UNION
Mezhdunarodnaya Kniga
Moscow G—200

SWEDEN
Almquist and Wiksell
Gamla Brogatan 26
S—101 20 Stockholm

USA
F. W. Faxon Co. Inc.
15 Southwest Park
Westwood Mass. 02090
Stechert Hafner Inc.
31. East 10th Street
New York, N. Y. 10003

VIETNAM
Xunhasaba
19, Tran Quoc Toan
Hanoi

YUGOSLAVIA
Forum
Vojvode Mišića broj 1
Novi Sad
Jugoslovenska Knjiga
Terazije 27
Beograd

15. VI. 1973.

Index: 26.007

ACTA CHIMICA

ACADEMIAE SCIENTIARUM HUNGARICAE

ADIUVANTIBUS

V. BRUCKNER, GY. DEÁK, K. POLINSZKY,
E. PUNGOR, G. SCHAY, Z. G. SZABÓ

REDIGIT

B. LENGYEL

TOMUS 76 FASCICULUS 4

AKADÉMIAI KIADÓ, BUDAPEST

1973

ACTA CHIM. (BUDAPEST) ACASA 76 (4) 339–449 (1973)

ACTA CHIMICA

A MAGYAR TUDOMÁNYOS AKADÉMIA KÉMIAI TUDOMÁNYOK OSZTÁLYÁNAK IDEGEN NYELVŰ KÖZLEMÉNYEI

SZERKESZTI

LENGYEL BÉLA

TECHNIKAI SZERKESZTŐK

DEÁK GYULA és HARASZTHY-PAPP MELINDA

Az Acta Chimica német, angol, francia és orosz nyelven közöl értekezéseket a kémiai tudományok köréből.

Az Acta Chimica változó terjedelmű füzetekben jelenik meg, egy-egy kötet négy füzetből áll. Évente átlag négy kötet jelenik meg.

A közlésre szánt kéziratok a szerkesztőség címére (Budapest 112/91 Műegyetem) küldendők.

Ugyanerre a címre küldendő minden szerkesztőségi levelezés. A szerkesztőség kéziratokat nem ad vissza.

Megrendelhető a belföld számára az „Akadémiai Kiadó"-nál (1363 Budapest Pf 24. Bankszámla 215 11488), a külföld számára pedig a „Kultúra" Könyv- és Hírlap Külkereskedelmi Vállalatnál (1389 Budapest 62, P.O.B. 149 Bankszámla: 218 10990) vagy annak külföldi képviseleteinél és bizományosainál.

Die Acta Chimica veröffentlichen Abhandlungen aus dem Bereiche der chemischen Wissenschaften in deutscher, englischer, französischer und russischer Sprache.

Die Acta Chimica erscheinen in Heften wechselnden Umfanges. Vier Hefte bilden einen Band. Jährlich erscheinen 4 Bände.

Die zur Veröffentlichung bestimmten Manuskripte sind an folgende Adresse zu senden:

Acta Chimica
Budapest 112/91 Műegyetem

An die gleiche Anschrift ist auch jede für die Redaktion bestimmte Korrespondenz zu richten. Abonnementspreis pro Band: $ 24,00.

Bestellbar bei dem Buch- und Zeitungs-Außenhandels-Unternehmen »*Kultúra*« (1389 Budapest 62, P.O.B. 149 Bankkonto Nr. 218 10990) oder bei seinen Auslandsvertretungen und Kommissionären.

Acta Chimica Academiae Scientiarum Hungaricae, Tomus 76 (4), pp. 339–343 (1973)

STUDY ON THE SOLUBILITIES OF SILVER HALIDES IN SOME AQUEOUS AND NON-AQUEOUS SOLVENT MIXTURES

N. A. KAZARJAN and E. PUNGOR

(Mendeleev Institute of Chemical Technology, Moscow and Institute for General and Analytical Chemistry of the Technical University, Budapest)

Received June 12, 1972

A simple method is suggested for the determination of the solubility products of silver chloride, silver bromide and silver iodide and the data obtained in mixtures of water with methanol, ethanol, *n*-propanol, iso-propanol, acetone and dimethylformamide are reported.

In our earlier works [1, 2] the silicone rubber based ion-selective electrodes were studied in alcohol–water, in acetone–water, and dimethylformamide–water mixtures from the point of view of swelling of the electrodes in these solvents. The swelling to a bigger extent dislocates the connections of the active particles in the membrane and so the electrode response ceases. The results enabled us to conclude that the heterogeneous membrane electrodes are applicable in a wider range of these mixed solvents.

To study the theoretical basis of the application of the membrane electrodes it is necessary to determine the solubility products [3] of the appropriate precipitates in these solvents. For the determination of these data several methods are available. In our present investigation we used the potentiometric method applying an iodide electrode.

Experimental

The potentiometric measurements were carried out on a precision pH meter (Model OP 205, Radelkis, Budapest) with an expanded scale having a high input resistance of 10^{12} Ohm. The electrodes for the determination of iodide, bromide and chloride were manufactured by Radelkis. The reference electrode was in every case a saturated calomel electrode and the connection of the two half cells was assured by a saltbridge containing potassium nitrate. The data were registered by using a millivolt recorder.

The solubility products were measured in the knowledge of the original halide concentration (X_0) by the titration procedure. After the end-point the excess amount of the silver (Ag_s) is known too. The potential difference between the points of overtitration and beginning stage of the titration can be measured. At the end-point of the titration the halide and silver concentrations are equal (X_e, Ag_e). So

$$\Delta E = 0.059(pX_e - pX_0) + 0.059(pAg_e - pAg_s)$$

From that

$$pX_e = \frac{\Delta E}{2 \cdot 0.059} + 1/2(pX_0 + Ag_s)$$

From the pX_e values the solubility product is calculated. The application of this simple equation is based on the assumption that the potential response of the electrodes during the whole titration is a Nernstian one. This assumption was strengthened through many experiments carried out in aqueous and non-aqueous solvents in our laboratories.

Mixtures of water with methanol, ethanol, propanol, iso-propanol, acetone and dimethylformamide, respectively, were used as solvents.

Results and discussion

The results of our investigations for the six organic solvents mixed with water in various proportions are compiled in Tables I—III. The tables contain

Table I

Solubility products of silver chloride in mixtures of water with different organic solvents

Solvent	Solvent (v/v %)	p^8AgCl		
		Measured values	Mean values	Previous values
H_2O	100	9.8_2 9.9_8	9.9_0	9.8_2
CH_3OH	10	10.0_2 10.1_0	10.0_6	10.1_0
	40	10.4_0 10.3_0	10.3_5	10.4_0
	60	10.7_2 10.7_4 11.3_2	10.9_3	10.7_0
	90	11.5_0 11.6_4	11.5_7	11.5_0
C_2H_5OH	10	10.1_0		
	40	10.4_0		
	60	10.7_4		
	90	11.5_0		
i-C_3H_7OH	10	9.8_8		
	20	10.1_6		
	30	10.2_0		
	40	10.2_8		
n-C_3H_7OH	10	9.9		
	20	9.9_2		
	30	9.9_2		
	40	10.0_0		
$(CH_3)_2CO$	10	9.8_0 9.8_0	9.8_0	9.8_0
	20	9.7_2 10.0_6	9.8_9	10.0_6
	30	9.5_2 10.2_4	9.8_8	10.2_4
	40	9.2_6 10.5_0	9.8_8	10.5_0
$HON{=}C{-}(CH_3)_2$	10	10.0_4		
	40	10.3_2		
	60	10.6_6		

the experimental data and the mean values of our latest measurements of the solubility products at 25 °C and our previous values obtained with laboratory made halide electrodes.

Table II

Solubility products of silver bromide in mixtures of water with different organic solvents

Solvent	Solvent (v/v %)	p^8AgBr					
		Measured values				Mean values	Previous values
H_2O	100	12.3_6	12.2_8			12.3_2	12.3_6
CH_3OH	10	12.4_8				12.4_8	
	40	13.0_0				13.0_0	
	60	13.4_2	13.3_0			13.4_1	13.3_8
	90	14.6_4	14.3_0			14.4_7	14.4_0
C_2H_7OH	10	10.3_2	12.5_4	12.6_4	13.1_0	12.6_5	12.5_4
	40	12.7_4	12.8_0			12.7_7	12.9_0
	60	13.1_2	13.3_0	13.5_2		13.3_1	13.2_6
	90	14.3_2	14.2_6	14.4_8		14.3_5	14.3_0
i-C_3H_7OH	10	12.4_0	12.3_0			12.5_5	12.3_0
	20	12.4_8				12.4_8	12.4_8
	30	12.6_4				12.6_4	12.6_4
	40	12.7_8				12.7_8	12.7_8
n-C_3H_7OH	10	12.2_0	12.5_0			12.3_5	12.5_0
	20	12.6_6	12.7_0			12.6_8	12.6_6
	30	12.7_4				12.7_4	12.7_4
	40	12.8_2				12.8_2	12.8_2
$(CH_3)_2CO$	10	12.2_0	12.4_6	12.6_0		12.4_2	12.4_6
	20	12.6_0	12.7_2	11.6_0		12.3_1	12.6_0
	30	11.2_0	12.6_2			11.9_1	12.6_2
	40	10.0_8	12.6_4			11.2_8	12.6_4
$HON{=}C{-}(CH_3)_2$	10	12.2_2					
	40	12.5_0					
	60	12.7_0					

D. FEAKINS *et al.* [4] and H. A. PARTON *et al.* [5] respectively, determined the solubility product of silver chloride in various methanol–water mixtures. The data for comparison are given in Table IV. It can be seen that our data are close to the literature values.

Table III

Solubility products of silver iodide in mixtures of water with different organic solvents

Solvent	Solvent (v/v %)	pS_{AgI} Measured values				Mean	Previous values
H_2O	100	15.9_6	15.8_6			15.9_1	$15,9_6$
CH_3OH	10	16.1_2	16.1_4	16.3_0		16.1_9	16.1_2
	40	16.3_0	16.4_8	16.5_8	16.6_4	16.5_0	16.4_8
	60	16.6_4	16.7_2	16.8_0	17.1_6	16.8_3	16.7_2
	90	17.1_6	17.4_2	17.7_0		17.4_3	17.4_2
C_2H_5OH	10	16.1_0	16.0_6	16.1_6		16.1_1	16.1_6
	40	16.3_2	16.6_6			16.4_9	16.4_0
	60	16.6_6	16.8_4			16.7_5	16.6_0
	90	17.1_2	17.3_0	17.4_2		17.2_8	17.3_0
i-C_3H_7OH	10	16.0_6	16.2_6			16.1_4	16.0_4
	20	16.1_2	16.4_0			16.2_6	16.1_2
	30	16.2_0				16.2_0	16.2_0
	40	16.2_8				16.2_8	16.2_8
n-C_3H_7OH	10	16.0_0	16.2_0	16.2_0	16.1_4	16.1_4	16.2_0
	20	16.2_0	16.2_4			16.2_2	16.2_4
	30	16.2_0	16.3_2			16.2_6	16.3_2
	40	16.2_0	16.4_0			16.3_0	16.4_0
$(CH_3)_2CO$	10	16.0_0	16.1_2	16.2_8		16.1_3	16.2_0
	20	16.0_0	16.0_4	16.1_8	16.2_8	16.1_3	16.2_8
	30	16.0_0	16.0_4	16.2_4		16.0_9	16.2_4
	40	16.0_6	16.2_0			16.1_3	16.2_0
$HON{=}C{-}(CH_3)_2$	10	15.9_6	16.0_0			15.9_8	15.9_6
	40	15.8_0	15.7_6			15.7_8	15.7_6
	60	15.4_4	15.3_4			15.3_9	15.3_4

We determined for each electrode the standard deviation of the pS values. For this calculation we have used the values for every solvent mixture and found that the standard deviation for iodide electrode is 0.12 pS, for the bromide electrode 0.40 pS and for the chloride electrode 0.28 pS.

Table IV

Solubility exponents in methanol–water mixtures

Methanol-water g/g %	pS_{AgCl} (25 °C)			
	measured by Feakins and coworkers	measured by Parton and coworkers	this work	
			mean value	previous value
8.2			10.0_6	10.1_0
10	9.99_2	10.0_3		
20.2_2	10.23_3	10.2_4		
33.4	10.56_6			
34.5			10.3_5	10.4_0
43.1_2	10.83_0			
54.2			10.9_3	10.7_4

REFERENCES

1. KAZARJAN, N. A., PUNGOR, E.: Anal. Chim. Acta **51,** 213 (1970)
2. KAZARJAN, N. A., PUNGOR, E.: Acta Chim. Acad. Sci. Hung. **66,** 183 (1970)
3. PUNGOR, E., TÓTH, K.: Anal. Chim. Acta **47,** 291 (1969)
4. FEAKINS, D., LAWRENCE, K. G., VOICE, P. J., WILLMOTT, A. R.: J. Chem. Soc. (A), **5,** 837 (1970)
5. PARTON, H. A., DAVIS, D. J., HURST, F., GEMMEL, G. D.: Trans. Faraday Soc. **41,** 575 (1945)

Nelly Arisovna KAZARJAN; Cand. Chem. Sci.
Mendeleev Institute of Technology, Moscow, USSR

Ernő PUNGOR; 1111 Budapest, Gellért tér 4.

Acta Chimica Academiae Scientiarum Hungaricae, Tomus 76 (4), pp. 345—357 (1973)

ON SOME RELATIONS BETWEEN VARIATIONAL PRINCIPLES IN IRREVERSIBLE THERMODYNAMICS

I. J. KUMAR and L. N. GUPTA

(Defence Science Laboratory, Delhi-6, India)

Received February 28, 1972

Some relations between various variational principles in irreversible thermodynamics have been derived. It is shown that GYARMATI's principle and the local potential principle of PRIGOGINE and GLANSDORFF are equivalent when the phenomenological coefficients are correlated by extended ONSAGER relations. A Lagrangian function for the generalized Navier–Stokes equations is derived through the local potential approach and, by its comparison with the corresponding Lagrangian function derived from GYARMATI's principle, it is shown that the two functions are equivalent except for their method of representation. Such equivalence has also been demonstrated in the case of the Lagrangian's for heat conduction equation and Fick's equation for multicomponent diffusion. BIOT's variational principle is a particular case of the local potential principle. A particular form of ZIEGLER's principle is derived from GYARMATI's integral principle.

1. Introduction

The variational formulation of a problem, when possible, provides the powerful tool of direct methods of variational calculus for obtaining an approximate solution to the problem. There have been several attempts [1, 2, 3] to interpret ONSAGER's relations by means of variational principles. This resulted in several variational principles in irreversible thermodynamics, for example, ONSAGER's principle of least dissipation of energy [1], the principle of minimum production of entropy formulated by PRIGOGINE [4] and the principle of least irreversible force given by ZIEGLER [3, 5, 6]. For the class of non-linear and non-self-adjoint equations to which the non-steady conservation equations of mass, momentum and energy with variable coefficients belong, a variational formulation in the classical sense is not possible, and recourse is, therefore, made to looser or extended variational formulations based on functions having some physical meaning. GYARMATI's principle [7], the local potential principle [8] and BIOT's variational principle [2, 9] are examples of such approaches.

GYARMATI [7, 10, 11] has treated the variational principles of non-equilibrium thermodynamics. In these papers he has clarified the relation between PRIGOGINE's principle [4] and GYARMATI's principle [7], giving an alternative description for the principle of least dissipation of energy. He has also asserted

[7] that every variational principle in which the potential functions exist can be derived from GYARMATI's principle. GYARMATI [12] has formulated his principle in a general manner and has shown that it can be applied to certain types of quasilinear and non-linear equations, where the extended ONSAGER relations hold true. VERHÁS [13] and BÖRÖCZ [14] have applied GYARMATI's principle to generalized Navier—Stokes equations in which convection type terms are also present. GYARMATI [12] has discussed the relation of his principle to VOJTA's functional variational principle and has shown that the two different formulations are but two alternative representations of a single general principle. VERHÁS [15] has applied GYARMATI's principle to plastic flow. SÁNDOR [16, 17] has given many applications of the universal form of GYARMATI's principle to non-linear problems and also to some quasilinear problems.

The object of this paper is to show that GYARMATI's principle [12] and the local potential principle formulated by GLANSDORFF and PRIGOGINE [8, 18] are equivalent when relations of the type $L_{ik}(\Gamma) = L_{ki}(\Gamma)$ and $L_{ikj} = L_{kij} = \ldots = L_{jki}$ are valid (the variables Γ are state parameters or internal parameters with respect to the forces). Generally, the application of GYARMATI's principle depends upon the existence of these ONSAGER type relations. In section 3 of this paper Lagrangian functions derived for some quasi-linear and non-linear equations are given and the local potential is derived for generalized NAVIER—STOKES equations. It will be shown that the Lagrangian functions derived by the two approaches, *viz.* those of GYARMATI and of the local potential are equivalent except in their method of representation. In sections 4 and 5, BIOT's variational principle [9, 19] is derived from the local potential principle and a special form of ZIEGLER's principle [3] is derived from GYARMATI's integral principle [12].

2. Relation between Gyarmati's principle and the local potential principle

In this section it will be shown that GYARMATI's variational principle [12] and the local potential principle [20, 21] are equivalent when ONSAGER type relations $L_{ik}(\Gamma) = L_{ki}(\Gamma)$ and $L_{ikj} = L_{kij} = \ldots = L_{jki}$ are valid. Let δF be the variation of time-dependent local potential given by GLANSDORFF [20]

$$\delta F = \sum_{\alpha} \int_{V} \delta J_{\alpha} \cdot \delta X_{\alpha} \, dV \tag{2.1}$$

where J_α denotes fluxes X_α — forces and V — volume. The validity of the local potential principle depends upon whether or not δF in Eq. (2.1) is a total differential in the extended sense of PRIGOGINE and GLANSDORFF [18];

here the parameters with superscript 'O' refer to the reference state with respect to which variations are taken, and thus are not to be varied. The basic state may either be stationary or time-dependent. However, δF in Eq. (2.1) may be an exact differential even if L_{ik} are functions of the parameters and, in some cases, even if ONSAGER type relations are not valid. Moreover, if ONSAGER type relations are satisfied, Eq. (2.1) will be an exact variation and δF can be written as

$$\delta F = \delta \int_V \left[\sum_\alpha J_\alpha X_\alpha - \frac{\partial(\varrho^0 e^0)}{\partial t} T^{-1} + \frac{\partial \varrho_r^0}{\partial t} \mu_r T^{-1} + \frac{\partial v_i^0}{\partial t} \cdot \frac{\varrho^0}{T^0} \cdot v^i \right] dV, \quad (2.2)$$

where ϱ denotes density, e—energy per unit mass, t—time, T—temperature, v—velocity and μ—chemical potential. Therefore, the corresponding Lagrangian function is given by

$$L = \sum_\alpha J_\alpha X_\alpha - \frac{\partial(\varrho^0 e^0)}{\partial t} T^{-1} + \frac{\partial \varrho_r^0}{\partial t} \cdot \mu_r T^{-1} + \frac{\partial v_i^0}{\partial t} \cdot \frac{\varrho^0}{T^0} \cdot v_i . \quad (2.3)$$

For energy only, Eq. (2.3) takes the form

$$L = \sum_\alpha J_\alpha X_\alpha - \frac{\partial(\varrho^0 e^0)}{\partial t} \cdot T^{-1}, \quad (2.4)$$

since

$$\frac{ds}{dt} = T^{-1} \frac{de}{dt}, \quad (2.5)$$

$$L = \sum_\alpha J_\alpha X_\alpha - \varrho^0 \frac{ds}{dt} . \quad (2.6)$$

Here $L(T, T^0, \mu_r, \mu_r^0, v_i, v_i^0)$.

In general, there will be a surface integral too, but if the intensive parameters, whose gradients are forces, are kept fixed at the surface or the flux at the surface is zero, then the surface integral term will vanish. With the above conditions of variation, the EULER—LAGRANGE equations (2.2) will be the conservation equations with the subsidiary conditions that

$$T = T^0, \quad \mu_r = \mu_r^0 \quad \text{and} \quad v_i = v_i^0. \quad (2.7)$$

GYARMATI [12] has given a very general form of his principle, which can be written as

$$\delta \int_V [\sigma - (\psi + \Phi)] \, dV = 0, \quad (2.8)$$

with integration over the total volume V of the continuum.

Here

$$\sigma(J, X) = \sum_{\alpha} J_\alpha X_\alpha \geqslant 0 \tag{2.9}$$

and Φ and ψ are the dissipation potentials.

In the case of transport processes the forces can always be generated as the gradients of certain variables 'Γ' which are state parameters or internal parameters with respect to the forces, *i.e.*

$$X_i = \nabla \Gamma_i. \tag{2.10}$$

Utilizing the entropy balance equation

$$\varrho \dot{s} + \nabla \cdot J_s = \sigma. \tag{2.11}$$

Eq. (2.8) can be formulated in an alternative way as

$$\delta \int_V [\varrho \dot{s} + \nabla \cdot J_s - (\psi + \Phi)]\, dV = 0 \tag{2.12}$$

Also

$$\Phi = \psi = \frac{\sigma}{2}. \tag{2.13}$$

In the case of linear processes Φ and ψ are homogeneous quadratic functions

$$\psi(X, X) \equiv \frac{1}{2} \sum_{i,k=1}^{b} L_{ik} X_i X_k \geqslant 0, \tag{2.14}$$

$$\Phi(J, J) \equiv \frac{1}{2} \sum_{i,k=1}^{b} R_{ik} J_i J_k \geqslant 0. \tag{2.15}$$

Eq. (2.12) can also be written as

$$\delta \int_V [\varrho \dot{s} - (\psi + \Phi)]\, dV + \delta \int_S J_s \cdot dS = 0. \tag{2.16}$$

Since the variation is with respect to variables Γ which are state parameters or internal parameters with respect to the forces, Eq. (2.16) can be reduced to

$$\delta \int_V (\varrho \dot{s} - \sigma)\, dV + \delta \int_S J_s \cdot dS = 0. \tag{2.17}$$

If the parameters at the surface are kept fixed or the flux at the surface is zero, the surface integral will vanish, thus the Lagrangian function derived by GYARMATI's approach will be $\varrho\dot{s} - \sigma$ which we denote by L_G

$$L_G = \varrho\dot{s} - \sigma . \tag{2.18}$$

It can be seen that the variation in both approaches is with respect to state parameters or internal variables; time derivatives are not varied in either approach and the Lagrangian functions are equivalent. The difference between the Lagrangian functions is in their method of representation: while one is

$$L(T, T^0, \mu_r, \mu_r^0, v_i, v_i^0),$$

the other is $L_G(\Gamma_i)$, where the Γ_i's correspond to T, μ and v_i respectively. From Eqs (2.6) and (2.18)

$$L = -L_G . \tag{2.19}$$

Therefore, $\delta L = -\delta L_G$

$\delta L = 0$ if and only if $\delta L_G = 0$.

From the above discussion it is also clear that the local potential principle is derivable from GYARMATI's principle and *vice versa*. GYARMATI [12] has shown that Eq. (2.8) is applicable to quasi-linear equations if

$$L_{ik}(\Gamma_1, \Gamma_2, \ldots \Gamma_n) = L_{ki}(\Gamma_1, \Gamma_2, \ldots \Gamma_n), \tag{2.20}$$

and to non-linear equations if

$$\begin{aligned} L_{ik} &= L_{ki} \\ L_{ikj} = L_{kij} &= \ldots = L_{jki} \\ &\vdots \\ L_{ikj} \ldots n &= L_{kij} \ldots n \ldots = L_{n\ldots jki}, \end{aligned} \tag{2.21}$$

and

$$\begin{aligned} R_{ik} &= R_{ki} \\ R_{ikj} = R_{kij} &\ldots = R_{jki} \\ &\vdots \\ R_{ikj} \ldots n &= R_{kij} \ldots n \ldots = R_{n\ldots jki}, \end{aligned} \tag{2.22}$$

whereas the local potential principle is applicable whenever δF is a total differential in the extended sense of PRIGOGINE and GLANSDORFF [18]; it is applicable when the above relations hold true.

3. Derivation of the local potential for generalized Navier—Stokes equations

In this section the local potential for generalized NAVIER—STOKES equations will be derived. The Lagrangian function derived in this way will be compared with that deduced by BÖRÖCZ [14] and VERHÁS [13]. Some other Lagrangian functions, *e.g.* for heat conduction [13] and Fick's equation [13] will be compared. The generalized NAVIER—STOKES equations are given by [14]

$$\varrho \frac{dv}{dt} + \operatorname{grad} p - \varrho F - \eta \Delta v - \left(\frac{1}{3}\eta + \eta_v\right) \operatorname{grad} \operatorname{div}(v) - \\ - \eta_r \operatorname{rot}(2\omega - \operatorname{rot} v) = 0\,, \tag{3.1}$$

and

$$\varrho \Theta \frac{d\omega}{dt} - 2\eta_r (\operatorname{rot} v - 2\omega) = 0, \tag{3.2}$$

where v denotes velocity, ϱ—density, p—pressure, F—external force per unit mass, η is the coefficient of viscosity, η_v the coefficient of bulk viscosity, η_r the coefficient rotational viscosity, ω denotes the mean angular velocity which is determined in every point of the fluid by the rigid rotation of the particles, Θ denotes the mean internal moment of inertia per unit mass of the constituent particles.

By proceeding in the same way as HAYS [22] and KUMAR [23], the local potential function can be derived. Now consider a volume V of an isotropic fluid with the boundary surface S. The family of velocity distributions in the volume considered may be thought of as having the appropriate macroscopic velocity distribution v^0 plus small and arbitrary variations of the velocity δv around the macroscopic distribution, Similarly the mean angular velocity ω can be regarded as a sum of ω^0 and $\delta\omega$:

$$v = v^0 + \delta v \tag{3.3}$$

$$\omega = \omega^0 + \delta\omega\,. \tag{3.4}$$

If we assume ϱ, η, η_v, η_r to be constants, the Lagrangian function for Eqs (3.1) and (3.2) can be derived in the following way. By multiplying both sides of Eqs (3.1) and (3.2) by δv and $\delta\omega$, respectively, and taking $\omega = \omega^0$ in Eq. (3.1) and $v = v^0$ in Eq. (3.2) one obtains

$$\varrho\, \delta \frac{\partial v}{\partial t} \cdot \delta v = \left(\varrho \frac{\partial v^0}{\partial t} - \operatorname{grad} p + \varrho F\right) \delta v + \\ + \operatorname{div}\left\{2\eta (\operatorname{grad} v)^s + \left(\eta_v - \frac{2}{3}\eta\right) \operatorname{div}(v)\right\} \delta v + \\ + \operatorname{rot}\left\{\eta_r (2\omega^0 - \operatorname{rot}(v)\right\} \delta v\,, \tag{3.5}$$

and

$$\varrho\,\delta\frac{\partial\omega}{\partial t}\cdot\delta\omega=\varrho\Theta\frac{\partial\omega^0}{\partial t}\cdot\delta\omega+2\eta_r(\mathrm{rot}\,v^0-2\omega)\,\delta\omega, \tag{3.6}$$

since

$$\delta F_1=-\frac{1}{2}\int_V(\delta v)^2\,dV \quad\text{and}\quad \delta F_2=-\frac{1}{2}\int_V(\delta\omega)^2\,dV,$$

$$\delta F=\delta F_1+\delta F_2\leqslant 0\,. \tag{3.7}$$

Consequently, the required velocity distribution v, and the mean angular velocity ω are characterized by the extremum conditions

$$\left(\frac{\delta F}{\delta v}\right)_{v^0}=0 \text{ and } \left(\frac{\delta F}{\delta\omega}\right)_{\omega^0}=0\,, \tag{3.8}$$

with the subsidiary conditions $v=v^0$ and $\omega=\omega^0$ (3.9). Therefore, the Lagrangian function as derived from the local potential is

$$\begin{aligned}L=&\left(\varrho\frac{dv^0}{dt}+\mathrm{grad}\,p^0-\varrho F\right)v+\frac{1}{2}\left(\eta_v-\frac{2}{3}\eta\right)(\mathrm{div}\,v)^2+\\&+\frac{\eta}{4}\sum_{i,J=1}^{3}\left(\frac{\partial v_i}{\partial x_J}+\frac{\partial v_j}{\partial x_i}\right)^2+\varrho\Theta\omega\frac{d\omega^0}{dt}-\frac{\eta_r}{2}(2\omega^0-\mathrm{rot}\,v^0)^2.\end{aligned} \tag{3.10}$$

Thus the Lagrangian functions derived from GYARMATI's principle by VERHÁS [13] and BÖRÖCZ [14] are the same as Eq. (3.10) except for their representations. The actual form of the Lagrangian function for some equations as derived from GYARMATI's principle [7] and the local potential principle is given below. For heat conduction

$$L_G=\varrho CvT\frac{\partial T}{\partial t}+\frac{\lambda}{2}(\nabla T)^2\,. \tag{3.11}$$

Eq. (3.11) has been given by GYARMATI [7],

$$L=\varrho CvT\frac{\partial T^0}{\partial t}+\frac{\lambda}{2}(\nabla T)^2\,, \tag{3.12}$$

Eq. (3.12) is quoted by HAYS [22].

Similarly in the case of Fick's equation of multicomponent diffusion, VERHÁS [13] and SÁNDOR [16] have given

$$L_G=\varrho\sum_{k=1}^{K-1}(\mu_k-\mu_K)\frac{dc_k}{dt}+\frac{1}{2}\sum_{i,k=1}^{K-1}L_{ik}\nabla(\mu_i-\mu_K)\cdot(\mu_K-\mu_K)\,. \tag{3.13}$$

This can be easily derived also by the local potential method giving

$$L = \varrho \sum_{k=1}^{K-1} (\mu_k - \mu_K) \frac{dc_k^0}{dt} + \frac{1}{2} \sum_{i,k=1}^{K-1} L_{ik} \nabla(\mu_i - \mu_K) \cdot \nabla(\mu_k - \mu_K). \tag{3.14}$$

Thus it can be seen that the Lagrangian functions are the same except for their way of representation.

Thus it appears that GYARMATI's integral principle and the local potential principle are equivalent; the basic difference between the two is their starting point. While GYARMATI has started from ONSAGER's relationships and developed a variational principle from which the equations of irreversible thermodynamics follow, the approach of GLANSDORFF and PRIGOGINE [8] is to start from the equations and construct a principle from which these follow. Neither variational principle is a variational principle in the classical sense; both depend on the cognizance of two types of variables, the ones which are varied and the others which are kept fixed while performing the variation. In our opinion, both lead to the necessary extension of the classical variational calculus so as to include processes involving mechanical dissipation.

4. Derivation of Biot's variational principle from the local potential principle

In this section it will be shown that BIOT's variational principle can be derived from the local potential principle. BIOT's variational principle is based on ONSAGER's reciprocal relations, but BIOT [19] has shown that even if ONSAGER's relations are not valid his variational principle is still applicable to certain types of non-linear problems. BIOT [2] has also shown that his variational principle reduces to the solution of equations of the type

$$\frac{\partial V}{\partial q_i} + \frac{\partial D}{\partial \dot{q}_i} = Q_i \tag{4.1}$$

where V is the potential energy, D is the dissipation function and Q is the work done at the surfaces; q_i are the generalized coordinates, $\dot{q}_i$ denote the differential of q_i with respect to time:

$$V = \frac{1}{2} \sum_{i,J} a_{iJ} q_i q_J , \tag{4.2}$$

$$D = \frac{1}{2} \sum_{i,J} b_{iJ} \dot{q}_i \dot{q}_J . \tag{4.3}$$

In irreversible thermodynamics, the principle is developed through the use of a heat flow vector H whose rate of change with time, $\dot{H}$, is the heat flux across an area normal to it:

$$\dot{H} = \frac{\partial H}{\partial t} . \tag{4.4}$$

In the case of isotropic conduction as given by BIOT [9] the variational formulation has the form

$$\delta V + \delta D = -T \cdot \delta H , \tag{4.5}$$

where

$$V = \int_x \int_T (CT)\, dT\, dx , \tag{4.6}$$

$$D = \int_x \frac{1}{2K} (\dot{H})^2\, dx . \tag{4.7}$$

If the heat flow vector H is defined in terms of time-dependent generalized coordinates q_i as

$$H = H(q_i, x, t) \qquad i = 1, 2, \ldots n, \tag{4.8}$$

then, as shown by BIOT [9], the transient heat conduction equation with temperature dependent specific conductivity and specific heat is equivalent to Eq. (4.1). In a subsequent paper BIOT [19] has shown that even if a convection term is present, a suitable definition of V and D reduces it to Eq. (4.1). Eq. (4.1) can also be written as

$$\frac{\partial D}{\partial \dot{q}_i} = Q_i - \frac{\partial V}{\partial q_i} . \tag{4.9}$$

If

$$X_i = Q_i - \frac{\partial V}{\partial q_i} , \tag{4.10}$$

then Eq. (4.9) takes the form

$$\frac{\partial D}{\partial \dot{q}_i} = X_i , \tag{4.11}$$

where X_i is total disequilibrium force. BIOT [2] has defined the function

$$P = D - \sum_i X_i \dot{q}_i , \tag{4.12}$$

and has shown that his variational principle is equivalent to P being an extremum when $\dot{q}_i$ are fixed and q_i are varied and, conversely, if q_i are fixed and $\dot{q}_i$ are varied. Upon re-writing Eq. (4.12) in GYARMATI's notation, we have

$$D = \frac{1}{2}\sigma = \psi\,, \tag{4.13}$$

$$\sum_i X_i \dot{q}_i = \sum_i X_i J_i = \sigma\,. \tag{4.14}$$

Therefore, Eq. (4.12) takes the form

$$P = (\psi - \sigma), \tag{4.15}$$

which is the same as the Lagrangian function defined by GYARMATI [7]. Also the conditions of variation are similar to a particular form of GYARMATI's integral principle [7]. Therefore, it follows that BIOT's variational principle is derivable from GYARMATI's integral principle. Also in section 2 of this paper we have shown that the GYARMATI principle [12] and the local potential principle [18] are equivalent except for their physical meanings. Thus it follows that BIOT's variational principle is derivable from the local potential principle.

From BIOT's work [9] it is evident that his discussion is based on a hypothesis that is correct from the viewpoint of mathematics but is physically empty. The displacement vector H introduced by BIOT [9] has no physical meaning. Theoretically BIOT's variational principle is applicable to problems in two and three dimensions, too, but in practice it can be applied to one-dimensional problems only, owing to the presence of the divergence term

$$\int_V c\,dT = h = -\nabla \cdot H\,. \tag{4.16}$$

5. Relation between Gyarmati's principle and Ziegler's principle of least irreversible force

In this section it will be shown that a special form of ZIEGLER's principle of least irreversible force [3] can be derived from GYARMATI's principle. ZIEGLER [3] has stated the principle of least irreversible force and has given its alternative forms as the principle of maximum rate of entropy production and the principle of maximum rate of dissipation work. One of the forms of the principle of least irreversible force is equivalent to

$$X_k^i (\dot{x}_k - \dot{x}_k^0) \geqslant 0 \tag{5.1}$$

in which X_k^i denotes the actual irreversible force, $\dot{x}_k$ — the actual velocity, M — the corresponding value of the dissipation function $D(\dot{x}_k)$, and $\dot{x}_k^0$ is any other velocity with a dissipation function $D(\dot{x}_k^0) \leq M$. The equality sign holds whenever $\dot{x}_k^0$ is another solution. Also dual forms of the principle exist in force space where the forces are kept fixed and the variation is carried out with respect to velocities. In other cases, velocities are kept fixed and the forces varied. ZIEGLER's principle is based on statistical foundations and it can be applied to both linear and non-linear problems.

The approach of ZIEGLER [3] is similar to the local potential approach where one considers the variation around an average state and the two types of functions become equal when they represent an actual solution. If we assume that the dissipation function as well as all the other functions involved are continuous and have continuous derivatives, D is positive semidefinite and D satisfies the relation

$$\frac{\partial D}{\partial \dot{x}_k} \dot{x}_k = f(D), \tag{5.2}$$

then D is quasi-homogeneous and f is an arbitrary function. ZIEGLER [3] has defined the following quantities

$$\Phi = \int \frac{D}{f(D)} dD, \tag{5.3}$$

$$X_k^i = \frac{\partial \Phi}{\partial \dot{x}_k}, \tag{5.4}$$

$$\psi = \int \frac{D'}{g(D')} \alpha D', \tag{5.5}$$

$$\dot{x}_k = \frac{\partial \psi}{\partial X_k^i}. \tag{5.6}$$

Also ZIEGLER [3] has shown that if the velocities $\dot{x}_k$ can be defined, then

$$\Phi + \psi = \sum_k X_k^i \dot{x}_k. \tag{5.7}$$

Now we will derive Eq. (5.7) from GYARMATI's principle [12]. GYARMATI [12] has given a global form of the universal principle as

$$\delta \int_V [\sigma - (\psi + \Phi)] \mathrm{d}V = 0. \tag{5.8}$$

Therefore, the corresponding Lagrangian function is given by

$$L = \sigma - (\psi + \Phi), \tag{5.9}$$

where

$$\sigma = \sum_i X_i J_i = \sum_k X_k^i \dot{x}_k \,. \tag{5.10}$$

Thus it can be seen that Eqs (5.7) and (5.9) are equal in a local case, and under these conditions the ZIEGLER principle is derivable from GYARMATI's principle. It is necessary to define the velocities but in general this is not possible for continuous media. However, in the case of non-continuous media, ONSAGER [1] and ONSAGER and MACHLUP [24] have shown that ONSAGER's 'α_k' parameters and the fluxes can be obtained from the internal parameters by means of the time derivative operator d/dt, *i.e.* for example

$$J_k \equiv \frac{\mathrm{d}}{\mathrm{d}t}\alpha_k \equiv \frac{\mathrm{d}}{\mathrm{d}t}\begin{pmatrix}\text{internal parameter}\\ \text{or}\\ \text{state variable}\end{pmatrix}. \tag{5.11}$$

Thus it can be seen that in such cases the x_k parameters of ZIEGLER [3] are identical with the α_k parameters of ONSAGER. Also VOJTA [25, 26] applied the flux representation of ONSAGER [1] to continua and non-local media. Thus with some difficulty ZIEGLER's representation in Eq. (5.7) can be applied to continua with the aid of a functional formalism. Also in section 2 of this paper it has been shown that the GYARMATI principle [12, 27] is equivalent to the local potential principle. Therefore, it can also be seen that in this special case ZIEGLER's principle is derivable from the local potential principle. Moreover, the similarity in these principles is the occurrence of two types of functions (T and T^0, where T^0 is at the average state).

FINLAYSON and SCRIVEN [28] have critically examined the mathematical formulation of the variational principles of BIOT [29] and of GLANSDORFF and PRIGOGINE [18]. It has been shown that the above variational principles are outside the scope of classical variational calculus and are closely related to the method of weighted residuals. While agreeing with the observation of the above authors, it is felt that the physical meaning of the GLANSDORFF—PRIGOGINE [18] method has a definite advantage over that of the method of weighted residuals and its formulation has led to the extension of classical variational calculus to non-linear and quasi-linear problems and also to problems where convection or inertia effects exist.

Doubtless, formulations (2.1) and (2.8) can be considered the most general principles of the dissipative process. Also Eq. (2.8) is very closely related to VOJTA's [25] principle. But the special advantage of the local potential over other variational principles is that it is supported by the fluctuation theory. It may be stated that the very existence of the local potential expresses the stability of an arbitrary macroscopic state with respect to small fluctua-

tions. Moreover, KRUSKAL [30] has used the local potential to construct a satisfactory condition for convergence and, owing to the existence of two types of functions, it can be applied in practice more easily than other variational principles. The use of local potentials has proved to be of real practical interest because it opens the way to the use of variational techniques in most non-linear and quasi-linear problems.

*

The authors are grateful to Prof. I. GYARMATI for many useful suggestions and for bringing to the notice of the authors some very recent literature. The authors thank Dr. R. R. AGGARWAL for his interest in the work, and the Director of Defence Science Laboratory for his permission to publish this paper.

REFERENCES

1. ONSAGER, L.: Phys. Rev., **37,** 405 (1931)
2. BIOT, M. A.: Phys. Rev., **97,** 1463 (1955)
3. ZIEGLER, H.: Some Extremum Principle in Irreversible Thermodynamics with Application to Continuum Mechanics. Progress in Solid Mechanics, Vol. IV. Edited by J. N. Sheddon and R. Hill. North-Holland Publishing Co., Amsterdam 1963
4. PRIGOGINE, I.: Introduction to Thermodynamics of Irreversible Processes, Charles C. Thomas Publisher, Springfield, Illinois, U.S.A. 1955
5. ZIEGLER, H.: Ing. Arch., **30,** 410 (1961)
6. ZIEGLER, H.: Ing. Arch., **31,** 317 (1962)
7. GYARMATI, I.: Acta Chim. Acad. Sci. Hung., **43,** 353 (1965)
8. GLANSDORFF, P., PRIGOGINE, I.: Physica, **30,** 351 (1964)
9. BIOT, M. A.: Variational Principles in Heat Transfer. A Unified Lagrangian Analysis of Dissipative Phenomena, Oxford Clarendon Press 1970
10. GYARMATI, I.: Z. Phys. Chem., **239,** 133 (1968)
11. GYARMATI, I.: Zhurn. Fiz. Khim., **39,** 1489 (1965)
12. GYARMATI, I.: Ann. Phys., **23,** 353 (1969)
13. VERHÁS, J.: Z. phys. Chem., **234,** 226 (1967)
14. BÖRÖCZ, SZ.: Proc. Conference on Some Aspects of Physical Chemistry, Budapest 1966
15. VERHÁS, J.: Proc. 2nd Conference on Applied Physical Chemistry, Vol. 2. Akadémiai Kiadó, Budapest 1971
16. SÁNDOR, J.: Zhurn. Fiz. Khim., **46,** 2727 (1970)
17. SÁNDOR, J.: Acta Chim. Acad. Sci. Hung., **67,** 303 (1971)
18. PRIGOGINE, I., GLANSDORFF, P.: Physica, **31,** 1242 (1965)
19. BIOT, M. A.: J. Aerospace Sci. 568 (1962)
20. GLANSDORFF, P.: Nonequilibrium Thermodynamics, Variational Techniques and Stability. Edited by Donnely, Herman and Prigogine. University of Chicago Press, Chicago 1966
21. PRIGOGINE, I.: Nonequilibrium Thermodynamics, Variational Techniques and Stability. Edited by Donnely, Herman and Prigogine. University of Chicago Press, Chicago 1966
22. HAYS, D. F.: Nonequilibrium Thermodynamics, Variational Techniques and Stability. Edited by Donnely, Herman and Prigogine, University of Chicago Press, Chicago 1966
23. KUMAR, I. J.: Int. J. Heat and Mass Transfer, 1971
24. ONSAGER, L., MACHLUP, S.: Phys. Rev., **91,** 1505 (1953)
25. VOJTA, G.: Acta Chim. Acad. Sci. Hung., **54,** 55 (1967)
26. VOJTA, G., ABHANAL, DT.: Akad. Wiss., **1,** 183 (1967)
27. GYARMATI, I.: Nonequilibrium Thermodynamics, Field Theory and Variational Principles. Springer-Verlag, Berlin—Heidelberg, New York 1970
28. FINLAYSON, B. A., SCRIVEN, L. E.: J. Heat Mass Transfer **10,** 799 (1967)
29. BIOT, M. A.: J. Aerospace Sci., **24,** 857 (1957)
30. KRUSKAL, M.: Nonequilibrium Thermodynamics, Variational Techniques and Stability. Edited by Donnely, Herman and Prigogine. University of Chicago Press, Chicago 1966.

I. J. KUMAR
L. N. GUPTA
Defence Science Laboratory, Delhi-6, India.

Acta Chimica Academiae Scientiarum Hungaricae, Tomus 76 (4), pp. 359–374 (1973)

BETRACHTUNGEN ZUM KOALESZENZPROZESS ZWISCHEN UNGLEICHARTIGEN TEILCHEN*

H. SONNTAG

(Deutsche Akademie der Wissenschaften zu Berlin, Zentralinstitut für Physikalische Chemie Berlin-Adlershof)

Eingegangen am Mai 2, 1972

Die verschiedenen Mechanismen der Koaleszenzstabilität im Dreiphasensystem wurden für mischbare und nichtmischbare disperse Phasen vom theoretischen Standpunkt aus betrachtet und durch Experimente an verschiedenartigen dispersen Systemen experimentell geprüft. Im Gegensatz zum Koaleszenzprozeß gleichartiger Teilchen können ungleichartige Teilchen gegen Koaleszenz im thermodynamischen Sinne stabil sein. Bei der thermodynamischen Betrachtung würde man diese Stabilität mit einer Zunahme der freien Grenzflächenenergie in Verbindung bringen, vom molekularphysikalischen Standpunkt dagegen durch die Vorzeichenänderung der Dispersionskräfte. Für die Erklärung der koaleszenzstabilisierenden Wirkung von Adsorptionsschichten werden zwei Mechanismen erörtert.

Während man zur Stabilisierung von Emulsionen und Schäumen unbedingt grenzflächenaktive oder makromolekulare Stoffe benötigt, kann man Feststoffdispersionen auch ohne grenzflächenaktive Zusätze stabilisieren. Bei der Wechselwirkung von ungleichartigen Teilchen, z. B. Gasbläschen auf Feststoffpartikeln in einer Flüssigkeit, kann man Koaleszenzstabilität je nach dem betrachteten System sowohl mit und ohne Adsorptionsschichten erreichen.

Die Wirkungsweise grenzflächenaktiver und makromolekularer Stoffe ist Gegenstand zahlreicher Untersuchungen gewesen, wobei die meisten Autoren versuchen, eine Korrelation zwischen den mechanischen Eigenschaften der Adsorptionsschichten und ihren Stabilisierungsvermögen zu finden [1—5]. Als Meßgröße verwendet man dabei meistens die Oberflächenscherviskosität oder die Scherfestigkeit, die man an ausgedehnten Phasengrenzen ermittelt.

Aus den publizierten Ergebnissen kann man entnehmen, daß in vielen Fällen eine hohe Scherfestigkeit der Adsorptionsschicht auch mit einer guten stabilisierenden Wirkung dieser Stoffe verbunden ist. Auf der anderen Seite gibt es dagegen auch eine Reihe von Tensiden, z. B. die Alkalisalze der Fettsäuren, die trotz äußerst geringer Scherfestigkeit sehr gute Stabilisatoren sind. Man hat deshalb in den letzten Jahren auch andere Methoden zur Klärung des Stabilsierungsvermögens grenzflächenaktiver Stoffe herangezogen, und zwar wurde die Oberflächenelastizität aus der Kapillarwellendämpfung [6, 7],

* Zum Teil vorgetragen auf der 1. Kolloidchemischen Konferenz, 24—26. Mai, 1971, Mátrafüred, Ungarn.

nach der Methode der Blasenschwingungen [8] und aus der Änderung der Filmspannung bei Expansion gemessen [9], außerdem wurde die Kompressions-Dilatationsviskosität [7] ermittelt. Alle diese Versuche ergaben, daß weder die Elastizität noch die Dilatationsviskosität von Adsorptionsschichten an ausgedehnten Phasengrenzen in Beziehung zur Schaum- oder Emulsionsstabilität stehen. Die Experimente ergaben weiterhin, daß zwischen dem Verlauf der Elastizitäts-Oberflächenkonzentrations-Isotherme von unlöslichen (z. B. Fettsäuren) und löslichen grenzflächenaktiven Stoffen keine Unterschiede bestehen, obwohl nur die letzteren als Stabilisatoren geeignet sind. Das legt nahe, daß man die Vorstellungen über die stabilisierende Wirkung von Tensiden neu durchdenken muß. Es soll deshalb die Frage aufgeworfen werden, ob man tatsächlich aus den Eigenschaften einer einzelnen Adsorptionsschicht auf die Wechselwirkung zweier Teilchen mit je einer Adsorptionsschicht rückschließen darf. Um das zu überprüfen, wurden von uns zahlreiche Koaleszenzuntersuchungen zwischen ungleichartigen Teilchen durchgeführt, weil man dabei die Wechselwirkung zweier Teilchen studieren kann, von denen nur eines eine Adsorptionsschicht trägt bzw. die unterschiedliche Adsorptionsschichten aufweisen.

Koaleszenzmechanismen

Zum leichteren Verständnis des Koaleszenzvorganges im dispersen Dreiphasensystem sollen zunächst die Koaleszenzmechanismen erörtert werden. Der einfachste Fall liegt vor, wenn beide Teilchensorten miteinander völlig mischbar sind (vgl. Abb. 1), denn die Koaleszenz führt hier unter Abnahme der Oberfläche zu einem neuen Teilchen. Da die Grenzflächenspannung bei den meisten Mischungen infolge der Grenzflächenaktivität einer der beiden Substanzen geringer ist als die der idealen Mischung, wird die Koaleszenz außerdem von einer Abnahme der Grenzflächenspannung begleitet. Anders liegen die Verhältnisse bei der Wechselwirkung zweier nicht mischbarer Teilchen. Hier sind verschiedene Fälle denkbar, und zwar das Teilchen 1 spreitet vollständig auf der 2. Partikel und inkludiert dieses (vgl. Abb. 2). Da die totale Oberfläche dabei zunimmt, kann der Prozeß nur freiwillig verlaufen, wenn die Grenzflächenspannungsänderung $\sigma_{21}—\sigma_{20}$ die Zunahme der freien Enthalpie mit der Oberflächenvergrößerung kompensiert. Bei unvollständiger Spreitung wird sich ein Zustand einstellen können, der in Abb. 3 schematisch dargestellt ist. Als Grenzfall muß man Abb. 4 ansehen, wenn sich nur noch ein punktförmiger Kontakt einstellt. Wesentlich ist nach unserer Meinung für die Koaleszenz, daß der Flüssigkeitsfilm des Dispersionsmediums zwischen den beiden Teilchen zerreißt, unabhängig davon, wie groß die Berührungsfläche zwischen den beiden Teilchen ist.

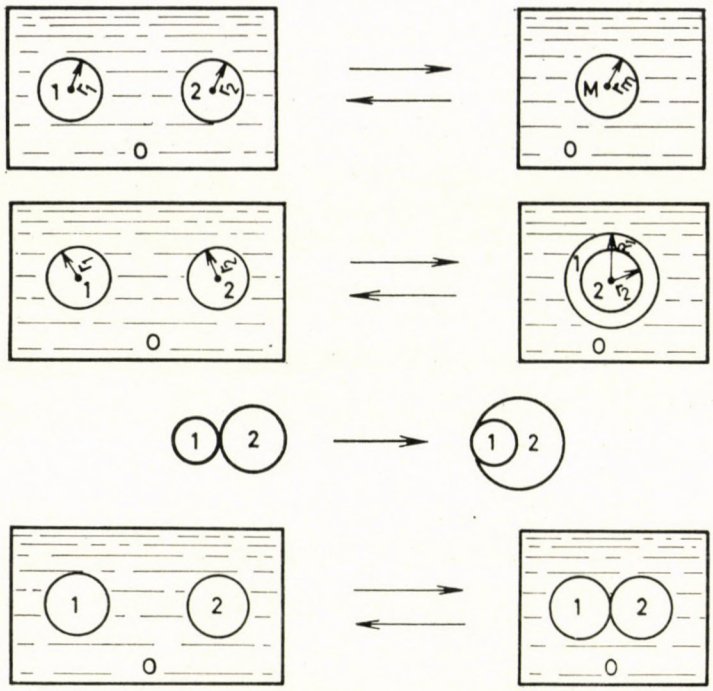

Abb. 1 - 4

Koaleszenzmessungen im System Quecksilber/Öl mit Tensid/Wasser

In einer früher beschriebenen Modellapparatur [10] werden ein Quecksilbertröpfchen mit einem Wassertröpfchen zur Wechselwirkung gebracht, die durch ein Ölmedium getrennt sind. In der Ölphase wird der grenzflächenaktive Stoff aufgelöst. Wasser- und Quecksilbertröpfchen im apolaren Medium stellen einen Kondensator dar und durch die sprunghafte Änderung der Kapazität beim direkten Kontakt von Quecksilber und Wasser kann man den Koaleszenzvorgang leicht verfolgen.

Gibt man der Ölphase als grenzflächenaktiven Stoff Ölsäure zu, so ist bekannt, daß die Ölsäure die Koaleszenz von Wassertröpfchen untereinander nicht verhindern kann [11]. Sie ist für W/O-Emulsionen kein Emulgator. Auf der anderen Seite vermag Ölsäure an der Quecksilber/Öl-Phasengrenze je nach der verwendeten Konzentration sehr dicke Adsorptionsschichten bis zu 40 nm auszubilden, die Quecksilber/Öl-Emulsionen hervorragend stabilisieren und eine hohe mechanische Scherfestigkeit aufweisen [12]. Bei der Wechselwirkung eines Wassertröpfchens mit einem Quecksilbertröpfchen in

ölsäurehaltigem Oktan bildet sich nur an einer der beiden Phasengrenzen eine dicke Adsorptionsschicht hoher Scherfestigkeit aus. Diese Adsorptionsschicht ist nicht in der Lage, die Koaleszenz des Wassers auf dem Quecksilber zu verhindern, auch nicht bei sehr hohen Ölsäurekonzentrationen. Die Koaleszenz zwischen Wassertropfen und Quecksilber ist am plötzlichen Abfall der Kapazität leicht zu erkennen. Man kann daraus schlußfolgern, daß die hohe Scherfestigkeit einer mehrmolekularen Adsorptionsschicht kein ausreichendes Stabilitätskriterium ist.

Koaleszenz im System Polymer/Wasser mit Tensid/Öl

Schon vor einigen Jahren hatten wir uns mit dem Waschvorgang beschäftigt [13] und dabei das Koaleszenzverhalten von polaren und unpolaren Öltropfen auf verschiedenartigen Polymerfolien studiert. Die Ergebnisse dieser Untersuchungen sind für die Betrachtungen über die Ursachen der Koaleszenzstabilität wieder interessant. Vergleicht man nämlich die Konzentrationen ein und desselben grenzflächenaktiven Stoffes, die man zur Stabilisierung von Öltröpfchen untereinander und von Öltröpfchen gegen die Polymerphase benötigt (Tab. I), so sieht man ebenfalls deutlich, daß eine stabile Adsorptionsschicht an nur einer Phasengrenze — in diesem Fall an der Öl/Wasser-Phasengrenze — nicht die Koaleszenz verhindern kann. Die Stabilisierungskonzentra-

Tabelle I

Stabilisierungskonzentration von Tensiden für Cyclohexantröpfchen untereinander und gegen verschiedene Polymerphasen

System	c_s Mol/l
C_6H_{12}/H_2O + NP 20* /C_6H_{12}	$2 \cdot 10^{-5}$
C_6H_{12}/H_{20} + NP 20/Polyamid	$1{,}4 \cdot 10^{-4}$
C_6H_{12}/H_2O + 20/Polyester	$1{,}2 \cdot 10^{-4}$
C_6H_{12}/H_2O + NP 20/Polyäthylen	instabil
C_6H_{12}/H_2O + NP 20/Teflon	$1{,}5 \cdot 10^{-4}$
C_6H_{12}/H_2O + NaDS**/C_6H_{12}	$4 \cdot 10^{-5}$
C_6H_{12}/H_2O + NaDS/Polyamid	$5 \cdot 10^{-3}$
C_6H_{12}/H_2O + NaDS/Polyester	$5 \cdot 10^{-3}$
C_6H_{12}/H_2O + NaDS/Polyäthylen	instabil
C_6H_{12}/H_2O + NaDS/Teflon	$7 \cdot 10^{-3}$

* NP 20 Nonylphenoläthylenoxidaddukt 20
** NaDS Na-dodecylsulfat-1

tion der Tenside für Öltröpfchen gegen Polymer liegen um eine bzw. zwei Größenordnungen höher als für die Öltröpfchen allein. Gegen Polyäthylen können die beiden verwendeten Tenside überhaupt keine Stabilität erzeugen. Die Stabilisierungskonzentration der beiden Tenside gegen die Polymeren liegt in der Größenordnung der kritischen Konzentration der Mizellbildung (cmc für NP 20 = $1{,}4 \cdot 10^{-4}$ Mol/l, cmc für NaDS = $8 \cdot 10^{-3}$ Mol/l).

Zerstörung von W/O-Emulsionen durch Deemulgatoren

Der Prozeß der chemischen Deemulgierung zeigt nach unserer Meinung ebenfalls sehr deutlich, daß die Koaleszenzstabilität stets an das Vorhandensein zweier Adsorptionsschichten (d. h. an den beiden wechselwirkenden Teilchen je eine) einer sogenannten »Sandwich«schicht gebunden ist. Denken wir z. B. an die Wasser/Erdöl-Emulsionen, in der die Wassertröpfchen durch Feststoffpartikeln von etwa 25 nm Teilchengröße stabilisiert werden [14, 15]. Bekanntlich kann man diese Emulsionen zerstören, wenn man im Erdöl deemulgatorhaltiges Wasser emulgiert. Der Deemulgator ist stärker grenzflächenaktiv als der Stabilisator in der Erdölphase und verhindert somit die Anreicherung des Stabilisators an der Wasser/Öl-Phasengrenze. Diese Wassertröpfchen, die keine stabilisierende Adsorptionsschicht aufweisen, da der Deemulgator W/O-Emulsionen nicht zu stabilisieren vermag, können ohne Schwierigkeiten mit den stabilisierten Wassertröpfchen koaleszieren. Der Grund dafür ist wieder, daß eine »formal stabile« Adsorptionsschicht für die Koaleszenzstabilisierung zweier Teilchen nicht ausreichend ist.

Kompression von Sandwichschichten

Die oben genannten Beispiele machen es verständlich, daß die Untersuchungen der mechanischen Eigenschaften an ausgedehnten Phasengrenzen zur Erklärung der Koaleszenz nicht zum Erfolg führen kann. Mit anderen Worten ausgedrückt, die Entstehung eines Loches in der Adsorptionsschicht als Ursprung des Zerreißens kann nicht der entscheidende Schritt der Koaleszenz sein. Die Aufgabe besteht vielmehr darin, nach Methoden zu suchen, mit denen man die mechanischen Eigenschaften der Sandwichschichten bestimmen kann. An Quecksilbermodelldispersionen in Ölmedien [16] kann man die Sandwichschichten zwischen zwei Tröpfchen einfach dadurch komprimieren, daß man ein äußeres elektrisches Feld an die Tröpfchen anlegt und die Kompression der Schicht kapazitiv mißt. Aus der reversiblen Dickenänderung bei Kompression durch das elektrische Feld berechneten wir die Elastizität senkrecht zur Phasengrenze. Für polymolekulare »Sandwich«-schichten aus Ölsäure erhielten wir je nach der verwendeten Ölsäurekonzentra-

tion stabile Schichtdicken von 20 und 80 nm, mit einer dickenunabhängigen Elastizität von 10^5 dyn/cm^2 und für extrem dünne Ölsäureschichten von 5,4 nm Dicke einen Wert von 10^6 dyn/cm^2. Zwischen 5,4 nm und 20 nm konnten keine koaleszenzstabilen Schichten erhalten werden. Das ist verständlich, wenn man annimmt, daß nur die extrem dünnen, die sogenannten schwarzen Filme eine so hohe Elastizität aufweisen, während alle dickeren Schichten einen Wert von 10^5 dyn/cm^2 besitzen. Die elastischen Kräfte senkrecht zur Phasengrenze müssen nämlich die Dispersionsanziehungskräfte kompensieren können. Nur wenn sie größer als diese sind, können sie die weitere Annäherung und damit die Koaleszenz verhindern. Der Vergleich mit den Dispersionskräften zwischen den Teilchen [16] zeigt, daß unterhalb 20 nm Abstand der Teilchen die Dispersionskräfte pro Flächeneinheit größer als 10^5 dyn/cm^2 werden. Daraus resultiert, daß kleinere Adsorptionsschichten nicht stabil sein können, was experimentell auch gefunden wird.

Eine mögliche Ursache der Koaleszenzstabilität von Adsorptionsschichten grenzflächenaktiver oder makromolekularer Stoffe besteht also darin, daß sie bei Druckbeanspruchung infolge der zwischenpartikularen Kräfte sich elastisch verformen, so daß durch Kompression der Moleküle oder durch gegenseitiges Durchdringen der orientierten Adsorptionsschichten eine Abstoßung stattfindet. Das ist aber nur eine Möglichkeit der koaleszenzstabilisierenden Wirkung von Adsorptionsschichten. Betrachtet man an Stelle von Quecksilber/Öl-Emulsionen Wasser/Öl-Emulsionen, so kann man ebenfalls wieder die Dickenänderung als Funktion eines äußeren Druckes untersuchen. Für Wassertröpfchen, die mit Span 80 stabilisiert wurden, erhielten wir beständige Schichten von etwa 40 nm Dicke. Bei einer äußeren Kompression kann man nur eine geringe Dickenänderung nachweisen, bis plötzlich bei einem bestimmten Druck die Sandwichschicht zerstört wird. Die Ursache liegt nach unserer Meinung darin begründet, daß die Tensidadsorptionsschicht dem äußeren Druck ausweicht und in die wäßrige Phase abgedrängt wird, d. h. die von außen angelegte Energie entspricht der Desorptionsenergie der Alkylreste aus der Ölphase und der Umorientierungsenergie der Wassermoleküle beim Einbringen der Alkylreste in die Wasserphase.

Wenn man diesen Mechanismus als zweite Möglichkeit der Koaleszenzstabilität von Adsorptionsschichten annimmt, erhält man eine zwanglose Deutung der Bancroft'schen Regel, nach der ein Tensid immer die dispersen Teilchen stabilisiert, in denen es nicht löslich ist. Die Bancroft'sche Regel kann man dagegen nicht erklären, wenn man die alte Vorstellung zu Grunde legt, daß die Ursache der Stabilität auf der Ausbildung einer gelartigen Adsorptionsschicht mit hoher Scherfestigkeit beruht. In diesem Falle sollte es nämlich unwichtig sein, ob sich die gelartige Schicht vom Dispersionsmedium her oder von der dispersen Phase her ausbildet und somit müßten beide Emulsionstypen stabil sein.

Thermodynamisch stabile Systeme

Eine dritte Möglichkeit der Emulsionsstabilität hat man vorzulegen, wenn das Tensid in der Öl- und Wasserphase etwa in gleichem Maße löslich ist. In diesem Fall wird bei geeigneter Tensidkonzentration die Dispersionsenergie so gering, daß zwischen den Tröpfchen praktisch keine Dispersionskräfte mehr auftreten. Man kann bei diesem Beispiel von einer quasithermodynamischen Stabilität sprechen.

Eine echte thermodynamische Stabilität kann man nur bei der Wechselwirkung ungleichartiger Teilchen beobachten.

Während der Koaleszenz gleichartiger Teilchen verringert sich die Oberfläche, sie stellt somit einen freiwillig unter Abnahme der freien Enthalpie verlaufenden Prozeß dar. Anders liegen die Verhältnisse bei der Koaleszenz ungleichartiger Teilchen. Dieser Vorgang muß nicht von einer Abnahme der freien Enthalpie begleitet werden, einmal weil dabei die Grenzfläche nicht zwangsläufig verkleinert werden muß und zum anderen, weil die Änderung der Grenzflächenspannungen zu einer Vergrößerung der freien Enthalpie führen kann. Flüssigkeitsfilme zwischen verschiedenartigen dispersen Teilchen können somit in einem thermodynamisch stabilen Zustand vorliegen.

Betrachten wir den Koaleszenzvorgang zwischen ungleichartigen Teilchen im System dreier nicht miteinander mischbarer Phasen, wie das in Abb. 4 schematisch angedeutet ist. Die Größe der Kontaktfläche kann dabei je nach der Deformierbarkeit der dispersen Teilchen in weiten Grenzen schwanken. Solange die Teilchen nicht aufeinander spreiten, kann man die Flächenänderung bei der Koaleszenz vernachlässigen. Die Bedingung für thermodynamische Stabilität läßt sich dann durch die Ungleichung darstellen:

$$\sigma_{12} > \sigma_{20} + \sigma_{10}$$

Drei charakteristische Beispiele, an denen von uns experimentelle Arbeiten durchgeführt wurden, sollen nachfolgend analysiert werden.

a) *Wechselwirkung im System Polymer/Wasser/Öl-Modell für das Schmutztragevermögen*

Verwenden wir als Polymerphase Stoffe wie Polyamid oder Polyester [9], so ist die Grenzflächenspannung zur Ölphase (σ_{12}) sehr klein und nur wenig von 0 verschieden, so daß immer Koaleszenz eintritt. Eine Stabilisierung ist, wie oben ausgeführt wurde, nur mit Tensiden möglich. Bei polaren Polymeren, wie z. B. Cellulosederivaten, wird die Grenzflächenspannung σ_{10} sehr klein und wässrige Filme auf dieser Polymerphase sind thermodynamisch stabil wenn $\sigma_{12} > \sigma_{20}$ ist.

b) *Wechselwirkung im System Quecksilber/Öl/Wasser*

Für die Auswahl dieses Systems waren verschiedene Gründe maßgebend, einmal standen uns zu den dazugehörigen symmetrischen Systemen,

Quecksilber/Öl- und Wasser/Öl-Emulsionen, ausreichend Versuchsergebnisse zur Verfügung und zum anderen gestatten die hohen Grenzflächenspannungen σ_{12} und σ_{10} eine breite Variierung.

Durch die Wahl des Ölmediums und durch Zugabe von Tensiden, die bevorzugt ander Phasengrenze Quecksilber/Öl adsorbiert werden, kann man die Grenzflächenspannung so verändern, daß thermodynamisch stabile Ölfilme zwischen Wasser und Quecksilbertropfen auftreten, die bei jeder Dicke beständig bleiben. Die Stabilitätsbedingung lautet:

$$\sigma_{Hg/H_2O} > \sigma_{Hg/Öl} + \sigma_{H_2O/Öl}$$

σ_{Hg/H_2O} = Grenzflächenspannung Hg gegen Wasserphase

$\sigma_{H_2O/Öl}$ = Grenzflächenspannung Wasser gegen Ölphase

$\sigma_{Hg/Öl}$ = Grenzflächenspannung Hg gegen Ölphase

Die Grenzflächenspannung nach dem Koaleszenzvorgang, d. h. im obigen Beispiel Quecksilber mit adsorbierter Tensidschicht gegen Wasser, kann man direkt messen. Die Grenzflächenspannungen Öl/Wasser wurden nach der Methode des hängenden Tropfens oder nach de Nouy bestimmt. Die Grenzflächenspannung Hg/Öl bzw. Hg mit Monofilm/Wasser ermittelten wir nach einer in [20] angegebenen modifizierten Wilhelmymethode mittels einer amalgamierten Platinplatte. Der adsorbierte Monofilm bleibt nach dem Absaugen der tensidhaltigen Ölphase an der Quecksilberoberfläche zurück. Die mit der

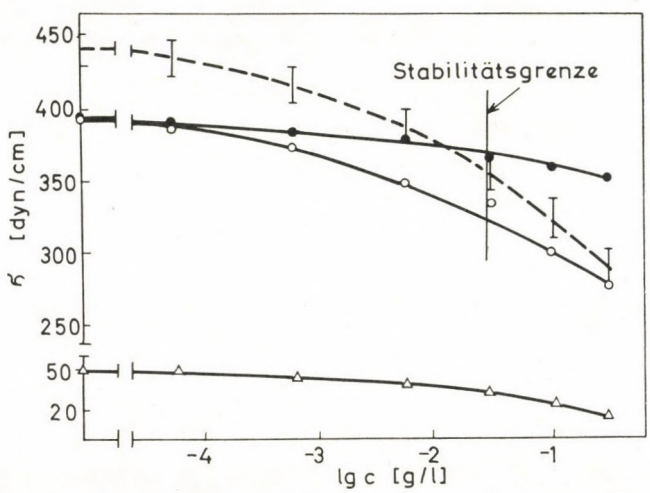

Abb. 5. σ-c-Kurven von Ölsäure-Monoglyzerid in Oktan. ● σHg + Monofilm/H_2O, ○ σHg/Oktan, △ σH_2O/Oktan, − − − σH_2O/Oktan + σHg/Oktan

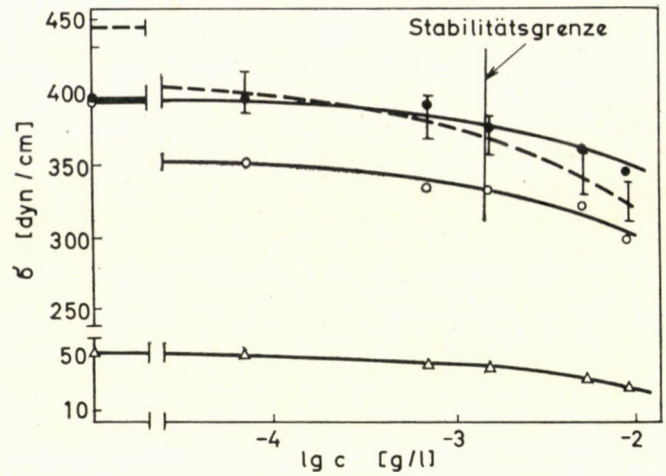

Abb. 6. σ-c-Kurven von Span 80 in Oktan. ● σHg + Monofilm/H_2O, ○ σHg/Oktan, △ σH_2O/Oktan, – – – σH_2O/Oktan + σHg/Oktan

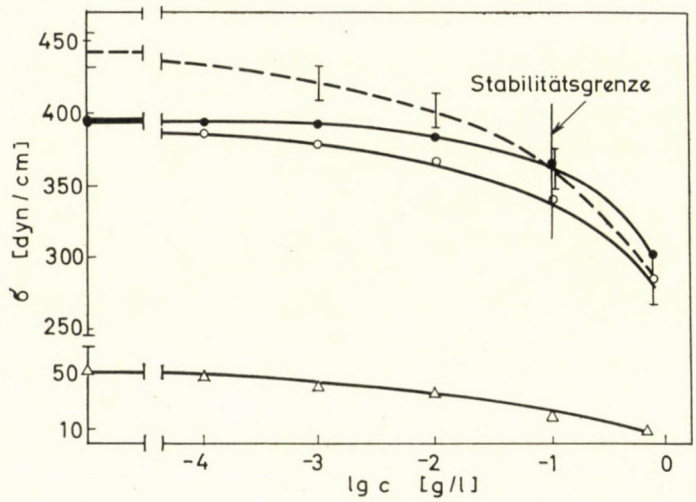

Abb. 7. σ-c-Kurven von Span 65 in Oktan, ● σHg + Monofilm/H_2O, ○ σHg/Oktan, △ σH_2O/Oktan, – – – σH_2O/Oktan + σHg/Oktan

Adsorptionsschicht bedeckte Hg-Oberfläche wurde danach mit der wäßrigen $5 \cdot 10^{-2}$ *n*KCl-Lösung überschichtet und in üblicher Weise die Grenzflächenspannung bestimmt.

Aus den folgenden Diagrammen, in denen die einzelnen Grenzflächenspannungen des Quecksilber/Öl/Wasser-Systems als Funktion des Tensidgehaltes dargestellt sind, geht hervor, daß eine Stabilisierung im thermodynamischen Sinne möglich ist, wenn Tenside der Ölphase zugesetzt werden (Abb. 5—7). Bei geringen Tensidkonzentrationen ist das System thermody-

namisch instabil, denn die Summe der Grenzflächenspannungen Quecksilber/Öl und Wasser/Öl, die als gestrichelte Kurve in den Diagrammen eingezeichnet wurde, liegt unterhalb der Grenzflächenspannungskurve Quecksilber mit Monoschicht/Wasser. Steigern wir die Tensidkonzentration, so schneiden sich die beiden Kurven. Das System erfüllt die oben angegebene Ungleichung, d. h. es wird im thermodynamischen Sinne stabil.

Vergleichen wir die durch die Grenzflächenspannungsmessungen ermittelten Stabilisierungskonzentrationen der Tenside mit den am Versuchsmodell erhaltenen, die in den Diagrammen mit einem senkrechten Strich dargestellt

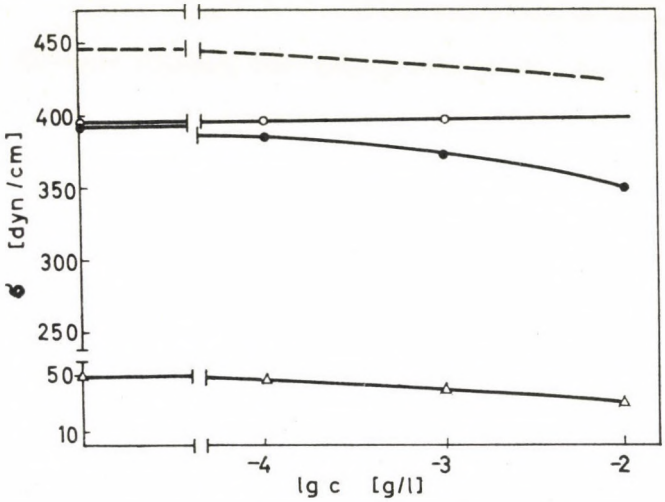

Abb. 8. σ-c-Kurven von Natriumdecylbenzolsulfonat in Wasser mit Oktan als Ölphase. ● σHg/Wasser, ○ σHg/Oktan, △ H_2O/Oktan, — — — σH_2O/Oktan + σHg/Oktan

sind, so stellen wir im Rahmen der Fehlergrenze Übereinstimmung fest. Daraus folgt, daß zumindest bei den Stabilisierungskonzentrationen das System Quecksilber/Öl/Wasser im thermodynamischen Sinne stabil ist, ob bei höheren Tensidkonzentrationen noch zusätzlich eine Koaleszenzstabilisierung durch stabile Adsorptionsschichten auftritt, kann durch das Verhalten bei der Komprimierung der stabilen Filme bzw. der Adsorptionsschichten durch Anlegen zusätzlicher Anziehungskräfte, z. B. durch ein äußeres elektrisches Feld, entschieden werden [10].

Eine Stabilisierung von Heterosystemen ist prinzipiell nicht nur durch Zugabe von Tensiden in die Ölphase möglich, sondern kann auch durch eine tensidhaltige wäßrige Phase erreicht werden.

Aus den Abb. 8 und 9 geht jedoch hervor, daß die von uns gewählten Ölphasen bzw. tensidhaltigen Wasserphasen nach den gemessenen Grenzflächenspannungen und auch *de facto* nicht thermodynamisch stabil sind.

c) *Wechselwirkung im System Gas/Flüssigkeit I/Flüssigkeit II*

In der in Abb. 10 gezeigten Meßzelle wurden Cyclohexanfilme auf Wasser ausgebildet und die Dicke der Cyclohexanfilme interferometrisch [3] untersucht. In dem Glasring von 1 mm Stärke befindet sich eine Bohrung von 5 mm. Diese Bohrung wird zunächst völlig mit dem Ölmedium gefüllt. Zum Absau-

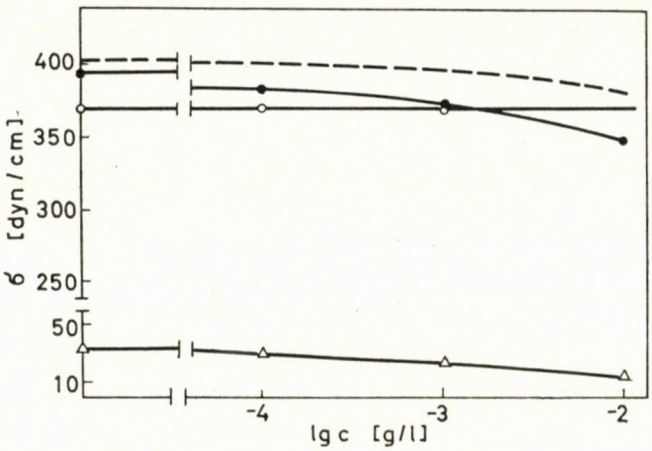

Abb. 9. σ-c-Kurven von Natriumdecylbenzolsulfonat in Wasser mit *m*-Xylol als Ölphase. ● σHg/Wasser, ○ σHg/Xylol, △ σH_2O/*m*-Xylol, — — — σH_2O/*m*-Xylol + σHg/*m*-Xylol

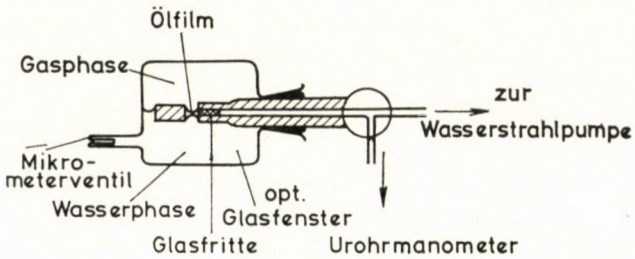

Abb. 10

gen des Ölfilmes und zum Erzeugen eines definierten Unterdrucks ist seitlich eine Kapillare angesetzt. Die Austrittsöffnung der Kapillare wird mit Glaspulver gefüllt und zu einer Fritte zusammengesintert. Von der Porenweite dieser Fritte hängt der Maximalwert des Unterdruckes ab und kann somit im gewünschten Maße eingestellt werden. Bevor mit dem Absaugen begonnen werden kann, wird die wäßrige Phase mit Hilfe des Mikroventils luftblasenfrei mit der Ölphase in Kontakt gebracht. Saugt man nun die Ölphase aus der Bohrung aus, entsteht ein kreisförmiger Ölfilm auf Wasser. Ein Unterdruck entsteht erst, wenn die gesamte Öffnung des Glasringes mit einem kreisförmigen Film bedeckt ist. Der Unterdruck wird mit einem U-Rohrmanometer gemessen.

Besondere Aufmerksamkeit schenkten wir den Heterosystemen Öl/Wasser/Luft und Wasser/Öl/Luft, weil zu den dazugehörigen symmetrischen Dispersionen, den Emulsionen und Schäumen ebenfalls zahlreiche Publikationen vorliegen.

Den Koaleszenzvorgang zwischen Gasbläschen und Öltröpfchen sowie zweier Öltröpfchen in wäßrigen Tensidlösungen untersuchten wir mit der in [21] beschriebenen Frittenzelle. Zur Messung der Schaumstabilität benutzten wir eine Glasringzelle, wie sie von SCHELUDKO und MITARBEITERN [22] beschrieben wird. Die Stabilität von Ölfilmen zwischen Wassertröpfchen und Gasphase studierten wir mit der in Abb. 10 skizzierten Meßzelle.

Je nach der verwendeten Ölphase sollten entweder Ölfime zwischen Gasblase und Wasserphase bzw. Wasserfilme zwischen Gasbläschen und Öltröpfchen thermodynamisch stabil sein können. Allerdings muß man bemerken, daß die Beurteilung der thermodynamischen Stabilität allein aus den Grenzflächenspannungsmessungen zu Fehlinterpretationen führen kann. Zum Beispiel stehen Benzol oder Ölsäurelinsen auf einer Wasseroberfläche mit einem Monofilm der jeweiligen Ölphase im Gleichgewicht, d. h. beim Zerreißen des instabilen Ölfilmes zwischen Gasblase und Wassertröpfchen verbleibt ein stabiler Monofilm. Man muß deshalb als Endwert der Grenzflächenspannung nach dem Zerreißen des Ölfilmes die Grenzflächenspannung — bzw. Filmspannung–Wasser + Ölmonofilm/Luft verwenden und diese sind natürlich aus Grenzflächenspannungsmessungen mit den üblichen Methoden nicht erhältlich. Bei Ölsäure kann man die Filmspannung auf einer Langmuirwaage direkt messen, bei organischen Lösungsmitteln dagegen ist die Messung so nicht durchführbar.

Zur Beurteilung, ob thermodynamische Stabilität vorliegt oder nicht, sollte man deshalb nicht von den Grenzflächenspannungswerten ausgehen, sondern sollte die Ursache auf die zwischenpartikularen Kräfte zurückführen. Im dispersen Dreiphasensystem können die Dispersionskräfte zwischen den verschiedenartigen Teilchen ihr Vorzeichen ändern, d. h. die Dispersionskräfte sind Abstoßungskräfte und *keine* Anziehungskräfte. Das ist molekularphysikalisch schwierig zu verstehen, folgt aber sowohl aus der makroskopischen als auch mikroskopischen Theorie der Dispersionkräfte zwischen Partikeln [22].

Für die Dispersionskräfte, bezogen auf die Flächeneinheit (Π_D), zwischen den plattenförmigen Teilchen 1 und 2 in einem Dispersionsmedium erhält man gemäß der makroskopischen Theorie von Lifschitz [1] für Abstände, die kleiner als die Londonsche Wellenlänge sind, die Näherungsgleichung:

$$\Pi_D = \frac{h}{16\pi^3 d^3} \int_0^\infty \frac{(\varepsilon_1-\varepsilon_0)(\varepsilon_2-\varepsilon_0)}{(\varepsilon_1+\varepsilon_0)(\varepsilon_2+\varepsilon_0)}\, d\xi \qquad (1)$$

h = Plancksches Wirkungsquantum, d = Abstand der beiden Teilchen, ε_1, ε_2 = komplexe Dielektrizitätskonstante der Teilchen, ε_0 = komplexe DK des Dispersionsmediums, ξ = imaginärer Teil der komplexen Kreisfrequenz.

Nach Gleichung 1 erhält man positive Dispersionskräfte, wenn die Differenzen der komplexen DK-Werte $(\varepsilon_1 - \varepsilon_0)$ und $(\varepsilon_2 - \varepsilon_0)$ ungleiches Vorzeichen besitzen.

Nach der mikroskopischen Theorie von Hamaker erhält man für die Wechselwirkung plattenförmiger Teilchen bei Abständen kleiner als die Londonsche Wellenlänge

$$\Pi_D = \frac{A^*}{6\pi d^3} \,. \tag{2}$$

A^* ist die zusammengesetzte Hamaker-Konstante. Die zusammengesetzte Hamaker-Konstante läßt sich darstellen durch

$$A^* = A_0 + A_{12} - A_{10} - A_{20}$$

A_0 ist die Hamaker-Konstante des Dispersionsmediums, A_{12} die Hamaker-Konstante für die beiden Teilchen und A_{20} und A_{10} charakterisieren die Wechselwirkung zwischen den Teilchen und dem Dispersionsmedium. Da in der Regel außer über den A_0-Wert keine Angaben über die Größe der Hamaker-Konstanten gemacht werden können, sind Voraussagen über die Vorzeichenänderung der Dispersionskräfte nur selten möglich. Aus den Untersuchungen über die Spreitung von Flüssigkeiten auf festen oder flüssigen Trägern ist bekannt, unter welchen Bedingungen sich multimolekulare Flüssigkeitsschichten ausbreiten. Von diesen Experimenten her kann aber nicht auf das Vorliegen positiver Dispersionskräfte geschlossen werden. Metastabile »dicke« Flüssigkeitsfilme erhält man auch in Gegenwart elektrostatischer Abstoßungskräfte, wie aus den Stabilitätsmessungen an Schaumfilmen und Emulsionströpfchen bekannt ist.

Die Gleichgewichtsdicke des Ölfilms auf Wasser ohne Veränderung des äußeren Druckes wird vom Krümmungsdruck Π_σ und von der Summe der Wechselwirkungskräfte, bezogen auf die Flächeneinheit, bestimmt:

$$\Pi_\sigma = \Sigma \Pi (d) .$$

Aus den Untersuchungen über die Stabilität in apolaren Medien ist bekannt, daß sowohl für Schaumfilme als auch für W/O-Emulsionen die elektrostatischen Kräfte vernachlässigbar klein sind, so daß wir die $\Sigma\Pi$ zunächst nur auf die van der Waals-Kräfte zurückführen wollen.

Bei Kenntnis des Krümmungsdruckes könnte man für einen d-Wert die Wechselwirkungskräfte ermitteln. Allerdings ist der Krümmungsdruck

in unserer Meßanordnung nicht konstant, sondern hängt vom Radius (R) der kreisförmigen Berührungsfläche ab.

Zum Nachweis, ob tatsächlich die Dispersionskräfte die dominierende Rolle spielen, wurde durch Veränderung des äußeren Druckes (Π_a) die Gleichgewichtsdicke variiert und geprüft, ob die Gleichung

$$\Pi_a + \Pi_\sigma = \frac{A^*}{6\pi d^3}$$

erfüllt ist (vgl. Abb. 11).

Die Ergebnisse zeigen, daß bis etwa 35 nm Schichtdicke, das entspricht Unterdrucken von etwa 2400 dyn/cm² abstoßende Dispersionskräfte die dominierende Rolle spielen. Aus der Steigung der Geraden errechnet man eine

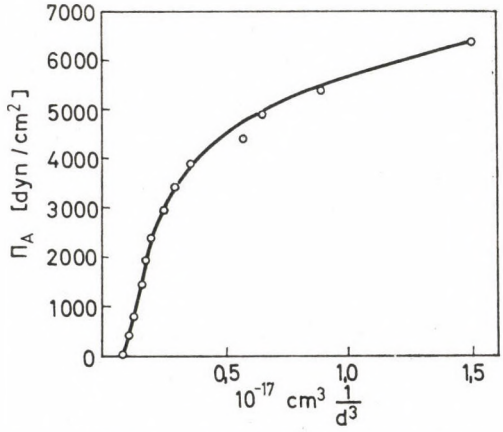

Abb. 11. Änderung der Gleichgewichtsdicke ($1/d^3$) mit dem angelegten Druck

Hamaker-Konstante von $3{,}8 \cdot 10^{-12}$ erg. Für unser Beispiel setzt sich die Hamaker-Konstante A^* zusammen aus der Differenz $A_{\text{Öl}} - A_{\text{Öl/Wasser}}$. Da die Dispersionskräfte positives Vorzeichen tragen, wird die Dispersionswechselwirkung allein von der gegenseitigen Wechselwirkung der Wasser- und Ölmoleküle bestimmt. Das ist zunächst überraschend, denn die Adhäsion zwischen Wasser und Ölphase ist sehr gering. Man entnimmt aber Abb. 11, daß bei kleineren Abständen die Gleichgewichtsdicke des Ölfilmes mit wachsendem Druck viel stärker abnimmt. Daraus muß man schlußfolgern, daß in diesem Dickenintervall zusätzliche Anziehungskräfte wirksam werden, über deren Natur wir aber zunächst keine Angaben machen können. Es konnte aber experimentell gezeigt werden, daß auch bei kleinen Abständen stets die Abstoßungskräfte überwiegen, d. h. daß keine sprunghaften Dickenänderungen — Zerreißdicken im symmetrischen Fall [23—25] — im Ölfilm auftreten.

Ähnlich wie in Cyclohexanfilmen auf Wasser existieren auch in Alkanfilmen bis zum Oktan auf Wasser positive Dispersionskräfte, bei den höheren Alkanen tritt eine Vorzeichenumkehr ein. Für Oktanfilme auf Wasser berechneten wir aus der Π_A-Abstandsisotherme eine Hamaker-Konstante von $4{,}8 \cdot 10^{-12}$ erg. Auch beim Oktan tritt keine Zerreißdicke auf, d. h. Oktanfilme sind ebenfalls bis zum Monofilm hinab stabil. In Ölfilmen von Aromaten wie Benzol oder Xylol treten ebenfalls wie bei den höheren Alkanen negative Dispersionskräfte auf.

Aus diesen Versuchen kann man gewisse Rückschlüsse auf die komplexe *DK* des Wassers ziehen. Vergleicht man die in Tab. II angegebenen statischen *DK*-Werte — für unpolarisierbare organische Verbindungen sind statische und komplexe *DK* gleich — mit der Vorzeichenänderung der Dispersionskräfte, so kann man feststellen, daß die komplexe *DK* des Wassers bei $\sim$2,0 liegen muß.

Tabelle II

Statische DK-Werte für verschiedene organische Lösungsmittel und Vorzeichen der Dispersionskräfte für diese Ölfilme auf Wasser

Lösungsmittel	stat. *DK*	Dispersionskräfte
Heptan	1,92	positiv
Octan	1,95	positiv
Decan	1,99	negativ
Cyclohexan	2,02	positiv
Decalin	2,13	negativ
Benzol	2,28	negativ

Entsprechend dem Wert der komplexen Dielektrizitätskonstanten für Wasser und Dekalin sollten Wasserfilme zwischen Gasphase und Dekalintropfen stabil sein, weil Dispersionsabstoßungskräfte auftreten. Auf der anderen Seite ist nach HARKINS [23] bekannt, daß Wasser auf Dekalin nicht spreitet, mit anderen Worten, es sollten keine Dispersionsabstoßungskräfte vorhanden sein. Diesen scheinbaren Widerspruch konnten wir auf experimentellem Wege aufklären. Gemäß der Theorie der zwischenpartikularen Kräfte erhält man bei größeren Schichtdicken Dispersionsabstoßungskräfte, im Unterschied jedoch zu den Untersuchungen mit Cyclohexan (vgl. Abb. 11) und Octan auf Wasser überwiegen bei kleinen Abständen die Anziehungskräfte, deren Natur wir noch nicht vollständig aufklären konnten, gegenüber den Dispersionsabstoßungskräften. Die Folge davon ist, daß Wasserfilme auf Dekalin nur in einem begrenzten Dickenintervall thermodynamisch stabil sind. Bei kleineren Filmdicken zerreißen dann die Wasserfilme. Diese Er-

scheinung ist sehr wichtig, weil sie zeigt, daß zur Berechnung der Wechselwirkung zwischen zwei Teilchen bei kleinen Abständen die ausschließliche Berücksichtigung von elektrostatischen und Dispersionskräften zu Fehlinterpretationen führt. Sie zeigt weiter, daß große Anstrengungen unternommen werden müssen, die Natur und Gesetzmäßigkeiten dieser zusätzlichen Anziehungskräfte aufzuklären.

LITERATUR

1. REHBINDER, P. A.: Kolloid-Z. (Moskau) **20,** 527 (1958)
2. REHBINDER, P. A., TRAPEZNIKOW, A. A.: Acta physicochim. URSS **9,** 257 (1938)
3. REHBINDER, P. A., TAUBMAN, A. B.: Kolloid-Z. (Moskau) **23,** 359 (1961)
4. BISWAS, A. B., HAYDON, D. A.: III. Int. Kongr. f. grenzfl. Stoffe. Bd. II, 580 (1960)
5. SONNTAG, H.: Z. physik. Chemie **225,** 284 (1964)
6. LUCASSEN, E. H., LUCASSEN, J.: Adv. Colloid Interf. Sci. **2,** 347 (1969)
7. KRETZSCHMAR, G., LUNKENHEIMER, K.: **74,** (1970) 1064
8. FRIESE, P.: Dissertation, Humboldt-Universität (1971)
9. PLATIKANOW, D., PANAJOTOW, I.: Ann. Univ. Sofia **60,** 85 (1968)
10. BUSKE, N., SONNTAG, H.: Kolloid-Z. Z. Polymere **249,** 1133 (1971)
11. KLARE, H.: Dissertation. Humboldt-Universität (1967)
12. STRENGE, K.: Dissertation. Humboldt-Universität (1969)
13. SONNTAG, H., STRENGE, K.: Tenside **4,** 129 (1967)
14. NEUMANN, H. J.: Erdöl und Kohle **18,** 865 (1965)
15. SONNTAG, H., KLARE, H.: Kolloid-Z. Z. Polymere **195,** 35 (1964)
16. STRENGE, K., SONNTAG, H.: Tenside **6,** 61 (1969)
17. TORZA, S., MASON, G.: Science **163,** 813 (1969)
18. TORZA, S., MASON, G.: J. Coll. & Interf. Sci. **33,** 67 (1970)
19. SONNTAG, H.: Studia biophysica **26,** 109 (1971)
20. SONNTAG, H., STRENGE, K.: J. Coll. & Interf. Sci. **32,** 159 (1970)
21. SONNTAG, H., NETZEL, J., UNTERBERGER, B.: Spec. Discuss. Far. Soc. on Thin Liquid Films and Boundary Layers 57 (1971)
22. SCHELUDKO, A., PLATIKANOW, D., MANEW, E.: Discuss. Far. Soc. **40,** 253 (1965)
23. HARKINS, W. D.: J. Chem. Phys. **9,** 552 (1941)

H. SONNTAG; 1199 Berlin-Adlershof, Rudoweg Chaussee 5. DDR.

Acta Chimica Academiae Scientiarum Hungaricae, Tomus 76 (4) pp. 375—379 (1973)

HYDROGEN-BONDED PYRIDINIUM-PYRIDINE SYSTEM STUDIED BY EXTENDED HÜCKEL METHOD

A. SÜTŐ and M.-M. HEGYHÁTI

(Central Research Institute for Physics, Budapest)

Received July 31, 1972

The hydrogen-bonded pyridinium–pyridine system is examined using the extended Hückel method. With a simplex minimization for two variables it is confirmed that the total electron energy reaches no minimum as a function of the N...N and H...N distances. Taking the distance of the N atoms at a fixed value of 3.85 Å, a polarizing effect of the moving proton on the valence electrons was observed.

The hydrogen bond in pyridinium-pyridine

A REIN—HARRIS type calculation performed for pyridinium–pyridine [1, 2] raised the question whether the method provides the expected bond distances under the restrictions that the rings of the two molecules be coplanar and the H-bond linear. The calculation yielded a symmetrical double-well potential but the energy of the complex increased monotonously as the pyridine and the pyridinium approached one another. This calculation is repeated here treating the valence electrons with the extended Hückel method and using a more detailed variation of geometry. The numbering of the atoms is shown in Fig. 1. The coordinates of the pyridine molecule are taken from SUTTON's tables [3]. The ionization potentials and the Slater exponents of the atomic orbitals are collected in Table I. The calculations were carried out with $K=1.45$.

To find the N...N and H...N distances corresponding to the minimal energy, the usual treatment would be to fix the H...N distance at its equilibrium value in the separated pyridinium and to vary only the N...N dis-

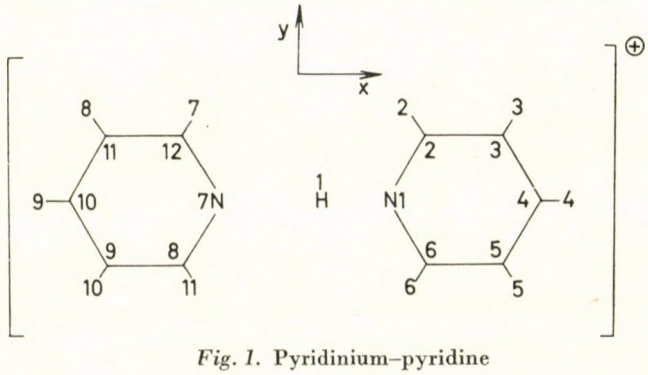

Fig. 1. Pyridinium–pyridine

tance. But a more correct way of obtaining the most energetically favourable geometry is minimization in two variables. Here the simplex procedure (see Appendix) has been applied for this purpose. The points of the simplex with the corresponding energy values are shown in Fig. 2. One can see that at a H...N distance of 0.8 Å the energy is almost constant and is equal to the sum of the energies of the separated pyridinium and pyridine (—1003.729 eV).

Table I

Slater exponents and ionization potentials
(eV)

	Exponents	1 *s*	2 *s*	2 *p*
H	1.000	13.60		
	0.5		3.40	3.40
C	1.625	—	21.40	11.40
N	1.950	—	26.00	13.40

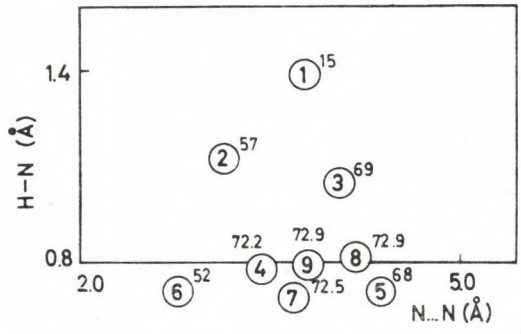

Fig. 2. Simplex minimization for two variables. Numbers above the circles are in units of 10^{-2} eV. The integer part of the energy is —1003. eV

The simplex does not converge to a single point. Hence, according to our calculation linear and coplanar pyridinium-pyridine does not exist — in agreement with the result of the previous calculation [2]. We obtained 0.8 Å for the H...N distance in pyridinium.

We were also interested in the proton potential in the hydrogen bond and the polarization effect of the proton on the electronic system. The effective proton potential picked up at a N...N separation of 3.85 Å is shown in Fig. 3. Table II compares the atomic charges on pyridine alone, pyridine in the complex, and pyridinium alone. The only remarkable changes are on the nitrogen, the hydrogen and — to a smaller degree — on the alfa carbon. This last is

interesting, because it implies that the electron charge increases on this C-atom as the proton approaches the nitrogen. The same phenomenon has been observed by others also [4]. The increase in the N—C_α overlap population (Table II) corresponds with that of the frequency of the skeletal oscillation in the pyridinium, in relation to the pyridine. Table III shows in detail the change in the electron population of the nitrogen orbitals under protonation. One can see that the drop in charge is concentrated on the $2p_x$ orbital, as would be

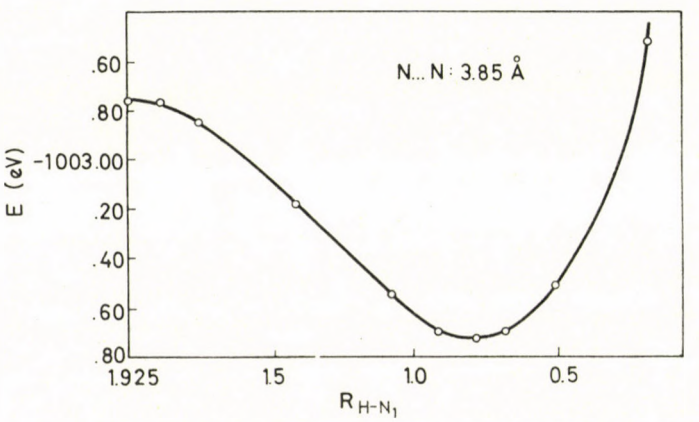

Fig. 3. The total electron energy as a function of the proton position

Table II

Atomic charges and overlap populations between the core atoms and the proton of the H-bond

	N–H(Å)	H	C_α	C_β	C_γ	H	N...H	N–C_α	C_α–C_β	C_β–C_γ
Pyridine	—	—1.2393	0.4422	—0.1565	0.0419	—	—	0.7636	1.0305	0.9822
Pyridine in the complex (N . . . N : 3.85 Å)	3.05Å	—1.2379	0.4422	—0.1565	0.0419	0.4779	0.0015	0.7636	1.0305	0.9822
	2.75	—1.2327	0.4421	—0.1564	0.0419	0.3761	0.0061	0.7636	1.0305	0.9822
	2.25	—1.1363	0.4408	—0.1531	0.0418	0.1667	0.0554	0.7660	1.0298	0.9822
	1.925	—0.8313	0.4424	—0.1320	0.0433	0.0572	0.1726	0.7812	1.0213	0.9835
	1.60	—0.5593	0.4308	—0.1286	0.0422	0.1667	0.3556	0.7926	1.0240	0.9830
	1.40	—0.5299	0.4186	—0.1383	0.0413	0.2616	0.4632	0.7937	1.0309	0.9821
	1.20	—0.5336	0.4079	—0.1446	0.0412	0.3385	0.5612	0.7959	1.0353	0.9816
	1.10	—0.5620	0.4035	—0.1472	0.0412	0.3761	0.5957	0.7963	1.0367	0.9815
	0.80	—0.6218	0.3918	—0.1516	0.0413	0.4779	0.6806	0.7974	1.0396	0.9816
Pyridinium	0.80	—0.6203	0.3917	—0.1515	0.0413	0.4777	0.6815	0.7975	1.0396	0.9816

expected, for this orbital is directed towards the hydrogen atom. There is a minimal charge on the nitrogen and its $2p_x$ orbital at 1.3—1.4 Å, which is also manifested in the N$2p_x$ net orbital population.

Calculations including the $2s$ and $2p$ orbitals of the bonding hydrogen atom were also carried out. No electron population was found on these orbitals, all population numbers are negative.

Table III

Electron numbers on the nitrogen orbitals

	N—H Å	$2s$	$2p_x$	$2p_y$	$2p_z$
Pyridine	—	1.7221	1.7963	1.1566	1.5643
Pyridine in the complex (N . . . N: 3.85 Å)	3.05	1.7220	1.7950	1.1566	1.5643
	2.75	1.7217	1.7899	1.1566	1.5643
	2.25	1.7195	1.6958	1.1566	1.5643
	1.925	1.7142	1.3965	1.1566	1.5643
	1.6	1.7031	1.1352	1.1566	1.5643
	1.4	1.6933	1.1157	1.1566	1.5643
	1.2	1.6814	1.1312	1.1566	1.5643
	1.1	1.6754	1.1656	1.1566	1.5643
	0.8	1.6560	1.2449	1.1566	1.5643
Pyridinium	0.8	1.6559	1.2434	1.1566	1.5643

Appendix: The simplex method

Suppose we may calculate the function

$$f_i = f(x_i) = f(x_{i_1} \ldots, x_{i_n})$$

on an area of the n variables. We do not know the explicit form of the function and we have to determine its minimum point, if one exists. We calculate the function in $n + 1$ points which form a non-degenerate n-dimensional simplex. This simplex may also be regular provided we transform the variables to dimensionless units. The coordinates of such a regular simplex centered at the origin are given in the rows of the matrix below:

$$\begin{pmatrix} r_1 & r_2 & r_3 & \ldots & r_n \\ -R_1 & r_2 & r_3 & \ldots & r_n \\ 0 & -R_2 & r_3 & \ldots & r_n \\ 0 & 0 & -R_3 & \ldots & r_n \\ \vdots & & & & \\ 0 & 0 & 0 & \ldots & -R_n \end{pmatrix}$$

where $r_i = 1/\sqrt{2i\,(i+1)}$

$R_i = i \cdot r_i$

$i = 1, \ldots, n$

By replacing these points with better ones, *i.e.* with points in which the value of the function is smaller, we get simplexes progressively approaching the minimum. The only rules are: 1. to replace only with a better point, 2. to replace always the worst point. To do this, we calculate the function in all the n points and arrange them in the order

$$f_0 < f_1 < \cdots < f_n$$

The worst point (x_n) will then be reflected to the center of the others:

$$x^*_{nj} = \frac{2}{n} \sum_{k=0}^{n-1} x_{kj} - x_{nj} \,. \tag{1}$$

If the new value

$$f^*_n < f_n \tag{2}$$

we change x_n with x^*_n. The points are rearranged and the process repeated. If (2) fails, the criterion has to be applied to the next largest subscript. We finish when (2) fails for n = zero subscript. The process may be continued around x_0 with a smaller simplex.

The minimum can be reached more rapidly if we give up the regularity of the simplex and use instead of (1)

$$x^*_{ni} = 2 \frac{\sum_{k=0}^{n-1} (f_n - f_k)\, x_{ki}}{\sum_{k=0}^{n-1} (f_n - f_k)} - x_{ni} \,. \tag{1a}$$

The computer program of a variant of the simplex method is available [5, 6].

*

We are indebted to Dr. J. HOLDERITH for useful discussions about the simplex method.

REFERENCES

1. REIN, R., HARRIS, F. E.: J. Chem. Phys. **41,** 3393 (1964)
2. SABIN, J. R.: Int. Quant. Chem. **II.** 23 (1968)
3. Tables of Interatomic Distances (Ed. L. E. Sutton), The Chemical Society, London, 1958
4. ADAM, W., GRIMINSON, A., HOFFMAN, R., DE ORTIZ, C. Z.: J. Am. Chem. Soc. **90,** 1509 (1968)
5. NELDER, J. A., MEAD, R.: Comput, J. **7,** 308 (1965)
6. CHANDLER, J. P.: Simplex Method, Quantum Chemical Program Exchange, Indiana University, 1969

András SÜTŐ
Magdolna HEGYHÁTI
1525 Budapest, Konkoly Thege M. út.

Acta Chimica Academiae Scientiarum Hungaricae, Tomus 76 (4), pp. 381—392 (1973)

MECHANISM OF ELASTIC AFTER-EFFECT IN DILUTE STRUCTURIZED AQUEOUS BENTONITE SUSPENSIONS*

E. D. SHCHUKIN and P.A. REKHBINDER**

(Disperse Systems Department, Institute of Physical Chemistry, Academy of Sciences of the USSR, Moscow)

Received August 28, 1972

1. The micromechanism of the reversible after-effect in dilute colloidal bentonite suspensions has been considered to involve fast and slow stages of elastic deformation (with time constants of the order of a few hundredths of a second and of 10^2 sec, respectively). Approximate quantitative estimates are given for the main parameters describing this process, *viz.* the equilibrium elastic module and the viscosities, which agree with the experimental data.

2. As a mechanism explaining the existence of reversible deformations under small shear stresses, the manifestation of the preferential mutual orientation of anisometric particles in the coagulation structure is considered; an increase of the entropy connected with this texturization permits to estimate the value of the equilibrium module of elasticity ($\sim 10^4$ dyne/cm^2).

3. The two observed stages of reversible after-effect can be described by the KELVIN model (with the given value of the equilibrium module of high elasticity) as involving two various mechanisms for the change of mutual particle orientation; the coiling of particles against each other and the sliding of contact points over a particle surface. In the first case, the viscosity of the elastic after-effect estimated on the basis of the model of immobilized dispersion medium (water) flowing from cell to cell in the random network of particles, amounts to (10^4—10^5) η_w, where η_w is the viscosity of water; in the second case, the viscosity of the elastic after-effect obtained on the basis of estimating the viscous resistance in coagulation contacts under conditions of sliding, reaches 10^8 η_w.

SERB-SERBINA *et al.* [1—3] have shown that thixotropic coagulation structures formed in aqueous suspensions of clays, especially of bentonite, display elastic after-effect, a peculiarly high elasticity. Under the influence of a constant shearing stress deformation is observed in these structures, characterized by a slow increase in time and a continuous decrease after removal of the load. These effects were explained in terms of their entropic nature [4, 5].

The rheological properties of highly disperse (colloidal) suspensions of bentonite in water with a low content of the solid phase (3% by volume) were thoroughly studied by FEDOTOVA [6]. The coagulation structures developed — three-dimensional networks of particles — are capable of reversible restoration after collapse, *i.e.* possess thixotropic properties. The dependence of a uniform shear deformation rate on the applied stress in steady-state flow reveals typical regions different in their physical nature.

* Lecture held by E. D. SHCHUKIN at the 1st Conference of Colloid and Surface Chemistry, May 24—26, 1971, Mátrafüred, Hungary.

** Died on July 12, 1972.

Over the stress range of about 50 to 500 dyne/cm^2 a slow creep appears — Shvedov's region with a maximum constant plastic viscosity of η_0 10^9 poise. This is characteristic of a rigid structure in which the fraction of destroyed contacts between particles at the given moment is small, *i.e.* the structure has time to restore thixotropically in a flow process. Under the conditions of higher stress a viscous plastic flow with significant deformation rates (Bingham region) takes place. With the increase of stress, the effective viscosity drops sharply, reaching the minimum constant value $\eta_m \approx 0.1$ poise; this corresponds to viscous flow of the system (according to Einstein) with a totally destroyed structure.

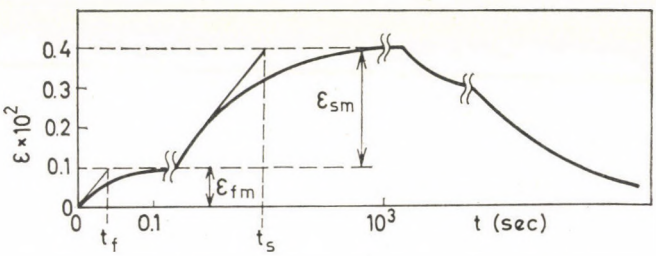

Fig. 1. Dependence of shear deformation on time in the process of elastic after-effect at stages of fast and slow elastic deformations

Under the conditions of small shear stresses below 40—50 dyne/cm^2, creep in the systems examined is practically absent. The above deformations are truly reversible (in value) and develop, up to their equilibrium value in correspondence with the applied stress, *i.e.* they are purely elastic deformations of the elastic after-effect. The dependence of shear deformation, ε*, on time with a stress of $\tau \approx 50$ dyne/cm^2 (slightly lower), corresponding to the initial part of the rheological curve where residual deformations are absent, is shown schematically in Fig. 1. This dependence reveals strongly pronounced stages of 'fast' and 'slow' elastic deformations. Both can be described, as a first approximation, by the Kelvin after-effect, *i.e.* by the exponential increase of deformation after loading (and its exponential decrease after unloading) with characteristic time constants. For the first, fast stage this time constant t_f is about 1/100; for the second, slow stage it amounts to $t_s \approx 10^2$ sec. The final, equilibrium value of the reversible deformation reached at the above stress τ at the first stage is approximately $\varepsilon_{fm} \approx 0.1\%$. At the second stage, the value of elastic deformation is somewhat greater: $\varepsilon_{sm} \approx 0.3\%$. Thus the module of high elasticity equals $\sim 10^4$—10^5 dyne/cm^2.

* The quantity characteristic of shear deformation, ε, corresponds in the mechanics of continua to the value usually called 'technical shear', γ, *i.e.* to the double value of 'pure shear'.

This distinctive behaviour of colloidal suspensions strikingly displayed even in dilute systems has been explained [4, 5] as follows.

The reversibility of deformations under these conditions (when the 'usual' elasticity peculiar to solids and characterized by high modules of the order of 10^{10} to 10^{12} dyne/cm^2 cannot be observed) is attributed to entropy effects due to changes in the mutual orientation of particles, similarly to the description of the high elasticity of polymers caused by the statistics of the configurations of macromolecular chains [7]. Moreover, the relatively rapid, first stage of the after-effect may be connected to the coiling of particles without linear displacement relative to each other, while the second, slow stage

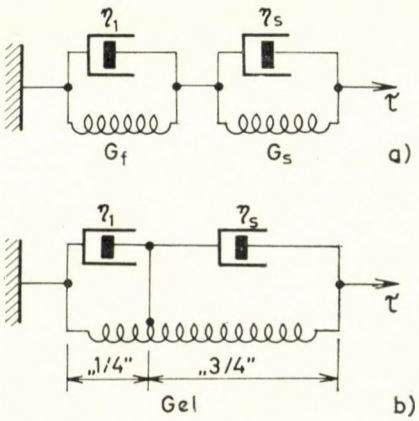

Fig. 2. Rheological models describing the two stages of highly elastic after-effect

corresponds to the subsequent reorientation process which involves mutual sliding of the particles, *i.e.* gradual displacement of the points of coagulation contacts over the particle surface.

These processes of the elastic after-effect may be described by a simple rheological model consisting of two KELVIN cells in series (it should be emphasized that this model shown in Fig. 2a refers apparently only to the region of small stresses before the development of SHVEDOV's creep).* According to this model, we have the following values of fast and slow elastic deformation modules:

$$G_f = \frac{\tau}{\varepsilon_{fm}} \approx \frac{50}{10^{-3}} = 5 \times 10^4 \quad \text{dyne/cm}^2;$$

$$G_s = \frac{\tau}{\varepsilon_{sm}} \approx \frac{50}{3 \times 10^{-3}} = 1.7 \times 10^3 \quad \text{dyne/cm}^2.$$

* We use the combination of the simplest models of KELVIN's elastic after-effect, taking into account mainly the analysis of equilibrium states (the superposition described) and the estimation of conventional time constants for the after-effect. The kinetics of the development and decrease of deformation are usually more complicated then in this simplest model [8].

In accordance with the ideas developed, in both cases we deal with a similar reversibility of deformation (entropy factor), therefore it is more expedient to consider one 'common' module of high elasticity, G_{el}, determined by the sum of equilibrium deformations

$$\varepsilon_m = \varepsilon_{fm} + \varepsilon_{sm} \approx 0.1 + 0.3 = 0.4\%, \textit{ viz.}$$

$$G_{el} = \frac{\tau}{\varepsilon_m} \approx \frac{50}{4 \times 10^{-3}} = 1.25 \times 10^4 \text{ dyne/cm}^2.$$

The deformabilities at the two stages indicated, corresponding to two different elements with viscosities η_f and η_s are different and contribute about 1/4 and 3/4, respectively (see Fig. 2).

Since the constant of elastic after-effect is the ratio of viscosity to the corresponding module of high elasticity, the values of the above two viscosities are given by the following expressions:

$$\eta_f = G_f \cdot t_f \approx 5 \times 10^4 \times 10^{-2} = 5 \times 10^2 \text{ poise};$$
$$\eta_s = G_s \cdot t_s \approx 1.7 \times 10^4 \times 10^2 = 1.7 \times 10^6 \text{ poise}.$$

Consequently, the effective viscosity of the structure at the stage of fast, high elasticity is 10^4 to 10^5 times greater than the viscosity of the dispersion medium–water; at the stage of slow elastic deformations this ratio reaches 10^8.

On the basis of the concepts about microprocesses in the thixotropic coagulation structures, the following approximate description is possible for the macrorheological parameters corresponding to the behaviour of colloidal disperse suspensions at small shear stresses.

Module of high elasticity

Consider structurized system under the conditions of uniform shear at constant temperature T, and stress τ replacing in this case the pressure p. The behaviour of this system can be described by the thermodynamic potential per unit volume:

$$\Phi(T, \tau) = U - ST - \tau\varepsilon ,$$

where the deformation is $\varepsilon = \varepsilon(T, \tau)$ and the sign of term $\tau\varepsilon$ corresponds to the condition that the work is positive if it is performed on the system. True

elastic deformations are neglected because they are very small under the given stress and only the high elastic deformations connected with changes in the mutual arrangement of particles are considered. Then we assume that

$$U = \text{const}\,;\; S = S_1 + S_2(\varepsilon)\,,$$

where S_1 does not depend on deformation ε, but $S_2 = S_2(\varepsilon)$ is the 'configurational' entropy component; let us assume that $\varepsilon = 0$ and $S_2 = 0$ if $\tau = 0$.

At constant T and τ, an equilibrium in the system considered corresponds to the minimum of potential Φ. The only variable parameter is deformation ε:

$$\left(\frac{\partial \Phi}{\partial \varepsilon}\right)_{T,\tau} = -T\frac{\partial S_2}{\partial \varepsilon} - \tau = 0\,.$$

Since ε and τ have the same sign, this corresponds to a decrease in entropy with increasing deformation.

The following expression proves that the extremum is, in fact, a minimum:

$$\left(\frac{\partial^2 \Phi}{\partial \varepsilon^2}\right)_{T,\tau} = -T\frac{\partial^2 S_2}{\partial \varepsilon^2} > 0\,.$$

This means that the entropy decreases with increasing deformation no less sharply than does $-\varepsilon^2$.

As a model of the coagulation structure, we examine a system of similar anisometric particles with linear dimensions δ. For a pronounced anisometry of particles, sticks or platelets, let us take $\delta = l$, where l is the largest size; for particles with slightly pronounced anisometry let $\delta = l - d$, where l and d are the largest and the smallest size, respectively.

In accordance with the proposed method [4] developed in this laboratory by PERTSOV and YUSHCHENKO [9], a system at equilibrium in the absence of stress is in a random arrangement with equally probable orientations of particles; in addition, the average projection $\bar{z}$ of particle size δ for every direction has the same magnitude

$$\bar{z} = \frac{1}{N}\sum z_i = \frac{\delta}{2}\,;$$

where N is the number of particles of the disperse phase per unit volume of the system.

Indeed, in coordinates ϑ and φ, the projection of the particle size onto a polar axis $\bar{z} = \delta \sin \vartheta$ (Fig. 3). In the element of space angle $\mathrm{d}\omega = \cos \vartheta\, \mathrm{d}\vartheta\, \mathrm{d}\varphi$, the number of particles is

$$\mathrm{d}N = \frac{N}{2\pi}\cos \vartheta\, \mathrm{d}\vartheta\, \mathrm{d}\varphi$$

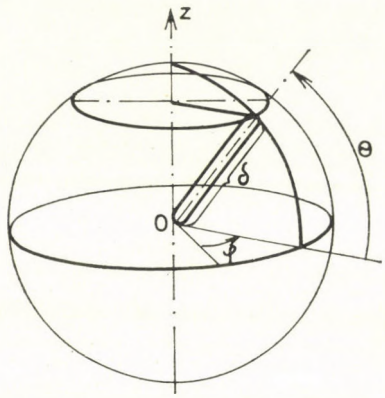

Fig. 3. Estimation of particle size projection onto a given axis

(here a hemisphere is, naturally, considered: $0 < \varphi < 2\pi$ and $\delta < \vartheta < \pi/2$). Hence it follows that the average value of the projections of all particles onto the selected axis is

$$\bar{z} = \frac{1}{N} \cdot \int \delta \sin \vartheta \, \mathrm{d}N = \frac{1}{N} \cdot \frac{N\delta}{2\pi} \iint \sin \vartheta \, \cos \vartheta \, \mathrm{d}\vartheta \, \mathrm{d}\varphi = \frac{\delta}{2} .$$

Within the range $\mathrm{d}z = \delta \cos \vartheta \, \mathrm{d}\vartheta$, *i.e.* in 'spherical segment' $\mathrm{d}\omega' = 2\pi \cos \vartheta \, \mathrm{d}\vartheta$, the fraction of particles is given by

$$\frac{\mathrm{d}N}{N} = \frac{1}{2\pi} \cdot 2\pi \cos \vartheta \, \mathrm{d}\vartheta = f(z) \, \mathrm{d}z = f(z) = \delta \cos \vartheta \, \mathrm{d}\vartheta ;$$

consequently, the distribution function will have the following form

$$f(z) = \text{const} = 1/\delta,$$

and the dispersion of value z is determined by the following equation:

$$\sigma_z^2 = \int (z - \bar{z})^2 f(z) \, \mathrm{d}z = \frac{1}{\delta} \int_0^{\delta} \left(z - \frac{\delta}{2} \right)^2 \mathrm{d}z = \frac{1}{12} \delta^2.$$

Let us suppose now that as a result of stress applied in the direction of the selected polar axis, a partial mutual orientation of the particles ('texturization') in the given direction will take place and the mean projection of particle dimensions onto this direction will increase. To determine the proba-

bility of such a state of the system, we use the following approach (developed by YUSHCHENKO).* Since the projection of each particle, z, is a chance value, LYAPUNOV's central limit theorem is applicable to the system, and the distribution of the mean projection $\bar{z}$ is a normal distribution with a mathematical expectation of $\mu = \delta/2$ and a dispersion of $\sigma^2 = \sigma^2/N = \delta^2/12N$.

Thus the function

$$f(\bar{z}) = \frac{1}{\sqrt{2\pi}\,\sigma} e^{-(\bar{z}-\mu)^2/2\sigma^2} = \sqrt{\frac{6}{\pi}} \cdot \frac{\sqrt{N}}{\delta} e^{-\frac{3}{2}N\left(\frac{\bar{z}-\delta/2}{\delta/2}\right)^2}$$

expresses the probability of this deviation of the mean projection of particle sizes onto the selected axis from the most probable mean value in the absence of coorientation $\delta/2$.

Besides, this deviation (owing to its physical meaning) may be considered as a value close to the deformation in the system:**

$$\frac{\bar{z} - \delta/2}{\delta/2} \approx \varepsilon .$$

In this case the probability of deformation ε caused by the coorientation of particles is determined by the distribution function

$$\sqrt{\frac{6}{\pi}} \cdot \frac{\sqrt{N}}{\delta} e^{-\frac{3}{2}N\varepsilon^2},$$

and the change in the logarithm of probability upon transition from $\varepsilon = 0$ to some definite ε will be:

$$\Delta \ln W = -\frac{3}{2} N\varepsilon^2 ;$$

This corresponds to a change in the entropy of the system given by

$$\Delta S_2 = -\frac{3}{2} Nk\varepsilon^2 .$$

* Acad. A. N. KOLMOGOROV has called our attention to this way of evaluation.

** A case of 'strong' anisometry of particles is supposed. If the anisometry of particles is less expressed, it can be supposed that deformation ε is related in a definite way to the characteristic degree of anisometry. In the simplest case with linear connection we have $\varepsilon \sim \left(\frac{\delta}{l}\right) \cdot \frac{z - \delta/2}{\delta/2}$, where l — maximum size of particles.

Along a curve corresponding to the minimum of thermodynamic potential Φ, *i.e.* along the equilibrium curve $\varepsilon = \varepsilon(\tau)$, we obtain:

$$\tau = -T\frac{\partial S_2}{\partial \varepsilon} = 3NkT\varepsilon\,;$$

hence, the equilibrium module of high elasticity is

$$G_{el} = \tau/\varepsilon = 3\,NkT\,.$$

The particles of the colloidal bentonite suspension examined are thin plates. Let us assume that their largest dimension $l \approx 100$—200 Å, thickness $d \approx$ ≈ 10 Å, and the volume concentration $C = 3\%$. Then for the number of particles in unit volume we find:

$$N \approx \frac{C}{l^2\,d} \approx 10^{17}\,\mathrm{cm}^{-3}\,.$$

The equilibrium module of high elasticity (at room temperature) will be:

$$G_{el} \approx 3 \times 10^{17} \times 4 \times 10^{-14} = 1.2 \times 10^4\ \mathrm{dyne/cm^2};$$

which agrees with the above experimental value (1.25×10^4 dyne/cm^2). Here, indeed, importance should be attached only to agreement in the order of magnitude. This agreement may be considered as corroboration of the concept developed for the mechanism of the observed reversible deformation.

Viscosity of elastic after-effect

The analysis of this quantity also requires the introduction of a definite model. First we shall discuss the initial stage of after-effect, *i.e.* the fast elastic deformation connected with the manifestation of an elastic after-effect viscosity $\eta_f \approx (10^4$—$10^5)\cdot\eta_w$, where η_w—viscosity of water (dispersion medium).

The deformation of coagulation structure cells, caused by mutual turns of particles (plates without the sliding of contact points) is schematically shown in Fig. 4a, b.

The contact is assumed to be an 'ideal joint' requiring no work, thus 'coorientation', *i.e.* the increase of the mean projection of particles in a given direction, is observed. It is quite evident, however, that in this 'regular' model there is no reason for a significant increase of the effective viscosity relative to the viscosity of the dispersion medium, immobilized water, since the deformation of each cell occurs through the same uniform shears to which the whole system is exposed.

A possible increase of viscosity in small volumes of the liquid owing to contact with the particle surface is not considered here; this factor requires special examination. However, it should be noted that this factor in itself cannot explain the fact that the effective viscosity of the system exceeds the viscosity of water by many orders of magnitude. The observed thixotropic reversibility of the examined structures proves this. Indeed, in the case of complete collapse of the network, the viscosity of these systems sharply falls and the remaining relatively small difference from the viscosity of the dispersion medium, not exceeding one order of magnitude, conforms to the concept of Einstein flow. The mean 'cell' size in the dispersion medium remains

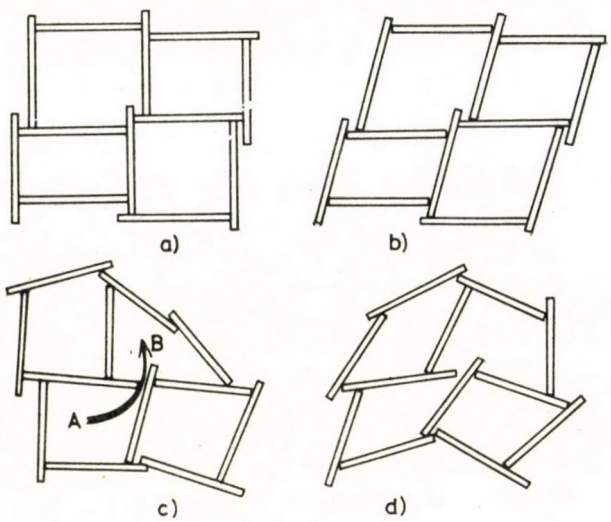

Fig. 4. Shear deformation in idealized (*a*, *b*) and real (*c*, *d*) coagulation structures

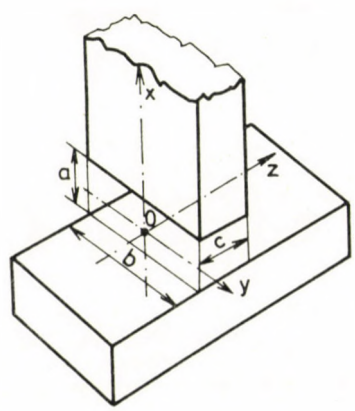

Fig. 5. Scheme of flow in a gap

approximately the same, in this case of the order of 100 Å, *i.e.* the whole volume of the dispersion medium remains essentially a thin boundary layer, a few tens of an Å in thickness; if the main cause of a high effective viscosity of the system were the influence of a boundary solid phase upon these layers, then destruction of the network would not cause such a significant decrease in the viscosity.

If the shear ε acts during a period of time t at an average rate of $\dot{\varepsilon} = \varepsilon/t$ then the work of viscosity forces in unit volume is determined by the value of $\eta\dot{\varepsilon}\varepsilon \approx \eta\varepsilon^2/t$; for a cell of volume $\approx l^3$ it is

$$W \approx \frac{\eta\varepsilon^2 l^3}{t} .$$

An obvious solution of this contradiction is an examination of the true, random particle structure in which cell deformation is connected with the flow of immobilized water from one cell into another through relatively narrow gaps (see Fig. 4c, d). Following this method, we assume that the shear changes the volume approximately by $\pm l^3\varepsilon$ and, consequently, makes some water flow through gaps between the cells: $V = \beta l^3\varepsilon$, where β is a factor of the order of a few units, taking into account that a microprocess of in the random 'irregular' structure of particles extends to some neighbouring elementary volumes.

If the flow occurs in a gap, a in thickness, b in width and c in length (Fig. 5), then the average flow rate is $w = \beta l^3\varepsilon/abt$. The flow rate distribution is described generally by the parabolic law:

$$w(x) = \frac{1}{2} \frac{\Delta p}{c\eta_W} \left(\frac{a}{2}\right)^2 \left[1 - \left(x \Big/ \frac{a}{2}\right)^2\right],$$

where Δp is the pressure drop over the gap c. It is easy to show that

$$\Delta p = 3\eta_W \frac{c}{\left(\frac{a}{2}\right)^2} W = 3\eta_W \frac{c}{\left(\frac{a}{2}\right)^2} \frac{\beta l^3 \varepsilon}{abt} .$$

The dissipation of energy in the gap is

$$W_f = \Delta p \beta l^3 \varepsilon = 12\eta_W \cdot \frac{c}{ba^3} (\beta l^3 \varepsilon)^3 \cdot \frac{1}{t} .$$

If this expression is equated to $\eta_f\varepsilon^2 l^3/t$, then we find the effective viscosity η_f under the conditions of 'fast', highly elastic deformation:

$$\eta_f/\eta_W = 12\beta^2 \frac{c}{ba^3} l^3 .$$

Now let us assume that the thickness and length of the gap are approximately equal to the thickness of the particles (platelets) while the gap width — to the maximum particle size: $a = c \approx d$, $b \approx l$. Hence one obtains

$$\eta_f/\eta_W \approx 12\,\beta^2 \left(\frac{l}{d}\right)^2.$$

Let factor β be equal to a few units, and the ratio l/d be approximately equal to 10 (or a few times); the effective viscosity of a fast, highly elastic deformation should exceed the viscosity of water by 10^4—10^5. This correctly predicts the order of magnitude of the above experimental results.

At the same time it is necessary to emphasize the tentative character of the estimate of η_f. In particular, the ratio obtained obviously does not include the concentration of the disperse phase. Nevertheless, this concentration is specified by the model used: it equals several (n) particles per volume βl^3, where also $\beta \approx n$; consequently, the volume concentration of the disperse phase is supposed to be approximately

$$\frac{nl^2 d}{\beta l^3} \approx \frac{d}{l},$$

i.e. of the order of 10^{-1} or somewhat less, in agreement with the experimental conditions [6].

The above evaluation of fast, highly elastic deformation viscosity may be simply applied also to the second stage of after-effect involving a considerably higher viscosity. In this case, the mutual sliding of particles, *i.e.* a slight displacement of contact points over the particle surface without destruction of the majority of the contact may be considered as a proposed mechanism for the increase of particle coorientation relative to each other [5]. This sliding process may be approximately described in the same terms of viscous flow of a dispersion medium in a gap. However, in this case the gap is considerably narrower; in the first case, we have assumed it to be roughly equal to the thickness of the platelets ($a \approx d$ is of the order of 10 Å or slightly more), but now we assume that the gap thickness is only a few Å, *i.e.* $a = \vartheta d$, where factor $\vartheta \approx 10^{-1}$. Substitution of this value into the expression of effective viscosity gives at the stage of slow elasticity:

$$\eta_s/\eta_W \approx 12\,\beta^2 \frac{1}{\delta^3} \left(\frac{l}{d}\right)^2,$$

i.e. approximately by three orders of magnitude more than at the first stage. This value ($\approx 10^6$ poise) has been experimentally determined.

However, the last estimate includes some elements of conditionality and requires further, more accurate calculations. In particular, certain changes in the properties of the liquid in a narrow gap which are of great importance, should be taken into account, because the layers equal only a few molecules in thickness. At the same time a special analysis is required for the above ratio of 'deformabilities' at the stages of fast and slow elastic deformations:

$$\varepsilon_{fm} : \varepsilon_{sm} \approx 1 : 3 .$$

REFERENCES

1. SERB-SERBINA, N. N., REKHBINDER, P. A.: Kolloidn. Zhurn., **9,** 381 (1947)
2. ABDURAGHIMOVA, L. A., REKHBINDER, P. A., SERB-SERBINA, N. N.: Kolloidn. Zhurn., **17,** 184 (1955)
3. REKHBINDER, P. A.: in New Methods for the Physico-chemical Study of Surface Phenomena, 1st Edition, p. 5. Izd. AN USSR 1950. REKHBINDER, P.: Disc. Faraday Soc., **18,** 151 (1954)
4. SHCHUKIN, E. D., REKHBINDER, P. A.: Vth National Conference on Colloid Chemistry. Proceedings, p. 166. Izd. AN USSR 1962
5. REKHBINDER, P. A.: in Physico-chemical Mechanics of Disperse Structures, p. 3. Hauka 1966
6. FEDOTOVA, V. A., KHODZHAEVA, KH., REKHBINDER, P. A.: Dokl. AN USSR, **170,** 1133 (1966); **177,** 155 (1967)
7. VOLKENSTEIN, M. V.: Configurational Statistics of Polymeric Chains. Izd. AN USSR, 1959
8. REKHBINDER, P. A., IVANOVA-CHUMAKOVA, L. V.: in Advances in the Chemistry and Technology of Polymers, Vol. 2, p. 146. Goskhimizdat 1957; Z. phys. Chem., **209,** 1 (1958)
9. PERTSOV, A. V.: Thesis, Moscow, 1967

E. D. SHCHUKIN
P. A. REKHBINDER
Disperse Systems Department, Institute of Physical Chemistry, Academy of Sciences of the USSR, Moscow, USSR.

Acta Chimica Academiae Scientiarum Hungaricae, Tomus 76 (4), pp. 393—398 (1973)

FORMATION OF GLUCOSE-1,2-ORTHOESTERS FROM TETRA-O-ACETYL-α-D-GLUCOPYRANOSYL BROMIDE UNDER THE EFFECT OF PHOSPHORANES

I. PINTÉR, J. KOVÁCS and A. MESSMER

(Central Research Institute for Chemistry of the Hungarian Academy of Sciences, Budapest)

Received February 7, 1972

Glucose-1,2-orthoesters are formed from tetra-O-acetyl-α-D-glucopyranosyl bromide under the effect of ethoxycarbonylmethylenetriphenylphosphorane or cyanomethylenetriphenylphosphorane in alcohol-containing solvents. The absence of the BESTMANN reaction (formation of acetylaldosylphosphoranes) can be attributed to strong steric hindrance from the triphenylphosphine group.

Application of the Staudinger reaction to aceto-azido sugars resulted in new types of acetylaldosylphosphine imines (**I**) which proved to be advantageous for use as starting material in the preparation of acetylaldosylcarbodiimides and, from these, different N-glucosides [1].

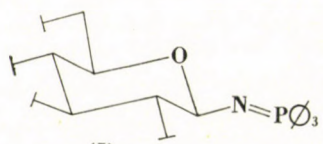

(I)

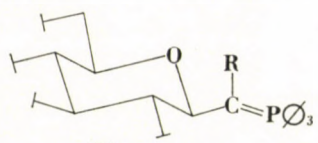

(II)

Similar favourable synthetic properties can be expected in the case of the analogous sugar phosphoranes [(**II**): like(**I**), CR instead of N] — unknown up to now — therefore the application of the BESTMANN reaction [2] to carbohydrates has been attempted.

In the case of the resonance-stabilized phosphoranes the BESTMANN reaction takes place only with acyl halides [3] or highly reactive primary alkyl halides [2], because of the decreased nucleophilicity of the ylide carbon atom. Similarly, it can be expected that only the more reactive acylglycosyl halides will undergo this reaction, while structurally similar but non-activated secondary halides will fail to react.

In our experience, ethoxycarbonylmethylenetriphenylphosphorane (**III**) and *sec*-butyl bromide or cyclohexyl bromide do not react with each other, and the phosphorane can be recovered almost quantitatively.

At the same time, the boiling of 1 mol of 2,3,4,6-tetra-O-acetyl-α-D-glucopyranosyl bromide (**IV**) with 2 moles of the phosphorane in chloroform resulted in the hydrobromide of the starting phosphorane, *i.e.*, ethoxycarbo-

nylmethyltriphenylphosphonium bromide (**VI**) was obtained. As the other product, strikingly, the well-known [4] compound 1,2-ethylorthoacetyl-3,4,6-triacetyl-α-D-glucopyranose (**V**) was isolated in 68% yield, instead of the expected acetylglucosylphosphorane.

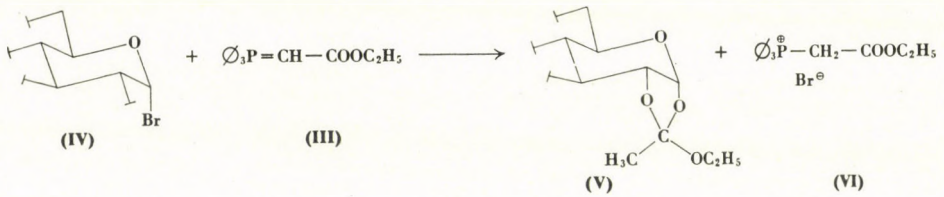

Evidently, the ethanol present in small amounts in the chloroform solution and not the ethoxycarbonyl group of the reagent is responsible for the ethoxy group in the orthoester **V**. This is confirmed by the fact that under otherwise identical conditions cyanomethylenetriphenylphosphorane (**VII**) gave the same 1,2-orthoester in 69% yield; in this case the by-product was cyanomethyltriphenylphosphonium bromide (**VIII**). In alcohol-free chloroform the formation of orthoesters could not be detected.

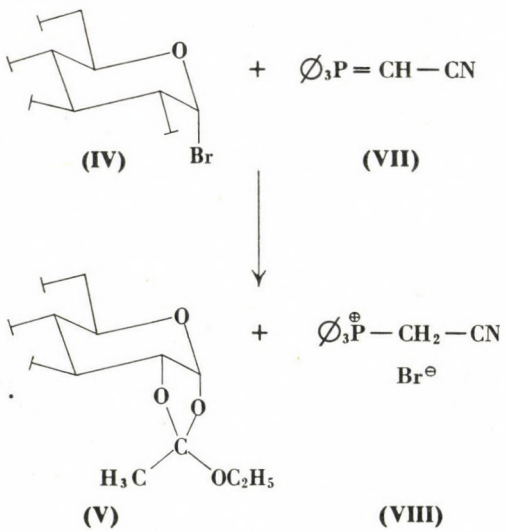

In accordance with this, in benzene solutions containing ethanol, isopropanol or *t*-butanol, the corresponding 1,2-alkylorthoacetyl derivatives were obtained. The data of the products from the phosphorane reactions are summarized in Table I; the physical constants reported in the literature [5, 6] for these orthoesters are given in brackets.

Table I

Alcohol	1,2-Alkylorthoacetyl-3,4,6-triacetyl-α-D-glucopyranose				Phosphonium salt	
	Yield, %	M.p., °C	$[\alpha]_D(CHCl_3;\ c = 1)$		Yield, %	M.p., °C
Ethanol	66	95—6 (95—6)	+31.0°	(+31°)	84	158—9
Isopropanol	57	118—20 (120—21)	+28.5°	(+30°)	93	156—9
t-Butanol	42	149—51 (152.5—154.5)	+34.0°	(+34.5°)	92	156—8

In order to explain the reaction, two possible mechanisms can be considered. LEMIEUX [5] showed that the formation of an 1,2-orthoester from tetra-O-acetyl-α-D-glucopyranosyl bromide on the effect of bases starts with anomerization (conversion of the α-anomer (**IV**) into the β-anomer (**IX**)); the intermediate acetoxonium cation **X** is formed by means of neighbouring-group participation of the C-2 acetoxy group in the pyranose ring, and **X** gives then the orthoester (**XI**) with the alcohol present.

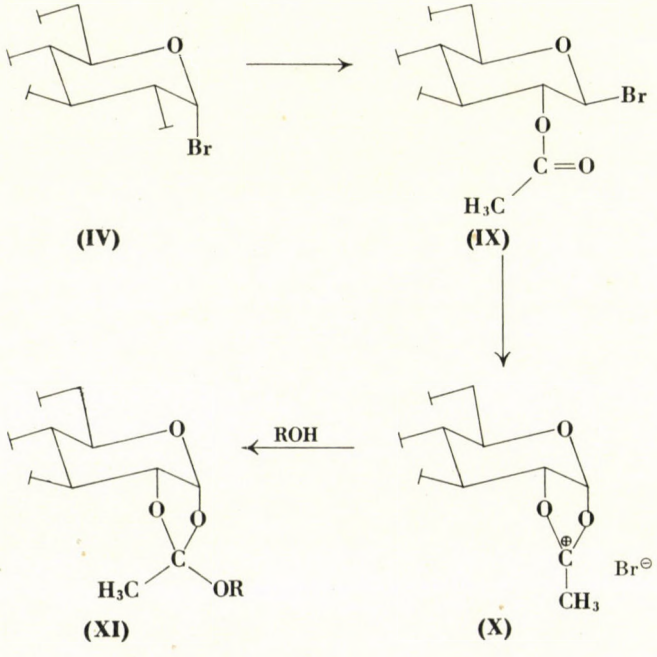

On the other hand, KHORLIN, BOCHKOV and KOCHETKOV [7] suggested that the synthesis of orthoesters in ethyl acetate starts with S_N2 (nucleophilic

backside) attack by the carbonyl oxygen of ethyl acetate (**XII**) on the C-1 atom. The resulting intermediary complex (**XIII**) is then converted into the orthoester with alcohol *via* the acetoxonium cation **X**, involving again C-2 acetoxy participation.

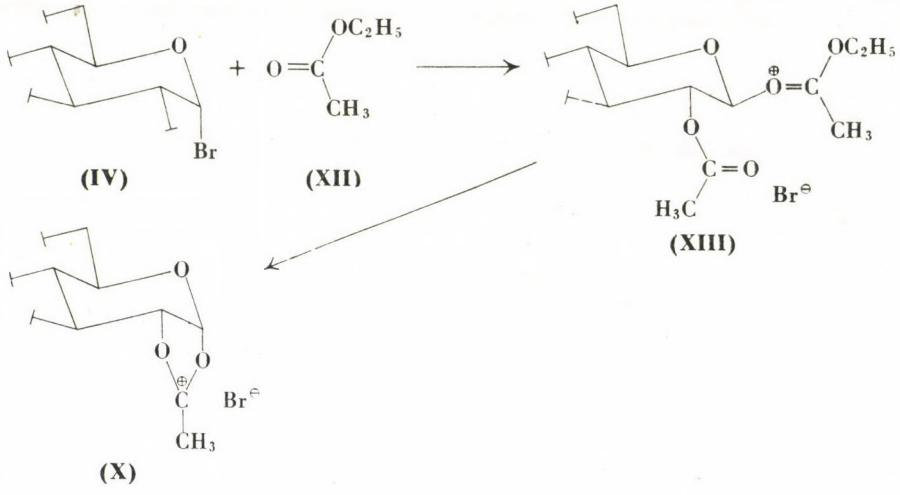

In the case examined by us it must be supposed that the mechanism of the reaction is analogous to that suggested by KOCHETKOV. In the first step, the nucleophilic betainic oxygen atom of ethoxycarbonylmethylenetriphenylphosphorane (**III**) or, in the case of the cyano derivative (**VII**) its nitrogen atom, attacks by S_N2 mechanism on the C-1 atom. (A similar but stable phosphonium salt was isolated from the reaction of ethyl iodide and acylphosphoranes [8]). From the unstable intermediate **XIV**, the phosphorane will again

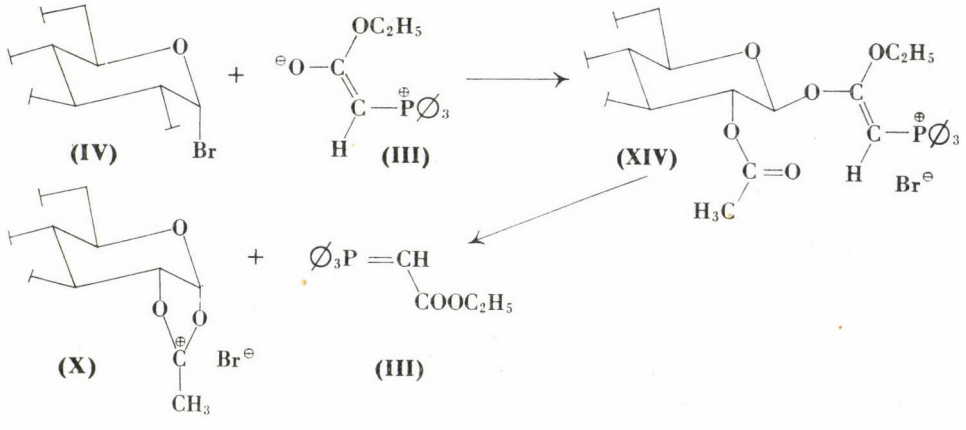

be eliminated on the effect of the neighbouring C-2 acetoxy group, giving rise to the acetoxonium cation **X**. The final step is again the reaction with alcohol, yielding the orthoester, while the phosphorane reacts with the hydrogen bromide liberated.

Thus, in the interaction of the acylglycosyl halide and the phosphorane, it is probably not the ylide carbon atom of the phosphorane but its betainic hetero atom that launches the nucleophilic attack. This is explained by the fact that in this case the hetero atom has stronger nucleophilic character than the ylide carbon atom, owing to the electron delocalization. Furthermore, the three phenyl groups attached to the phosphorus atom have such a strong steric effect on the ylide carbon atom that it prevents effective collisions on the C-1 carbon atom.

Experimental

Of the reagents used in the experiments, tetra-O-acetyl-α-D-glucopyranosyl bromide [9], ethoxycarbonylmethylenetriphenylphosphorane [10], and cyanomethylenetriphenylphosphorane [11] were prepared as described in the literature.

Ethoxycarbonylmethylenetriphenylphosphorane and sec-butyl bromide

sec-Butyl bromide (0.69 g; 5 mmoles) and the phosphorane (3.48 g; 10 mmoles) were refluxed in dry benzene (30 ml) for 15 hrs. No precipitation of salt was observed. After evaporation to dryness, 80% of the phosphorane was recovered unchanged; m. p. 127—8 °C. No m. p. depression occurred in admixture with the original sample.

Ethoxycarbonylmethylenetriphenylphosphorane and cyclohexyl bromide

Cyclohexyl bromide (0.82 g; 5 mmoles) and the phosphorane (3.48 g; 10 mmoles) were refluxed in benzene (30 ml) for 20 hrs. No precipitation of salt occurred. After evaporation to dryness 78% of the phosphorane could be recovered unchanged; m. p. 127—9 °C (no m. p. depression with the original sample).

1,2-Ethylorthoacetyl-3,4,6-triacetyl-α-D-glucopyranose

(a) Tetra-O-acetyl-α-D-glucopyranosyl bromide (12.33 g; 3 cmoles) and ethoxycarbonylmethylenetriphenylphosphorane (20.91 g; 6 cmoles) were refluxed in chloroform solution (100 ml) for 12 hrs, then anhydrous ether (450 ml) was added, and the wall of the vessel was scraped. A crystalline salt (13.7 g) separated which gave pure ethoxycarbonylmethyltriphenylphosphonium bromide (11.0 g; 86%) on dissolution in chloroform and precipitation with ether; m. p. 158—9 °C. No m. p. depression occurred with an authentic sample.

The oil which remained after the evaporation of the mother liquor was treated with cold absolute ether (150 ml) to obtain the starting phosphorane (4.35 g; 21%). On crystallization of the evaporation residue of the ethereal mother liquor from alcohol (30 ml), 1,2-ethylorthoacetyl-3,4,6-triacetyl-α-D-glucopyranose (7.7 g; 68%) separated, m. p. 92—4 °C. It was recrystallized from cyclohexane (60 ml) to give the pure product (7.2 g; 64%); m. p. 94—96 °C; $[\alpha]_D + 30°$ (chloroform, $c = 1$).

The mother liquor of crystallization was evaporated to dryness and recrystallized from cyclohexane to yield triphenylphosphine oxide (3.1 g; 37%), m. p. 155—7 °C.

(b) Tetra-O-acetyl-α-D-glucopyranosyl bromide (4.11 g; 1 cmole) and cyanomethylenetriphenylphosphorane (6.02 g; 2 cmoles) were refluxed in chloroform (50 ml) for 11 hrs. After cooling, cyanomethyltriphenylphosphonium bromide (3.40 g; 98%) was obtained as

crystals, m.p. 256—8 °C. No m.p. depression occurred with an authentic sample. Evaporation and treatment of the chloroform filtrate with ether yielded further 11% of the phosphonium salt.

The mother liquor of the ethereal reaction mixture was evaporated to dryness and the residue crystallized from ethanol (18 ml) to give crystalline 1,2-ethylorthoacetyl-3,4,6-triacetyl-α-D-glucopyranose (2.6 g; 69%), m.p. 92—4 °C. The mixed m.p. and the infrared spectrum showed perfect identity with the product obtained in the former reaction; $[\alpha]_D + 31.0°$ (chloroform, $c = 1$).

The processing of the mother liquors of crystallization yielded a total amount of 1.45 g (52%) of triphenylphosphine oxide, m.p. 153—6°C.

(c) Tetra-O-acetyl-α-D-glucopyranosyl bromide (4.11 g; 1 cmole) and ethoxycarbonylmethylenetriphenylphosphorane (6.97 g; 2 cmoles) were refluxed in 5% benzene solution of ethanol (100 ml) for 6 hrs, and the ethoxycarbonylmethyltriphenylphosphonium bromide which separated on cooling was filtered off. The evaporation residue of the mother liquor was recrystallized to obtain crystalline 1,2-ethylorthoacetyl-3,4,6-triacetyl-α-D-glucopyranose (66%), m.p. 95—6 °C; $[\alpha]_D + 31.0°$ (chloroform, $c = 1$).

1,2-Isopropylorthoacetyl-3,4,6-triacetyl-α-D-glucopyranose

Tetra-O-acetyl-α-D-glucopyranosyl bromide (1 cmole) and ethoxycarbonylmethylenetriphenylphosphorane (2 cmoles) were refluxed in benzene containing 5% of isopropanol for 6 hrs, cooled and the crystalline ethoxycarbonylmethyltriphenylphosphonium bromide removed by filtration. Processing of the mother liquor yielded the pure product in 57% yield, m.p. 118—120 °C; $[\alpha]_D + 28.5°$ (chloroform, $c = 1$).

1,2-t-Butylorthoacetyl-3,4,6-triacetyl-α-D-glucopyranose

Tetra-O-acetyl-α-D-glucopyranosyl bromide (1 cmole) and ethoxycarbonylmethylenetriphenylphosphorane (2 cmoles) were refluxed in benzene containing 5% of *t*-butanol for 6 hrs. The reaction mixture was processed according to the above procedure to obtain the product in 42% yield; m.p. 149—51 °C; $[\alpha]_D + 34.0°$ (chloroform, $c = 1$).

REFERENCES

1.a. MESSMER, A., PINTÉR, I., SZEGŐ, F.: Angew. Chem. **76,** 227 (1964)
b. MESSMER, A., PINTÉR, I., SZEGŐ, F.: MTA Kém. Tud. Oszt. Közl. **25,** 1 (1966)
2. BESTMANN, H. J.: Chem. Ber. **95,** 58 (1962)
3. BESTMANN, H. J., ARNASON, B.: Chem. Ber. **95,** 1513 (1962)
4. LEMIEUX, R. U., CIPERA, J. D. T.: Can. J. Chem. **34,** 906 (1956)
5. LEMIEUX, R. U., MORGAN, A. R.: Can. J. Chem. **43,** 2199 (1965)
6. SCHULZ, M., STEINMAUS, H.: Zeitschr. Naturforschg. **193,** 263 (1964)
7. KHORLIN, A. YA., BOCHKOV, A. F., KOCHETKOV, N. K.: Izv. Akad. Nauk. SSSR **1964,** 2214
8. GRIGORENKO, A. A., SEVCHUK, M. J., DOMBROVISKII, A. V.: Zhur. Obshch. Him. **36,** 506 (1966)
9. BÁRCZAI-MARTOS, M., KŐRÖSY, F.: Nature **165,** 369 (1950)
10. ISLER, O., GUTMANN, H., MONTAVON, M., RÜEGG, R., RYSER, G., ZELLER, P.: Helv. Chim. Acta **40,** 1242 (1957)
11. SCHIEMENZ, G. P., ENGELHARD, H.: Chem. Ber. **94,** 578 (1961)

István PINTÉR
József KOVÁCS
András MESSMER
1025 Budapest, Pusztaszeri út 57—69.

Acta Chimica Academiae Scientiarum Hungaricae, Tomus 76 (4), pp. 399—407 (1973)

N-GYCOSIDES, XVII

PREPARATION AND STRUCTURE OF N-NITROSO-N-ARYLGLYCOSYLAMINES

R. BOGNÁR and M. M. PUSKÁS

(Institute of Organic Chemistry, L. Kossuth University, Debrecen)

Received February 14, 1972

Stable, crystalline N-nitroso derivatives (**II**) of secondary N-arylglycosylamine O-acetates (**I**) and methyl ethers have been prepared. Non-acetylated N-nitroso compounds (**III**) containing an aldo-hexose sugar component are non-crystalline and strongly hygroscopic, while the aldopentose derivatives are crystalline substances. They can be re-acetylated and give crystalline benzal derivatives (**IV**).

The N-nitroso structure of the compounds was confirmed by the acid hydrolysis of **III** and by azo-coupling reaction. The structures of the non-sugar decomposition or conversion products obtained (**III** A—G) could be traced back to primary aromatic N-nitrosamines. The reaction of compounds **III** with β-naphthol resulted in the corresponding dyes of phenylazo-β-naphthol type (**V**).

A significant structural difference between secondary N-glycosides and secondary amines is that the nitrogen atom of a secondary N-glycosylamine is involved in forming a mixed O,N-acetal with one of its covalent bonds. Therefore this bond, and therewith the glycosyl group can be readily split off hydrolytically, even if the other substituent on the nitrogen atom is an electron-withdrawing aryl or substituted aryl group.

In the course of our investigations on N-arylglycosylamines, the reactivity of the NH group of these compounds has been studied from several points of view (hydrolysis, stability, acylation, alkylation, quaternization, nitrosation, etc.).

In the present paper the nitrosation reactions of secondary N-arylglycosylamines, as well as the preparation, properties and structure determination of N-nitroso derivatives are reported.

Preparation of N-nitroso derivatives of N-arylglycosylamines

Because of the sensitivity of free-N-glycosides to acids [1, 2], their O-acetates were used in the nitrosation reactions, which were effected with sodium nitrite in glacial acetic acid. It is known that in glacial acetic acid medium the actual nitrosating agent is N_2O_3 formed by the interaction of nitrite ion and self-protonated nitrous acid; the nucleophilic attack of N_2O_3 may result in C-, N- or O-nitroso derivatives [3, 4, 5]. In the case of N-glycosides of aromatic primary amines, the possibility of nitrosation in the *para* or *ortho* positions of the aromatic ring should also be taken into account, in addition to the reaction with the NH group. In the compounds examined, however, this process was shown to play no part, and the products obtained were N-nitroso derivatives.

The O-acetylated N-nitrosoglycosylamines (**II**) are crystalline substances obtainable in high yields. They can be saponified with sodium methoxide according to ZEMPLÉN, to give acetyl-free N-nitroso derivatives (**III**). Of these, however, only the free N-nitroso-N-arylglycosylamines containing pentose (arabinose or xylose) were isolated as crystalline products; the aldohexose derivatives are strongly hygroscopic amorphous substances. Re-acetylation gave, however the crystalline starting acetates, and crystalline benzal derivatives (**IV**) could also be prepared from the free N-nitroso derivatives [12].

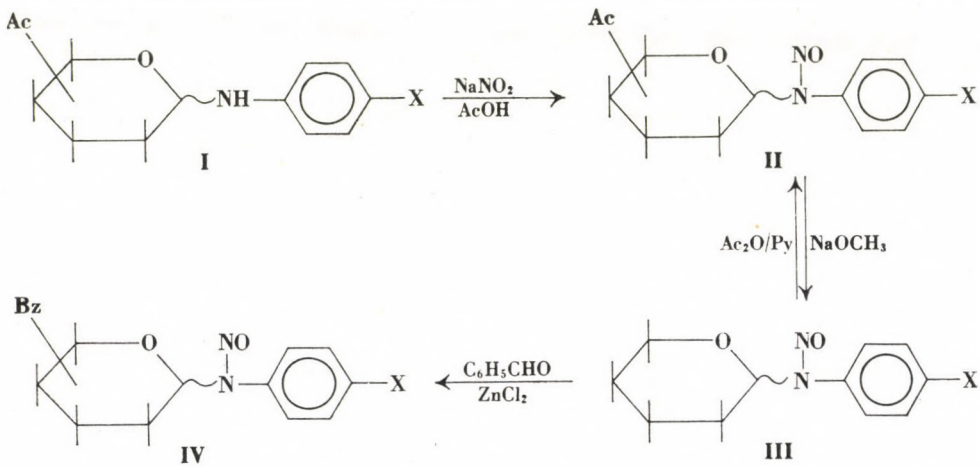

Similarly to N-glycosides acetylated in the sugar moiety, the O-methyl ether derivatives can also be nitrosated.

Catalytic hydrogenation with Pd/C removed the nitroso group from compound **3b** (Table I) and N-*p*-tolyl-tetra-O-acetyl-D-glucosylamine was obtained.

In the infrared spectra of both the free and acetylated or benzal-N-nitroso derivatives characteristic N—N=O bands appear at 1420—1380 cm^{-1}, 1240—1260 cm^{-1}, 1300—1330 cm^{-1} and 1130 cm^{-1} frequency values

The absorption maxima of their ultraviolet spectra are shifted towards shorter wavelengths by 25—70 nm as compared with the parent compounds; thus, N-nitrosation results in a hypsochromic shift.

The data in Table I show that laevorotatory β-anomeric O-acetates give dextro-rotatory compounds on both N-acetylation and N-nitrosation; further on, identical N-nitroso and N-acetyl derivatives are obtained on the acetylation or nitrosation of either α- or β-anomeric N-aryl-glycosylamine O-acetates.

Chemical evidence of the N-nitroso structure of the compounds

In addition to the analytical, infrared and ultraviolet spectroscopic results, the structures of the compounds were also proved chemically; *e.g.*, in the case of N-nitroso-N-*p*-nitrophenyl-D-glucopyranosylamine, this was car-

Table I

Specific rotations of N-glycoside derivatives

No.	Compound	$[\alpha]_D$ values						
		a	*b*	*c*	*d*	*e*	*f*	*g*
1.	N-Phenyl-D-glucopyranosylamine	+216	+24	+63			+145	+88*
2.	N-Phenyl-α-D-galactopyranosylamine	+205	+48	+96				
	N-Phenyl-β-D-galactopyranosylamine	— 34.1	+48	+96				
3.	N-*p*-Tolyl-D-glucopyranosylamine	— 78	+17	+64.2		+58		
4.	N-*p*-Tolyl-D-galactopyranosylamine	— 53	+36	+82		+66		
5.	N-*p*-Bromophenyl-α-D-glucopyranosylamine	+168	+16	+64				
	N-*p*-Bromophenyl-β-D-glucopyranosylamine	— 65	+16	+64		+51		
6.	N-*p*-Bromophenyl-α-D-galactopyranosylamine	+189	+36	+85				
	N-*p*-Bromophenyl-β-D-galactopyranosylamine	— 53	+36	+85		+70	—123.3	+110*
7.	N-*p*-Nitrophenyl-D-glucopyranosylamine	—204	+93	+115		+87		
8.	N-*p*-Nitrophenyl-D-glucopyranosylamine	— 70	+125	+160				
9.	N-*p*-Tolyl-D-xylopyranosylamine	— 25	+26.5	+32	—128			
10.	N-*p*-Bromophenyl-D-xylopyranosylamine	— 23	+6.5	+36	—62	+36		
11.	N-*p*-Bromophenyl-L-arabinopyranosylamine	+ 70	+48	—71	+72	—73		
12.	N-*p*-Chlorophenyl-D-xylopyranosylamine	— 25	+7	+35	—62	+35		
13.	N-*p*-Chlorophenyl-L-arabinopyranosylamine	+ 75	+56.5	—90	+66.8	—90		
14.	N-*p*-Nitrophenyl-D-xylopyranosylamine	— 37	+15.6	+117	+79			
15.	N-*p*-Nitrophenyl-L-arabinopyranosylamine	+130	+171.4	+140	+257			

* $c = 1$, in 96% ethanol; $c = 1$, in pyridine

The values of optical rotation in the columns refer to:

(*a*) Compound, acetylated in the sugar moiety [6—10]; (*b*) N-nitroso, acetylated in the sugar moiety; (*c*) N-acetyl, acetylated in the sugar moiety; (*d*) N-nitroso, non-acetylated; (*e*) N-acetyl, non-acetylated in the sugar moiety [13—15]; (*f*) methylated in the sugar moiety [11]; (*g*) N-nitroso-N-glycosides methylated in the sugar moiety.

ried out as follows. The free N-nitroso-N-glycoside, obtained by saponification of the O-acetate with CH_3ONa, was treated with dilute acid; nitric acid was liberated and a precipitate separated at room temperature, or more readily on heating. In the course of the reaction, D-glucose, nitrobenzene, *p*-nitrophenol, *p*-nitroaniline and 4,4'-dinitrodiazoaminobenzene were formed.

The compounds were identified as described in Experimental.

The ratio and amounts of the products formed depended on the conditions of the hydrolysis (temperature and time of heating). For example, the amount of *p*-nitrophenol increases with increasing temperature and duration of heating at the expense of the diazo compound.

The formation of the decomposition products takes place according to the following reaction equations:

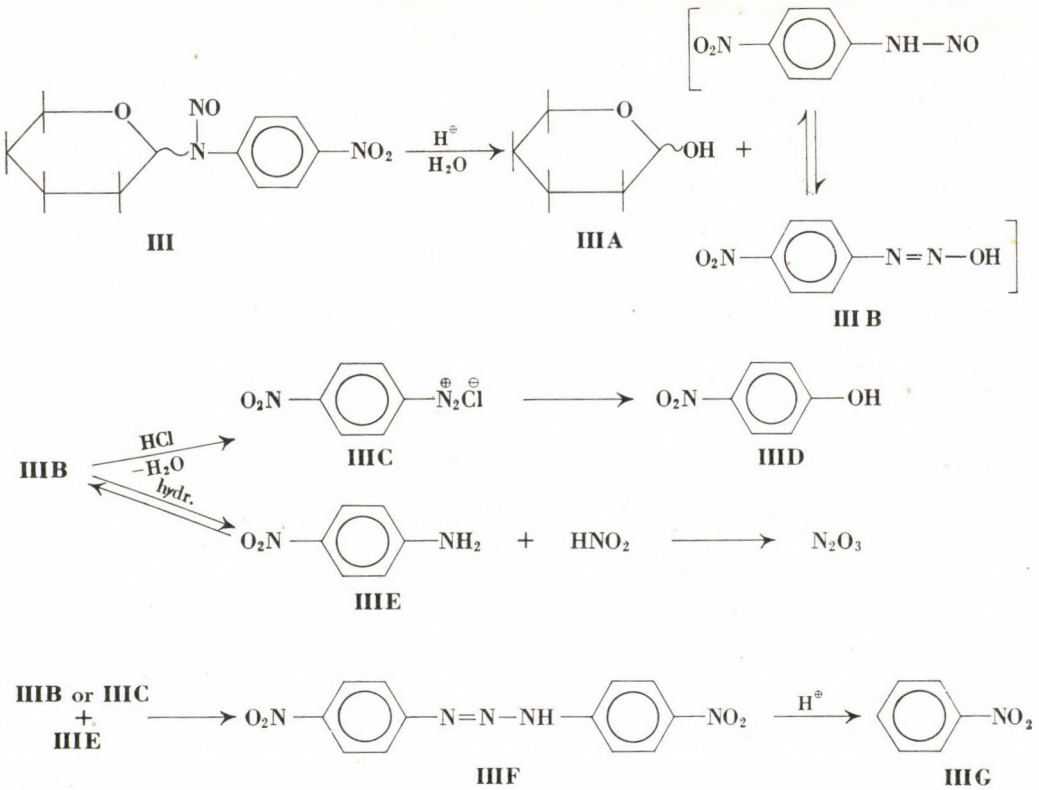

The hydrolysis products, N-nitroso-*p*-nitroaniline and its tautomeric form, isonitrosamine (**IIIB**), are not stable even at room temperature [16]. Treatment with dilute hydrochloric acid gives partly *p*-nitrophenyldiazonium chloride (**IIIC**) which is hydrolyzed to *p*-nitrophenol (**IIID**); on the other hand, in aqueous medium (**IIIB**) is decomposed in an equilibrium reaction to yield

p-nitroaniline (**IIIE**) and nitrous acid. The reaction of *p*-nitroaniline with N-nitroso-*p*-nitroaniline or *p*-nitrophenyldiazonium chloride results in 4,4'-dinitrodiazoaminobenzene (**IIIF**). The latter is hydrolyzed by hot acid to nitrobenzene (**IIIG**).

The other compounds in Group *d* of Table I also decompose in a similar way on treatment with hot dilute aqueous acids.

The N-nitroso structure of the compounds and the first step of the above hydrolytic reaction, *i.e.*, the formation of nitrosamine or isonitrosamine and the diazonium salt, are also confirmed by the experimental fact that the acetyl-free compounds *1d* and *7d* can be coupled with β-naphthol in the same way as usual in the preparation of azo dyes; the reaction results in the corresponding azo dyes, *i.e.*, phenylazo-β-naphthol and *p*-nitrophenylazo-β-naphthol.

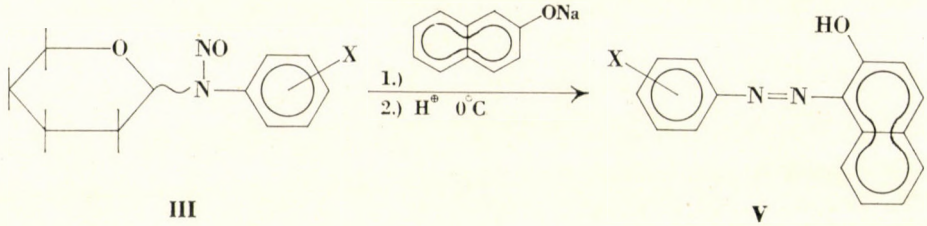

III V

X: H: NO_2

The reactions discussed verify unambiguously that the site of nitrosation is the nitrogen atom of the N-glycoside, and nitrosation of the benzene ring at *para* position does not occur in the case of N-phenyl-D-glycosylamine derivatives, either.

Further investigations on this group of compounds, as well as the elucidation of the anomerism conditions by means of spectroscopic methods are in progress and will be reported in a forthcoming paper.

Experimental

Preparation of N-nitroso-N-arylglycosylamines acetylated in the sugar moiety

The β-anomer or an anomeric mixture of the N-glycoside-O-acetate (0.01 mole) was dissolved in five parts of glacial acetic acid and solid sodium nitrite (0.03 mole) was added to the solutions, with stirring, during 1 hr at room temperature. The reaction mixture was poured onto 100 parts of crushed ice, under stirring; the yellowish product which precipitated was filtered off and washed with cold water until free from acid. The air-dry product was recrystallized from ethanol in the presence of decolorizing carbon (Table II).

Preparation of N-nitroso-N-arylglycosylamines

The N-nitroso-N-arylglycosylamine acetylated in the sugar moiety was dissolved in a minimum amount of absolute methanol or a mixture of absolute chloroform at room temperature and it was saponified with a catalytic amount of 0.1*N* sodium methoxide. The reaction mixture was allowed to stand at room temperature for 30 min, then at 0 °C for 24 hrs. After

Table II

Symbol	Compound	Yield, %	M.p., °C	N %		C %		H %	
				Calcd.	Found	Calcd.	Found	Calcd.	Found
1b	N-Nitroso-N-phenyl-2,3,4,6-tetraacetyl-D-glucosylamine	78	105	6.19	6.16	53.09	53.20	5.34	5.24
2b	N-Nitroso-N-phenyl-2,3,4,6-tetraacetyl-D-galactosylamine	76	102	6.19	6.24	53.09	53.23	5.34	5.12
3b	N-Nitroso-N-*p*-tolyl-2,3,4,6-tetraacetyl-D-glucosylamine	69	115—6	6.01	6.05	54.07	53.97	5.61	5.73
4b	N-Nitroso-N-*p*-tolyl-2,3,4,5-tetraacetyl-D-galactosylamine	75	105	6.01	6.00	54.07	54.27	5.61	5.78
5b	N-Nitroso-N-*p*-bromophenyl-2,3,4,6-tetraacetyl-D-glucosylamine	68	132	5.27	5.20	45.19	45.28	4.36	4.34
6b	N-Nitroso-N-*p*-bromophenyl-2,3,4,6-tetraacetyl-D-galactosylamine	62	116	5.27	5.29	45.19	45.38	4.36	4.43
7b	N-Nitroso-N-*p*-nitrophenyl-2,3,4,6-tetraacetyl-D-glucosylamine	72	160	8.41	8.43	48.29	48.41	4.66	4.69
8b	N-Nitroso-N-*p*-nitrophenyl-2,3,4,6-tetraacetyl-D-galactosylamine	65	142	8.41	8.30	48.29	48.26	4.66	4.49
9b	N-Nitroso-N-*p*-tolyl-2,3,4-triacetyl-D-xylosylamine	56	100	7.10	7.28				
10b	N-Nitroso-N-*p*-bromophenyl-2,3,4-triacetyl-D-xylosylamine	67	121	6.10	6.25				
11b	N-Nitroso-N-*p*-bromophenyl-2,3,4-triacetyl-L-arabinosylamine	58	119—20	6.10	5.98				
12b	N-Nitroso-N-*p*-chlorophenyl-2,3,4-triacetyl-D-xylosylamine	74	119—21	6.75	7.00				
13b	N-Nitroso-N-*p*-chlorophenyl-2,3,4-triacetyl-L-arabinosylamine	60	108—9	6.75	6.92				
14b	N-Nitroso-N-*p*-nitrophenyl-2,3,4-triacetyl-D-xylosylamine	78	161	9.88	9.69				
15b	N-Nitroso-N-*p*-nitrophenyl-2,3,4-triacetyl-L-arabinosylamine	70	131—2	9.88	9.75				
1g	N-Nitroso-N-phenyl-2,3,4,6-tetra-O-methyl-D-glucosylamine	58	82.5—83.5	8.23	8.31				
5g	N-Nitroso-N-*p*-bromophenyl-2,3,4,6-tetra-O-methyl-D-galactosylamine	65	87—88	6.67	6.52				

this the solution was neutralized with glacial acetic acid and evaporated to dryness on a water bath at 40 °C in vacuum. In the presence of aldohexose sugar components, hygroscopic yellow foams were obtained which could not be crystallized. If the sugar component was an aldopentose, the solid residue was dissolved in pyridine, treated with decolorizing carbon and evaporated to dryness in vacuum; then some absolute ethanol was added to it repeatedly, and the mixture was evaporated to dryness to remove pyridine. Finally the product was crystallized (Table III).

Table III

Symbol	Compound	M.p., °C
9d	N-Nitroso-N-*p*-tolyl-D-xylosylamine	162
10d	N-Nitroso-N-*p*-bromophenyl-D-xylosylamine	156
12d	N-Nitroso-N-*p*-chlorophenyl-D-xylosylamine	147
14d	N-Nitroso-N-*p*-nitrophenyl-D-xylosylamine	
11d	N-Nitroso-N-*p*-bromophenyl-L-arabinosylamine	
12d	N-Nitroso-N-*p*-chlorophenyl-L-arabinosylamine	
15d	N-Nitroso-N-*p*-nitrophenyl-L-arabinosylamine	136

Re-acetylation of N-nitroso-N-arylglycosylamines

The N-nitroso-N-arylglycosylamine was acetylated with 10 parts of acetic anhydride and 10 parts of absolute pyridine at room temperature for 24 hrs; the N-nitroso-N-arylglycosylamines acetylated in the sugar moiety were obtained in high yields. The reaction mixture was poured onto 100 parts of crushed ice, the product which separated was filtered off and washed with cold water until free from acid. The air-dry product was recrystallized from ethanol or methanol using decolorizing carbon.

Benzal derivatives of N-nitroso-N-aryl-D-glycosylamines

The N-nitroso-N-aryl-D-glycosylamine (0.003 mole) was shaken with freshly distilled benzaldehyde (0.025 mole) and freshly ignited zinc chloride (0.005 mole) in a closed vessel for 5 hrs. Ice-water, then petroleum ether were added to the mixture. The solid product was filtered off and washed with cold water and petroleum ether. The air-dry substance was treated with decolorizing carbon and recrystallized from ethanol. The data of the compounds are given in Table IV.

Hydrolysis of N-nitroso-N-arylglycosylamines

N-Nitroso-N-arylglycosylamines can be hydrolyzed in 1—5% aqueous hydrochloric acid solution by heating on a water bath at 80 °C for 5 min, then allowing the mixture to stand at room temperature. During hydrolysis a copious precipitation occurs, accompanied by a characteristic smell. The nitrous acid formed was detected with a paper impregnated with potassium iodide and starch. The hydrolysate was cooled to 0 °C and filtered.

The sugar content of the filtrate was examined quantitatively by means of paper chromatography. Schleicher—Schüll 2043 b Mgl paper and *n*-butanol–pyridine–water (6 : 4 : 3) solvent mixture were used; the development took 28 hrs; the spots were detected with aniline hydrogen phthalate, and heating to 105 °C for 10 min; the expected amount of D-glucose was found by means of measuring the spot weight.

The filtrate was extracted with ether, treated with decolorizing carbon, concentrated to one-fourth of its volume, and the corresponding phenols were identified after recrystallization on the basis of their melting points and mixed melting points; TLC was used for the identification of the amines (Merck Kieselgel G layer; benzene developing solvent; 1% aqueous $FeCl_3$ reagent for the detection of phenols; diazotization and dye-coupling reactions were used for the detection of amines, beside standard substances).

The precipitate was crystallized from methanol, acetone or benzene after repeated treatment with decolorizing carbon. The orange-yellow product had indicator properties. Its 0.1% alcoholic solution had lemon-yellow and cherry-red colours in acid and alkaline media,

Table IV

No.	Compound	Yield, %	M.p., °C	$[\alpha]_D^{20}$	N %		C %		H %	
					Calcd.	Found	Calcd.	Found	Calcd.	Found
1.	N-Nitroso-N-phenyl-4,6-benzal-D-glucosylamine	45	123	—84	7.51	7.39				
2.	N-Nitroso-N-*p*-tolyl-4,6-benzal-D-glucosylamine	38	86	—46.6	7.25	6.96				
3.	N-Nitroso-N-*p*-bromophenyl-4,6-benzal-D-glucosylamine	35	80	—70	6.20	5.98				
4.	N-Nitroso-N-*p*-bromophenyl-4,6-benzal-D-galactosylamine	40	92	—18	6.20	6.00				
5.	N-Nitroso-N-*p*-nitrophenyl-4,6-benzal-D-glucosylamine	49	176	+37.3	10.07	10.02	52.41	52.50	4.87	4.80

respectively. The pH range of the colour change was 11.07—11.57 determined in glycine NaCl NaOH buffer solution according to Sörensen. The compound was found to be 4,4'-dinitrodiazoaminobenzene by comparison of its TLC, IR, UV and melting point data with an authentic sample.

Preparation of phenylazo-β-naphthol from N-nitroso-N-phenylglycosylamines

N-Nitroso-N-phenylglycosylamine (0.001 mole) was dissolved in 10% hydrochloric acid (2.5 ml) and the solution was cooled to 0 °C. β-Naphthol (0.144 g; 0.001 mole) was dissolved in 10% sodium hydroxide (0.83 ml) and the solution placed into an ice bath. The cold acid solution of the N-nitroso compound was added to it slowly, dropwise, under stirring. A red colour appeared, then a red substance precipitated. The reaction mixture was allowed to stand in ice for 30 min, then filtered off and the precipitate washed with cold water. The air-dry product was recrystallized from ethanol after treatment with decolorizing carbon, to obtain 0.03 g of the product, m.p. 130 °C (lit. m.p. 131 °C). The substance was run on a Kieselgel G thin layer in benzene together with authentic phenylazo-β-naphthol; the samples were found to be identical.

***p*-Nitrophenylazo-β-naphthol** (Para Red)

This compound was obtained from N-nitroso-N-*p*-nitrophenylglycosylamines according to the procedure given for the preparation of Para Red [17]. Recrystallization from toluene gave 0.05 g of the product, m.p. 246 °C (lit. m.p. 246—48 °C). The product was identical with an authentic sample on the basis of TLC (Kieselgel G; benzene).

Preparation of N-nitroso-N-arylglycosylamines methylated in the sugar moiety

Nitrosation was carried out in the same way as in the case of acetyl derivatives. The nitroso derivatives were extracted with $CHCl_3$ after having poured the reaction mixture onto ice. The combined extracts were dried over Na_2SO_4 and evaporated to dryness on a water bath at 40 °C in vacuum. The residue was dissolved in petroleum ether, b.p. 60—80 °C, treated with decolorizing carbon, and the crystalline product was obtained on cooling.

*

The authors' thanks are due to the Hungarian Academy of Sciences for supporting this work, to Dr. É. Dávid-Rákosi for the analyses, and to Mr. G. Horváth for his assistance in the work on pentosides.

REFERENCES

1. Isbell, H. S., Frush, H. L.: Am. Chem. Soc. **72,** 1043 (1950)
2. Bayne, S., Holmes, W. H.: J. Chem. Soc. **1952,** 4347
3. Austin, A. T.: Science Progress XLIX 196 (1961)
4. Challis, B. C., Butler, A. R.: The Chemistry of the Amino Group (Ed. S. Patai), p. 305. J. Wiley & Sons, London—New York—Sydney, 1968
5. Turney, T. A., Wright, G. A.: Chem. Rev. **59,** 497 (1959)
6. Weisz, E.: Preparation of acetylated glycosides containing nitrogen. (In Hungarian). Doctoral Thesis, Budapest, 1940
7. Bognár, R., Nánási, P.: J. Chem. Soc. **1955,** 189
8. Bognár, R., Nánási, P.: Acta Chim. Acad. Sci. Hung. **22,** 301 (1960)
9. Nánási, P., Bognár, R.: J. Chem. Soc. **1961,** 323
10. Nánási, P., Bognár, R.: Acta Phys. et Chim. Debrecina VIII 49 (1962)
11. Bognár, R., Nánási, P., Lipták, A.: Acta Chim. Acad. Sci. Hung. **45,** 47 (1965)
12. Freudenberg, K., Toepffer, H., Andersen, C. Chr.: Chem. Ber. **61,** 1750 (1928)
13. Sokolowski, J., Fialkiewicz, Z., Smiatacz, Z., Wasielewski, C.: Roczniki Chem. **37,** 515 (1963)
14. Sokolowski, J., Szafranek, J.: Roczniki Chem. **37,** 735 (1963)
15. Smiatacz, Z., Sokolowski, J.: Roczniki Chem. **40,** 1473 (1966)
16. Müller, E., Haiss, H.: Chem. Ber. **96,** 570 (1963)
17. Organikum, VEB Deutscher Verlag der Wissenschaften, 502 B, Berlin, 1962

Rezső Bognár
Mária M. Puskás
4010 Debrecen 10. Hungary.

Acta Chimica Academiae Scientiarum Hungaricae, Tomus 76 (4), pp. 409—415 (1973)

STUDY OF THE TRANSFORMATIONS OF DIOLS AND CYCLIC ETHERS, XXXI*

DEHYDRATION OF 1,3-DIOLS ON METAL CATALYSTS

M. BARTÓK and Á. MOLNÁR

(Department of Organic Chemistry, A. József University, Szeged)

Received February 21, 1972

The experimental results of the dehydration of 1,3-diols of various structures on copper catalysts are reported. The experimental work leads to the finding that a suitably prepared copper catalyst catalyzes the dehydration of 1,3-diols. Depending on the structure of the diol, three main reactions take place: the formation of oxo compounds with the same number of carbon atoms as those of the diol, 1,2-elimination and fragmentation processes.

It has been experimentally confirmed that the transformation of the diols with the accompanying formation of oxo compounds can be observed not only on the vicinal diols but, with the change of the experimental conditions, on certain types of 1,3-diols too.

In this paper we deal with the investigation of the transformations of 1,3-diols on metal catalysts. This is a timely problem, not only because of its practical importance, but also because at the beginning of our studies both the general regularities of the dehydration of 1,3-diols and the dehydrating abilities of metal catalysts were often discussed and interpreted in the literature in an incorrect manner. With a few exceptions, the reason for this is seen in the lack of suitable experimental data and in the fact that the experimental results which had been obtained were not analyzed in the best way.

Up to the present no regularities of general validity have been put forward for the possible transformations of 1,3-diols (we disregard the incorrect assertion often cited in organic chemistry textbooks that under condition of dehydration 1,3-diols are converted mainly to cyclic ethers). It must be stressed at once that the dehydration of 1,3-diols mostly does not lead to the formation of cyclic ethers. It is possible, however, to find literature data [1—4] which describe the formation of unsaturated alcohols, dienes, oxo compounds and various fragments on the dehydration of 1,3-diols.

From a survey of the literature it can be established that there have been attempts in the field of 1,3-diols to systematize the various experimental data and to draw certain general conclusions from these [5, 6]. This work did not succeed, however, due to the contradictory experimental results. Since new experimental data related to this were not obtained, it was not possible either to study for example whether the pinacol type rearrangement can be extended to the entire family of diols. It is certain that progress is not assisted

* Part XXX: Acta Phys. et Chem. Szeged, **18**, 85 (1972)

by findings such as those which consider the transformation of 1,2-diols with the accompanying formation of oxo compounds as a feature of vicinal diols, separate vicinal glycols quite rigorously from other diols, and hence try to compare the transformations of 1,3-diols particularly to the reactions of 1,4- and 1,5-diols.

Detailed accounts were given in our earlier work [7—10] of the experimental results on the dehydration of 1,3-propanediol and 1,3-butanediol in the presence of various metal catalysts. This work has led to the finding that the most active of the Raney type metal catalysts is Cu/Al. In order to prove the catalytic role of the copper, and also for preparative purposes, a study was made of the dehydration of 1,3-butanediol with copper catalysts on aluminium oxide and silica gel supports. It turned out during these studies that as regards its activity, cycle-time and life-time, the copper catalyst on a silica gel support prepared by a suitable chosen method is better than the Cu/Al catalyst, and its selectivity does not decrease either. It could thereby be proved that the catalytic effect can be attributed to the appropriate form of copper. On the above basis a procedure was developed [11] for the preparation of methyl ethyl ketone from the C_3 fraction: by means of the PRINS reaction [12] the propylene content of the C_3 fraction is converted with formaldehyde to 1,3-butanediol, using cation-exchange resins as catalyst.

The 1,3-butanediol can be dehydrated to methyl ethyl ketone and butyraldehyde on a Cu/SiO_2 catalyst at 200—250 °C.

The present paper reports the experimental results of the dehydration of 1,3-diols of various structures on metal catalysts. The following model compounds were selected for the study of the dehydration of the 1,3-diols. Some of these (**I, IV—VIII, X—XIV**) were commercial products, while others (**II, III, IX, XV—XVII**) were prepared by ourselves on the basis of literature methods.

Diprimary 1,3-diols [13]:

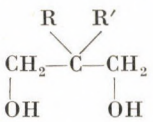

	I	II	III	IV	V	VI	VII
R	H	i-Pr	Bu	Me	Me	Et	Et
R′	H	H	H	Me	Pr	Et	Bu

Primary-secondary 1,3-diols:

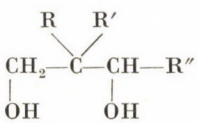

	VIII	IX	X	XI
R	H	H	H	Me
R′	H	H	Et	Me
R″	Me	Ph	Pr	i-Pr

Disecondary 1,3-diols:

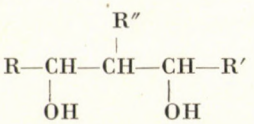

	XII	XIII	XIV
R	Me	Me	Me
R′	Me	Me	Me
R″	H	Me	Pr

Primary-tertiary, secondary-tertiary and ditertiary 1,3-diols:

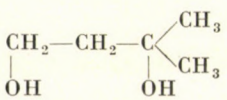

XV

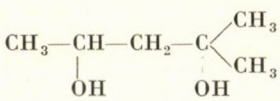

XVI

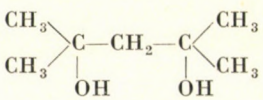

XVII

The dehydration of the 1,3-diols listed was studied mainly on Cu/Al and Cu/SiO_2, and also on Pt/C catalysts. The reactions were carried out in a continuous system at 150—300 °C in the apparatus described earlier [7]. The description of the method of investigation and the preparation of the catalysts can also be found in earlier papers [7, 11, 14]. In addition to the above, we also carried out the transformation of 1,3-butanediol on platinum, palladium and rhodium catalysts on a thermolite (T) carrier, using an impulse technique.

The experimental results are summarized below. During the transformation of the 1,3-diols on Cu/Al and Cu/SiO_2 catalysts it was possible to observe, depending on the structure of the diol, the three main reaction paths outlined in the following scheme:

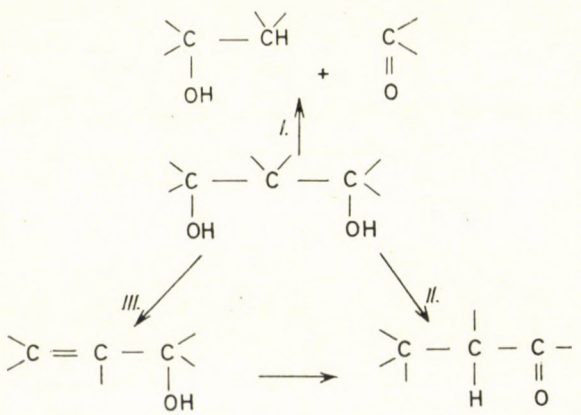

I. Splitting of the molecule into two parts; this is the characteristic direction of decomposition in the transformation mainly of polysubstituted 1,3-diols on Cu/SiO_2 and Cu/Al catalysts. The probability of the occurrence of

this process increases with the order of both the carbon atoms bearing the hydroxyl groups (with the exception of the ditertiary diols), and the carbon atom at position 2.

II. Intramolecular dehydration accompanied by the formation of oxo compounds with the same number of carbon atoms as the diols; this process is characteristic for the primary-secondary, disecondary and primary-tertiary diols, mainly in those cases where there are no substituents on the carbon atom at position 2.

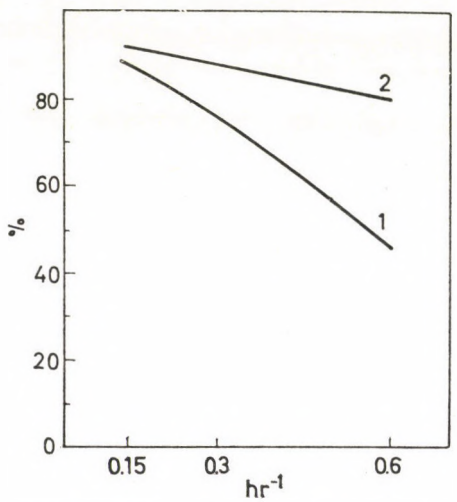

Fig. 1. Variation of the conversion of 2-methyl-2,4-pentanediol (1) and 2,4-dimethyl-2,4-pentanediol (2) as a function of the volume flow rate, on a Cu/Al catalyst, at 224 °C

III. 1,2-elimination processes resulting in the formation of α,β-unsaturated alcohols and dienes; these can be observed only in the case of ditertiary diols not containing substituents on the carbon atom at position 2.

The experimental results serving as the basis of the above conclusions can be found in Table I, for some of the model compounds.

From a comparison of the data relating to compounds **XVI** and **XVII** of Table I with the experimental data given in Fig. 1, it can be seen that for those 1,3-diols (ditertiary 1,3-diols) where as a result of the structure of the molecule dehydrogenation is a hindered process, the elimination of water leading to the formation of unsaturated alcohols and dienes becomes the determining reaction direction and is faster than the fragmentation, even in the case of metal catalysts.

The three primary processes given above (I, II, III) are followed by the hydrogenation, dehydrogenation, decarbonylation, dehydration (formation of dienes in the case of ditertiary diols), and decomposition of the primary products, and by intermolecular hydrogenation–dehydrogenation processes

Table I

Main directions of the transformation of 1,3-diols on a Cu/Al catalyst (volume flow rate 0.1 hr^{-1}; temperature 200—250 °C; conversion 100%)

Formula		Yield of fragmentation products (%)	Yield of oxo compounds with same number of carbon atoms as diol (%)
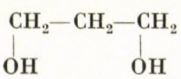	I	10	80
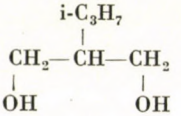	II	40	60
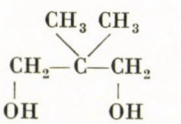	IV	90	0
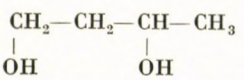	VIII	min.	95
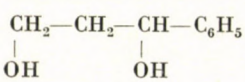	IX	30	60
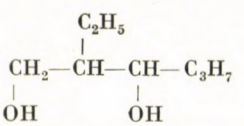	X	85	15
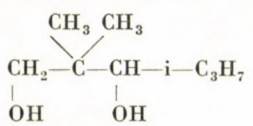	XI	90	0
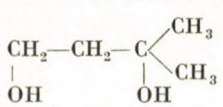	XV	75	15
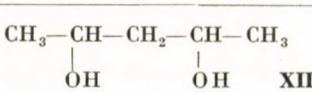	XII	35	65

Table I (cont.)

Formula	Yeld of fragmentation products (%)	Yield of oxo compunds vith same number of carbon atoms as diol (%)
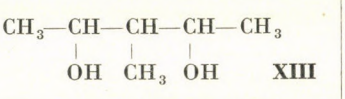 XIII	80	0
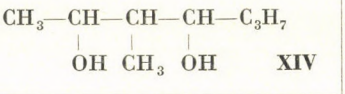 XIV	95	0
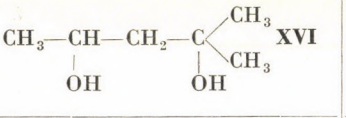 XVI	95	0
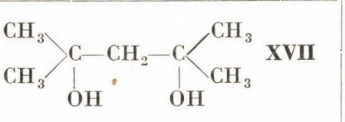 XVII	0	0*

* 40% dimethyl isobutenyl carbinol and 60% 2,4-dimethyl-1,3-pentadiene are formed.

as secondary reactions. The role of the secondary transformations becomes more important at higher temperatures.*

In the interpretation of the mechanism of dehydration of 1,3-diols on a Cu/Al catalyst importance is attached to the process of dehydrogenation of 1,3-butanediol observed at low conversions, in the course of which the formation of 1-butanol-3-one could be observed with high selectivity.

The experimental results of the transformations of 1,3-diols on Pt/C and Pt/T catalysts are summarized below. The activity of platinum catalysts is lower than those of Cu/Al and Cu/SiO_2 catalysts. In the case of the Pt/C catalyst the main directions of the transformations are essentially the same as those observed for copper catalysts. The lower activity of the Pt/C catalyst, however, requires a higher reaction temperature, and as a result of the increase of the rates of the secondary processes, therefore, the transformation proceeds with lower selectivity. A significant difference can be observed between the transformations of 1,3-butanediol on Pt/C and Pt/T catalysts. While methyl ethyl ketone is formed as the major product on a Pt/C catalyst in a continuous system, at the same time on a Pt/T catalyst (under the conditions of the impulse technique) in addition to the formation of methyl ethyl ketone (20%) a much larger amount of acetone (40%) is also obtained.

* It should be noted that in the absence of catalysts, but under otherwise identical experimental conditions, the diols studied do not react.

REFERENCES

1. BAUER, F.: Monatsh., **25,** 1 (1904)
2. KADIERA, V.: Monatsh., **25,** 332 (1904)
3. WINFIELD, M. E.: Catalysis, Vol. VII, (Ed. Emmett, P. H.) Reinhold, New York 1960
4. Glycols. ACS Monograph Ser. No. 114 (Ed. Curme, G. O., Johnston, F.) Reinhold, New York 1952
5. BARBOT, A.: Ann. Chim. **11,** 599 (1939)
6. MATHIEU, J., ALLAIS, A., VALLS, J.: Cahiers de synthèse organique, Vol. VI, Masson et Cie., Paris 1960
7. BARTÓK, M., KOZMA, B.: Acta Phys. et Chem. Szeged, **9,** 116 (1963)
8. BARTÓK, M., ZALOTAI, L.: Acta Phys. et Chem. Szeged, **14,** 39 (1968)
9. ZALOTAI, L., BARTÓK, M.: Acta Phys. et Chem. Szeged, **14,** 47 (1968)
10. BARTÓK, M., PRÁGAI, B.: Acta Phys. et Chem. Szeged, **16,** 85 (1972)
11. BARTÓK, M., KORÁNYI, GY., KOVÁCS, K., NOTHEISZ, F.: Patent application, 8 Sept. 1971
12. PRINS, H. J.: Chem. Weekbl., **14,** 267, 932 (1917); J. Chem. Soc., **114,** 261 (1918)
13. BARTÓK, M., KOZMA, B., GILDE, A. S.: Acta Phys. et Chem. Szeged, **11,** 35 (1965)
14. BARTÓK, M., FÉNYI, SZ.: Acta Phys. et Chem. Szeged, **12,** 157 (1966)

Mihály BARTÓK
Árpád MOLNÁR } 6701 Szeged, Dóm tér 8. Hungary.

Acta Chimica Academiae Scientiarum Hungaricae, Tomus 76 (4), pp. 417—429 (1973)

STUDY OF THE TRANSFORMATIONS OF DIOLS AND CYCLIC ETHERS, XXXII

STUDY OF THE TRANSFORMATIONS OF 2-METHYL-OXACYCLOALKANES ON METAL CATALYSTS

M. BARTÓK, I. TÖRÖK and I. SZABÓ

(Department of Organic Chemistry, A. József University, Szeged)

Received February 21, 1972

The reactions of 2-methylethylene oxide, 2-methyloxethane, 2-methyltetrahydrofuran and 2-methyltetrahydropyran have been studied in the presence of Pt/T, Pd/T, Rh/T, Cu/Al, Ni/Al and Zn/Al catalysts, under identical experimental conditions, by the impulse technique. In the experimental work an analysis was made of the reaction directions which depend on the ring size and the catalyst: isomerizations to the corresponding aldehydes, ketones and unsaturated alcohols, and hydrogenolysis with the formation of the corresponding alcohols.

Under the influence of metal catalysts oxacycloalkanes can in principle isomerize to oxo compounds and unsaturated alcohols, while on the action of catalytically activated hydrogen they may undergo hydrogenolysis, with the formation of alcohols. Before our investigations were begun (1958) only the isomerization reactions of epoxides had been reported and, therefore, the opinion had evolved that these were characteristic of epoxides in general [1]. Our aim which arose from this (and towards which we worked in cooperation with the Organic Catalysis Group, Organic Chemistry Institute, Academy of Sciences of the USSR) was the study of the regularities of the isomerization and hydrogenolysis of oxacycloalkanes containing low numbers of carbon atoms in the rings. In the course of this joint research we demonstrated the general character of the isomerization of the oxacycloalkanes to oxo compounds [2—8]. It must be stressed that, in spite of the fact that reference can be found in the patent literature to the isomerization of oxacycloalkanes, this process had previously been experimentally confirmed and hence was a scientifically accepted reaction only for epoxides [9—11].

In the present paper we wish to report our more recent studies which were carried out with regard to the isomerization of 2-methyl-oxacycloalkanes in the presence of various metal catalysts, and which made use of the possibilities provided by the impulse technique. In our earlier work the isomerization of the oxacycloalkanes had been established only qualitatively and in its main outlines, and only the isomerizing activity of platinum catalysts had been studied. Investigations were not made to study the transformations of oxacycloalkanes of various ring-sizes under the same experimental conditions, nor with the experimental parameters ensured by the impulse technique.

On the above basis our aim was to study the behaviour of 2-methylethylene oxide, 2-methyloxacyclobutane, 2-methyltetrahydrofuran and 2-methyltetrahydropyran in the presence of platinum, palladium and rhodium catalysts on thermolite supports, and of Raney type copper, zinc and nickel catalysts (in the following metal/T and metal/Al) at 150—400 °C. The studies were carried out with the impulse technique, using hydrogen as carrier gas. The impulse technique described earlier [12] was modified merely in that Rasotherm glass was selected as the structural material of the microreactor. The description of the preparation of the catalysts used in the experimental work and of their individual properties can be found in our earlier publications [12—14]. In the experimental work we generally used 1 ml of the thermolite supported catalysts containing 10% metal, and 0.2 ml of the Raney type catalysts. The internal diameter of the microreactor was 6 mm. The experimental method consisted in the study of the selected oxacycloalkanes under identical experimental parameters. The extent of conversion of the individual compounds was measured as a function of temperature, and the products formed were determined both qualitatively and quantitatively.

An account of the experimental results now follows. In the presence of both Pt/T, Pd/T, Rh/T and Ni/Al, Cu/Al, Zn/Al catalysts the conversion of the

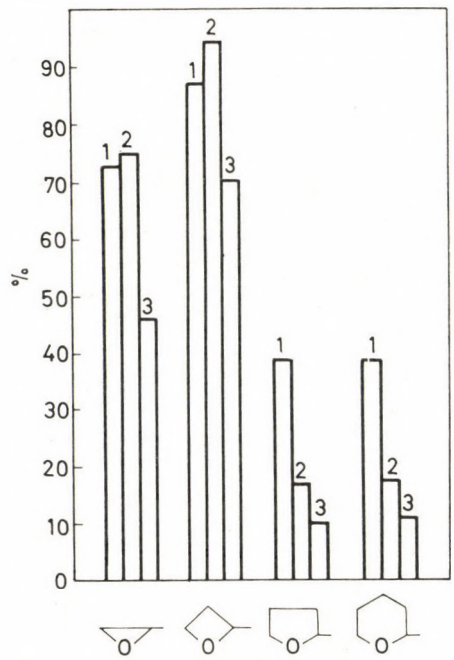

Fig. 1. Conversion (%) of 2-methyloxacycloalkanes at 250 °C on various catalysts (1: Pt/T; 2: Rh/T; 3: Pd/T)

2-methyloxacycloalkanes varies in the following order: $4 > 3 > 5 \approx 6$ (where the numbers are the numbers of atoms in the ring) (Fig. 1).

Because of the greater strain of the three- and four-membered rings and the easy fragmentation of the latter, the above order for the rate of decomposition can readily be explained. As will be seen later, the different effects of the catalysts on the stabilities of the cyclic ethers can be correlated mainly with the various transformating directions. The most active are the hydrogenating Pt/T, Rh/T and Ni/Al catalysts.

The main products of 2-methyloxacycloalkanes on the above catalysts in the presence of hydrogen can be seen from the following schemes.

The main products of the transformation of 2-methylethylene oxide:

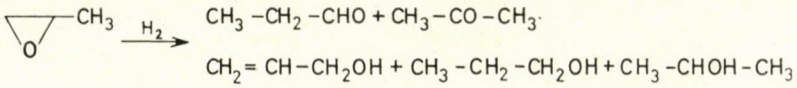

The main products of the transformation of 2-methyloxacyclobutane:

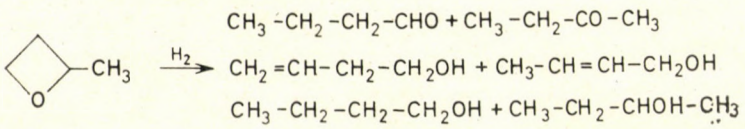

A high degree of selectivity can be observed in the transformations of 2-methyltetrahydrofuran and 2-methyltetrahydropyran on the individual catalysts:

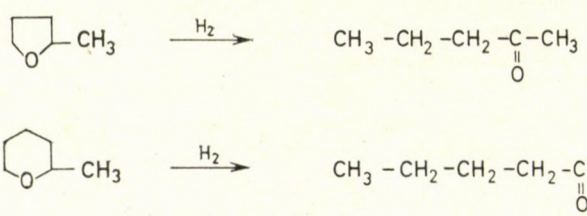

The main directions of transformation, therefore, are isomerizations accompanied by the formation of oxo compounds and unsaturated alcohols, and hydrogenolysis resulting in the formation of saturated alcohols. The extents to which the main processes take place are determined decisively by the ring size and the catalysts. Before a more detailed discussion of these questions some characteristic plots are given for the four model compounds: the variation of the product composition as a function of temperature (Figs 2—11). The

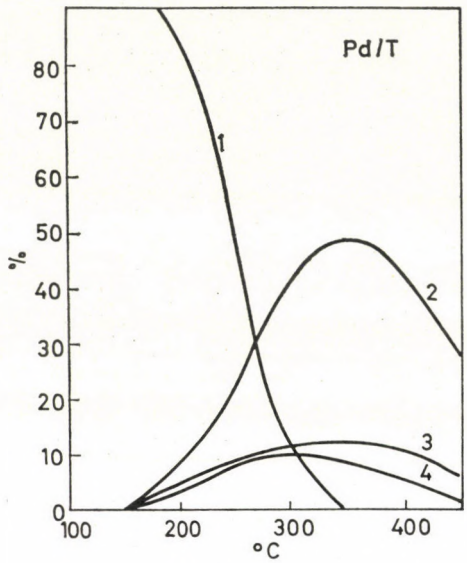

Fig. 2

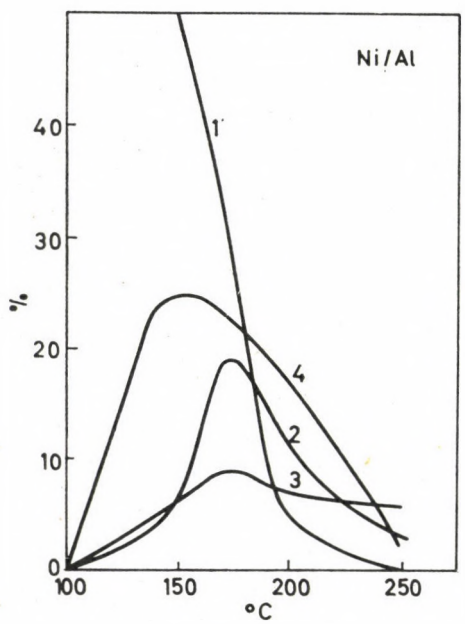

Fig. 3

Figs 2 and 3: Variation of the product composition as a function of temperature in the transformation of propylene oxide (1: propylene oxide; 2: propionaldehyde; 3: acetone; 4: 1-propanol)

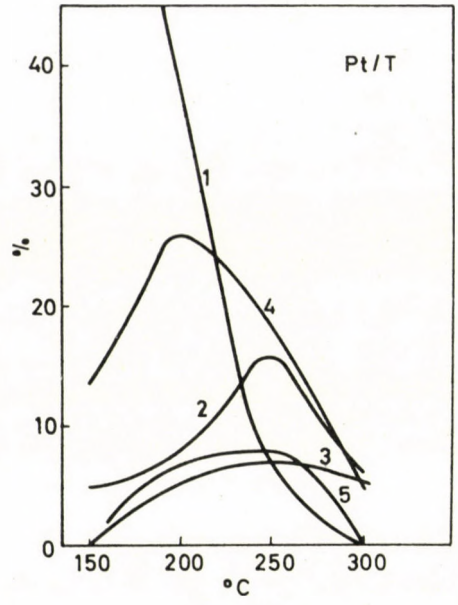
Pt/T
40
30
20
10
0
%
1
2
3
4
5
150
200
250
300
°C

Fig. 4

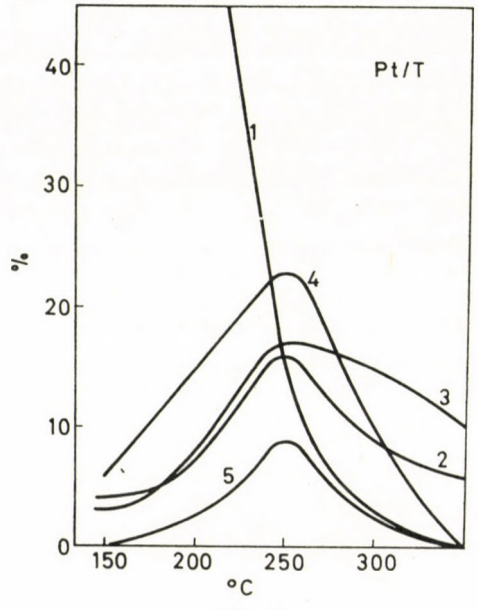
Pt/T
40
30
20
10
0
%
1
2
3
4
5
150
200
250
300
°C

Fig. 5

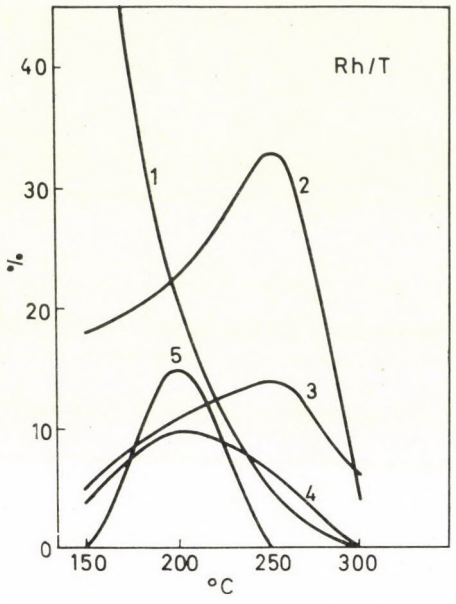
Rh/T
40
30
20
10
0
%
1
2
3
4
5
150
200
250
300
°C

Fig. 6

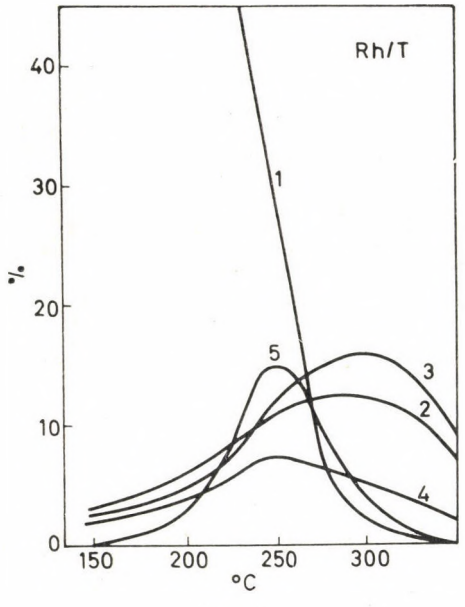
Rh/T
40
30
20
10
0
%
1
2
3
4
5
150
200
250
300
°C

Fig. 7

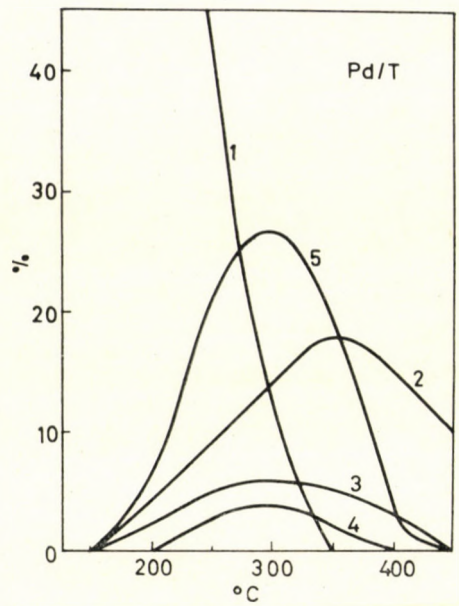

Fig. 8

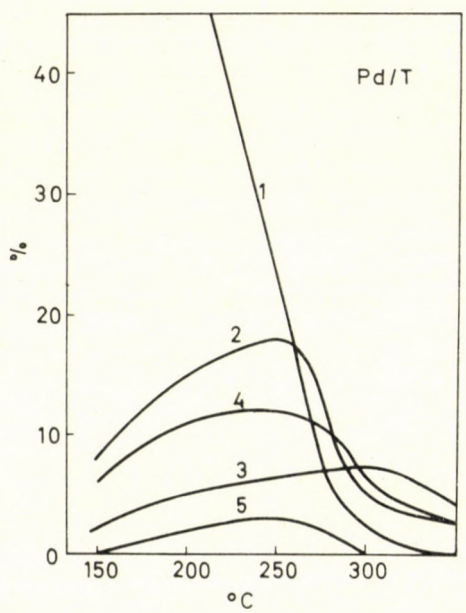

Fig. 9

Figs 4—9. Variation of the product composition as a function of temperature in the transformation of 2-methyloxacyclobutane (1: 2-methyloxacyclobutane; 2: butyraldehyde; 3: methyl ethyl ketone; 4: 1-butanol + 2-butanol; 5: allyl carbinol + crotyl alcohol)

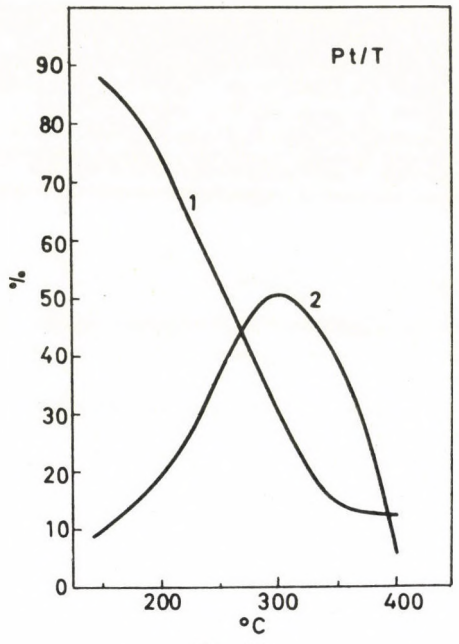

Fig. 10

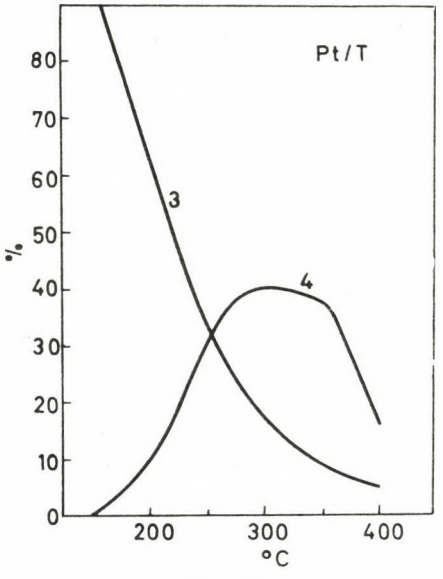

Fig. 11

***Figs* 10—11.** Variation of the product composition as a function of temperature in the transformations of 2-methyltetrahydrofuran and 2-methyltetrahydropyran (1: 2-methyltetrahydropyran; 2: methyl propyl ketone; 3: 2-methyltetrahydropyran; 4: methyl butyl ketone)

amounts of products formed vary with temperature according to a maximum curve; this can understandably be explained by the secondary transformation of the primary products. The study of these secondary processes was not included in our programme.

The figures for the parallel experiments in the case of 2-methyloxacyclobutane draw attention to the effect of the nature of the active sites of the catalysts on the directions of transformation. It appears that the surface state of the catalysts, and hence their activity and selectivity, change during the experiments. It seems justified to study not only the role of the catalysts without support but also the structures of the catalysts during the reaction and the effects of these on the reaction directions. In our experimental work the change of the activity of the Pt/T catalyst was studied as a function of the number of impulses. With the exception of the first one or two impulses, however, no essential change was observed, not even after 50 impulses. If these observations are compared with the data for the parallel experiments reported above, it seems likely that the changes caused in the activities of the catalysts have a substantial effect on the surface states of the catalysts.

The individual characteristics of the transformations of cyclic ethers, depending on the catalysts and the ring size, can be readily explained on the basis of Figs 12—17. In these figures the maximum yields of aldehydes, ketones and unsaturated alcohols formed by isomerization, and the alcohols resulting from hydrogenolysis, are plotted in the temperature range studied as a function of the catalyst and the ring size.

As a summary of the experimental data, in the following we report the main characteristics of the transformations of 2-methyloxacycloalkanes. For all six catalysts the transformation of three- and four-membered cyclic ethers in the presence of hydrogen is a complex process, with the formation of several products, and essentially all the mentioned reaction directions can be observed. In the case of the five- and six-membered cyclic ethers, however, of the studied reaction directions only the isomerization to the corresponding ketones takes place.

Propylene oxide isomerizes mainly to propionaldehyde. However, isomerization to acetone and hydrogenolysis are also appreciable. In the case of 2-methyloxacyclobutane, each reaction direction can be observed, the proportions being affected considerably by the nature of the catalyst and by the quality and state of its active sites. With 2-methyltetrahydrofuran the most considerable reaction is the isomerization to methyl ethyl ketone under the action of platinum. Rh/T has a similar role, but on the other catalysts various decomposition processes (mainly dehydration), not yet studied, can be observed only at higher temperatures. Similar observations can be made for the transformation of 2-methyltetrahydropyran, with the difference that the isomerization to ketone proceeds on Pd/T too.

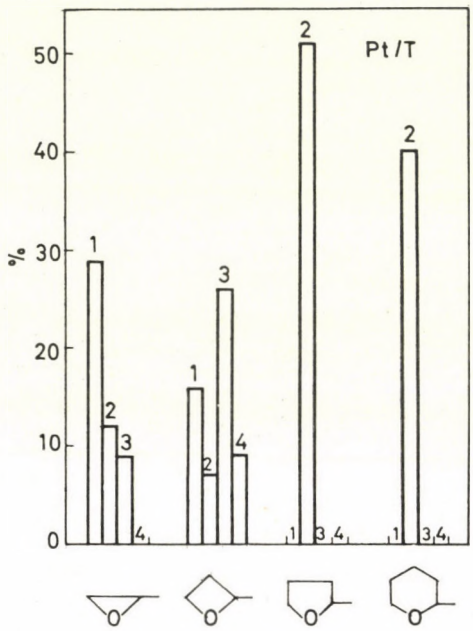

Fig. 12

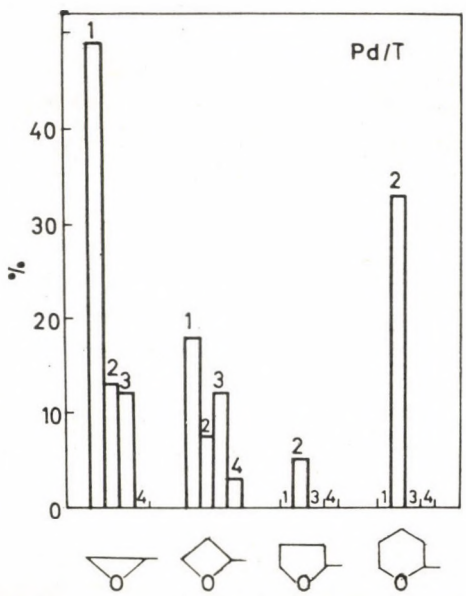

Fig. 13

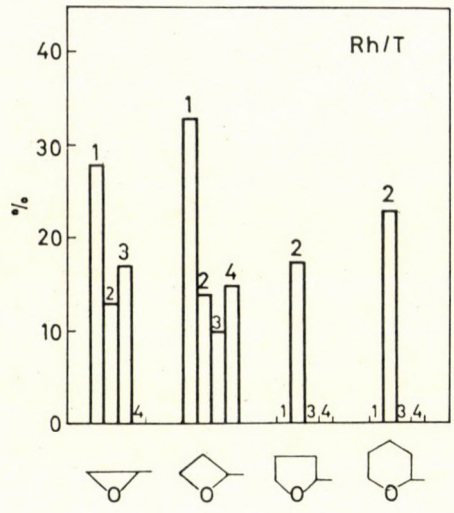

Fig. 14

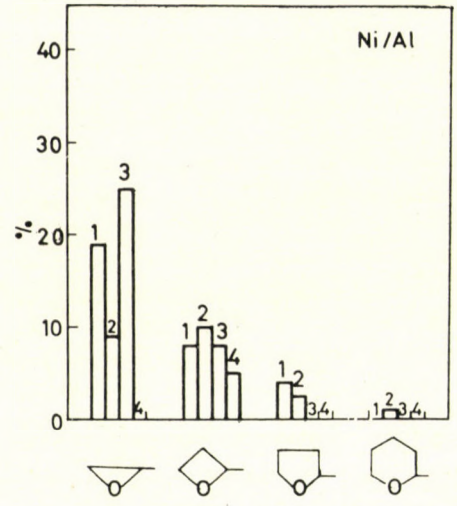

Fig. 15

The dependence of the reaction directions on the ring size can be summarized as follows.

Variation of the isomerization to aldehyde: $3 > 4$; the formation of aldehydes was not observed for the five- and six-membered cyclic ethers.

Variation of the isomerization to ketone: $5 \sim 6 > 4 \sim 3$.

Isomerization to unsaturated alcohols can be observed only for 2-methyloxacyclobutane on all catalysts with the exception of Ni/Al (it should be noted that in the case of propylene oxide allyl alcohol can be detected on the Zn/Al catalyst too).

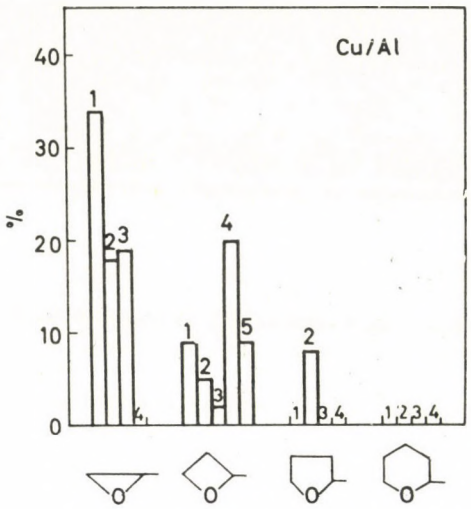

Fig. 16

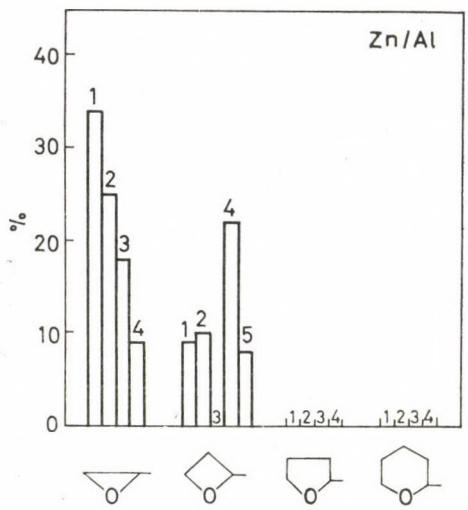

Fig. 17

Fig. 12—17. Maximum yields of isomerization and hydrogenolysis products of 2-methyloxacycloalkanes on various metal catalysts (1: aldehyde; 2: ketone; 3: alcohols; 4: unsaturated alcohols; 5: methyl vinyl ketone)

Hydrogenolysis can be observed only in the cases of three- and four-membered cyclic ethers, to an extent depending on the nature of the catalyst (it must be noted that on the action of superactive catalysts 2-methyltetrahydropyran too undergoes hydrogenolysis).

Although the catalysts studied by us can be systematized on the basis of their effects on the directions of transformation of 2-methyloxacycloalkanes,

such a classification nevertheless had to be passed over since without making the experimental data more accurate significant changes cannot be established. There is, however, one clear conclusion: the isomerization of cyclic ethers with the formation of ketones is catalyzed by the platinum group metals studied (although it has to be noted that in the case of the five-membered cyclic ether palladium does not exhibit the necessary activity), while their hydrogenolysis is catalyzed by the above metals and by nickel too.

The relative amounts of the products formed by the splitting of the two C—O bonds in the 2-methyloxacycloalkanes are given in the following table:

Table I

	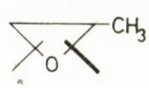				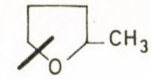		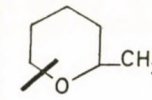	
Catalyst	1	2	1	2	1	2	1	2
Ni/Al	1	2	1	1	0	0	0	0
Cu/Al	1	3	1	2	min	0	0	0
Zn/Al	1	4	1	2	0	0	0	0
Rh/T	1	4	1	2	1	0	1	0
Pd/T	1	6	1	3	min	0	1	0
Pt/T	1	4	1	4	1	0	1	0

REFERENCES

1. MALINOVSKII, M. S.: Okisi olefinov i ih proizvodnie. GHI, Moscow 1961
2. SHUYKIN, N. I., BELSKII, I. F.: Dokl. AN SSSR, **120,** 548 (1958)
3. BELSKII, I. F., SHUYKIN, N. I.: Dokl. AN SSSR, **127,** 91 (1959)
4. SHUYKIN, N. I., BARTÓK, M., KOVÁCS, Ö., BELSKII, I. F.: Izv. AN SSSR, Ser. Khim., **1962,** 1653
5. SHUYKIN, N. I., KOVÁCS, Ö., BELSKII, I. F., BARTÓK, M.: Acta Chim. Acad. Sci. Hung., **38,** 115 (1963)
6. SHUYKIN, N. I., APJOK, J., BARTÓK, M., BELSKII, I. F., KARAKHANOV, R. A.: Izv. AN SSSR, Ser. Khim., **1964,** 746
7. SHUYKIN, N. I., BELSKII, I. F., KARAKHANOV, R. A., KOZMA, B., BARTÓK, M.: Izv. AN SSSR, Ser. Khim., **1964,** 747
8. BARTÓK, M.: Kémiai Közl., **28,** 79 (1967)
9. KASHIRSKII, M.: Zhur. russk. fiz. khim. obshch., **13,** 76 (1881)
10. KRASUSKII, K. A.: Zhur. russk. fiz. khim. obshch., **34,** 537 (1902)
11. IPATYEV, V. N., LEONTOVICH, V.: Chem. Ber., **36,** 2016 (1903)
12. BARTÓK, M., FÉNYI, Sz.: Acta Phys. et Chem. Szeged, **12,** 157 (1966)
13. BARTÓK, M., KOZMA, B.: Acta Phys. et Chem. Szeged, **9,** 116 (1963)
14. BARTÓK, M., APJOK, J., KARAKHANOV, R. A., KOVÁCS, K.: Acta Chim. Acad. Sci. Hung., **61,** 315 (1969)

Mihály BARTÓK
István TÖRÖK
Imre SZABÓ
} 6701 Szeged, Dóm tér 8. Hungary.

Acta Chimica Academiae Scientiarum Hungaricae, Tomus 76 (4), pp. 431—436 (1973)

SYNTHESIS OF A HEXAPEPTIDE, A POTENTIAL INHIBITOR OF GH-RH* LIBERATION

S. BAJUSZ, I. FAUSZT and J. BORVENDÉG

(Research Institute for Pharmaceutical Chemistry, Budapest)

Received June 16, 1972

Structural resemblance indicates that GH-RH is formed from the β-chain of hemoglobin, being the amino-terminal 1—10 fragment of the latter. It is reasonable to suppose that the liberation of GH-RH may be inhibited by peptides containing the β-chain 10—11 sequence in their amino-terminal. For a study of this possibility the 10—15 hexapeptide fragment of the β-chain in human hemoglobin has been prepared, starting with Trp-NH_2, by stepwise synthesis.

The peptide with growth hormone releasing hormone (GH—RH) activity was isolated from porcine hypothalamus [1] and proved to be H-Val-His-Leu-Ser-Ala-Glu-Glu-Lys-Ala-OH** (**I**) [2]. The synthesis of decapeptide **I** has recently been published by the Peptide Group of Merck Sharp and Dohme Research Laboratories (Rahway, New Jersey) [3]. In this report it was pointed out that "a striking similarity exists between **I** and the proposed amino-terminal sequence of the β-chain of hemoglobin"*** . . . "suggesting that **I** may be derived from hemoglobin as angiotensin I arises from an α_2-globulin" (*i.e.* angiotensinogen or renin substrate). If the structural resemblance is not a freak of chance and GH-RH is indeed derived from hemoglobin, there must be a proteolytic enzyme exhibiting a highly selective specificity for cleaving the β-chain between positions 10 and 11. That means that the GH-RH liberating enzyme should display its function analogously to renin, which removes angiotensin I from angiotensinogen —by cleavage of the leucyl-leucyl bond at positions 10 and 11.

It is known that renin-catalysed liberation of angiotensin I from angiotensinogen can be inhibited by smaller peptides containing the leucyl-leucyl

* Growth hormone releasing hormone.

** The symbols follow the Tentative Rules of the IUPAC-IUB Commission on Biochemical Nomenclature (J. Biol. Chem. 247, 977 (1972)). The following additional abbreviations have been used: OPCP — pentachlorophenyloxy, DCHA — dicyclohexylamine, DMF — dimethylformamide.

*** Namely (Val.His.Leu.Ser.Ala.Glx-Glx.(Lys)Ala.Glx.Val..) where parentheses enclose a region, the composition but not the sequence of which has been determined experimentally. A period between amino acids within the parentheses indicates that the amino acid to its left has been placed in what seems to be the most probable position [4]. The sequence of the first eight residues as given above (**I**) has recently been confirmed by EDMAN dansyl degradation studies [3].

sequence at the amino-terminus [5] on account of splitting leucine from these peptides instead of angiotensin I from the renin substrate. Relying upon these findings it can be supposed that GH-RH formation from hemoglobin might be similarly inhibited by peptides comprising residues 10 and 11 of the β-chain on their amino-terminal.

The structure of a potential GH-RH inhibiting peptide could be designed taking into consideration the sequence of the β-chain of human hemoglobin which had been determined experimentally [4]. It can be seen (Fig. 1) that residues at the critical positions are alanine and valine. Therefore an alanyl-valyl-peptide, namely the sequence covering positions 10—15 (italicized in

H-Val-His-Leu-Thr-Pro-Glu-Glu-Lys-
1 2 3 4 5 6 7 8

-Ser-*Ala-Val-Thr-Ala-Leu-Trp*-Gly-Lys-Val-
9 10 11 12 13 14 15 16 17 18

-Asn-Val-Asp-Glu-Val-Gly-Gly-
19 20 21 22 23 24 25

Fig. 1. The amino-terminal sequence of the β-chain of human hemoglobin. The arrow indicates the bond cleaved by the supposed enzyme, liberating GH-RH

Fig. 1) was synthesized in the form of a hexapeptide amide, H-Ala-Val-Thr-Ala-Leu-Trp-NH_2 (**II**). The sequence of **II** includes, besides Ala-Val — marked for the proteolytic cleavage — a tryptophan residue, which is expected to improve the binding capacity of the hexapeptide. The terminal amide group was chosen to render a neutral environment to the side chain of tryptophan, as there is no free carboxyl group in the β-chain, the first acidic amino acid to its left being at position 21.

The synthesis of hexapeptide **II** was accomplished by the stepwise approach (Fig. 2) starting from crystalline tryptophan amide oxalate (**III**) obtained from the appropriate carbobenzoxy derivative. The protected dipeptide amide **IV** was prepared by the mixed anhydride method. It was found that in the presence of a catalytic amount of N-methylmorpholine the dicyclohexylamine salt of carbobenzoxy-leucine could be converted directly into a mixed anhydride. In this reaction the N-acyl-N-methylmorpholiniumchloride complex is the anhydride-forming agent, as proposed by ANDERSON [6], since in the absence of a tertiary amine (such as N-methylmorpholine) anhydride formation was very slow or did not occur at all. Catalytic hydrogenation of **IV** afforded the corresponding free dipeptide amide (**V**) isolated as a crystalline oxalate. Coupling of **V** with pentachlorophenyl carbobenzoxy-alaninate yielded the protected tripeptide amide **VI**, and this was condensed after deblocking by hydrogenation with pentachlorophenyl carbobenzoxy-threoninate to give the protected tetrapeptide amide **VIII**. The free tetrapeptide (**IX**) ob-

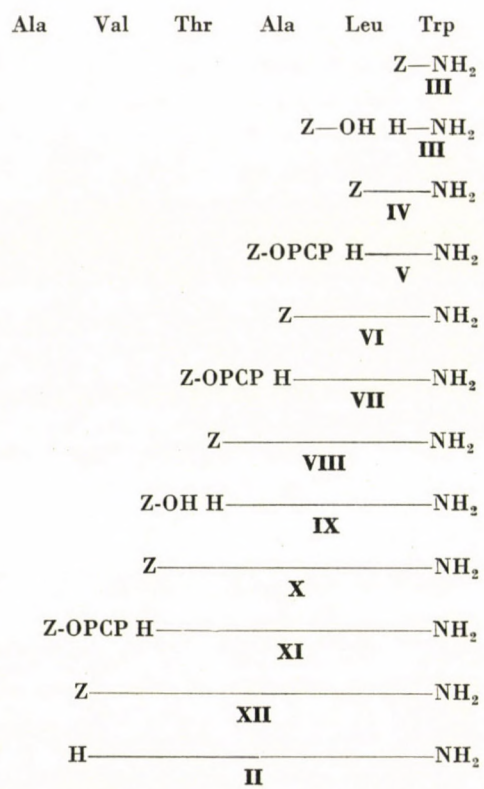

Fig. 2. Synthesis of hexapeptide amide

tained by catalytic hydrogenation of **VIII** was allowed to react with a mixed anhydride of carbobenzoxy-valine to afford the protected pentapeptide amide **X**, which was converted into **XI** by hydrogenation. The free pentapeptide amide was acylated with the aforementioned pentachlorophenyl carbobenzoxy-alaninate to yield the protected hexapeptide amide **XII**, the terminal amino group of which was liberated by catalytic hydrogenation. The hexapeptide amide **II** was isolated as the acetate salt, with satisfactory elemental and amino acid analysis, in a yield of 51.6%, calculated for the amino acid derivatives used in the coupling reactions [7]. The results of biological studies with this hexapeptide amide will be published elsewhere.

Experimental

All melting points are uncorrected. TLC were performed on silica (Kieselgel G, Merck). R_f values refer to the following solvent systems; R_f^1: ethyl acetate–pyridine–acetic acid–water (240 : 20 : 6 : 11). R_f^2: ethyl acetate–pyridine–acetic acid–water (120: 20 : 6 : 11). R_f^3: ethyl acetate–pyridine–acetic acid–water (60 : 20 : 6 : 11).

H-Trp-$NH_2 \cdot (COOH)_2$ (III)

Carbobenzoxy-tryptophan amide [9] (3.37 g; 10 mmoles) in methanol (100 ml) was deprotected by hydrogenation in the presence of palladized charcoal. The catalyst was removed by filtration and the solution was evaporated to dryness. The residue was dissolved in a mixture of ethanol–benzol and evaporated again to dryness. The product was redissolved in methanol (30 ml) and after adding oxalic acid (0.9 g; 10 mmoles) the solution was evaporated. The resulting oxalate was crystallized with ether to yield 2.91 g (96%) of **III**; m.p. 189—191 °C; R^3_f 0.37; $[\alpha]_D^{20}$ + 4.78 (c = 1, ethanol).

$C_{13}H_{15}O_5N_3$ (293.28). Calcd.C 53.24; H 5.15; N 14.32; O 27.27. Found C 53.28; H 5.20; N 14.30; O 27.30%.

Z-Leu-Trp-NH_2 (IV)

(A) Carbobenzoxy-leucine liberated from its DCHA salt (4.9 g; 11 mmoles) was dissolved in DMF (10 ml) and treated successively at —10° with N-methylmorpholine (1.22 ml; 11 mmoles), isobutyl chloroformate (1.45 ml, 11 mmoles) and, after 10 min, with a pre-cooled solution of tryptophan amide oxalate (**III**; 2.93 g; 10 mmoles) in DMF (10 ml) containing N-methylmorpholine (2.22 ml; 20 mmoles). After stirring at —10 °C for 30 min and at 0 °C for 1 hr, the mixture was kept at room temperature overnight, then filtered and evaporated under reduced pressure. The residue was stirred with ethyl acetate (10 ml) and water (5 ml) for 10—20 min. The suspension was filtered, the solid was washed with ethyl acetate and water and dried to obtain 4.1 g (91%) of **IV**; m.p. 210—213 °C, R^1_f 0.8; $[\alpha]_{20}^{D}$ —17.7° (c = 1, DMF).

$C_{25}H_{30}O_4N_4$ (450.54). Calcd. C 66.64; H 6.71; N 12.43; O 14.20. Found C 66.70; H 6.69; N 12.42; O 14.17%.

(B) DCHA salt of carbobenzoxy-leucine (4.9 g; 11 mmoles) was suspended in DMF (10 ml) and treated successively at —10 °C with methylmorpholine (0.122 ml; 1.1 mmoles), isobutyl chloroformate (1.45 ml; 11 mmoles) and, after 10 min, the mixed anhydride formed was allowed to react with tryptophan amide oxalate (**III**; 2.93 g; 10 mmoles) as described above, to yield 3.8 g (84.5%) of **IV**; m.p. 210—213 °C; R^1_f 0.8.

Z-Ala-Leu-Trp-NH_2 (VI)

The carbobenzoxy dipeptide amide **IV** (4.1 g; 9.1 mmoles) was hydrogenated in methanol (60 ml) in the presence of palladized charcoal. After completion of deblocking (checked by TLC), the catalyst was filtered off and washed with methanol. The solution and washings were combined and, after addition of oxalic acid (0.8 g; 9.1 mmoles), concentrated under reduced pressure. The residue was crystallized with ether, filtered, washed with ether and dried; yield 3.55 g (99%); m.p. 115 °C (decomp.); R^2_f 0.5. The free dipeptide amide (**V**) obtained was dissolved in DMF (10 ml) containing N-methylmorpholine (2.0 ml; 18 mmoles). The stirred solution was treated successively at room temperature with pentachlorophenyl carbobenzoxy-alaninate (4.66 g; 9.9 mmoles) and N-methylmorpholine (1.1 ml; 9.9 mmoles) added in five portions during 30 min. Stirring was continued until dissolution occurred and, after being kept at room temperature overnight, the reaction mixture was concentrated under reduced pressure. The residue was stirred with ethyl acetate (10 ml) and water (5 ml). The resulting suspension was filtered off, washed with ethyl acetate and water and dried; yield 4.31 g (92%); m.p. 188—190 °C; R^1_f 0.68; $[\alpha]_D^{20}$ —24.6° (c = 1, DMF).

$C_{28}H_{35}O_5N_5$ (521.63). Calcd. C 64.47; H 6.76; N 13.42; O 15.33. Found C 64.37; H 6.77; N 13.35; O 15.48%.

Z-Thr-Alal-Leu-Trp-NH_2 (VIII)

The protected tripeptide amide **VI** (4.31 g; 8.28 mmoles) was dissolved in methanol (50 ml) and hydrogenated over palladized charcoal. The catalyst was removed by filtration and the solution was concentrated under reduced pressure. The residue was triturated with ether, filtered, washed with ether and dried to yield 3.07 g (96%) of **VII**; m.p. 108—112 °C (decomp.); R^3_f 0.5. The free tripeptide amide (7.95 mmoles) was dissolved in DMF (8 ml) and treated successively with pentachlorophenyl carbobenzoxy-threoninate (4.39 g; 8.75 mmoles) as described in the preparation of **VI**. After being kept at room temperature overnight, the reaction mixture was concentrated under reduced pressure and the residue was triturated with ether. The

suspension was filtered, the solid was washed with ether and water and dried to obtain 4.53 g (91.5%) of **VIII**; m.p. 218—220 °C; R_f^2 0.8; $[\alpha]_D^{20}$ —16.0° (c = 1, DMF).

$C_{32}H_{42}O_7N_6$ (622.73). Calcd. C 61.71; H 6.79; N 13.49; O 17.98. Found C 61.54; H 6.89; N 13.56; O 18.02%.

Z-Val-Thr-Ala-Leu-Trp-NH_2 (X)

The protected tetrapeptide amide **VIII** (4.53 g; 7.26 mmoles) was hydrogenated in methanol (40 ml) in the presence of palladized charcoal. The catalyst was filtered off and the solution was concentrated under reduced pressure. The residue was triturated with ether, filtered, washed with ether and dried to yield 3.52 g (99%) of the free tetrapeptide amide **IX**; m.p. 193—195 °C; R_f^3 0.47. The product was dissolved in DMF (10 ml) and, after cooling to —10 °C, it was added to the mixed anhydride. The latter was prepared from the DCHA salt of carbobenzoxy-valine (3.42 g; 7.92 mmoles) and isobutyl chloroformate (1.075 ml; 7.92 mmoles) in the presence of N-methylmorpholine (0.088 ml; 0.792 mmoles) according to procedure *(B)* in the preparation of compound **IV**. The filtered reaction mixture was concentrated under reduced pressure and the residue was triturated with ether and suspended in ethanol (20 ml). The suspension was boiled for 10—20 min, cooled and filtered, washed with cooled ethanol and dried; yield 4.25 g (82%); m.p. 245—247 °C (decomp.); R_f^2 0.73; $[\alpha]_D^{20}$ —18.7°. (c = 1, DMF).

$C_{37}H_{51}O_8N_7$ (721.87). Calcd. C 61.56; H 7.12; N 13.58; O 17.71. Found C 61.47; H 7.18; N 13.58; O 17.77%.

Z-Ala-Val-Thr-Ala-Leu-Trp-NH_2 (XII)

The protected pentapeptide amide **X** (3.74 g; 5.18 mmoles) in DMF (50 ml) was deblocked by hydrogenolysis in the presence of palladized charcoal. The catalyst was filtered off and the filtrate was concentrated to 20 ml. The solution containing the free peptide (**XI**) was treated successively with pentachlorophenyl carbobenzoxy-alaninate (2.68 g; 5.7 mmoles) and N-methylmorpholine (0.632 ml; 5.7 mmoles) as described in the preparation of **VI**. The mixture was kept at room temperature overnight, then concentrated under reduced pressure and the residue was triturated with ether. The resulting crude product was suspended in ethanol (40 ml) and boiled for 20—30 min. The cooled suspension was filtered, the solid washed with cold ethanol, and dried; yield 3.65 g (89%); m.p. 243—246 °C; R_f^2 0.8; $[\alpha]_D^{20}$ —13.2° (c = 0.23 DMF).

$C_{40}H_{56}O_9N_8$ (792.95). Calcd. C 60.59; H 7.11; N 14.13; O 18.16. Found C 60.43; H 7.20; N 14.09; O 18.20%.

H-Ala-Val-Thr-Ala-Leu-Trp-$NH_2 \cdot CH_3COOH$ (II)

The protected hexapeptide amide **XII** (3.65 g; 4.61 mmoles) was dissolved in a mixture of DMF (50 ml) and 80% acetic acid (10 ml). The solution was hydrogenated in the presence of palladized charcoal. The catalyst was removed by filtration and washed with water. The filtrate and washings were combined and concentrated to about 50 ml under reduced pressure, when the free hexapeptide amide acetate separated. The cooled suspension was filtered, the precipitate was washed with cold DMF and acetone, and dried to obtain 3.05 g (94.3%) of **II**; m.p. 226—230 °C; R_f^3 0.35; $[\alpha]_D^{20}$ —24.3° (c = 1, acetic acid) and —33.9° (c = 1, 80% acetic acid).

$C_{32}H_{50}O_7N_8 \cdot CH_3COOH$ (718.87). Calcd. C 56.90; H 7.57; N 15.62; O 20.03. Found C 56.82; H 7.67; N 15.58; O 19.89%.

Amino acid analysis: Thr 0.98 (1); Ala 2.0 (2) Val 1.02 (1) Leu 1.01 (1) NH_3 0.99 (1).

REFERENCES

1. SCHALLY, A. V., SAWANO, S., ARIMURA, A., BARETT, J. F., WAKABAYASHI, I., BOWERS, C. Y.: Endocrinology **84,** 1493 (1969)
2. SCHALLY, A. V., BABA, Y., NAIR, R. M. G., BENETT, C. D.: J. Biol. Chem. **246,** 6647 (1971)
3. VEBER, D. F., BENETT, C. D., MILKOWSKI, J. D., GAL, G., DENKEWALTER, R. G., HIRSCHMANN, R.: Biochem. Biophys. Res. Commun. **45,** 235 (1971)
4. DAYHOFF, M. O.: Atlas of Protein Sequence and Structure **4,** D-49 (1969)
5. KOKUBU, T., UEDA, E., FUJIMOTO, S., HIWADA, K., KATO, A., AKUTSU, H., YAMAMURA, Y., SAITO, S., MIZOGUCHI, T.: Nature **217,** 456 (1968)
6. ANDERSON, G. W., CALLAHAN, F. M., ZIMMERMANN, J. E.: J. Am. Chem. Soc. **89,** 178 (1967)
7. BAJUSZ, S., FAUSZT, I.: Acta Chim. Acad. Sci. Hung. (In press).

Sándor BAJUSZ
Irén FAUSZT
János BORVENDÉG

1325 Budapest, P. O. Box 82,
Szabadságharcosok u. 47—49.

Acta Chimica Academiae Scientiarum Hungaricae, Tomus 76 (4), pp. 437—440 (1973)

PROMOTED HYDROGENOLYSIS OF CARBOBENZOXYAMINO ACIDS IN THE PRESENCE OF ORGANIC BASES

(SHORT COMMUNICATION)

H. MEDZIHRADSZKY-SCHWEIGER

(Research Group for Peptide Chemistry, Hungarian Academy of Sciences, Budapest)

Received June 29, 1972

The hydrogenolysis of carbobenzoxyamino acids has been investigated in the presence of organic bases and the reaction velocities compared with decarbobenzoxylations effected in acetic or neutral medium. In all cases a 4—5 times more rapid cleavage was found in the presence of bases.

In an earlier investigation [1] we have shown that the hydrogenolysis of the carbobenzoxy protecting group of methionine-containing peptides proceeds readily in the presence of organic bases (cyclohexylamine, triethylamine), *i.e.* the poisoning effect of methionine is eliminated. The base stabilizes by salt formation the unstable, intermediate carbamic acid produced by the hydrogenolysis of the carbobenzoxyamino acid, so that peptides containing free amino group will not be formed in the reaction mixture.

The hydrogenolysis of a carbobenzoxy compound is characterized by the following equation:

$$C_6H_5CH_2OCO{-}NH{-}CH(R){-}COOH + H_2 \xrightarrow{H_2/Pd}$$

$$\rightarrow [HOOC{-}NH{-}CH(R){-}COOH] + C_6H_5CH_3 \rightarrow CO_2 + H_2N{-}CH(R){-}COOH$$

Hydrogenolysis in the presence of cyclohexylamine or triethylamine leads to the corresponding salt of the carbamic acid, which is stable if excess base is used.

$$HOOC{-}NH{-}CH(R){-}COOH + C_6H_{11}NH_2 \rightleftharpoons$$

$$\rightleftharpoons C_6H_{11}\overset{\oplus}{N}H_3 \; \overset{\ominus}{O}OC{-}NH{-}CH(R){-}COOH$$

From these facts one could come to the conclusion that only methionine compounds containing a free amino group possess inhibitory effect. This conclusion seemed to be proved by the easy hydrogenolysis of carbobenzoxyglycine in the presence of acetylmethionine and cyclohexylamine, but it was in contrast with the fact that acetylmethionine had a significant poisoning effect in neutral medium.

Besides the carbamic acid stabilizing effect, we have thus supposed some other reaction between the base and carbobenzoxy compound which also contributes to the elimination of the poisoning effect of methionine peptides.

The question arose whether the hydrogenolysis of carbobenzoxyamino acids containing no sulfur could be influenced by the addition of bases. This reaction is usually performed in the presence of one equivalent of hydrochloric acid or in diluted acetic acid; to our knowledge there is no data in the literature for the use of bases in hydrogenolysis experiments. Therefore we decided to

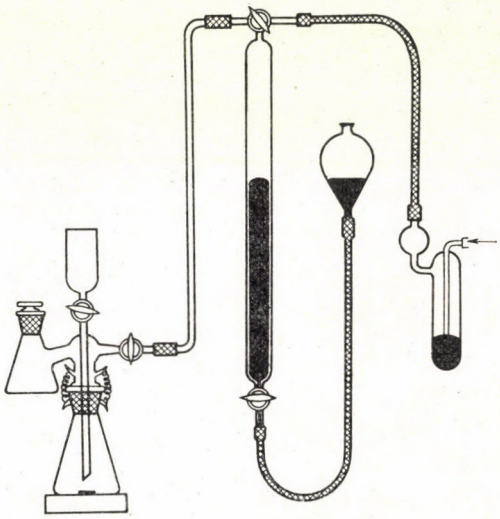

Fig. 1

investigate the hydrogenolysis of different carbobenzoxyamino acids in the presence of cyclohexylamine and triethylamine, and compared the measured reaction velocities with those observed without bases, in neutral and acidic solvents. For these investigations we selected the carbobenzoxyamino acids in such a way, that all major groups were represented: carbobenzoxyglycine, carbobenzoxyalanine as neutral, carbobenzoxyaspartic acid, carbobenzoxyglutamic acid as aminodicarboxylic, dicarbobenzoxylysine, dicarbobenzoxyornithine as basic and carbobenzoxyserine as hydroxyamino acid derivatives.

The measurements were performed under otherwise identical conditions, with one mmole of the carbobenzoxyamino acids in absolute methanol solution. The catalyst was 10% palladium-on-charcoal, amounting to 10% of the carbobenzoxyamino acid. For the hydrogenolyses in basic medium a fourfold excess of cyclohexylamine or triethylamine was used, based on the carbobenzoxyamino acid; the hydrogenolysis experiments in acidic medium were performed in the presence of one equivalent hydrochloric acid.

The apparatus used for the reactions is shown in Fig. 1. The absorption compartment filled with sodium hydroxide absorbed the carbon dioxide liberated spontaneously during the hydrogenolysis in neutral or acidic medium, thus ensuring the exact measurement of the hydrogen consumption.

In order to compare the hydrogenolyses made in different media, the hydrogen consumption, in percentage of the theoretical value, were plotted against the time. All of the investigated carbobenzoxyamino acids showed qualitatively and nearly quantitatively identical curves, therefore only the progress of hydrogenolysis of carbobenzoxyglycine is illustrated in Fig. 2.

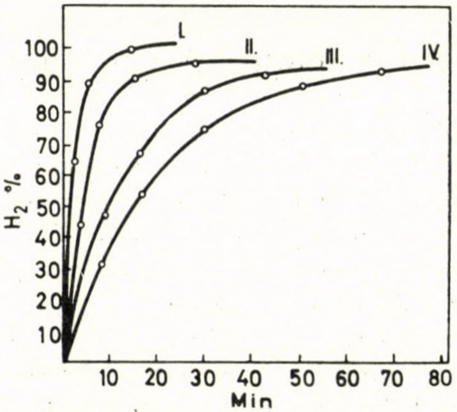

Fig. 2. Carbobenzoxyglycine. I: anhydrous methanol + cyclohexylamine; II: anhydrous methanol + triethylamine; III: anhydrous methanol + HCl; IV: anhydrous methanol

As it is evident from the Figure, a more rapid reaction was found in the presence of cyclohexylamine or triethylamine than in acidic or neutral medium. The time needed for quantitative reaction was reduced in all cases to one-fifth or one-fourth, and the velocity of the reaction depended practically on the intensity of stirring.

The significant difference between the two reaction velocities can be attributed to the probable formation of the deprotonated iminohydrin tautomeric form of the amino acid derivative in the presence of a base. The iminohydrin form is well known in aromatic carbobenzoxyamino acids [2], and bases evidently favour its formation:

$$C_6H_5CH_2OCO{-}NH{-}CH(R){-}COOH \rightleftharpoons$$

$$\rightleftharpoons C_6H_5CH_2{-}O{-}\underset{\displaystyle OH}{\underset{|}{C}}{=}N{-}CH(R){-}COOH$$

The speed-up effect of polarization near the bond to be hydrogenolyzed was mentioned earlier by FRANKEL *et al.* [3]. They investigated the hydrogenolysis of the —NH—O— linkage of amino-oxypeptides and observed, that the reaction proceeded 5—6 times more rapidly in case of esters than with the free acids. In their opinion, the ease of hydrogenolysis of the amino-oxy linkage was due to enolate ion formation:

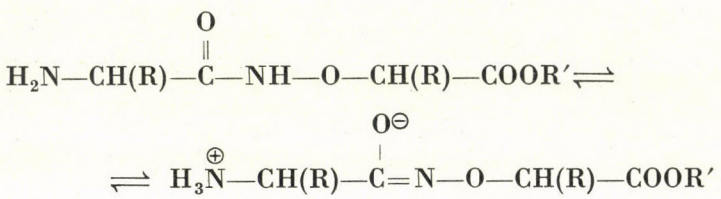

The charged amino-oxy group of esters forms an internal salt with the α-amino group. Elimination of the enolic charge from the amino-oxy group of esters by the addition of hydrochloric acid, results in much more difficult hydrogenolysis.

On the basis of these investigation it can be established that the use of organic bases in the hydrogenolysis of the carbobenzoxy group of amino acids and peptides has some advantages. Removal of the volatile bases from the reaction mixture does not cause any difficulty. The use of bases is problematic only with dipeptide esters, because the formation of the cyclic diketopiperazines occurs very easily. The basic medium is very favourable in the hydrogenolysis of trytophan-containing peptides: the decomposition of the indole ring of tryptophan — observed in the presence of acids — can be avoided.

REFERENCES

1. MEDZIHRADSZKY-SCHWEIGER, H., MEDZIHRADSZKY, K.: Acta Chim. Acad. Sci. Hung. **50,** 339 (1966)
2. SCHRÖDER, E., LÜBKE, K.: The Peptides, Vol. I. p. 23. Academic Press, New York, 1965
3. FRANKEL, M., ZVILICHOVSKY, G., KNOBLER, Y.: J. Chem. Soc. **1964,** 3931

Hedvig MEDZIHRADSZKY-SCHWEIGER; 1088 Budapest, Múzeum krt. 4/b.

RECENSIONES

Electronic Structure of Organic Compounds

(Fortschritte der Chemischen Forschung, Volume 24 for topics in Current Chemistry)

Springer-Verlag, Berlin–Heidelberg–New York, 1971, 54 pages

The volume consists of two parts. The first part (32 pages) was written by Professor Dr. Hans FISCHER (Zürich) with the title: Chemically Induced Dynamic Nuclear Polarization.

The CIDNP effect (which in the course of lectures is often jokingly mentioned as the "kidnap" effect) was discovered in 1967. This phenomenon, observable by high resolution NMR spectroscopy, is produced by radical reaction products during the course of the reaction or immediately following it. In recent years, chemists have intensively studied the CIDNP effect, as it furnishes important information on radical reactions and on the structure of products.

After a short introduction, FISCHER discusses over 10 pages the theoretical background, and demonstrates the scope of applications by examples. Both the theoretical and practical parts are written in a simple and lucid style, offering a very good introduction for those who read the chapter in order to get acquainted with the nature and applications of this effect.

The second part of the book "Critique of the Notion of Aromaticity" is the work of the authors Dr. Jean-Francois LABARRE and Dr. Francois CRASNIER (20 pages). The study is not divided into sub-chapters, as it also appears unnecessary for the treatment of the subject. As it is foreshadowed by the title, the authors stir up a nest of hornets. Indeed, the dispute on 'aromaticity' and the many concepts associated with it *(e.g.* pseudo-aromaticity, quasi-aromaticity, anti-aromaticity, non-aromaticity, homo-aromaticity, etc.) must prickle from every side the person dealing with this question.

The authors do not claim closing of the dispute; they deal with this complicated, far-flung complex of problems expressing only their own point of view, in the form of an entertaining essay.

Both chapters are completed with an extensive list of references.

Cs. SZÁNTAY

The Chemistry of Nonbenzoenoid Aromatic Compounds

Symposium Editor: Michinori Oki, Butterworths, London, 1971. 287 pages

The book contains the specially invited lectures presented at the international symposium organized by IUPAC in Sendai, August 24—28, 1970.

The first lecture, "Quantitative studies on aromaticity and antiaromaticity", was presented by R. BRESLOW (USA) (20 pages). The author discusses first the concept and definition of aromaticity and antiaromaticity. He is of the opinion that this problem is so simple that every repetition would seem superfluous; however, remarkably, there are still chemists, who contest that the two concepts can be defined in a meaningful way. Following this, BRESLOW sets forth the properties of the cyclopropenyl cation, anion and derivatives, and discusses then other antiaromaticity systems (*e.g.* cyclobutadiene) in a very interesting way.

The paper by F. GERSON (Switzerland) has the title "ESR studies of some nonbenzoid radical ions" (21 pages). The problem is discussed by the author in two groups: (1) nonalternant hydrocarbons, and (2) bridged [10]- and [14]annulenes.

K. HAFNER (W. Germany) lectured on the "Structure and reactivity of polycyclic cross-conjugated π-electron systems" (27 pages). To test the correctness of the theoretical

considerations, several nonbenzoid bicyclic as well as tri- and tetracyclic pericondensed π-electron systems were synthesized and their structures and reactivity investigated.

"The theoretical design of novel stabilized systems" is the title of the paper by R. HOFFMAN (USA) (13 pages). The co-author of the WOODWARD— HOFFMANN rule draws conclusions from simple symmetry considerations and detailed MO circulation concerning three stabilized systems of novel type.

TAKESHI NAKAJIMA (Japan) reports under the title "Bond distortion in nonalternant hydrocarbons" (19 pages) on the results of his semiempirical ICAO-SCF-MO calculations.

A. W. JOHNSON (UK) presented a paper (23 pages) dealing with the "Aromaticity in macrocyclic polypyrrolic ring systems", according to which the aromatic character of [18] annulene is maintained also in porphin.

The lecture of TETSUO NOZOE (Japan) is entitled "Recent advances in the chemistry of troponoids and related compounds in Japan" (41 pages) and surveys the results of the last five years.

The next lecture in the book is that of H. PRINZBACH (W. Germany): "Cyclic cross-conjugated π-systems: α,ω-cycloaddition reactions" (50 pages). The author discusses in five sub-chapters the new results concerning the cyclic cross-conjugated systems (1) calicene, (2) pentafulvalene, (3) sesquifulvalene, (4) fidecene, (5) pentaphenafulvalene.

In his paper "Recent progress in the annulene field" (23 pages), F. SONDERHEIMER (UK) gives an account of recent progress made in the synthesis of annulenes containing an odd number of carbon atoms in the ring.

The lecture by F. VOGEL (W. Germany) "Aromatic and non-aromatic 14-π-electron systems" (23 pages) discussed the 1,6-methano[10]annulenes and their analogues containing a heteroatom.

The last paper with the title "Conjugated cyclic chlorocarbons: trichlorocyclopropenium ion, heptachlorotropenium ion, and octachlorofulvalene" (18 pages) was presented by R. WEST (USA).

As compared with the original lectures, the treatment of the material has been made easier not only by its presentation in written form, but also by the completion of each chapter with detailed references. Thus, by the publishing in book-form of the lectures of the IUPAC symposium, a very important source of knowledge has been made available to chemists interested in this field.

CS. SZÁNTAY

H. KÖNIG: *Neuere Methoden zur Analyse von Tensiden*

Springer Verlag, Berlin— Heidelberg— New York, 1971, 239 Seiten

Für Fachleute, die sich mit Tensiden befassen, ist das Buch des Professors der Mainzer Universität Hans KÖNIG nützlich und lehrreich. Das zur rechten Zeit erschienene Buch füllt eine bestehende Lücke, denn seit dem Zeitpunkt des Erscheinens von Hummels Buch über dasselbe Thema sind fast 10 Jahre vergangen. In den letzten Jahren blieb die Entwicklung von Analysemethoden für Tenside gewissermaßen hinter der Entwicklung ihrer Produktion und Anwendung zurück. Literaturangaben über die Analyse von bestimmten Tensiden (z. B. Sulfobernsteinsäureester, Alkylphosphate, amphotere Tenside) sind kaum oder überhaupt nicht aufzufinden.

Die analytischen Methoden für Tenside werden im Buch in zwei Hauptteilen behandelt. Das Thema des ersten Teiles ist die Trennung und qualitative Bestimmung (Identifizierung) von Tensiden bzw. ihren Gemischen (177 Seiten), während sich der zweite Teil (49 Seiten) mit der quantitativen Bestimmung befaßt.

Im ersten Teil gruppiert der Verfasser die Tenside nach ihrer Ionenaktivität. Diese Gruppen werden dann nach dem hydrophilen bzw. innerhalb dessen nach dem hydrophoben Molekülteil in Untergruppen geteilt, die in vier Tabellen zusammengefaßt sind. Im weiteren werden die einzelnen analytischen Methoden gemäß dieser Einteilung diskutiert. Außer einem kritischen Überblick über die einschlägige Literatur werden bei jeder Methode die Reproduzierbarkeit sowie der Zeit- und Arbeitsbedarf angegeben.

Zum Trennen von Tensiden bzw. Tensidgemischen empfiehlt der Verfasser verschiedene chromatographische Verfahren (Ionenaustausch-, Säulen-, Papier-, Dünnschicht- und Gaschromatographie). Die Ergebnisse der dünnschichtchromatographischen Untersuchungen werden in sechs zusammenfassenden Tabellen und sechs Abbildungen anschaulich gemacht. Ein besonderes Kapitel befaßt sich mit der Trennung von nichtionischen Tensiden nach dem

Oxyäthylierungs- bzw. Oxypropylierungsgrad bzw. mit ihrer Trennung von anderen nichtionischen Verbindungen.

Die Tenside werden auf Grund von UV-, IR- und NMR-Spektren identifiziert. Der Verfasser und seine Mitarbeiter waren die ersten, die NMR-spektroskopische Aufnahmen zur Identifizierung von ionischen Tensiden verwendeten.

Vier Tabellen, welche die Handelsnamen, die chemische Zusammensetzung und die Herstellerfirmen der geprüften 57 Handelprodukte enthalten, bilden einen wertvollen Teil des Buches. Die Spektrensammlungen am Ende der einzelnen Kapitel enthalten die IR- und NMR-Spektren der untersuchten 57 Tenside, mit Angabe der Strukturformeln und genauer Bezeichnung der zu den einzelnen Molekülteilen gehörenden Absorptionsbanden.

Im zweiten Teil des Buches behandelt der Verfasser die quantitative Bestimmung der Tenside. Auch hier werden die analytischen Verfahren nach der Ionenaktivität gruppiert.

Außer den allgemeinen Methoden werden in einem besonderen Kapitel die quantitativen Bestimmungsmethoden für Sulfobernsteinsäure-Halbester und -Diester (gegenwärtig noch kaum oder überhaupt nicht in der Literatur veröffentlicht) sowie für Phosphorsäureester von Fettalkoholen und oxyäthylierten Fettalkoholen behandelt.

In einem anderen Kapitel wird ein neues und wertvolles Verfahren zur Bestimmung des Oxyäthylierungs- bzw. Oxypropylierungsgrades bei oxyäthylierten bzw. oxypropylierten nichtionischen Tensiden aufgrund ihrer IR-Spektren bzw. integrierten NMR-Spektren bekanntgegeben.

Der Aufbau des Buches ist logisch und gut übersichtlich. Die einzelnen Kapitel können auch für sich studiert werden. Das Verständnis des Buches wird durch den klaren, gut lesbaren aber dennoch knappen Stil erleichtert.

J. MORGÓS

Proceedings of the Fourth International Congress on Catalysis, Vols. 1 and 2

Akadémiai Kiadó, Budapest 1971 (pp. 1150, in English)

The publication of these two volumes containing the text of the 9 plenary lectures, the 86 session papers and the relevant discussion material of the 4th International Congress on Catalysis held in Moscow, 1968, is a long expected event. As known for specialists in the field of catalysis, since 1956 the International Congress on Catalysis is organized every 4 year and it constitutes a significant event followed with great interest. The Proceedings following the congresses attract an even greater attention since these include, in addition to the full text of session papers (which are distributed among the participants in the form of preprints) also the full plenary lectures and the discussion material. It is in this way that the rapidly published Proceedings furnish an up-to-date cross section of catalysis research throughout the world. Unfortunately, the condition of rapid publication has not been fulfilled in the present case owing to reasons beyond the control of the Publisher: the book appears 3 years after the congress. (The Proceedings of the Amsterdam Congress held in 1964 were published in the first half of 1965).

The main objective of the 1968 Congress was the 'prediction' of catalytic activity. However, this topic proved to be rather narrow. As reflected by the material of the Congress, in addition to this problem, other interesting directions were also well represented. The 6 plenary lectures, viz. (in their order of presentation) by J. H. DEBOER (The Netherlands), S. Z. ROGINSKII (USSR), D. A. DOWDEN (England), C. KEMBALL (England), G. RIENÄCKER (GDR) and Y. YONEDA (Japan), discussed the general relationships of catalysis. The subjects of the plenary lectures were, in the above order, the correlation between mass transport in the pores and the catalytic selectivity; electronic factors and internal kinetics as related to the prediction of catalytic activity; application of the crystal and ligand field theories to heterogeneous catalysis; structure and stability of hydrocarbon intermediates on the catalyst surface; metal catalysis and linear free energy relationships. In the reviewer's opinion, it would have been more expedient to place the plenary lectures at the beginning of the Proceedings, rather than hide them among the session papers which may cause some difficulties in locating them.

The 86 session papers are given in the order of their presentation, the discussion material is combined for units of 3 papers. As for the types of catalysts, 45% of the papers were devoted to semiconductors and oxides, 35% to metal catalysts and 10% to zeolites, the remaining lectures were concerned with various theoretical problems. A special merit of the books is the

presentation of figures and references introduced in the course of the discussion, thus facilitating orientation in this important part of the volumes.

The quality of printing is suitable and, in spite of its delayed publication, these volumes will, in all probability, become a useful item on the bookshelves of scientists dealing with catalysis.

L. GUCZY

Handbuch der analytischen Chemie. Elemente der dritten Hauptgruppe. Aluminium

Zweite Auflage, bearbeitet von H. Bensch, mit 47 Abbildungen. Springer-Verlag, Berlin–Heidelberg–New York, 1972

Der Band Aluminium des Handbuches der analytischen Chemie befaßt sich mit der Chemie eines Elementes, das sowohl für das praktische Leben als auch für die theoretische Forschung von gleich großer Bedeutung ist. Die wichtigsten Kapitel des 716 Seiten umfassenden Buches sind die folgenden:

Grundlagen der Chemie von wäßrigen Lösungen der Aluminiumionen; nach einer kurzgefaßten theoretischen Einleitung werden hier die organischen Komplexe des Aluminiums behandelt.

Im zweiten Teil werden die Bestimmungsmethoden ausführlich behandelt; in vielen Fällen wird auch die Rezeptur für das analytische Verfahren angegeben. Die gravimetrischen Verfahren nehmen einen Umfang von etwa 130 Seiten ein; es werden — außer den mit anorganischen Komponenten gebildeten Niederschlägen — auch Niederschläge mit organischen Reagenzien angeführt.

Auf dem Gebiet der titrimetrischen Methoden wird ausführlich auf die Meßtechnik der Säure-Basen-Bestimmung des Aluminiums eingegangen; außerdem werden komplexchemische Bestimmungsmethoden behandelt und indirekte Bestimmungsverfahren vorgeführt, z. B. die Bestimmung des Sauerstoffgehalts in Aluminiumoxinat zwecks Bestimmung des Aluminiumions.

Es soll als lobenswerter Zug des Buches hervorgehoben werden, daß innerhalb der einzelnen Verfahrensgruppen die klassischen und instrumentalen Verfahren stets nebeneinander behandelt werden.

Auf dem Gebiet der photometrischen Verfahren wird der Gebrauch der die wichtigsten Farbreaktionen liefernden Verbindungen bei der Bestimmung des Aluminiums neben verschiedenen Substanzen beschrieben. Dieses ist das längste Kapitel des Buches.

Im Kapitel über Fluorimetrie werden diejenigen Aluminiumkomplexe behandelt, die sich für Fluoreszenzmessungen eignen.

Einige nephelometrische Methoden werden vorgeführt, ebenso auch polarographische und amperometrische Methoden und die Anwendung der Flammenspektrometrie und innerhalb dieser die Meßtechnik der Atomabsorption wird beschrieben. Weiterhin wird die Spektralanalyse und Röntgenfluoreszenzanalyse sowie die Anwendung von radiochemischen Methoden behandelt.

Die Trennverfahren werden in einem Umfang von ungefähr 100 Seiten behandelt; hier werden Verfahren der Niederschlagsbildung, Komplexbildung, Extraktion und die chromatographische Trennung beschrieben.

Das letzte Kapitel des Buches befaßt sich mit speziellen Bestimmungen und Methoden; ihre gesonderte Behandlung ist durch die Besonderheit der zu bestimmenden Substanz bzw. durch die Ungewöhnlichkeit der Meßtechnik gerechtfertigt.

Das Buch ist ein unentbehrliches Handbuch für alle Analytiker, die mit Aluminium arbeiten.

E. PUNGOR

The Porous Structure of Catalysts and Transport Processes in Heterogeneous Catalysis

(The Fourth International Congress on Catalysis, Symposium III, Novosibirsk)

Editor: G. K. Boreskov. Akadémiai Kiadó, Budapest, 1972, 498 pages

The Fourth International Congress on Catalysis held in the Soviet Union in 1968 dealt with questions of the predetermination of catalytic effects. Three special symposia of the congress each considered one narrower field of the general theme: (1) the mechanism and kinetics of complex catalytic reactions, (2) electronic structural considerations of catalysis and chemisorption on semiconductors, (3) the porous structure of catalysts and the role of transport processes in heterogeneous catalysis. The book in question contains the material presented at this latter symposium, and includes the introductory plenary lecture and the complete text of 27 other lectures, together with the discussions.

This symposium material now presented in book form is still topical. Research in this field progresses more slowly, and such spectacular, break-through results are not encountered as in many other areas of catalysis. The problems of material and heat transfer processes are primarily of importance in connection with industrial procedures, this being attributable to the larger catalyst particles used in large-scale reactors. It is generally strived in laboratory catalyst investigations to avoid the disturbing effect of transport processes.

The lectures touched upon all of the more important questions relating to this topic. They thus dealt with the porous structure of the catalyst, and with material and heat transfer, that is with the development of concentration and temperature conditions in the space around the catalyst particle and particularly inside the catalyst particle, and finally the exact evaluation of the pore-diffusion hindrance was introduced for a number of reactions.

In his introductory lecture G. K. Boreskov gave a thorough account on the transport processes occurring in porous catalyst particles. In essence he had summarized all those questions which were dealt with more closely by the subsequent lectures with regard to the recent research results. It is especially noteworthy that in his lecture he reported the case of heterogeneous pore distribution in exact form, together with the development of the temperature gradient inside the particle and the practical consequences of these.

The majority of the lectures concerned with exothermic reactions, for which relations obtained by the joint consideration of material and heat transfer conditions were reported, together with conclusions drawn from them. Theoretical considerations were used to show the effects of increase of the pore-diffusion hindrance on the efficiency of the catalyst particle, on the apparent activation energy, and on the stability of operation of the catalyst particle. The latter is appreciably similar to the stability conditions of catalytic reactors in the case of exothermic reactions. A very comprehensive theoretical treatment of this question can be found in papers 6 (V. S. Beskov, O. A. Malinovskaya), 7 (P. Schneider, P. Mitschka) and 8 (L. M. Piesmen, Yu. I. Harkats, V. G. Levich), while the theoretical conclusions are checked experimentally in the lectures 1 (P. Hugo, W. Wicke), 3 (J. J. Carberry) and 22 (A. A. Ivanov, G. K. Boreskov, V. S. Beskov).

Several lectures present the concrete study of some catalytic reactions, including the analysis of the pore-diffusion hindrance. Thus, the oxidation of SO_2 on supported vanadium pentoxide catalysts is reported in papers 20 (B. Kadlec, A. Regner, J. Vosolsobe, V. Pour), 21 (A. A. Ivanov, G. K. Boreskov, V. S. Beskov) and 22 (S. Weychert, A. Urbanek), the hydrogenation of CO_2 to methane on Ni/Cr_2O_3 in paper 23 (V. Pour),the isomerization of *n*-butane on aluminium silicate in paper 24 (P. Fejes, D. Kalló, G. Schay), and the oxidation of furfurol to maleic anhydride in paper 26 (E. J. Paulane *et al.*). Questions of pore-diffusion hindrance on the liquid-phase hydrogenation of aromatic compounds are dealt with in paper 25 (N. C. Nahas, J. E. Stice), and during the polymerization of ethylene on chromic oxide in paper 27 (V. R. Gurevich *et al.*). In some of these latter lectures (23, 24) theoretical and experimental evidence is to be found that a number of particle efficiencies must be reckoned with simultaneously in multi-component systems.

Many of the lectures deal exclusively with the determination of those quantities which exert a fundamental effect on the diffusion kinetics. Of these the pore structure and the effective diffusion constant of the porous particle are the most important.

It is evident from the investigations that the values obtained for the porosity depend appreciably on the method applied. Lecture 11 (G. A. Grachev *et al.*) provides evidence that

completely different pictures of the porosity are given by mercury-porosimetric, capillary-condensation, electron-microscopic and gas-permeability measurements. In the case of polydisperse, that is, completely disordered, heterogeneous pore structures the values of the porosity depend to a considerable extent on the method of determination. Thus, it is not surprising to find in paper 9 (N. WAKAO) that pore diffusion is different in reactive and unreactive systems. In the former every accessible pore plays a part, while in the latter only the permeable pores between opposite surfaces of the porous particle come into consideration. According to the author, it is not the material transport which can be explained on the basis of the pore texture, but *vice versa*. In essence this also happens when catalyst particles of heterogeneous pore distribution are approximated to particles with two pore sizes (paper 2, M. G. SLINKO); over a wide range of conversion this permits the interpretation of the experimental results on the basis of the theoretically obtained exact relations (paper 10, R. MONTARNAL). Purely for the sake of interest, mention must be made of paper 4 (M. BACCAREDDA *et al.*) dealing with the theoretical investigation of the effects expected to be exerted on the pore-diffusion material-transport by tapering, narrowing or widening, of the pores.

What could be said as to the pore structure of the catalyst also holds for the 'effective diffusion constant' too: the value depends on the method applied. In order to obtain the correct value, that is the one which is valid according to paper 13 (B. R. DAVIS, D. S. SCOTT) in the given catalytic transformation, the determination must be carried out under the given reaction conditions; the experiments indicated that this is possible by studying the change of the material impulse passing through a column containing the catalyst in question. At such time too, the error which occurs in measurements made on a single, but perhaps not the most characteristic particle, is eliminated. The method is otherwise very widely used in which the conditions corresponding to Fick's First Law hold: the sides of a cylindrical porous particle are closed, and the gas space between the end-plates is separated; stationary diffusion material transport through the particle is ensured by continuous gas flow in the two spaces. This principle is essentially the same as that used in the apparatus of A. PARATELLA and I. SORGATO (paper 14), in which the effective diffusion constant was determined up to 600 atm.

Several papers give an account of how diffusion material-transport within the particle may be determined by physisorption measurements. In paper 12 (P. SCHNEIDER, J. M. SMITH) frontal gas chromatography is described as the method of measurement; the diffusion within the particle is calculated from the results obtained, and also the separate contributions due to the Knudsen diffusion and the surface migration. Calculation of the diffusion constant from 'sorption rate' is found in paper 18 (L. H. RICKERT). The possibility exists for the direct determination of the surface migration itself by the NMR examination of the absorbed phase (paper 15: D. FREUDE, D. GESCHKE, H. PFEIFER, H. WINKLER; paper 17: R. HAUL, B. BODDENBERG). The participation of surface migration in the diffusion material-transport within the particle is at times very considerable, and therefore the knowledge of it is of great importance.

The book has a pleasant appearance, and the duplication of the typewritten material is typographically satisfactory. Unfortunately, however, errata are fairly frequent, and often lead to difficulties in understanding, particularly of the equations. Unfortunately the discussions following the lectures are not always complete, the authors' replies generally being missing.

It is a credit to the Akadémiai Kiadó that this collection has appeared, since to date this is the only material on the Fourth International Congress on Catalysis to be available in book form.

D. KALLÓ

B. W. COOK and K. JONES: *A Programmed Introduction to Infrared Spectroscopy*

Heyden and Son Ltd., London, New York, Rheine, 1972, XVI + 192 pp

If the volume with the title above were to be classified, perhaps a "teaching machine in book form" would be the best term for characterizing it. Use of the book by the reviewer according to the introduction would not show the merits and faults of the book, the reviewer himself being reasonably conversant with infrared spectroscopy. The use of a statistical test, *e.g.* the "criterion test" in the book was, however, impossible in Hungary owing to language problems. Thus finally a single criterion test was made, where the person selected has passed his "matriculation" and his "University entrance examination", had a good knowledge of

English, but no detailed knowledge of the technique. His test figures showed 89% efficiency. This may be regarded as evidence that the book is a very good aid for people trying to get their fundamental knowledge in IR spectroscopy.

The structure of the book is very simple. After a short text a question is given with three answers. Each answer directs the learner to a specific page. If the answer is correct, further text and a further question with answers follow. If the answer was incorrect, the learner is directed back with a comment on his mistake.

By this method the student is taken through an introduction, a chapter on spectrometer components, the setting up of a spectrometer, basic theory, sample preparation, quantitative analysis, fault recognition and interpretation. These last are especially interesting, although the text on interpretation does not go beyond the ester grouping. The book includes the Colthup correlation table, and other group frequencies, with illustrative spectra, occur in other chapters. Appendices on attenuated total reflection, sample preparation and fault finding, a short guide to IR literature and a brief summary complete the volume, which is an excellent book for English speaking beginners in the field.

M. VAJDA

J. H. VAN DER MAAS: *Basic Infrared Spectroscopy*. Second edition

Heyden and Son Ltd., London, New York, Rheine. 1972, X + 109 pp

As G. DIJKSTRA mentions in his Foreword, "The book is an attempt to bring an understanding of the methods one uses in a reasoned approach to the interpretation of spectra of large molecules".

The main advantage of the book is the very careful selection of the subject matter, the almost ascetic concentration on necessary material and a sufficiently detailed treatment of the essential parts. These qualities make it an excellent "first book on IR spectroscopy" which will also provide sufficient stimuli and a good grounding for further study.

After a short introduction, touching on electromagnetic radiation, refraction, dispersion, absorption, selection rules and the dissipation of absorbed energy, the theory of vibrational and rotational spectra of diatomic molecules is treated. The anharmonicity of vibrations is mentioned and the intensity of vibrational and rotational bands is dealt with. After the short paragraph on the vibrating rotator, molecular interaction, the sources of line broadening are discussed. The paragraphs on triatomic molecules, combination bands, degeneracy and isotope effect follow, and the theoretical part is concluded with a short discussion of polyatomic molecules and large molecules (polymers, steroids, etc.).

The third chapter deals with spectrophotometers, their setting up and use. The excellent figures, demonstrating the effects of the various good or bad settings are a great help for the novice. Chapter 4 discusses sampling and the effects of sample preparation on the appearance of the spectra and the problems of quantitative analysis. A short discussion on attenuated total reflection concludes this chapter.

The last chapter deals with the main points of the interpretation of spectra and also gives hints for the use of the appendices, which are very good. The reviewer would like to call special attention to the excellent set of band contours.

M. VAJDA

MTP International Review of Sciences, Inorganic Chemistry Series One

Consultant Editor: H. J. Emélius. (Vol. 5. Transition Metals — Part I)

Edited by D. W. A. SHARP (Univ. of Glasgow) Butterworth et Co. London, 1972, 396 pages. £ 10.00

The Medical and Technical Publishing Co. intends to publish a series giving a systematic and critical survey on the results of recent years from various branches of science, written by selected experts. First, the most important results of chemical research in the period from 1967 to 1971 will be published in the series of Inorganic Chemistry, Physical Chemistry and Organic Chemistry in 33 volumes, together with 3 index volumes.

The volume discussed here is the 5th volume of the Inorganic Chemistry Series, surveying primarily the field of the simple binary and ternary compounds of the transition metals, but it contains also complementary chapters on transition metal complexes, which otherwise are dealt with in Volume 6. This compilation is justified by the multitude of results obtained in the last five years in the field of coordination compounds, owing to which a division of equal extent between binary and coordination compounds could not be made.

The authors of the individual chapters were asked by the editor to evaluate the recent developments of a special field critically emphasizing the most important results, without seeking completeness.

The volume contains 9 chapters, discussed in detail in the following.

Chapter 1 is 31 pages, written by R. E. HESTER (Univ. of York), deals with the salts of oxyacids, in the order of the groups of transition metals, from the scandium group to the zinc group. Each group is discussed averagely in 1—2 pages, with clear illustrations, structural formulas and 229 references, involving predominantly the publications between 1966 and 1970. In the discussion of the subject, the author emphasizes the points of coordination chemistry. Structural problems of several novel coordination compounds are reported. However, in general one paper is dealt with only in a few sentences.

Chapter 2, on binary and complex oxides, has been compiled by J. D. M. MCCONNELL (Paisley College of Technology, Glasgow) in 30 pages, with 151 references. The structure of the chapter does not reflect a uniform viewpoint. After a short introduction, results concerning non-stoichiometric compounds and defect-structure compounds are reported, the following sub-chapter discusses the results obtained in vibrational spectroscopy (infrared and Raman spectra), while the fourth sub-chapter has the title: Physical Methods Applied to Oxides. In this chapter, results in Mössbauer spectroscopy, high-pressure techniques, high-temperature and the so-called matrix isolation techniques are dealt with. However, the short fifth and sixth sub-chapters, summarizing and evaluating the new structural versions, help to obtain a clear picture.

Chapter 3, of only 26 pages, dealing with metal alkoxides, mercaptides, dialkylamides and phosphides, has been written by D. C. BRADLEY (Queen Mary College, Univ. of London) and K. J. FISHER (Grinnell College, Iowa). The part on alkoxides discusses systematically the novel compounds, and reports then in separate sub-chapters on crystal structure and the results obtained by NMR, ESR, magnetochemistry, electron absorption and reflection spectroscopy, infrared spectroscopy and thermochemistry. — On the other hand, the part on mercaptides describes only in a grouping according to the periodic system, from the titanium group to the copper group, recent results. The part dealing with dialkylamides describes their preparation, reactions and physical properties. The phosphido compounds occupy only 1 page. (150 ref.)

Chapter 4 of 78 pages, compiled by Roland WARD (Univ. of Connecticut) on the structural chemistry of the condensed systems of transition metals, gives a very good impression. An excellently systematised survey, illustrated by several figures, is given based on the most recent results concerning the problems of the lattice structure of transition metals and some of their alloys, their hydrides, borides, carbides, silicides and phosphides. (108 ref.)

Chapter 5 discusses the complexes of ligands containing nitrogen and oxygen. The author of this chapter is S. M. NELSON (Queen's Univ., Belfast). The chapter is divided into 3 parts, dealing with the complexes of ligands containing oxygen, nitrogen, and with the complexes of pseudohalide ions. The chapter is very compact, indicated also by the fact that the number of references, 455, is remarkably large, as compared to the text of only 53 pages.

A separate chapter of 40 pages, written by J. A. MCGINNETY (Yale Univ.) discusses nitrogen and oxygen complexes. The four main sections deal with the complexes of molecular oxygen, nitrosyl complexes, complexes of molecular nitrogen, and finally, with other complexes. The arrangement and systemisation of the individual sections was done primarily on the basis of structural aspects. (209 ref.)

Halogenides are divided into two chapters. Chapter 7, written by J. M. WINFIELD (Univ. of Glasgow), discusses the fluorides in 21 pages (224 ref.), while chlorides, bromides and iodides are treated in Chapter 8 in 38 pages (237 ref.) by R. COLTON (Univ. of Melbourne). The two chapters differ substantially with respect to classification and mode of discussion. Though this is partly justified by the nature of the compounds, it cannot be considered as fortunate. On the other hand, it explains the division of the subject into two chapters.

The last Chapter 9 discusses sulfides, selenides, and tellurides. The author is F. JELLINEK (Rijksuniv., Groningen). It is a concise, informative and clearly systematised summary of the recent results (57 pages, 747 ref.).

As can be seen also from the detailed review given above, in accordance with the aim set, the book tries to give an as far as possible brief but manysided survey on recent results,

obtained in the last five years, in the field of the simple compounds and some of the coordination compounds of the transition metals. Actually, it makes possible a quick orientation in diverse fields, and facilitates indeed the work of the researchers by its immense bibliography (2582 references!). The increasing difficulties in following continuously new results are well known.

Though discussion of the subjects is by far not uniform, which obviously is not to be expected in view of the difference in concept of the various reviewers. Even in view of the different nature of the individual parts of the subject, the whole work can be excellently used. Its versatility and easy comparison of several different viewpoints, contribute largely in making the volume highly useful. The book, published in photoprint, is very easy to read and has a nice presentation.

P. SZARVAS

INDEX

Printed in Hungary

A kiadásért felel az Akadémiai Kiadó igazgatója — Műszaki szerkesztő: Zacsik Annamária

A kézirat nyomdába érkezett: 1972. XII. 14. — Terjedelem: 10,15 (A/5) ív, 53 ábra

73.74441 Akadémiai Nyomda, Budapest — Felelős vezető: Bernát György

ACTA CHIMICA
ТОМ 76—ВЫП. 4

РЕЗЮМЕ

Исследование растворимости галоидов серебра в смесях воды с некоторыми неводными растворителями

Н. А. КАЗАРЯН и Э. ПУНГОР

Описывается простой метод определения продуктов растворимости, а также приводятся данные для продуктов растворимости хлористого, бромистого и йодистого серебра в смесях вода с метанолом, этанолом, норм.-пропанолом, изопропанолом, ацетоном и диметилформамидом.

О некоторых зависимостях между вариационными принципами в необратимой термодинамике

И. Й. КУМАР и Л. Н. ГУПТА

Были получены некоторые зависимости между различными вариационными принципами в необратимой термодинамике. Было показано, что принцип Дьярмати и принцип местного потенциала Пригогина и Гландсдорфа являются эквивалентными, если феноменологические коэффициенты взаимосвязаны согласно расширенным функциям Онсагера. Функция Лагранжа для обобщенного уравнения Навьера—Стокса была получена через приближение локального потенциала, и на основе сравнения ее с соответсвующей функцией Лагранжа, полученной на основе принципа Дьярмати, было показано, что две функции эквивалентны, за исключением метода их изображения. Такое подобие было продемонстрировано также в случае уравнения Лагранжа для теплопроводимости и уравнения Фика для мультикомпонентной диффузии. Вариационный принцип Байота же является частным случаем принципа местного потенциала. Частный случай принципа Циглера, в свою очередь, может быть выведен из интегрального принципа Дьярмати.

Процесс коалесценции между неоднородными частицами

ФОН Х. ЗОНТАГ, Н. БУСКЕ и К. ШТРЕНГЕ

Различные механизмы стабильности к коалесценции в трехфазных системах обсуждаются теоретически для смешиваемых и несмешиваемых дисперсных фаз и экспериментально проверяются на различных дисперсных системах. В противоположность процессу коалесценции однородных частиц, неоднородные частицы могут быть термодинамически стабильными по отношению к коалесценции. С термодинамической точки зрения, эту стабильность можно связать с повышением свободной энергии поверхности раздела, а с точки зрения молекулярной физики, — с изменением знака дисперсионных сил. Для объяснения стабилизирующего влияния адсорбционных слоев выдвигается два механизма.

Исследование системы пиридиниум — пиридин с водородными мостиками с помощью метода Хюккеля

А. ШЮТЁ и М. М. ХЕДЬХАТИ

Система пиридиниум — пиридин с водородными мостиками была изучена с помощью обобщенного метода Хюккеля. С помощью симплексной минимализации для двух переменных было доказано, что зависимость общей электронной энергии от расстояний N . . N и N . . H не имеет минимума. Принимая для расстояния атомов N определенную величину (3,85 Å), наблюдалось поляризующее влияние движущихся протонов на валентные электроны.

Механизм эластичного пост-эффекта в структурированных водных суспензиях бентонита низких концентраций

Е. Д. ЩУКИН и П. А. РЕКНБИНДЕР

1. Микромеханизм обратимого пост-эффекта в коллоидально-дисперсных суспензиях бентонита низкой концентрации рассматривался как совокупность ступеней быстрой и медленной эластичных деформаций (с постоянными времени порядка нескольких сотых секунды и 10^2 сек, соответственно). Приводится приближенное количественное определение основных параметров, описывающих данный процесс: равновесных эластичных модулей и вязкостей, согласующихся с экспериментальными данными.

2. В качестве механизма, объясняющего существование обратимых деформаций под влиянием небольших напряжений сдвига, полагается проявление предпочитаемой взаимной ориентации анизометричных частиц в коагулированной структуре; увеличение энтропии системы, связанной с этой текстуризацией, позволяет определить величину равновесного модуля эластичности ($\sim 10^4$ дин/см^3).

3. Две наблюдаемые ступени обратимого пост-эффекта могут быть описаны моделью Кельвина (с заданной величиной равновесного модуля высокой эластичности) как два различных механизма изменения взаимной ориентации частиц: как результат поворота друг против друга, и вследствие скольжения — смещения точек контакта по поверхности частицы. В первом случае, вязкость эластичного пост-эффекта определяется на основе модели неподвижной дисперсной среды (вода), протекающей из ячейки в ячейку с произвольной решеткой частиц и составляет (10^4—10^5) η_w, где η_w — вязкость воды; во втором случае, вязкость эластичного пост-эффекта может быть определена на основе определения вязкостного сопротивления в коагулированных контактах в условиях сдвига и достигает величины 10^8 d_w.

Образование 1,2-ортоэфиров глюкозы из тетра-О-ацетил-α-О-глюкопиранозилбромида под влиянием фосфоранов

И. ПИНТЕР, Й. КОВАЧ и А. МЕССМЕР

Образование 1,2-ортоэфиров глюкозы из тетра-О-ацетил-α-О-глюкопиранозилбромида происходит под влиянием этоксикарбонилметилен- и цианметилен-трифенилфосфоранов в растворителе, содержащем спирт. Отсутствие реакции Бестманна (т. е. образования ацетилальдозилфосфорана) может быть вызвано сильным стерическим препятствием, оказываемым трифенилфосфиновой группой.

N-Гликозиды, XVII

Синтез и строение N-нитрозо-N-арилгликозиламинов

Р. БОГНАР и М. ПУШКАШ

Были синтезированы О-ацетали вторичных N-арилгликозиламинов (I) и их метиловые эфиры, а также стабильные кристаллические N-нитрозо-производные (II). N-Нитрозосоединения, не содержащие ацетильной группы (III), в случае альдогексозы как сахарной компоненты являются некристаллическими, сильно гигроскопическими соединениями, в то время как в случае альдопентозных производных — это кристаллические соединения. Они могут быть ацетилированы, давая при этом кристаллические бензальные производные (IV).

Строение N-нитрозо-соединений было доказано, подвергая III кислому гидролизу и азотированию. Были получены продукты разложения и превращений, свидетельствующие о наличии структур первичных ароматических N-нитрозоаминов, наряду с сахарами. Соединения III при взаимодействии с β-нафтолом дают соответствующие краски типа фенилазо-β-нафтола (V).

Исследование превращений диолов и циклических эфиров, XXXI

Дегидрирование 1,3-диолов на металлических катализаторах

М. БАРТОК и А. МОЛНАР

Исследована дегидратация 1,3-диолов различного строения на некоторых медных катализаторах. На основе экспериментальных данных было показано, что дегидратацию 1,3-диолов катализирует специально приготовленный медный катализатор. В зависимости от структуры диола, происходят три основные реакции: образование оксосоединений с тем же самым числом углеродных атомов как и в диоле, процесс 1,2-отщепления и процессы фрагментации.

Экспериментально было доказано, что превращения диолов, сопровождаемые образованием оксосоединений, наблюдаются не только в случае вицинальных диолов, но, при изменении некоторых экспериментальных условий, и в случае некоторых типов 1,3-диолов.

Исследование превращений диолов и циклических эфиров, XXXII

Исследование превращений 2-метил-оксациклоалканов на металлических катализаторах

М. БАРТОК, И. ТЁРЁК и И. САБО

Были исследованы превращения 2-метил-этиленоксида, 2-метил-оксина, 2-метил-тетрагидрофурана и 2-метил-тетрагидропирана в присутствии катализаторов Pt/T, Pd/T, Rh/T, Cu/Al, Ni/Al и Zn/Al при идентичных экспериментальных условиях с помощью метода импульсной техники. Экспериментально анализировались направления реакций, зависящие от величины кольца и катализатора: изомеризация до соответствующих альдегидов, кетонов и ненасыщенных спиртов, а также гидрогенолиз с образованием соответствующих спиртов.

Синтез гексапептидамида, потенциально препятствующего выделению GH—RH*

Ш. БАЮС, И. ФАУСТ и Й. БОРВЕНДЕГ

На основе структурного подобия можно заключить, что GH—RH образуется из β-цепи гемоглобина и является его N-конечным 1—10 фрагментом. Полагалось, что выделение GH—RH может быть заторможено такими пептидами, на N-конце которых содержится 10—11 дипептидная секвенция β-цепочки. Для изучения данной проблемы был получен 10—15 гексапептидный фрагмент β-цепочки гуманного гемоглобина, исходя из Trp—NH_2 с помощью ступенчатого синтеза.

* Гормон, выделяющий гормон роста

The Acta Chimica publish papers on chemistry, in English, German, French and Russian.

The Acta Chimica appear in volumes consisting of four parts of varying size, 4 volumes being published a year.

Manuscripts should be addressed to

Acta Chimica
Budapest 112/91 Műegyetem

Correspondence with the editors should be sent to the same address.

The rate of subscription is $ 24.00 a volume.

Orders may be placed with "*Kultúra*" Foreign Trade Company for Books and Newspapers (1389 Budapest 62, P.O.B. 149 Account No. 218 10990) or with representatives abroad

---

Les Acta Chimica paraissent en français, allemand, anglais et russe et publient des mémoires du domaine des sciences chimiques.

Les Acta Chimica sont publiés sous forme de fascicules. Quatre fascicules seront réunis en un volume (4 volumes par an).

On est prié d'envoyer les manuscrits destinés à la rédaction à l'adresse suivante:

Acta Chimica
Budapest 112/91 Műegyetem

Toute correspondance doit être envoyée à cette même adresse.

Le prix de l'abonnement est de $ 24,00 par volume.

On peut s'abonner à l'Entreprise pour le Commerce Extérieur de Livres et Journaux «*Kultúra*» (1389 Budapest 62, P.O.B. 149 Compte-courant N°. 218 10990) ou à l'étranger chez tous les représentants ou dépositaires.

«*Acta Chimica*» издают трактаты из области химической науки на русском, французском, английском и немецком языках.

«*Acta Chimica*» выходят отдельными выпусками разного объема. 4 выпуска составляют один том. 4 тома публикуются в год.

Предназначенные для публикации рукописи следует направлять по адресу:

Acta Chimica
Budapest 112/91 Műegyetem

По этому же адресу направлять всякую корреспонденцию для редакции.

Подписная цена – $ 24,00 за том.

Заказы принимает предприятие по внешней торговле книг и газет «*Kultúra*» (1389 Budapest 62, P.O.B. 149 Текущий счет № 218 10990) или его заграничные представительства и уполномоченные.

Reviews of the Hungarian Academy of Sciences are obtainable at the following addresses:

ALBANIA

Drejtorija Qändrone e Pärhapjes
dhe Propagandimit të Librit
Kruga Konferenca e Päzes
Tirana

AUSTRALIA

A. Keesing
Box 4886, GPO
Sydney

AUSTRIA

GLOBUS
Höchstädtplatz 3
A-1200 Wien XX

BELGIUM

Office International de Librairie
30, Avenue Marnix
1050 Bruxelles
Du Monde Entier
162, Rue du Midi
1000 Bruxelles

BULGARIA

HEMUS
11 pl Slaveikov
Sofia

CANADA

Pannonia Books
2, Spadina Road
Toronto 4, Ont.

CHINA

Waiwen Shudian
Peking
P. O. B. 88

CZECHOSLOVAKIA

Artia
Ve Smečkách 30
Praha 2
Poštovní Novinová Služba
Dovoz tisku
Vinohradská 46
Praha 2
Mad'arská Kultura
Václavské nám. 2
Praha 1
SLOVART A. G.
Gorkého
Bratislava

DENMARK

Ejnar Munksgaard
Nörregade 6
Copenhagen

FINLAND

Akateeminen Kirjakauppa
Keskuskatu 2
Helsinki

FRANCE

Office International de Documentation
et Librairie
48, rue Gay-Lussac
Paris 5

GERMAN DEMOCRATIC REPUBLIC

Deutscher Buch-Export und Import
Leninstraße 16
Leipzig 701
Zeitungsvertriebsamt
Fruchtstraße 3—4
1004 Berlin

GERMAN FEDERAL REPUBLIC

Kunst und Wissen
Erich Bieber
Postfach 46
7 Stuttgart S.

GREAT BRITAIN

Blackwell's Periodicals
Oxenford House
Magdalen Street
Oxford
Collet's Subscription Import
Department
Dennington Estate
Wellingsborough. Northants.
Robert Maxwell and Co. Ltd.
4—5 Fitzroy Square
London W. 1

HOLLAND

Swetz and Zeitlinger
Keizersgracht 471—478
Amsterdam C.
Martinus Nijhof
Lange Voorhout 9
The Hague

INDIA

Hind Book House
66 Babar Road
New Delhi 1

ITALY

Santo Vanasia
Via M. Macchi 71
Milano
Libreria Commissionaria Sansoni
Via La Marmora 45
Firenze
Techna
Via Cesi 16
40135 Bologna

JAPAN

Kinokuniya Book-Store Co. Ltd.
826 Tsunohazu 1-chome
Shinjuku-ku
Tokyo
Maruzen and Co. Ltd.
P. O. Box 605
Tokyo-Central

KOREA

Chulpanmul
Phenjan

NORWAY

Tanum-Cammermeyer
Karl Johansgt 41—43
Oslo 1

POLAND

RUCH
ul. Wronia 23
Warszawa

ROUMANIA

Cartimex
Str. Aristide Briand 14—18
Bucureşti

SOVIET UNION

Mezhdunarodnaya Kniga
Moscow G—200

SWEDEN

Almquist and Wiksell
Gamla Brogatan 26
S—101 20 Stockholm

USA

F. W. Faxon Co. Inc.
15 Southwest Park
Westwood, Mass. 02090
Stechert Hafner Inc.
31. East 10th Street
New York, N. Y. 10003

VIETNAM

Xunhasaba
19, Tran Quoc Toan
Hanoi

YUGOSLAVIA

Forum
Vojvode Mišića broj 1
Novi Sad
Jugoslovenska Knjiga
Terazije 27
Beograd

25. VI. 1973 Index: 26.007